
Development and Evaluation of a Performance Modeling Flight Test Approach Based on Quasi Steady-State Maneuvers

Thomas R. Yechout and Keith B. Braman

Grant NSG-4028
April 1984

Development and Evaluation of a Performance Modeling Flight Test Approach Based on Quasi Steady-State Maneuvers

Thomas R. Yechout and Keith B. Braman

Flight Research Laboratory, University of Kansas Center for Research, Inc., Lawrence, Kansas 66045

Prepared for
Ames Research Center
Dryden Flight Research Facility
Edwards, California
under Grant NSG-4028

1984



National Aeronautics and
Space Administration

Ames Research Center

Dryden Flight Research Facility
Edwards, California 93523

TABLE OF CONTENTS

	<u>Page</u>
LIST OF FIGURES.	viii
LIST OF TABLES	xii
LIST OF SYMBOLS.	xiv
LIST OF ACRONYMS	xviii

CHAPTER

1. INTRODUCTION.	1
1.1 BACKGROUND	1
1.2 OBJECTIVE.	4
2. PROJECT HISTORY	6
3. APPROACH.	8
3.1 GENERAL.	8
3.2 ANALYSIS TECHNIQUES.	12
3.2.1 Concept	12
3.2.1.1 Aerodynamic Characteristics.	14
3.2.1.2 Engine Characteristics	24
3.2.1.3 Summary.	40
3.2.2 Data Flow	42

TABLE OF CONTENTS (continued)

<u>CHAPTER</u>	<u>Page</u>
3.2.3 Conventional Data Reduction	52
3.2.3.1 Stabilized Points.	53
3.2.3.2 Pull-Up, Push-Over, Pull-Up.	55
3.2.4 Performance Modeling.	57
3.2.4.1 ITERATE Program.	58
3.2.4.2 MODEL Program.	62
3.2.5 Error Analysis.	65
3.2.6 Accelerometer Corrections	69
3.2.7 Structural Flexibility.	70
3.3 CALIBRATION TESTS.	72
3.3.1 Instrumentation Transducers	72
3.3.2 Thrust Run.	73
3.3.3 Pitot-Static System, Temperature Probe and Angle of Attack	77
3.3.4 Weight and Balance.	84
3.3.5 Accelerometer Alignment	85
3.4 FLIGHT TESTS AND PROCEDURES.	86
3.4.1 General	86
3.4.2 Description of Tests.	87
3.5 INSTRUMENTATION.	93
4. RESULTS	97
4.1 CALIBRATION TESTS.	97
4.1.1 Instrumentation Transducers	97
4.1.2 Thrust Run.	98

TABLE OF CONTENTS (continued)

<u>CHAPTER</u>	<u>Page</u>
4.1.3 Pitot Static System, Temperature Probe and Angle of Attack	106
4.1.4 Weight and Balance.	110
4.2 BASELINE CHARACTERISTICS	112
4.2.1 Aerodynamic	112
4.2.1.1 C_{L_s} versus α	112
4.2.1.2 C_{D_s} versus α	116
4.2.2 Engine.	121
4.2.2.1 F_g/δ_{t_2} versus $N_1/\sqrt{\theta}_{t_2}$	121
4.2.2.2 $W_f/\sqrt{\theta}_{t_2} \delta_{t_2}^N$ versus $N_1/\sqrt{\theta}_{t_2}$	123
4.2.2.3 $W_a \sqrt{\theta}_{t_2} / \delta_{t_2}$ versus $N_1/\sqrt{\theta}_{t_2}$	125
4.3 CONVENTIONAL DATA REDUCTION.	127
4.3.1 Stabilized Points	127
4.3.2 Push-Pull Maneuvers	130
4.4 PERFORMANCE MODELING	138
4.4.1 Cruise Performance Prediction	138
4.4.2 Flight Trajectory Performance Prediction.	156
4.4.2.1 Climbs	158
4.4.2.2 Accelerations/Decelerations.	166
4.5 ERROR ANALYSIS	173
4.6 DATA REPEATABILITY	189
5. ESTIMATED FLIGHT TIME SAVINGS	190
5.1 CONVENTIONAL EVALUATION.	191
5.2 PERFORMANCE MODELING, APPROACH I (CONSERVATIVE).	193

TABLE OF CONTENTS (continued)

<u>CHAPTER</u>	<u>Page</u>
5.3 PERFORMANCE MODELING, APPROACH II (ANTICIPATED) . . .	194
5.4 PERCENT REDUCTION IN FLIGHT TIME	195
5.5 SUMMARY.	196
6. FUTURE WORK	197
7. CONCLUSIONS AND RECOMMENDATIONS	199
7.1 CONCLUSIONS.	200
7.2 RECOMMENDATIONS.	204
8. REFERENCES.	207

APPENDICES

A. SUPPORT ORGANIZATIONS	210
B. TRIGONOMETRIC RELATIONSHIPS FOR THRUST AND C.G. CORRECTION.	214
C. SOFTWARE DOCUMENTATION.	217
D. TFE 731-2 ENGINE PREDICTION DECK FINAL THRUST, FUEL FLOW AND AIRFLOW CHARACTERISTICS.	315
E. LEAR 55 THRUST RUN.	320
F. DATA PLOTS: BASELINE AERODYNAMIC CHARACTERISTICS	326
G. LEAR 55 BASELINE ENGINE CHARACTERISTICS	342
H. LEAR 35 BASELINE ENGINE CHARACTERISTICS	360
I. FLIGHT TRAJECTORY PREDICTIONS	390

LIST OF FIGURES

<u>Number</u>	<u>Title</u>	<u>Page</u>
2.1	Program Schedule	7
3.1	Gates Learjet Model 35 Aircraft.	9
3.2	Gates Learjet Model 35 Three-View.	10
3.3	Gates Learjet Model 35 Flight Envelope	11
3.4	Aircraft Force Balance Diagram	15
3.5	Thrust Moment Vectors.	18
3.6	Moment Arms for C.G. Standardization	20
3.7	Engine Deck Corrected Thrust Characteristics, M = .45.	28
3.8	Engine Deck Corrected Airflow Characteristics, M = .45.	29
3.9	Engine Deck Corrected Fuel Flow Characteristics, M = .45.	30
3.10	Engine Deck Nonstandard Corrected Fuel Flow Characteristics, M = .45, N = .96.	32
3.11	Engine Deck Nonstandard Corrected Fuel Flow Characteristics, M = .45, N = .88.	33
3.12	Data Management System	43
3.13	Performance Modeling Data Flow	46
3.14	Sample Mach History of C_{D_s} , 95% N_1 Accel at 73000 W/ δ	50
3.15	Sample Mach History of C_{L_s} , 95% N_1 Accel at 73000 W/ δ	51

LIST OF FIGURES (continued)

<u>Number</u>	<u>Title</u>	<u>Page</u>
3.16	ITERATE Program Flow Chart	59
3.17	Thrust Run Load Cell/Tie Down Configuration.	74
3.18	Thrust Run Hardware.	75
3.19	Trailing Cone Assembly	80
3.20	Noseboom Installation of Angle of Attack and Sideslip Vanes	82
3.21	Typical Test Sequence.	90
3.22	Instrumentation System Installation.	96
4.1	Thrust Run Corrected TSFC Data	100
4.2	TSFC Correction Parameter, η	101
4.3	Thrust Run Corrected Thrust Data	103
4.4	Thrust Run Nonstandard Corrected Fuel Flow Data.	104
4.5	Thrust Run Corrected Airflow Data.	105
4.6	Pitot Static System Calibration.	107
4.7	Temperature Probe Recovery Factor Calibration.	108
4.8	Angle of Attack Upwash Calibration	109
4.9	Aircraft C.G. Travel	111
4.10	Lift Coefficient Characteristics, $M \geq .65$	114
4.11	Lift Coefficient Characteristics, $M \leq .65$	115
4.12	Drag Coefficient Characteristics, $M \geq .6$	118
4.13	Drag Coefficient Characteristics, $M \leq .55$, 90 and 95% N_1	119
4.14	Drag Coefficient Characteristics, $M \leq .55$, 50 to 90% N_1	120

LIST OF FIGURES (continued)

<u>Number</u>	<u>Title</u>	<u>Page</u>
4.15	Corrected Gross Thrust Characteristics, $M = .55$	122
4.16	Nonstandard Corrected Fuel Flow Characteristics, $M = .55$	124
4.17	Corrected Airflow Characteristics, $M = .55$	126
4.18	Lift Coefficient Push-Pull Data, Flight 185, Run 10	133
4.19	Lift Coefficient Push-Pull Data, Flight 185, Run 13	134
4.20	Drag Coefficient Push-Pull Data, Flight 185, Run 10	135
4.21	Drag Coefficient Push-Pull Data, Flight 185, Run 13	136
4.22	Boom Bending Correction Estimate.	137
4.23	ITERATE Corrected RPM Prediction, $W/\delta = 22000$ lbs . . .	140
4.24	ITERATE Corrected RPM Prediction, $W/\delta = 40000$ lbs . . .	141
4.25	ITERATE Corrected RPM Prediction, $W/\delta = 60000$ lbs . . .	142
4.26	ITERATE Corrected RPM Prediction, $W/\delta = 80000$ lbs . . .	143
4.27	ITERATE Standardized Range Factor Prediction, $W/\delta = 22000$ lbs.	144
4.28	ITERATE Standardized Range Factor Prediction, $W/\delta = 40000$ lbs.	145
4.29	ITERATE Standardized Range Factor Prediction, $W/\delta = 60000$ lbs.	146
4.30	ITERATE Standardized Range Factor Prediction, $W/\delta = 80000$ lbs.	147
4.31	ITERATE Standardized Specific Range Prediction, $W/\delta = 22000$ lbs.	148
4.32	ITERATE Standardized Specific Range Prediction, $W/\delta = 40000$ lbs.	149

LIST OF FIGURES (continued)

<u>Number</u>	<u>Title</u>	<u>Page</u>
4.33	ITERATE Standardized Specific Range Prediction, W/ δ = 60000 lbs.	150
4.34	ITERATE Standardized Specific Range Prediction, W/ δ = 80000 lbs.	151
4.35	ITERATE Specific Range Parameter Prediction, W/ δ = 22000 lbs.	152
4.36	ITERATE Specific Range Parameter Prediction, W/ δ = 40000 lbs.	153
4.37	ITERATE Specific Range Parameter Prediction, W/ δ = 60000 lbs.	154
4.38	ITERATE Specific Range Parameter Prediction, W/ δ = 80000 lbs.	155
4.39	MODEL Time Prediction, Profile 1	160
4.40	MODEL Fuel Used Prediction, Profile 1.	161
4.41	MODEL Time Prediction, Profile 2	162
4.42	MODEL Fuel Used Prediction, Profile 2.	163
4.43	MODEL Time Prediction, Profile 3	164
4.44	MODEL Fuel Used Prediction, Profile 3.	165
4.45	MODEL Time Prediction, Profile 6	167
4.46	MODEL Fuel Used Prediction, Profile 6.	168
4.47	MODEL P _s Prediction, Profile 6	169
4.48	MODEL Time Prediction, Profile 7	170
4.49	MODEL Fuel Used Prediction, Profile 7.	171
4.50	MODEL P _s Prediction, Profile 7	172

LIST OF TABLES

<u>Number</u>	<u>Title</u>	<u>Page</u>
1	Lear 35 Specifications	8
2	Wetted Areas and Characteristic Lengths Applicable to Skin Friction Drag Correction	23
3	Test Runs for Engine Deck Combined with Installation Effects	26
4	Power of δ_{t_2} , N, Used for Nonstandard Corrected Fuel Flow.	34
5	Sensitivity Analysis Parameters.	66
6	Sensitivity Analysis Maneuvers	68
7	Test Points for Pitot Static System, Temperature Probe and Angle of Attack Calibration.	78
8	Flight Test Summary.	86
9	Performance Modeling Maneuvering Sequences	89
10	Instrumentation Parameter List	94
11	Thrust Run Summary	99
12	Stable Point Summary	128
13	ITERATE Stable Point Prediction Cases.	129
14	Flight Trajectory Summary.	157
15	Maximum Relative Error Analysis for Lift Coefficient (C_{L_s}).	176
16	Maximum Absolute Error Analysis for Lift Coefficient (C_{L_s}).	177
17	Maximum Relative Error Analysis for Drag Coefficient (C_{D_s}).	178
18	Maximum Absolute Error Analysis for Drag Coefficient (C_{D_s}).	179

LIST OF TABLES (continued)

<u>Number</u>	<u>Title</u>	<u>Page</u>
19	Maximum Relative Error Analysis for Corrected Gross Thrust (F_g/δ_{t_2})	180
20	Maximum Absolute Error Analysis for Corrected Gross Thrust (F_g/δ_{t_2})	181
21	Maximum Relative Error Analysis for Corrected Airflow ($W_a\sqrt{\theta_{t_2}}/\delta_{t_2}$)	182
22	Maximum Absolute Error Analysis for Corrected Airflow ($W_a\sqrt{\theta_{t_2}}/\delta_{t_2}$)	183
23	Maximum Relative Error Analysis for Gross Thrust (F_g)	184
24	Maximum Absolute Error Analysis for Gross Thrust (F_g)	185
25	Maximum Relative Error Analysis for Airflow (W_a) . . .	186
26	Maximum Absolute Error Analysis for Airflow (W_a) . . .	187
27	Error Analysis Summary Based on Instrumentation Accuracy	188
28	"Speed Power" Estimate	191

LIST OF SYMBOLS

<u>Symbol</u>	<u>Definition</u>
a_x	acceleration along x axis
a_z	acceleration along z axis
c.g.	center of gravity
\bar{c}	mean aerodynamic chord
C_D	drag coefficient
C_{D_S}	drag coefficient corrected for skin friction variation
$C_{D_{SF}}$	drag coefficient due to skin friction
C_L	lift coefficient
C_{L_0}	zero α lift coefficient
C_{L_α}	$\partial C_L / \partial \alpha$
C_{L_S}	lift coefficient corrected for thrust moment effect and nonstandard c.g.
$C_{L_{A/C}}$	lift coefficient with thrust vector removed
$C_{L_{T_{A/C}}}$	lift coefficient corrected for thrust moment effects
C_f	skin friction coefficient
D	drag
F_g	gross thrust
F_r	engine ram drag
F_{ex}	excess thrust
F_x	forces along x axis
F_z	forces along z axis
g	acceleration due to gravity, load factor
h	pressure altitude
h_g	geometric altitude

LIST OF SYMBOLS (continued)

<u>Symbol</u>	<u>Definition</u>
h_e	energy height
h_r	F_r moment arm about c.g.
$H_{c.g.}$	horizontal c.g. position
I_{yy}	aircraft moment of inertia about y axis
K	proportionality constant for induced drag ($C_D = C_{D_0} + KC_L^2$); temperature probe recovery factor
C_{m_q}	variation of pitching moment coefficient with pitch rate
$C_{m_{\dot{\alpha}}}$	variation of pitching moment coefficient with the rate of change of angle of attack
$C_{m_{\delta_e}}$	variation of pitching moment coefficient with elevator deflection
L	lift
l	distance between c.g. and nose boom angle of attack vane
l_{tail}	tail lift moment arm about c.g.
M_{ic}	instrument corrected Mach number
M	true Mach number, pitching moment
m	aircraft mass
\dot{m}_e	total engine mass flow rate
n_x	load factor along x axis
n_z	load factor along z axis
N	power of δ_{t_2}
N_1	engine fan RPM
N_2	engine core RPM
P_s	specific excess power

LIST OF SYMBOLS (continued)

<u>Symbol</u>	<u>Definition</u>
P_s	test system static pressure
p	pressure
P_t	total pressure measured by pitot tube
\bar{q}	dynamic pressure
q	pitch rate
R_e	Reynolds number
S	wing reference area
T	absolute temperature
T_{ic}	instrument corrected total temperature
t	time
V	aircraft true velocity
$V_{c.g.}$	vertical c.g. position
V_∞	engine exhaust velocity downstream from nozzle
W	aircraft weight
W_a	engine airflow
W_e	total engine weight flow rate
W_f	fuel flow
Z_{thrust}	F_g moment arm about c.g.

Greek Symbol

α	angle of attack
β	sideslip
δ	$P_{ambient}/P_{sea\ level}$ (pressure ratio)
δ_e	elevator deflection
λ	aircraft thrust inclination angle

LIST OF SYMBOLS (continued)

<u>Symbol</u>	<u>Definition</u>
η	TSFC correction parameter
γ	flight path angle; ratio of specific heat for air
θ	$T_{\text{ambient}}/T_{\text{sea level}}$ (temperature ratio); pitch attitude angle
ρ	air density

Subscript

A	average for two engines
a	ambient.
body	body axis system
D	deck predicted
L	left engine
R	right engine
s	standardized
std	standard
T	total for two engines
t	test; total property
TRP	thrust run predicted
w	wind axis system
x	longitudinal axis
y	lateral axis
z	normal axis
2	compressor face conditions
S.L.	sea level value

LIST OF ACRONYMS

<u>Acronym</u>	<u>Definition</u>
A/C	Aircraft
AFB	Air Force Base
AFFTC	Air Force Flight Test Center
CRINC	University of Kansas Center for Research, Inc.
D.E.	Doctor of Engineering
FTDB	Flight Test Data Base
GLC	Gates Learjet Corporation
KSR	Kohlman Systems Research
K.U.	University of Kansas
KU-FRL	University of Kansas Flight Research Lab
MAC	Mean Aerodynamic Chord
M.E.	Master of Engineering
NASA	National Aeronautics and Space Administration
NM	Nautical Mile
PRF	Pressure Recovery Factor
R.A.	Research Assistant
RPM	Revolutions Per Minute
SEL	Systems Engineering Laboratories
TSFC	Thrust Specific Fuel Consumption

1. INTRODUCTION

1.1 BACKGROUND

A large number of flight test hours have been required to define the performance characteristics of modern aircraft using classical flight test techniques. Typically, cruise performance has been defined by generating extensive speed-power data while acceleration and flight trajectory performance has been defined from acceleration, climb, and descent tests throughout the flight envelope. An alternate method is to develop and verify a performance model using only a limited amount of acceleration/deceleration (quasi steady-state maneuvering) data to predict the overall one g performance characteristics of an aircraft. A substantial saving in flying hours as well as data reduction time would be realized compared to classical methods. In addition, the performance modeling approach would result in definition of baseline aircraft and engine performance characteristics allowing flexible application of the technique to a variety of situations and direct use of the data in applications such as aircraft simulation and correlation of wind tunnel results.

Studies have been conducted by NASA and the Air Force to establish the potential of the performance modeling concept. Performance modeling was used by NASA with an F-104G and a YF-12C aircraft [1 and 2] and by NASA and AFFTC with an F-111A aircraft [3, 4]. These efforts used acceleration, deceleration, and climb maneuvers at full military power and/or maximum (afterburner) power to generate a model which was used to predict flight trajectory performance characteristics for "off-test"

conditions at military or maximum power. Good correlation was achieved between the model and actual aircraft climb/acceleration performance, and recommendations were made for further development and evaluation of this concept in a dedicated flight test program which would define prediction accuracy and extend application of the model to partial power conditions. The effort outlined in this report was designed to satisfy those recommendations by extending development of the concept, developing all applicable software and techniques, and conducting the needed flight test program.

A survey of applicable background literature was accomplished to review past work in performance flight testing, including the methods used, data acquisition, and data reduction techniques [5]. The use of acceleration techniques to determine aircraft baseline performance characteristics has received increasing attention during the past 10 years. Many of the references advocated the dynamic push-over, pull-up maneuver as an evaluation technique in addition to the quasi steady-state accel/decel maneuvers. However, because of the need for certain stability and control derivatives along with the I_{yy} moment of inertia when using push-over, pull-up maneuvers, this program concentrated primarily on the quasi steady-state acceleration/deceleration maneuvers. Thus, the methods developed in this program were dependent on a minimum of additional information. Many of the references reduced dynamic data to drag polar form; however, inclusion of both power effects and Mach effects in the drag polar was not found in any of the literature. In addition, the use of baseline characteristics input to a modeling program for prediction of stabilized cruise performance as a check on the

overall process was also not addressed. The effort outlined in this report provided a straightforward method for determining aircraft performance which required limited instrumentation and knowledge of the aircraft but yet was capable of providing accurate results and significantly reducing flight time. It should therefore be applicable to a wide range of users including general aviation as well as highly sophisticated aircraft.

1.2 OBJECTIVE

The objective of this program was to develop, evaluate, and verify a generalized aircraft performance modeling technique based on a limited amount of quasi steady-state flight test data. The performance model was then used to predict steady-state (cruise) and flight trajectory performance throughout the one g flight envelope. Evaluation and verification of the modeling techniques were accomplished by comparing model predicted performance with in-flight results.

This effort was designed to advance the state of technology by

1. Developing an overall methodology to improve performance modeling accuracy over techniques used in the past.
2. Developing and evaluating a flight test technique capable of defining power-dependent lift and drag characteristics for the full range of power settings. (Successful definition of power effects was a fundamental requirement for developing the accurate performance predictions typically needed for flight manuals, engineering documentation and simulators.)
3. Developing a modeling technique to predict the stabilized cruise performance characteristics of the aircraft directly from acceleration/deceleration data.
4. Extending application of performance modeling to acceleration, deceleration and climb maneuvers at any power setting so that realistic flight trajectories involving variable airspeed/altitude/throttle setting conditions can be accurately predicted.

5. Developing and evaluating a simplified in-flight thrust and airflow calculation method which was not dependent on extensive engine instrumentation.
6. Defining the accuracies associated with the above techniques based on comparison of model predictions to actual in-flight data.
7. Developing an overall methodology for realistic utilization of the modeling approach which includes requirements for instrumentation and flight maneuvers, definition of calibration tests, application of the engine performance prediction deck, and definition of applicable software.

2. PROJECT HISTORY

This program began with the submission of a proposal to NASA Ames-Dryden Flight Research Facility in February 1982. The proposal outlined a three-phase effort consisting of

1. Phase I: Planning and Development of Analytical Tools.
2. Phase II: Flight Test.
3. Phase III: Reporting.

A detailed task breakdown for each phase is presented in Reference 6.

Funding for Phase I was requested in the initial proposal and was received from NASA Ames-Dryden, via Grant NSG 4028, with work officially beginning in late spring of 1982. Phase I was concluded in October 1982 with the submission of a detailed Flight Test Plan, KU-FRL-577-1 [5].

A proposal covering the Phase II effort was submitted in July 1982.

Approval for this effort was received in late 1982 via a continuation of Grant NSG 4028. Phase II was completed in August 1983.

Phase III was primarily directed at preparation of the Final Report. It began with a presentation of preliminary flight test results to a review group at NASA Ames-Dryden in August 1983. Comments from this review were then used to assist in the Final Report writing effort. Submission and presentation of the Final Report were the last major efforts in Phase III required to bring the program to completion. The overall program schedule is presented in Figure 2.1. The support organizations which played a direct role in this effort are discussed in Appendix A.

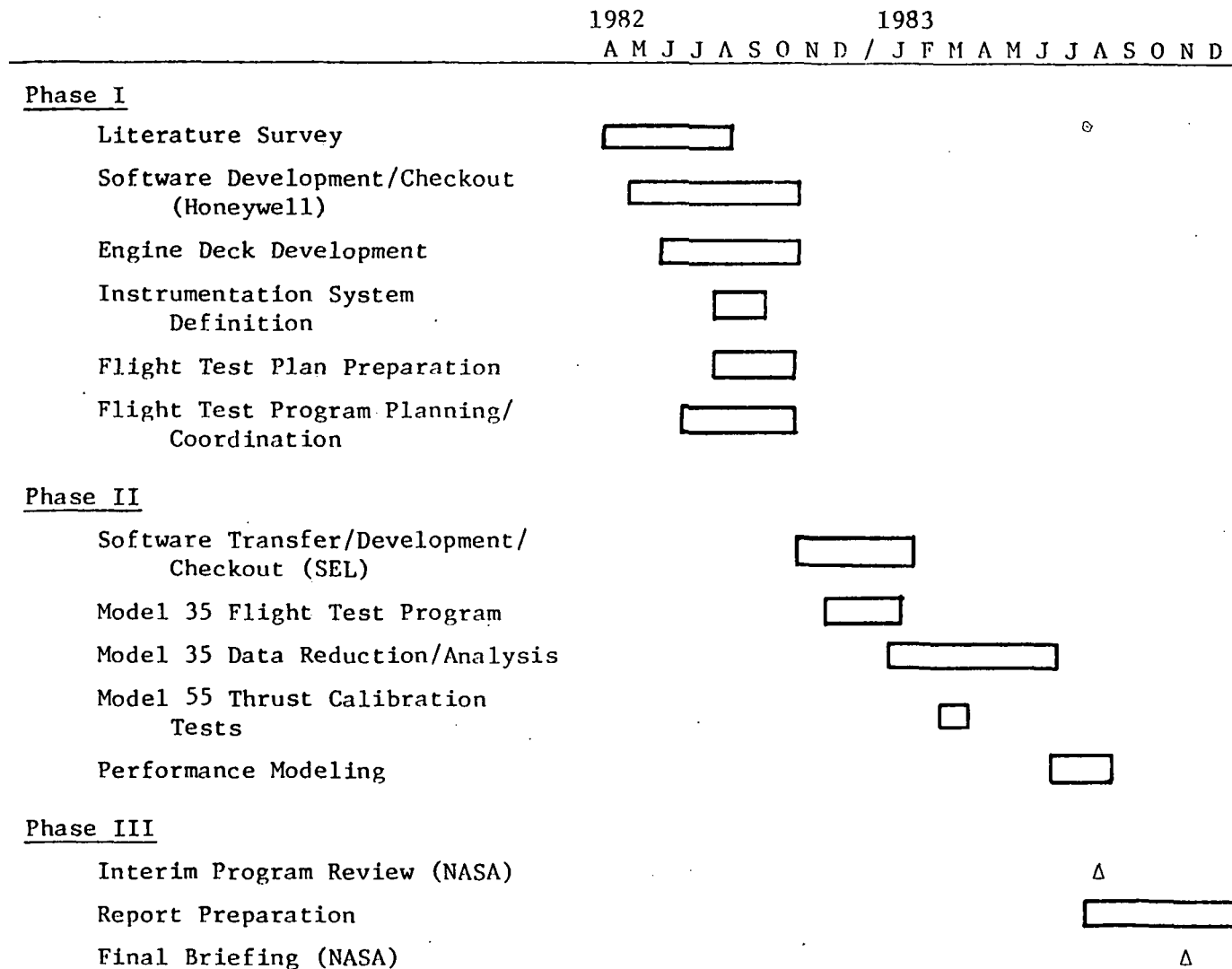


Figure 2.1: Program Schedule

3. APPROACH

3.1 GENERAL

The flight test program consisted of 17.4 flight hours with an instrumented Learjet Model 35 business jet (Figure 3.1) in the cruise configuration to develop and evaluate the performance modeling approach. The Lear 35 is a subsonic, twin-jet aircraft, certified to FAR 25. A three-view drawing is presented in Figure 3.2. The aircraft has a swept wing with low drag laminar flow airfoil, tip tanks, twin Garrett Air Research TFE 731-2 turbofan engines which are pod mounted on the aft fuselage, and a completely flush-riveted fuselage and wing structure. The TFE 731-2 engine is a twin spool turbofan with a 2.67 bypass ratio and a maximum thrust of 3,5000 lbs each. The Lear 35 has a maximum gross weight of approximately 18,000 lbs, and the flight envelope is presented in Figure 3.3. Table 1 presents additional Lear 35 specifications. The test aircraft was equipped with a flight test nose boom and was operated by the Gates Learjet Corporation. The aircraft was based at the Learjet facility in Wichita, Kansas, during the program.

Table 1: Lear 35 Specifications

Maximum Mach Number	.83
Long Range Cruise Mach Number	.73
Normal Cruise Mach Number	.77
Maximum Certificated Operating Altitude	45,000 ft.
Service Ceiling	42,500 ft.
Usable Fuel Capacity	6172 lbs.



Figure 3.1: Gates Learjet Model 35 Aircraft

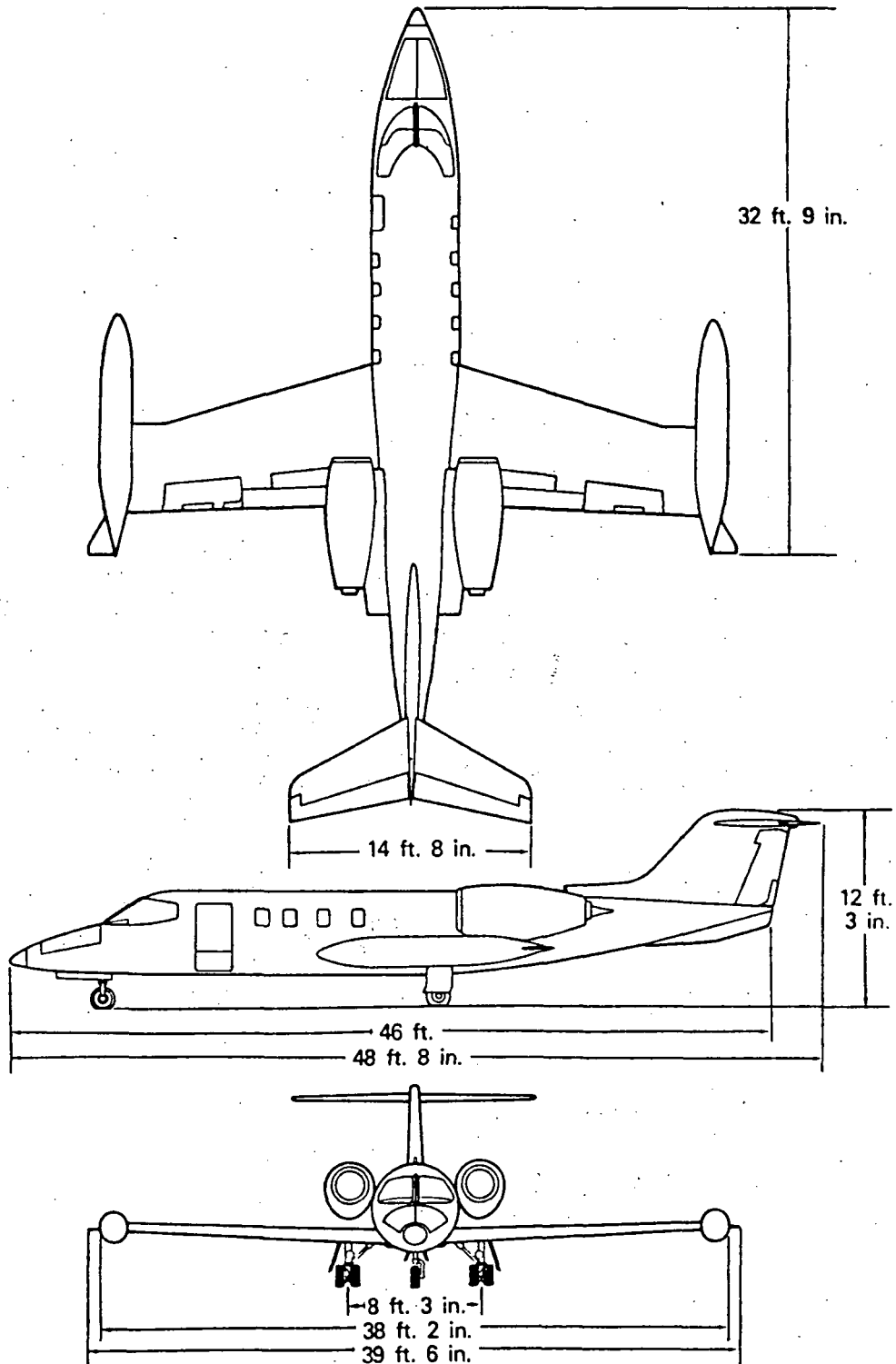


Figure 3.2: Gates Learjet Model 35 Three-View

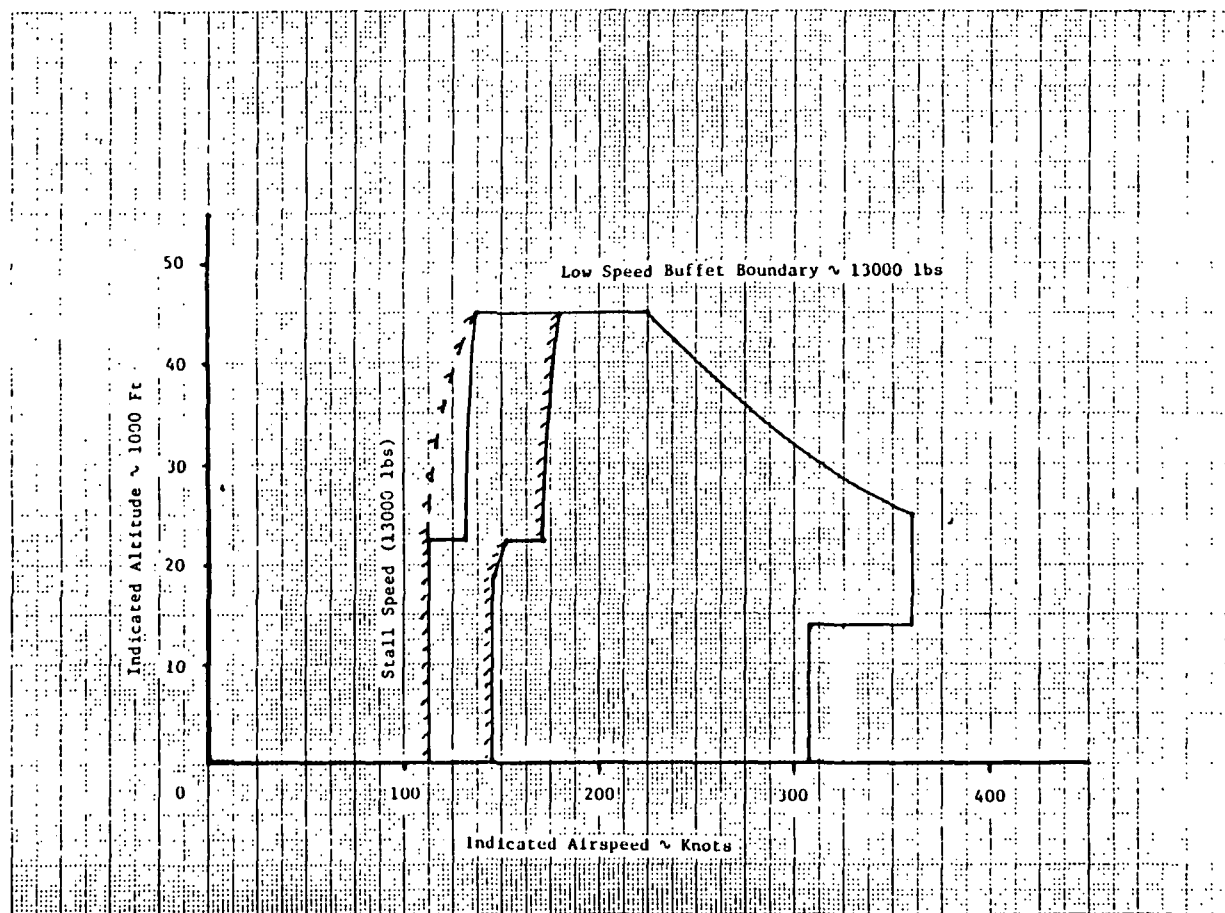


Figure 3.3: Gates Learjet Model 35 Flight Envelope

3.2 ANALYSIS TECHNIQUES

3.2.1 CONCEPT

The first step in developing an overall aircraft performance model was the definition of baseline aerodynamic and propulsion system characteristics. Baseline aerodynamic characteristics consisted primarily of the lift and drag models, while baseline engine characteristics included the gross thrust, fuel flow and airflow models.

A new dimension of this program concerned in-flight definition of the aerodynamic effect of thrust level on lift and drag characteristics which heretofore had not been possible. Normally lift and drag measurements are accomplished using a series of stabilized points throughout the aircraft flight envelope. A wide range of engine power settings are used to achieve the stabilized conditions from which lift and drag may be determined given an in-flight thrust and airflow model along with normally instrumented aircraft parameters such as weight and angle of attack. Unfortunately, the flow field around the aircraft may be significantly altered by the airflow through the engine(s) which will result in the lift and drag characteristics being directly dependent on engine power. If the stabilized point method is used on an aircraft where power effects are significant, use of the resulting data to predict nonstabilized (i.e. excess thrust not equal to zero) performance characteristics will be susceptible to significant error. As a result, this program developed a flight test technique to evaluate efficiently the effect of engine power setting on the lift and drag characteristics of an aircraft. The technique utilized quasi steady-

state maneuvers (level accelerations and decelerations) at selected power settings throughout the Mach range of the aircraft to define lift and drag coefficient variation as a function of angle of attack, Mach number and power setting.

3.2.1.1 Aerodynamic Characteristics

Development of the lift and drag characteristics from quasi steady-state maneuvers began with consideration of the forces acting on the aircraft. The aircraft force balance equations resolved parallel and perpendicular to the flight path (assuming zero sideslip, wings level, and constant mass) are, from Figure 3.4,

$$F_{x_w} = ma_{x_w}$$

$$F_g \cos(\alpha + \lambda) - F_r - D = W\left(\frac{a_{x_w}}{g} + \sin\gamma\right)$$

$$F_{z_w} = ma_{z_w}$$

$$L + F_g \sin(\alpha + \lambda) = W\left(\frac{a_{z_w}}{g} + \cos\gamma\right)$$

As discussed in Reference 6, the flight path load factors resolved along the x and z wind axes are

$$n_{x_w} = \frac{a_{x_w}}{g} + \sin\gamma$$

$$n_{z_w} = \frac{a_{z_w}}{g} + \cos\gamma$$

The force balance equations may be expressed as

$$F_g \cos(\alpha + \lambda) - F_r - D = Wn_{x_w} \quad (1)$$

$$L + F_g \sin(\alpha + \lambda) = Wn_{z_w} \quad (2)$$

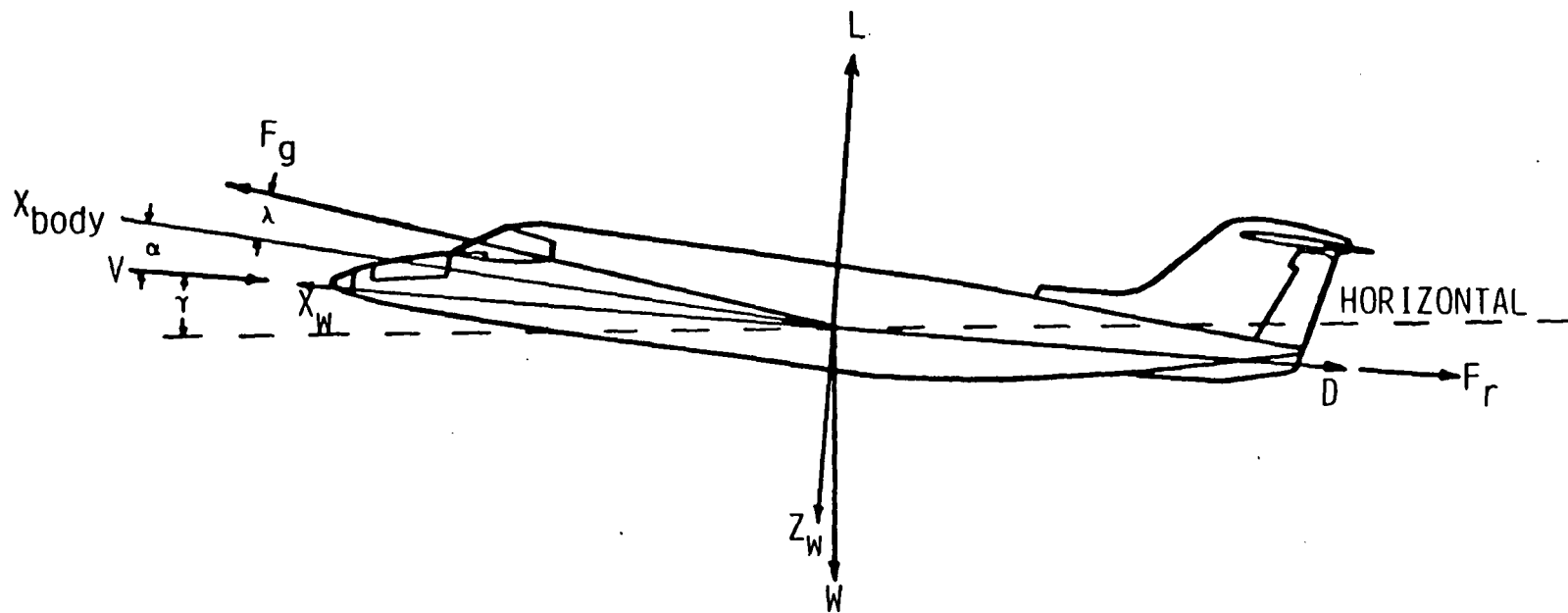


Figure 3.4: Aircraft Force Balance Diagram

Since

$$V \sin \gamma = \frac{dh_g}{dt} = \text{Rate of Climb}$$

and

$$a_{x_w} = \frac{dV}{dt},$$

Equation (1) can also be written in terms of rate of change of energy height as

$$\frac{(F_g \cos(\alpha + \lambda) - F_r - D)V}{W} = \frac{dh_g}{dt} + \frac{V}{g} \frac{dV}{dt} = \dot{h}_e \quad (3)$$

From Equation (3), the excess thrust, $F_g \cos(\alpha + \lambda) - F_r - D$, is seen to be a direct function of rate of climb and the acceleration/deceleration of the aircraft. Consequently, acceleration and deceleration maneuvers were used to define the excess thrust throughout the flight envelope; and the drag could in turn be determined after F_g and F_r were defined. By also calculating the lift utilizing Equation (2), a wide range of C_L and C_D points could be generated in a single accel/decel maneuver; and several of these maneuvers were combined to establish lift and drag characteristics as a function of Mach number, angle of attack, and power setting.

To determine F_g and F_r , contractor-predicted data which incorporated installation effects and which were adjusted with a ground thrust run were used. Overall development of the engine model is discussed in Section 3.2.1.2.

With the methodology established for calculating F_g and F_r , the lift and drag coefficients for a particular data point could be calculated utilizing Equations (1), (2), and (3) combined with flight path acceleration data:

$$C_{L_{A/C}} = \frac{Wn_{z_w} - F_{g_T} \sin(\alpha + \lambda)}{\frac{1}{2} \gamma p_a M^2 S} \quad (4)$$

$$C_D = \frac{F_{g_T} \cos(\alpha + \lambda) - F_{r_T} - Wn_{x_w}}{\frac{1}{2} \gamma p_a M^2 S} \quad (5)$$

or

$$C_D = \frac{F_{g_T} \cos(\alpha + \lambda) - F_{r_T} - \frac{W}{V} (\dot{h}_e)}{\frac{1}{2} \gamma p_a M^2 S} \quad (6)$$

where F_{g_T} and F_{r_T} refer to the total values of gross thrust and ram drag for both engines. The A/C subscript on C_L refers to "power off" conditions, since the effect of the thrust force was considered in the calculation. Wind axis load factors were determined from accelerometers mounted on the body axis of the aircraft using appropriate angular transformations. Trim adjustments to $C_{L_{A/C}}$ have not yet been made for thrust moment effects or nonstandard c.g.

To remove thrust effects completely, the effect of the associated moments created by the thrust (F_{g_T}) and ram drag (F_{r_T}) about the c.g. must be removed. From Figure 3.5, this moment is given by

$$\Delta M_{\text{thrust}} = -F_{g_T} Z_{\text{thrust}} + F_{r_T} h_r.$$

To counteract this moment, an incremental lift at the tail is needed, such that

$$-\Delta L_{\text{tail}} \ell_{\text{tail}} - F_{g_T} Z_{\text{thrust}} + F_{r_T} h_r = 0$$

and the change in lift coefficient which must be added to $C_{L_{A/C}}$ is

$-\Delta L_{\text{tail}}/\bar{q}S$, or

$$\Delta C_{L_{\text{thrust moment}}} = \frac{(F_{g_T} Z_{\text{thrust}} - F_{r_T} h_r)}{\ell_{\text{tail}} \bar{q} S} \quad (7)$$

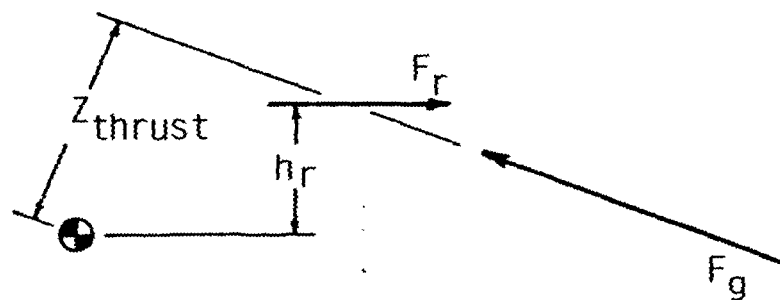
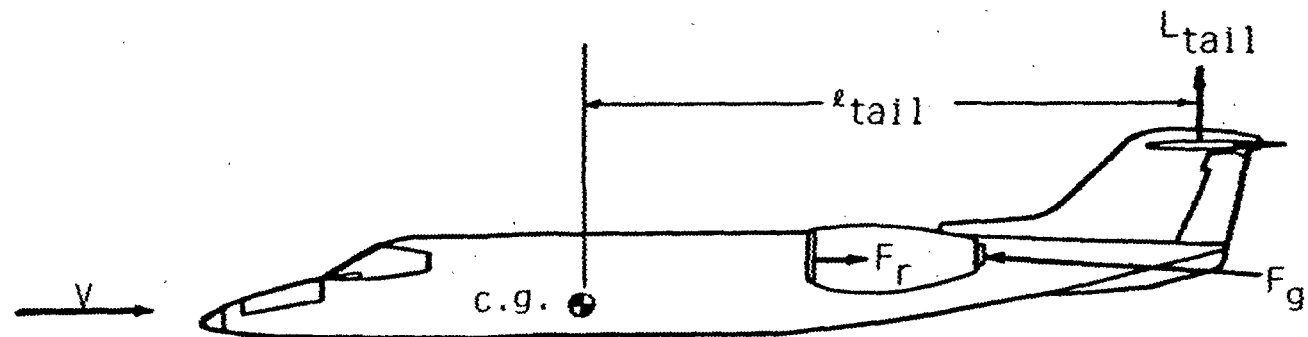


Figure 3.5: Thrust Moment Vectors

The trimmed lift coefficient ($C_{L_{T_{A/C}}}$) then becomes

$$C_{L_{T_{A/C}}} = C_{L_{A/C}} + \Delta C_{L_{\text{thrust moment}}} \quad (8)$$

The distance Z_{thrust} is a function of c.g. and airframe geometry, while h_r and ℓ_{tail} are also functions of angle of attack. A detailed derivation of the required trigonometric relationship is presented in Appendix B. A thrust moment correction to C_D was not made, since in this program the correction was very small and aircraft drag characteristics were defined as a function of power setting. A review of the flight test data showed that this was justified, since the maximum value of $\Delta C_{L_{\text{thrust moment}}}$ experienced was .003, which resulted in a "worst case" impact on C_D of less than two drag counts (.0002).

$C_{L_{T_{A/C}}}$ was standardized to a particular c.g. location so that all data were "normalized" to the same c.g. configuration. From Figure 3.6 and the Appendix B diagram for ℓ_{tail} , this correction begins with a moment balance:

$$AL_{\text{wing}} = L_{\text{tail}} \ell_{\text{tail}} \quad [\text{test c.g.}]$$

$$L_{\text{wing}} (A - \Delta \text{c.g.}) = Z (L_{\text{tail}} + \Delta L_{\text{tail}}) \quad [\text{standard c.g.}]$$

where ΔL_{tail} is the change in tail lift required for a standard c.g.

Since

$$Z = \ell_{\text{tail}} + \Delta \text{c.g.} \quad [\Delta \text{c.g. measured parallel to } V]$$

$$L_{\text{tail}} \ell_{\text{tail}} - L_{\text{wing}} \Delta \text{c.g.} = (\ell_{\text{tail}} + \Delta \text{c.g.}) L_{\text{tail}} + (\ell_{\text{tail}} + \Delta \text{c.g.}) \Delta L_{\text{tail}}$$

With the total aircraft lift (L) given by

$$L = L_{\text{wing}} + L_{\text{tail}}$$

for the test condition, we have

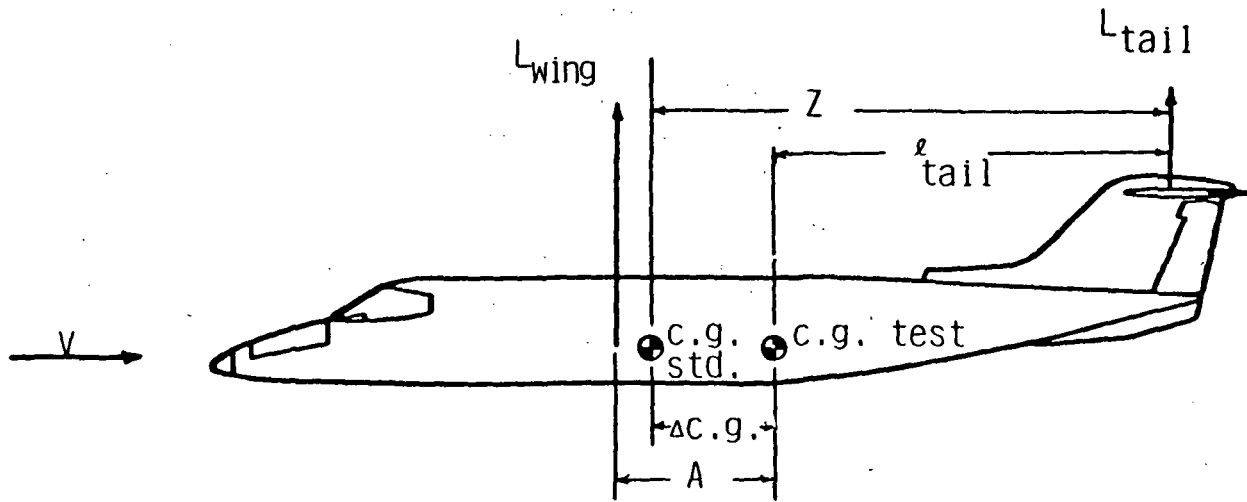


Figure 3.6: Moment Arms for C.G. Standardization

$$-L(\Delta c.g.) = (\ell_{tail} + \Delta c.g.) \Delta L_{tail}$$

$$\Delta L_{tail} = \frac{-L(\Delta c.g.)}{\ell_{tail} + \Delta c.g.}$$

In coefficient form

$$\Delta C_{L_{c.g.}} = \frac{-C_{L_{T_{A/C}}} (\Delta c.g.)}{(\ell_{tail} + \Delta c.g.)}, \quad (9)$$

and the standardized C_L corrected for thrust moment effects and to a standard c.g. is

$$C_{L_S} = C_{L_{T_{A/C}}} + \Delta C_{L_{c.g.}} \quad (10)$$

Reference 6 provides a method for correcting C_D for nonstandard c.g. which utilizes wind-tunnel data to predict the trim drag increment based on $\Delta C_{L_{c.g.}}$. Since this correction is generally small and the required wind-tunnel data were not available, a trim drag correction to C_D was not made for nonstandard c.g. in this program. The $H_{c.g.}$ variation during testing was generally less than ± 1 percent MAC, and consequently the error was considered negligible. The flight data confirmed that the assumption was valid. The maximum value of $\Delta C_{L_{c.g.}}$ experienced was .005, which resulted in a "worst case" impact of less than 3 drag counts (.0003) on C_D .

A correction to the drag coefficient was then made for skin friction variation as a function of Reynolds number. Schlichting's formula for the skin friction coefficient assuming turbulent flow [7] was used.

$$C_f = \frac{.455}{(\log_{10} R_e)^{2.58} (1 + .144 M^2)^{.65}}$$

$$R_e = \frac{\rho V \ell}{\mu}; \quad \begin{array}{l} \ell = \text{characteristic length;} \\ \mu = \text{viscosity coefficient.} \end{array}$$

The drag coefficient due to skin friction was then

$$C_{D_{SF}} = C_f \left[\frac{\text{Wetted Area}}{S} \right]$$

where the drag contribution of the aircraft components was broken down according to Table 2. The Reynolds number calculation used the characteristic length for each component, and the applicable wetted area was used to calculate $C_{D_{SF}}$. The skin friction drag contributions were then standardized to an altitude of 25000 feet by computing $C_{f_{25000'}}$ and $C_{D_{SF_{25000'}}}$ and defining the incremental change in drag coefficient due to skin friction variation for off-standardized conditions as

$$\Delta C_{D_{SF}} = C_{D_{SF_{25000'}}} - C_{D_{S.F.t}}$$

This methodology was used for each of the aircraft components; and the total skin friction drag correction, $\Delta C_{D_{SF_{total}}}$, was obtained by summing the contribution of each component.

$$\begin{aligned} \Delta C_{D_{SF_{total}}} = & \Delta C_{D_{SF_{fuselage}}} + \Delta C_{D_{SF_{wing}}} + \Delta C_{D_{SF_{h. tail}}} + \Delta C_{D_{SF_{v. tail}}} \\ & + \Delta C_{D_{SF_{pylon}}} + \Delta C_{D_{SF_{nacelles}}} + \Delta C_{D_{SF_{ventral fin}}} \\ & + \Delta C_{D_{SF_{tank}}} + \Delta C_{D_{SF_{tank fin}}} \end{aligned}$$

The standardized drag coefficient, C_{D_S} , was then

$$C_{D_S} = C_D + \Delta C_{D_{SF_{total}}} \quad (11)$$

An altitude of 25000 feet was chosen for standardization, since it was approximately in the middle of the altitude envelope of the aircraft. As a result, the magnitude of $\Delta C_{D_{SF}}^{\text{total}}$ was relatively small with a maximum absolute value of less than 12 drag counts (.0012), which was determined from flight test data throughout the program.

Table 2: Wetted Areas and Characteristic Lengths
Applicable to Skin Friction Drag Correction*

<u>Component</u>	<u>Wetted Area (Ft²)</u>	<u>Characteristic Length (Ft)</u>
Fuselage	520	46.2
Wing	402	6.8
Horizontal tail	107	3.7
Vertical tail	73	7
Engine pylons	25	7
Engine nacelles	140	7.8
Ventral fin	11	7
Tip tanks	125	14.4
Tank fins	7	1.1

*Figures provided by Gates Learjet Corporation, January 12, 1983.

C_{L_S} and C_{D_S} versus angle of attack characteristics were defined from a series of test points obtained during accel/decel maneuvers. As discussed previously, these characteristics were defined as a function of power setting (based on eight specific test values of N_1) and Mach number. The needed C_L range was obtained through variation of the weight-pressure ratio (W/δ). By determining the lift and drag characteristics as a function of eight test power settings, the power-dependent effects could be defined when comparing data for the same Mach number and angle of attack.

3.2.1.2 Engine Characteristics

Prediction of in-flight thrust and airflow is essential to the definition of aircraft lift and drag characteristics as seen in Section 3.2.1.1. The three most commonly used approaches for determining in-flight engine characteristics are

1. The direct application of the engine manufacturer's theoretical engine prediction deck,
2. The application of a gas generator analysis,
3. The measurement of thermodynamic parameters at the inlet and exit stations of the propulsion system.

The first method is the easiest to implement but the least accurate because it may not include engine installation effects and represents only the performance of the manufacturer's nominal engine, not the one(s) installed on the test aircraft. The second method requires many measurements internal to the engine which are then used to compute the exhaust conditions and hence the thrust. The last and oldest is the direct measurement of inlet and exit pressure and temperature to estimate the thrust without regard to what takes place in between these two stations. This method also requires considerable instrumentation including a tail pipe probe.

A simplified in-flight thrust and airflow prediction technique was developed as part of this effort which was called "Thrust Modeling." It was designed to complement the overall performance modeling approach and provide several advantages over the other methods. However, the performance modeling methodology developed herein can utilize the other methods as well, and thus future programs are not constrained to manda-

tory use of the "Thrust Modeling" technique. "Thrust Modeling" required few special sensors and provided answers that were believed to closely approach the accuracies of the gas generator and tail pipe probe method without their associated complications.

The in-flight engine model consisted of 1) corrected thrust (F_g/δ_{t_2}), 2) corrected fuel flow ($W_f/\sqrt{\theta_{t_2}} \delta_{t_2} N$), and 3) corrected airflow ($W_a \sqrt{\theta_{t_2}}/\delta_{t_2}$) which were calculated and plotted versus corrected RPM ($N_1/\sqrt{\theta_{t_2}}$) for constant Mach number. Curve fits and table look-ups were used to represent these data as a function of Mach number throughout the Mach range.

"Thrust Modeling" consisted of three distinct steps:

1. Simplified representation of corrected thrust, fuel flow, and airflow as a function of corrected RPM and Mach number based on engine deck predictions,
2. Correction of the engine deck model to the individual characteristics of each test engine based on a ground thrust run,
3. In-flight correction of thrust and airflow predictions based on actual fuel flow and an accurate specific fuel consumption prediction.

In the first step, an engine prediction deck for the TFE 731-2 engine was obtained from the Garrett Turbine Engine Company; and engine installation effects consisting of the inlet pressure recovery factor, bleed requirements and horsepower extraction were defined by the Gates Learjet Corporation. The engine prediction deck was a computer program developed by Garrett which predicted thrust, fuel flow and airflow characteristics given altitude, Mach number, RPM and installation effects. The engine deck was run for the conditions presented in Table 3, and the output data were corrected to standard form (F_g/δ_{t_2} ,

Table 3: Test Runs for Engine Deck Combined
with Installation Effects

Mach	Altitude				
	0	10K	25K	35K	43K
0	X	X			
.05	X	X			
.1	X	X			
.15	X	X			
.2	X	X			
.25	X	X			
.3	X	X	X		
.35	X	X	X		
.4	X	X	X	X	
.45	X	X	X	X	
.5	X	X	X	X	X
.55	X	X	X	X	X
.6	X	X	X	X	X
.65		X	X	X	X
.7		X	X	X	X
.75			X	X	X
.8			X	X	X
.85			X	X	X

Note:

Each run included

- a) N_1 incrementing by 5% from idle to 21000 RPM
- b) Matching on idle power
- c) Matching on max continuous power.

$W_f / \sqrt{\delta_{t_2}} \delta_{t_2}^N$, $W_a \sqrt{\delta_{t_2}} / \delta_{t_2}$) and then plotted versus corrected RPM ($N_1 / \sqrt{\delta_{t_2}}$) for a constant Mach number. The conditions presented in Table 3 were designed to evaluate the engine throughout its Mach, altitude and RPM ranges. For corrected thrust and corrected airflow, Mach number and corrected RPM were the only two independent variables present; and consequently the deck predictions formed one curve for a constant Mach number. Figures 3.7 and 3.8 present typical data for corrected thrust and corrected airflow at .45 Mach. An averaging program and cubic spline program as described in Appendix C were then used to define appropriate table look-up values at every 500 RPM increment of corrected RPM. This approach was not successful for engine deck fuel flow predictions due to altitude dependency after reduction to standard corrected form. Figure 3.9 illustrates this problem for Mach .45. The altitude dependency for fuel flow was discussed with the Garrett Turbine Engine Company. Representatives of Garrett stated that the altitude dependency was due to bleed valve scheduling in the near-idle RPM range and to Reynolds number effects. To maintain all engine data in a similar format and preserve the analysis methodology, a unique representation for corrected fuel flow characteristics was developed to collapse altitude variations onto one curve as a function of corrected RPM and Mach. This representation consisted of defining a nonstandard corrected fuel flow in the form $W_f / \sqrt{\delta_{t_2}} \delta_{t_2}^N$, where N is a function of Mach number and represents the power of delta required to eliminate the altitude dependency of corrected fuel flow. An empirical approach was used to determine the most desirable value of N for each cardinal Mach number. (A cardinal Mach number was each even .05 Mach increment as defined in Table 3.)

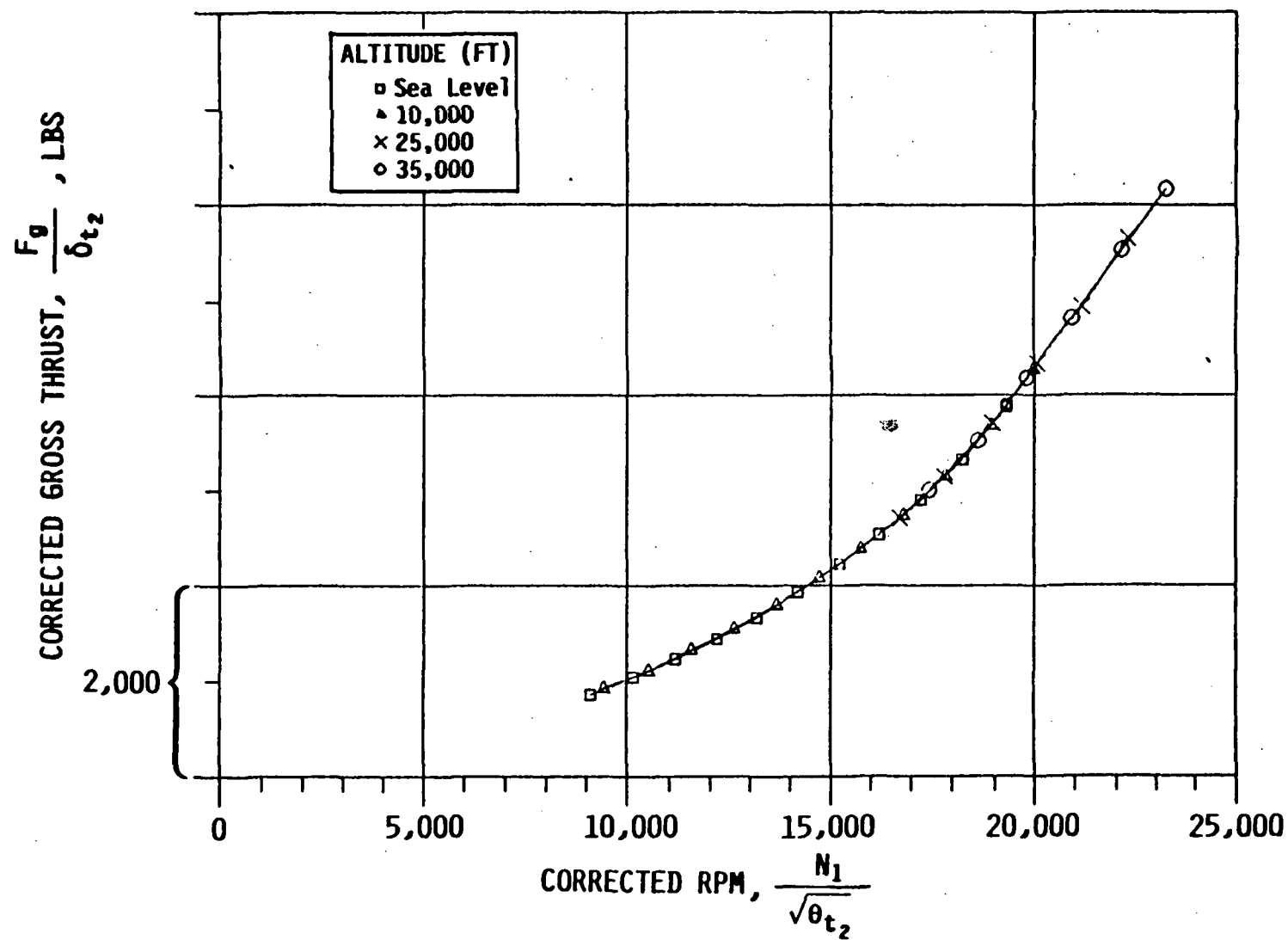


Figure 3.7: Engine Deck Corrected Thrust Characteristics
 $M = .45$

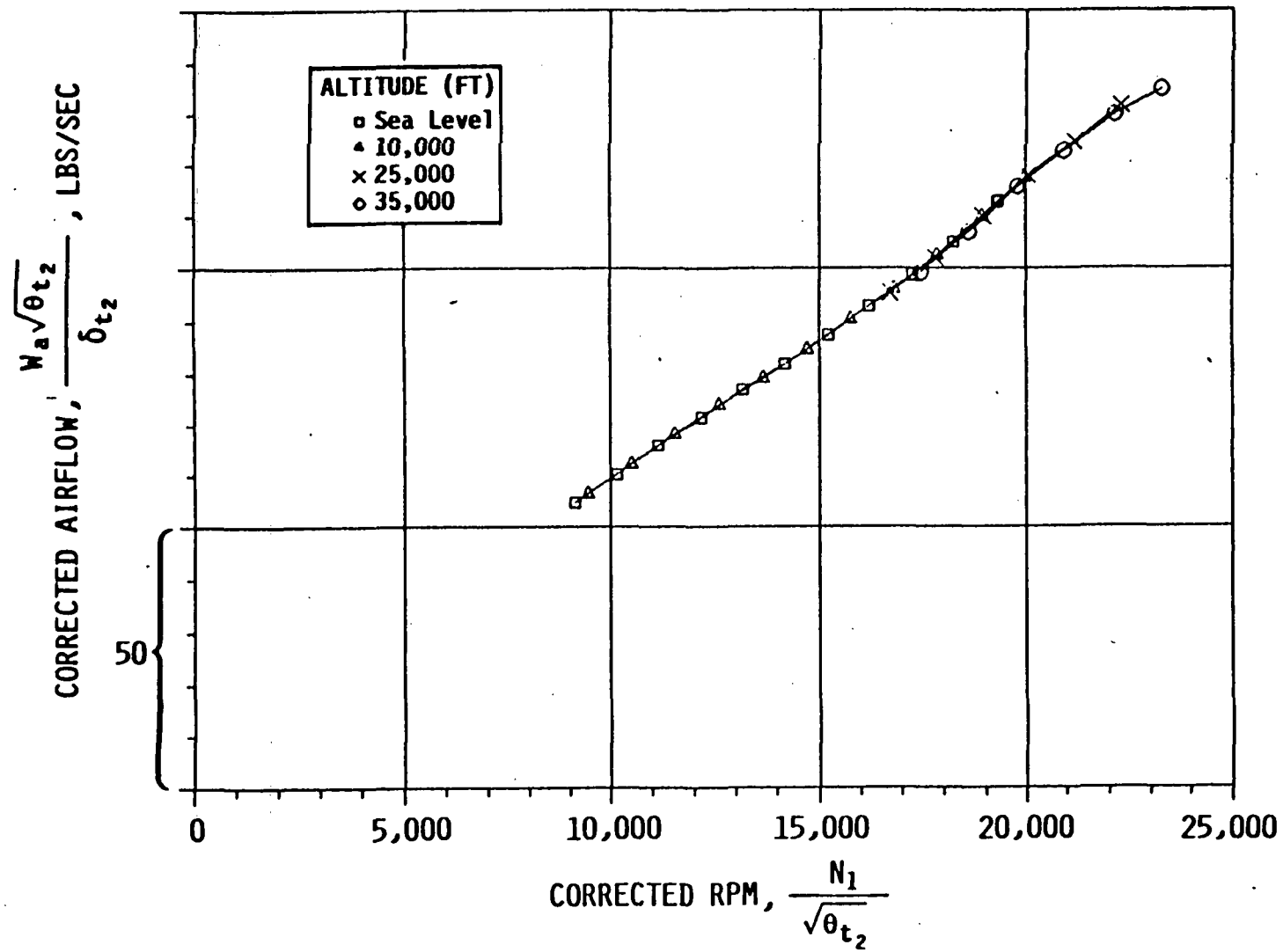


Figure 3.8: Engine Deck Corrected Airflow Characteristics
 $M = .45$

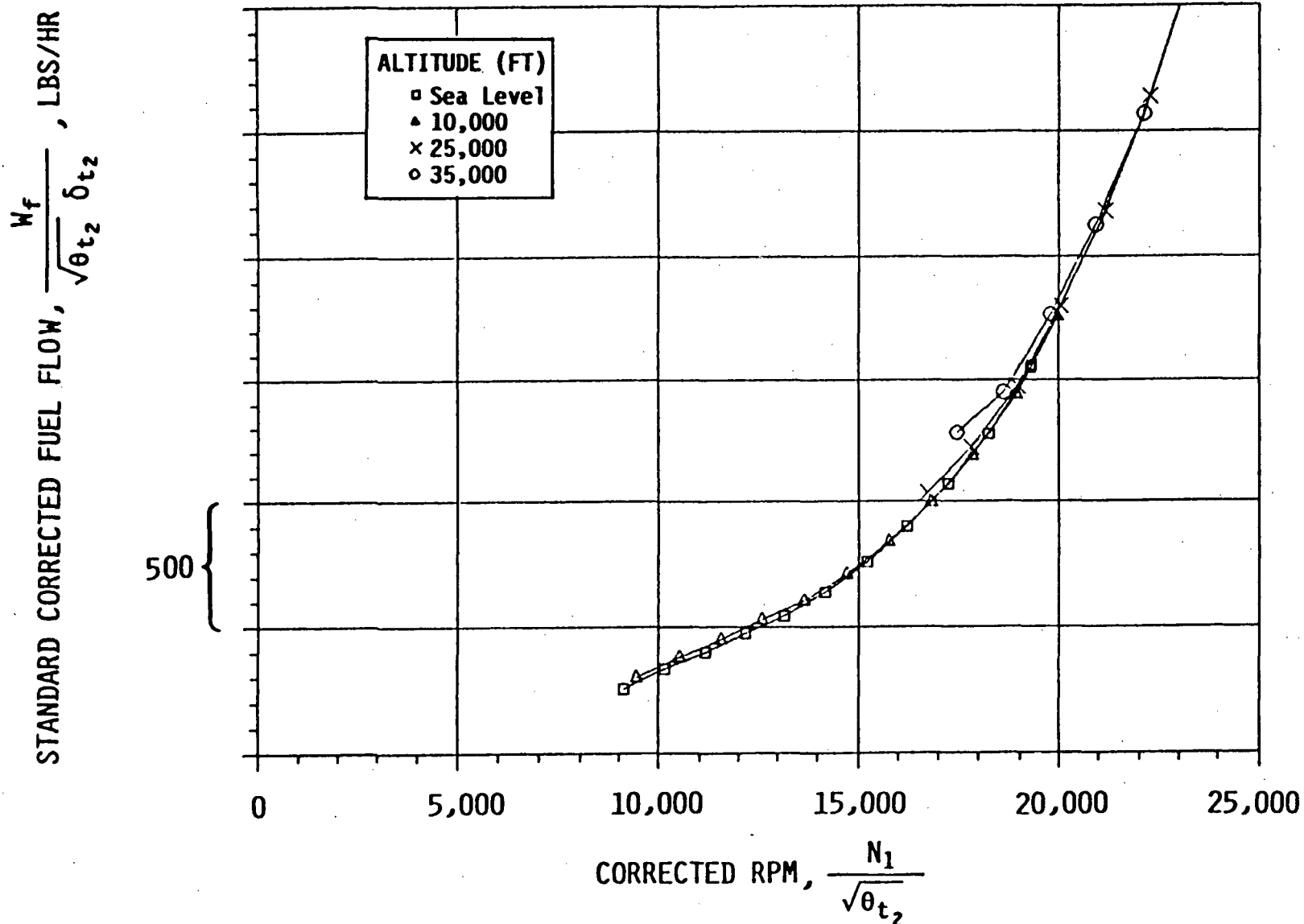


Figure 3.9: Engine Deck Corrected Fuel Flow Characteristics, $M = .45$

Figure 3.10 illustrates how the nonstandard corrected fuel flow was used for $N = .96$ to eliminate the altitude dependency seen in Figure 3.9 for .45 Mach. Figure 3.11 presents the fuel flow plot for .45 Mach and $N = .88$ which was also evaluated in leading up to the final selection of .96 for N . Table 4 presents the optimum values of N determined during this program as a function of Mach number. The final deck thrust, airflow and fuel flow curves are presented in Appendix D. The three engine parameters were then available in table look-up format as a function of corrected RPM and Mach which eliminated dependency of the flight test data reduction software on in-line engine deck computations. This greatly improved data turnaround and reduced computer time as well as provided the engine deck data in a format suitable for the corrections applied in the next two steps.

Step two consisted of modifying the engine deck curves based on the individual characteristics of each test engine recorded during a ground thrust run. This step was needed, since the engine deck predictions represented an average engine, and significant variation from average engine characteristics is common due to the wear and uniqueness of each individual engine. The thrust run procedure and results are documented in Sections 3.3.2 and 4.1.2. A correction parameter, η , was developed based on the ratio of thrust run specific fuel consumption to engine deck specific fuel consumption which could easily and accurately be used to adjust the deck predictions throughout the Mach range based on the thrust momentum equation. The correction parameter was defined as

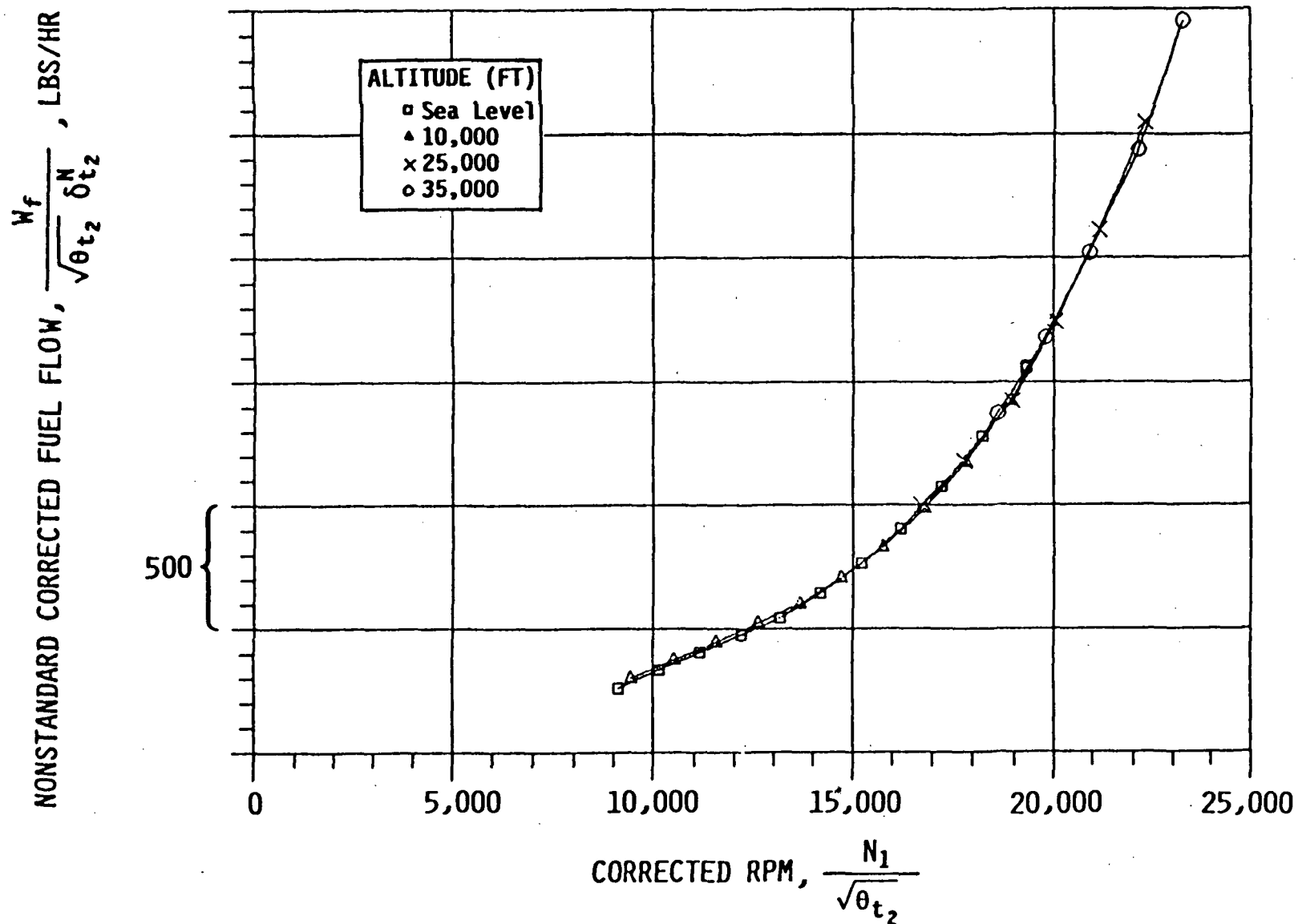


Figure 3.10: Engine Deck Nonstandard Corrected Fuel Flow Characteristics,
 $M = .45$, $N = .96$

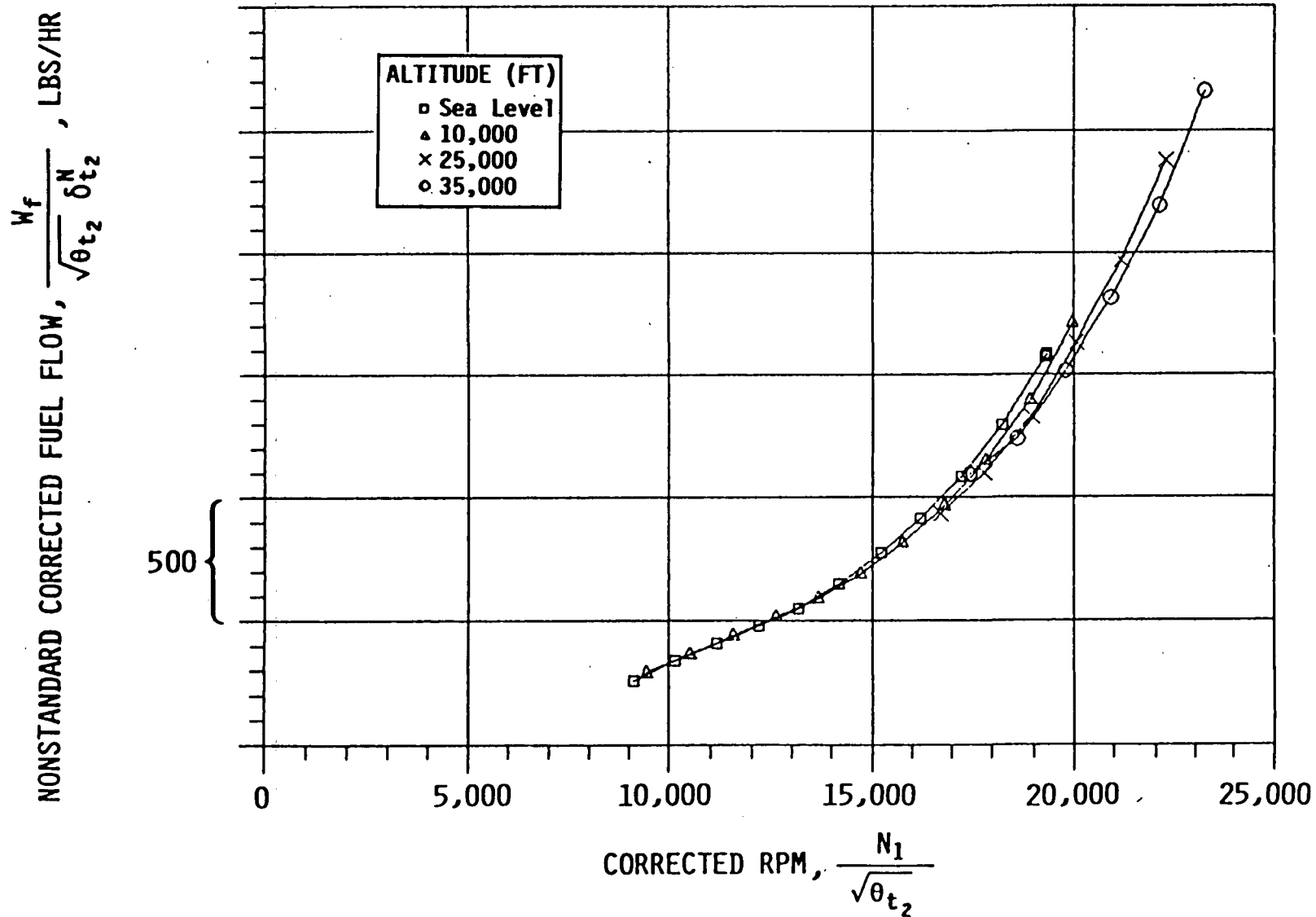


Figure 3.11: Engine Deck Nonstandard Corrected Fuel Flow Characteristics,
 $M = .45$, $N = .88$

Table 4: Power of δ_{t_2} , N, Used for
Nonstandard Corrected Fuel Flow

<u>Mach</u>	<u>N</u>
0	.97
0.05	.98
0.10	.98
0.15	.98
0.20	.98
0.25	.97
0.30	.97
0.35	.96
0.40	.96
0.45	.96
0.50	.96
0.55	.96
0.60	.91
0.65	.91
0.70	.91
0.75	.91
0.80	.91
0.85	.91

$$\eta = \frac{\text{TSFC}_{\text{TRP}}}{\text{TSFC}_D} = \frac{W_{f_{\text{TRP}}} F_{g_D}}{W_{f_D} F_{g_{\text{TRP}}}} \quad (12)$$

where TRP = thrust run predicted

D = engine prediction deck.

" η " was defined as a function of corrected RPM from the thrust run data. Actual adjustment of the corrected thrust, fuel flow and airflow engine deck curves based on the thrust run was accomplished in conjunction with the in-flight correction discussed in step three. A unique feature of using the η correction parameter was that airflow as well as fuel flow and thrust corrections to the engine deck predictions could be made using one correction parameter as shown in the next paragraph.

The third step applied a final correction to thrust and airflow based on actual in-flight measured fuel flow. The procedure recommended in Reference 1 was used to correct the thrust run predicted (TRP) data based on the ratio of test fuel flow to predicted fuel flow. Experience with in-flight thrust measurements on the XB-70 showed that the predicted specific fuel consumption was generally accurate within 5 percent of the measured value, even though the measured thrust did not usually agree with the predicted thrust. The TSFC prediction was considered the most accurate prediction available and formed the basis for the final correction applied to the thrust characteristics. This correction procedure was also used by the F-104G and F-111 programs. The following relationships can be derived from the fundamental assumption that predicted that TSFC is accurate.

$$\text{TSFC}_{\text{TRP}} = \frac{W_{f_{\text{TRP}}}}{F_{g_{\text{TRP}}}} \approx \frac{W_{f_t}}{F_{g_t}} \quad (13)$$

$$F_{g_t} = \frac{W_{f_t}}{W_{f_{TRP}}} F_{g_{TRP}} \quad (14)$$

Prediction of the ram drag, F_r , is directly dependent on the airflow which must be subjected to the same analysis. Since, from the thrust momentum equation,

$$F_g = \dot{m}_e V_\infty = \frac{W_e V_\infty}{g} = \frac{(W_a + W_f) V_\infty}{g}$$

$$F_{g_{TRP}} = \frac{(W_{a_{TRP}} + W_{f_{TRP}}) V_\infty}{g}$$

and

$$F_{g_t} = \frac{W_{f_t}}{W_{f_{TRP}}} F_{g_{TRP}} = \frac{W_{f_t}}{W_{f_{TRP}}} \frac{(W_{a_{TRP}} + W_{f_{TRP}}) V_\infty}{g}$$

$$F_{g_t} = \frac{\left(\frac{W_{f_t}}{W_{f_{TRP}}} W_{a_{TRP}} + W_{f_t} \right) V_\infty}{g} \quad (15)$$

The ∞ subscript refers to the section of the engine wake where the pressure of the engine exhaust gases is first equal to the pressure of the surrounding atmosphere. From Equation (15), consistent application of the TSFC assumption (13) requires that contractor-predicted airflow also be corrected with the ratio of test to predicted fuel flow.

$$W_{a_t} = \frac{W_{f_t}}{W_{f_{TRP}}} W_{a_{TRP}} \quad (16)$$

and the ram drag is

$$F_{r_t} = \frac{W_a V}{g} = \left(\frac{W_{f_t}}{W_{f_{TRP}}} \right) \frac{W_{a_{TRP}} V}{g} \quad (17)$$

(Reference 6)

where V is the free-stream velocity.

Combining the above results with definition of the correction parameter η , Equation (14) becomes

$$F_{g_t} = \frac{W_{f_t}}{W_{f_{TRP}}} F_{g_{TRP}} = \frac{W_{f_t} F_{g_D}}{\eta W_{f_D}} \quad (18)$$

and, for each engine,

$$F_{g_{t_R}} = \frac{W_{f_{t_R}} F_{g_D}}{\eta_R W_{f_D}}$$

$$F_{g_{t_L}} = \frac{W_{f_{t_L}} F_{g_D}}{\eta_L W_{f_D}}$$

where $R \rightarrow$ Right engine

$L \rightarrow$ Left engine.

As seen from the above equations, prediction of in-flight thrust was only dependent on the engine deck predictions of thrust and fuel flow, measurement of test fuel flow and the correction parameter η . Development of the in-flight airflow equation begins with consideration of the thrust momentum equation for the engine deck predictions:

$$F_{g_D} = \frac{W_e V_\infty}{g} = \frac{(W_{a_D} + W_{f_D}) V_\infty}{g} .$$

Since

$$F_{g_{TRP}} = \frac{W_{f_{TRP}} F_{g_D}}{\eta W_{f_D}} \quad \text{and,}$$

using a development similar to that for F_{g_t} , the equation becomes

$$F_{g_{TRP}} = \frac{W_{f_{TRP}}}{\eta W_{f_D}} \frac{(W_{a_D} + W_{f_D}) V_{\infty}}{g}$$

or

$$F_{g_{TRP}} = \left[\frac{W_{f_{TRP}} W_{a_D}}{\eta W_{f_D}} + \frac{W_{f_{TRP}}}{\eta} \right] \frac{V_{\infty}}{g}$$

Solving for V_{∞} ,

$$V_{\infty} = \frac{F_{g_{TRP}} g}{\left[\frac{W_{f_{TRP}} W_{a_D}}{\eta W_{f_D}} + \frac{W_{f_{TRP}}}{\eta} \right]} \quad (19)$$

Since

$$F_{g_{TRP}} = \frac{[W_{a_{TRP}} + W_{f_{TRP}}] V_{\infty}}{g} = \frac{W_{a_{TRP}} V_{\infty} + W_{f_{TRP}} V_{\infty}}{g},$$

the equation may be solved for the airflow experienced during the thrust

run, $W_{a_{TRP}}$,

$$W_{a_{TRP}} = \frac{g}{V_{\infty}} \left[F_{g_{TRP}} - \frac{W_{f_{TRP}} V_{\infty}}{g} \right] = \frac{g F_{g_{TRP}}}{V_{\infty}} - W_{f_{TRP}}.$$

Substituting in Equation (19),

$$W_{a_{TRP}} = W_{f_{TRP}} \left[\frac{W_{a_D}}{\eta W_{f_D}} + \frac{1}{\eta} - 1 \right] \quad (20)$$

and from Equation (16),

$$W_{a_t} = \frac{W_{f_t}}{W_{f_{TRP}}} W_{a_{TRP}} = W_{f_t} \left[\frac{W_{a_D}}{\eta W_{f_D}} + \frac{1}{\eta} - 1 \right] \quad (21)$$

For each engine:

$$W_{a_{t_R}} = W_{f_{t_R}} \left[\frac{W_{a_D}}{\eta_R W_{f_D}} + \frac{1}{\eta_R} - 1 \right]$$

$$W_{a_{t_L}} = W_{f_{t_L}} \left[\frac{W_{a_D}}{\eta_L W_{f_D}} + \frac{1}{\eta_L} - 1 \right] .$$

Prediction of in-flight airflow was then only dependent on the engine deck prediction of airflow and fuel flow, measurement of test fuel flow and the correction parameter η . Development and implementation of the airflow prediction technique was unique to this program. It provided a more accurate prediction of airflow than total reliance on engine deck predictions and did not require extensive inlet instrumentation. When implementing Equations (20) and (21), careful attention must be given to balancing units. Airflow is normally expressed in lbs/sec; and, as a result, W_{f_t} and W_{f_D} must be converted to lbs/sec for the units to balance. Fuel flow is normally defined in lbs/hr.

3.2.1.3 Summary

The data analysis procedures outlined offered several advantages over conventional analysis techniques. Flight test data from level acceleration and deceleration maneuvers are normally used primarily to predict standardized climb and acceleration performance in the form of P_s (specific excess power) plots and rate of climb versus airspeed/attitude plots. Aircraft motion in the form of climb and/or acceleration is both the observed and the "end product" parameter; and consequently, the flight test data must be corrected for nonstandard temperatures, wind, acceleration, and weight effects to obtain standardized performance (Reference 8). The analysis procedures used in this program went one level beyond the aircraft motion parameters of climb and acceleration. Aerodynamic data were reduced to lift and drag coefficient form; and engine data were reduced to the normalized F_g , W_f , and W_a form. Consequently, it was not necessary to standardize the aircraft motion parameters; and a great amount of information regarding all aspects of aircraft performance was available. Cruise performance, flight trajectory performance, and climb/acceleration characteristics could be determined using the performance modeling programs discussed in Section 3.2.4; and the data were in an ideal format for input to aircraft simulations. In addition, the in-flight thrust and airflow prediction technique ("Thrust Modeling") provided three principal advantages over methods in the past:

1. Extensive engine instrumentation such as that needed with the gas generator method was not required.

2. The need for on-line engine deck computations as part of the flight test data reduction software was eliminated.
3. A significant improvement in accuracy was achieved over methods which rely completely on engine deck predictions.

The logical next step in the further validation of the "Thrust Modeling" technique is the evaluation of test engine performance characteristics in an altitude test cell such as the NASA Lewis Facility. This effort would establish the accuracy of the prediction technique with a one-to-one comparison of test cell and in-flight data. Based on data obtained from the F-104G, F-111 and YF-12 programs (References 1-3), "Thrust Modeling" was believed to have an accuracy of three to five percent, which is generally considered in the state-of-the-art range.



3.2.2 Data Flow

The flight test instrumentation system recorded all performance related parameters in a digital format at a sampling rate of approximately 10 samples/sec. A detailed description of the instrumentation system, calibration routines, and initial data processing is presented in Section 3.5. An overall flow diagram for the data management system is illustrated in Figure 3.12. The top four blocks accomplished standard calibration and sensor compensation procedures to transform raw data to appropriate engineering units format in the Flight Test Data Base (FTDB) file. This subsection will primarily discuss data flow and methodology beginning with the FTDB and extending to definition of baseline aerodynamic and engine data products. At this point, the performance modeling programs could be exercised using the baseline data products as primary inputs.

A detailed flow diagram of data reduction from the FTDB to baseline data is presented in Figure 3.13. The Flight Test Data Base contained 36 time-varying performance parameters, and an aircraft I.D. file provided an additional 8 aircraft unique constants as shown in Figure 3.13. The gross thrust (F_g) in the FTDB has had the fuel flow and η corrections applied in accordance with Equation (18), and airflow (W_a) had the same corrections applied in accordance with Equation (21). Ram drag was calculated with Equation (17), and the body axis accelerations ($n_{x_{body}}$, $n_{y_{body}}$, $n_{z_{body}}$) had been corrected for off-c.g. location of the accelerometers (Section 3.2.6). Parameters from the FTDB and aircraft I.D. file were processed according to the methodology shown in Section 3.2.1 to form Performance Data File I. The START program presented in Appendix C was used for these computations.

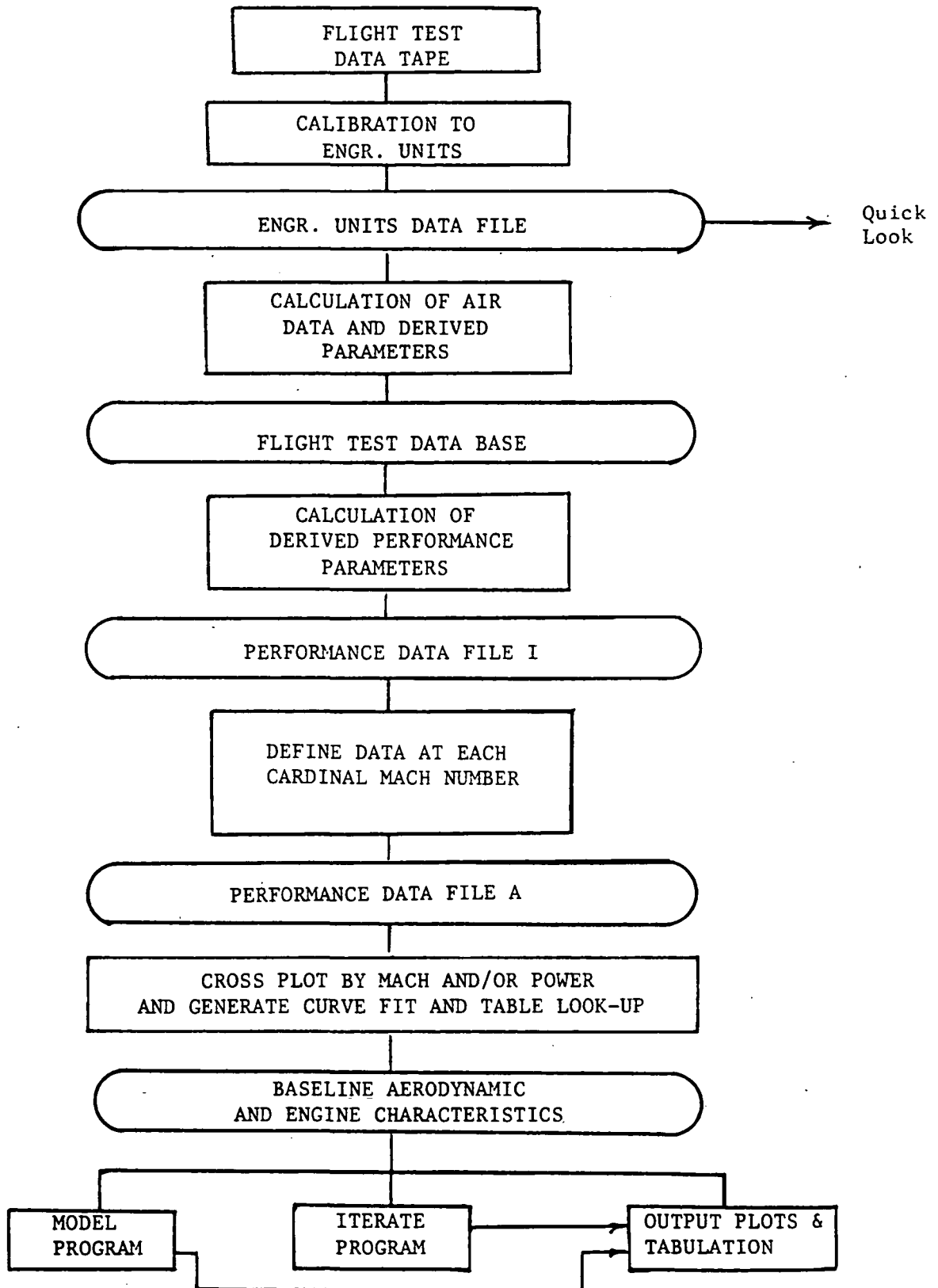


Figure 3.12: Data Management System

The parameters in Data File I were calculated for each sample time during a performance maneuver and stored. Data File I was continually expanded as additional flights were accomplished.

The next step in the data flow was to plot and curve-fit selected parameters from Data File I versus Mach number for an entire maneuver. This served two purposes. First, a continuous Mach history was produced for a maneuver based on limited segments of data (see Figures 3.14 and 3.15). Since the acceleration/deceleration maneuvers were typically quite long in duration (up to 8 minutes), only limited segments of data were recorded periodically throughout a maneuver so as not to saturate the data recording system. Second, occasional difficulties with noise and/or turbulence could be readily detected and smoothed. Each parameter was then recorded at each cardinal Mach within a given maneuver. Cardinal Mach numbers were from .25 to .8 in .05 Mach increments. Data File A consisted of twelve subfiles, each for a cardinal Mach, which were expanded as each maneuver was reduced.

The next step was to access all data from File A at a specific Mach number and plot

- a) F_g / δ_{t_2} vs $N_1 / \sqrt{\theta_{t_2}}$
- b) $W_f / \sqrt{\theta_{t_2}} \delta_{t_2}^N$ vs $N_1 / \sqrt{\theta_{t_2}}$
- c) $W_a \sqrt{\theta_{t_2}} / \delta_{t_2}$ vs $N_1 / \sqrt{\theta_{t_2}}$

A curve was then fit through each data plot to define the applicable engine characteristics. The lift and drag coefficient data were also accessed from File A for a specific Mach number and were then separated

by power setting based on N_{1A} . For each power setting, C_{L_s} versus α and C_{D_s} versus α were plotted and a best fit curve applied. The power effects on C_{L_s} and C_{D_s} were then analyzed and defined. Next, the Mach number was incremented and the same procedure followed for the entire Mach range.

The data flow provided a logical processing of flight test data and a timely comparison and assessment of "new" data in relation to data that had been obtained on previous flights. This allowed an awareness of important trends in the data and also served as a check on the instrumentation system and other factors that directly affected data quality.

FLIGHT TEST DATA BASE

$p, q, r, \theta, \phi, T_{a_t}, \alpha, B, V, h, W_{f_R}, W_{f_L}$
 $N_{1_R}, N_{1_L}, N_{2_R}, N_{2_L}, M, W, H_{c.g.}, V_{c.g.}, \delta_{t_2},$
 $W_{a_R}, W_{a_L}, \delta, \theta, \theta_{t_2}, F_{g_R}, F_{g_L}, F_{r_R}, F_{r_L}, n_{x_{body}},$
 $n_{y_{body}}, n_{z_{body}}, \text{time, flight, maneuver}$

ACCESS AIRCRAFT I.D. FILE

FOR

$S, \lambda, MAC, ZT, XRD, ZRD, H_{tail}, V_{tail}$

PROCESS DATA AT EACH TIME INCREMENT

AND

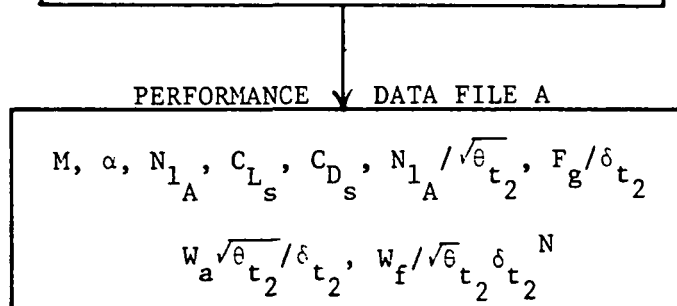
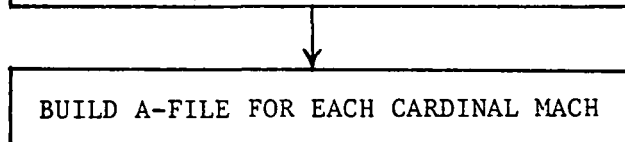
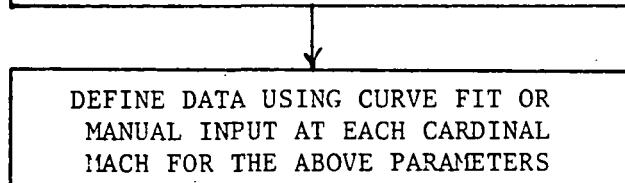
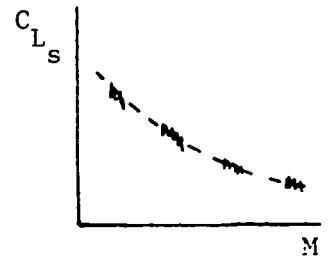
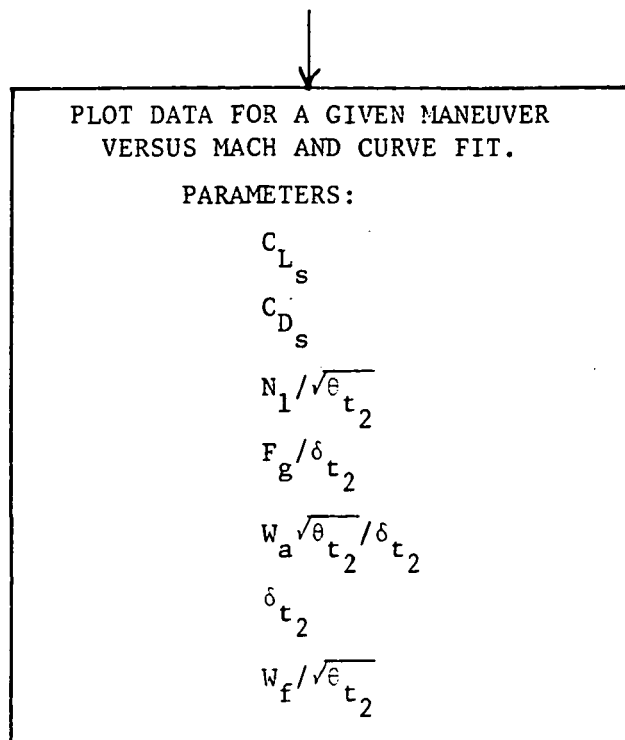
STORE

(using START program)

PERFORMANCE DATA FILE I

$M, C_{L_s}, C_{D_s}, \alpha, N_{1_A}, N_{2_A}, N_{1_A}/\sqrt{\theta_{t_2}},$
 $N_{2_A}/\sqrt{\theta_{t_2}}, F_{g_T}/\delta_{t_2}, \theta_{t_2}, \delta_{t_2}, W/\delta, W_{a_T}\sqrt{\theta_{t_2}}/\delta_{t_2}$
 $W_{f_T}/\sqrt{\theta_{t_2}}, RE, \text{time, flight, maneuver}$

Figure 3.13: Performance Modeling Data Flow



A

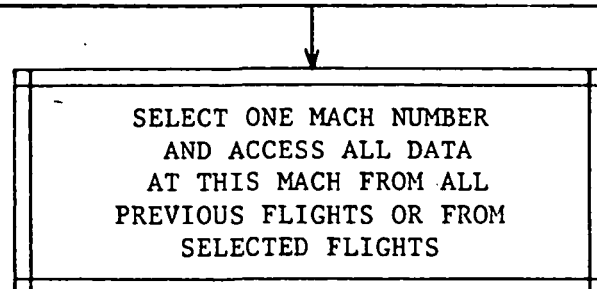


Figure 3.13: (continued)

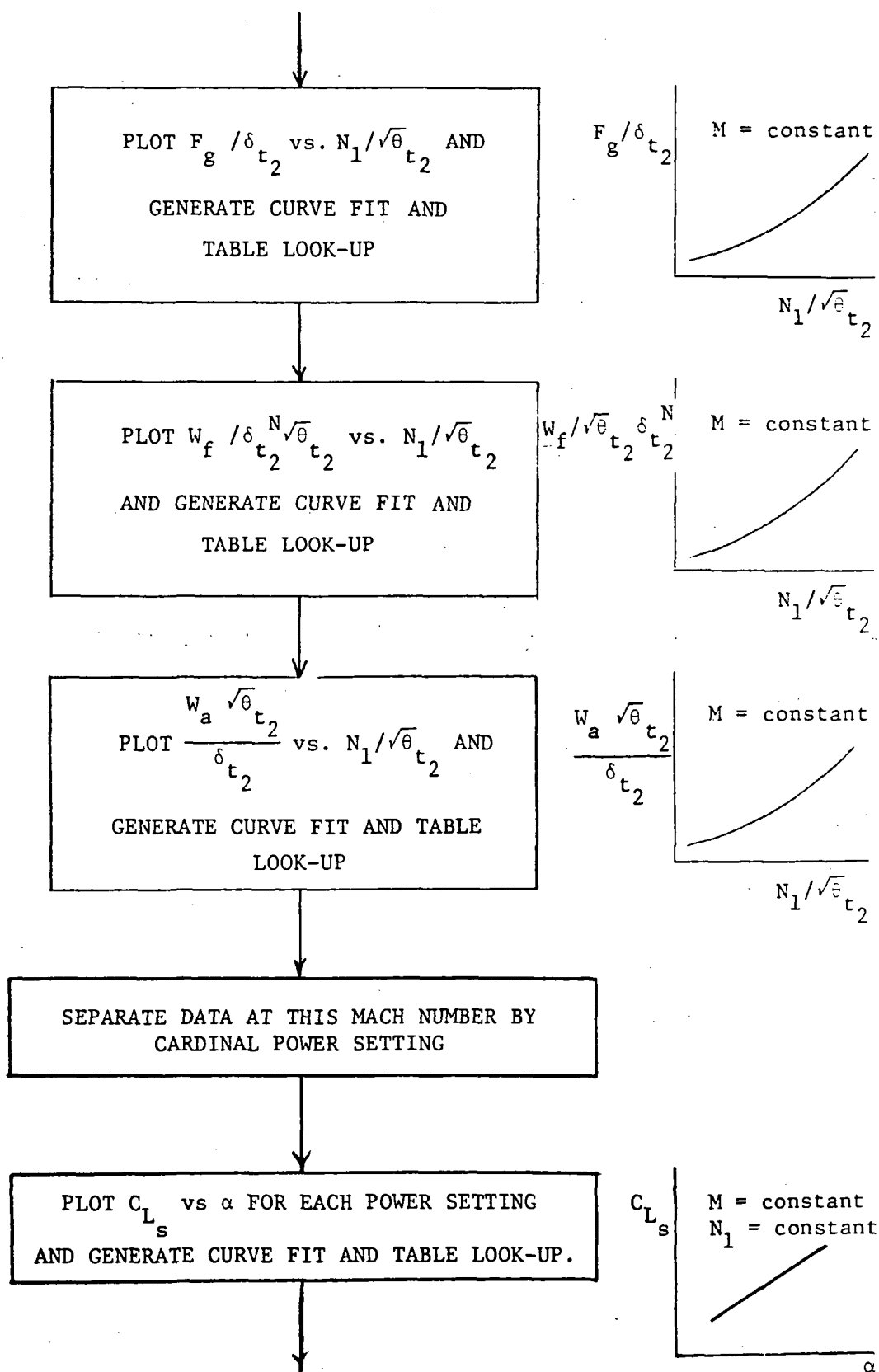


Figure 3.13: (continued)

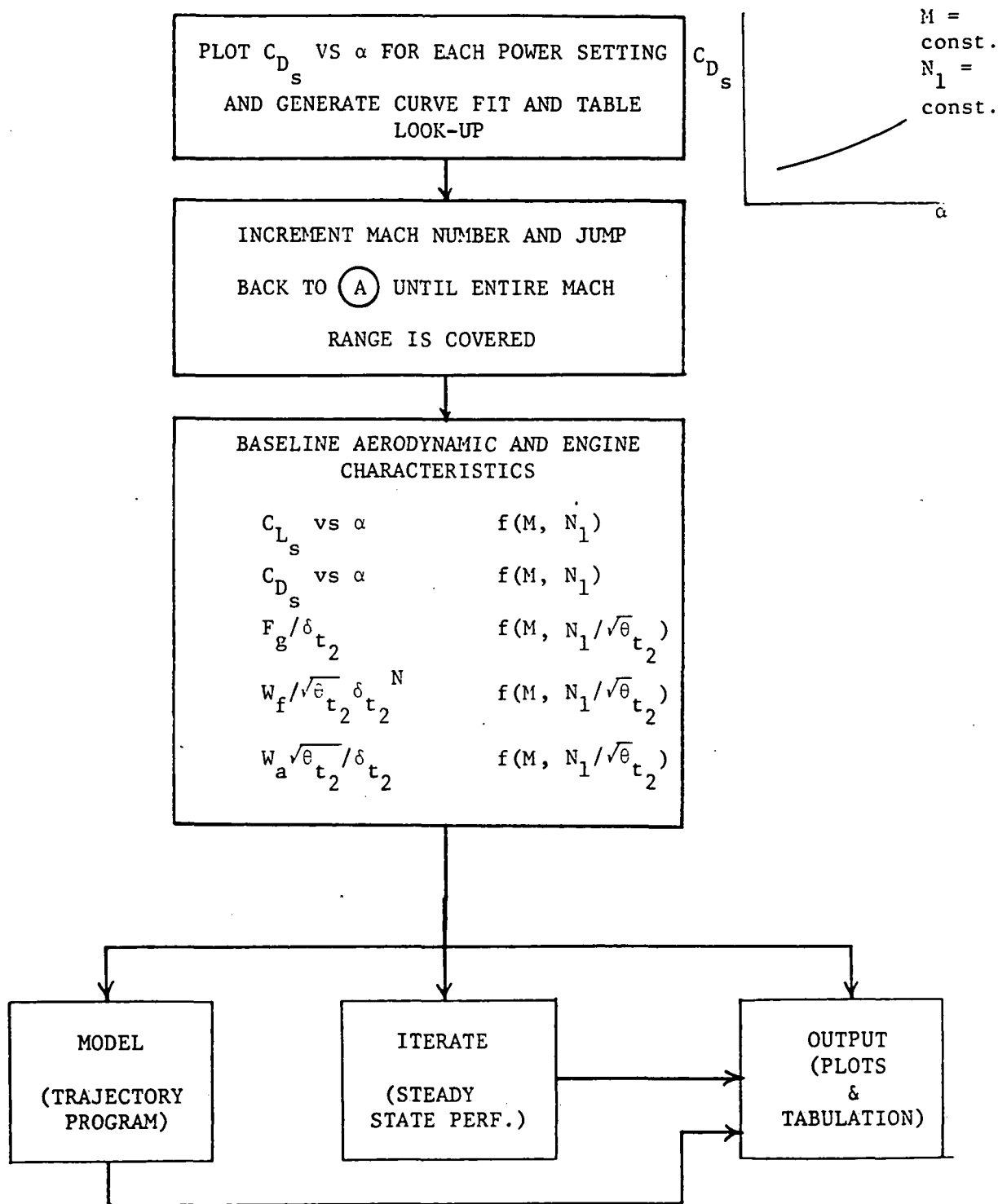


Figure 3.13: (concluded)

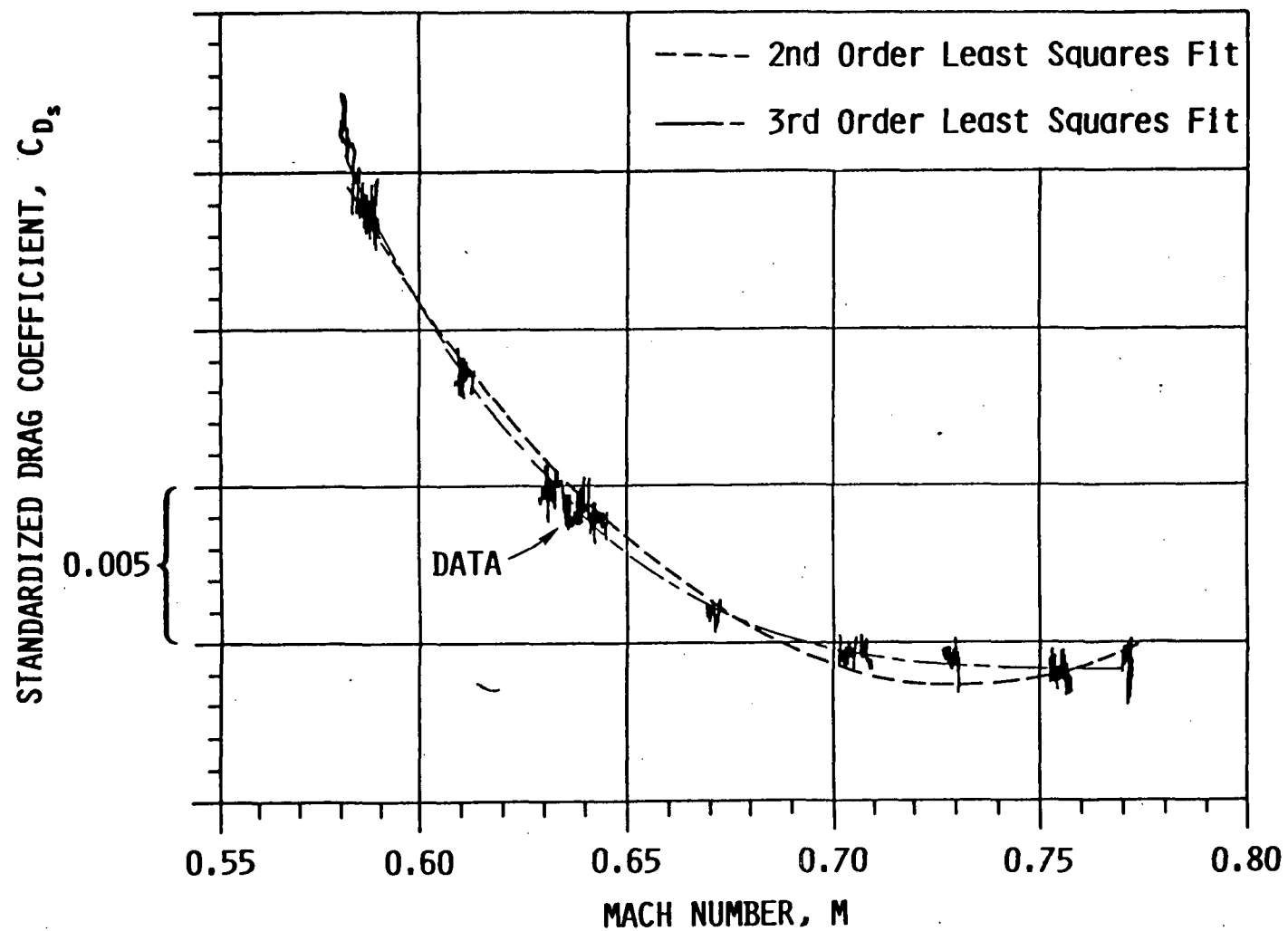


Figure 3.14: Sample Mach History of C_{D_s} , 95% N_1 Accel at 73000 $\frac{W}{\delta}$

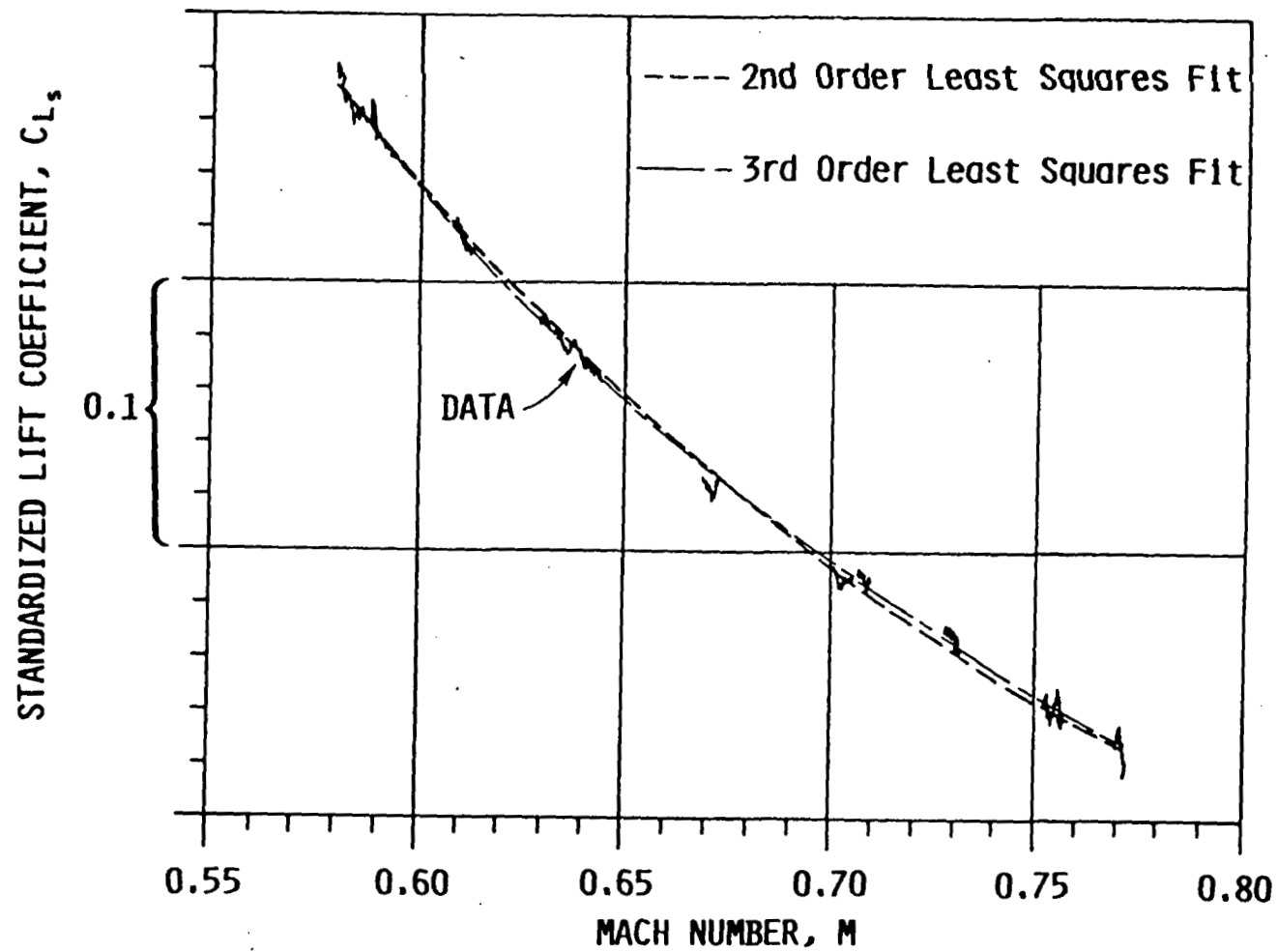


Figure 3.15: Sample Mach History of C_{L_s} , 95% N_1 Accel at 73000 W/δ

3.2.3 Conventional Data Reduction

In addition to the data reduction techniques developed in Sections 3.2.1 and 3.2.2, conventional data analysis techniques were applied to the stable point and pull-up, push-over, pull-up maneuvers for comparison with the performance modeling predictions. These maneuvers are described in Section 3.4.

3.2.3.1 Stabilized Points

Stabilized point data were used to define steady-state cruise performance characteristics in terms of corrected RPM ($N_1/\sqrt{\theta_{t_2}}$), range factor, specific range, and specific range parameter versus Mach for constant W/δ values. The range parameters were defined by

$$\text{Range Factor (RF)} = \frac{VW}{W_{fT}}$$

$$\text{Specific Range (SR)} = \frac{V}{W_{fT}}$$

$$\text{Specific Range Parameter (SRP)} = \frac{V\delta}{W_{fT}}$$

where V = true velocity in knots.

W_{fT} = total in-flight fuel flow for both engines in lbs/hr.

W = aircraft weight in pounds.

Since the stable points were obtained for a range of pressure and temperature conditions as W/δ was held approximately constant, a nominal altitude was chosen for each target value of W/δ and associated standard values of δ and θ defined so that range factor and specific range could be standardized. Standardization began by defining standard values of fuel flow and true velocity as

$$W_{f_{std}} = \left(\frac{W_{fT}}{\delta_{t_2} \sqrt{\theta_{t_2}}} \right)_{test} (\delta_{t_2})_{std} (\sqrt{\theta_{t_2}})_{std}$$

$$V_{std} = V_{test} \sqrt{\frac{\theta_{std}}{\theta_{test}}} \quad (\text{Reference 9}).$$

Standardized range factor and specific range were then defined as

$$RF_{std} = \frac{V_{std} W}{W_{f_{std}}} = RF_{test} \left(\frac{\delta_{test}}{\delta_{std}} \right) \quad (22)$$

$$SR_{std} = \frac{V_{std}}{W_{f_{std}}} = SR_{test} \left(\frac{\delta_{test}}{\delta_{std}} \right) \quad (23)$$

All stable point data were standardized using these equations so that valid comparisons could be made with the ITERATE program (Section 3.2.4.1) predictions. Standardization was not required on corrected RPM, since

$$N_1 / (\sqrt{\theta} t_2)_{test} = N_1 / (\sqrt{\theta} t_2)_{std}$$

as discussed in Reference 9. In addition, specific range parameter did not require standardization, since

$$(SRP)_{std} = \frac{V_{std} \delta_{std}}{W_{f_{std}}} = (SR)_{std} \delta_{std} = (SRP)_{test}.$$

The test value of W/δ was held to within $\pm 1\%$ in flight, which made the corrections for off- W/δ negligible.

3.2.3.2 Pull-Up, Push-Over, Pull-Up

Push-pull data were used to obtain additional definition of C_{L_s} and C_{D_s} versus angle of attack characteristics over a wide range of angle of attack. Although the techniques developed in Section 3.2.1 were used to reduce the data to coefficient form, the push-pull maneuvers were included in the conventional data reduction section, since they were not specifically necessary to the overall definition of one g performance characteristics using the performance modeling approach. Push-pull aerodynamic data were compared with those obtained from accel/decel maneuvers to evaluate the correlation between techniques. Since a push-pull maneuver involved angular rates and accelerations which required an incremental change in elevator deflection (δ_e) to sustain the maneuver, a correction was made to standardize the data. From Reference 10, the change in elevator position may be determined from the equation

$$\Delta\delta_e = \frac{(C_{m_q} + C_{m_{\dot{\alpha}}})q\bar{c}}{C_{m_{\delta_e}}2V} - \frac{I_{yy}\dot{q}}{\bar{q}S\bar{c}C_{m_{\delta_e}}}} - \frac{\Delta M_{c.g.}}{\bar{q}S\bar{c}C_{m_{\delta_e}}}}.$$

The first term in the above equation gives the change in δ_e needed to account for a pitch rate (q), the second for a pitch acceleration (\dot{q}) and the third for a nonstandard center of gravity. During this program, the push-pull maneuvers were deliberately performed very smoothly and slowly to minimize the pitch angular acceleration and consequently reduce the second term to near zero. Since the moment of inertia (I_{yy}) may typically not be known with a great deal of accuracy, this was considered a practical approach for comparison purposes. In

addition, the third term was eliminated, since the correction for nonstandard c.g. was already made in the normal data flow (Equation 9).

As a result, the equation for $\Delta\delta_e$ simplified to

$$\Delta\delta_e = \frac{(C_{m_q} + C_{m_{\dot{\alpha}}})q\bar{c}}{C_{m_{\delta_e}} 2V}$$

and

$$\Delta C_{L_{\Delta\delta_e}} = C_{L_{\delta_e}} \Delta\delta_e$$

$$C_{L_s} = C_{L_{s_{\text{push pull}}}} + \Delta C_{L_{\Delta\delta_e}},$$

where C_{m_q} , $C_{m_{\dot{\alpha}}}$, $C_{m_{\delta_e}}$ and $C_{L_{\delta_e}}$ as a function of Mach, were obtained from predictions.* A similar correction to C_{D_s} was not made due to the negligible magnitude of $C_{D_{\delta_e}}$. The angle of attack was also corrected for angular rate using

$$\Delta\alpha = \tan^{-1} \frac{q\ell}{V}$$

and

$$\alpha_{\text{rate corrected}} = \alpha + \Delta\alpha$$

where ℓ represents the distance between the c.g. and the nose boom angle of attack vane.

*Aerodynamics Document for the Gates Learjet Model 35A/36A, Kohlman Aviation Corporation, by D. L. Kohlman, Report 82-01, March 1982, proprietary.

3.2.4 Performance Modeling

The baseline aircraft/engine data presented in Figure 3.13 formed the basis for calculating overall aircraft performance. The baseline data were utilized in two computer prediction programs for this purpose. The first program, ITERATE, calculated steady-state cruise performance in terms of corrected RPM ($N_1/\sqrt{\theta_{t_2}}$), range factor, specific range and specific range parameter versus Mach for constant values of W/δ . The second program, MODEL, calculated time histories of aircraft performance for selected trajectories (climb/accel/decel) throughout the flight envelope.

3.2.4.1 ITERATE Program

This program was developed to calculate steady-state, constant weight-pressure ratio (W/δ) cruise performance from aircraft engine/aerodynamic characteristics generated from flight test quasi steady-state maneuvers. Since steady-state performance parameters cannot be explicitly solved for, it was necessary to develop an iterative routine which would converge upon the steady-state solution. This routine iterated on lift coefficient to obtain steady-state values of C_D , C_L , F_g , F_n , F_r , α , SR, SRP, R.F., and $N_1/\sqrt{\theta}_{t_2}$ at a constant W/δ for the entire Mach envelope. The overall computational flow of ITERATE is shown schematically in Figure 3.16.

The routine normally started with desired steady-state values of W/δ , h , N_1 , and Mach number. The iteration began by first approximating lift coefficient with Equation (24).

$$C_L = \frac{W}{\delta} \left(\frac{2}{P_{S.L.} \gamma M^2 S} \right) \quad (24)$$

However, this value of lift coefficient did not take into account the thrust moment effects and was not a steady-state value. Therefore, the objective of the iteration routine was to solve for a steady-state value of lift coefficient.

The iteration routine next calculated aircraft angle of attack based on the last approximation of lift coefficient. This was accomplished with a table look-up of the baseline C_{L_s} vs α characteristics. This look-up was a function of power setting for Mach numbers less than .65 and a function of Mach for Mach numbers greater than .65 for the Lear 35, as discussed in Section 4.2.1.

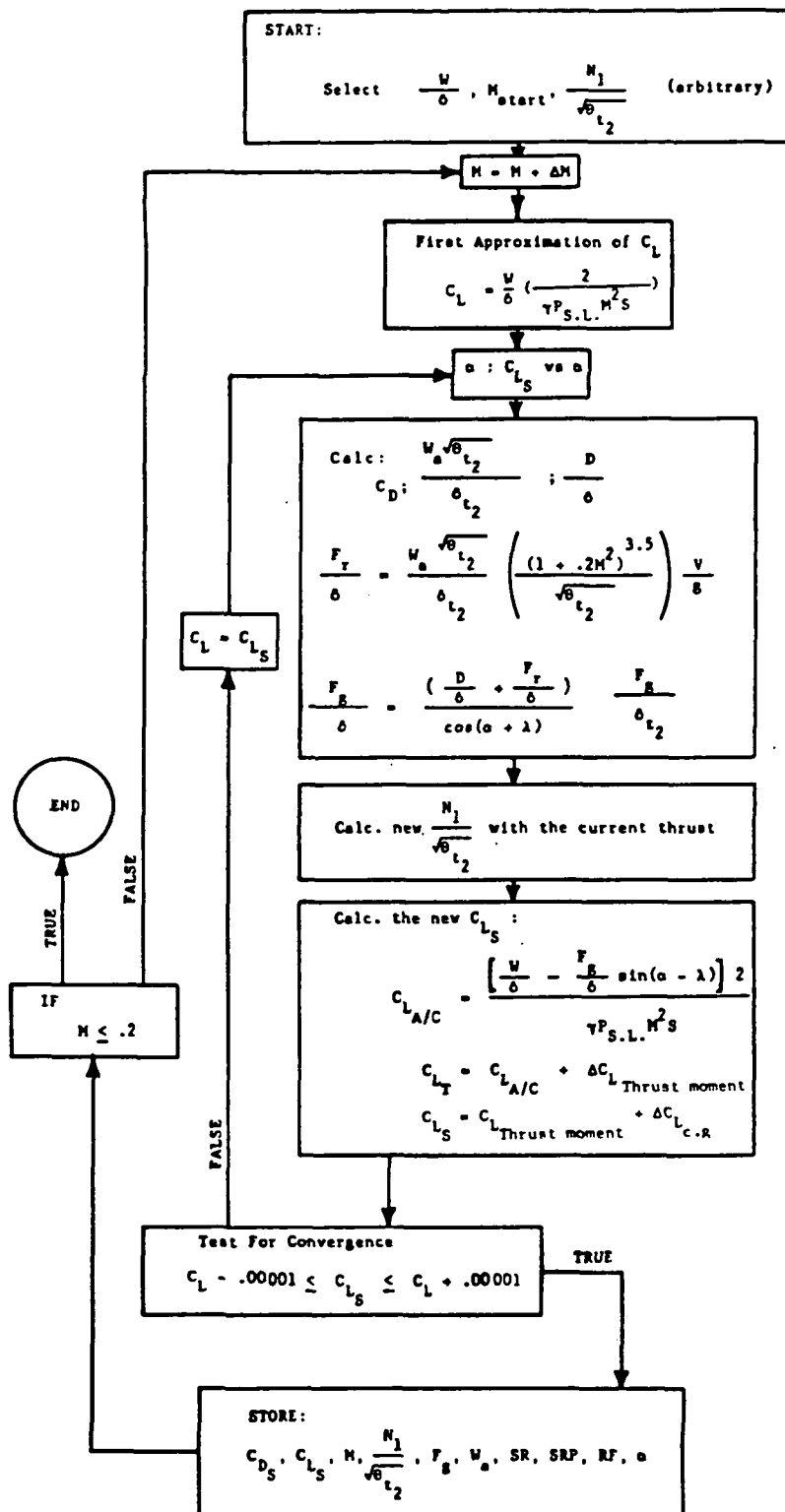


Figure 3.16: ITERATE Program Flow Chart

With angle of attack defined, the drag coefficient could then be determined. For Mach numbers greater than or equal to .60, a table look-up routine was used to interpolate the drag coefficient characteristics for angle of attack and Mach number, as discussed in Section 4.2.1. For Mach numbers less than .60, a table look-up on angle of attack and power was used. Drag over delta was then calculated with Equation (25).

$$\frac{D}{\delta} = \frac{C_D \gamma^P S.L. SM^2}{2} \quad (25)$$

A table look-up for test engine airflow was performed, using corrected RPM and Mach. Corrected ram drag was then calculated with

$$\frac{F_r}{\delta_{t_2}} = \frac{W_a V/g}{\delta_{t_2}} = \left[\frac{\left(\frac{W_a \sqrt{\theta}}{\delta_{t_2}} \right) Ma}{\sqrt{\theta} \frac{g}{\delta_{t_2}}} \right];$$

where M is Mach number, a is the local speed of sound, and $W_a \sqrt{\theta} / \delta_{t_2}$ is the corrected airflow from the table look-up. The above ram drag calculation was for one engine and was therefore multiplied by two to represent the combined total of both engines. At the same time the total pressure correction was multiplied out, yielding F_r / δ , which was used to calculate gross thrust in the next step.

With the values of drag over delta and ram drag over delta defined, the gross thrust over delta could then be calculated:

$$\frac{F_g}{\delta} = \frac{D/\delta + F_r/\delta}{\cos(\alpha + \lambda)};$$

and the corrected thrust was

$$\frac{F_g}{\delta_{t_2}} = \frac{F_g/\delta}{(1 + .2[M^2])^{3.5} \times PRF}$$

where PRF was the engine inlet pressure recovery factor. Next, a new power level (N_1) was defined. This was accomplished using the baseline gross thrust model ($N_1/\sqrt{\theta_{t_2}}$ vs F_g/δ_{t_2} and M).

Finally, the lift coefficient was updated,

$$C_{L_{A/C}} = \frac{W/\delta - F_g/\delta \sin(\alpha + \lambda)}{1/2 \gamma P_{S.L.} S M^2},$$

and corrected for thrust moment effect and c.g. position:

$$C_{L_{T_{A/C}}} = C_{L_{A/C}} + \Delta C_{L_{\text{thrust moment}}}$$

$$C_{L_s} = C_{L_{T_{A/C}}} + \Delta C_{L_{c.g.}}$$

With two lift coefficients defined, a test for convergence was then performed. For the first iteration, a comparison of the approximated C_L (Equation 24) to the value of C_{L_s} computed with the above equation was made. If convergence was not achieved, C_L was set equal to C_{L_s} ; and the iteration continued with a new calculation of angle of attack. Agreement between the last iteration and the present iteration was required to be within ± 0.00001 for convergence. When the lift coefficient did converge, the new steady-state values of C_{D_s} , C_{L_s} , F_g , F_n , F_r , range factor, specific range, specific range parameter and $N_1/\sqrt{\theta_{t_2}}$ were stored. Mach number was then incremented and the iteration performed again. The process continued until the entire Mach envelope had been defined. Additional information for the ITERATE program is presented in Appendix C. A typical number of iterations for convergence was three.

3.2.4.2 MODEL Program

The MODEL program was an adaptation of the Air Force Flight Test Center Digital Performance Simulation (DPS) computer program [11]. MODEL evaluated defined trajectories to simulate aircraft performance characteristics. The output included a time history of weight, speed, altitude, and distance. Many other parameters such as load factor, angle of attack, bank angle, heading, gross thrust, specific excess thrust, and certain aerodynamic variables were also determined. The program was capable of computing a number of performance trajectories, including four types of wing level climbs and an acceleration/deceleration maneuver. The aircraft was described to the program by tables of baseline aerodynamic and propulsion characteristics.

The general approach used in MODEL was to compute the time required to accelerate, climb, or cruise over a small fixed interval of velocity, altitude, or distance and then progressively sum these increments. This was accomplished by first evaluating the total energy of the aircraft which is equal to the potential and kinetic energy.

$$E = Wh_g + \frac{1}{2} mV^2.$$

Defining the energy height as $h_e = E/W$, assuming no wind (or a constant wind), and an inertial reference frame, the energy height becomes

$$h_e = h_g + \frac{V^2}{2g}. \quad (26)$$

The rate of change of specific energy was defined by differentiating Equation (26):

$$\frac{dh_e}{dt} = \frac{dh_g}{dt} + \frac{VdV}{gdt}.$$

Recalling that the specific excess power is defined as

$$P_s = \frac{\Delta h_e}{\Delta t} = \frac{F_{ex} V}{W} \quad (27)$$

Solving Equation (27) for Δt , the change in time is equal to the ratio of the change in energy height to the average specific excess power, or

$$\Delta t = \frac{\Delta h_e}{(P_s)_{avg}} \quad (28)$$

where

$$(P_s)_{avg} = \left(\frac{F_{ex} V}{W} \right)_{avg} = \frac{F_{ex_{avg}} V_{avg}}{W_{avg}}$$

and

$$F_{ex_{avg}} = \frac{F_{ex_1} + F_{ex_2}}{2}$$

$$V_{avg} = \frac{V_1 + V_2}{2}$$

$$W_{avg} = \frac{W_1 + W_2}{2}$$

The subscripts 1 and 2 refer to the conditions at the beginning and end of an interval. By generating Δh_e from Equation (26), Equation (28) becomes

$$\Delta t = \frac{h_{g_2} - h_{g_1} + \frac{V_2^2 - V_1^2}{2g}}{\frac{F_{ex_{avg}} V_{avg}}{W_{avg}}}$$

which simplifies to

$$\Delta t = \frac{W_{avg}}{F_{ex_{avg}}} \left[\frac{r_{g_2} - h_{g_1}}{V_{avg}} + \frac{V_2 - V_1}{g} \right]. \quad (29)$$

An estimate of the time, Δt_{est} , required to accelerate and/or climb during the interval was initially set to an arbitrary value. All parameters at point 1 were known, and the weight of the aircraft at point 2 was then computed as

$$W_2 = W_1 - W_{f_{avg}} \Delta t_{est} \quad (30)$$

Since V_2 and h_{g_2} were set by the program, W_{avg} , $F_{ex_{avg}}$, and V_{avg} could be computed and Equation (29) used to solve for Δt . Δt_{est} was then compared with Δt in a test for convergence and another iteration performed using $\Delta t_{est} = \Delta t$ if the convergence test failed. If convergence was achieved, the values of W , F_{ex} , and Δt were stored and evaluation of the next increment begun.

The simplifying assumptions made in MODEL were

- (1) spherical, nonrotating earth (no centrifugal effect from the force of gravity),
- (2) constant gravity ($g = 32.174 \text{ ft/sec}^2$), and
- (3) no accelerations caused by wind gradients.

3.2.5 Error Analysis

A sensitivity analysis was accomplished to determine the effect that errors in key instrumentation parameters had on selected flight test data base and baseline aerodynamic/engine characteristics. Table 5 summarizes the instrumentation parameters which were analyzed and the associated characteristics. N_1 and W_f were analyzed for both the right and left engine due to the small difference in engine performance identified during the thrust run. The analysis was conducted in two phases. First, the effect of a one percent error in each instrumentation parameter listed in Table 5 was evaluated. Actual data from four representative maneuvers consisting of 17 data runs were used to determine the absolute error and relative error for each of the Table 5 affected variables that resulted from a one percent error. Each instrumentation parameter was varied separately, resulting in a total of 816 conditions being analyzed (17 runs x 48 instrumentation parameter/affected variable combinations). The four test maneuvers chosen are summarized in Table 6 which covered representative weight, altitude, Mach and power conditions experienced throughout the test program. The nominal and one percent error case were analyzed for each condition using the standard data reduction software to determine the absolute error and relative error as defined below.

Absolute Error = Nominal Case - Error Case.

Relative Error = $\frac{\text{Absolute Error}}{\text{Nominal Case}}$.

The maximum absolute and relative errors experienced were then identified for each of the 48 instrumentation parameter/affected variable

Table 5: Sensitivity Analysis Parameters

INSTRUMENTATION Parameter Varied	Affected Variable					
	C_{L_s}	C_{D_s}	F_g/δ_{t_2}	$W_a\sqrt{\theta}/\delta_{t_2}$	F_g	W_a
Engine RPM N_{1R}	X	X	X	X	X	X
N_{1L}	X	X	X	X	X	X
Fuel Flow W_{fR}	X	X	X	X	X	X
W_{fL}	X	X	X	X	X	X
Longitudinal Accel $n_{x_{body}}$	X	X				
Normal Acceleration $n_{z_{body}}$	X	X				
Angle of Attack	X	X				
Static Pressure	X	X	X	X	X	X
Dynamic Pressure	X	X	X	X	X	X
Air Temperature	X	X	X	X	X	X

combinations by reviewing data from each run. These maximum errors were then tabulated so that the relative impact of a one percent error could be compared for each instrumentation variable to assist in identification of instrumentation requirements for future programs.

The second phase of the error analysis evaluated the maximum relative and absolute error associated with the actual instrumentation accuracies defined for the data acquisition system used during the program. The most critical instrumentation parameters were identified from the phase one analysis, and the accuracy specified for each of these transducers was used in a separate analysis to determine the anticipated errors associated with this program. The instrumentation transducers used during this program were generally of very high quality with state-of-the art or close to state-of-the art accuracies. As a result, the effect of high quality instrumentation transducers may be readily assessed by comparing the results of the phase one and phase two error analysis. Results are presented in Section 4.5.

Table 6: Sensitivity Analysis Maneuvers

<u>Flt</u>	<u>Maneuver No.</u>	<u>Runs</u>	<u>W/δ (lbs)</u>	<u>Condition</u>	<u>Power (N₁)</u>
184	1	3	22000	ACCEL	95%
184	2	5-10	22000	DECEL	50%
187	1	23-26	60000	ACCEL	95%
187	6	50, 51, 60-63	60000	DECEL	80%

3.2.6 Accelerometer Corrections

Since flight path accelerations were a primary factor in the calculation of C_{L_s} and C_{D_s} , two corrections to body axis accelerometer data had to be considered. The first, angular misalignment between the measurement axis of each accelerometer and its respective aircraft body axis, was negligible in this program due to the accelerometer alignment procedures discussed in Section 3.2.5. The second, a correction for angular velocity and acceleration inputs due to the location of the accelerometer not being at the aircraft c.g., is developed in Reference 5. The magnitude of this correction was minimized by locating each accelerometer as close to the test c.g. range as possible.

3.2.7 Structural Flexibility

The Lear 35 was considered a rigid aircraft for purposes of this program. Provision was not made in the analysis techniques to account for structural flexibility, since discussions conducted with the Learjet Corporation and consultants to the company indicated that the Model 35 was highly rigid and that flexibility effects related to the performance modeling work would be insignificant. The excellent repeatability of data experienced during the program confirmed that this assumption was valid.

Application of performance modeling techniques to an aircraft with significant structural flexibility would require additional information about the aircraft. Specifically, definition of the significant flexibility modes of the aircraft would be needed along with the aerodynamic influence coefficient matrix and the structural influence coefficient matrix as defined in Reference 12. Since the aircraft mass distribution directly affects the lift and drag coefficient characteristics of a flexible aircraft, a standard mass distribution would have to be defined and a correction applied to the lift and drag coefficient data based on the actual mass distribution of the aircraft. The correction would be developed in a manner similar to the other coefficient corrections discussed in Section 3.2.1. For example:

$$\Delta C_{L_{\text{flexibility}}} = C_{L_{\text{std mass}}} - C_{L_{\text{test mass}}}$$

and

$$C_{L_{\text{flexibility}}}^{\text{corrected}} = C_{L_s} + \Delta C_{L_{\text{flexibility}}}.$$

The mass distribution of the aircraft throughout a test flight would have to be known accurately and approximate prediction equations developed for lift and drag coefficient based on the significant flexibility modes of the aircraft. Reference 12 presents the approach for the case of angular flexibility about the y body axis resulting from forces in the z body axis direction. It may be possible to minimize the corrections by restricting the mass distribution variation during the data acquisition phases of flight test.

3.3 CALIBRATION TESTS

3.3.1 Instrumentation Transducers

A description of the instrumentation system and instrumentation transducers is presented in Section 3.5. All transducers were calibrated prior to the flight test program and also calibrated after completion of the program to check for calibration shifts. All calibrations were accomplished by Learjet and KSR personnel at the Learjet Wichita facility with the exception of the fuel flow transducers, which were calibrated by Flow Technology, Inc., Phoenix, Arizona. The accelerometers were calibrated using an Ideal-Aerosmith, Inc., tilt table (part no. 221300-3); and the rate gyros were calibrated on a Genisco, Inc., rate table (part no. 223E314P1). Specifically designed angular boards were used for the angle of attack, sideslip and surface position calibrations. The pressure transducers were calibrated using a Ruska Instrument Corporation Model 6000 pressure calibration instrument. An HP 3325A synthesizer/function generator was used for the engine RPM calibrations.

3.3.2 Thrust Run

A ground thrust run was made to determine the actual thrust, fuel flow and airflow (using Equation 20) characteristics of each engine. The thrust run configuration consisted of restraining the aircraft in the forward horizontal direction by attaching a cable between the main landing gear strut and a ground tie-down with a load cell located directly in the load bearing path as illustrated in Figures 3.17 and 3.18. Each engine was evaluated separately with the tie-down hardware attached to the respective gear strut. This arrangement was possible, since the landing gear struts were located directly beneath each engine as shown in Figure 3.2. Test points for each engine consisted of five stabilized conditions based on N_1 which were chosen throughout the RPM range. The engine was stabilized for approximately three minutes at each test condition with fuel flow, N_1 , and thrust (using the load cell) being recorded along with ambient pressure and temperature. The data were then reduced to corrected form so that the η curve could be defined as discussed in Sections 3.2.1.2 and 4.1.2.

It was desired to obtain at least nine evenly spaced test points for each engine throughout the RPM range to improve definition of the TSFC curve. Program constraints would not allow this for the Lear 35 program; however, a very extensive thrust run was accomplished on the Lear 55 aircraft which included a total of 20 stabilized points for each engine as discussed in Appendix E. This is the recommended approach for future programs. The load cell/tie-down arrangement was calibrated during the Lear 55 thrust run in which the aircraft was

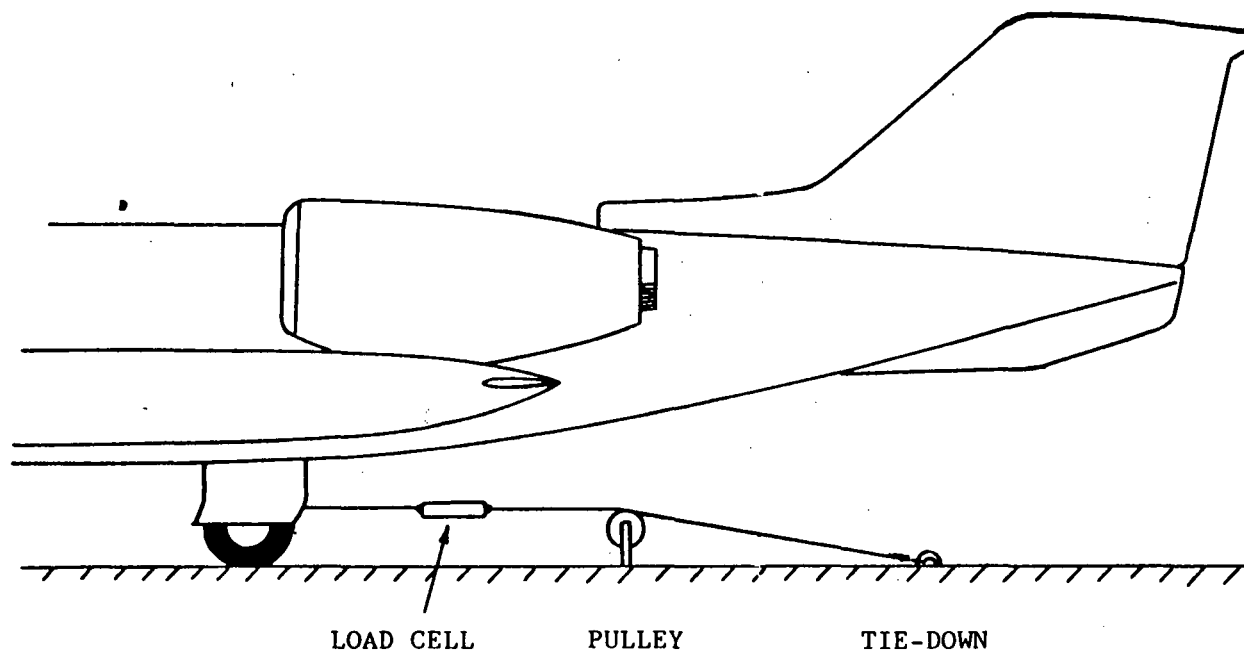


Figure 3.17: Thrust Run Load Cell/Tie-Down Configuration



Figure 3.18: Thrust Run Hardware

restrained using the same hardware as shown in Figure 3.18 while on the Edwards AFB thrust table, an internationally recognized facility for determining engine thrust characteristics. A correction curve was developed for the load cell/tie-down arrangement based on the Edwards thrust table as discussed in Appendix E.

3.3.3 Pitot Static System, Temperature Probe and Angle of Attack

The aircraft pitot-static system, temperature probe and angle of attack transducer were calibrated during the initial two test flights. Calibration maneuvers consisted of a series of stabilized points conducted throughout the airspeed range at three test altitudes: 11,000, 35,000 and 43,000 feet. A test summary of these points is presented in Table 7. The test points were selected to cover the C_L , W/δ and Mach ranges of the aircraft as well as representative altitude conditions.

The pitot-static system calibrations were accomplished to define static port position error characteristics using a trailing cone which extended approximately one fuselage length behind the aircraft on a flexible tube. A rigid tube with several static ports was inserted ahead of the cone as shown in Figure 3.19 to record the actual static pressure. The cone was used to stabilize the tube assembly behind the aircraft. The actual static pressure was recorded at each test point as well as the static pressure measured by the "test system" which consisted of four static ports located approximately 8 1/2 inches aft of the pitot tube tip on the nose boom. To record these measurements, the aircraft was stabilized at a test condition and a switching valve was used to measure "test system" and cone pressure with the same pressure transducer. Since the difference between the test system and actual static pressure ($\Delta p_p = p_s - p_a$) was needed, utilization of the same pressure transducer eliminated transducer offset errors that would be present if two separate transducers had been used. Data were taken under well-stabilized conditions to prevent pneumatic lag from influencing the measure-

Table 7: Test Points for Pitot Static System
Temperature Probe and Angle of Attack
Calibration

<u>Pressure Altitude</u>	<u>Indicated Velocity (KIAS)</u>	<u>Indicated Mach</u>
11,000	150	-
	200	-
	250	-
	300	-
	350	-
35,000	-	.55
	-	.59
	-	.63
	-	.67
	-	.71
	-	.75
	-	.79
43,000	-	.60
	-	.70
	-	.78

ments. These data were analyzed using standard techniques contained in Reference 13. The position error was defined using the parameter $\Delta p_p / q_{cic}$ as a function of lift coefficient ($C_{L_{ic}}$) where

$$\Delta p_p = p_s - p_a$$

$$q_{cic} = p_t - p_s$$

$$C_{L_{ic}} = \frac{W}{1/2 \gamma p_s M_{ic}^2}$$

Results are presented in Section 4.1.3.

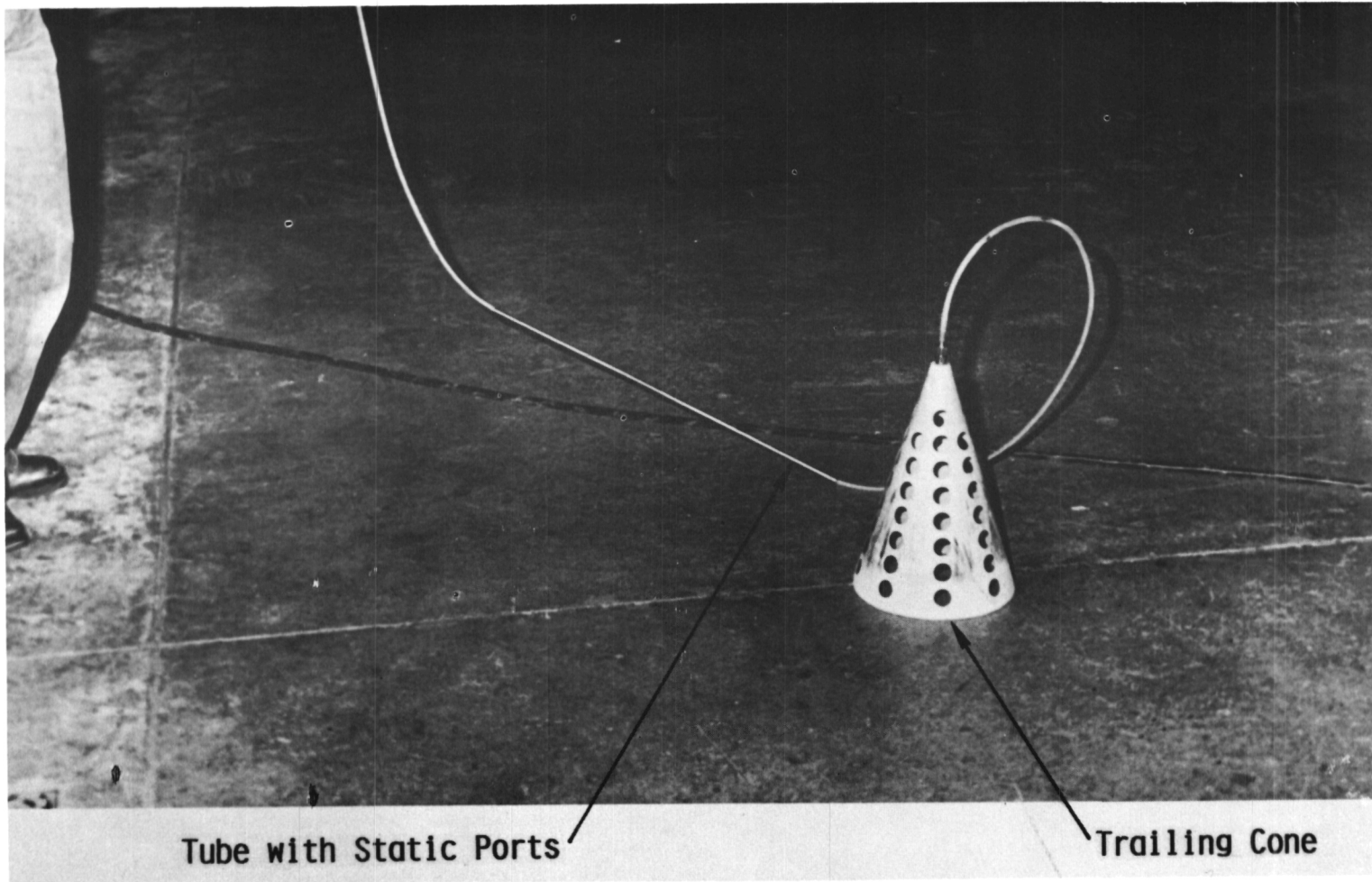


Figure 3.19: Trailing Cone Assembly

The air temperature probe was calibrated by defining the temperature probe recovery factor (K) from data obtained at the same test points as those presented in Table 7. By conducting each test series at the same altitude and assuming the tests were flown in the same air mass (same T_a), the probe recovery factor was determined using the fact that

$$T_{ic} = T_a(1 + .2KM_{ic}^2) \quad (18)$$

which may be rearranged in the form

$$\frac{1}{T_{ic}} = \frac{1}{T_a} - .2K \frac{M_{ic}^2}{T_{ic}}.$$

When $1/T_{ic}$ is plotted versus $.2M_{ic}^2/T_{ic}$ for a fixed altitude, the slope of the resulting line will be equal to -K. Results are presented in Section 4.1.3.

The angle of attack was measured by sensing the position of a vane which extended out from the side of the nose boom aft of the pitot static probe (Figure 3.20). A correction for the flow disturbance due to the bow wave of the aircraft fuselage was defined from data obtained at the same stabilized points presented in Table 7. To determine the actual angle of attack, data from the longitudinal and vertical body-mounted accelerometers were used along with the equation

$$\theta = \alpha_{true} + \gamma = \tan^{-1} \frac{\bar{n}_{x_{body}}}{\bar{n}_{z_{body}}}.$$

Thirty data points (approximately 3 seconds of data) were used from each stabilized point to compute averaged values of each acceleration:

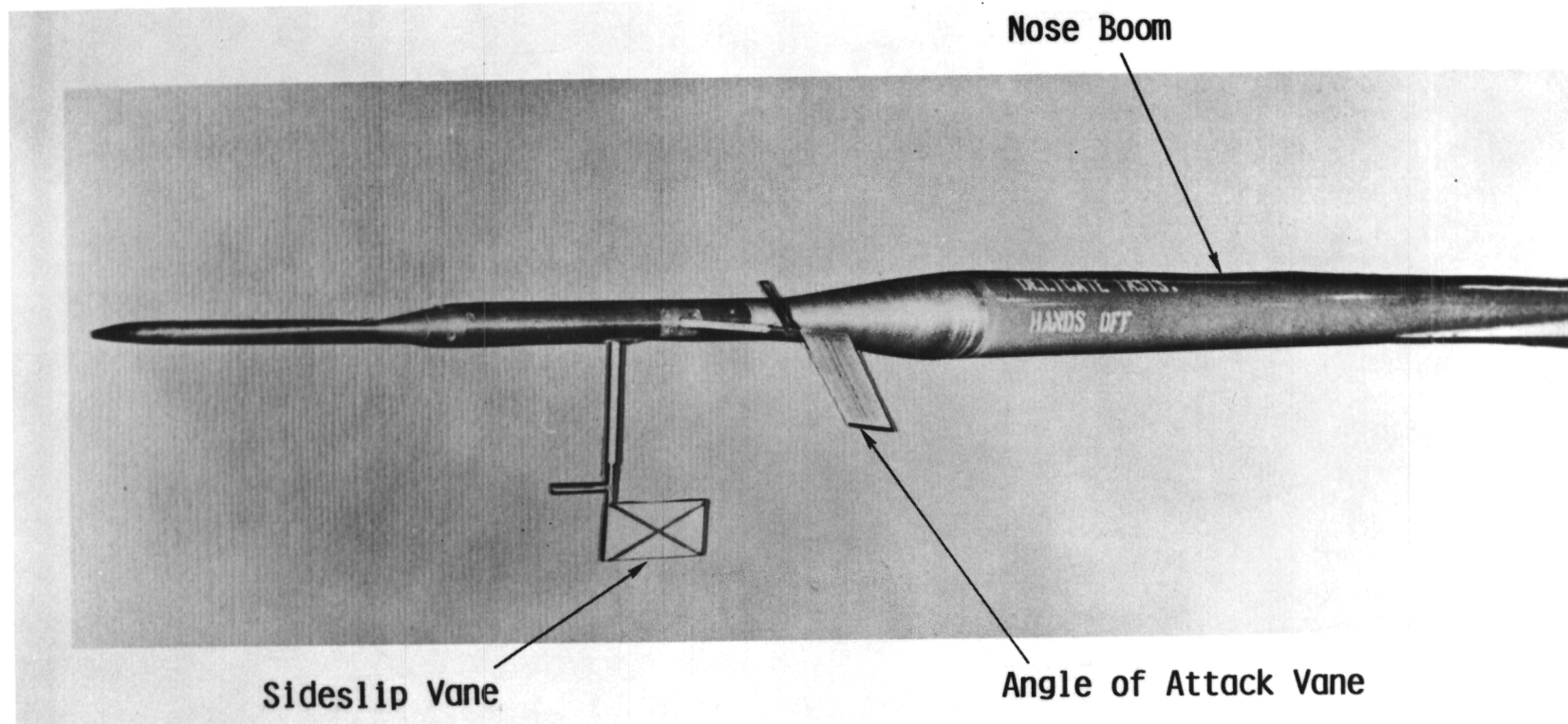


Figure 3.20: Noseboom Installation of Angle of Attack and Sideslip Vanes

$$\bar{n}_{x_{\text{body}}} = \frac{\sum_{n=1}^{30} n_{x_{\text{body}}}}{30}$$

$$\bar{n}_{z_{\text{body}}} = \frac{\sum_{n=1}^{30} n_{z_{\text{body}}}}{30} .$$

The flight path angle γ was estimated by

$$\gamma = \sin^{-1} \frac{\dot{h}_g}{V}$$

where

$$\dot{h}_g = \frac{dh}{dt} \frac{\bar{T}_{a_t}}{\bar{T}_{a_s}} .$$

dh/dt was estimated using a linear curve fit for h versus time with

\bar{T}_{a_t} and \bar{T}_{a_s} being averaged quantities over 30 points similar to $\bar{n}_{x_{\text{body}}}$ and $\bar{n}_{z_{\text{body}}}$. The values obtained for dh/dt were very small,

as would be expected for a stabilized point. The actual angle of attack was then determined by

$$\alpha_{\text{true}} = \tan^{-1} \frac{\bar{n}_{x_{\text{body}}}}{\bar{n}_{z_{\text{body}}}} - \sin^{-1} \frac{\dot{h}_g}{V_t} .$$

For each test condition, the parameter

$$\Delta\alpha = \alpha_{\text{true}} - \alpha_{\text{boom}}$$

was plotted versus α_{boom} to define the angle of attack correction.

Results are presented in Section 4.1.3.

3.3.4 Weight and Balance

The aircraft was weighed before each test flight to determine the gross weight and horizontal c.g. position. The procedure consisted of raising the aircraft on jacks and recording the load at each jack point through load cells which were an integral part of each jack. Post-flight weighings were made after the initial three performance flights to establish confidence in the fuel burn estimations for both weight and c.g. variation during flight.

3.3.5 Accelerometer Alignment

Since accurate measurement of flight path acceleration was critical in the calculation of lift and drag from quasi steady-state maneuvers, considerable attention was given to precise alignment of the body axis accelerometers during the initial installation. This procedure began with leveling of the aircraft on jacks such that the x and y body axes were aligned in the horizontal plane. The accelerometers were then installed as nearly orthogonal to each other as possible in the aircraft with alignment adjustments made until the longitudinal and lateral accelerometers read zero and the normal accelerometer read one g. The aircraft was then rolled to approximately 6.5 degrees left wing down while maintaining x body axis alignment in the horizontal plane. Alignment of the longitudinal accelerometer was then adjusted until a zero reading was obtained. Following this adjustment, the aircraft was re-leveled in the x-y plane and all accelerometers checked for the appropriate reading. No alignment adjustments were necessary at this point, since the longitudinal and lateral accelerometers read zero and the normal accelerometer read one g. If these readings had not resulted, additional alignment adjustments would have been necessary and the procedure repeated until acceptable alignment was achieved.

3.4 FLIGHT TESTS AND PROCEDURES

3.4.1 General

A total of 17.42 hours were flown during the test program, which included instrumentation evaluation, pitot-static system calibration and takeoff/landing/ground effect evaluation as well as performance modeling. Table 8 presents a breakdown of the flight test program.

Table 8: Flight Test Summary

<u>Flt. No.</u>	<u>Date</u>	<u>Flt. Time</u> <u>(hrs:mins)</u>	<u>Mission</u>
175	Dec. 16, '82	1:45	Instrumentation checkout, pitot static cal.
176	Dec. 17, '82	2:15	Pitot static cal., test maneuver familiarization
184	Jan. 5, '83	1:50	22,000 W/δ
185	Jan. 6, '83	2:10	40,000, 47,000 W/δ
187	Jan. 7, '83	3:20	60,000, 73,000 W/δ
188	Jan. 10, '83	3:30	67,000, 80,000 W/δ; 60,000 repeat (partially completed)
189	Jan. 11, '83	2:35	53,000 W/δ, 60,000 repeat (complete)

All flights were flown from the Gates Learjet Corporation Wichita Facility with a flight crew consisting of a Learjet pilot and copilot and KSR flight test engineer. The flight crew was briefed concerning procedures and test maneuvers by CRINC personnel. The test aircraft was owned and operated by Learjet.

3.4.2 Description of Tests

Four types of maneuvers were flown during the program:

1. Approximately constant altitude accelerations and decelerations (quasi steady-state maneuvers) at constant power based on N_1 .
2. Stabilized points at constant W/δ .
3. Pull-up, push-over, pull-up (push-pull) profiles initiated from a stabilized point.
4. Flight trajectory profiles throughout the Mach and altitude envelope of the aircraft.

The primary maneuver used for performance modeling was the quasi steady-state acceleration/deceleration which provided sufficient data to completely define the baseline aerodynamic and engine characteristics as discussed in Section 3.2.1. Stabilized points and flight trajectory profiles were used for evaluation of the stabilized point and flight trajectory predictions provided by the performance modeling programs ITERATE and MODEL. The push-pull profiles were obtained to spot-check the accel/decel data and extend the angle of attack range.

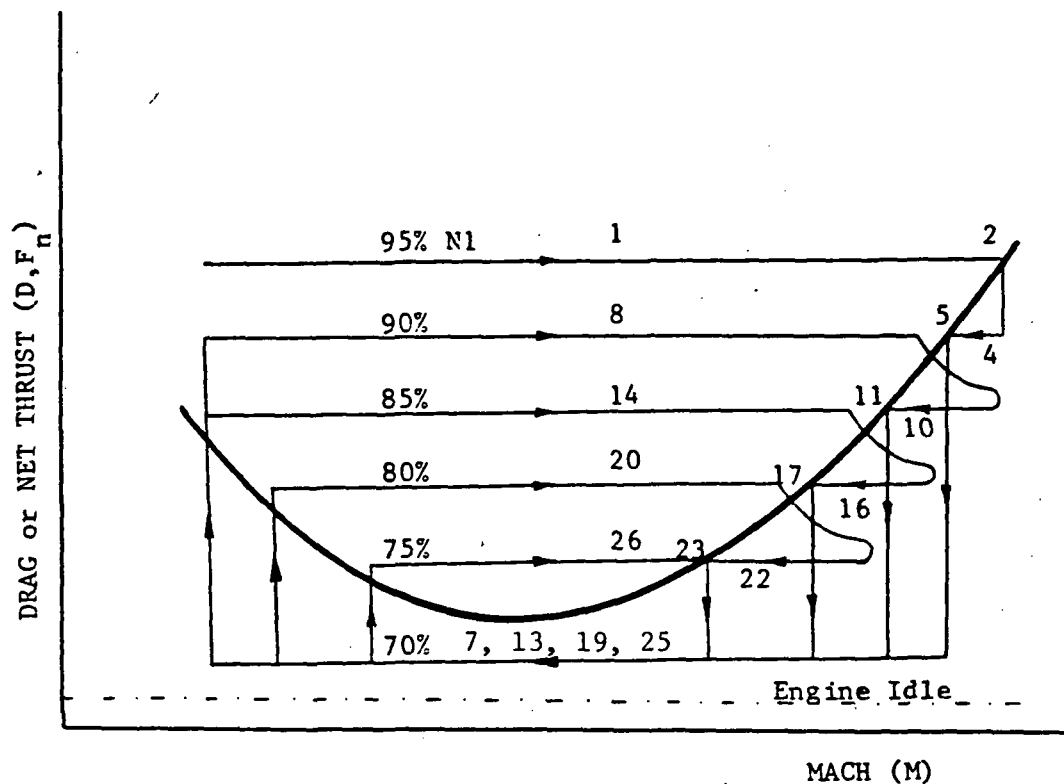
The accel/decel maneuvers were conducted at nearly constant altitude using the altitude hold mode of the autopilot. Normally less than a 60 foot excursion from the start altitude was experienced during a maneuver. Eight cardinal power settings were evaluated consisting of 95, 90, 85, 80, 75, 70, 60 and 50 percent N_1 . The N_1 was chosen as the variable to represent power because of the relatively high bypass ratio of these engines and the resulting high correlation to engine

airflow. This technique allowed determination of the power-dependent lift and drag characteristics. An accel/decel was conducted at a cardinal power setting by holding N_1 to within $\pm 1/2$ percent during a maneuver. A range of weight-pressure ratio (W/δ) within the aircraft envelope was designated to provide a C_L variation for a given Mach number so that Mach effects could be defined. For example, eight values of W/δ were evaluated as shown in Table 9. These eight values of W/δ provided eight evenly spaced points on a constant Mach drag polar in the mid-Mach range. Each accel/decel was then conducted at an approximately constant power setting and W/δ . At each value of W/δ , an accel/decel sequence was performed which included maneuvers at all cardinal power settings above idle. As W/δ increased, the number of available power settings decreased due to increasing idle RPM with increasing altitude. For example at 40,000 feet only the 95, 90 and 85 percent power settings could be evaluated. As a result, the largest amount of data was obtained for the higher power settings. Primary cruise performance characteristics such as $N_1/\sqrt{\theta_{t_2}}$ versus Mach, and range factor versus Mach are also a function of W/δ . These characteristics were evaluated in a conventional manner from a series of stabilized points conveniently located within an overall accel/decel maneuvering sequence. Maneuvering sequences at W/δ values of 22,000, 40,000, 60,000 and 80,000 pounds were chosen to include stable points, as shown in Table 9. Approximately four stable points were obtained at each value of W/δ . To evaluate repeatability of the data, the maneuvering sequence at 60,000 W/δ was repeated on different flights.

Table 9: Performance Modeling Maneuvering Sequences

<u>W/δ</u> <u>(lbs)</u>	<u>Nominal</u> <u>Altitude</u> <u>(ft)</u>	<u>Stable Points</u> <u>Included</u>	<u>Repeat</u>
22,000	10,000	X	
40,000	23,000	X	
47,000	26,000		
53,000	29,000		
60,000	32,000	X	X
67,000	35,000		
73,000	38,000		
80,000	40,000	X	

A typical maneuvering sequence is illustrated in Figure 3.21 which assumes the drag curve and engine idle level are as shown for a particular W/ δ configuration. The sequence includes stabilized points and push-pull maneuvers. A sequence began by slowing the aircraft to an acceptable minimum speed (for the Lear 35 this was an airspeed slightly above stick shaker speed) at an altitude based on the target value of W/ δ . A 95 percent accel was then performed followed by a stabilized point and a push-pull. Approximately two to four minutes were spent at each stabilized point to assure that the aircraft had stabilized. A push-pull consisted of a very slow roller coaster maneuver between approximately .5 g and 2.5 g or buffet with angular acceleration kept to a minimum. After the push-pull, the throttles were retarded to 90% and a decel performed into another stabilized point. The sequence then continued as shown in Figure 3.21. Altitude adjustments were made at convenient times in the sequence to maintain



<u>Sequence</u>	<u>Power Setting</u>	<u>Maneuver</u>	<u>Data Recorded</u>
1	95	Accel	Yes
2	95	Stabilized Point	Yes
3	95	Push-pull	Yes
4	90	Decel	Yes
5	90	Stabilized Point	Yes
6	90	Push-pull	Yes
7	70	Decel	Yes
8	90	Accel	Yes
9	95	Accel	No
10	85	Decel	Yes
11	85	Stabilized Point	Yes
12	85	Push-pull	Yes
13	70	Decel	Yes
14	85	Accel	Yes
15	95	Accel	No
16	80	Decel	Yes
17	80	Stabilized Point	Yes
18	80	Push-pull	Yes
19	70	Decel	Yes
20	80	Accel	Yes
21	95	Accel	No
22	75	Decel	Yes
23	75	Stabilized Point	Yes
24	75	Push-pull	Yes
25	70	Decel	Yes
26	75	Accel	Yes

Figure 3.21: Typical Test Sequence

W/δ within approximately ± 1 percent as weight decreased. The majority of the stabilized points were obtained following a decel which allowed for faster stabilization. Although not specifically shown in the Figure 3.21 diagram, a high power setting as indicated in sequence 15 was used to accelerate past the last stabilized point so that the decel as shown in sequence 16 could be obtained. The general guideline used was to accelerate far enough past the last stabilized point so that the engine would achieve stabilization on the subsequent decel before reaching the Mach number of the last stabilized point. Data were taken periodically throughout an accel/decel rather than continually to keep the volume of data to a manageable level. Ideally, approximately a twenty-second burst of data was recorded as the aircraft passed through each cardinal Mach. For maneuver sequences which did not include stabilized points or push-pull maneuvers, an accel/decel was continued until the absolute value of acceleration was generally below a quarter knot per second. The actual test sequence performed at each W/δ condition depended directly on the location of the drag curve with respect to the net thrust levels. For example, if two cardinal power settings were located between engine idle and the bottom of the drag curve, then at least one decel would be performed at each of these power settings. The maneuver sequence was designed to acquire the needed data in a time-efficient manner and also be easily accomplished by the flight crew. It clearly met these objectives. For planning purposes, 90 minutes were estimated for a maneuver sequence with stabilized points and push-pulls, and 45 minutes were estimated for a sequence without these maneuvers.

Flight trajectory profiles were flown during the program which consisted of climb, accel and decel maneuvers throughout the airspeed, altitude and power range of the aircraft. A detailed description of these tests is presented in Section 4.4.2.



3.5 INSTRUMENTATION

A multichannel digital data acquisition system (DAS) was installed in the test aircraft to record all applicable aircraft parameters. The DAS utilized a Honeywell 5600C magnetic tape recorder and a 10-bit processor/multiplexer. All data were sampled at a minimum rate of ten samples per second. Preflight and post-flight calibrations were performed before and after each test mission. Table 10 summarizes the range and approximate accuracy for each instrumented parameter used for the performance modeling effort. The instrumentation system was designed and transducer accuracies specified in accordance with the recommendations made in Reference 14. The instrumentation system incorporated a start/stop switch for the copilot as well as an in-flight readout of selected parameters such as aircraft weight to aid in achieving test conditions and assuring critical transducers were functional. The majority of the system including the signal conditioning and magnetic tape recorder were installed in the main cabin area as shown in Figure 3.22. Individual transducers were installed in a location appropriate to their function. For example, the accelerometers were installed as close to the aircraft c.g. as possible to minimize off-c.g. corrections.

Table 10: Instrumentation Parameter List

<u>Parameter</u>	<u>Units</u>	<u>Range</u>	<u>Resolution</u>
1. Altitude (boom static pressure)	psia	0 - 15 psia	.00075 psia (\sim 1.5 ft)
2. Airspeed (boom differential q_{cic} pressure)	psid	0-6 psid	± 0.25 kt ($\pm .002$ psid)
3. Air temperature	$^{\circ}\text{C}$	-70 to 350°C	$\pm .25^{\circ}\text{C}$
4. Longitudinal acceleration	g	+1.0 to -1.0	± 0.001 g
5. Lateral acceleration	g	+1.0 to -1.0 g	± 0.001 g
6. Normal acceleration	g	+5.0 to -5.0 g	± 0.005 g
7. Pitch rate	$^{\circ}/\text{sec}$	$\pm 200^{\circ}/\text{sec}$	$\pm 0.3^{\circ}/\text{sec}$
8. Roll rate	$^{\circ}/\text{sec}$	$\pm 200^{\circ}/\text{sec}$	$\pm 0.3^{\circ}/\text{sec}$
9. Yaw rate	$^{\circ}/\text{sec}$	$\pm 200^{\circ}/\text{sec}$	$\pm 0.3^{\circ}/\text{sec}$
10. Pitch angle	deg	$\pm 60^{\circ}$	$\pm 0.75^{\circ}$
11. Roll angle	deg	$\pm 90^{\circ}$	$\pm 0.75^{\circ}$
12. Boom vane α	deg	$\pm 30^{\circ}$	0.1°
13. Fuel flow left	gal/hr	0 to 2050 lb/hr	10 lb/hr
14. Fuel flow right	gal/hr	0 to 2050 lb/hr	10 lb/hr
15. Engine RPM-N1-left	%	0 to 110%	0.2%
16. Engine RPM-N1-right	%	0 to 110%	0.2%
17. Engine RPM-N2-left	%	0 to 110%	0.2%
18. Engine RPM-N2-right	%	0 to 110%	0.2%
19. Fuel used totalizer	lb	0 to 6500 lb	5 lb
20. Fuel temperature left	$^{\circ}\text{F}$	-50° , $+75^{\circ}\text{C}$	0.1°C

Table 10: Instrumentation Parameter List (continued)

<u>Parameter</u>	<u>Units</u>	<u>Range</u>	<u>Resolution</u>
21. Fuel temperature right	°C	-50°, +75°C	0.1°C
22. Turbine temperature left	°C	150° to 1000°C	±1°C
23. Turbine temperature right	°C	150° to 1000°C	±1°C
24. Flap position	deg	Up/T.O./Ldg.	---
25. Spoiler position	deg	---	---
26. Pilot/Engineer status byte	---	---	---
27. Clock (binary-real time)	sec	---	---
28. Boom vane β	deg	+30°	0.1°

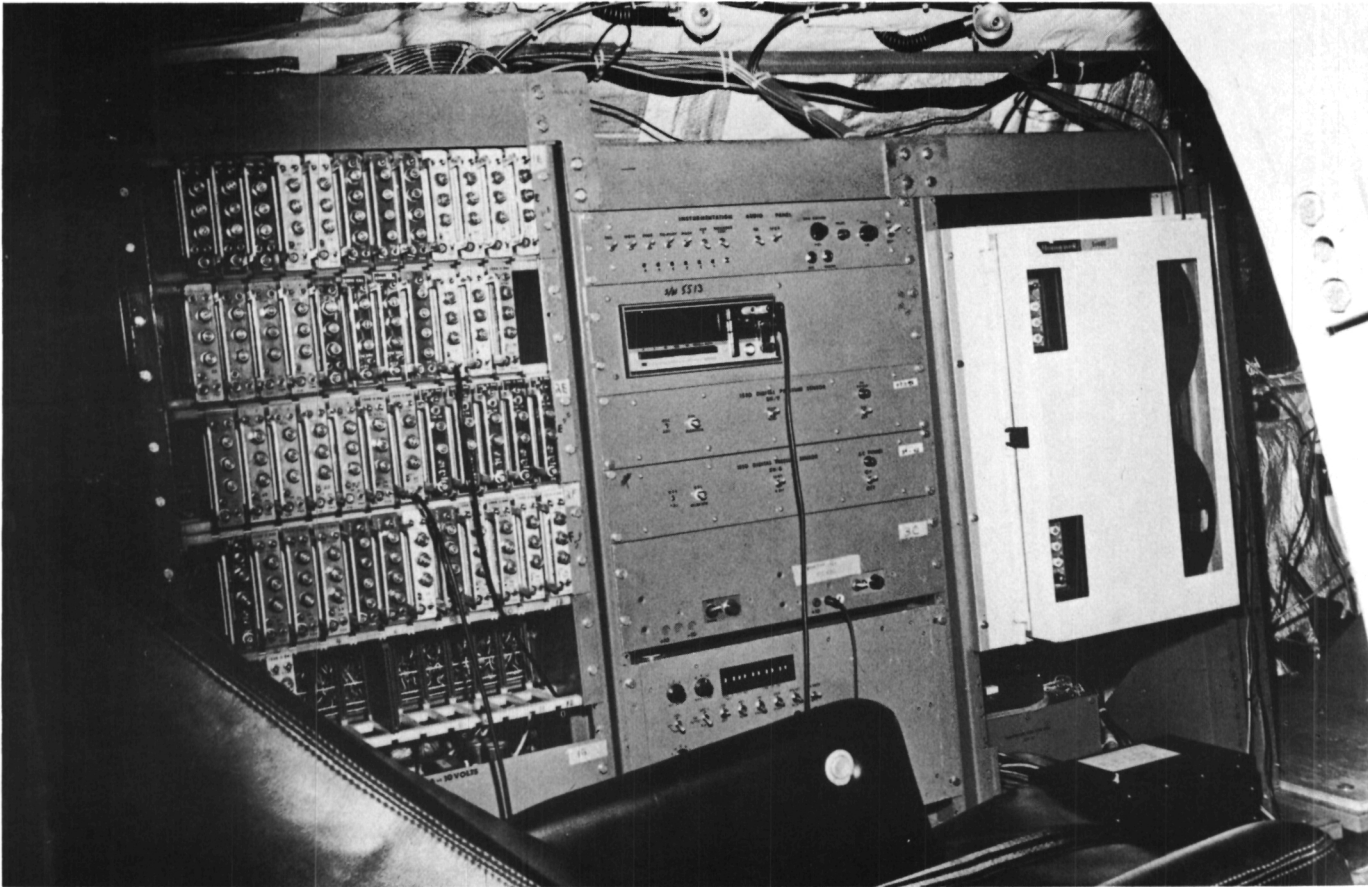


Figure 3.22: Instrumentation System Installation

4. RESULTS

Results of the overall program are presented in this chapter. The baseline aerodynamic and engine data were proprietary to the Link Division of the Singer Corporation; and, as a result, the actual numbers are not presented. However, the scaling of each baseline characteristic graph is included to provide the necessary interpretation of the data.

4.1 CALIBRATION TESTS

4.1.1 Instrumentation Transducers

Results of the calibration tests for each transducer were reviewed and incorporated into the data reduction software. These calibration curves were used to convert raw data to engineering units format as the first step in the overall data reduction process. The pre- and post-program calibration for all transducers had excellent agreement (within the specified transducer accuracy).

4.1.2 Thrust Run

Table 11 presents a summary of the thrust run conditions for each engine. The thrust calibration friction correction as discussed in Appendix E was used to arrive at the actual thrust values, and computer program F.TABLE described in Appendix C was used to convert the raw data to corrected form. Determination of η , the ratio of thrust run TSFC to engine prediction deck TSFC, began by plotting thrust run corrected TSFC versus corrected RPM, as shown in Figure 4.1. Corrected TSFC was obtained from the ratio of $W_f/\sqrt{\theta} \delta^{.97}$ and F_g/δ , since $N = .97$ for the zero Mach case as discussed in Section 3.2.1.2. The engine prediction deck corrected TSFC was also included for comparison, and then a curve was faired through the thrust run data using the engine deck curve as a guide for extrapolation in the high corrected RPM range that could not be reached during ground operation. In the less critical low corrected RPM range, the extrapolation was based on the trends observed with the Lear 55 thrust run where a crossover was found. The low RPM region was considered less critical, since all flight test data were obtained at corrected RPM values generally above 11000; and the majority of the flight test conditions called for corrected RPM's above 14,000. It is desirable, however, to obtain thrust run points in this range as accomplished on the Lear 55 program rather than to rely on extrapolation. The ratio (η) of the thrust run corrected TSFC curve to the engine deck corrected TSFC curve was then obtained as a function of corrected RPM as presented in

Table 11: Thrust Run Summary

Right Engine				Left Engine			
N_1 (RPM)	$\frac{N_1}{\sqrt{\theta}}$ (RPM)	T (°F)	P_a (psia)	N_1 (RPM)	$\frac{N_1}{\sqrt{\theta}}$ (RPM)	T (°F)	P_a (psia)
14477	14846	33.6	14.26	14541	14966	30.0	14.26
16672	17101	33.4	14.26	16774	17258	30.4	14.26
17832	18286	33.7	14.26	17737	18231	31.4	14.26
18738	19212	33.8	14.26	18692	19220	32.0	14.26
19068	19541	34.3	14.26	19111	19631	32.0	14.26

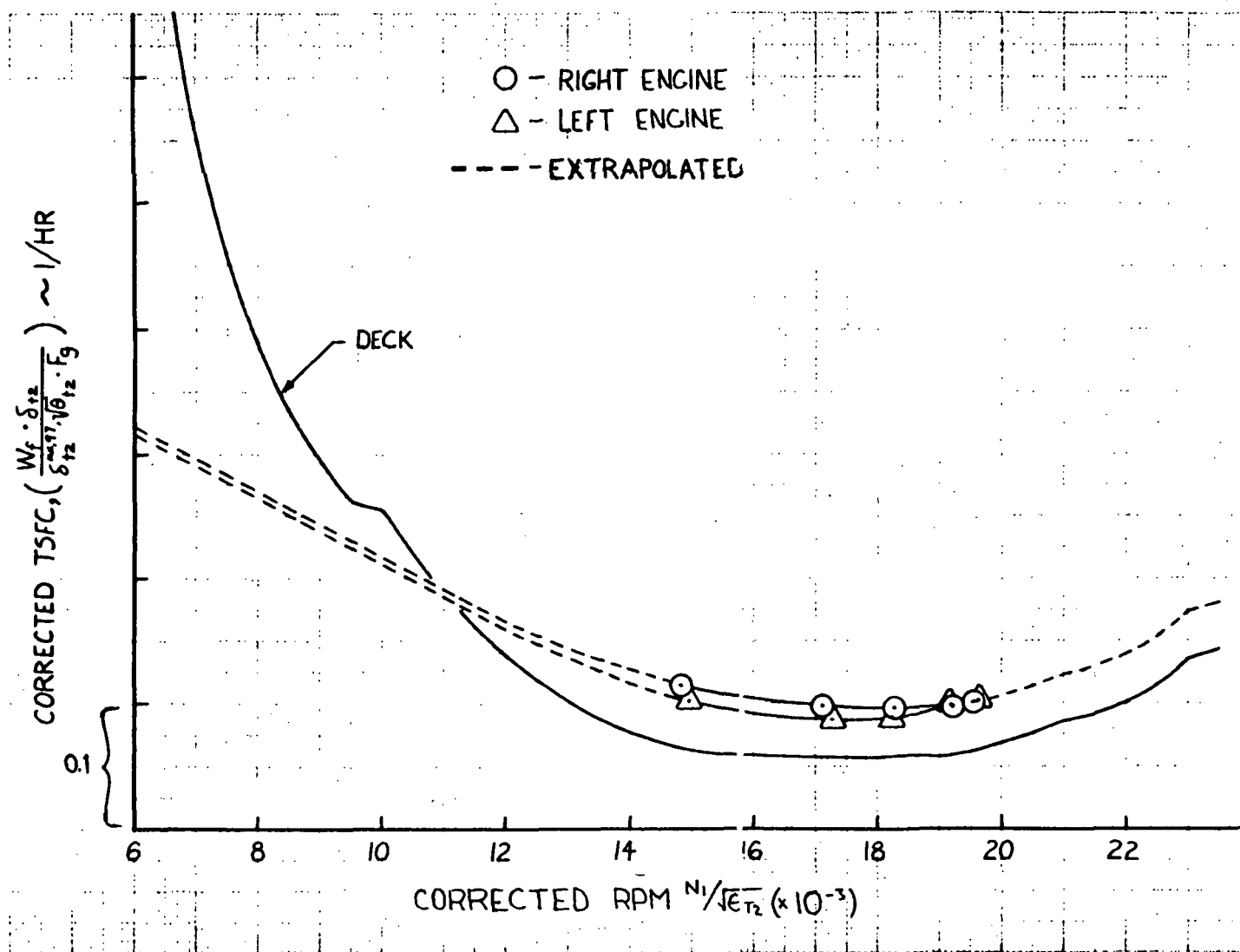


Figure 4.1: Thrust Run Corrected TSFC Data

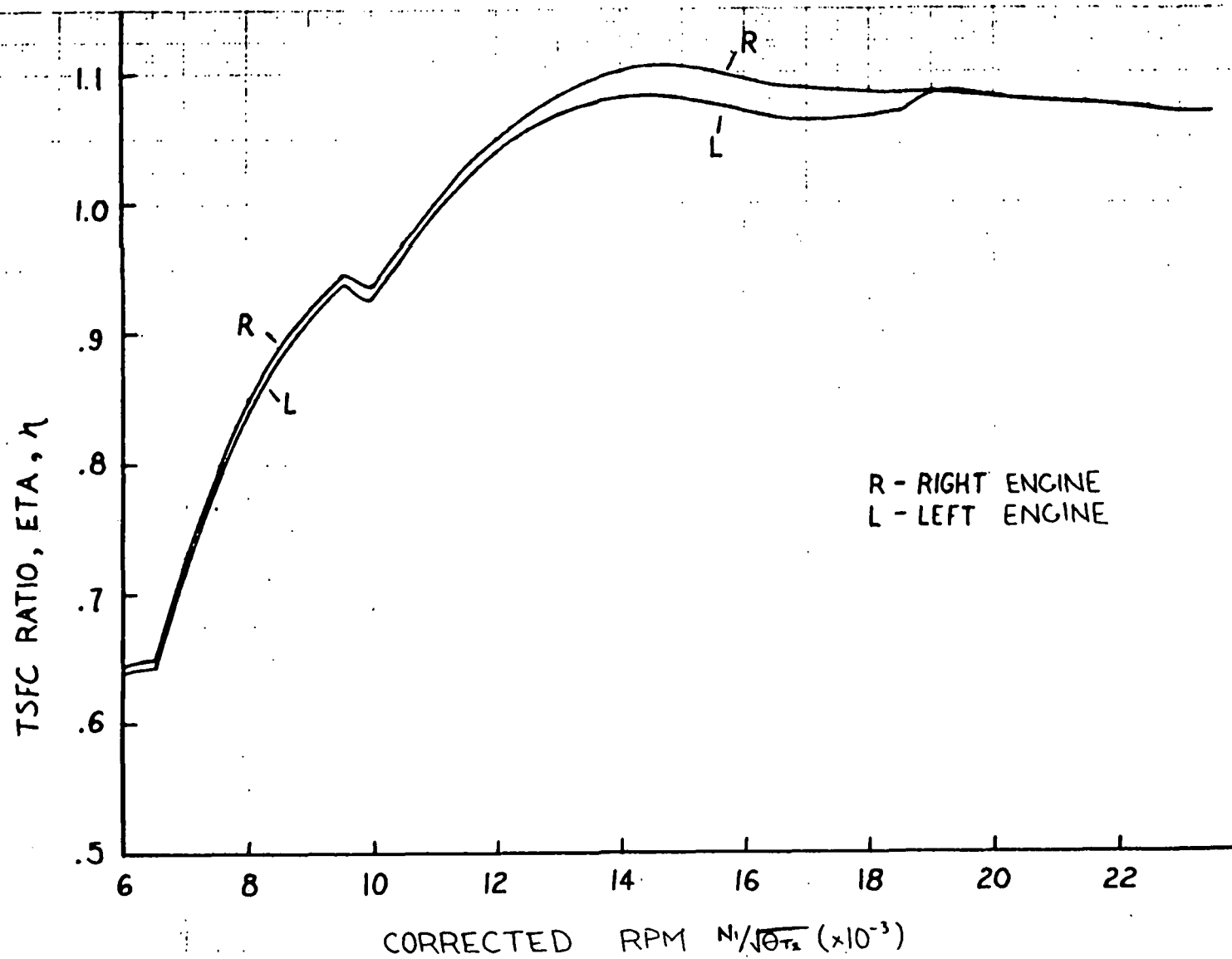


Figure 4.2: TSFC Correction Parameter, η

Figure 4.2 for each engine. Figures 4.3, 4.4 and 4.5 present the thrust run corrected thrust, fuel flow and airflow data points with the engine prediction deck curve superimposed for comparison. The airflow data in Figure 4.5 were calculated using Equation (20) and the η characteristics. The thrust run data clearly showed that each of the test engines had higher TSFC values than the deck predictions in the critical RPM range and followed the general trend of the deck in this range.

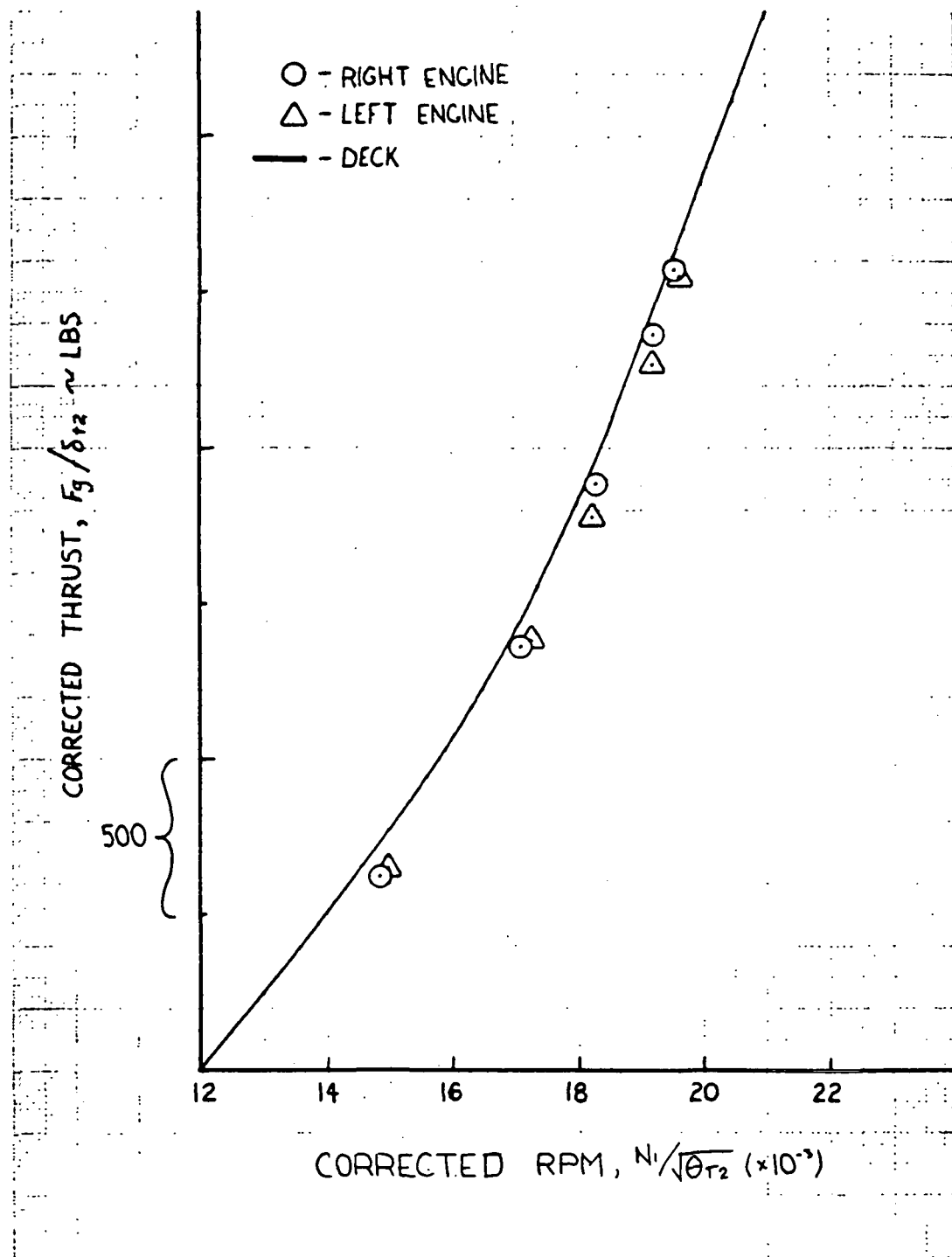


Figure 4.3: Thrust Run Corrected Thrust Data

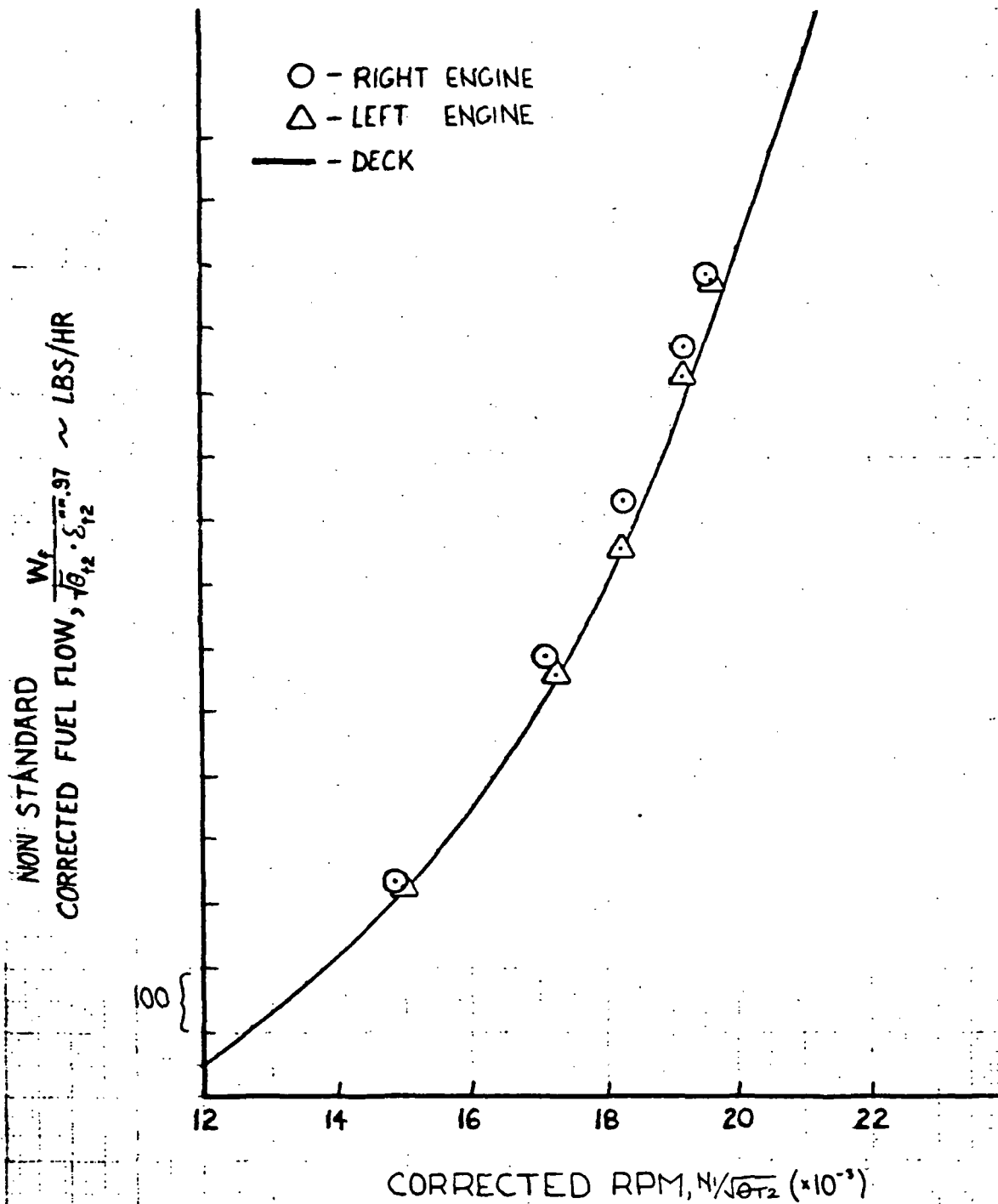


Figure 4.4: Thrust Run Nonstandard Corrected Fuel Flow Data

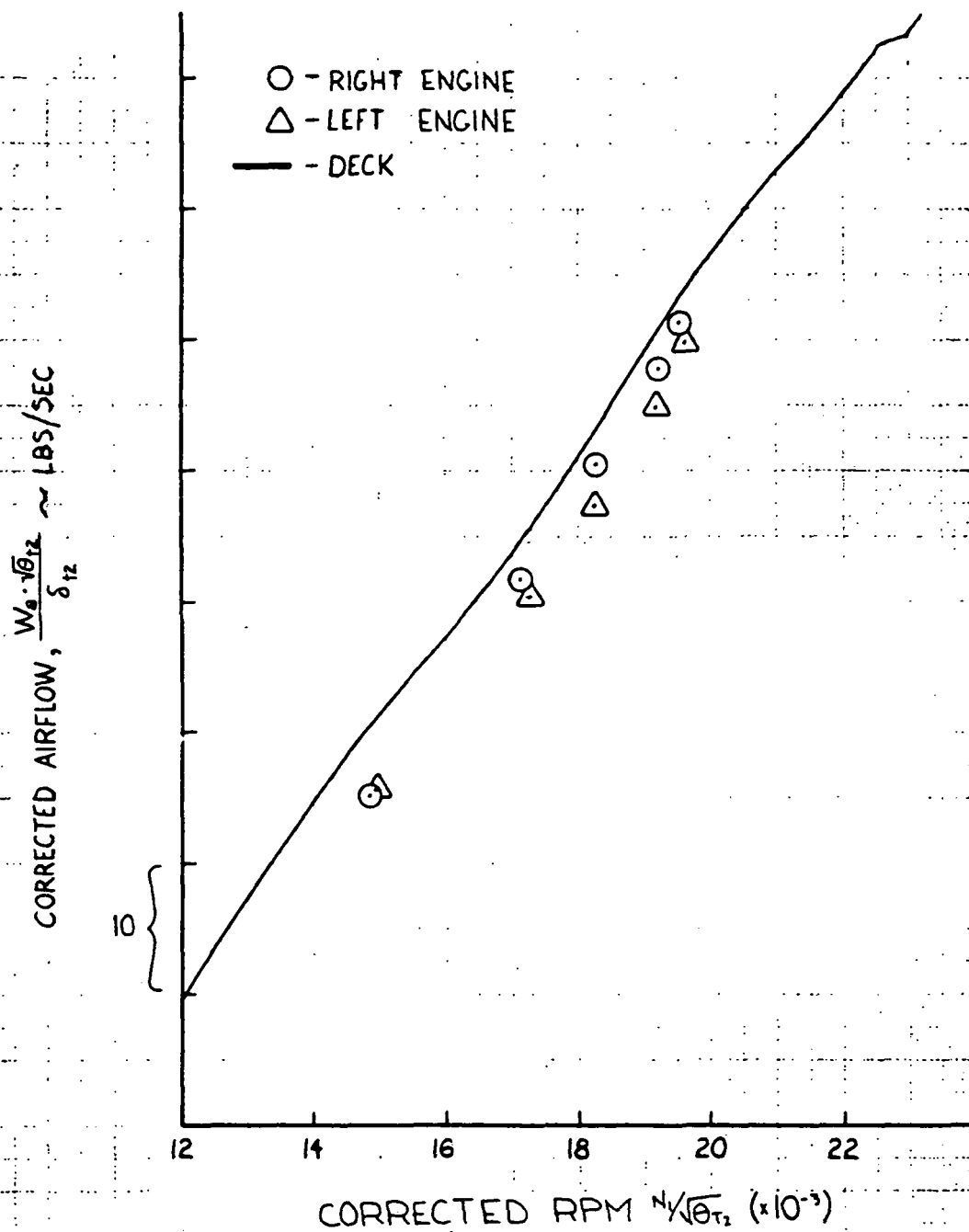


Figure 4.5: Thrust Run Corrected Airflow Data

4.1.3 Pitot Static System, Temperature Probe and Angle of Attack

Results of the pitot static system calibration are presented in Figure 4.6. The position error parameter $\Delta p_p/q_{cic}$ for each test point is plotted versus C_L along with a "best fit" fairing of the data. The maximum error due to data scatter was equivalent to ± 1.5 knots over the entire range. The curve was then input to the overall data reduction software to correct for position error.

The temperature probe recovery factor was defined from the slope of $1/T_{ic}$ versus $.2 M_{ic}^2/T_{ic}$ as outlined in Section 3.3.3. A linear curve fit was defined for two test altitudes as presented in Figure 4.7. A temperature probe recovery factor of .963 was determined for the temperature probe installation and input to the data reduction software.

Results of the angle of attack calibration are presented in Figure 4.8. A "best fit" fairing of the data is included. As seen from the figure, a gradually increasing upwash correction was needed with angle of attack up to approximately $4.5^\circ \alpha_{boom}$ and then remained approximately constant at the maximum value of $-.75^\circ$. All data fell within a scatter band of $\pm 1.5^\circ$. This correction was also incorporated in the data reduction software.

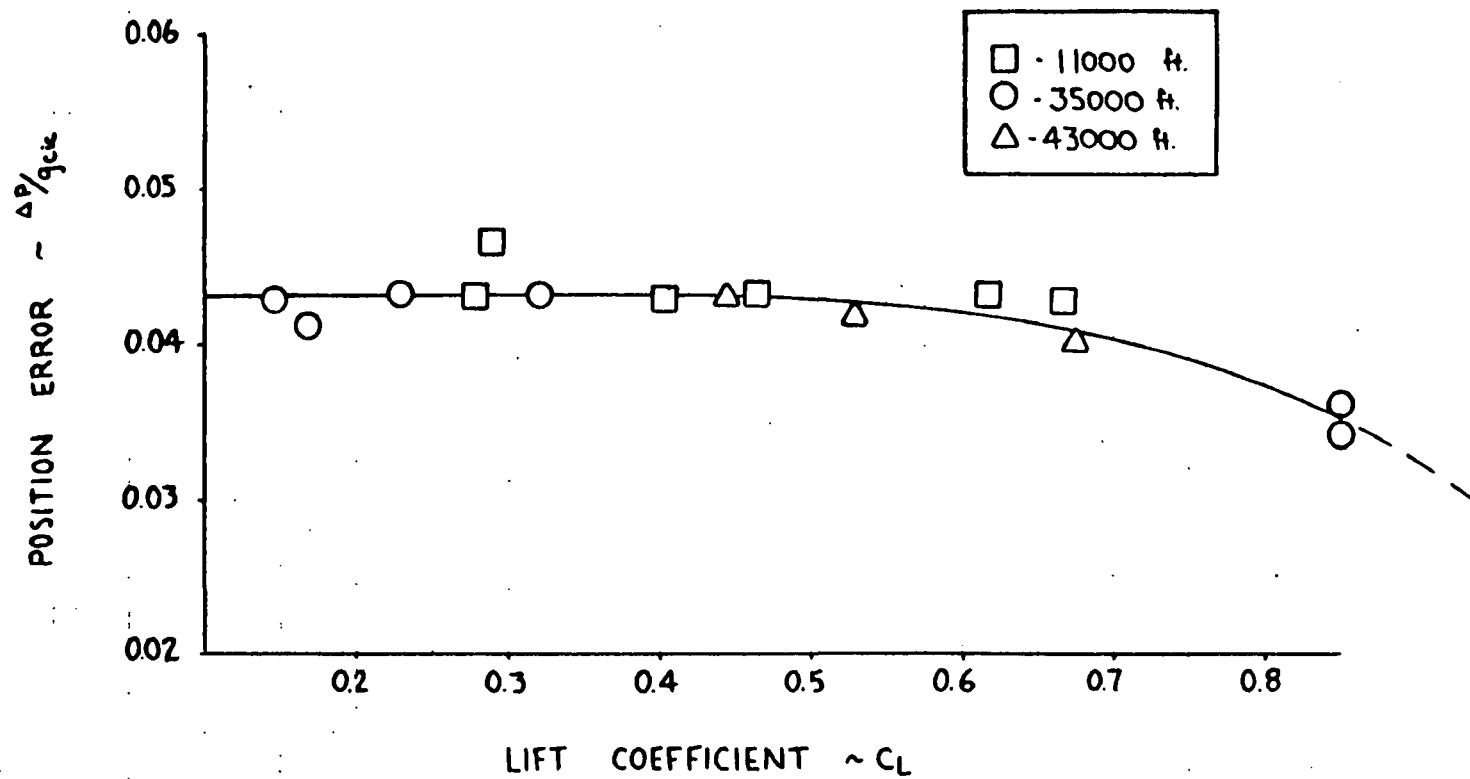


Figure 4.6: Pitot Static System Calibration

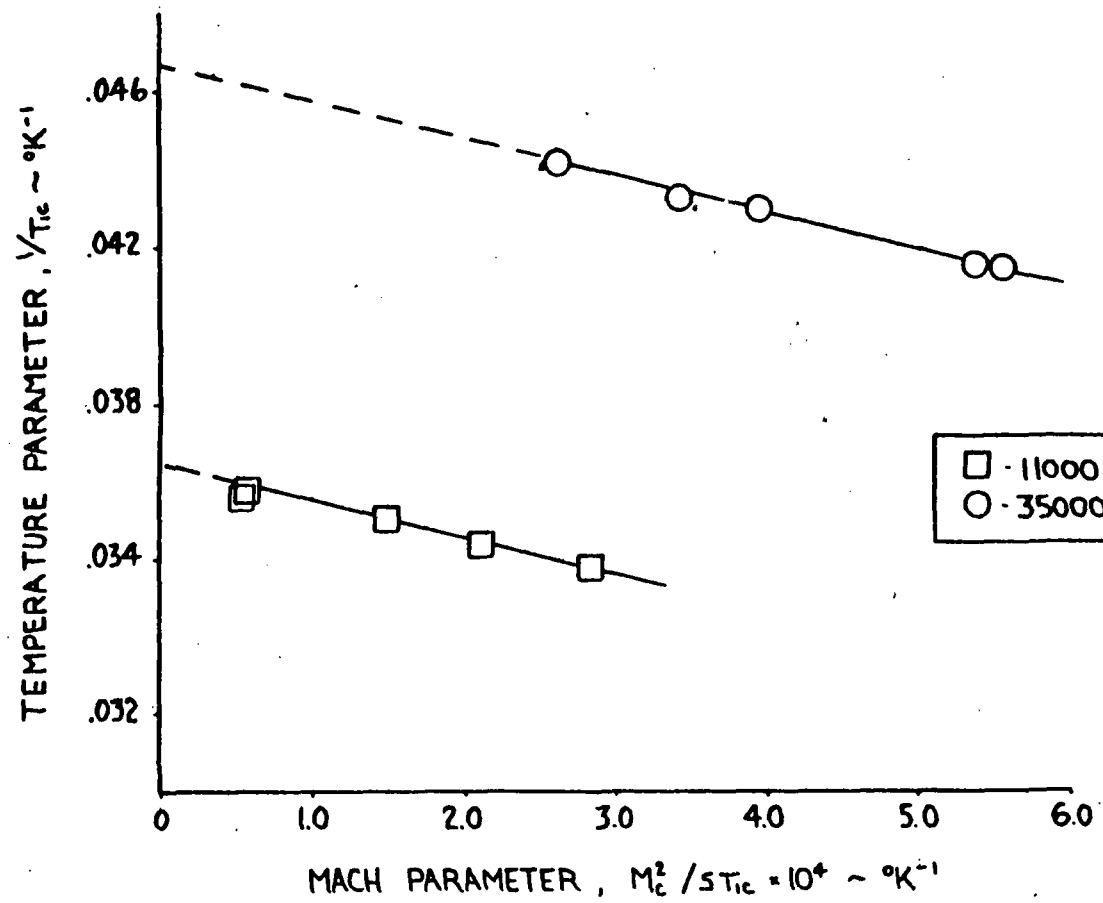


Figure 4.7: Temperature Probe Recovery Factor Calibration

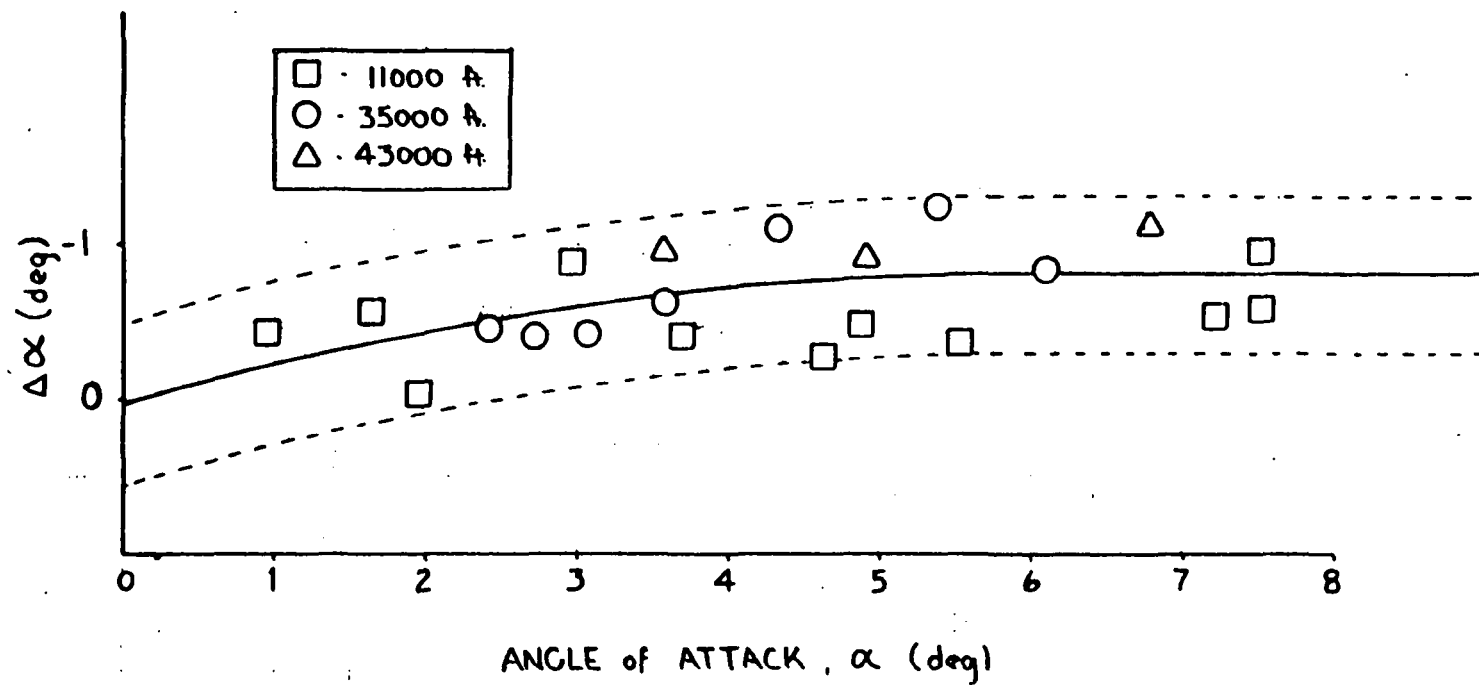


Figure 4.8: Angle of Attack Upwash Calibration

4.1.4 Weight and Balance

The c.g. travel as a function of aircraft weight is presented in Figure 4.9 for each of the test flights. The flights were designed to generally keep the c.g. location to within $\pm 1\%$ of the standard 25% MAC location during the data acquisition phases as seen from the c.g. travel diagram. The Lear 35 was an excellent aircraft for tightly controlling c.g., since the majority of fuel was located in two wing tanks with a centroid very close to the standard position.

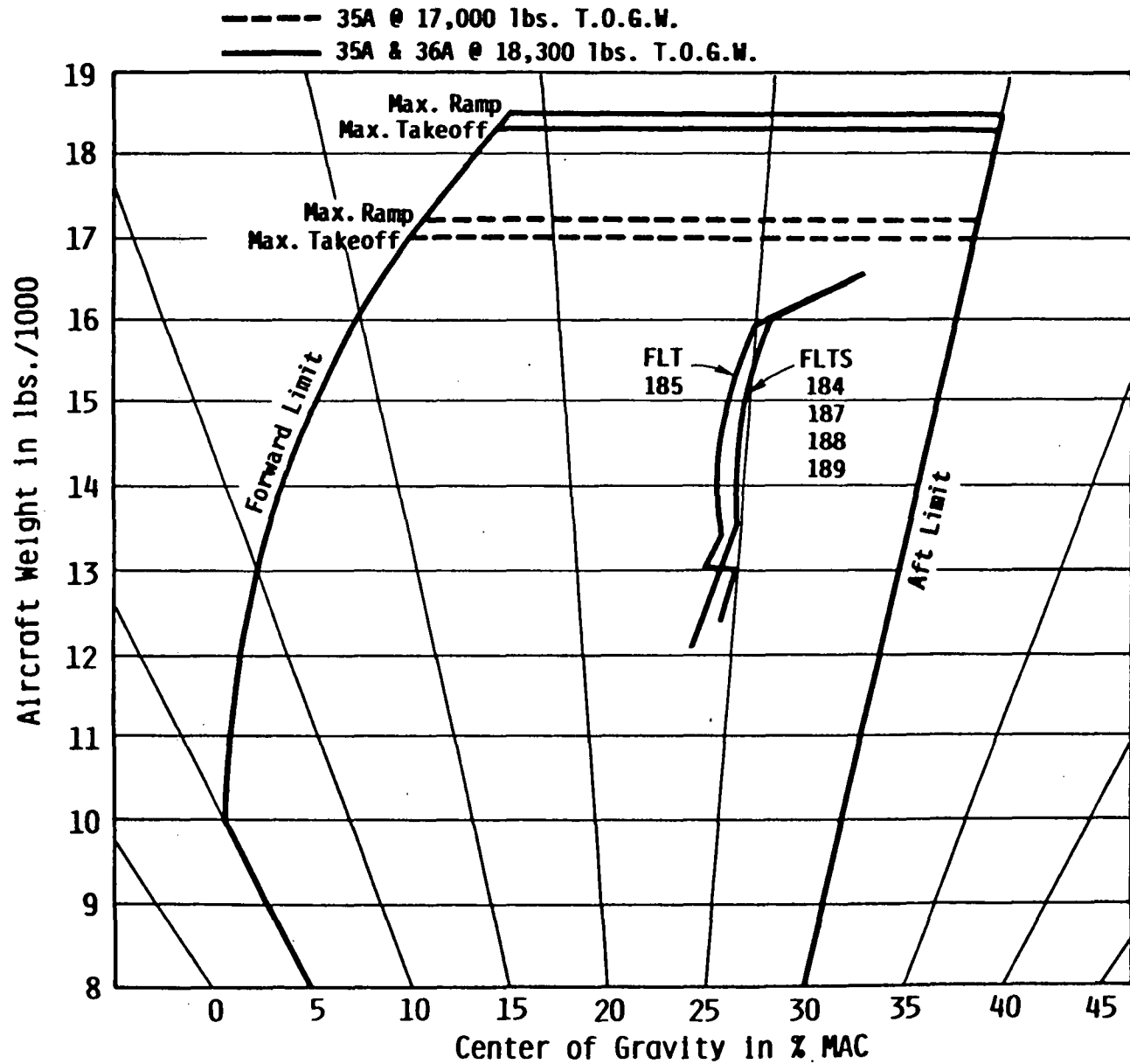


Figure 4.9: Aircraft C. G. Travel

4.2 BASELINE CHARACTERISTICS

4.2.1 Aerodynamic

4.2.1.1 C_{L_s} versus α

The C_{L_s} versus angle of attack characteristics fell into two distinct categories. Above .65 Mach, power effects were negligible; but distinct Mach effects were identified. A summary of the standardized lift coefficient characteristics in this high Mach region is presented in Figure 4.10, where an increase in Mach number resulted in an increase in C_{L_s} as well as the slope C_{L_α} . The extrapolated portions of each curve are identified by the uniform dashed lines as indicated. The actual data plots used to determine these characteristics are presented in Appendix F, where a scatter band of approximately $\pm .02$ was found for C_{L_s} . Several overlays of the data were evaluated before the final curves were defined. Below .65 Mach, Mach effects were negligible, but power effects were found as presented in Figure 4.11. At power settings above 60%, a small but significant increase in C_{L_s} was observed. At 70% power, approximately a .01 increase in C_{L_s} resulted throughout the angle of attack range when compared to the data below the 60% power curve. As power was increased to 75% and above an additional increase of approximately .01 over the 70% curve was found. The power effects on C_{L_s} are thought to be directly related to the close proximity of the engine inlets above the inboard upper wing surface. Either of two effects could be present. First, the flow field around the wing/nacelle is fairly normal at high engine speed; however, at low engine speed, inlet spillage reduces the

lift over the inboard section of the wing by retarding the flow. Second, above 60% power, the increased airflow through the engine may alter the flow field in the engine/nacelle wing root area such that the overall circulation around the inboard wing section is increased, resulting in a corresponding increase in lift. This increase in lift did not continue with increasing power settings above 75% but rather remained constant at approximately the 75% value. The increase in airflow through the engine with increasing power may produce an increase in lift on the forward portion of the inner wing but could also result in flow starvation and separation near the trailing edge, producing an offsetting effect. Obviously, a flow field survey in the engine nacelle/wing root area is needed to help explain these power effects. Flow tufting in this area would be an excellent first step in understanding the power effects observed and could easily be accomplished concurrently with the quasi steady-state maneuvers used for performance modeling.

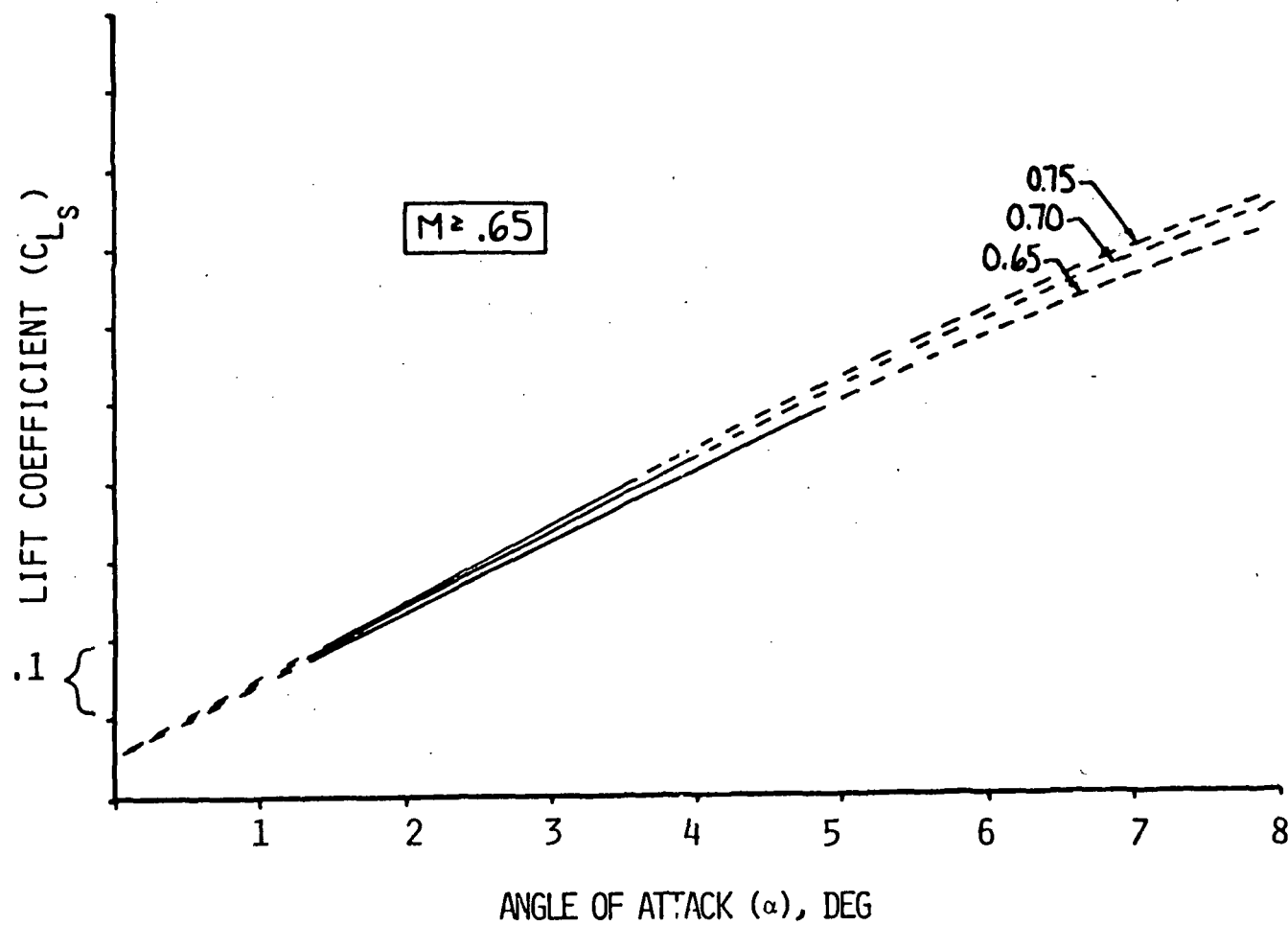


Figure 4.10: Lift Coefficient Characteristics, $M \geq .65$

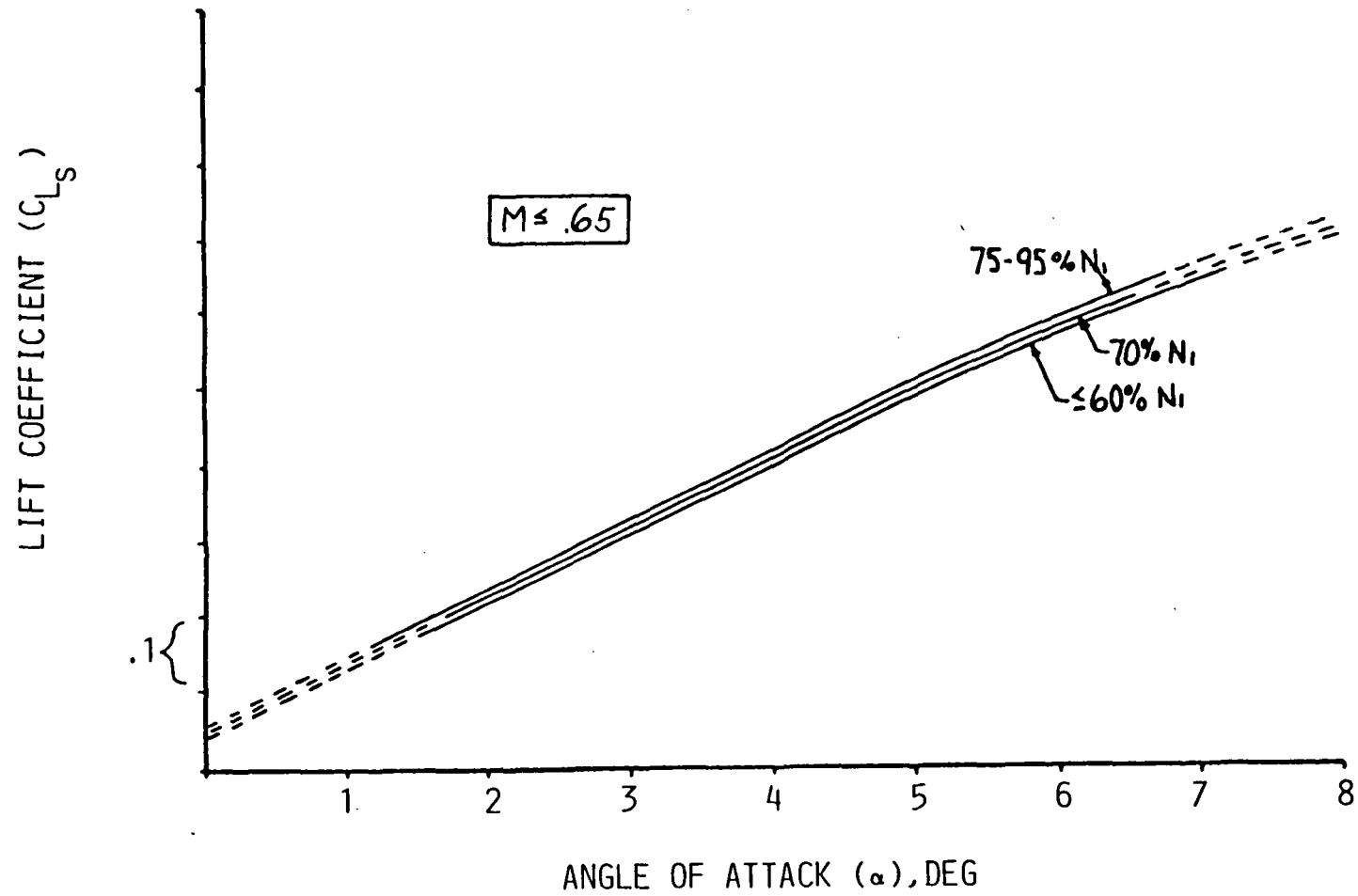


Figure 4.11: Lift Coefficient Characteristics, $M \leq .65$

4.2.1.2 C_{D_s} versus α

As with lift coefficient, the C_{D_s} versus angle-of-attack characteristics fell into two distinct and consistent categories. For .6 Mach and above, power effects were negligible but Mach effects were identified. A summary of the standardized drag coefficient characteristics in the high Mach region is presented in Figure 4.12 where an increase in Mach number generally resulted in an increase in C_{D_s} for a given angle of attack. The data plots used to determine these characteristics are presented in Appendix F. As shown in Figure 4.12, the largest increase in C_{D_s} with Mach number was projected above four degrees angle of attack. For .55 Mach and below, Mach effects were not significant but power effects were found throughout the Mach range. As presented in Figures 4.13 and 4.14, C_{D_s} generally decreased as power decreased, with approximately a 45 drag count band between 90% and 50% power in the mid angle-of-attack region. The 95% power curve intersected and crossed over the 90% curve at two locations and dropped below the 90% curve in the mid angle-of-attack region as shown. As with the lift coefficient curves, the complex flow interaction in the nacelle/wing root area must be analyzed to understand these characteristics. Normally it would be expected that lower drag would occur at higher power settings due to reduced inlet spillage. This trend is seen in the mid angle-of-attack region for 90% and 95% power (Figure 4.13). However, this is obviously not the only factor affecting the drag. Another possible interaction may be an increased pressure on the aft facing wing and fuselage surfaces (a drag reduction) resulting from

increased inlet spillage at the lower power settings. The close proximity of the engine nacelle to these surfaces make this occurrence quite feasible. In Figure 4.13, the crossover experienced by the 95% curve in the higher angle-of-attack region (lower speed) indicates that the increased pressure phenomenon may become predominant as the aft facing wing and fuselage surfaces increase with angle of attack and as propagation of the inlet spillage air also increases with lower speed. Another contributing factor may be increasing flow starvation and separation near the trailing edge of the wing with increasing power, as discussed in the lift section. This would account for the increased drag observed with increased power. The absence of power effects on drag at .6 Mach and above is probably due to the low propagation of inlet spillage air at higher speeds. Again, a flow field survey in the wing root/nacelle area would help clarify the causes of the identified drag characteristics.

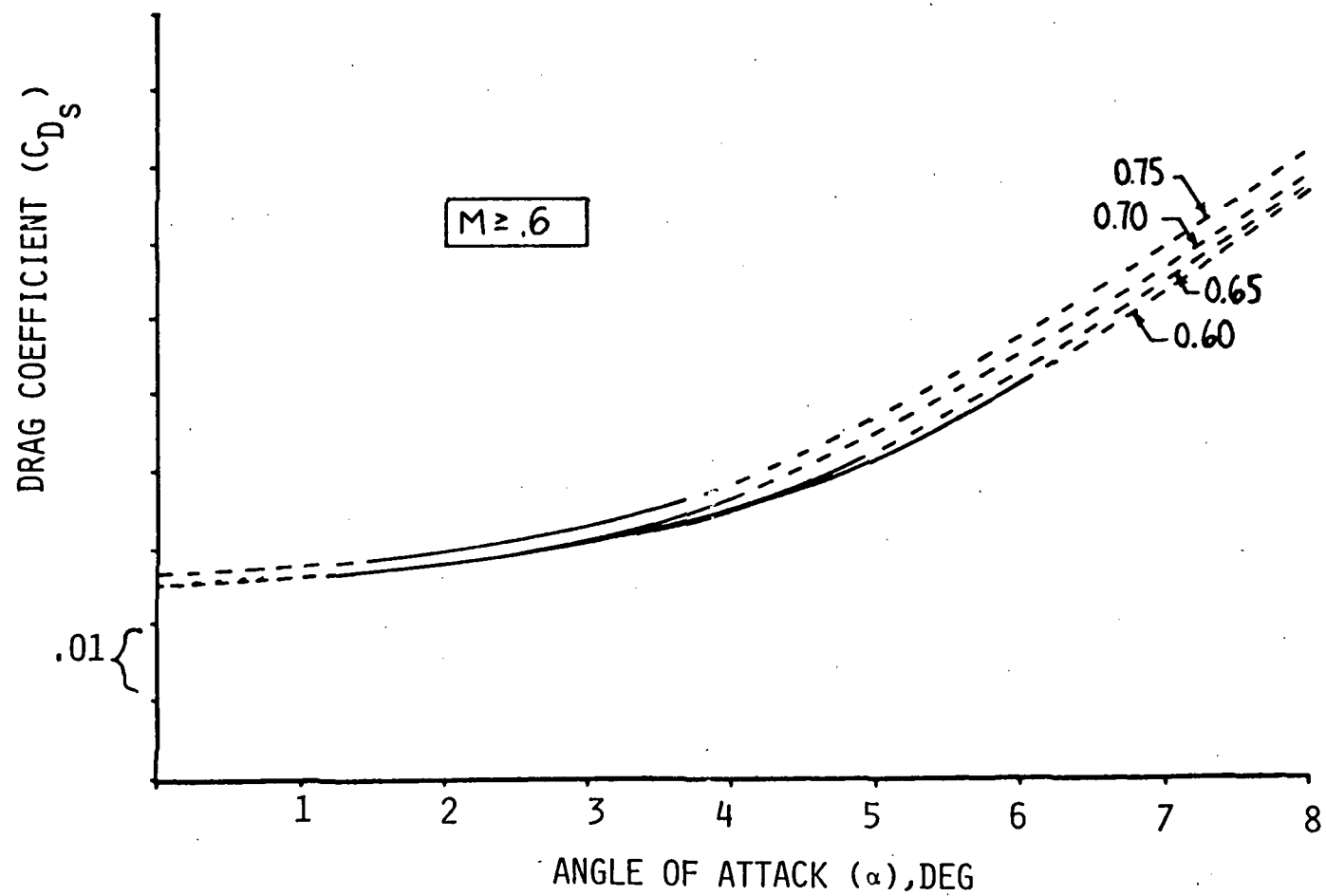


Figure 4.12: Drag Coefficient Characteristics, $M \geq .6$

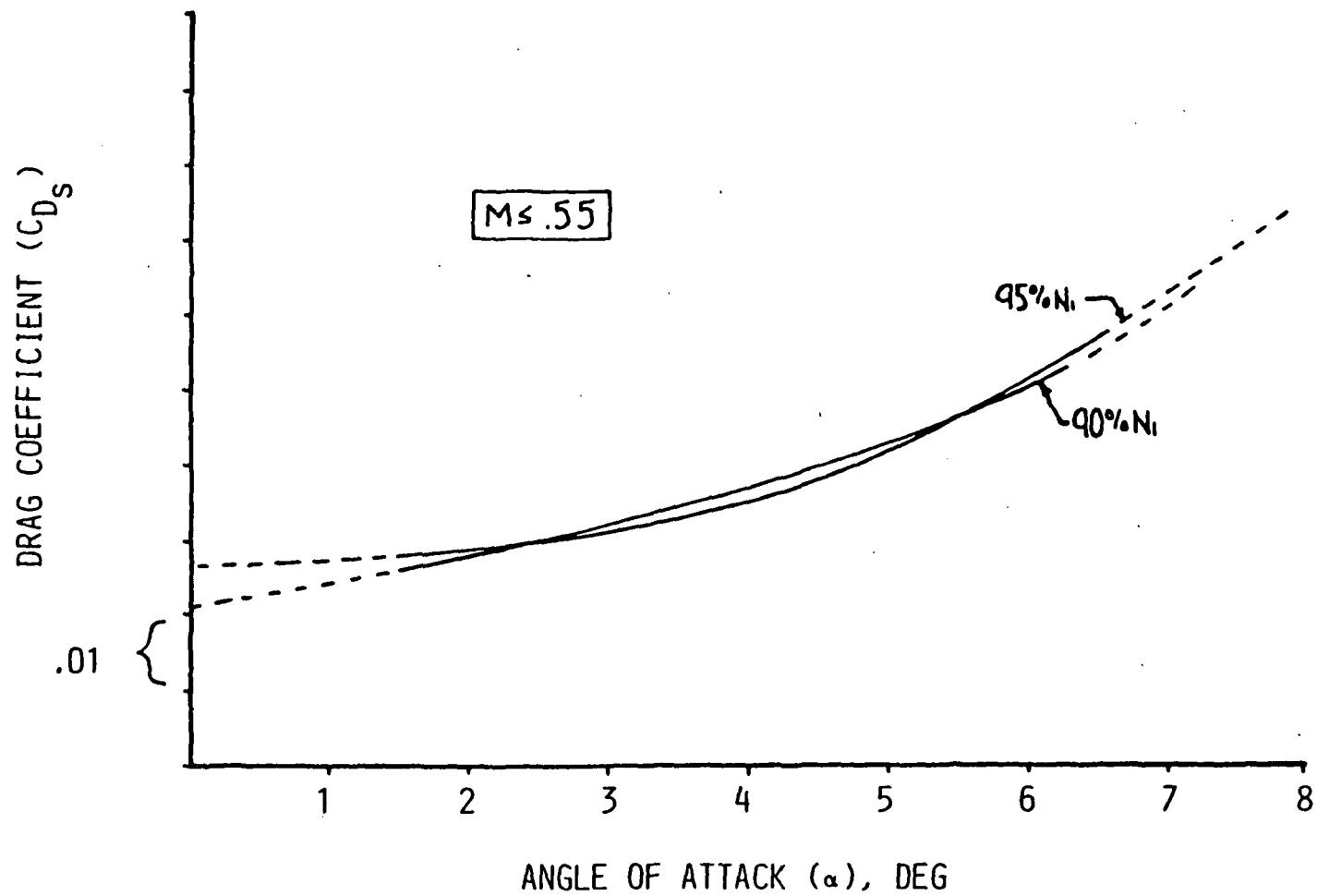


Figure 4.13: Drag Coefficient Characteristics, $M \leq .55$,
90 and 95% N_1

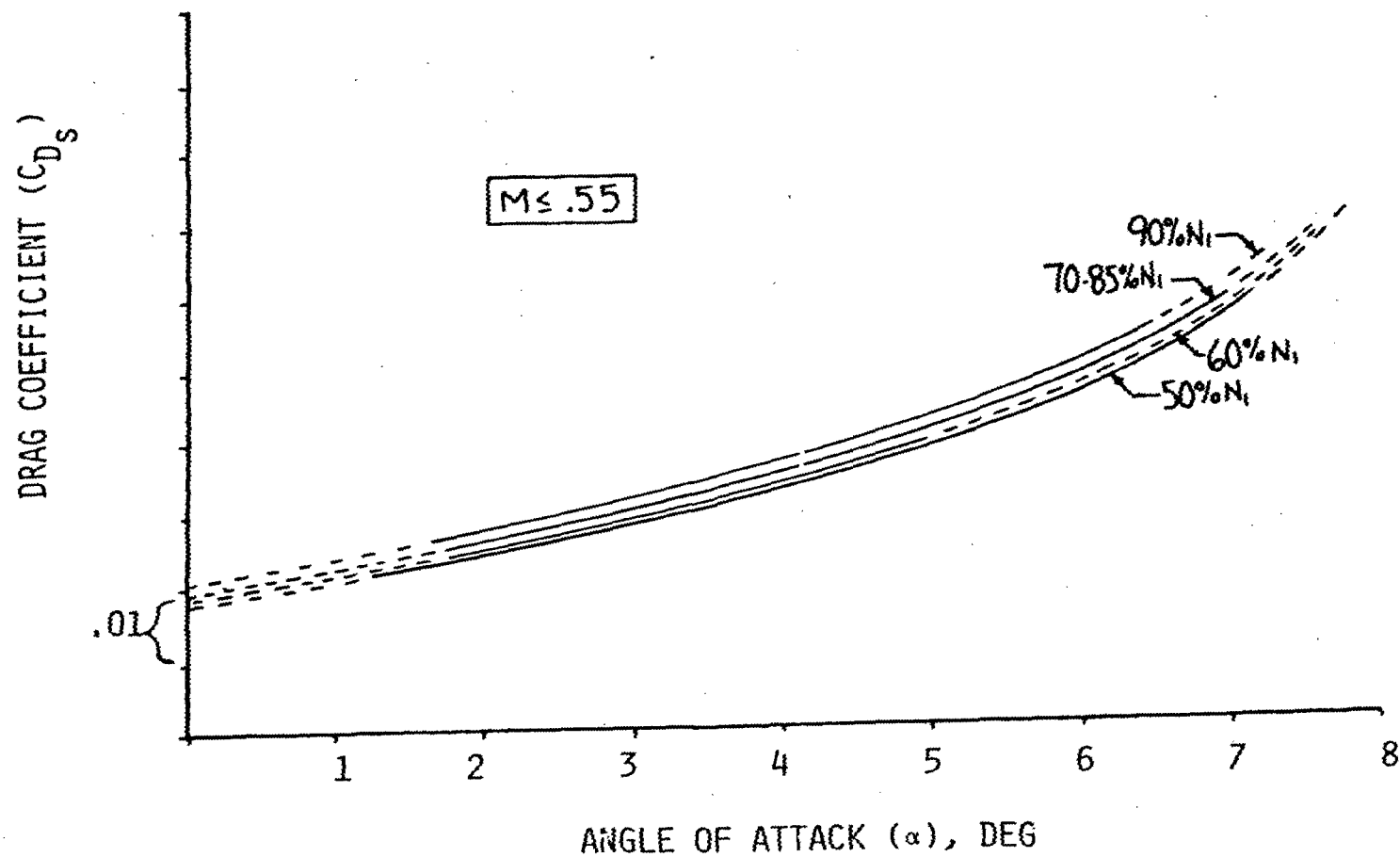


Figure 4.14: Drag Coefficient Characteristics, $M \leq .55$,
50 to 90% N_1

4.2.2 Engine

4.2.2.1 F_g/δ_{t_2} versus $N_1/\sqrt{\theta}_{t_2}$

Corrected gross thrust characteristics as a function of corrected RPM are presented in Figure 4.15 for the .55 Mach case. The engine prediction deck curve without the η or in-flight fuel flow correction applied is also shown for reference. The general trends of the prediction deck were found in the data with the absolute value of corrected thrust approximately 500 lbs below deck predictions. The lower in-flight thrust values were consistent with the thrust run results. A significant amount of scatter was found in the data as shown on the corrected thrust plots. This degree of scatter was not considered typical for the in-flight thrust prediction technique developed in the program based on the results of a similar flight test effort with the Lear 55 aircraft. Results of this effort are presented in Appendix G and show that a considerably tighter grouping of data can normally be expected with the method. The reason for the increased scatter band with the Lear 35 data has not been totally explained. Possible explanations include the lack of a thorough thrust run as accomplished on the Lear 55 (Appendix E) and small instrumentation errors during selected flights. In defining the engine curves, a significant attempt was made to keep the corrected thrust and corrected airflow curves consistent relative to the deviation from the prediction deck value. The remaining Lear 35 corrected gross thrust characteristics for .3 through .75 Mach are presented in Appendix H.

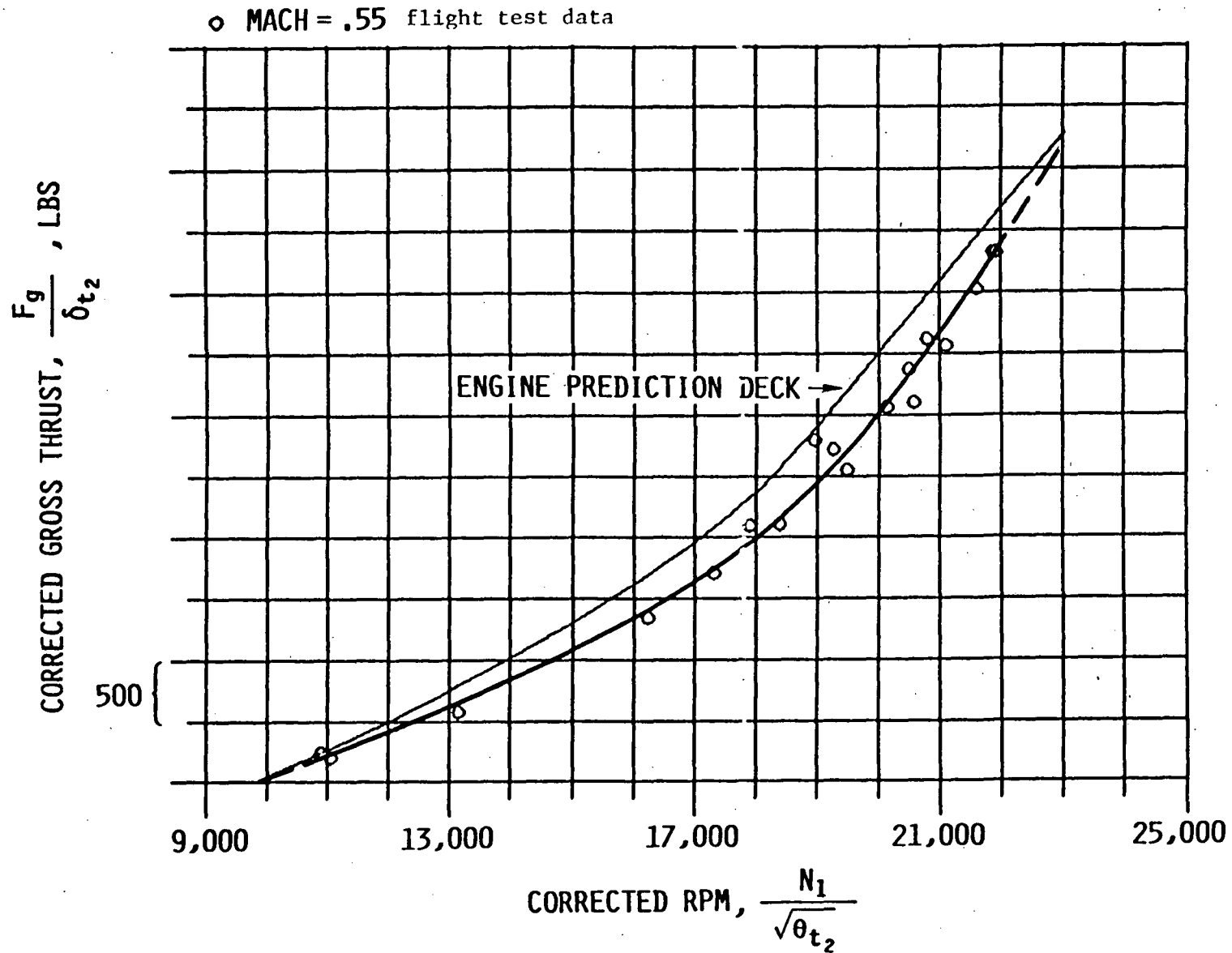


Figure 4.15: Corrected Gross Thrust Characteristics, M = .55

4.2.2.2 $W_f / \sqrt{\theta} t_2 \delta t_2^N$ versus $N_1 / \sqrt{\theta} t_2$

Nonstandard corrected fuel flow characteristics as a function of corrected RPM are presented in Figure 4.16 for the .55 Mach case. As with corrected thrust, the engine prediction deck curve is also shown for reference. The fuel flow data fell very close to the deck predictions with the maximum scatter observed approximately ± 100 lbs/hr about the final curves. Results of the Lear 55 (Appendix G) showed that this scatter was higher than should normally be expected. The remaining Lear 35 nonstandard corrected fuel flow characteristics for .3 through .75 Mach are presented in Appendix H.

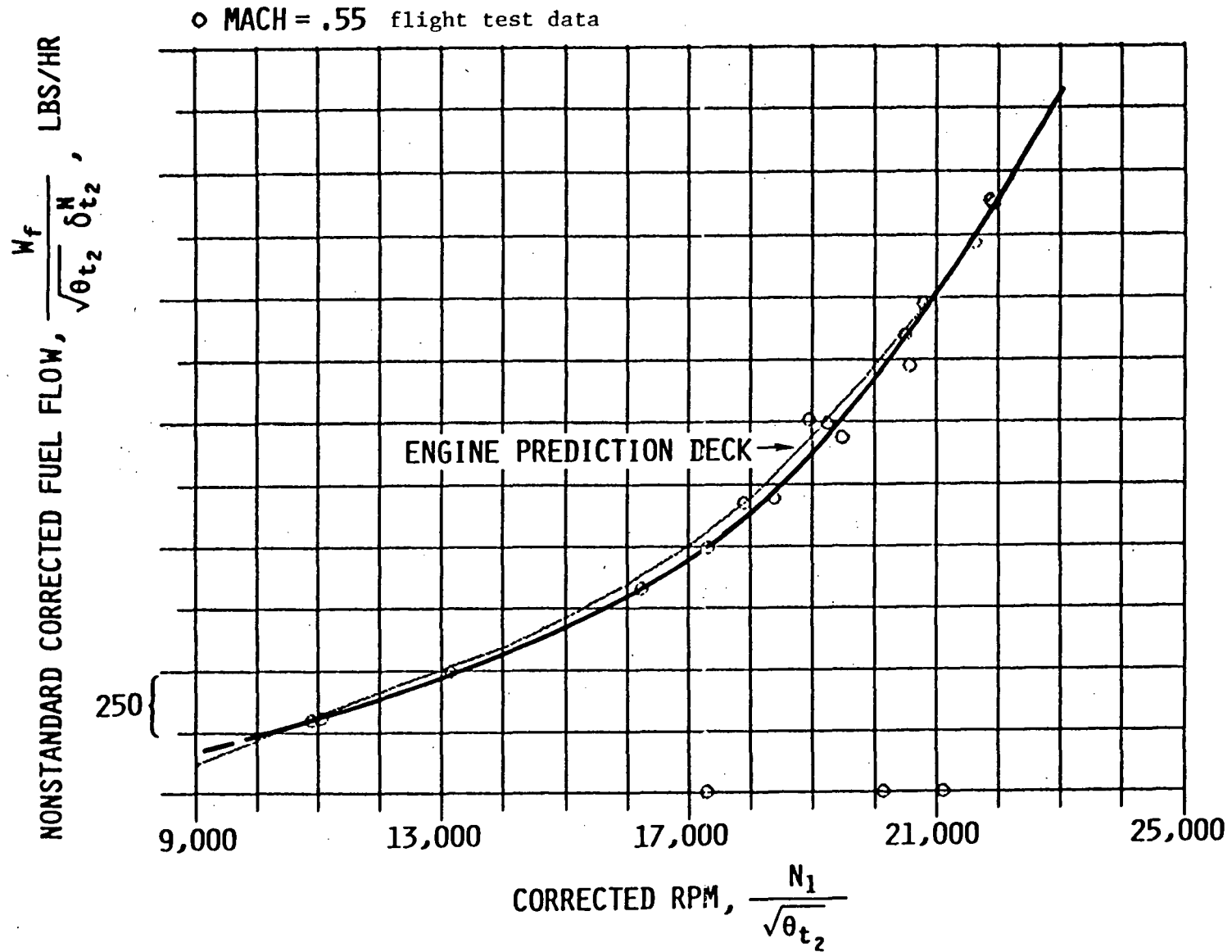


Figure 4.16: Nonstandard Corrected Fuel Flow Characteristics, M = .55

4.2.2.3 $W_a \sqrt{\theta_{t_2}} / \delta_{t_2}$ versus $N_1 / \sqrt{\theta_{t_2}}$

Corrected airflow characteristics as a function of corrected RPM are presented in Figure 4.17 for the .55 Mach case. Consistent with thrust, the airflow data generally fell below the deck predictions with a maximum scatter band of approximately +20, -5 lbs/sec relative to the faired curves. The faired curves were placed through the lower grouping of data for consistency with the thrust run and thrust data. Again the Lear 55 data in Appendix G indicated that considerably lower scatter would normally be expected. The remaining Lear 35 corrected airflow characteristics for .3 through .75 Mach are presented in Appendix H.

○ MACH = .55 flight test data

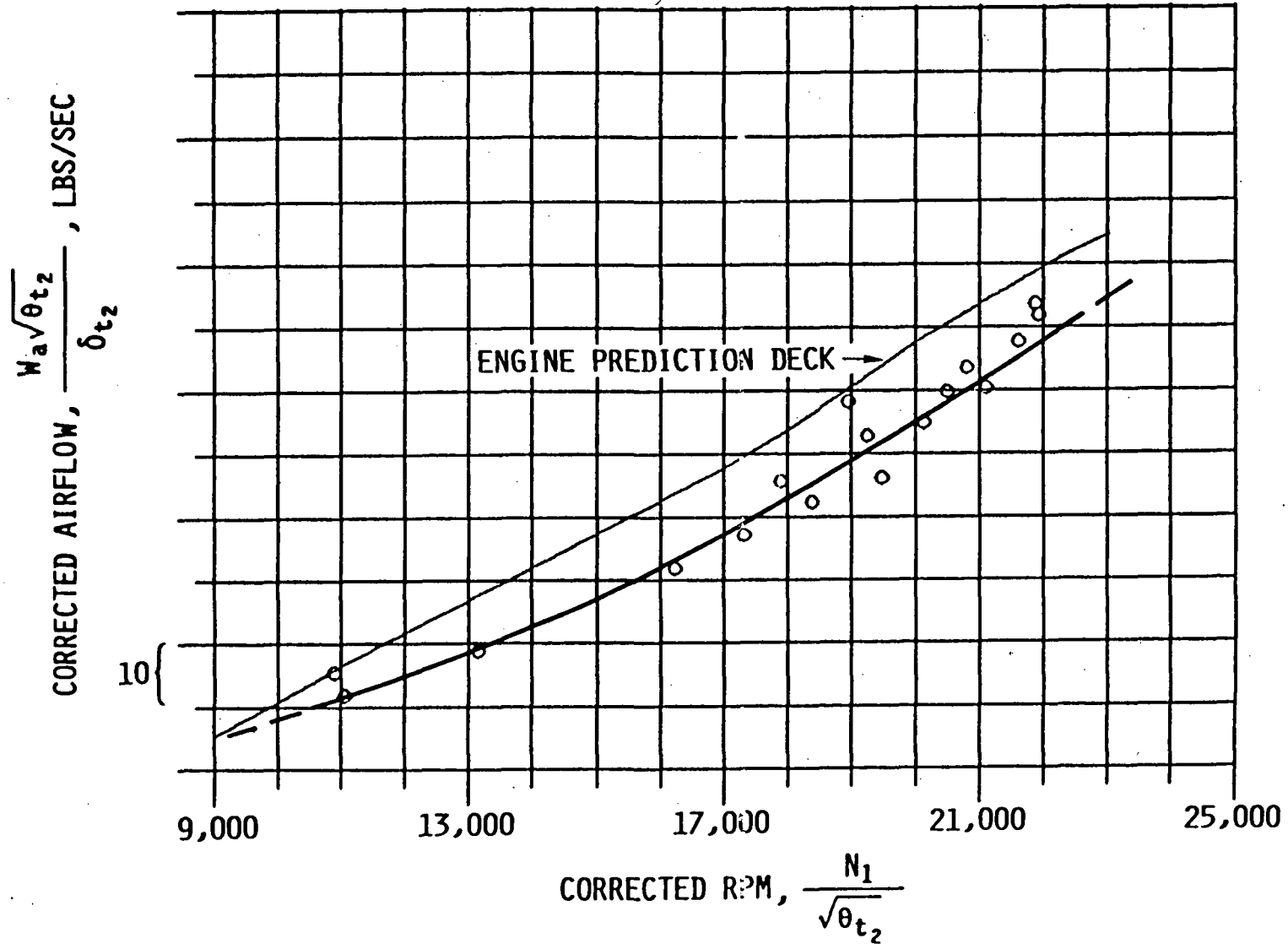


Figure 4.17: Corrected Airflow Characteristics, M = .55

4.3 CONVENTIONAL DATA REDUCTION

4.3.1 Stabilized Points

A total of twenty-one stabilized points were flown at four target values of W/δ (22,000, 40,000, 60,000 and 80,000 lbs) as discussed in Section 3.4.2. Table 12 presents a summary of the stabilized point data. Range factor and specific range were standardized using the δ_{std} and θ_{std} values presented in Table 13 and Equations (22) and (23). The nominal standard atmosphere altitude corresponding to δ_{std} and θ_{std} in Table 13 was selected based on an average of the stabilized point data for each W/δ condition. All of the actual test W/δ values were within ± 1 percent of the ITERATE W/δ values shown in Table 13 which were selected for use in the cruise performance modeling program ITERATE as discussed in Sections 3.2.4.1 and 4.4.1. Stabilized point corrected RPM, standardized range factor, standardized specific range and specific range parameter data are plotted versus Mach number in Section 4.4.1 (Figures 4.23-4.38). The data generally show the anticipated characteristics for each of these parameters.

Table 12: Stable Point Summary

Condition	Target W/ δ (lbs)	Test W/ δ (lbs)	Mach No.	Test δ	Test $N_1/\sqrt{\theta} t_2$ (RPM)	Test Range Factor (NM)	Std Range Factor (NM)	Test Specific Range (NM/lb)	Std Specific Range (NM/lb)	Specific Range Parameter (NM/lb)
1	22000	21498	.595	.722	18292	2808	2914	.181	.1879	.1307
2	22000	21240	.537	.715	17350	3003	3086	.1979	.2034	.1414
3	22000	21167	.477	.696	16347	3195	3195	.217	.217	.151
4	22000	21070	.422	.685	15335	3318	3267	.23	.226	.1574
5	22000	21240	.264	.663	13950	2613	2490	.1857	.177	.1231
6	40000	40100	.42	.359	16870	4200	3976	.291	.2755	.1045
7	40000	39600	.548	.372	17890	4735	4645	.321	.3149	.1196
8	40000	39747	.699	.387	19868	3990	4072	.2591	.2643	.1004
9	40000	40225	.755	.389	20920	3502	3592	.2241	.23	.0871
10	60000	59880	.473	.249	19060	4970	5016	.333	.336	.083
11	60000	60025	.499	.2397	19240	5050	4907	.354	.344	.0841
12	60000	59500	.64	.254	19475	5680	5848	.375	.386	.0955
13	60000	59600	.652	.247	19600	5635	5642	.3825	.3829	.9046
14	60000	59600	.72	.223	20550	5245	4742	.3775	.3412	.0842
15	60000	59750	.732	.257	20430	5200	5417	.3385	.3527	.0873
16	60000	60075	.734	.26	20400	5220	5502	.3343	.3523	.086
17	60000	59660	.785	.226	21475	4435	4063	.3288	.3012	.0744
18	80000	80025	.537	.182	21325	4920	4723	.3375	.324	.0615
19	80000	79230	.687	.186	20945	6000	5886	.4075	.4000	.0758
20	80000	80075	.723	.187	21215	5950	5869	.3975	.3920	.0741
21	80000	78900	.743	.195	21500	5680	5842	.3687	.3792	.0718

Table 13: ITERATE Stable Point Prediction Cases

<u>Case</u>	<u>Target W/δ (lbs)</u>	<u>"ITERATE" W/δ (lbs)</u>	<u>Nominal Altitude (ft)</u>	<u>δ std</u>	<u>θ std</u>
1	22000	21284	9700	.6957	.9333
2	40000	39912	24500	.3792	.8316
3	60000	59787	34000	.2467	.7662
4	80000	79487	39500	.1896	.7519

4.3.2 Push-Pull Maneuvers

Aerodynamic data from pull-up, push-over, pull-up (push-pull) maneuvers were compared to those obtained from accel/decel maneuvers to evaluate the correlation between techniques. Lift coefficient data for two representative maneuvers are presented in Figures 4.18 through 4.19, and drag coefficient data are presented in Figures 4.20 through 4.21. For each figure, the appropriate family of baseline curves, as determined from accel/decel maneuvers, is presented for reference. Data points from the push-pull maneuver are shown with symbols. The lift coefficient push-pull data crossed over the baseline curves with a point of intersection at approximately the one g condition. The drag coefficient push-pull data generally fell within 10 to 15 drag counts of the applicable baseline curve (solid line) and, in some cases, indicated that the extrapolated portion of the baseline curve may have been incorrect. The crossover experienced by the lift coefficient data was analyzed and theorized to be primarily due to bending of the nose boom with normal load factor. A correction to angle of attack was made for angular rate as discussed in Section 3.2.3.2, but a correction was not made for boom bending. For load factors greater than one, bending of the nose boom will result in an angle of attack reading smaller than the actual angle of attack; and a positive correction is necessary. A negative correction is needed for a load factor less than one. This correction would tend to bring the lift coefficient push-pull data in line with the baseline curves, since the point of intersection occurred

at approximately the one g condition. The push-pull drag coefficient data would also be slightly shifted with this correction but would continue to fall generally within 10 to 15 drag counts of the baseline curves due to the relatively small magnitude of the C_{D_s} versus α slope. Unfortunately, a boom bending calibration was not made when the aircraft was configured for the flight test program. An estimate of the boom bending angle of attack correction, $\Delta\alpha_{\text{boom bending}}$, as a function of normal load factor was made by analyzing the physical characteristics and configuration of the nose boom. Figure 4.22 presents this estimate along with data points from the two push-pull maneuvers showing the $\Delta\alpha_{\text{boom bending}}$ needed to bring the push-pull C_{L_s} data back in line with the baseline curves. The agreement between the estimated correction and these data is relatively close; and, as a result, the lack of agreement between the push-pull data and the baseline curves was primarily believed to be caused by the lack of a boom bending correction for angle of attack.

The results definitely showed that the push-pull maneuver could be very useful to any performance definition flight test program for an aircraft with negligible flexibility effects. The appropriate corrections to angle of attack must be defined, such as boom bending and angular rate. The push-pull maneuver can be used to efficiently extend the angle of attack range during definition of selected baseline aerodynamic characteristics and thus minimize the uncertainty of extrapolating baseline curves. It is not well suited to initial identification of power and Mach effects on lift and drag character-

istics, since the push-pull begins with a stable condition (at an appropriate power setting) and then experiences a limited Mach variation during the maneuver. It would be difficult, for example, to define the baseline aerodynamic characteristics for a high Mach, low power condition from a push-pull maneuver. The push-pull maneuver can definitely complement and serve as a cross-check on data obtained from accels and decels. In fact, the push-pull may be used in place of selected accels/decelers once the power and Mach effects have been identified. When using the push-pull, the accuracy of the angle of attack corrections should be checked by comparing data from both types of maneuvers across the angle of attack range.

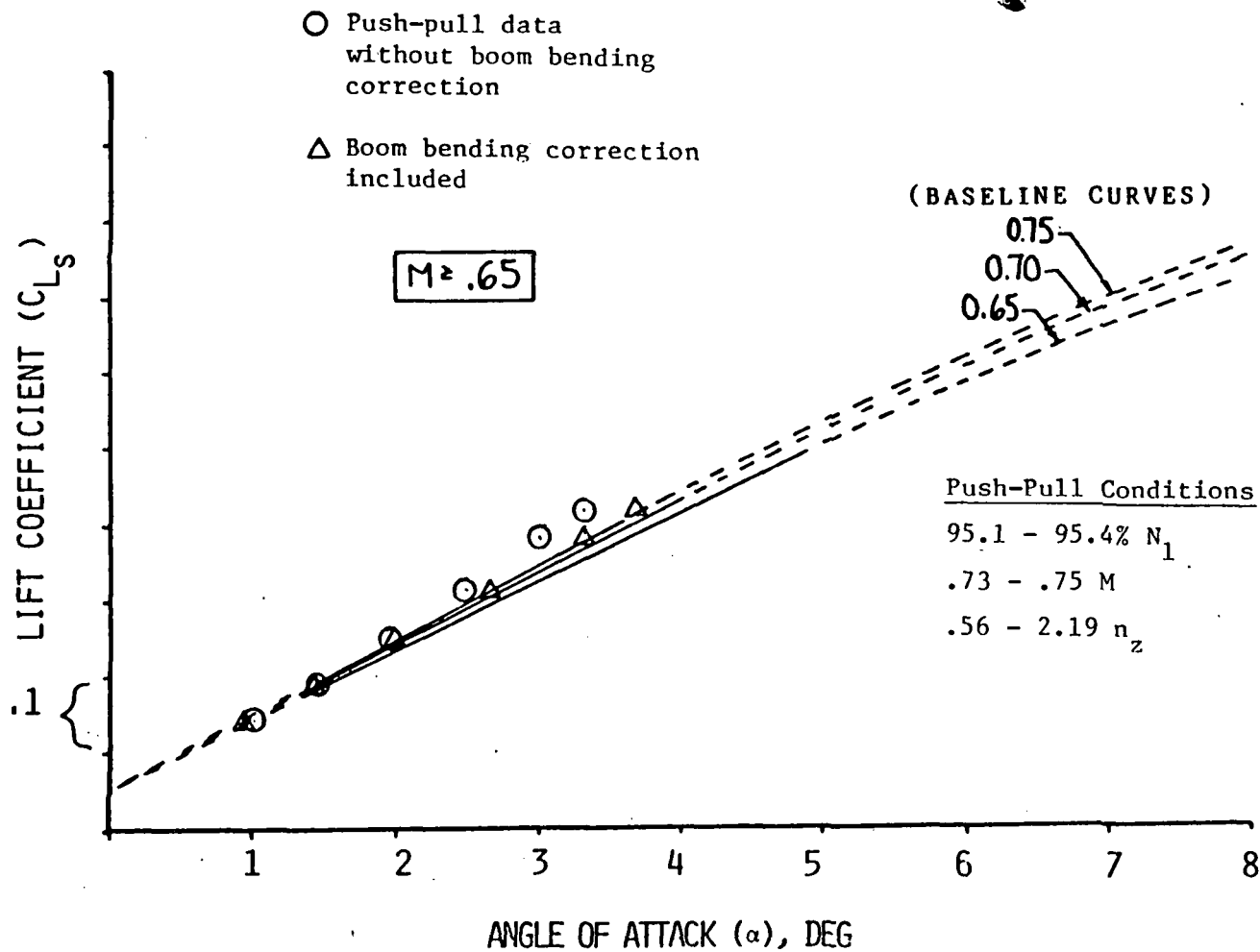


Figure 4.18: Lift Coefficient Push-Pull Data,
Flight 185, Run 10

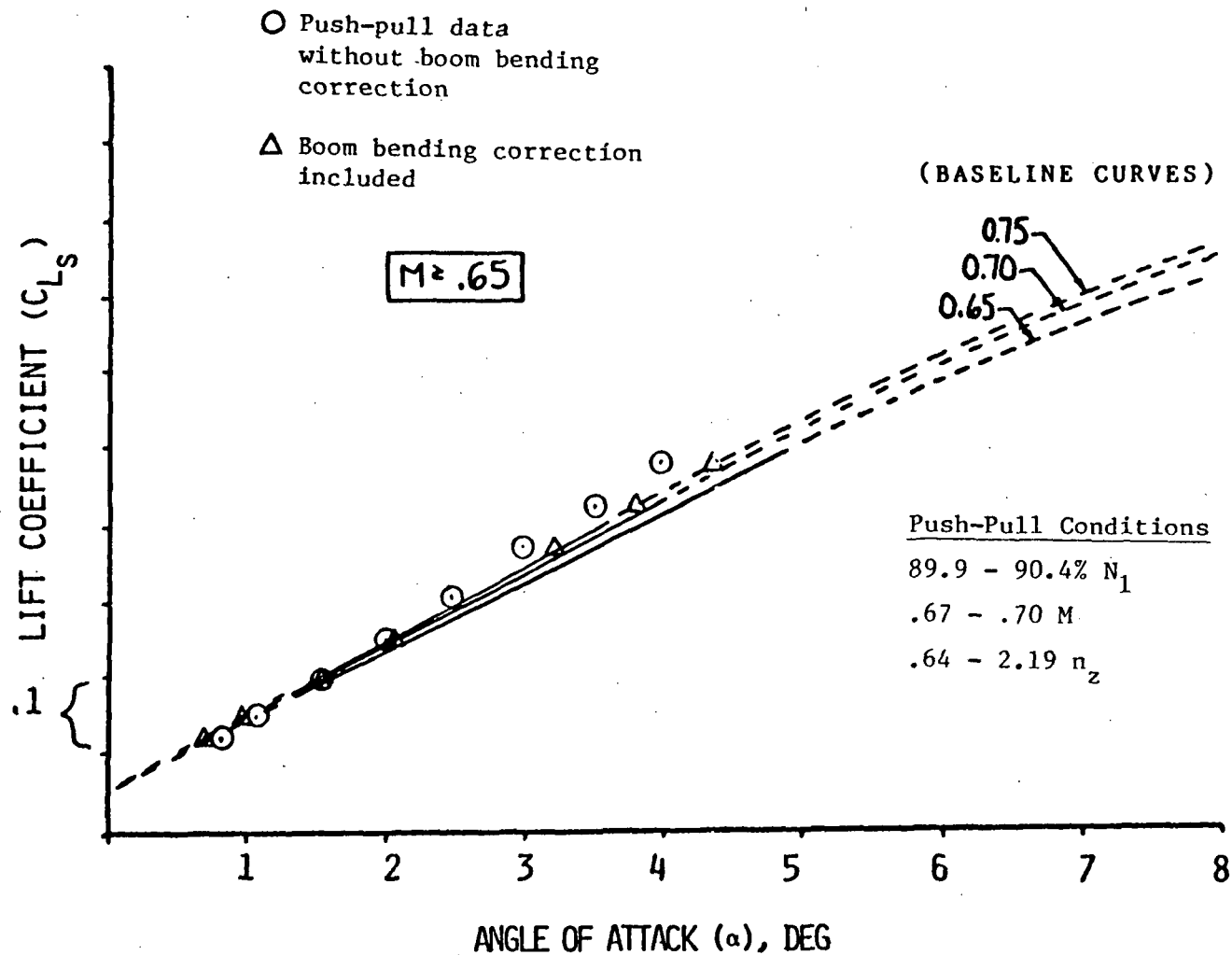


Figure 4.19: Lift Coefficient Push-Pull Data,
Flight 185, Run 13

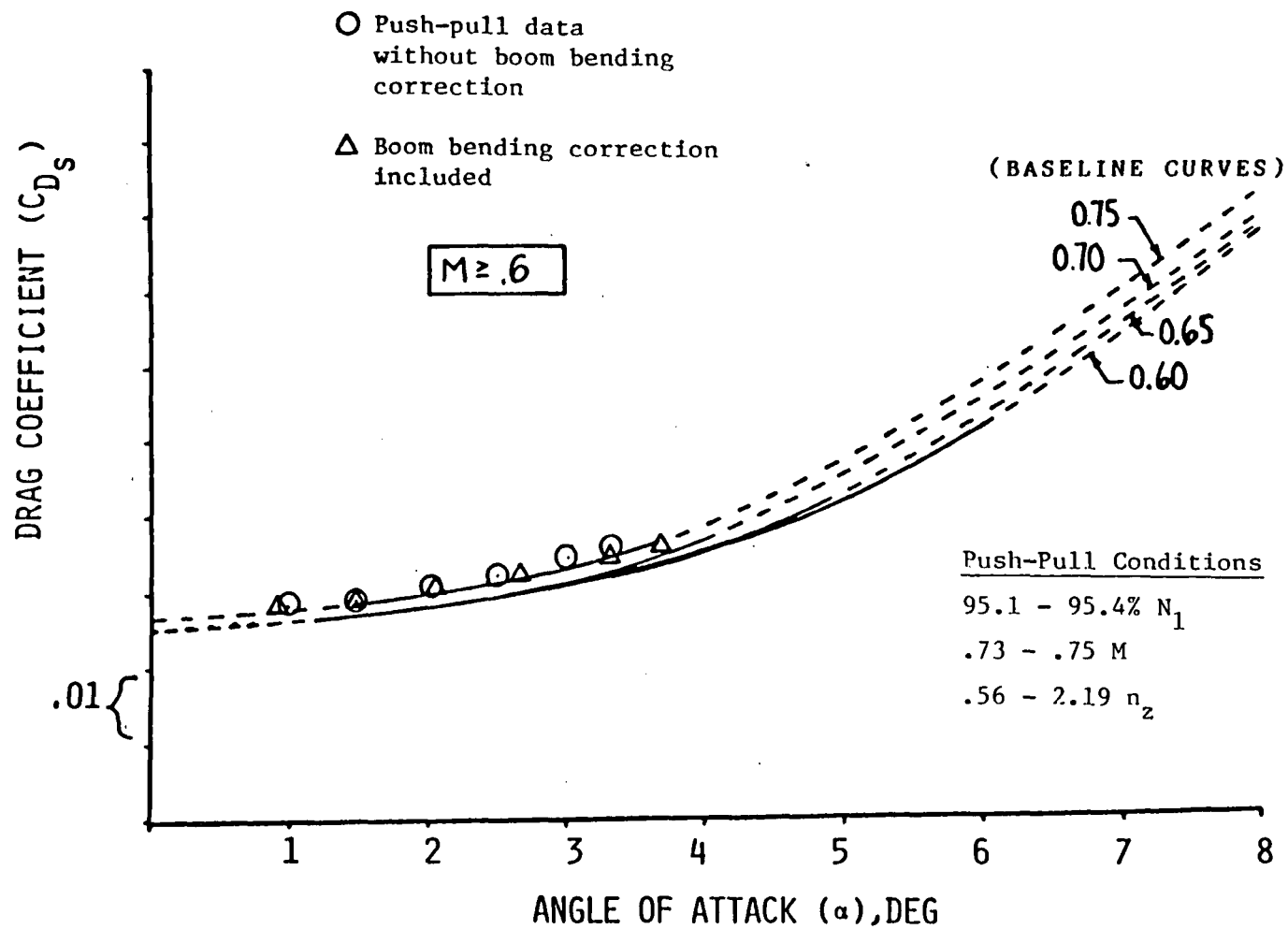


Figure 4.20: Drag Coefficient Push-Pull Data,
Flight 185, Run 10

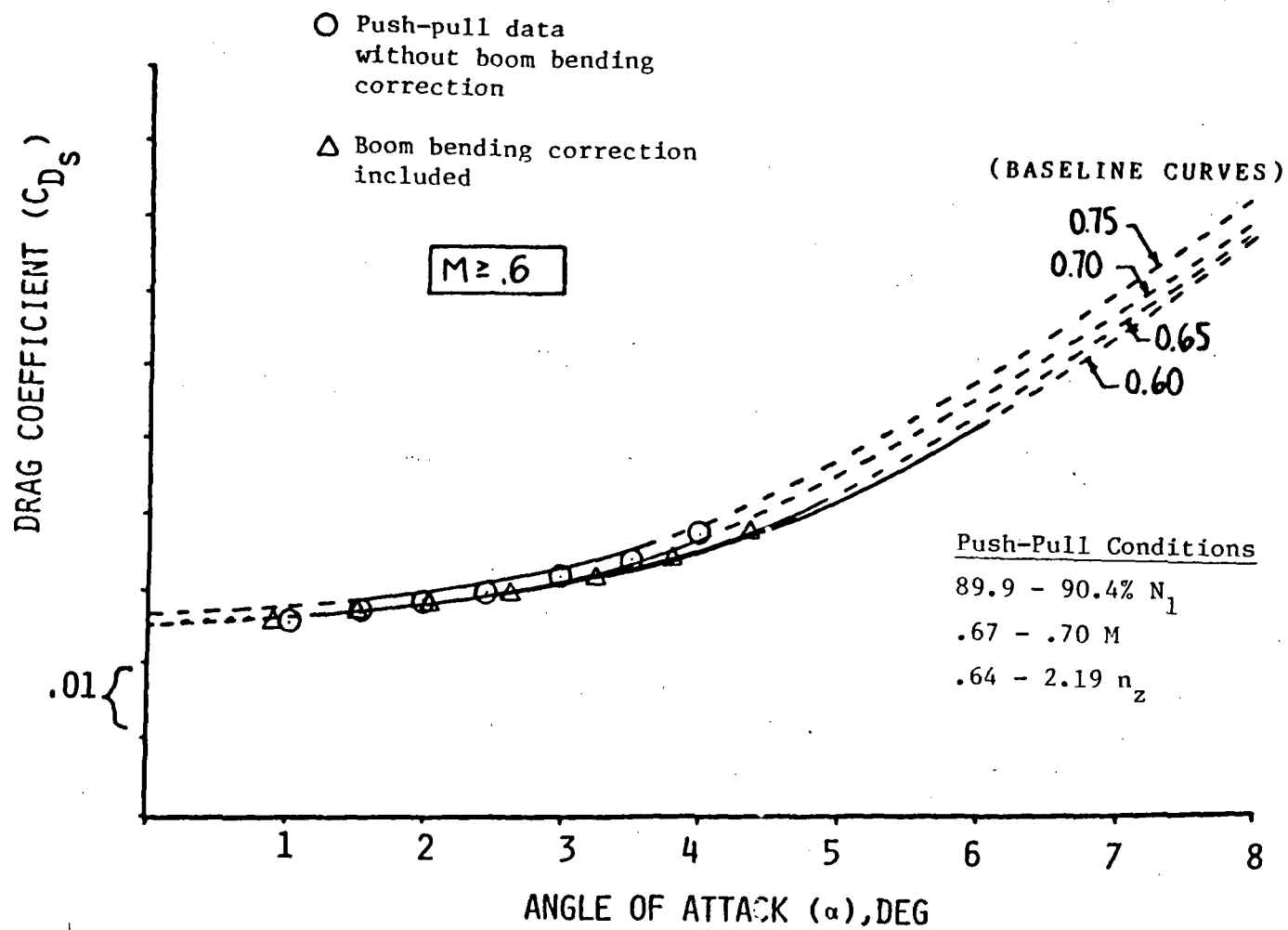


Figure 4.21: Drag Coefficient Push-Pull Data,
Flight 185, Run 13

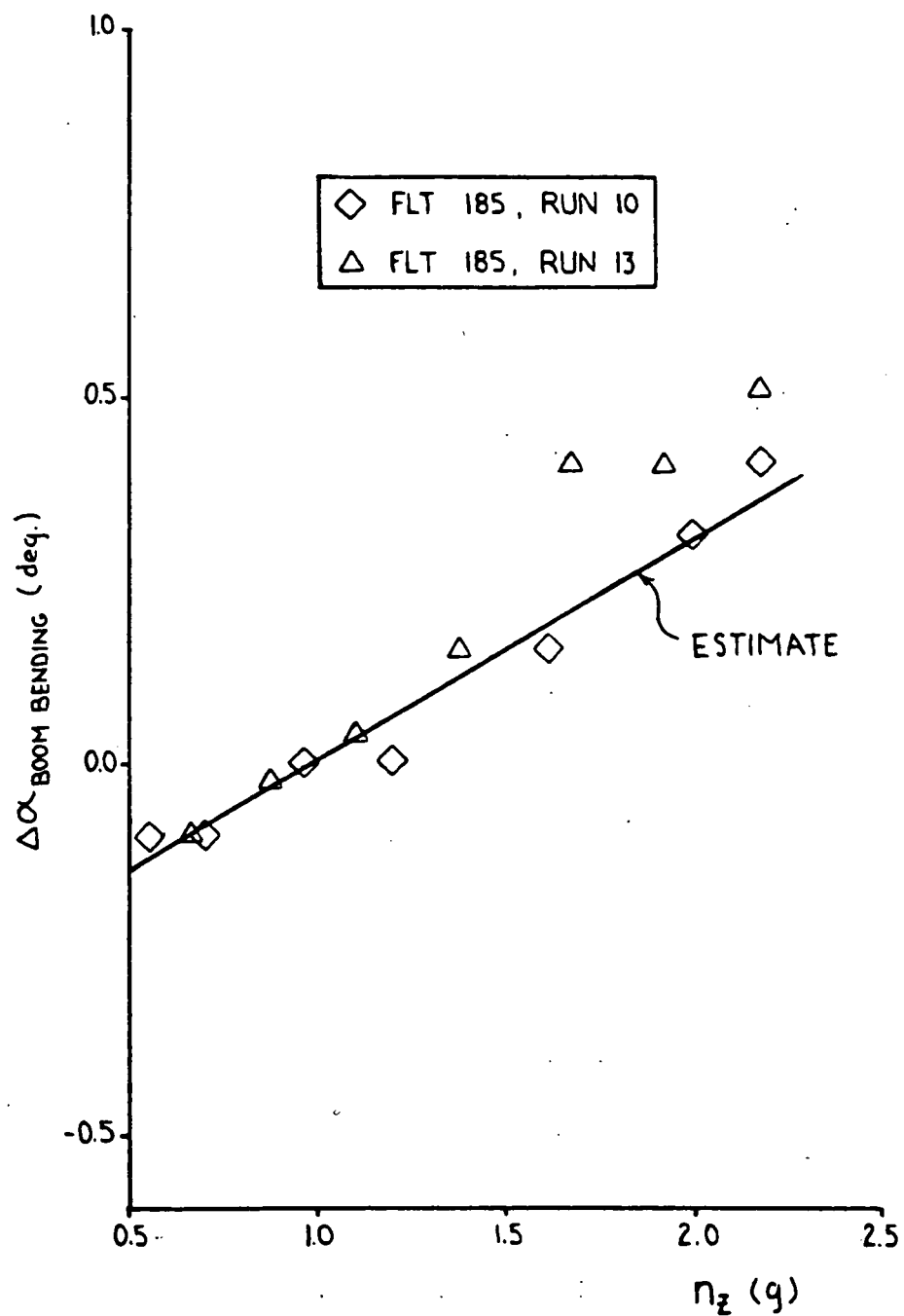


Figure 4.22: Boom Bending Correction Estimate

4.4 PERFORMANCE MODELING

4.4.1 Cruise Performance Prediction

The baseline aerodynamic and engine characteristics defined in Section 4.2 were digitized in table look-up format for use in the ITERATE cruise performance prediction program. Four W/δ cases were evaluated with the ITERATE program as summarized in Table 13. Figures 4.23 through 4.38 present the corrected RPM, range factor, specific range and specific range parameter predictions generated with ITERATE for these cases along with ± 5 and ± 10 percent error bands. The stabilized point data presented in Section 4.3.1 are included for comparison. The corrected RPM predictions generally were well within five percent of the stabilized point data. Exceptions to this were at the low Mach end of a particular W/δ Mach range where stabilized conditions are more difficult to achieve and cruise performance characteristics are of relatively low interest. For standardized range factor, the ITERATE predictions were generally within ten percent of the stabilized point data with the lower W/δ cases experiencing better prediction correlation than the higher W/δ cases. For the 60,000 W/δ case, where approximately twice as many stabilized points were available due to the duplicated tests, considerable scatter in the stabilized point data can be observed which indicates that a significant error band is associated with definition of range factor when using exclusively stabilized point data, the currently accepted practice. The ITERATE predictions for standardized specific range were also within 10 percent of the stabilized point data with all points within 5 percent

for the 22,000 and 40,000 W/ δ cases. The specific range parameter projections had similar characteristics when compared to the stabilized point data as those for standardized specific range.

Significant sources of error for comparison of the ITERATE predictions with stabilized point data include 1) the data scatter and resulting uncertainty associated with definition of the baseline aerodynamic and engine curves, 2) slightly off-stabilized test conditions for the stabilized point data and 3) possible instrumentation system errors which affected stabilized point and baseline characteristic data differently.

When evaluating the agreement between the ITERATE predictions and flight data, the above sources of error must be considered along with the error band associated with definition of the same cruise characteristics using exclusively stabilized point data. This error band was estimated to be at least 5%. In addition, the high sensitivity of all the cruise parameters to small variations in the fairing of baseline engine curves such as fuel flow is a significant consideration, since a larger scatter band was experienced for the engine data than should normally be expected. The ITERATE program may also be used in conjunction with stable point data to assist in defining the final baseline aerodynamic and engine curves when significant data scatter is present. Several trial fairings may be evaluated with ITERATE and then compared with stable point data to determine which fairing is the most realistic. The prediction correlation achieved was considered good in view of these factors and should improve on future programs where less data scatter is anticipated for the baseline engine characteristics.

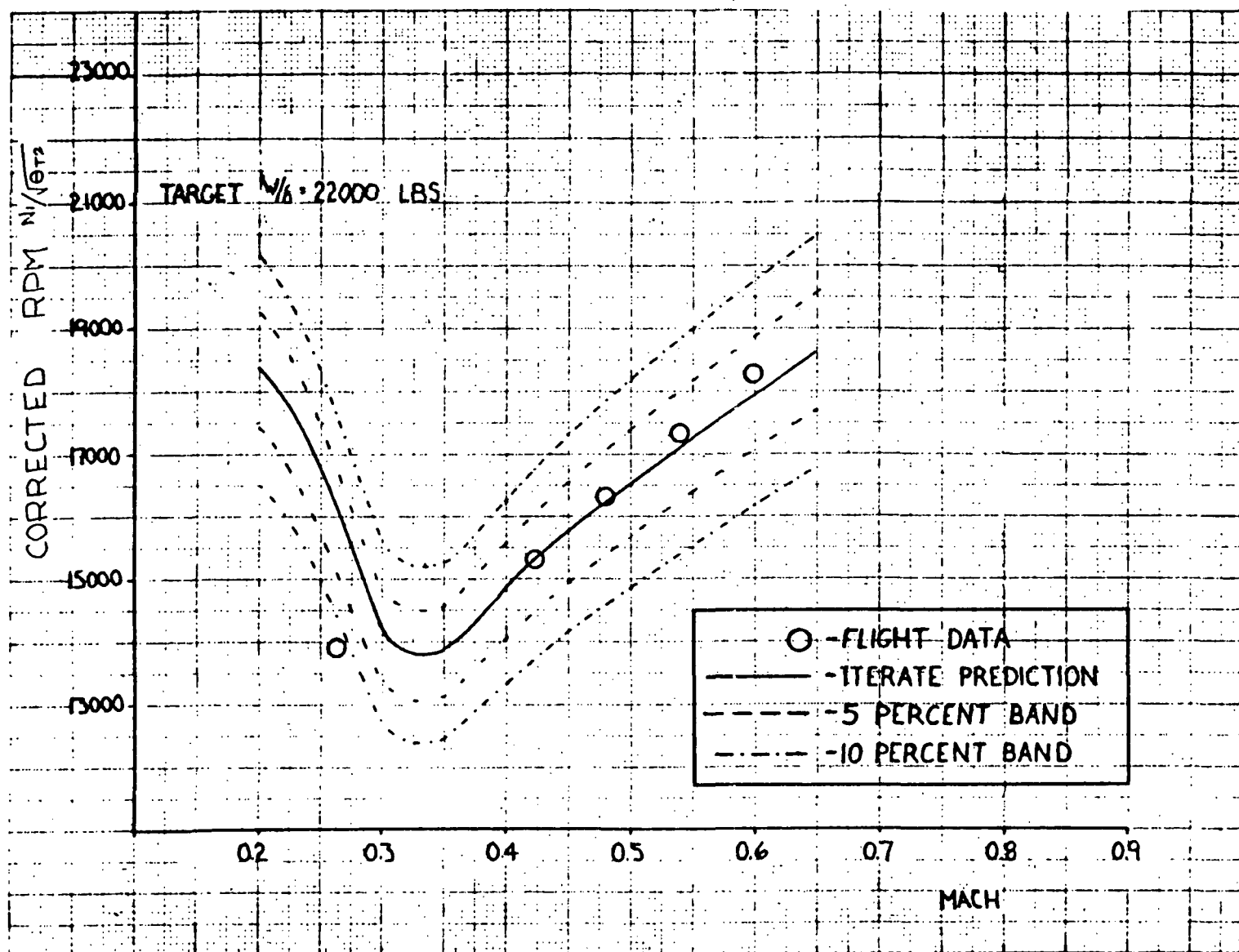


Figure 4.23: ITERATE Corrected RPM Prediction, $W/6 = 22000$ lbs

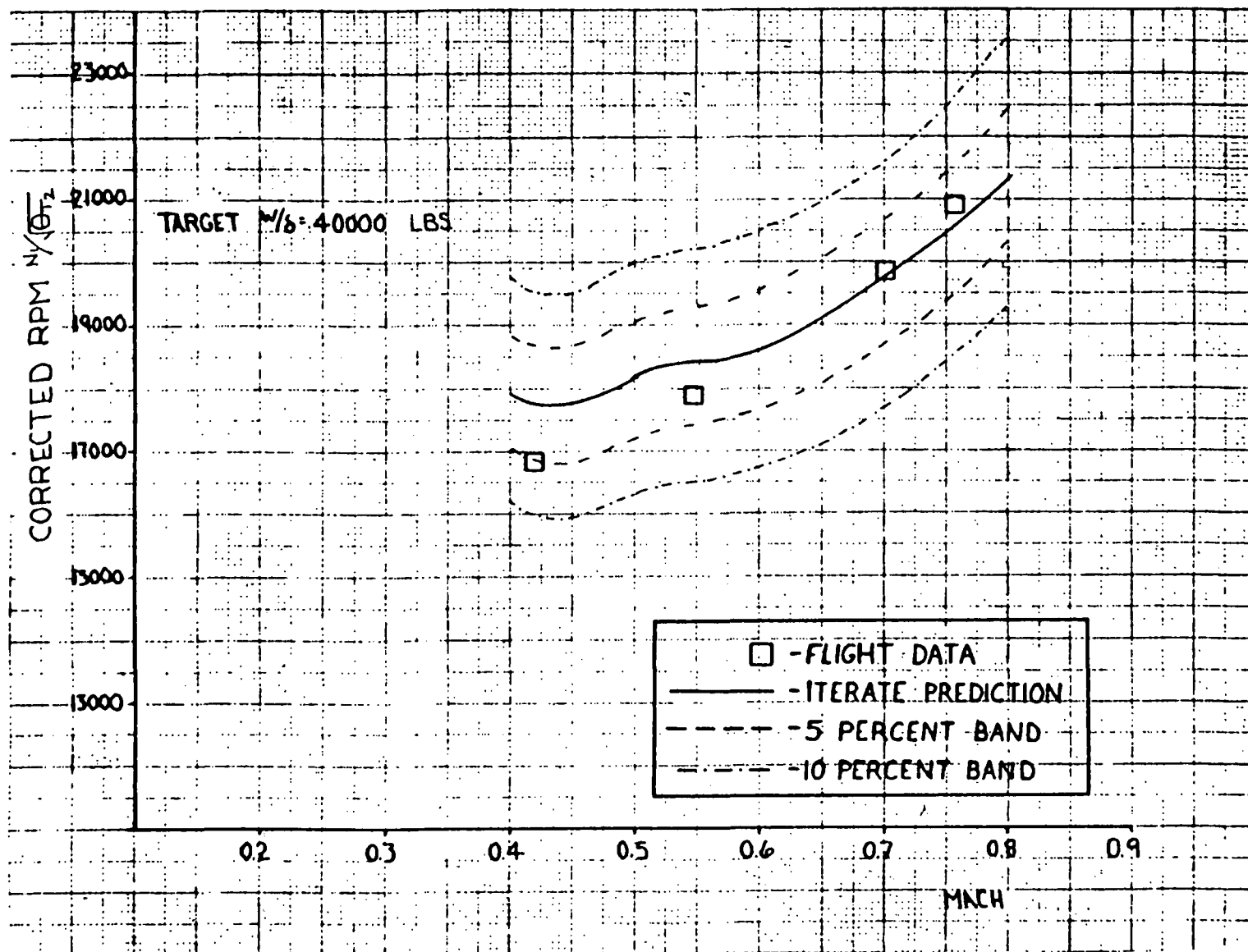


Figure 4.24: ITERATE Corrected RPM Prediction, $W/d = 40000$ lbs

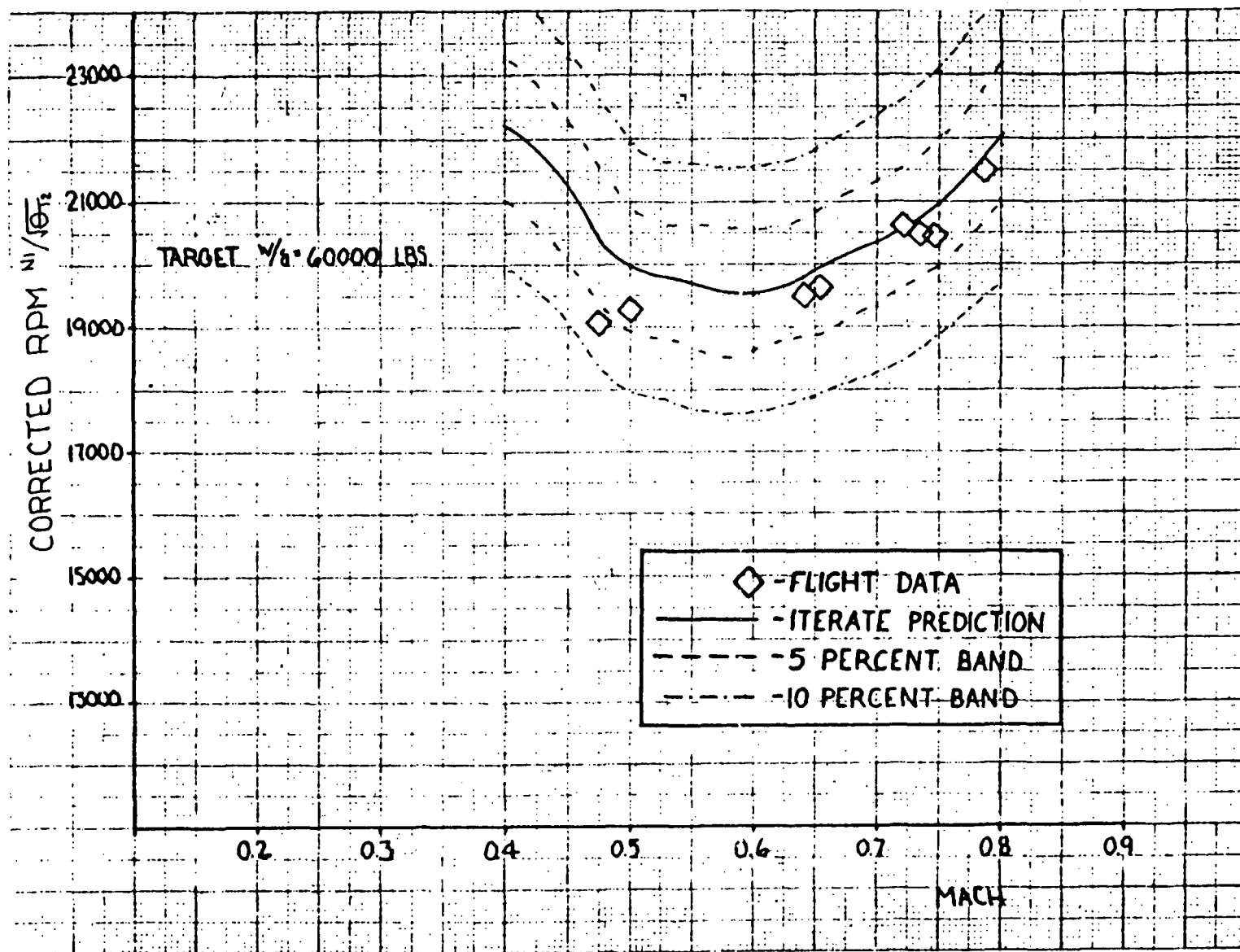


Figure 4.25: ITERATE Corrected RPM Prediction, $W/\delta = 60000$ lbs

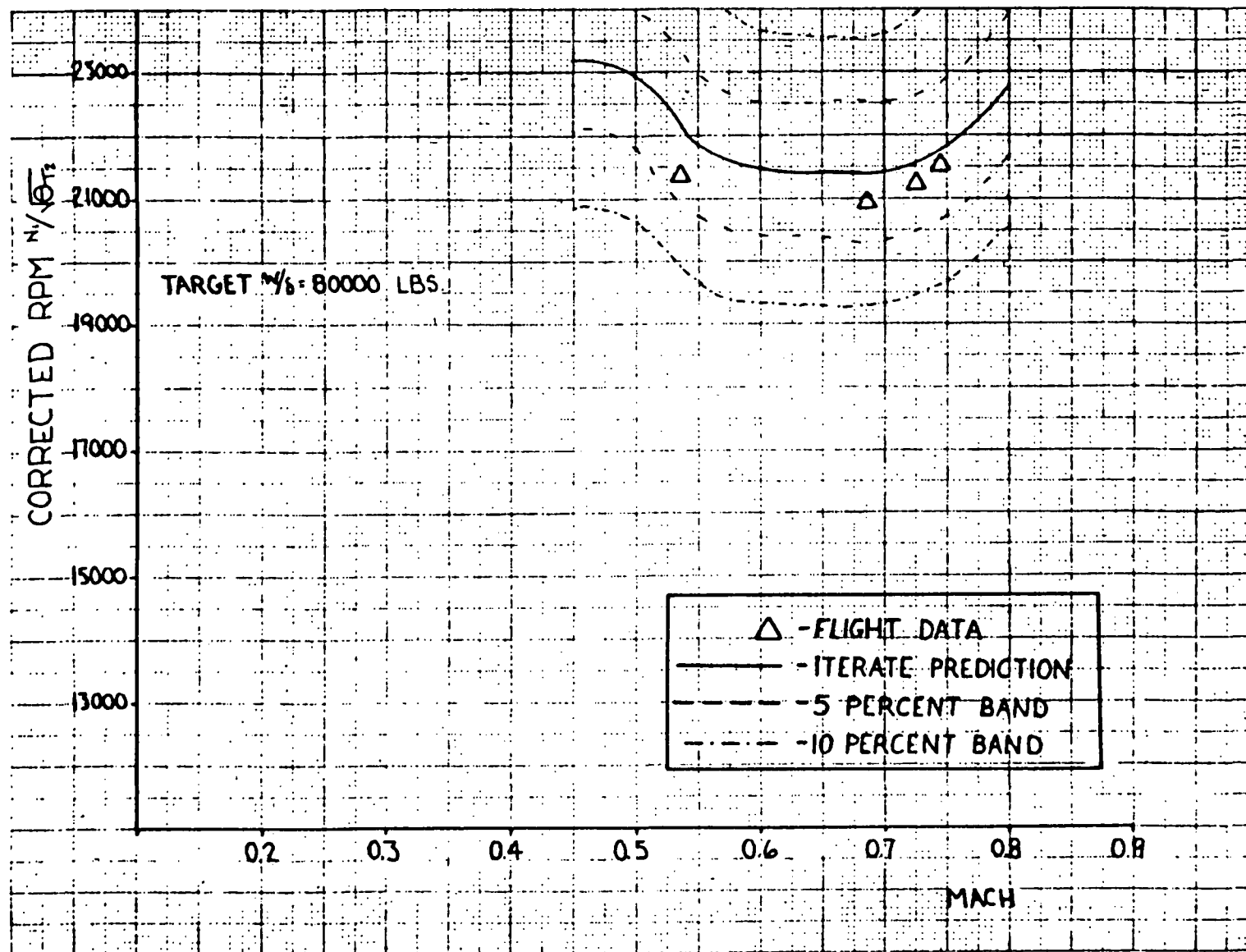


Figure 4.26: ITERATE Corrected RPM Prediction, $W/\delta = 80000$ lbs

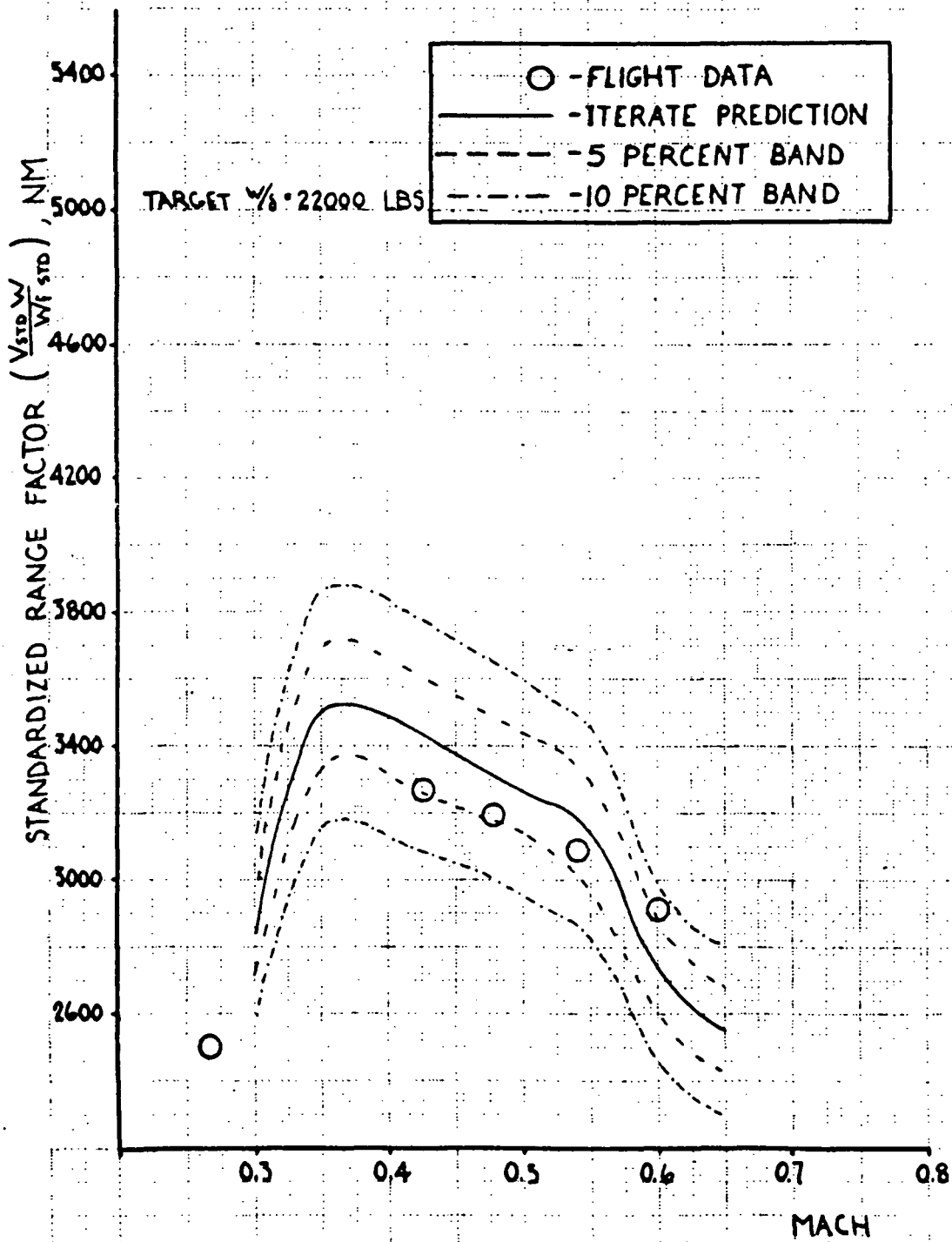


Figure 4.27: ITERATE Standardized Range Factor Prediction, $W/\delta = 22000$ lbs.

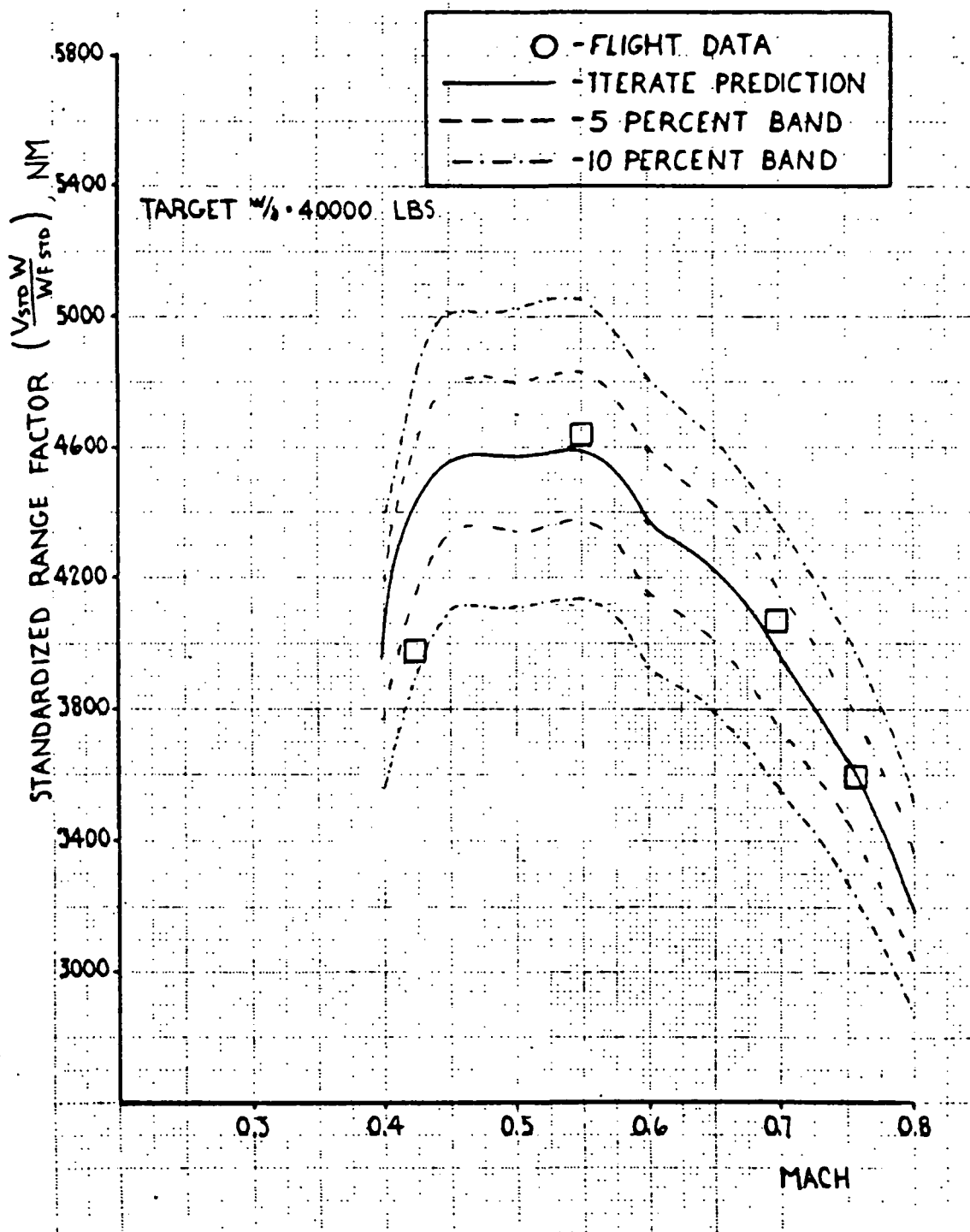


Figure 4.28: ITERATE Standardized Range Factor Prediction, $W/b = 40000$ lbs

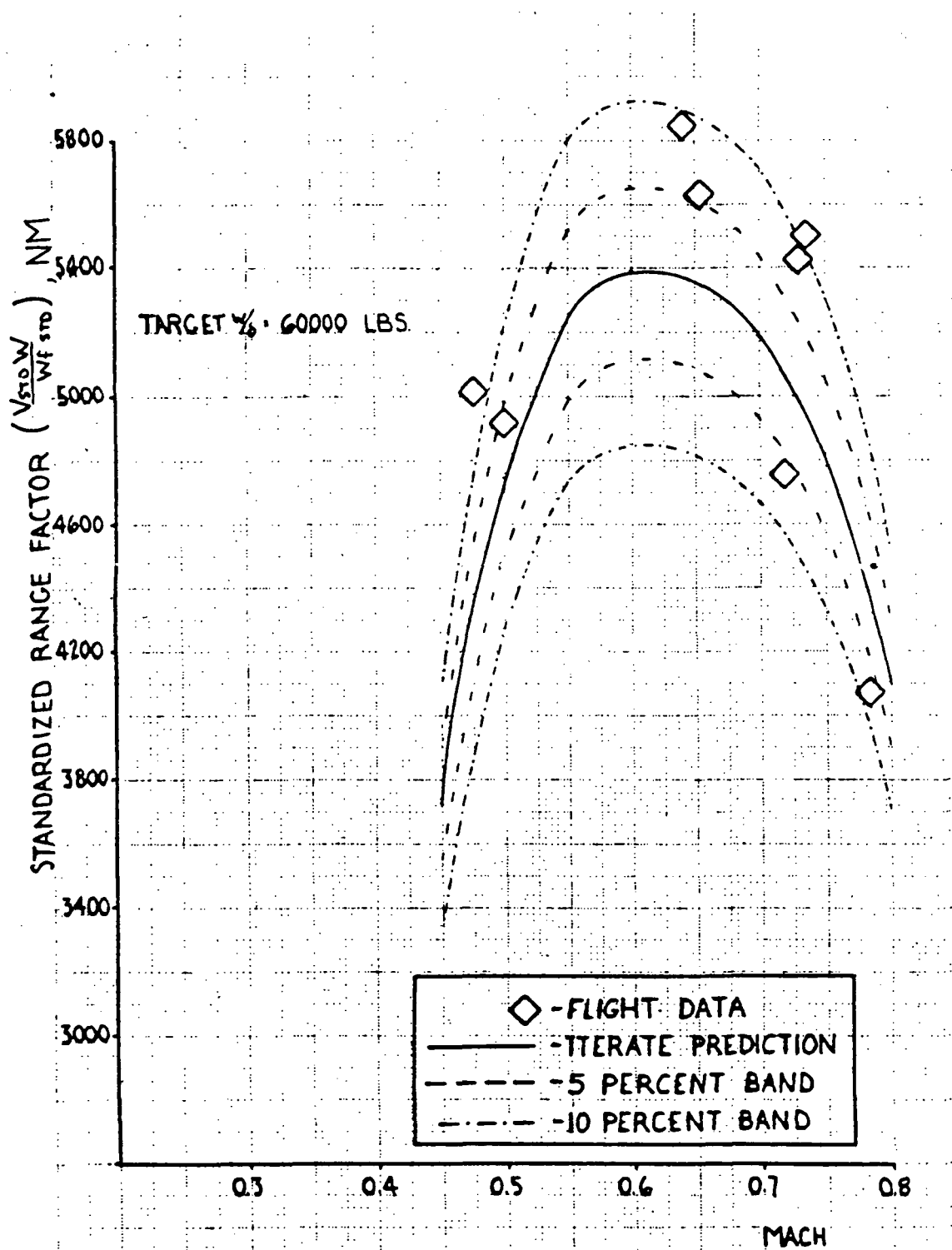


Figure 4.29: ITERATE Standardized Range Factor Prediction, $W/t = 60000$ lbs

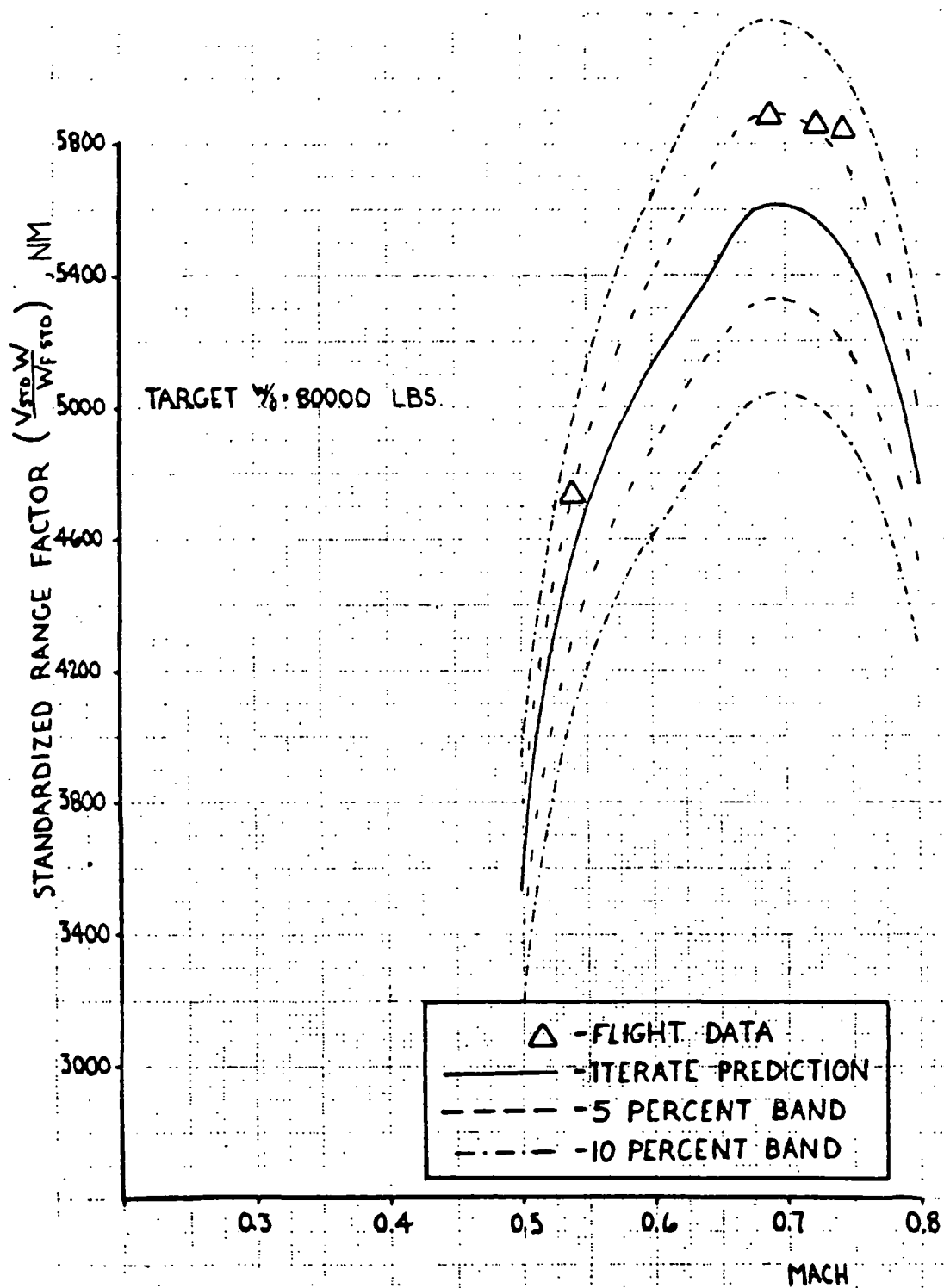


Figure 4.30: ITERATE Standardized Range Factor Prediction, $W/6 = 80000$ lbs

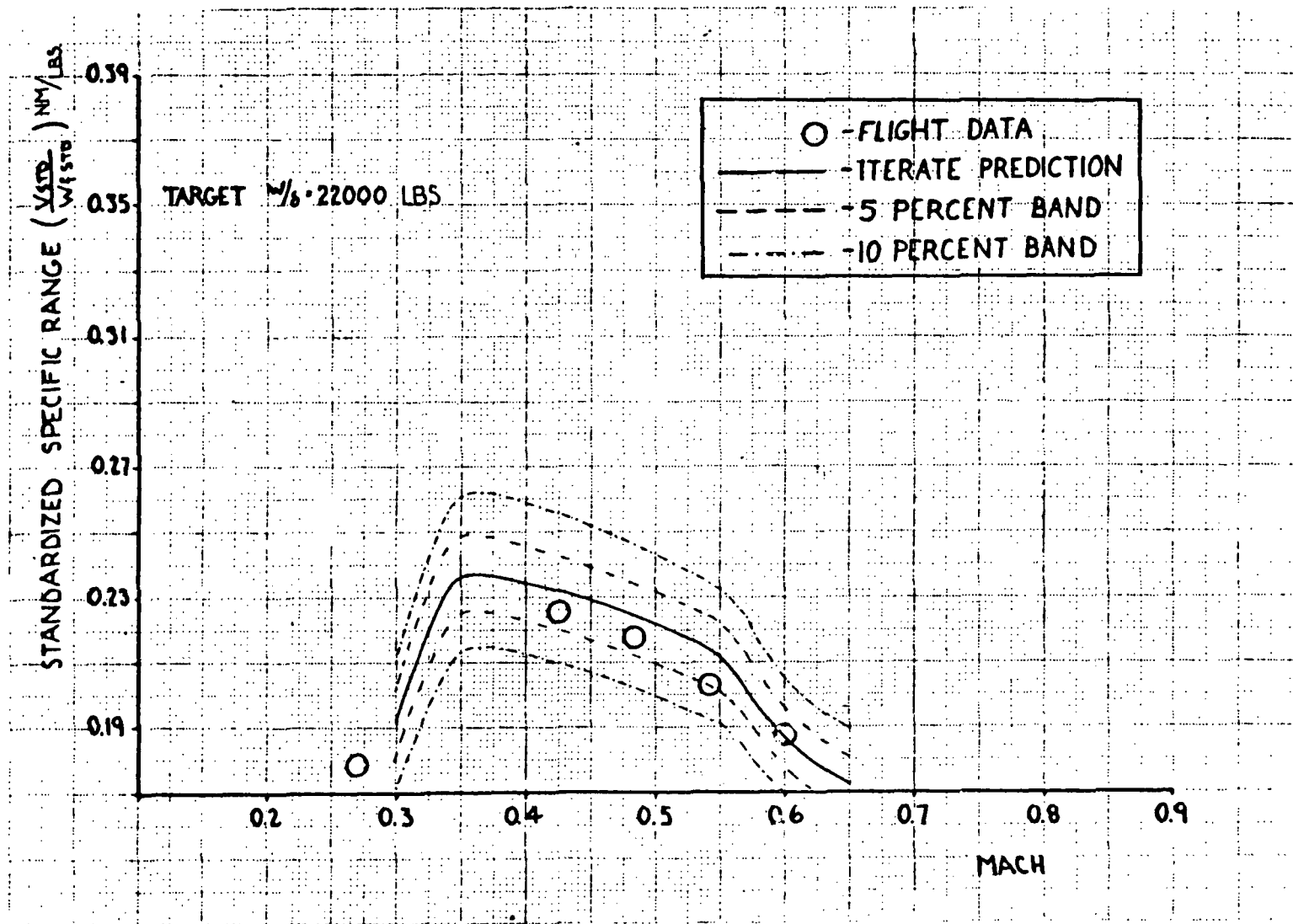


Figure 4.31: ITERATE Standardized Specific Range Prediction, $W/S = 22000$ lbs

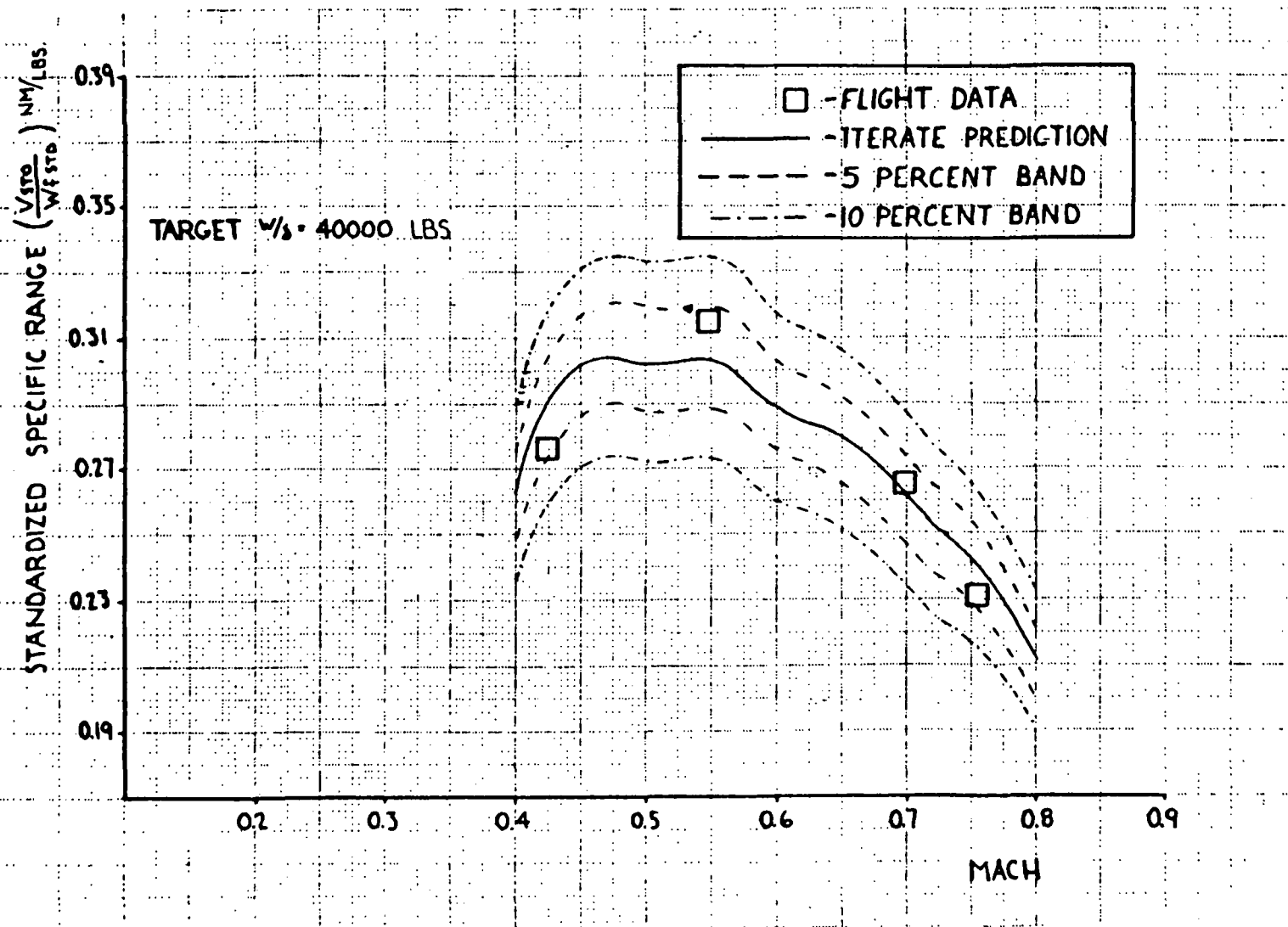


Figure 4.32: ITERATE Standardized Specific Range Prediction, $W/\delta = 40000 \text{ lbs}$

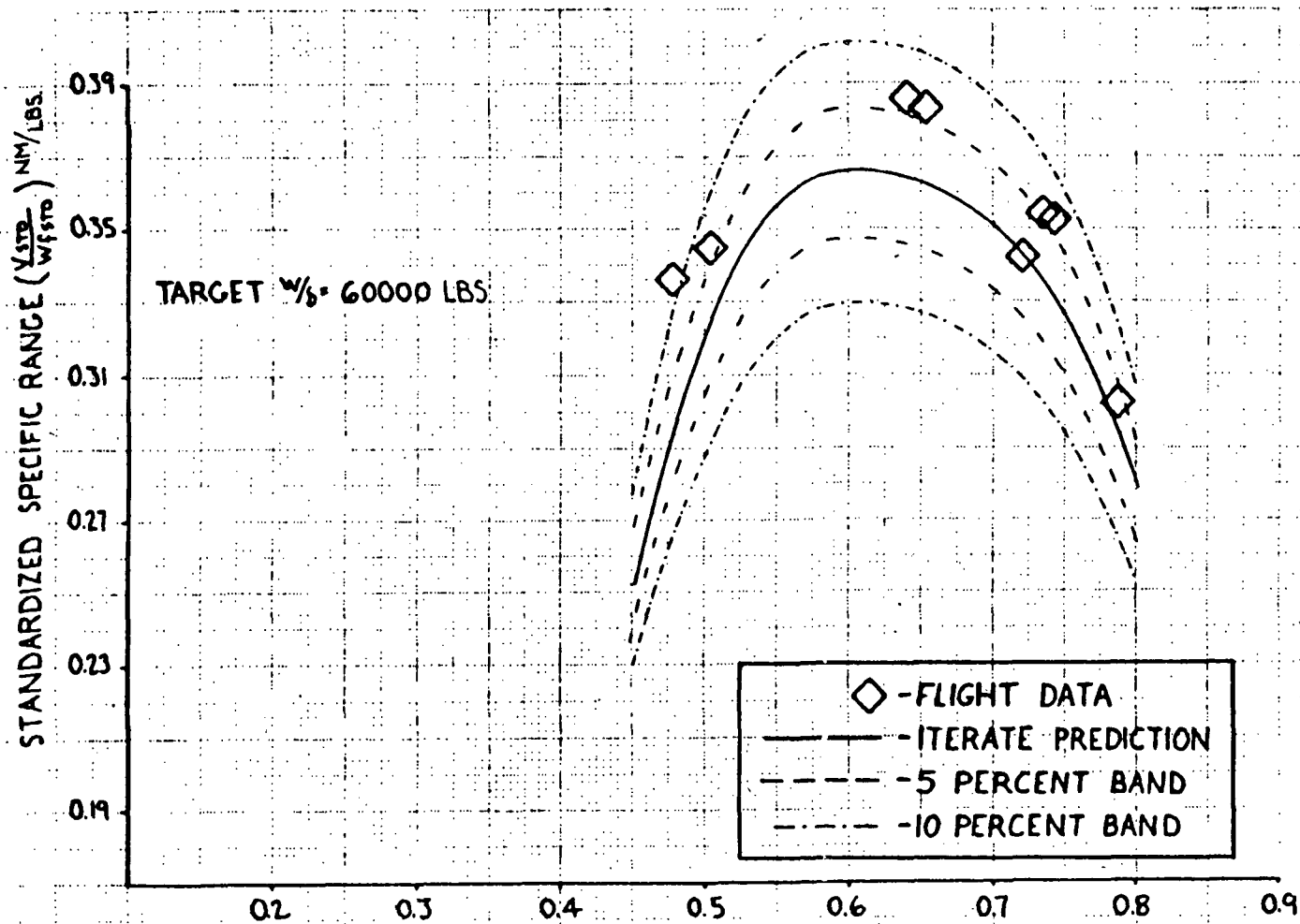


Figure 4.33: ITERATE Standardized Specific Range Prediction, $W/6 = 60000$ lbs

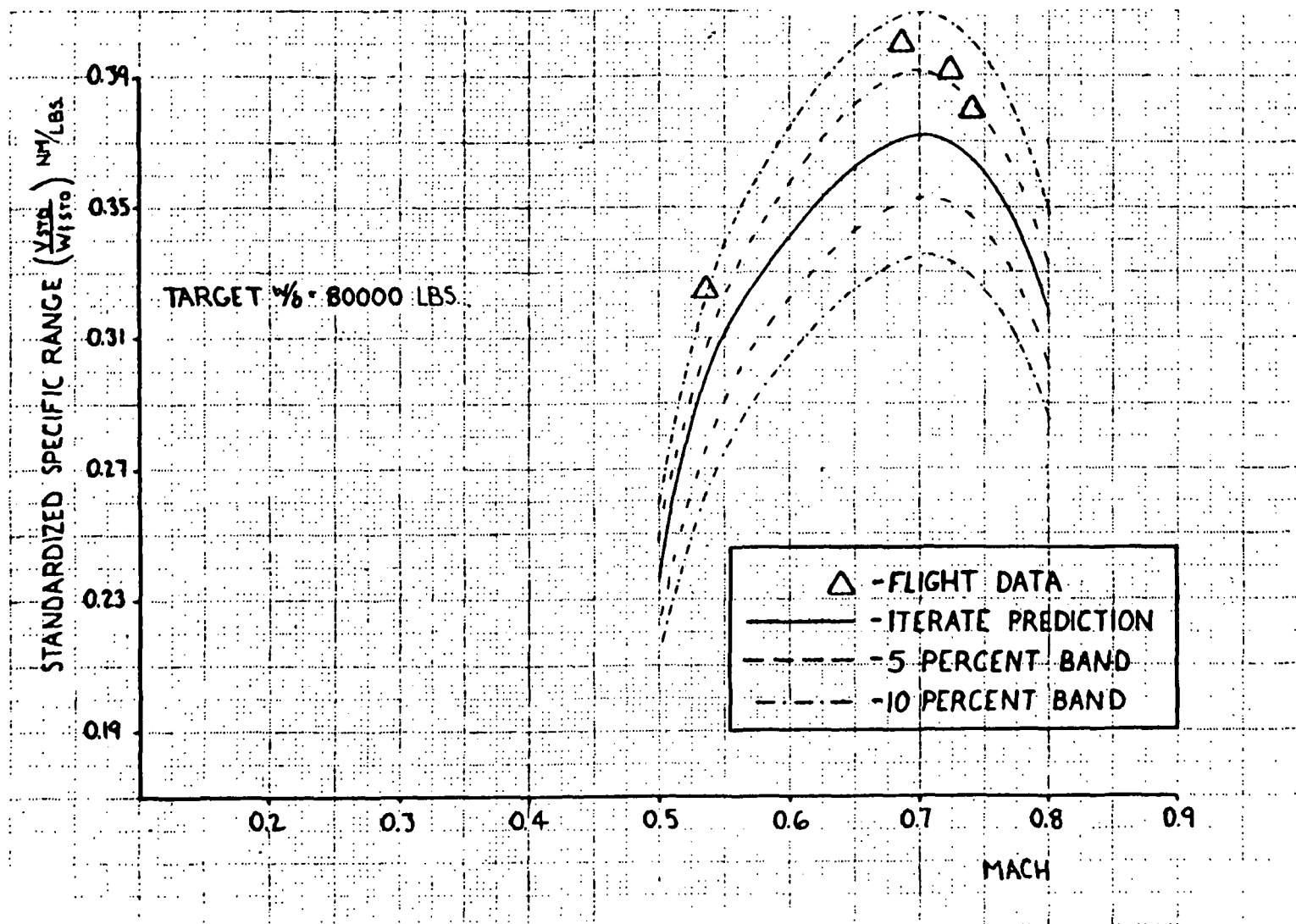


Figure 4.34: ITERATE Standardized Specific Range Prediction, $W/6 = 80000$ lbs

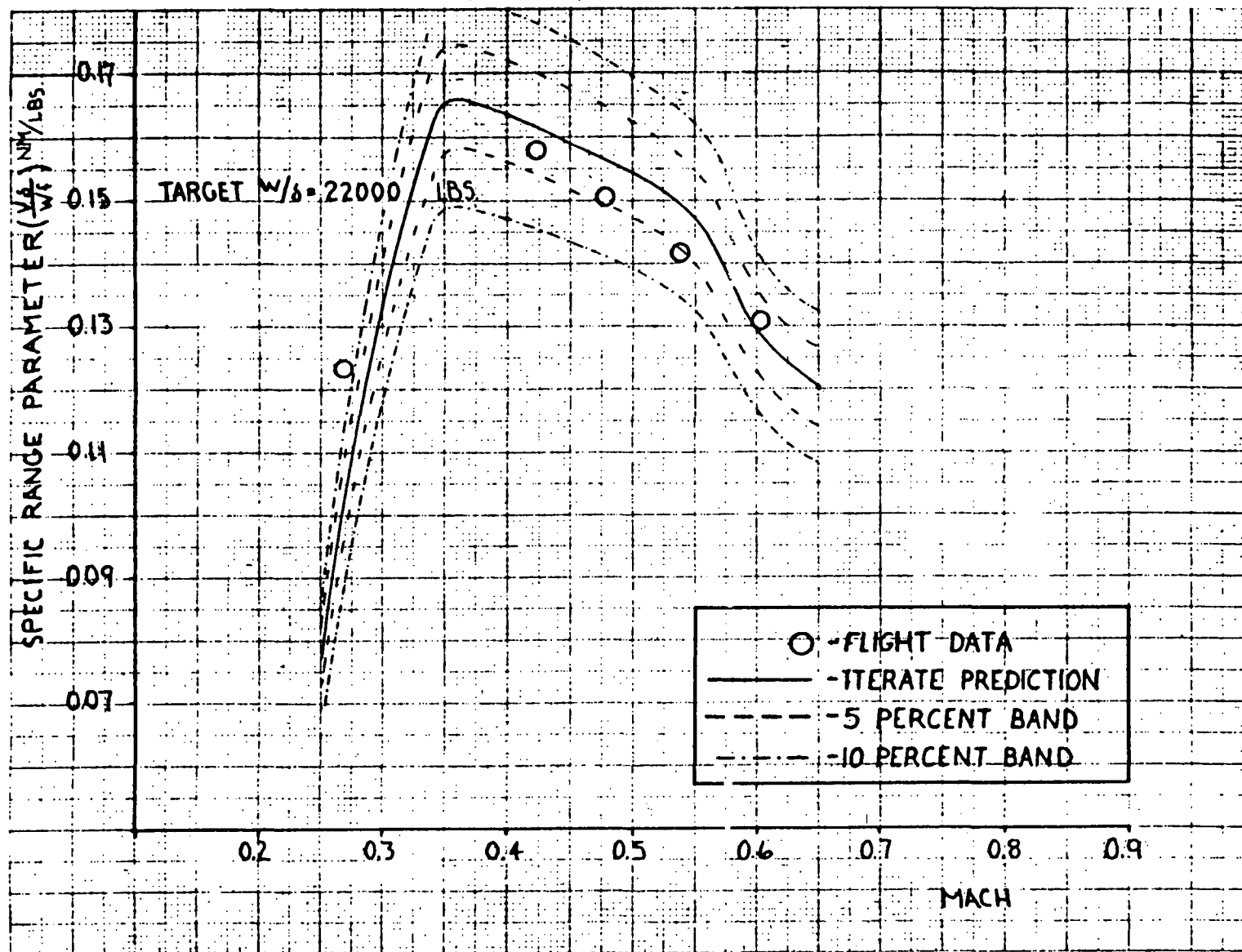


Figure 4.35: ITERATE Specific Range Parameter Prediction, $W/d = 22000$ lbs

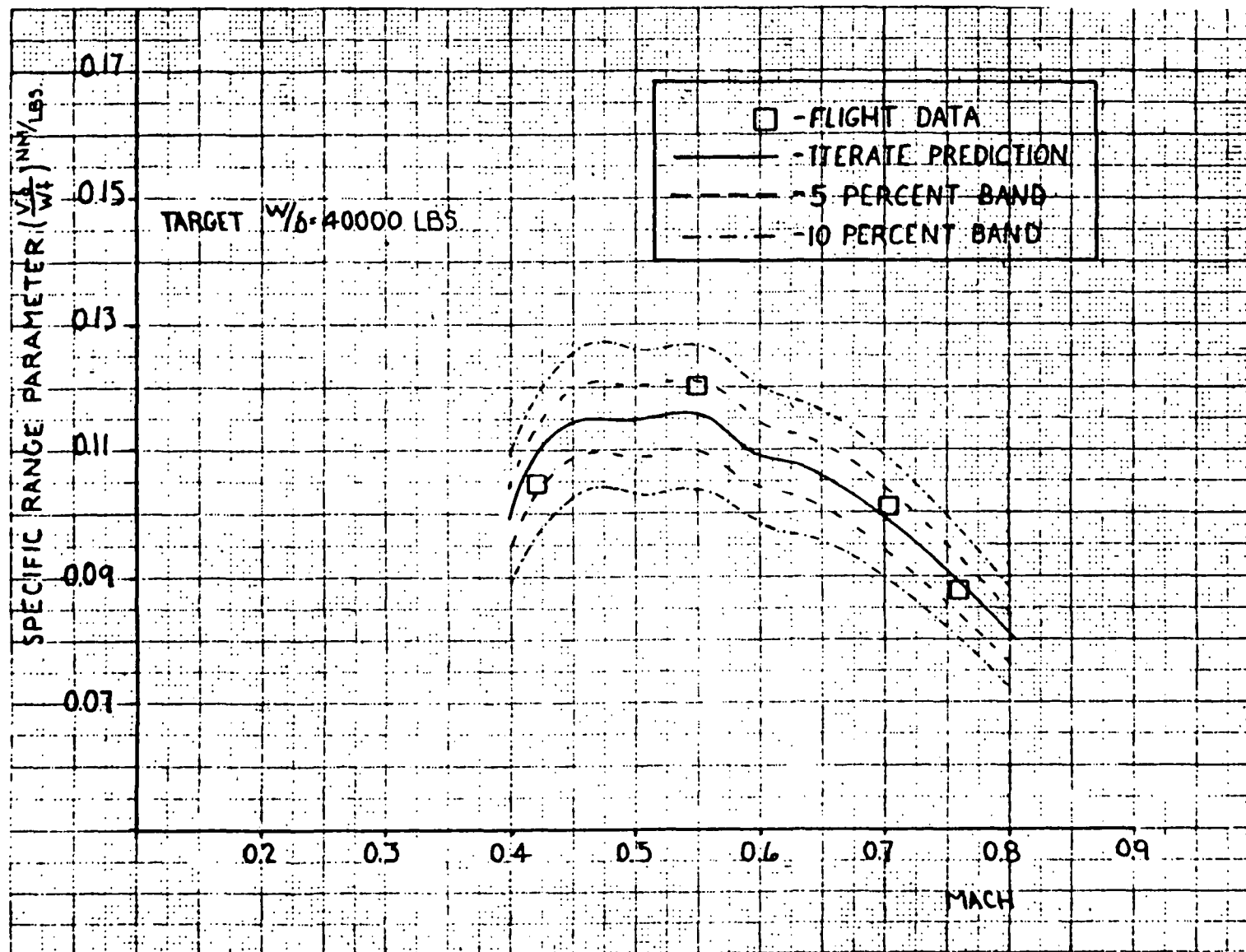


Figure 4.36: ITERATE Specific Range Parameter Prediction, $W/6 = 40000$ lbs

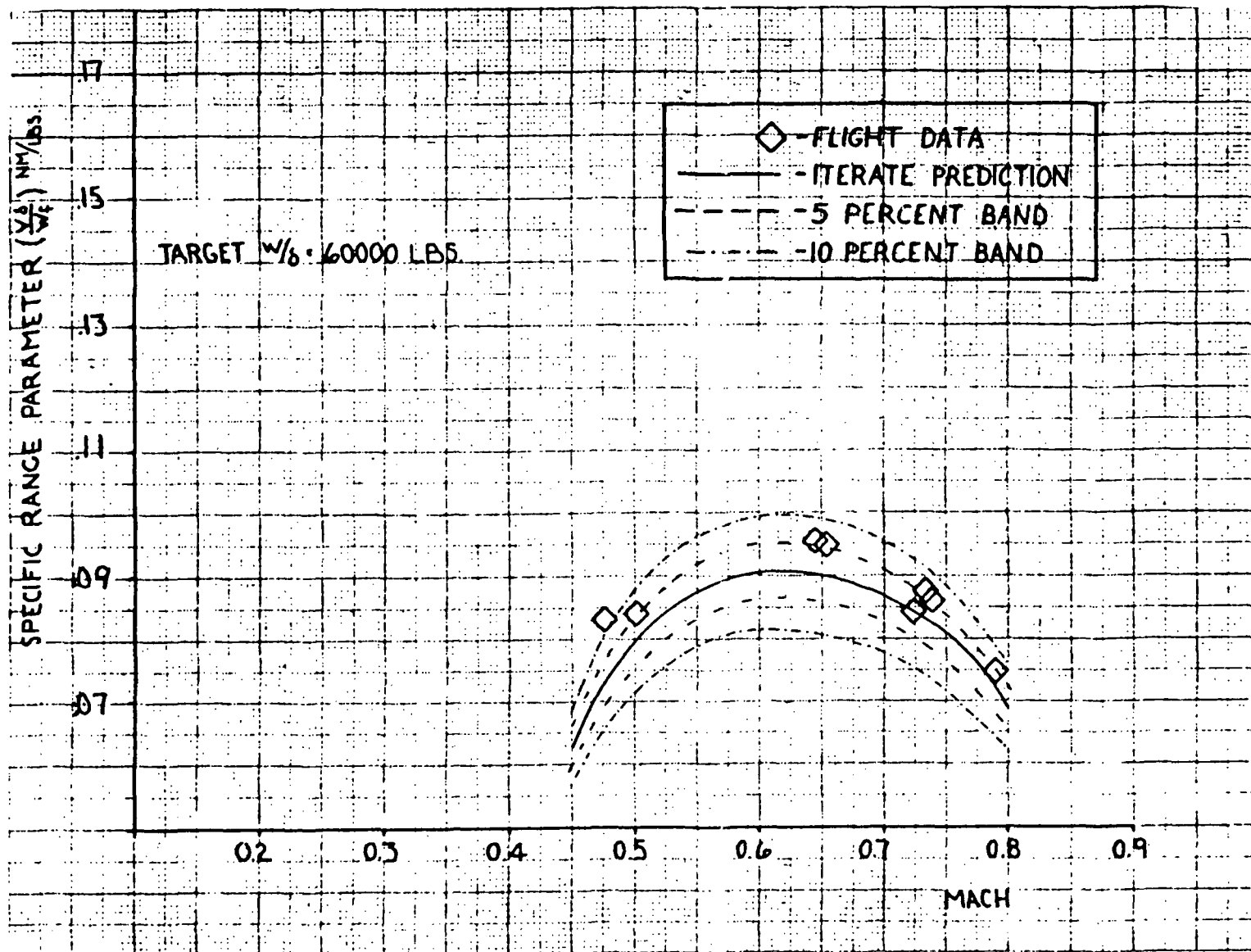


Figure 4.37: ITERATE Specific Range Parameter Prediction, $W/\delta = 60000 \text{ lbs}$

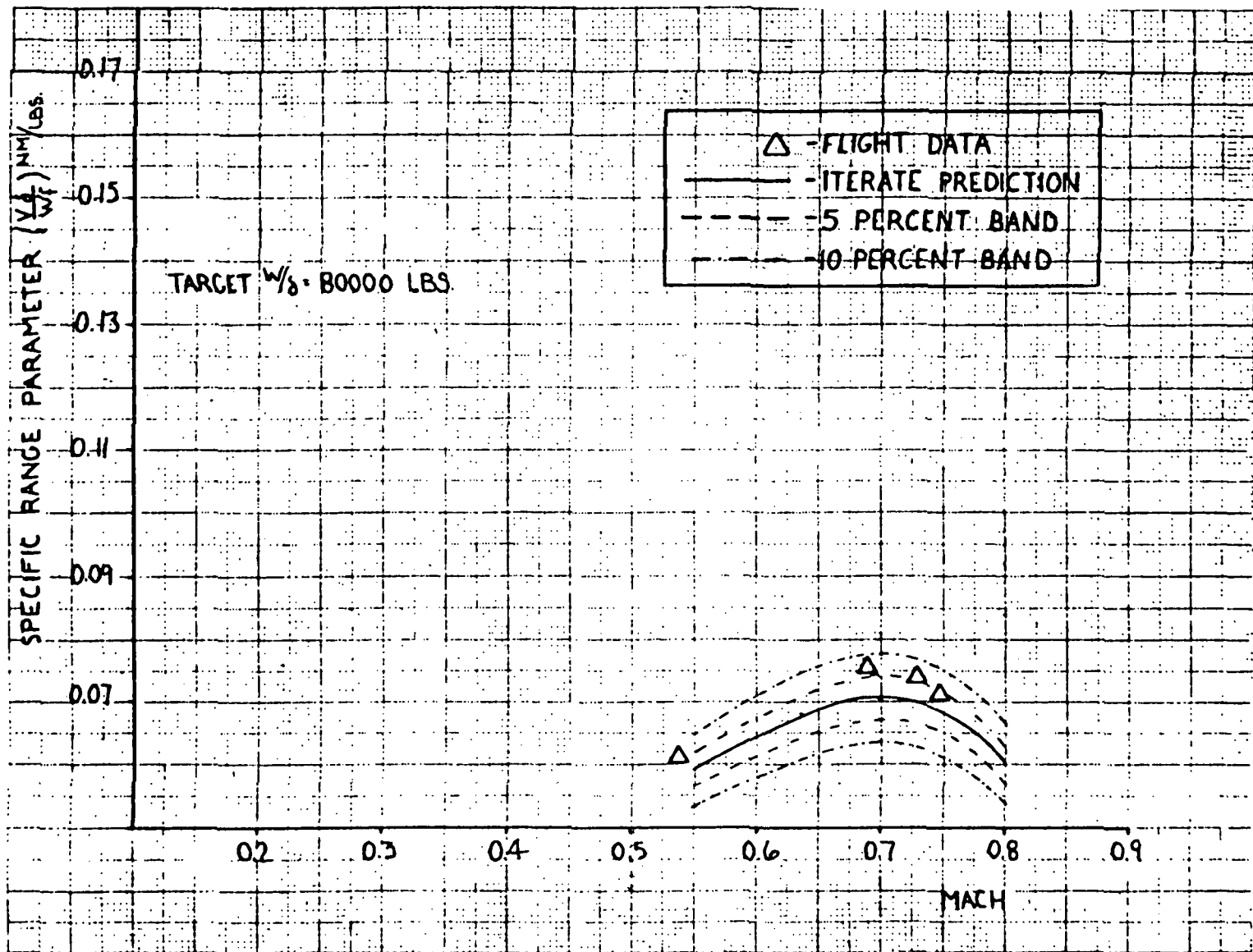


Figure 4.38: ITERATE Specific Range Parameter Prediction, $W/\delta = 80000 \text{ lbs}$

4.4.2 Flight Trajectory Performance Prediction

Several in-flight trajectories were flown so that a comparison between flight data and MODEL predictions could be made. These trajectories consisted of climbs and accelerations/decelerations as summarized in Table 14. Actual in-flight data for time, fuel used and specific excess power (for the accels/decel) were compared with predictions generated by the MODEL program for similar conditions. P_s for the in-flight data was computed with

$$P_s = n_x V$$

as shown in Reference 6.

Table 14: Flight Trajectory Summary

<u>PROFILE</u>	<u>MANEUVER</u>	<u>FLIGHT</u>	<u>RUN</u>	<u>ALTITUDE: START/END (ft)</u>	<u>MACH: START/END</u>	<u>WEIGHT: START/END (lbs)</u>
1	94% Climb	188	7	19041/20127	.483/.495	16254/16241
2	99% Climb	188	16	19939/24755	.710/.697	16029/15972
3	90% Climb	189	3	6880/10214	.430/.454	16331/16286
4	95% Accel	184	3	8757/8641	.326/.598	16029/15974
5	50% Decel	184	5	8628/8621	.559/.532	15927/15925
6	90% Accel	184	11	8669/8648	.291/.485	15892/15857
7	80% Accel	184	34	9525/9544	.266/.292	15032/15027
8	95% Accel	185	4	23911/23900	.414/.497	15842/15826
9	70% Decel	185	14	24530/24550	.676/.644	15259/15254
10	85% Decel	185	21	24542/24569	.715/.689	15083/15073

4.4.2.1 Climbs

MODEL predictions for time and fuel used as a function of altitude are presented in Figures 3.39 through 4.44 for the three climb profiles evaluated. Actual in-flight data are shown with symbols. The first two profiles generally agreed within ten percent when comparing MODEL and in-flight data. The MODEL predictions for Profile 3 (Figures 4.43 and 4.44) were less accurate but generally were less than 15 percent in error. The primary deviation in this profile occurred during the first 15 seconds, after which a fairly close approximation was obtained considering relative slopes of the MODEL and in-flight data. Although better agreement was hoped for, the results were considered reasonable considering three identified sources of error. First, the degree of data scatter present in defining the baseline engine curves (Section 4.2.2) was larger than should normally be expected, as shown with the Lear 55 program. As a result, the corrected thrust, airflow and fuel flow baseline curves were subject to a larger uncertainty. Second, the actual in-flight profiles were subject to significant airspeed, power and temperature variations which could not be totally accounted for within the MODEL program. For example, it was very straightforward to use MODEL for a constant Mach/constant power climb profile; but an actual flight profile could not realistically be flown exactly on these conditions. Modifications were made to MODEL to include variations in these parameters; however, precise input of each perturbation created unrealistic conditions for the MODEL program to follow precisely due to instrumentation accuracies and noise.

As a result, a small degree of smoothing was applied to the MODEL profile inputs. The smoothing combined with the instrumentation inaccuracies were a source of error which highlighted the difficulty of using an actual in-flight trajectory for comparison purposes. The third potential source of error concerned the effect of wind gradients which may have been present during flight evaluation of the actual profiles. This error source was also identified as part of the work conducted in Reference 4 and is almost impossible to account for due to the difficulty of obtaining accurate wind measurements. Despite these problems, reasonable predictions could be obtained for the Lear 35; and significantly improved correlation is anticipated for future programs which experience tighter data grouping on the baseline engine curves. Since future programs should be primarily interested in "on speed" and "on power" predictions, the inaccuracies resulting from attempting to follow precisely an actual in-flight profile should be eliminated for this type of application. Actual profiles should still be flown in selected cases for comparison purposes to estimate the correlation associated with a particular program; however.

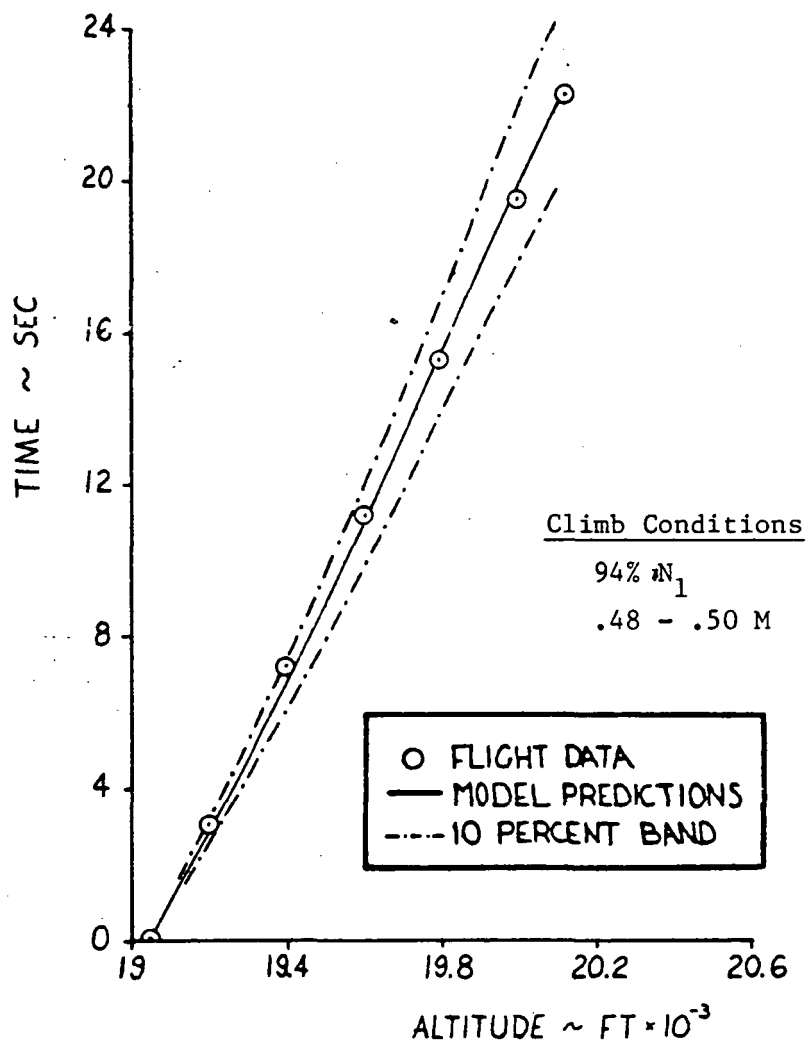


Figure 4.39: MODEL Time Prediction, Profile 1

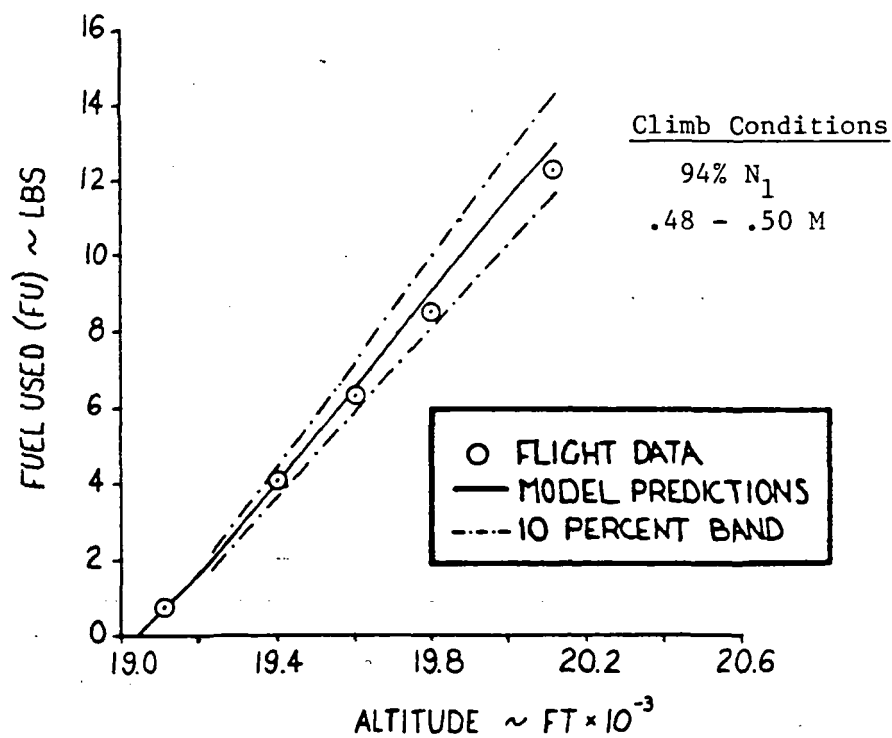


Figure 4.40: MODEL Fuel Used Prediction, Profile 1

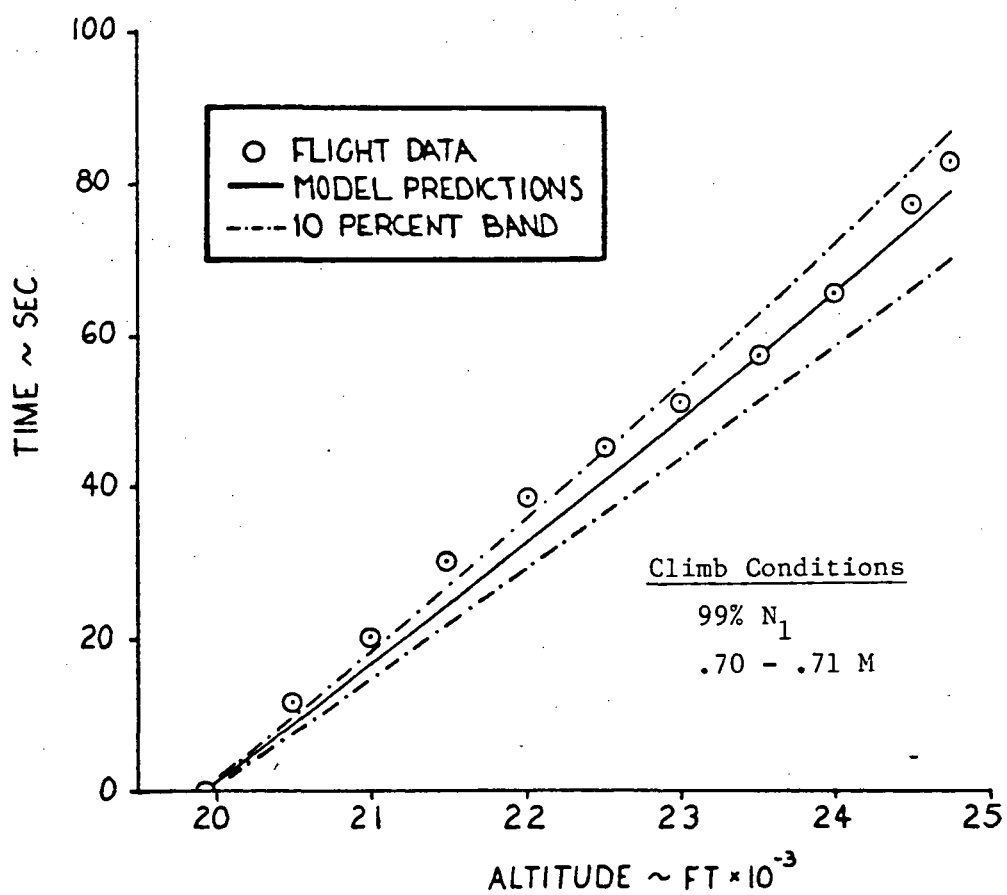


Figure 4.41: MODEL Time Prediction, Profile 2

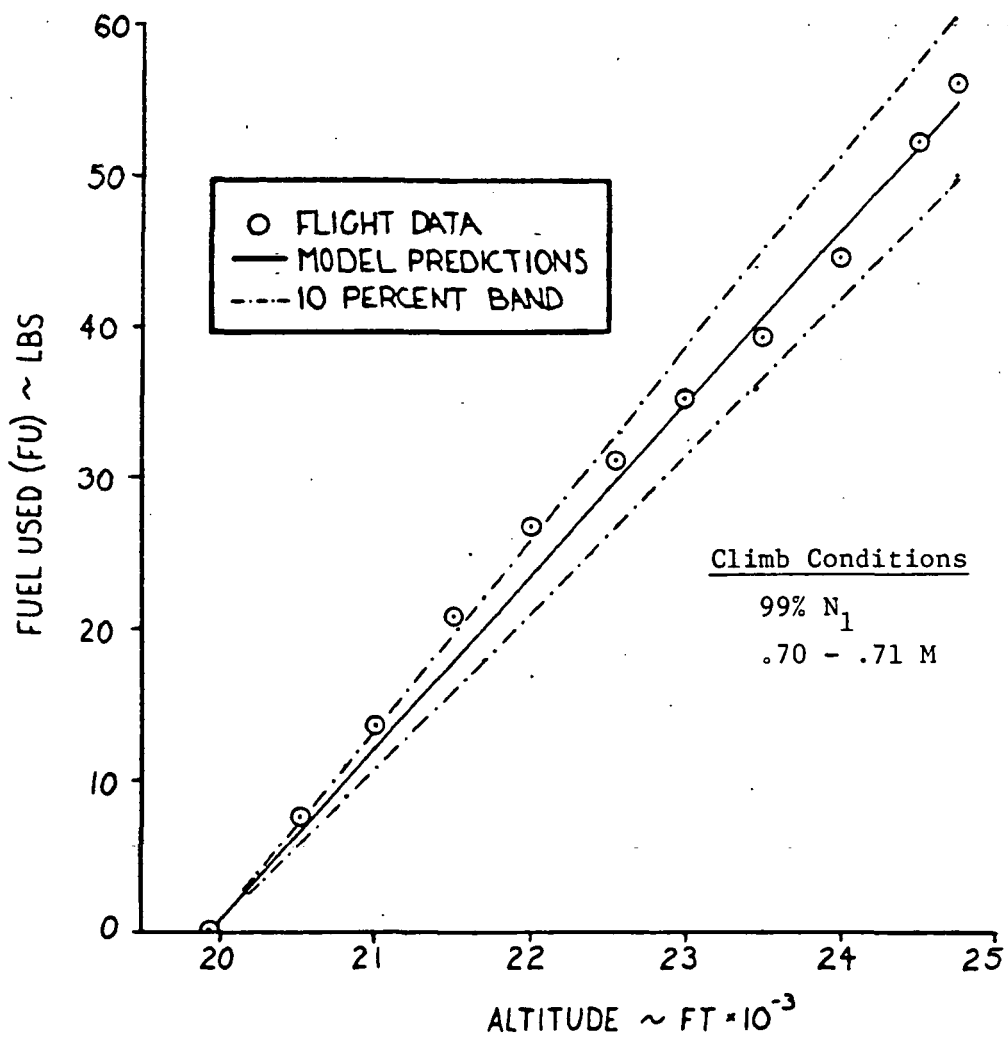


Figure 4.42 : MODEL Fuel Used Prediction, Profile 2

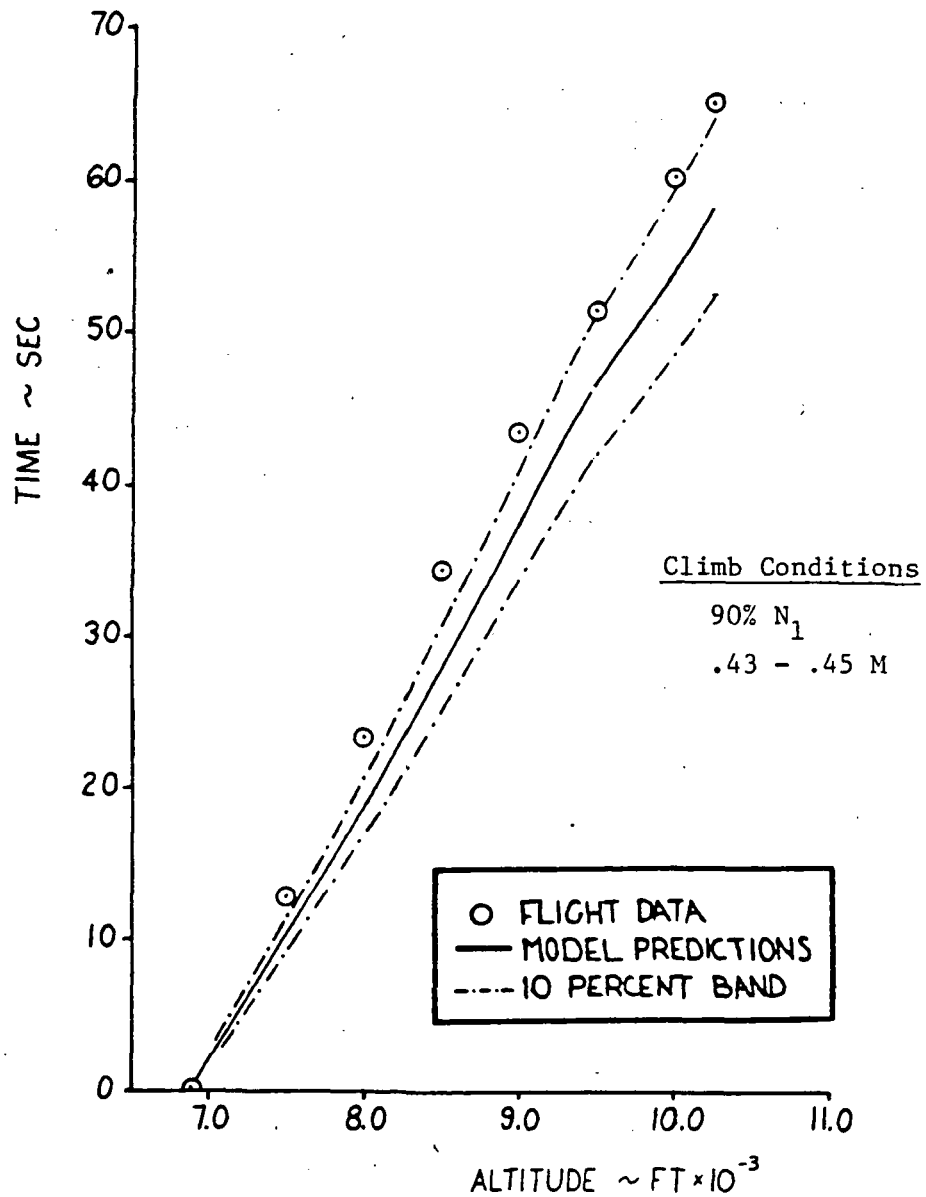


Figure 4.43: MODEL Time Prediction, Profile 3

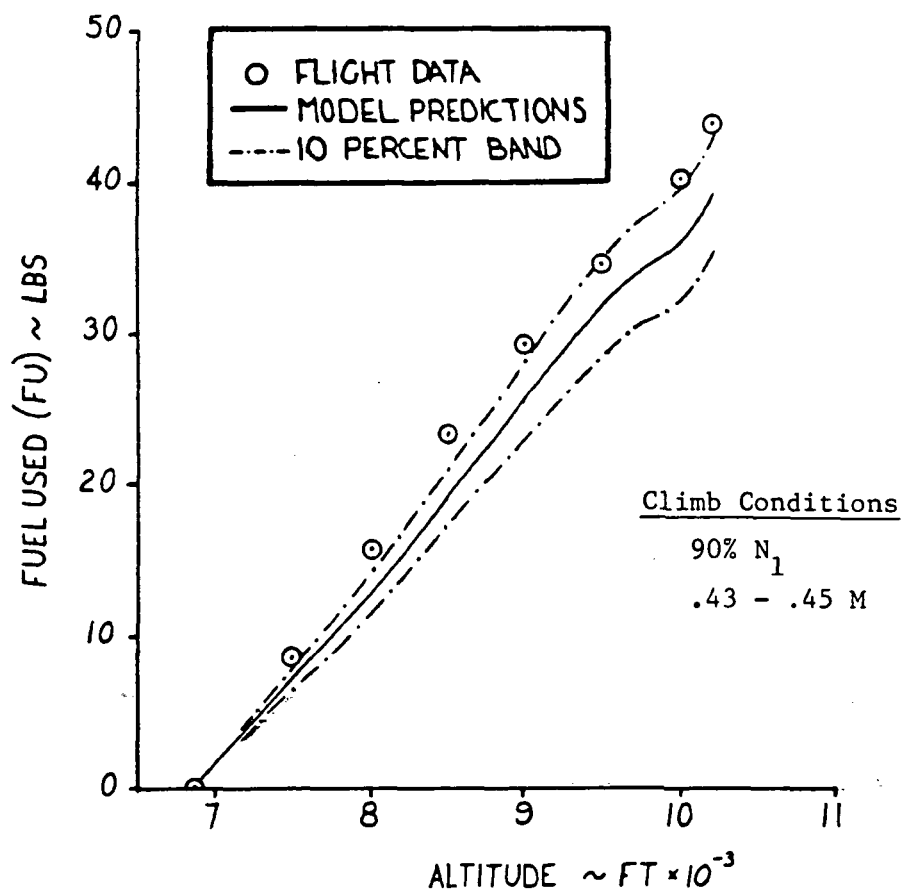


Figure 4.44 : MODEL Fuel Used Prediction, Profile 3

4.4.2.2 Accelerations/Decelerations

MODEL predictions for time, fuel used and specific excess power (P_s) as a function of Mach are presented in Figures 4.45 through 4.50 for two accel/decel profiles. These profiles represented approximately a "best" and "worst" case condition with the remaining accel/decel data plots presented in Appendix I. As with the climbs, actual in-flight data are shown with symbols. The majority of the in-flight data fell within 10 percent of the MODEL predictions with the worst case being a 26.6% error for P_s on Profile 7 (Figure 4.50). On this particular run, the maximum absolute error for P_s was approximately 4.8 ft/sec; and the large percentage error resulted due to the relatively low absolute magnitude of P_s (18 ft/sec) for this low speed flight condition. In addition, the baseline engine characteristics for this run were extrapolated, since the lowest Mach number for which baseline engine curves were defined was 0.3 and the actual test was conducted from .27 to .29 Mach. As with the climb trajectories, better agreement was hoped for; but the same sources of error identified in Section 4.4.2.1 were present. The acceleration and deceleration prediction results reemphasize the fact that actual profiles should still be flown for selected conditions to establish the correlation associated with a particular program. If the agreement between modeling predictions and flight data is acceptable, then a wide range of flight profiles may be modeled.

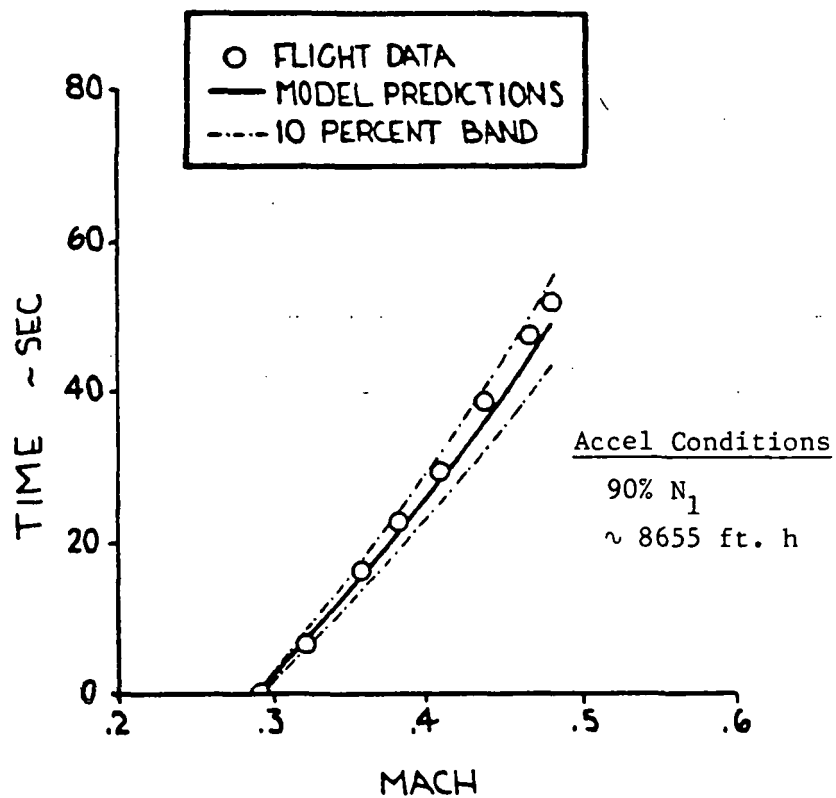


Figure 4.45: MODEL Time Prediction, Profile 6

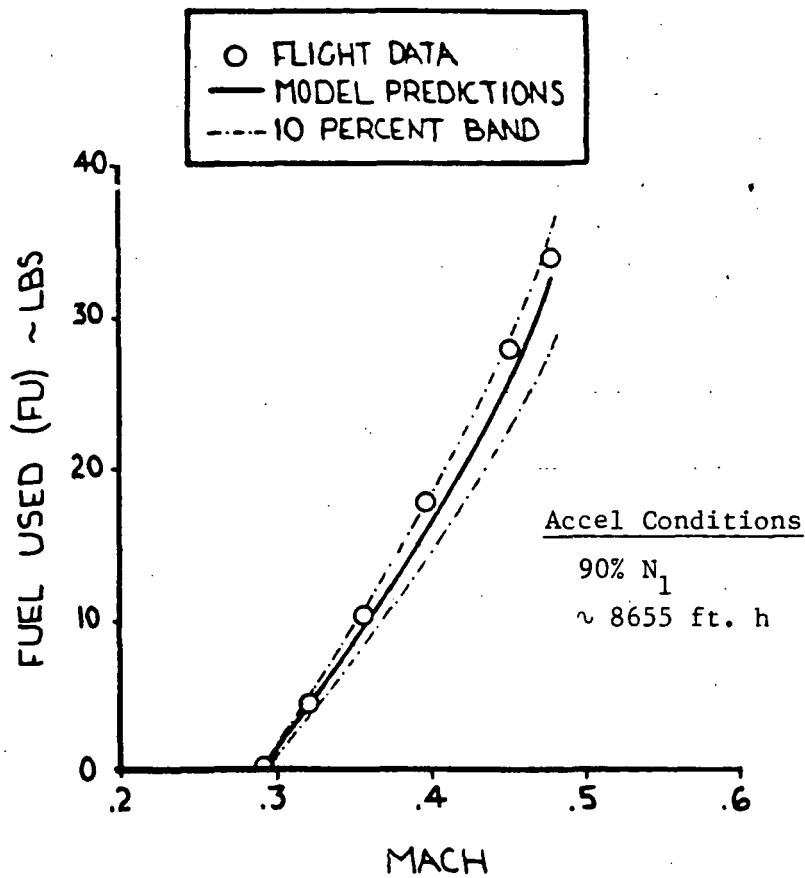


Figure 4.46: MODEL Fuel Used Prediction, Profile 6

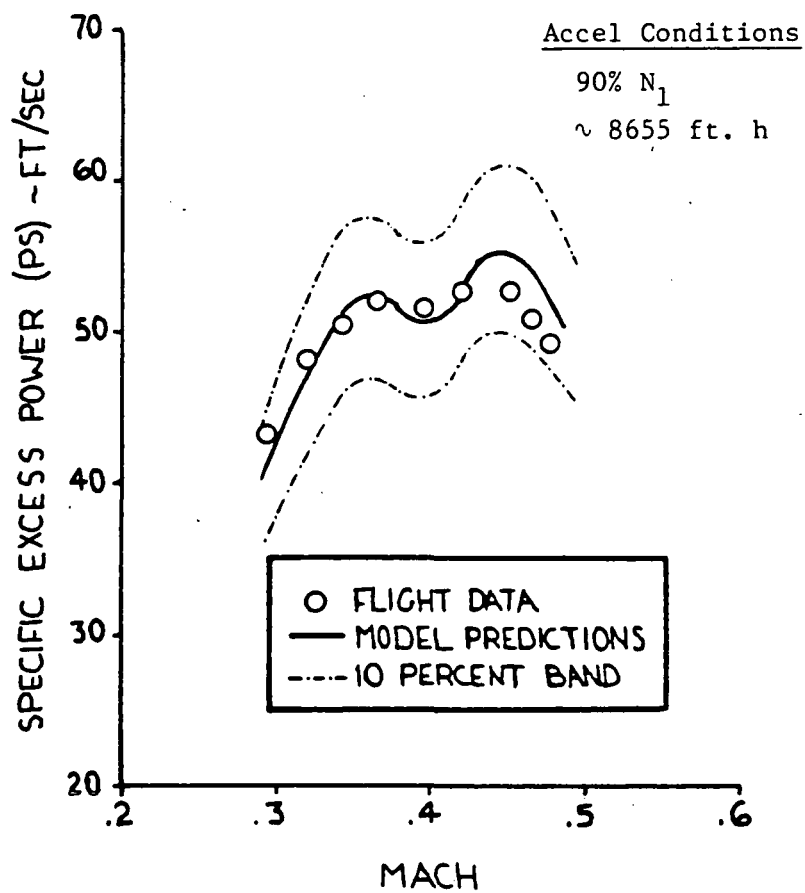


Figure 4.47: MODEL P_s Prediction, Profile 6

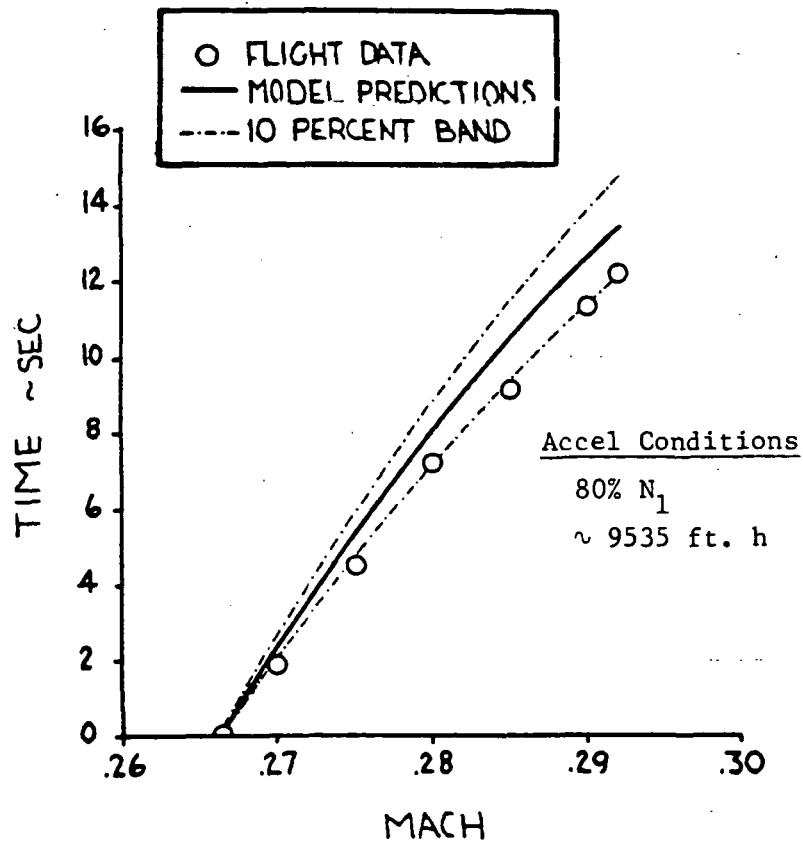


Figure 4.48: MODEL Time Prediction, Profile 7

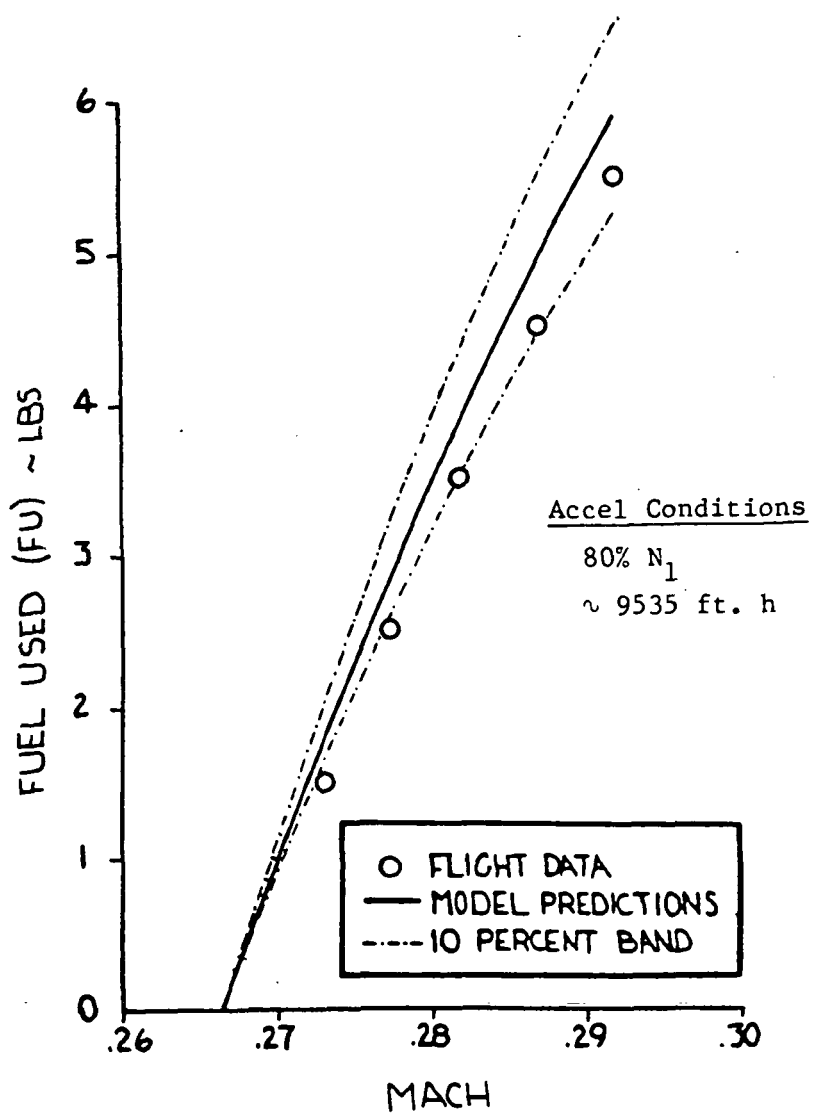


Figure 4.49: MODEL Fuel Used Prediction, Profile 7

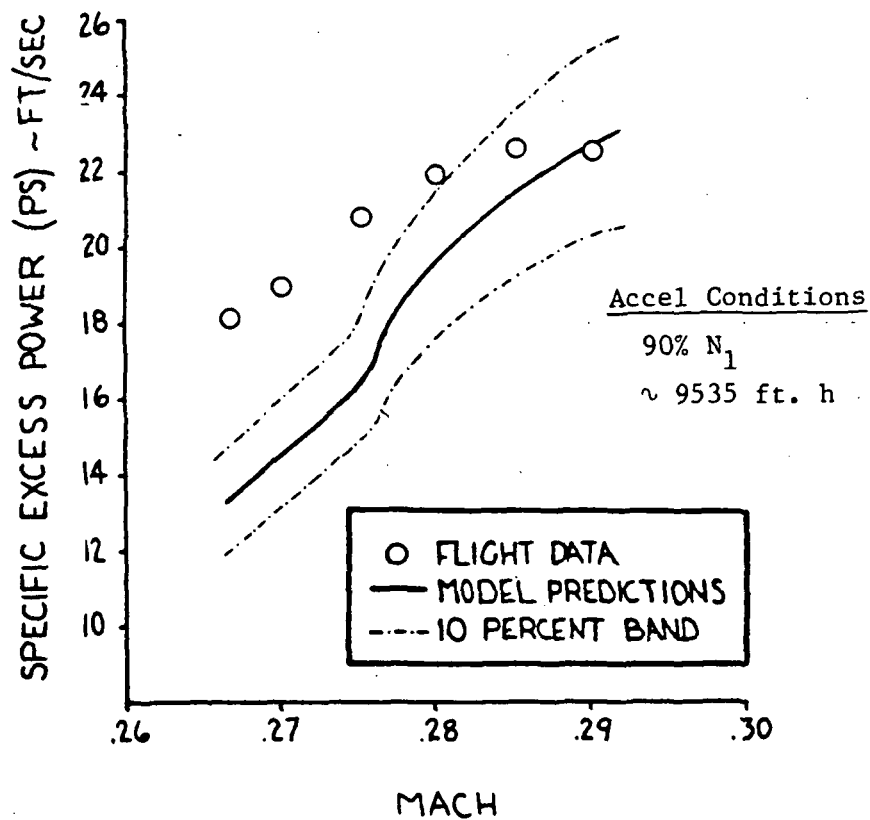


Figure 4.50: MODEL P_s Prediction, Profile 7

4.5 ERROR ANALYSIS

Results of the phase one error analysis as described in Section 3.2.5 are presented in Tables 15 through 26. The largest relative and absolute errors for lift coefficient resulting from a one percent error were found for $n_{z_{body}}$ and dynamic pressure which were approximately one percent and .008, respectively. For drag coefficient, fairly large relative errors were present for all the instrumentation parameters evaluated except total temperature, due to the small absolute value of C_{D_S} . In terms of drag counts, the maximum absolute error showed that angle of attack, $n_{x_{body}}$ and $n_{z_{body}}$ had the largest effect with a maximum absolute error of approximately 15 counts. Static pressure, N_1 , W_f and dynamic pressure had a significant effect on corrected and uncorrected thrust with a maximum relative error of 1.8 percent and a maximum absolute error of 109 pounds, resulting from static pressure on corrected thrust. The same instrumentation parameters had a significant effect on corrected and uncorrected airflow. A maximum relative error of 1.75 percent on corrected airflow resulted from static pressure, and a maximum absolute error of 3.33 lbs/sec resulted from N_1 . Careful review of Tables 15 through 26 will provide identification of the relative impact that a one percent error in each instrumentation variable had on baseline aerodynamic/engine characteristics.

Results of the phase two error analysis are presented in Table 27. The actual transducer accuracies available during the program for the most critical instrumentation parameters were used to estimate the relative and absolute errors associated with this program. For

lift coefficient, $n_{z_{body}}$ had the largest relative and absolute error of .525 percent and .004, respectively. The largest error contribution to drag coefficient was angle of attack, which had a relative and absolute error of 1.86 percent and 14 drag counts, respectively. The influence of fuel flow, longitudinal acceleration and vertical acceleration was also significant. Fuel flow was the primary source of error for the engine parameters as seen from the table.

Several conclusions may be drawn from the error analysis. The high quality static and dynamic pressure transducers used during the program greatly reduced the error potential of these two instrumentation parameters as identified in the phase one analysis. Accelerometers with at least the accuracy of those used during this program are important to keeping the resulting errors within acceptable levels. Angle of attack was the most critical parameter affecting drag even though its accuracy was considered the best available within the state of the art. A maximum absolute error of 14 drag counts resulted from an accuracy of $\pm 1^\circ$. As a result, considerable attention must be given to the accuracy of the angle of attack measurement when using the performance modeling approach. Fuel flow was also identified as a critical parameter, especially for the engine characteristics. As with angle of attack, the fuel flow accuracy of ± 10 lbs/hr was considered near the state of the art for a fuel flow transducer with the appropriate range needed in this program. When using the thrust and airflow prediction technique developed in this program (Section 3.2.1.2), the accuracy of the fuel flow transducer will probably determine the maximum prediction error and consequently high quality transducers are necessary to

the overall success of the technique. The engine RPM accuracy of $\pm 0.2\%$ was easily obtainable with standard "off-the-shelf" transducers and was sufficient to minimize the resulting errors on baseline characteristics. When establishing instrumentation requirements for an overall performance modeling flight test program, Tables 15 through 27 should be reviewed carefully. One limitation should be realized when attempting to project this analysis to another program. All of the error cases were evaluated within the Lear 35 performance envelope. The numerical results may change somewhat based on an expanded or contracted performance envelope, but the critical parameters identified should remain approximately the same.



Table 15: Maximum Relative Error Analysis for Lift Coefficient (C_{L_s})

PARAMETER VARIED	MAX RELATIVE ERROR (%)	ASSOCIATED ABSOLUTE ERROR	VALUE OF PARAMETER VARIED	FLIGHT CONDITION		
				$\frac{W}{\delta}$ (lbs)	MANEUVER	M
N_{1L}	.01	$.22 \times 10^{-4}$	95%	22000	95% Accel	.6
N_{1R}	.01	$.22 \times 10^{-4}$	95%	22000	95% Accel	.6
W_{fL}	.02	$.1 \times 10^{-3}$	$1474 \frac{\text{lbs}}{\text{hr}}$	22000	95% Accel	.33
W_{fR}	.02	$.1 \times 10^{-3}$	$1474 \frac{\text{lbs}}{\text{hr}}$	22000	95% Accel	.33
$n_{x_{\text{body}}}$.03	$.14 \times 10^{-3}$.27 g	22000	95% Accel	.33
$n_{z_{\text{body}}}$	1.01	$.52 \times 10^{-2}$.96 g	22000	95% Accel	.33
α	.03	$.2 \times 10^{-3}$	8.5°	60000	95% Accel	.48
Static Pressure	.14	$.37 \times 10^{-3}$	3.93 psi	60000	95% Accel	.79
Dynamic Pressure	.98	$.78 \times 10^{-2}$.54 psi	22000	50% Decel	.27
Total Temperature	<.001	$< 10^{-5}$				

Table 16: Maximum Absolute Error Analysis for Lift Coefficient (C_{L_s})

PARAMETER VARIED	MAX ABSOLUTE ERROR	ASSOCIATED RELATIVE ERROR (%)	VALUE OF PARAMETER VARIED	FLIGHT CONDITION		
				$\frac{W}{\delta}$ (lbs)	MANEUVER	M
N_{1L}	$.77 \times 10^{-4}$.01	95.8%	60000	95% Accel	.48
N_{1R}	$.52 \times 10^{-4}$.01	95.1%	60000	95% Accel	.48
W_{fL}	$.1 \times 10^{-3}$.01	$737 \frac{\text{lbs}}{\text{hr}}$	60000	95% Accel	.48
W_{fR}	$.1 \times 10^{-3}$.02	$1474 \frac{\text{lbs}}{\text{hr}}$	22000	95% Accel	.33
$n_{x_{\text{body}}}$	$.14 \times 10^{-3}$.03	.27 g	22000	95% Accel	.33
$n_{z_{\text{body}}}$	$.803 \times 10^{-2}$	1.00	1.005 g	22000	50% Decel	.27
α	$.2 \times 10^{-3}$.03	8.5°	60000	95% Accel	.48
Static Pressure	$.375 \times 10^{-3}$.06	3.55 psi	60000	80% Accel	.5
Dynamic Pressure	$.785 \times 10^{-2}$.98	.54 psi	22000	50% Decel	.27
Total Temperature	$< 10^{-5}$	$< .001$				

Table 17: Maximum Relative Error Analysis for Drag Coefficient (C_{D_s})

PARAMETER VARIED	MAX RELATIVE ERROR (%)	ASSOCIATED ABSOLUTE ERROR	VALUE OF PARAMETER VARIED	FLIGHT CONDITION		
				$\frac{W}{\delta}$ (lbs)	MANEUVER	M
N_{1L}	.57	$.133 \times 10^{-3}$	51%	22000	50% Decel	.55
N_{1R}	.58	$.137 \times 10^{-3}$	50.5%	22000	50% Decel	.55
W_{fL}	1.65	$.75 \times 10^{-3}$	$1474 \frac{\text{lbs}}{\text{hr}}$	22000	95% Accel	.33
W_{fR}	1.4	$.8 \times 10^{-3}$	$1508 \frac{\text{lbs}}{\text{hr}}$	22000	95% Accel	.33
$n_{x_{\text{body}}}$	3.4	$.15 \times 10^{-2}$.27 g	22000	95% Accel	.33
$n_{z_{\text{body}}}$	1.65	$.128 \times 10^{-2}$	1.008 g	22000	50% Decel	.27
α	1.82	$.137 \times 10^{-2}$	9.8°	22000	50% Decel	.27
Static Pressure	.6	$.28 \times 10^{-3}$	10.65 psi	22000	95% Accel	.33
Dynamic Pressure	1.4	$.7 \times 10^{-3}$	1.1 psi	22000	95% Accel	.33
Total Temperature	.10	5.88×10^{-4}	-48.3°C	60000	80% Decel	.5

178

Table 18: Maximum Absolute Error Analysis for Drag Coefficient (C_{D_s})

PARAMETER VARIED	MAX ABSOLUTE ERROR	ASSOCIATED RELATIVE ERROR (%)	VALUE OF PARAMETER VARIED	FLIGHT CONDITION		
				$\frac{W}{\delta(1bs)}$	MANEUVER	M
N_{1L}	$.199 \times 10^{-3}$.33	83.2%	60000	80% Decel	.5
N_{1R}	$.201 \times 10^{-3}$.34	82.6%	60000	80% Decel	.5
W_{fL}	$.75 \times 10^{-3}$	1.65	$1474 \frac{lbs}{hr}$	22000	95% Accel	.33
W_{fR}	$.8 \times 10^{-3}$	1.4	$1508 \frac{lbs}{hr}$	22000	95% Accel	.33
$n_{x_{body}}$	$.15 \times 10^{-2}$	3.4	.27 g	22000	95% Accel	.33
$n_{z_{body}}$	$.128 \times 10^{-2}$	1.65	1.008 g	22000	50% Decel	.27
α	$.137 \times 10^{-2}$	1.82	9.8°	22000	50% Decel	.33
Static Pressure	$.28 \times 10^{-3}$.6	10.65 psi	22000	95% Accel	.33
Dynamic Pressure	$.84 \times 10^{-3}$	1.1	.62 psi	60000	95% Accel	.48
Total Temperature	$.588 \times 10^{-4}$.10	$-48.3^\circ C$	60000	80% Decel	.5

Table 19: Maximum Relative Error Analysis for Corrected Gross Thrust $\left(\frac{F}{\delta t_2}\right)$

PARAMETER VARIED	MAX RELATIVE ERROR (%)	ASSOCIATED ABSOLUTE ERROR	VALUE OF PARAMETER VARIED	FLIGHT CONDITION		
				$\frac{W}{\delta}$ (lbs)	MANEUVER	M
N_{1L}	1.1	26.5 lbs	52%	22000	50% Decel	.55
N_{1R}	1.13	27 lbs	50.5%	22000	50% Decel	.55
W_{fL}	.55	12.2 lbs	$278 \frac{\text{lbs}}{\text{hr}}$	22000	50% Decel	.55
W_{fR}	.52	43 lbs	$442 \frac{\text{lbs}}{\text{hr}}$	60000	80% Decel	.72
Static Pressure	1.8	42 lbs	10.76 psi	22000	50% Decel	.55
Dynamic Pressure	.8	20 lbs	2.3 psi	22000	50% Decel	.55
Total Temperature	.022	1.8 lbs	36.4°	60000	80% Decel	.72

Table 20: Maximum Absolute Error Analysis for Corrected Gross Thrust $\left(\frac{F}{\delta t_2}\right)$

PARAMETER VARIED	MAX ABSOLUTE ERROR	ASSOCIATED RELATIVE ERROR (%)	VALUE OF PARAMETER VARIED	FLIGHT CONDITION		
				$\frac{W}{\delta}$ (lbs)	MANEUVER	M
N_{1L}	79 lbs	.67	95.4%	60000	95% Accel	.79
N_{1R}	74.5 lbs	.64	94.9%	60000	95% Accel	.79
W_{fL}	58 lbs	.50	788 $\frac{\text{lbs}}{\text{hr}}$	60000	95% Accel	.79
W_{fR}	58.2 lbs	.50	785 $\frac{\text{lbs}}{\text{hr}}$	60000	95% Accel	.79
Static Pressure	109 lbs	.95	3.87 psi	60000	95% Accel	.48
Dynamic Pressure	20 lbs	.80	2.3 psi	22000	50% Decel	.55
Total Temperature	1.8 lbs	.02	36.4°	60000	80% Decel	.72

Table 21: Maximum Relative Error Analysis for Corrected Airflow $(\frac{W_a \sqrt{\theta_{t_2}}}{\delta_{t_2}})$

PARAMETER VARIED	MAX RELATIVE ERROR (%)	ASSOCIATED ABSOLUTE ERROR	VALUE OF PARAMETER VARIED	FLIGHT CONDITION		
				$\frac{W}{\delta}$ (lbs)	MANEUVER	M
N_{1L}	1.65	$2.1 \frac{\text{lbs}}{\text{sec}}$	52%	22000	50% Decel	.55
N_{1R}	1.68	$2.15 \frac{\text{lbs}}{\text{sec}}$	50.5%	22000	50% Decel	.54
W_{fL}	.54	$.634 \frac{\text{lbs}}{\text{sec}}$	$268 \frac{\text{lbs}}{\text{hr}}$	22000	50% Decel	.55
W_{fR}	.52	$1.16 \frac{\text{lbs}}{\text{sec}}$	$456 \frac{\text{lbs}}{\text{hr}}$	60000	80% Decel	.72
Static Pressure	1.75	$2.2 \frac{\text{lbs}}{\text{sec}}$	10.76 psi	22000	50% Decel	.55
Dynamic Pressure	.8	$1.1 \frac{\text{lbs}}{\text{sec}}$	2.3 psi	22000	50% Decel	.55
Total Temperature	.08	$.217 \frac{\text{lbs}}{\text{sec}}$	45.2°	60000	95% Accel	.5

Table 22: Maximum Absolute Error Analysis for Corrected Airflow $(\frac{W_a \sqrt{\theta} t_2}{\delta t_2})$

PARAMETER VARIED	MAX ABSOLUTE ERROR	ASSOCIATED RELATIVE ERROR (%)	VALUE OF PARAMETER VARIED	FLIGHT CONDITION		
				$\frac{W}{\delta}$ (lbs)	MANEUVER	M
N_{1L}	$3.33 \frac{\text{lbs}}{\text{sec}}$	1.26	95.5%	60000	95% Accel	.5
N_{1R}	$3.28 \frac{\text{lbs}}{\text{sec}}$	1.24	95.5%	60000	95% Accel	.51
W_{fL}	$1.37 \frac{\text{lbs}}{\text{sec}}$.50	$724 \frac{\text{lbs}}{\text{hr}}$	60000	95% Accel	.48
W_{fR}	$1.36 \frac{\text{lbs}}{\text{sec}}$.5	$704 \frac{\text{lbs}}{\text{hr}}$	60000	95% Accel	.48
Static Pressure	$2.2 \frac{\text{lbs}}{\text{sec}}$	1.75	10.76 psi	22000	50% Decel	.55
Dynamic Pressure	$1.1 \frac{\text{lbs}}{\text{sec}}$.8	2.3 psi	22000	50% Decel	.55
Total Temperature	$.217 \frac{\text{lbs}}{\text{sec}}$.08	45.2°	60000	95% Accel	.5

Table 23: Maximum Relative Error Analysis for Gross Thrust (F_g)

PARAMETER VARIED	MAX RELATIVE ERROR (%)	ASSOCIATED ABSOLUTE ERROR	VALUE OF PARAMETER VARIED	FLIGHT CONDITION		
				$\frac{W}{\delta}$ (lbs)	MANEUVER	M
N_{1L}	.75	33.7 lbs	95.4%	60000	95% Accel	.79
N_{1R}	.8	16.5 lbs	52%	22000	50% Decel	.55
W_{fL}	.55	10.8 lbs	268 $\frac{\text{lbs}}{\text{hr}}$	22000	50% Decel	.55
W_{fR}	.52	14.7 lbs	456 $\frac{\text{lbs}}{\text{sec}}$	60000	80% Decel	.72
Static Pressure	1.0	20 lbs	10.76 psi	22000	50% Decel	.55
Dynamic Pressure	1.1	22 lbs	2.25 psi	22000	50% Decel	.53
Total Temperature	.02	.65 lbs	36.7°	60000	80% Decel	.72

Table 24: Maximum Absolute Error Analysis for Gross Thrust (F_g)

PARAMETER VARIED	MAX ABSOLUTE ERROR	ASSOCIATED RELATIVE ERROR (%)	VALUE OF PARAMETER VARIED	FLIGHT CONDITION		
				$\frac{W}{\delta}$ (lbs)	MANEUVER	M
N_{1L}	39 lbs	.48	95.5%	22000	95% Accel	.6
N_{1R}	40 lbs	.48	95.0%	22000	95% Accel	.6
W_{fL}	42 lbs	.5	1474 $\frac{\text{lbs}}{\text{hr}}$	22000	95% Accel	.6
W_{fR}	42 lbs	.50	1494 $\frac{\text{lbs}}{\text{hr}}$	22000	95% Accel	.6
Static Pressure	20 lbs	1.0	10.76 psi	22000	50% Accel	.55
Dynamic Pressure	28 lbs	.33	2.5 psi	22000	95% Accel	.6
Total Temperature	.65 lbs	.02	36.7°	60000	80% Decel	.72

Table 25: Maximum Relative Error Analysis for Airflow (W_a)

PARAMETER VARIED	MAX RELATIVE ERROR (%)	ASSOCIATED ABSOLUTE ERROR	VALUE OF PARAMETER VARIED	FLIGHT CONDITION		
				$\frac{W}{\delta}$ (lbs)	MANEUVER	M
N_{1L}	1.42	$1.48 \frac{\text{lbs}}{\text{sec}}$	95.4%	60000	95% Accel	.79
N_{1R}	1.38	$1.44 \frac{\text{lbs}}{\text{sec}}$	94.9%	60000	95% Accel	.79
W_{fL}	.54	$.58 \frac{\text{lbs}}{\text{sec}}$	$268 \frac{\text{lbs}}{\text{hr}}$	22000	50% Decel	.55
W_{fR}	.52	$.437 \frac{\text{lbs}}{\text{sec}}$	$449 \frac{\text{lbs}}{\text{hr}}$	60000	80% Decel	.72
Static Pressure	1.0	$1.1 \frac{\text{lbs}}{\text{sec}}$	10.76 psi	22000	50% Decel	.53
Dynamic Pressure	.95	$1.2 \frac{\text{lbs}}{\text{sec}}$	2.3 psi	22000	50% Decel	.53
Total Temperature	.03	$.031 \frac{\text{lbs}}{\text{sec}}$	44.8°	60000	95% Accel	.5

Table 26: Maximum Absolute Error Analysis for Airflow (W_a)

PARAMETER VARIED	MAX ABSOLUTE ERROR	ASSOCIATED RELATIVE ERROR (%)	VALUE OF PARAMETER VARIED	FLIGHT CONDITION		
				$\frac{W}{\delta}$ (lbs)	MANEUVER	M
N_{1L}	2.4	1.07	95%	22000	95% Accel	.6
N_{1R}	2.48	1.16	95%	22000	95% Accel	.6
W_{fL}	1.06	.50	1474 $\frac{\text{lbs}}{\text{hr}}$	22000	95% Accel	.6
W_{fR}	1.07	.50	1508 $\frac{\text{lbs}}{\text{hr}}$	22000	95% Accel	.6
Static Pressure	1.1 $\frac{\text{lbs}}{\text{sec}}$	1.0	10.76 psi	22000	50% Decel	.53
Dynamic Pressure	1.2 $\frac{\text{lbs}}{\text{sec}}$.95	2.3 psi	22000	50% Decel	.53
Total Temperature	.031 $\frac{\text{lbs}}{\text{sec}}$.03	44.8°	60000	95% Accel	.5

Table 27: Error Analysis Summary Based on Instrumentation Accuracy

BASELINE PARAMETER	MOST CRITICAL PARAMETER	SYSTEM ACCURACY	MAX RELATIVE ERROR (%)	ASSOC ABS ERROR	MAX ABS ERROR	ASSOC RELATIVE ERROR (%)
C_{L_s}	n_{z_body}	$\pm .005 \text{ g}$.525	$.271 \times 10^{-2}$	$.4 \times 10^{-2}$.496
	Dynamic pressure	$\pm .002 \text{ psi}$.364	$.291 \times 10^{-2}$	$.291 \times 10^{-2}$.364
C_{D_s}	W_f	$\pm 10 \frac{\text{lbs}}{\text{hr}}$	1.12	$.051 \times 10^{-2}$	$.051 \times 10^{-2}$	1.12
	n_{z_body}	$\pm .001 \text{ g}$	1.26	$.056 \times 10^{-2}$	$.056 \times 10^{-2}$	1.26
	n_{z_body}	$\pm .005 \text{ g}$.818	$.063 \times 10^{-2}$	$.063 \times 10^{-2}$.818
	α	$\pm .1^\circ$	1.86	$.14 \times 10^{-2}$	$.14 \times 10^{-2}$	1.86
	Dynamic pressure	$\pm .002 \text{ psi}$.355	$.027 \times 10^{-2}$	$.027 \times 10^{-2}$.355
$\frac{F_R}{\delta t_2}$	N_1	$\pm .2\%$.448	10.7 lbs	16.56 lbs	.14
	W_f	$\pm 10 \frac{\text{lbs}}{\text{hr}}$	1.97	43.9 lbs	73.6 lbs	.64
	Static pressure	$\pm .00075 \text{ psi}$.012	0.29 lbs	2.11 lbs	.018
	Dynamic pressure	$\pm .002 \text{ psi}$.07	1.74 lbs	1.74 lbs	.07
$\frac{W_s \sqrt{\delta t_2}}{\delta t_2}$	N_1	$\pm .2\%$.665	$.85 \frac{\text{lbs}}{\text{sec}}$	$.85 \frac{\text{lbs}}{\text{sec}}$.665
	W_f	$\pm 10 \frac{\text{lbs}}{\text{hr}}$	2.01	$2.37 \frac{\text{lbs}}{\text{sec}}$	$2.37 \frac{\text{lbs}}{\text{sec}}$	2.01
	Static pressure	$\pm .00075 \text{ psi}$.012	$.015 \frac{\text{lbs}}{\text{sec}}$	$.015 \frac{\text{lbs}}{\text{sec}}$.012
	Dynamic pressure	$\pm .001$.07	$.096 \frac{\text{lbs}}{\text{sec}}$	$.096 \frac{\text{lbs}}{\text{sec}}$.07
F_R	N_1	$\pm .2\%$.308	6.35 lbs	8.42 lbs	.101
	W_f	$\pm 10 \frac{\text{lbs}}{\text{hr}}$	2.05	40.3 lbs	40.3 lbs	2.05
	Static pressure	$\pm .00075 \text{ psi}$.007	0.139 lbs	.139 lbs	.007
	Dynamic pressure	$\pm .002$.098	1.96 lbs	2.24 lbs	.026
W_s	N_1	$\pm .2\%$.297	$.31 \frac{\text{lbs}}{\text{sec}}$	$.505 \frac{\text{lbs}}{\text{sec}}$.225
	W_f	$\pm 10 \frac{\text{lbs}}{\text{hr}}$	2.01	$2.16 \frac{\text{lbs}}{\text{sec}}$	$2.16 \frac{\text{lbs}}{\text{sec}}$	2.01
	Static pressure	$\pm .00075 \text{ psi}$.007	$.0077 \frac{\text{lbs}}{\text{sec}}$	$.0077 \frac{\text{lbs}}{\text{sec}}$.007
	Dynamic pressure	$\pm .002$.082	$.104 \frac{\text{lbs}}{\text{sec}}$	$.104 \frac{\text{lbs}}{\text{sec}}$.082

4.6 DATA REPEATABILITY

The entire maneuvering sequence for the 60000 W/δ case was repeated during the program to assess data repeatability. For the baseline aerodynamic characteristics, the data from each 60000 W/δ case easily fell within the scatter band experienced across all data and was usually in direct agreement with any slight variations explained by the variation of W/δ between flights. For example, a slightly higher W/δ on the repeated maneuver for a given Mach number and power setting would produce slightly higher lift and drag coefficients at a slightly higher angle of attack as would be expected. A slight variation of W/δ off the target test condition is normal due to the continuous weight change experienced during flight. The most important fact observed was that data from the repeated tests fell in line with the original data, and the same baseline curves would have been defined regardless of which test sequence was used. The same repeatability characteristics were found with the engine data. Slight variations were present, but these were easily explained due to temperature and pressure variations between flights. Again, the same baseline engine curves would have been defined regardless of which test sequence was used.

5. ESTIMATED FLIGHT TIME SAVINGS

One of the benefits of performance modeling is the amount of flight time saved in evaluating the performance characteristics of an aircraft when compared to conventional techniques. A significant amount of flight time will be saved for any program using performance modeling; however, the exact savings will depend on the particular aircraft characteristics and scope of the program along with the results of this effort. This program accomplished flight testing for both the conventional and performance modeling approaches so that the two methods could be compared. As a result, a considerable duplication of testing was included. To provide an estimate of the potential benefit, the flight time required to accomplish a conventional cruise/climb/accel performance evaluation on the Lear 35 was estimated and compared with the required flight time using performance modeling. Assumptions are clearly outlined. Two approaches using performance modeling are considered: first, a very conservative effort similar to that used in this program; and second, an approach typical of that expected for future programs.

Push-pull maneuvers are not included in the estimates for either the conventional or the performance modeling approaches, since they are typically added to either approach on an "as needed" basis. The modeling estimates include eight W/ δ performance modeling sequences, which is considered the minimum number to provide sufficient data throughout the Mach range. Flight trajectory profiles are not included in the estimates, since the correlation between modeling predictions and flight data must be established for a particular program.

5.1 CONVENTIONAL EVALUATION

Cruise

Assumptions:

1. Five W/ δ configurations required corresponding to the five nominal altitudes presented in Table 28.

Table 28: "Speed-Power" Estimate

<u>Nominal Altitude (ft)</u>	<u>S - P Points</u>	<u>S - P Time (min)</u>	<u>Increment Time (min)</u>	<u>Total (min)</u>
5000	18	72	51	123
15000	23	92	66	158
25000	19	76	54	130
35000	12	48	33	81
40000	8	32	21	<u>53</u>
				545 min =
				<u>9.08 hr</u>

2. Stabilized (four-minute) speed-power points required every 10-knot airspeed increment within the envelope (from buffet boundary to V_{\max} ; see Figure 3.3).
3. Three minutes required to increment from one stabilized point to the next.
4. Three flights required to accomplish the "speed power" points for an additional 45 minutes of takeoff, climb-out and return to base time. An additional 10 minutes will be required for two altitude changes during these flights.

"Speed Power" Estimate	545
Takeoff/Climb-Out/Return (15 minutes each flight)	45
2 Altitude Changes (5 minutes each change)	10
Total "Speed Power" Flight Time:	<hr/> 600 minutes.

Climb/Accel

Assumptions:

1. The same five nominal altitudes were used for level accels to evaluate specific excess power characteristics.
2. Three power settings were evaluated.
3. Each altitude evaluation required an average of 20 minutes.
4. One flight required.

Total Climb/Accel Time	100
Takeoff/Climb-Out/Return	15
4 Altitude Changes	20
Total Climb/Accel Flight Time:	<hr/> 135 minutes.

Total Conventional Flight Time = $600 + 135 = 735$ minutes
= 12.25 hours.

5.2 PERFORMANCE MODELING, APPROACH I (CONSERVATIVE)

Assumptions:

1. Eight W/ δ performance sequences
2. Four of the W/ δ sequences include five stabilized points each but no push-pull maneuvers.
3. Eight cardinal power settings evaluated.
4. Three flights required.

4 Sequences w/o stable points (45 mintes each)	180
4 Sequences w/stable points (80 minutes each)	320
Takeoff/Climb-Out/Return	45
5 Altitude Changes	25
Total:	<hr/> 570 minutes

Total Approach I Time = 570 minutes = 9.5 hours.

5.3 PERFORMANCE MODELING, APPROACH II (ANTICIPATED FOR FUTURE PROGRAMS)

Assumptions:

1. Eight W/ δ performance sequences
2. One of the W/ δ sequences includes five stabilized points
but no push-pull maneuvers.
3. Four cardinal power settings evaluated
4. Two flights required.

7 Sequences w/o stable points (25 minutes each)	175
1 Sequence w/stable points (60 minutes each)	60
Takeoff/Climb-Out/Return	30
6 Altitude Changes	30
Total:	295 minutes.

Total Approach II Time = 295 minutes = 4.92 hours.

5.4 PERCENT REDUCTION IN FLIGHT TIME

$$\text{Approach I: } \frac{12.25 - 9.5}{12.25} = \underline{22.4\%}.$$

$$\text{Approach II: } \frac{12.25 - 4.92}{12.25} = \underline{59.8\%}.$$

5.5 SUMMARY

The above estimates indicate that a reduction in flight time of between 22.4% and 59.8% can be expected when using the performance modeling approach. This reduction will result in considerable savings in the associated areas of calendar time, cost and manpower. Estimates of these savings are, of course, dependent on the particular factors affecting each individual program. Considerably more information is obtained with performance modeling than with the conventional approach. Definition of both Mach and power effects on the lift and drag coefficient characteristics along with the ability to model cruise and flight trajectory performance characteristics for the entire flight envelope are distinct advantages of performance modeling. Flight time estimates used in this section were based on the Lear 35 aircraft. A similar approach may be used for different aircraft with appropriate estimates for stable point requirements, takeoff/climb-out/return, etc., based on the aircraft envelope and performance characteristics.

6. FUTURE WORK

This program established the baseline concepts and techniques of the performance modeling approach to flight testing. These methods and applicable software were developed and verified to the extent that they have already been successfully used on several performance flight test programs for business jet class aircraft. Several additional areas surfaced during this program which would be worthwhile as objectives for future research. These include

- a. Follow-on evaluation of test engine performance characteristics in an altitude test cell facility to determine the correlation between the in-flight engine model defined using "Thrust Modeling" and the test cell results. The engines from an aircraft that had recently completed a performance modeling flight test program would be evaluated in a facility such as that at NASA Lewis to establish the accuracy of the engine model prediction technique used in the performance modeling approach.
- b. Expansion of performance modeling to the entire maneuvering flight envelope of the aircraft. This would involve additional emphasis on the push-pull maneuver and possibly definition and use of other maneuvers (i.e. the windup turn) to define aerodynamic characteristics for the entire range of angle of attack, Mach, and power. The MODEL program and AFFTC Performance Simulation Program currently have the capability to predict flight trajectory performance throughout

the maneuvering envelope of the aircraft given the expanded baseline characteristics. An ideal aircraft for the program would be a high performance fighter with a large "g" and Mach envelope.

- c. Development of a "real time" performance flight test data analysis capability using the performance modeling approach as the baseline. The performance modeling test approach and data reduction techniques developed in this program provided the needed tools to directly develop a "real time" analysis capability. Required efforts would include 1) cascading the existing data reduction software into one "straight through" program with appropriate logic and software modifications, 2) integration of the "real time" software with the flight test instrumentation system, 3) defining and developing "real time" display and test approach methodology, and 4) evaluation of the "real time" capability in a flight test program.
- d. Application of performance modeling to an aircraft with significant aeroelastic characteristics and a complex engine/nacelle including a variable geometry inlet and nozzle. An ideal aircraft would be a high performance fighter with well documented aerodynamic and structural influence coefficient matrices and a high Mach capability. In addition, an accurate engine prediction deck which included sound installation effect information would be needed.

7. CONCLUSIONS AND RECOMMENDATIONS

The most significant conclusions and recommendations resulting from this program are summarized in the following two subsections. Additional insight into a particular area may be gained by referring to the appropriate section of this report. Overall, all of the objectives and projected technology contributions established at the beginning of the program were satisfied or exceeded.



7.1 CONCLUSIONS

1. The performance modeling approach defined during this program provided a sound methodology for determining baseline aerodynamic and engine characteristics using exclusively quasi steady-state maneuvers.
2. The in-flight thrust and airflow prediction technique provided three principal advantages over methods used in the past:
 - a) Extensive engine instrumentation such as a tail pipe probe was not required.
 - b) The need for in-line engine deck computation as part of the flight data reduction software was eliminated.
 - c) An improvement in accuracy was achieved over methods which rely completely on engine deck predictions.
3. The most critical instrumentation parameters affecting definition of baseline aerodynamic and engine characteristics were identified using two approaches. First, for the one percent error case, angle of attack, body accelerations and dynamic pressure had the largest influence on aerodynamic characteristics. Engine characteristics were primarily affected by static pressure, fan RPM, fuel flow and dynamic pressure. Second, the actual transducer accuracies available during the program were used to identify the most critical instrumentation parameters. The body accelerations, angle of attack and fuel flow were identified as having the

largest error contributions for the aerodynamic characteristics. Fuel flow was the primary source of error for the engine characteristics. Since the instrumentation accuracies of the body accelerations, angle of attack and fuel flow were at or near state-of-the-art values, these parameters will probably have a significant influence on the errors associated with any performance modeling flight test effort.

4. The push-pull maneuver may be used to efficiently extend the angle of attack range during definition of selected baseline aerodynamic characteristics for a nonflexible aircraft if the appropriate corrections to measurement of angle of attack have been defined, such as boom bending and angular rate. The push-pull can definitely complement data obtained from accels and decels by serving as a cross-check and minimizing the uncertainty in extrapolating baseline curves. However, it is not well suited to initial identification of power and Mach effects on lift and drag characteristics due to the limited Mach variation experienced for each power setting.
5. The flight test maneuvers and methodology developed during this program were able to define the power as well as Mach and angle of attack effects on baseline aerodynamic characteristics. Significant power effects were identified for both lift and drag on the Learjet Model 35 aircraft and should be anticipated for any aircraft with jet engines mounted on the aft fuselage above the inboard wing section.

Definition of power effects is essential to accurate prediction of nonstabilized (i.e., excess thrust not equal to zero) performance characteristics such as in aircraft simulator applications.

6. Prediction of stabilized cruise performance characteristics agreed with flight data within 10 percent and was usually well within five percent. This determination was made by comparing the cruise predictions from ITERATE with actual stabilized point data. Since the error band associated with stabilized point data was approximately five percent, the ITERATE prediction correlation was considered good. In addition, since the baseline aerodynamic and engine characteristics used in ITERATE were defined from quasi steady-state maneuvers, greater emphasis on these time efficient maneuvers appears justified when compared to the stabilized point method for definition of cruise performance characteristics.
7. Prediction of flight trajectory performance characteristics generally agreed with flight data within 10 percent, but several of the comparisons between in-flight data points and performance modeling predictions were well in excess of 10 percent error with the worst case being a 26.6 percent discrepancy. Sources of error included abnormally high data scatter associated with definition of the baseline engine characteristics, wind effects and difficulty in modeling an actual in-flight trajectory subject to airspeed, altitude, power and temperature variations. Improved trajectory pre-

diction correlation with flight data is anticipated for future programs, but the degree of correlation should be established for each particular effort (see Recommendation 8).

8. A significant reduction in flight test time was projected when using the performance modeling approach compared to the more conventional stabilized point method. Estimates for the Learjet Model 35 aircraft showed a reduction in test time of between 22 and 60 percent. In addition, considerably more information was obtained from the performance modeling approach along with the ability to predict a nearly infinite number of cruise and flight trajectory conditions.

7.2 RECOMMENDATIONS

1. The number of cardinal power settings selected for a program should be based on the relative susceptibility of the particular aircraft configuration to power effects and the acceptable error associated with interpolating between cardinal power settings. It is anticipated that between four and eight cardinal power settings are adequate for most aircraft with significant flight time savings resulting from a lower number of settings.
2. A limited number of stabilized points should be included as part of any performance modeling flight test program as a check on overall data quality. The baseline aerodynamic and engine characteristics should be input to the ITERATE program so that stabilized point predictions can be made and compared with the actual stabilized point data.
3. A ground thrust run consisting of approximately 9 stabilized points for each engine across the RPM range should be accomplished to define the TSFC correction parameter, η , as part of the overall engine model development. The recommended thrust run procedure is similar to that accomplished on the Learjet Model 55 aircraft (Appendix F). Due to program constraints with the Model 35, only a five point thrust run was accomplished for each engine, which was considered barely adequate.

4. A flow field survey should be accomplished in the engine nacelle/wing root area of an aircraft such as the Learjet Model 35 with an overwing engine mounting to assist in understanding power effects on lift and drag characteristics. Flow tufting in this area would be an excellent first step. The Lear 35 would be an excellent aircraft for this work, since the power effects have been identified and documented as part of this program. The findings of such an effort could directly contribute to optimizing the engine location for aft fuselage mounted engine configuration during the initial aircraft design.
5. When selecting instrumentation transducers for a performance modeling flight test effort, results of the error analysis presented in Section 4.5 should be reviewed to assist in defining transducer accuracy. Special attention should be given to obtaining state-of-the-art accuracies for body accelerations, angle of attack and fuel flow, since these parameters were identified as critical during this program.
6. If the push-pull maneuver is used to complement data obtained from accels and decels, the accuracy of the angle of attack corrections such as boom bending and angular rate should be checked by comparing data from both types of maneuvers across the angle of attack range.
7. Future flight test programs using the performance modeling approach should include actual flight trajectory profiles

for selected conditions to establish the correlation associated with trajectory predictions. A comparison method similar to that used in this program is recommended. If acceptable agreement is established, then a wide range of flight profiles may be modeled with additional savings in flight time.

8. The areas identified in Chapter 6, Future Work, should be pursued in future research programs to extend application and definition of the performance modeling concept. These areas include 1) comparison of the in-flight engine model defined with "Thrust Modeling" to test cell results for the same engine(s), 2) expansion of performance modeling to include the entire maneuvering flight envelope of an aircraft, 3) development of a "real time" integrated performance flight test capability and 4) application of performance modeling to an aircraft with significant aeroelastic characteristics and a complex engine/nacelle.

8. REFERENCES

1. Marshall, Robert T., and Schweikhard, William G.: Modeling of Airplane Performance from Flight Test Results and Validation with an F-104G Airplane. NASA TN D-7137, 1973.
2. Redin, Paul C.: A Performance Model of the YF-12C Airplane. YF-12 Experiments Symposium, NASA CP-3054, Vol. 3, 1978, pp. 409-534.
3. Redin, Paul C.: Application of a Performance Modeling Technique to an Airplane with Variable Sweep Wings. NASA Technical Paper 1855, 1981.
4. Pihlgren, Wayne D.: Evaluation of Aircraft Predicted Performance Using Excess Thrust and Fuel Flow Modeling. AFFTC Flight Test Technology Branch Office Memo, 1981 (available from AFFTC/ENMT, Edwards AFB, California).
5. Yechout, T. R. and Braman, K. B.: Test Plan: Modeling of Aircraft Performance from Flight Test Results Using Quasi Steady-State Test Techniques. KU-FRL-577-1, The University of Kansas Center for Research, Inc., October 1982.
6. Simpson, William R.: The Accelerometer Methods of Obtaining Aircraft Performance from Flight Test Data. Professional Paper 245, Center for Naval Analysis, June 1979.
7. Schlichting H.: Boundary Layer Theory. McGraw-Hill, Inc., Sixth Edition, 1968.
8. Herrington, R. M., et al.: Flight Test Engineering Handbook. USAF Technical Report 6273, 1966.
9. Schweikhard, W. G. and Kohlman, D. L.: Flight Test Principles and Practices. University of Kansas, 1982.
10. Rawlings, Kenneth and Pritz, Wayne L.: Excess Thrust Modeling from Dynamic Maneuvers. SFTE Technical Paper (unnumbered), October 1978.
11. Olson, Wayne M.: An Aircraft Inflight Performance Simulation Computer Program. Performance and Flying Qualities Branch Office Memo, AFFTC, Edwards AFB, California, August 1979, revised July 1980 (available from AFFTC/ENFJ, Edwards AFB, California).
12. Roskam, Jan: Airplane Flight Dynamics and Automatic Flight Controls, Part II. Roskam Aviation and Engineering Corporation, Route 4, Box 274, Ottawa, Kansas 66067.

13. DeAnda, Albert G.: AFFTC Standard Airspeed Calibration, Procedures. AFFTC-TIH-68-1001, April 1966.
14. Renz, R. R. L. and Clarke, R.: A Literature Survey of Performance and Stability Flight Testing. University of Kansas Flight Research Lab report No. KU-FRL-407-1, July 1979.

APPENDIX A

SUPPORT ORGANIZATIONS

Several organizations played a direct role in the accomplishment of this program, as outlined in Figure A.1. A description of each organization's contribution to the overall program is presented here.

The Aeronautics Branch (OFA) in the Flight Support Division (OF) at NASA Ames-Dryden had responsibility for funding the development and analysis portion of the effort under NASA Grant NSG 4028. In addition, NASA Ames-Dryden provided Edwards AFB on-site facility support for calibrations. Mr. Paul Redin and Mr. F. W. Burcham (OFAP) were the project technical monitors of this grant.

The University of Kansas was responsible for overall technical development and program management. Professor William G. Schweikhard was the principal investigator for the project. Mr. Thomas R. Yechout (K.U. Doctor of Engineering Degree Candidate) was the principal research assistant/manager for the development and flight test efforts, and Mr. Keith B. Braman (K.U. Master of Engineering Degree Candidate) was responsible for the overall software area. The K.U. Honeywell 60/66 computer was used for initial development of the performance modeling software.

Kohlman Systems Research (KSR), Lawrence, Kansas, under Singer Corporation contract, provided the major portion of the computer time needed for software development and data analysis. A SEL 32/77 computer was used. KSR also provided personnel to assist with data reduction.

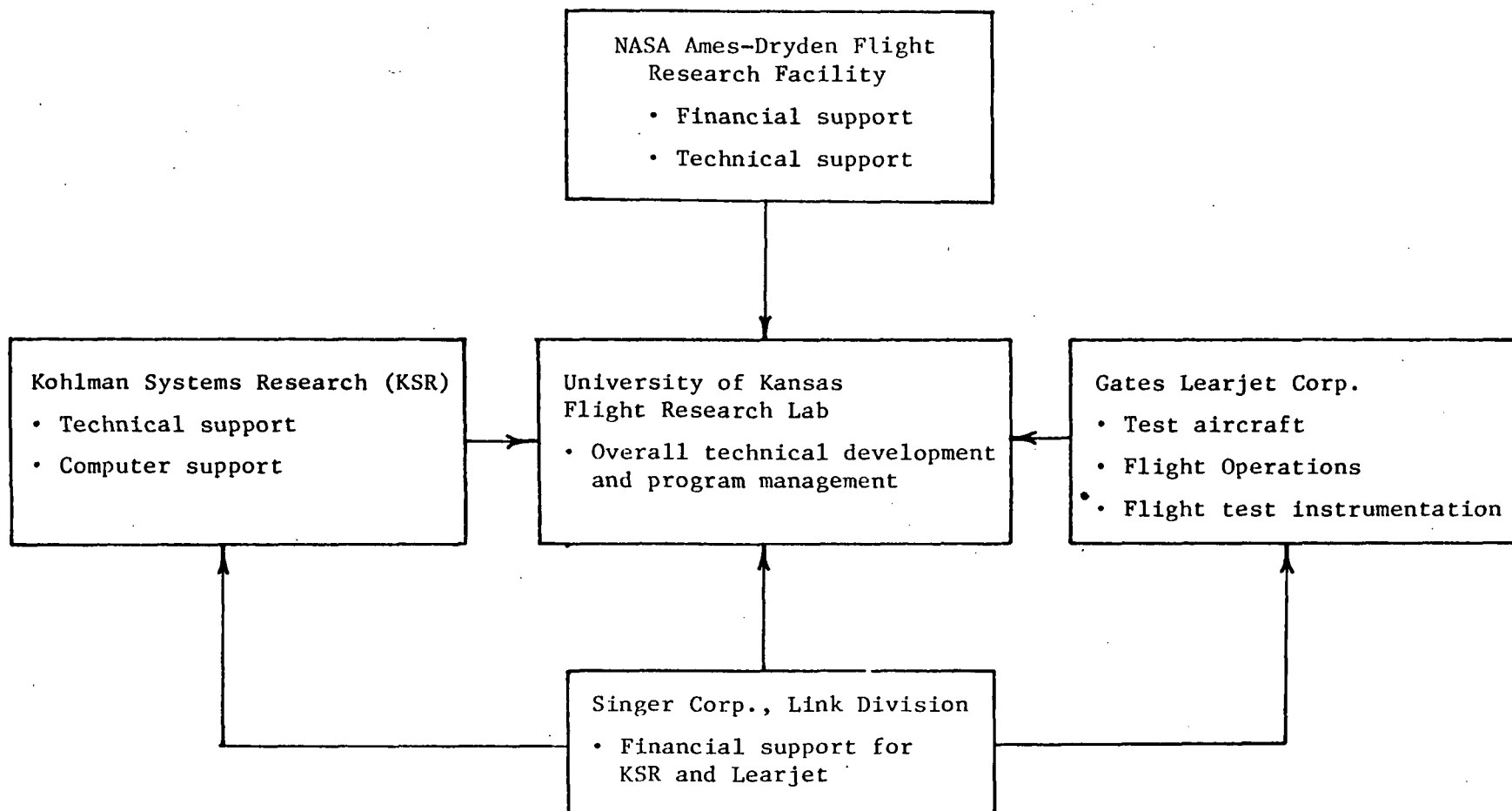


Figure A.1: Project Support Organization Chart

The Gates Learjet Corporation (GLC), Wichita, Kansas, under Singer Corporation contract, provided the test aircraft, instrumentation, and flight crew. Mr. Jim Dwyer was the GLC focal point for all flight operations during the program.

The Singer Corporation, Link Division, Binghamton, New York, funded the KSR and GLC efforts as part of an overall company program to define the flight characteristics of several general aviation aircraft for ground simulation applications. Mr. W. Day was the on-site Singer representative during the program.

The Air Force Flight Test Center, Edwards AFB, California and the Garrett Turbine Engine Company, Phoenix, Arizona also provided essential technical contributions to the overall effort.

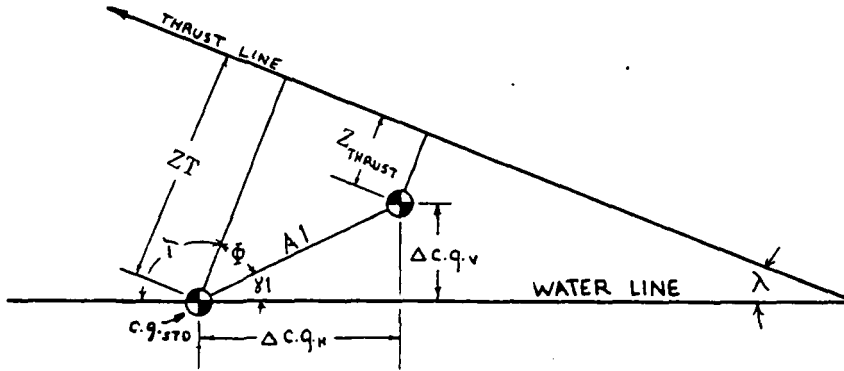
Page intentionally left blank

APPENDIX B

TRIGONOMETRIC RELATIONSHIPS FOR THRUST AND C.G. CORRECTIONS

The trigonometric relationships necessary to calculate Z_{thrust} , h_r , and ℓ_{tail} in Figure 3.5 will be presented.

1) Z_{thrust}



$$Al = \sqrt{\Delta c.g.H^2 + \Delta c.g.v^2}$$

$$\gamma_1 = \tan^{-1} \frac{\Delta c.g.v}{\Delta c.g.H}$$

ZT - known from
aircraft
geometry

$$\tau = 90^\circ + \lambda$$

$$\bar{\phi} = 180^\circ - \tau - \gamma_1 = 90^\circ - \lambda - \gamma_1$$

$$Z_{\text{thrust}} = ZT - Al \cos \bar{\phi}$$

$$\underline{Z_{\text{thrust}} = ZT - Al \sin(\lambda + \gamma_1)} \quad (\Delta c.g.H > 0)$$

If $\Delta c.g.H < 0$, then the geometry reduces to

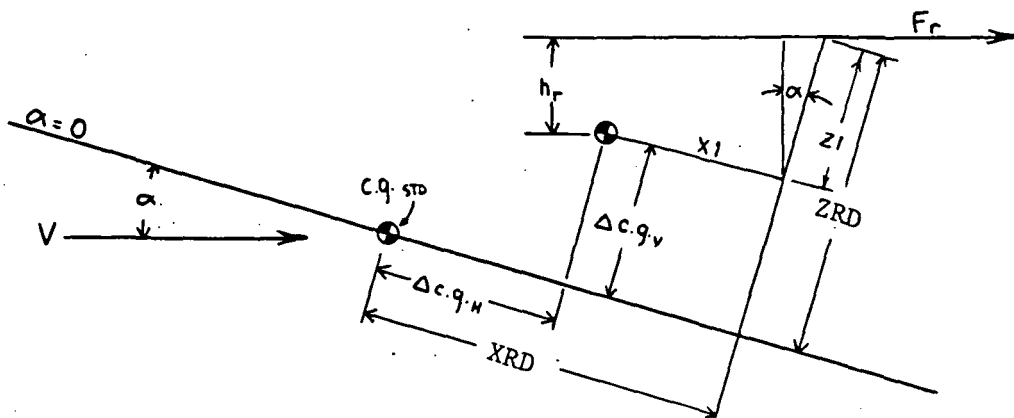
$$\underline{Z_{\text{thrust}} = ZT + Al \sin(\gamma_1 + \lambda)} \quad (\Delta c.g.H < 0)$$

If $\Delta c.g.$ equals zero, Z_{thrust} becomes

$$\underline{Z_{\text{thrust}} = ZT + Al \cos \lambda} \quad (\Delta c.g.v < 0)$$

$$\underline{Z_{\text{thrust}} = ZT - Al \cos \lambda} \quad (\Delta c.g.v > 0)$$

2) $\underline{h_r}$



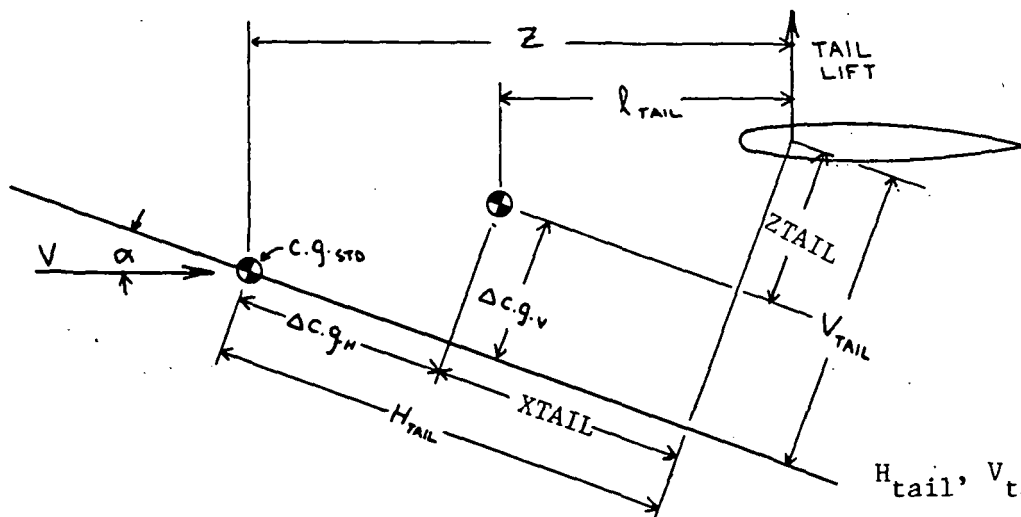
$$X1 = XRD - \Delta c.g.H$$

$$Z1 = ZRD - \Delta c.g.V$$

$$\underline{h_r = Z1 \cos \alpha - X1 \sin \alpha}$$

XRD, ZRD - known from aircraft geometry

3) $\underline{l_{tail}}$



H_{tail}, V_{tail} - known from aircraft geometry

(see next page)

$$XTAIL = H_{tail} - \Delta c.g._H$$

$$ZTAIL = V_{tail} - \Delta c.g._V$$

$$\underline{\ell_{tail} = XTAIL \cos \alpha + ZTAIL \sin \alpha}$$

4) $\Delta c.g. \rightarrow$ parallel to V

$$Z = H_{tail} \cos \alpha + V_{tail} \sin \alpha$$

$$\underline{\Delta c.g. = Z - \ell_{tail}}$$

Table B.1 presents the distances needed for the above calculations for the Lear 35 aircraft.

Table B.1: Lear 35 Thrust and C.G. Correction Distances

<u>Abbreviation</u>	<u>Distance (in)</u>
ZT	17.985
XRD	49.94
ZRD	17.11
H_{tail}	244.712
V_{tail}	80.635

Page intentionally left blank

APPENDIX C
SOFTWARE DOCUMENTATION

C.1 INTRODUCTION

The software development effort was divided into four areas. The first was concerned with the simplified representation of the engine manufactures prediction deck and development of the thrust run correction parameter, η . The second developed the algorithms needed for processing quasi steady-state performance data along with the analysis techniques for conventional performance maneuvers. The third area developed cruise and trajectory modeling techniques. Finally, a large number of utilities were written to aide in data analysis and processing for the overall program. The combined effort resulted in the development of over 30 programs and over 200 subroutines totaling over 10,000 lines of code. A summary of the primary program software is presented in Table C.1.

Table C.1: Software Summary

<u>SECTION</u>	<u>PROGRAM NAME</u>	<u>LINES OF CODE</u>
<u>Engine Model Development</u>		
C.2.1	F. TRIN	172
C.2.2	F. FUELCA	116
C.2.3	F. CONVR	311
C.2.4	F. BAVR	154
C.2.5	F. EXTRA	366
C.2.6	F. TABLE	532
<u>Flight Test Data Reduction</u>		
C.3.1	START	} 1058
C.3.1	PUSHPULL	
C.3.1.2	STAB	
C.3.2	MFIT	~1300
C.3.3	XPLOT	~700
<u>Cruise and Trajectory Modeling</u>		
C.4.1	ITERATE	570
C.4.2	MODEL	} 3393
C.4.2.1	DRAGA	
C.4.2.2	THRUST	
<u>Utilities</u>		
C.4.1	THRUST 1	145
C.4.2	REYNOLDS	95

C.2 ENGINE MODEL DEVELOPMENT

Figure C.1 presents the routines and order of implementation for developing the engine prediction deck curves in the simplified form required for the thrust modeling technique used in this program.

Figure C.2 presents the logic flow for the development of the thrust run correction parameter η .

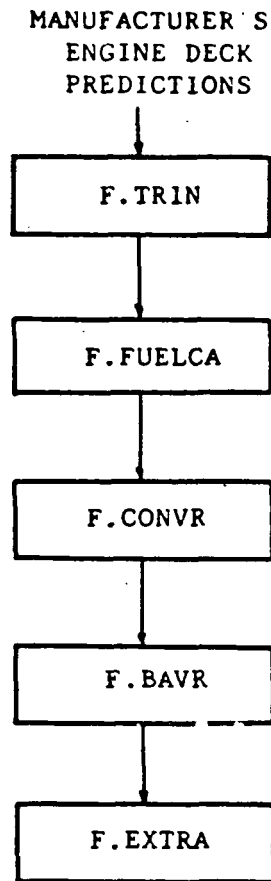


Figure C.1: Simplified Engine Deck Development Data Flow

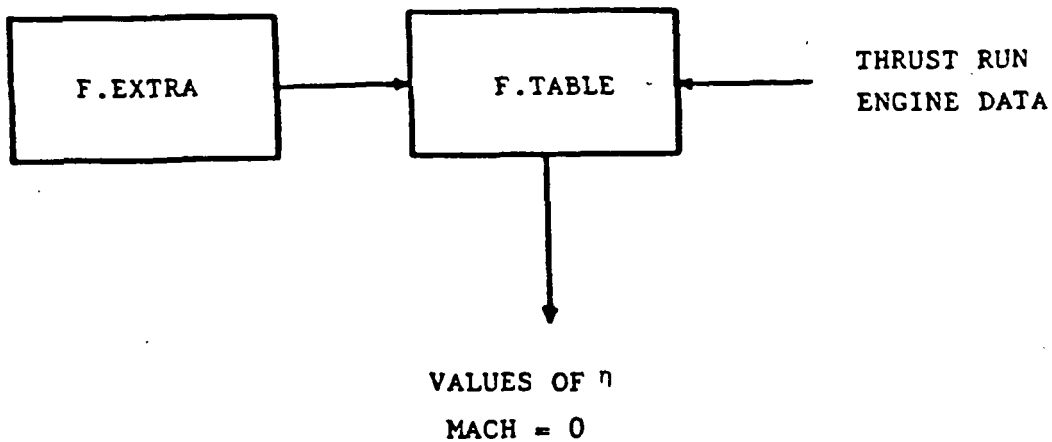


Figure C.2: Data Flow For Developing η curve

C.2.1 F. TRIN

PURPOSE:

To 1) provide for manual entry of raw engine prediction deck data onto the computer system, 2) apply the corrections for temperature and pressure to obtain the corrected form of the engine parameters, and 3) write out the initial engine prediction deck data files.

APPROACH:

The program first prompted the user for the total pressure and total temperature for which the predictions were calculated. Then all parameter values corresponding to one data point were entered by the user, corrected with the applicable equation, and written to the output file. This was repeated for each data file.

```

C *****
C *
C * ORGANIZATION: UNIVERSITY OF KANSAS CENTER FOR RESEARCH INC. *
C * PROGRAM : F.TRIN *
C * SUBROUTINE : *
C * AUTHOR : BRAMAN , KEITH *
C * COMPUTER : SEL 32/77 *
C * O/S : M.P.X. 1.3 *
C * COMPILER : ANSI-77 STANDARD FORTRAN (FORT77) *
C *
C * REVISIONS *
C *
C * I-----I-----I-----I-----I *
C * I PR# I VER/REV I NAME I DATE I *
C * I-----I-----I-----I-----I *
C * I I 1/0 I KEITH BRAMAN I 12/8/82 I *
C * I-----I-----I-----I-----I *
C *****
C
C THIS PROGRAM CALCULATES CORRECTED
C THRUST VALUES FROM THE ENGINE PREDICTION
C THRUST DECK INPUT
C
C CHARACTER*1 A
C CHARACTER*8 FILENAME
C TYPE *, '***** TO ABORT TYPE 9999 AT FN INPUT ****'
5 TYPE 6
6 FORMAT(/, 'S', 5X, 'INPUT THETA: ')
ACCEPT *, THETA
TYPE 200, THETA
CALL CHANGE (THETA, A)
IF (A.EQ.'Y') GO TO 5
10 TYPE 11
I=0
11 FORMAT(/, 'S', 5X, ' FILE NAME DATA IS TO BE STORED IN ; ')
ACCEPT 12, FILENAME
12 FORMAT (A8)
OPEN (UNIT=5, FILE=FILENAME, USER='BRAMAN',
&STATUS='NEW', FILESIZE =50, FORM='FORMATTED',
&BLOCKED=.TRUE., IOSTAT=11, ERR=13)
13 IF (I1.EQ.0) GO TO 15
IF (I1.EQ.1) GO TO 14
IF (I1.GT.1) GO TO 500
14 TYPE *, '***** FILENAME ALREADY EXISTS ****'
GO TO 10
15 TYPE 16
16 FORMAT(/, 'S', 5X, 'INPUT MACH #: ')
ACCEPT *, AM
TYPE 200, AM
CALL CHANGE (AM, A)
IF (A.EQ.'Y') GO TO 15
17 TYPE 18
18 FORMAT(/, 'S', 5X, 'INPUT TT2; ')
ACCEPT *, TT2

```

```

        TYPE 200,TT2
        CALL CHANGE(TT2,A)
        IF(A.EQ.'Y') GO TO 17
19      TYPE 20
20      FORMAT(/,'$',5X,'INPUT PT2: ')
        ACCEPT *,PT2
        TYPE 200,PT2
        CALL CHANGE(PT2,A)
        IF(A.EQ.'Y') GO TO 19
        SQTHETA = SQRT(TT2/518.7)
        DELT2 = (PT2/14.7)
C      WRITE TO DATA FILE
        WRITE(5,113)FILENAME
        WRITE(5,105)
        WRITE(5,100) AM,TT2,PT2
        WRITE(5,112)
        WRITE(5,110)
        WRITE(5,111)
        WRITE(5,112)
100     FORMAT (1X,3G15.7)
29      I=I+1
30      TYPE 31,I
31      FORMAT(/,'$',5X,'INPUT FN',I2,'= ')
        ACCEPT *,FN
        TYPE 200,FN
        IF(FN.EQ.9999) GO TO 10
        CALL CHANGE( FN,A)
        IF(A.EQ.'Y') GO TO 30
        IF(IFLAG.EQ.1)GO TO 50
32      TYPE 33,I
33      FORMAT(/,'$',5X,'INPUT WF',I2,'= ')
        ACCEPT *,WF
        TYPE 200,WF
        CALL CHANGE (WF,A)
        IF (A.EQ.'Y') GO TO 32
        IF(IFLAG.EQ.1)GO TO 50
34      TYPE 35,I
35      FORMAT(/,'$',5X,'INPUT WA', I2,'= ')
        ACCEPT *,WA
        TYPE 200,WA
        CALL CHANGE (WA,A)
        IF(A.EQ.'Y') GO TO 34
        IF(IFLAG.EQ.1)GO TO 50
36      TYPE 37,I
37      FORMAT(/,'$',5X'INPUT RPM',I2,'= ')
        ACCEPT *,RPM
        TYPE 201,RPM
        CALL CHANGE(RPM,A)
        IF(A.EQ.'Y') GO TO 34
        IF(IFLAG.EQ.1)GO TO 50
C
C      START CALL FOR CORRECTED VALUES
C
C      CORRECTED RPM
C      50  IFLAG=0

```

```

      CRPM= RPM/SQTHETA
C
C      CALL RAM DRAG
C
      FRAM = (WA*AM*1116.4*SQRT(THETA))/32.174
C
C      CALL GROSS THRUST
C
      FG= FRAM + FN
      FGODT2 = FG/DELT2
      CWF = WF/DELT2/SQTHETA
      CWA = (WA*SQTHETA)/DELT2
      TSFC=CWF/FGODT2
      TYPE 700
700  FORMAT(/,'$',5X,'LAST CHANCE FOR ANY CHANGES ; Y/N ')
      ACCEPT 2,A
      2    FORMAT(A1)
      IF(A.EQ.'Y')GOTO 710
      GO TO 600
710  TYPE *, 'THE VALUES ARE ;'
      TYPE *, '1   FN=',FN
      TYPE *, '2   WF=',WF
      TYPE *, '3   WA=',WA
      TYPE *, '4   RPM=',RPM
      TYPE *, '5   TSFC=',TSFC
      IFLAG=1
      TYPE 777
777  FORMAT(/,'$',5X,'INPUT VARIABLE NUMBER TO BE CHANGED;')
      ACCEPT *,J
      GO TO (30,32,34,36),J
C
C      WRITE DATA FILE
C
      600 WRITE(5,150) CRPM,FGODT2,CWF,CWA,TSFC
C 150 FORMAT(4X,F10.2,2X,F8.2,2X,F8.2,2X,F7.2,2X,F6.4)
      150 FORMAT(4X,5G15.7)
      GO TO 29
105  FORMAT(5X,'MACH #',7X,'TT2(DEG R)',6X,'PT2(Psia)')
110  FORMAT(10X,'CRPM', 7X,'FG/DELTA2', 6X,'CFUEL FLOW', 5X,
      & 'CAIR FLOW', 9X,'TSFC')
111  FORMAT(25X,'LBS',10X,'LBS/HR', 9X,'LBS/SEC')
112  FORMAT(' ')
200  FORMAT(17X,F10.4)
201  FORMAT(17X,F10.2)
500  TYPE *, '**** ERROR IN OPEN 5 ',I1
113  FORMAT(1X,'FILENAME ',A8)
      STOP
      END
      SUBROUTINE CHANGE(X,A)
      CHARACTER*1 A
      TYPE 1
1    FORMAT(/,'$',5X,'CHANGES? Y/N: ')
      ACCEPT 2, A
      2    FORMAT (A1)
      RETURN

```

END
SIFT ABORT EN
SCATALOG
CATALOG OM.TRIN U.50
SDEFNAME EN
SEOJ
SS

C.2.2 F. FUELCA

PURPOSE:

To investigate the effects of using a power of δ other than one to form corrected fuel flow. The program read F. TRIN output files and allowed the user to choose the power of delta

which was used to form:

$$\frac{W_f}{\sqrt{\theta}_{t_2} \delta_{t_2}^N}$$

APPROACH:

F. TRIN output files retained the values for temperature and pressure that were originally entered. These are used by F. TRIN to form CWF. Specifically,

$$CWF = \frac{W_f}{\delta_{t_2} \sqrt{\theta}_{t_2}}$$

In F. FUELCA, the values of CWF were multiplied by $\delta_{t_2}^{1-N}$, where N is the chosen power of δ_{t_2} . This resulted in

$$CWF = \frac{W_f}{\sqrt{\theta}_{t_2} \delta_{t_2}^N}$$

```

C *****
C *
C * ORGANIZATION: UNIVERSITY OF KANSAS CENTER FOR RESEARCH INC. *
C * PROGRAM : F.FUELCA *
C * SUBROUTINE : NONE *
C * AUTHOR : BRAMAN , KEITH *
C * COMPUTER : SEL 32/77 *
C * O/S : M.P.X. 1.3 *
C * COMPILER : ANSI-77 STANDARD FORTRAN (FORT77) *
C *
C * REVISIONS *
C *
C * I-----I-----I-----I-----I *
C * I PR# I VER/REV I NAME I DATE I *
C * I-----I-----I-----I-----I *
C * I I 1/0 I KEITH BRAMAN I 12/2/82 I *
C * I-----I-----I-----I-----I *
C *****
C
C THIS PROGRAM CHANGES THE POWER OF DELTA USED TO
C CORRECT FUEL FLOW IN THE ENGINE DECK PREDICTION
C FILES.
C
C REAL*4 CHF(100),Z1(100),Z2(100),Z3(100),XU(100),Z(100)
C CHARACTER*8 FILENAME
C CHARACTER*1 A
C TYPE 7
7 FORMAT(/,'$',5X,'INPUT THE FILENAME THE DATA HAS BEEN STORED',
& ' IN: ')
ACCEPT 332,FILENAME
OPEN(UNIT=5,FILE=FILENAME,USER='BRAMAN',STATUS='OLD',
& FORM='FORMATTED',BLOCKED=.TRUE.,ACCESS='SEQUENTAIL',
& IOSTAT=I3,ERR=997)
12 TYPE 9
9 FORMAT(/,'$',5X,'OUTPUT FILENAME TO STORE OUTPUT DATA IN ; ')
ACCEPT 332,FILENAME
OPEN(UNIT=6,FILE=FILENAME,USER='BRAMAN',STATUS='NEW',
& FILESIZE=3,FORM='FORMATTED',BLOCKED=.TRUE.,IOSTAT=IS,
& ERR=13,CLEAR=.TRUE.)
13 IF(IS.EQ.0)GO TO 3
IF(IS.GT.1) GO TO 995
IF(IS.EQ.1)TYPE 14;GO TO 12
14 FORMAT(/,5X,'**** FILE NAME ALREADY EXISTS ****')
3 OPEN(UNIT='UT')
C
C READ INPUT FILE AS STORED BY PROGRAM F.TRIN
C
C READ(5,175)
C READ(5,175)
C READ(5,110)AM,B,C
C READ(5,175)
C READ(5,175)
C READ(5,175)

```



```

      READ(5,175)
      DO I=1,100
        READ(5,150,END=15)XU(I),Z(I),CHF(I),Z2(I),Z3(I)
      END DO
15    TYPE *, 'FINISHED READ'
      NVAL=I-1
      TYPE *, '      INPUT DELTA POWER  > '
      ACCEPT *, APOWER
C     TYPE *, '      INPUT THETA POWER > '
C     ACCEPT *, TP
      TP=0.5
      THETAT2=SQRT(B/518.7)
      DELTAT2=C/14.7
      DELTAX=(DELTAT2/(DELTAT2**APOWER))
      DO I=1,NVAL
        Z1(I)=CHF(I)*(DELTAX)*(THETAT2/((B/518.7)**TP))
        Z3(I)=Z1(I)/Z(I)
      END DO
C
C WRITE OUTPUT VALUES OF FIT
C
C     WRITE('UT',444)FILENAME,APOWER
C     WRITE('UT',105)
C     WRITE('UT',110)AM,B,C
C     WRITE('UT',115)
C     WRITE('UT',120)
C     WRITE('UT',125)
C     WRITE('UT',115)
C     DO 70 I=1,NVAL
C 70  WRITE('UT',150)XU(I),Z(I),Z1(I),Z2(I),Z3(I)
C
C WRITE NEW DATA TO FILE
C
      WRITE(6,444)FILENAME,APOWER
      WRITE(6,105)
      WRITE(6,110)AM,B,C
      WRITE(6,115)
      WRITE(6,120)
      WRITE(6,125)
      WRITE(6,115)
      DO 80 I=1,NVAL
80  WRITE(6,150) XU(I),Z(I),Z1(I),Z2(I),Z3(I)
      CLOSE(UNIT=5)
      CLOSE(UNIT=6)
      GO TO 1
150  FORMAT(4X,5G15.7)
105  FORMAT(5X,'MACH #',7X,'TT2(DEG R)',6X,'PT2(PSIA)')
110  FORMAT(1X,3G15.7)
120  FORMAT(10X,'CRPM', 7X,'FG/DELTA2', 6X,'CFUEL FLOW', 5X,
&  'CAIR FLOW', 4X,'TSFC/THETA2')
125  FORMAT(25X,'LBS',10X,'LBS/HR', 9X,'LBS/SEC')
175  FORMAT(' ',A)
115  FORMAT(' ')
200  FORMAT(17X,F10.4)
332  FORMAT(A8)

```

```
201  FORMAT(17X,F10.2)
444  FORMAT(' FILENAME = ',A8,2X,' WF DELTA-T2 = ',F3.2)
997  TYPE *, '**** ERROR IN OPEN 5 ',I3
995  TYPE *, '**** ERROR IN OPEN 6 ',I3
      STOP
      END
```

C.2.3 F. CONVR

PURPOSE:

To interpolate the engine prediction deck data for corrected thrust, airflow, and fuel flow at a constant Mach number and altitude and to determine the appropriate curve value at even corrected RPM increments of 500 RPM using a cubic spline routine.

APPROACH:

After reading the input file (output from F. TRIN), the program created a new corrected RPM array which consisted of all even multiples of 500 RPM within the total RPM range of the input file. A subroutine then interpolated gross thrust, fuel flow, and air flow to each value in the new RPM array, and the output file was written.

```

C *****
C *
C * ORGANIZATION: UNIVERSITY OF KANSAS CENTER FOR RESEARCH INC. *
C * PROGRAM      : F.CONUR                                         *
C * SUBROUTINE   : WACSUB / WAC                                     *
C * AUTHOR      : BRAMAN , KEITH                                   *
C * COMPUTER    : SEL 32/77                                         *
C * O/S         : M.P.X. 1.3                                         *
C * COMPILER    : ANSI-77 STANDARD FORTRAN (FORT77)               *
C *
C *
C * REVISIONS
C *
C * I-----I-----I-----I-----I
C * I PR# I VER/REV I NAME I DATE I
C * I-----I-----I-----I-----I
C * I I 1/0 I KEITH BRAMAN I 12/2/82 I
C * I-----I-----I-----I-----I
C *
C *****
C
C THIS PROGRAM INPUTS THRUST DECK DATA TO BE BROKEN OUT AT EVEN
C BREAK POINTS WITH A CUBIC SPLINE ROUTINE
C
C DIMENSION X(100),Y(100),Z(50),X2(50),DY(150)
C DIMENSION Y1(100),Y2(100),Y3(100),Z1(100),Z2(100),Z3(100)
C DIMENSION XU(100),YU(100),Y1U(100),Y2U(100),Y3U(100)
C CHARACTER*8 FILENAME
C CHARACTER*1 A
1 TYPE 7
7 FORMAT(/,'$',5X,'INPUT THE FILENAME THE DATA HAS BEEN STORED',
& ' IN; ')
ACCEPT 332,FILENAME
OPEN(UNIT=5,FILE=FILENAME,USER='BRAMAN',STATUS='OLD',
& FORM='FORMATTED',BLOCKED=.TRUE.,ACCESS='SEQUENTIAL',
& IOSTAT=13,ERR=997)
12 TYPE 9
9 FORMAT(/,'$',5X,'OUTPUT FILENAME TO STORE OUTPUT DATA IN ; ')
ACCEPT 332,FILENAME
OPEN(UNIT=6,FILE=FILENAME,USER='BRAMAN',STATUS='NEW',
& FILESIZE=5,FORM='FORMATTED',BLOCKED=.TRUE.,IOSTAT=15,
& ERR=13)
13 IF(15.EQ.0)GO TO 3
IF(15.GT.1) GO TO 995
IF(15.EQ.1)TYPE 14;GO TO 12
14 FORMAT(/,5X,'**** FILE NAME ALREADY EXISTS ****')
3 OPEN(UNIT='UT')
C
C READ INPUT FILE AS STORED BY PROGRAM F.TRIN
C
C READ(5,175)
C READ(5,175)
C READ(5,110)AM,B,C
C READ(5,175)
C READ(5,175)

```

```

      READ(5,175)
      READ(5,175)
      READ(5,150,END=15)(X(I),Y(I),Y1(I),Y2(I),Y3(I),I=1,100)
      TYPE *, 'FINISHED READ'
15    NUAL=I-1
C
C    THE FOLLOWING LOOP 'FLIPS' THE DATA SO THAT THE
C    REST OF THE PROGRAM CAN COPE WITH THE NEW
C    UPSIDE-DOWN FORMAT
C
C    DO 17 I=1,NUAL
C      X(I)=XU(NUAL-(I-1))
C      Y(I)=YU(NUAL-(I-1))
C      Y1(I)=Y1U(NUAL-(I-1))
C      Y2(I)=Y2U(NUAL-(I-1))
C      Y3(I)=Y3U(NUAL-(I-1))
C    CONTINUE
C
C    CALC EVEN BREAK POINTS BEGINNING AT THE SMALLEST VALUE OF
C    X(I) AND ENDING AT THE HIGHEST VALUE OF X(I)
C
      XX=ANINT( X(1)/1000. )
      XX=XX*1000.
      IF(XX.LT.X(1))THEN
        XX=XX+500.
        GO TO 8
      END IF
      DO 40 I=1,50
        X2(I)=XX
        XX=XX+500.00000
        IF(X(NUAL).LT.XX)GO TO 41
      40 CONTINUE
      41 NN=I
C
C    PRINT OUT BREAK POINT AND X VALUES
C
C    CALL CUBIC SPLIN ROUTINE FOR ALL CONDITIONS
C
      CALL WACSUB(X,Y,Z,DY,X2,NN,IERR,NUAL)
      CALL WACSUB(X,Y1,Z1,DY,X2,NN,IERR,NUAL)
      CALL WACSUB(X,Y2,Z2,DY,X2,NN,IERR,NUAL)
      CALL WACSUB(X,Y3,Z3,DY,X2,NN,IERR,NUAL)
C
C    WRITE OUTPUT VALUES OF FIT
C
      WRITE('UT',444)FILENAME
      WRITE('UT',105)
      WRITE('UT',110)AM,B,C
      WRITE('UT',115)
      WRITE('UT',120)
      WRITE('UT',125)
      WRITE('UT',115)

```

```

C      DO 70 I=1,NN
C 70  WRITE('UT',150)X2(I),Z(I),Z1(I),Z2(I),Z3(I)
C
C  WRITE NEW DATA TO FILE
C
      WRITE(6,444)FILENAME
      WRITE(6,105)
      WRITE(6,110)AM,B,C
      WRITE(6,115)
      WRITE(6,120)
      WRITE(6,125)
      WRITE(6,115)
      DO 80 I=1,NN
80  WRITE(6,150) X2(I),Z(I),Z1(I),Z2(I),Z3(I)
      CLOSE(UNIT=5)
      CLOSE(UNIT=6)
      GO TO 1
C 150 FORMAT(4X,F10.2,2X,F8.2,2X,F8.2,2X,F7.2,2X,F6.4)
      150 FORMAT(4X,SG15.7)
      105 FORMAT(5X,'MACH #',7X,'TT2(DEG R)',6X,'PT2(PSIA)')
      110 FORMAT(1X,SG15.7)
      120 FORMAT(10X,'CRPM', 7X,'FG/DELTA2', 6X,'CFUEL FLOW', 5X,
      & 'CAIR FLOW', 4X,'TSFC/THETA2')
      125 FORMAT(25X,'LBS',10X,'LBS/HR', 9X,'LBS/SEC')
      175 FORMAT(' ',A)
      115 FORMAT(' ')
      200 FORMAT(17X,F10.4)
      332 FORMAT(A8)
      201 FORMAT(17X,F10.2)
      444 FORMAT(' FILENAME = ',BA)
      997 TYPE *, '**** ERROR IN OPEN 5 ',I3
      995 TYPE *, '**** ERROR IN OPEN 6 ',I5
      STOP
      END
      SUBROUTINE WACSUB(X,Y,Z,DY,X2,K,IERR,NVAL)
C      COMMON/ORDER/IDUM(4),NVAL
C      DOUBLE PRECISION AUGXL,AUGYL,FACTOR
      DIMENSION H(150),X(1),X2(1),Y(1),DY(1)
C
C      SCALE THE X DATA SO THAT THE X'S AND Y'S ARE OF THE SAME MAGNITUDE
C
      AUGXL=0.
      AUGYL=0.
      DO 10 I=1,NVAL
      AUGXL=AUGXL+ABS(X(I))
10  AUGYL=AUGYL+ABS(Y(I))
      AAUGXL=AUGXL/NVAL
      AUGYL=AUGYL/NVAL
      FACTOR=AUGXL/AUGYL
      DO 20 I=1,NVAL
20  X(I)=X(I)/FACTOR
      DO 30 I=1,K
30  X2(I)=X2(I)/FACTOR
      CALL WAC(NVAL,X,Y,K,X2,Z,DY,H,O,O,IERR)
      IF(IERR.EQ.O) GO TO 50

```

```

      K=NUAL
      DO 40 I=1,K
40 X2(I)=X(I)
C
C      SCALE THE X DATA BACK TO ITS ORIGINAL MAGNITUDE
C
50 DO 60 I=1,NUAL
60 X(I)=X(I)*FACTOR
      DO 70 I=1,K
70 X2(I)=X2(I)*FACTOR
      RETURN
      END
      SUBROUTINE WAC (M,XJ,YJ,N,XI,F,G,H,IFLAG,ISAVE,IERR)
C
C      ***STABILITY ANALYSIS***
C      CALLED BY STAB
C      NO CALLS
C
C      (1)
C      THIS SUBR (WEIGHTED ANGLE CUBIC) INTERPOLATES THE INPUT FUNCTION YJ
C      GIVEN AT THE M STATIONS XJ TO THE N OUTPUT STATIONS XI. F CONTAINS
C      THE FUNCTION,G ITS DERIV. AND H ITS INTEGRAL. THE METHOD IS CUBIC
C      THRU TWO POINTS WITH THE DERIVS GIVEN BY WEIGHTING THE ST LINE
C      ANGLES,NOT SLOPES. W IS THE WEIGHT FACTOR.
C
C      REF: TAPS PROGRAM MDC J7255 (CONTRACT: N00024-75-C-7205)
C
C      IMPLICIT REAL*8 (A-H , O-S, U-Z)
C      DIMENSION XJ(1),YJ(1),XI(1),F(1),G(1),H(1),A(150),B(150),
C      &C(150),D(150)
C      DATA Z0/0.000/,Z2/2.000/, Z3/3.000/, Z4/4.000/,Z6/6.000/
C      DATA Z0/0.0 //, Z2/2.0 //, Z3/3.0 //, Z4/4.0 //,Z6/6.0 /
C
C      M1=M-1
C      M2=M-2
C      N1=N-1
C
C      (3)
C*      STORE INTERVAL SIZES IN H AND ST LINE ANGLES IN F
C
C      DO 10 J=1,M1
C      H(J)=XJ(J+1)-XJ(J)
C      IF (H(J) .EQ. 0.) GO TO 20
C      U1 =YJ(J+1)-YJ(J)
C      F(J)= DATAN2(U1,H(J))
C      F(J)= ATAN2(U1,H(J))
C      D(J) = DSQRT( H(J)*H(J) + U1*U1)
C      D(J) = SQRT( H(J)*H(J) + U1*U1)
10 CONTINUE
      GO TO 40
C 20 WRITE (6, 30 ) J, (XJ(I),YJ(I),I=1,M)
C 30 FORMAT (1H0,38H***ERROR IN DATA GIVEN TO ROUTINE WAC.,
C 135H INTERVAL SIZE IN X IS ZERO AT THE ,I3,9HTH POINT. ,
C 2/,(2E16.5))
C      M = J-1

```

```

C      M1 = M-1
C      M2 = M-2
      20 IERR=1
      DO 11 I=1,M
11      CONTINUE
      RETURN
      40 CONTINUE
C
C*      NOW STORE G VALUES AND PUT INPUT VALUES INTO F (FOR CONVENIENCE)
C
      DO 50 J=2,M1
      U1 = (D(J)*F(J-1) + D(J-1)*F(J)) / ( D(J) + D(J-1) )
C      G(J)= DTAN(U1)
      G(J) = TAN(U1)
      F(J-1) = YJ(J-1)
50 CONTINUE
      F(M1) = YJ(M1)
      F(M) = YJ(M)
C
C*      NOW FIND CONSTS AND HOLD INTEGRAL AT J STATIONS IN YJ. FIRST AND (5)
C*      LAST ARE EXCEPTIONAL (QUADRATIC).
C
      IF (IFLAG .EQ. 0) GO TO 60
C*      FORCE FIRST POINT SLOPE TO ZERO IF IFLAG .NE. 0
      G(1) = Z0
      J1 = 1
      GO TO 70
60 J1 = 2
      A(1)=Z0
C*****
      B(1)=(F(1)-F(2)+G(2)*H(1))/(H(1)*H(1))
C*****
      C(1)=(Z2*(F(2)-F(1))-G(2)*H(1))/H(1)
      D(1)=F(1)
70 A(M1) = Z0
      B(M1)=(F(M)-F(M1)-G(M1)*H(M1))/(H(M1)*H(M1))
      C(M1)=G(M1)
      D(M1)=F(M1)
      D(M)=F(M)
      DO 80 J=J1,M2
      A(J)=(H(J)*(G(J+1)+G(J))-Z2*(F(J+1)-F(J)))/(H(J)**3)
      B(J)=(Z3*(F(J+1)-F(J))-H(J)*(G(J+1)+Z2*G(J)))/(H(J)*H(J))
      C(J)=G(J)
      D(J)=F(J)
80 CONTINUE
C
C*      (6)
C*      NOW CALC INTEGRAL.(SEE (5))
C
      YJ(1)=Z0
      YJ(2)=YJ(1)+H(1)*(F(1)+Z2*F(2)-G(2)*H(1)/Z2)/Z3
      DO 90 J=3,M1
      YJ(J)=YJ(J-1)+H(J-1)*(F(J-1)+F(J)+H(J-1)*(G(J-1)-G(J))/Z6)/Z2
90 CONTINUE
      YJ(M)=YJ(M1)+H(M1)*(Z2*F(M1)+F(M)+G(M1)*H(M1)/Z2)/Z3
C
C*      (7)

```



```

C*   DONE. NOW FOR FINAL INTERP VALUES
C
      I=0
      J=2
100  I=I+1
110  IF (XI(I).LE.XJ(J)) GO TO 120
      IF (J.EQ.M) GO TO L20
      J=J+1
      GO TO 110
120  ZI=XI(I)-XJ(J-1)
      ZI2=ZI*ZI
      ZI3=ZI2*ZI
      ZI4=ZI3*ZI
      UA=A(J-1)
      UB=B(J-1)
      UC=C(J-1)
      UD=D(J-1)
      G(I)=Z3*UA*ZI2+Z2*UB*ZI+UC
      F(I)=UA*ZI3+UB*ZI2+UC*ZI+UD
      H(I)=UA*ZI4/Z4+UB*ZI3/Z3+UC*ZI2/Z2+UD*ZI+YJ(J-1)
      IF (I.LT.N)GO TO 100
C
C**  RESTORE DESTROYED YJ VALUES
C
      IF (ISAVE .EQ. 1) GO TO 140
      DO 130 J=1,M
      YJ(J)=D(J)
130  CONTINUE
      RETURN
140  CONTINUE
C*   DUMP ANSWERS BACK INTO YJ ARRAY IF ISAVE = 1
      DO 150 J=1,N
      YJ(J) = F(J)
150  CONTINUE
      RETURN
      END

```

PURPOSE:

To average engine prediction deck data across the altitude range for each constant Mach and corrected RPM condition and to define the table look-up files for the engine deck predictions within the engine operating limits.

APPROACH:

Data for several altitudes, but one Mach, were read into a series of two dimensional arrays (one for each parameter). All data corresponding to each constant corrected RPM was averaged together, resulting in a series of one dimensional arrays which represented the corrected deck predictions for one Mach number.

```

C *****
C *
C * ORGANIZATION: UNIVERSITY OF KANSAS CENTER FOR RESEARCH INC. *
C * PROGRAM : F.BAUR *
C * SUBROUTINE : NONE *
C * AUTHOR : BRAMAN , KEITH *
C * COMPUTER : SEL 32/77 *
C * O/S : M.P.X. 1.3 *
C * COMPILER : ANSI-77 STANDARD FORTRAN (FORT77) *
C *
C * REVISIONS *
C *
C * I-----I-----I-----I-----I *
C * I PRN I UER/REV I NAME I DATE I *
C * I-----I-----I-----I-----I *
C * I I 1/O I KEITH BRAMAN I 3/21/83 I *
C * I-----I-----I-----I-----I *
C *
C *****
C
C DIMENSION RPM(40,18),FG(40,18),WF(40,18),WA(40,18),
& TSFC(40,18),AM(18),NVAL(18),K(18),KT(18),
& TFG(40),TWF(40),TWA(40),TTSFC(40),MC(40),
& AFG(40),AWF(40),AWA(40),ATSFC(40),ARPM(40)
C CHARACTER*8 FILENAME
C
C THIS LOOP READS THE FILES AND PUSHES THEM UP
C WITHIN THEMSELVES SO THAT ALL PARAMETERS
C CORRESPONDING TO THE SAME RPM HAVE THE SAME
C FIRST SUBSCRIPT.
C
20 CONTINUE
MC=0
TFG=TWF=TWA=TTSFC=0.0
TYPE*, 'HOW MANY FILES WILL BE READ?'
ACCEPT*, NNN
TYPE*, ' ***** ENTER FILES IN ORDER OF INCREASING ALTITUDE ***'
TYPE*, '
DO 10 J=1, NNN
TYPE 101
101 FORMAT(//, 5X, 'FILENAME=')
ACCEPT 200, FILENAME
OPEN(UNIT=5, FILE=FILENAME, USER='BRAMAN', STATUS='OLD',
& FORM='FORMATTED', BLOCKED=.TRUE., ACCESS='SEQUENTIAL',
& IOSTAT=19, ERR=300)
READ(5, 250)
READ(5, 250)
READ(5, 250)
READ(5, 220) AM(J), Q, R
READ(5, 250)
READ(5, 250)
READ(5, 250)
READ(5, 230, END=50) (RPM(I, J), FG(I, J), WF(I, J), WA(I, J),
& TSFC(I, J), I=1, 100 )

```

```

50   NVAL(J)=I-1
      GOTO 350
200   FORMAT(A8)
220   FORMAT(1X,3G15.7)
230   FORMAT(4X,5G15.7)
250   FORMAT(' ',A)
300   TYPE*, '*****ERROR IN OPEN 5*****', I3
350   CONTINUE
      CLOSE (UNIT=5)

C
      K(J)=ANINT((RPM(1,J)-4000)/500)
      KT(J)=40-(K(J)+NVAL(J))
      DO I=0,NVAL(J)-1
          FG(NVAL(J)-I+K(J),J)=FG(NVAL(J)-I,J)
          WF(NVAL(J)-I+K(J),J)=WF(NVAL(J)-I,J)
          WA(NVAL(J)-I+K(J),J)=WA(NVAL(J)-I,J)
          TSFC(NVAL(J)-I+K(J),J)=TSFC(NVAL(J)-I,J)
      END DO
      DO I=1,K(J)
          FG(I,J)=WF(I,J)=WA(I,J)=TSFC(I,J)=0.0
      END DO
      DO I=K(J)+NVAL(J)+1,40
          FG(I,J)=WF(I,J)=WA(I,J)=TSFC(I,J)=0.0
      END DO
10    CONTINUE

C
C
C   THE FOLLOWING NESTED LOOP SUMS THE VARIOUS
C   PARAMETERS AND DIVIDES BY THE NUMBER OF
C   POINTS AT EACH ALTITUDE TO CREATE THE
C   AVERAGES.
C
      MC=0
      DO I=1,40
          DO J=1,NNN
              IF( FG(I,J).NE.0.0) MC(I)=MC(I)+1
              TFG(I)=TFG(I)+FG(I,J)
              TWF(I)=TWF(I)+WF(I,J)
              TWA(I)=TWA(I)+WA(I,J)
              TTSFC(I)=TTSFC(I)+TSFC(I,J)
          END DO
          AFG(I)=TFG(I)/MC(I)
          AWF(I)=TWF(I)/MC(I)
          AWA(I)=TWA(I)/MC(I)
          ATSFC(I)=AWF(I)/AFG(I)
      END DO
      DO I=1,40
          IF(TFG(I).NE.0.0)GOTO 405
      END DO
405   M1=I
      DO I=M1,40
          IF(TFG(I).EQ.0.0)GOTO 410
      END DO
410   M2=I-1
C

```

```

DO I=1,40
  ARPM(I)=4000.+(I-1)*500.
END DO

C
C   THE FOLLOWING STATEMENTS ASK THE USER FOR A
C   FILE NAME AND CREATES THAT FILE.  THE AVERAGED
C   DATA IS STORED IN THE FILE.
C
245  TYPE 251,AM(NNN)
251  FORMAT(/,5X,'TYPE FILE NAME FOR MACH =',F5.3,' ')
      ACCEPT 1000, FILENAME
      OPEN(UNIT=6,FILE=FILENAME,USER='BRAMAN',STATUS='NEW',
&        FILESIZE=5,FORM='FORMATTED',BLOCKED=.TRUE.,
&        IOSTAT=15,ERR=301)
301  IF(15.EQ.0)GOTO 700
      IF(15.GT.1)GOTO 995
      IF(15.EQ.1)TYPE 305;GOTO 245
305  FORMAT(/,5X,'*****FILENAME ALREADY EXISTS*****')
700  CONTINUE
      WRITE(6,601)FILENAME
      WRITE(6,610)
      WRITE(6,620)
      WRITE(6,621) AM(NNN),Q,R
      WRITE(6,630)
      WRITE(6,640)
      WRITE(6,610)
      DO 750 I=M1,M2
      WRITE(6,650)ARPM(I) ,AFG(I),AWF(I),AWA(I),ATSFC(I)
750  CONTINUE
      CLOSE (UNIT=6)
      GOTO 20
601  FORMAT(4X,'FILENAME=',8A)
610  FORMAT(' ')
620  FORMAT(4X,'MACH NUMBER=')
621  FORMAT(1X,3G15.7)
630  FORMAT(10X,'CRPM',7X,'FG/DELTA2',6X,'CFUELFLOW',7X,
&        'CAIRFLOW',7X,'TSFC/THETA2')
640  FORMAT(25X,'LBS',10X,'LBS/HR',9X,'LBS/SEC')
650  FORMAT(4X,5G15.7)
995  TYPE*, 'ERROR IN OPEN 6',15
1000 FORMAT(A8)
1005 CONTINUE
      STOP
      END

```

C.2.5 F. EXTRA

PURPOSE:

To provide consistant extrapolation of each constant Mach engine prediction deck curve outside the normal engine operating envelope so that realistic interpolations could be accomplished between Mach numbers for conditions that were close to the limits of the engine envelope. Using this program, the table look-up files created with program F. BAVR were extended to the lowest and highest corrected RPM values anticipated.

APPROACH:

First, the engine prediction deck curve corresponding to the lowest Mach was extrapolated to the lower end of the desired RPM range and the high Mach curve to the upper end. Then, using a linearly extended difference between curves, each of the other curves was extrapolated to the limits.

```

C *****
C *
C * ORGANIZATION: UNIVERSITY OF KANSAS CENTER FOR RESEARCH INC. *
C * PROGRAM : F.EXTRA *
C * SUBROUTINE : LINEX / ORTHPY1 *
C * AUTHOR : BRAMAN , KEITH *
C * COMPUTER : SEL 32/77 *
C * O/S : M.P.X. 1.3 *
C * COMPILER : ANSI-77 STANDARD FORTRAN (FORT77) *
C *
C * REVISIONS *
C *
C * I-----I-----I-----I-----I *
C * I PR# I VER/REV I NAME I DATE I *
C * I-----I-----I-----I-----I *
C * I I 1/0 I KEITH BRAMAN I 2/22/83 I *
C * I-----I-----I-----I-----I *
C *****
C
C THE FOLLOWING CODE READS A NUMBER OF ENGINE
C PERFORMANCE DATA FILES WHICH HAVE BEEN CORRECTED
C FOR ALTITUDE EFFECTS AND AVERAGED. THE PARAMETERS
C CORRESPONDING TO THE LOWEST MACH NUMBER ARE
C EXTRAPOLATED AT THE LOWER END TO 4000 RPM; THOSE
C CORRESPONDING TO THE HIGHEST MACH NUMBER ARE
C EXTRAPOLATED AT THE UPPER END TO 23500 RPM.
C USING A LINEARLY EXTENDED DIFFERENCE BETWEEN
C MACH CURVES, THE REST OF THE DATA IS EXTRAPOLATED
C BASED ON THE UPPER AND LOWER CURVES.
C
C DIMENSION RPM(40,18),FG(40,18),WF(40,18),WA(40,18),
& TSFC(40,18),AM(18),K(18),KT(18),XVAL(40),
& YVAL1(40),YVAL2(40),YVAL3(40),YVAL4(40),
& M(4),X1(30),Z1(30),Z2(30),Z3(30),Z4(30),
& P(40,12),NVAL(18)
C CHARACTER*8 FILENAME
C IFLAG=0
C
C THIS LOOP READS THE FILES AND PUSHES THEM UP
C WITHIN THEMSELVES SO THAT ALL PARAMETERS
C CORRESPONDING TO THE SAME RPM HAVE THE SAME
C FIRST SUBSCRIPT.
C
C TYPE*, 'HOW MANY FILES WILL BE READ?'
C ACCEPT*, NNM
C TYPE*, ' **** ENTER FILES IN ORDER OF INCREASING MACH ****'
C TYPE*, ' '
C DO 10 J=1, NNM
C TYPE 101
101 FORMAT(//, 5X, 'FILENAME=')
C ACCEPT 200, FILENAME
C OPEN(UNIT=5, FILE=FILENAME, USER='BRAMAN', STATUS='OLD',
& FORM='FORMATTED', BLOCKED=.TRUE., ACCESS='SEQUENTIAL',
& IOSTAT=I3, ERR=300)

```

```

      READ(S,250)
      READ(S,250)
      READ(S,250)
      READ(S,220) AM(J),Q,R
      READ(S,250)
      READ(S,250)
      READ(S,250)
      READ(S,230,END=50)(RPM(I,J),FG(I,J),WF(I,J),WA(I,J),
&      TSFC(I,J),I=1,100 )
50    NVAL(J)=I-1
      DO I=1,NVAL(J)
        TSFC(I,J)=WF(I,J)/FG(I,J)
      END DO
      GOTO 350
200    FORMAT(A8)
220    FORMAT(1X,3G15.7)
230    FORMAT(4X,5G15.7)
250    FORMAT(' ',A)
300    TYPE*, '*****ERROR IN OPEN 5*****',I3
350    CONTINUE
      CLOSE (UNIT=5)

C
      K(J)=ANINT((RPM(1,J)-4000)/500)
      KT(J)=40-(K(J)+NVAL(J))
      DO I=0,NVAL(J)-1
        FG(NVAL(J)-I+K(J),J)=FG(NVAL(J)-I,J)
        WF(NVAL(J)-I+K(J),J)=WF(NVAL(J)-I,J)
        WA(NVAL(J)-I+K(J),J)=WA(NVAL(J)-I,J)
        TSFC(NVAL(J)-I+K(J),J)=TSFC(NVAL(J)-I,J)
      END DO
      DO I=1,K(J)
        FG(I,J)=WF(I,J)=WA(I,J)=TSFC(I,J)=0
      END DO
      DO I=1.40
        RPM(I,J)=3500+500*I
      END DO
10    CONTINUE

C
C    NOW THE FIRST AND LAST FILES ARE EXTRAPOLATED.
C    SPECIAL ARRAYS ARE SET UP FOR DATA TRANSFER
C    TO SUBROUTINE ORTHPY1.
C
      ND=(NVAL(NNN)/2)
      NE=KT(NNN)
      KE=NVAL(NNN)-ND+K(NNN)
      KX=KE+ND
      JE=NNN
      DO I=1,NE
        X1(I)=RPM(40-KT(NNN)+I,NNN)
      END DO
      TYPE*, 'WHAT ORDER FIT FOR UPPER END OF THE FOLLOWING CURVES;'
500    CONTINUE
      TYPE*, '          M FOR FG=?'
      ACCEPT*,M(1)
      TYPE*, '          M FOR WF=?'

```



```

ACCEPT*,M(2)
TYPE*, '          M FOR WA=?'
ACCEPT*,M(3)
TYPE*, '          M FOR TSFC=?'
ACCEPT*,M(4)
DO I=1,ND
  XUAL(I)=RPM(KE+I,JE)
  YUAL1(I)=FG(KE+I,JE)
  YUAL2(I)=WF(KE+I,JE)
  YUAL3(I)=WA(KE+I,JE)
  YUAL4(I)=TSFC(KE+I,JE)
END DO
CALL ORTHPY1(ND,XUAL,YUAL1,NE,X1,Z1,M(1),P)
CALL ORTHPY1(ND,XUAL,YUAL2,NE,X1,Z2,M(2),P)
CALL ORTHPY1(ND,XUAL,YUAL3,NE,X1,Z3,M(3),P)
CALL ORTHPY1(ND,XUAL,YUAL4,NE,X1,Z4,M(4),P)
DO I=1,NE
  FG(KX+I,JE)=Z1(I)
  WF(KX+I,JE)=Z2(I)
  WA(KX+I,JE)=Z3(I)
  TSFC(KX+I,JE)=Z4(I)
END DO
IF(IFLAG.EQ.10)GOTO 600
IFLAG=10
ND=(NUAL(1)/2)
NE=K(1)
KE=NE
KX=0
JE=1
DO I=1,NE
  X1(I)=RPM(I,1)
END DO
TYPE*, 'WHAT ORDER FIT FOR LOWER END OF THE FOLLOWING CURVES;'
GOTO 500
600 CONTINUE
C
CALL LINEX(FG,K,KT,NNN)
CALL LINEX(WF,K,KT,NNN)
CALL LINEX(WA,K,KT,NNN)
CALL LINEX(TSFC,K,KT,NNN)
C
C THIS LOOP CREATES THE TSFC EXTRAPOLATIONS
C FROM FG AND WF.
C
DO I=1,NNN
  DO J=1,40
    TSFC(J,I)=WF(J,I)/FG(J,I)
  END DO
END DO
C
C THIS LOOP CREATES A DATA FILE FOR EACH
C MACH NUMBER.
C
DO 1010 J=1,NNN
245 TYPE 251,AM(J)

```

```

251  FORMAT(//,5X,'TYPE FILE NAME FOR MACH =',F5.3,' ')
      ACCEPT 1000, FILENAME
      OPEN(UNIT=6,FILE=FILENAME,USER='BRAMAN',STATUS='NEW',
&        FILESIZE=5,FORM='FORMATTED',BLOCKED=.TRUE.,
&        IOSTAT=IS,ERR=301)
301  IF(IS.EQ.0)GOTO 700
      IF(IS.GT.1)GOTO 995
      IF(IS.EQ.1)TYPE 305;GOTO 245
305  FORMAT(/,5X,'*****FILENAME ALREADY EXISTS*****')
700  CONTINUE
      WRITE(6,601)FILENAME
      WRITE(6,610)
      WRITE(6,620)
      WRITE(6,621) AM(J),Q,R
      WRITE(6,630)
      WRITE(6,640)
      WRITE(6,610)
      DO 750 I=1,40
      WRITE(6,650)RPM(I,J),FG(I,J),WF(I,J),WA(I,J),TSFC(I,J)
750  CONTINUE
      CLOSE (UNIT=6)
      GOTO 1005
601  FORMAT(4X,'FILENAME=',8A)
610  FORMAT(' ')
620  FORMAT(4X,'MACH NUMBER=')
621  FORMAT(1X,3G15.7)
630  FORMAT(10X,'CRPM',7X,'FG/DELTA2',6X,'CFUELFLOW',7X,
&        'CAIRFLOW',7X,'TSFC/THETA2')
640  FORMAT(25X,'LBS',10X,'LBS/HR',9X,'LBS/SEC')
650  FORMAT(4X,5G15.7)
995  TYPE*, 'ERROR IN OPEN 6',IS
1000 FORMAT(A8)
1005 CONTINUE
1010 CONTINUE
      STOP
      END
      SUBROUTINE LINEX(ORD,K,KT,NNN)
      DIMENSION ORD(40,18),K(1),KT(1)

C
C      THIS SUBROUTINE CALCULATES THE LINEAR
C      RATE OF CHANGE OF THE DIFFERENCE BETWEEN
C      ADJACENT MACH CURVES AND EXTRAPOLATES
C      ALL CURVES ON THE BASIS OF THIS
C      APPROXIMATION.
C
      DO I=1,NNN-1
        DEL1=ORD(K(I+1)+1,I+1)-ORD(K(I+1)+1,I)
        DEL2=ORD(K(I+1)+2,I+1)-ORD(K(I+1)+2,I)
        DEL3=ORD(K(I+1)+3,I+1)-ORD(K(I+1)+3,I)
        DELD1=DEL1-DEL3
        DELD2=DEL2-DEL3
        DELD=(2*DELD1+DELD2)/6.0
        DEL=DEL3+3.0*DELD
        IF(DEL*DEL3.LE.0.0)DEL=0.0
        DO J=0,K(I+1)-1

```



```

C   4.  BCOEF(M)      COEF. FOR LEAST SQUARES POLY.
C   5.  ALPHA(M)     ALPHA COEF. FOR ORTH. POLY RECURRENCE RELATION
C   6.  BETA(M)      BETA COEF. FOR ORTH. POLY REC. REL.
C   7.  M            ORDER OF POLYNOMIAL FIT
C   8.  Z(K)         VECTOR OF SMOOTHED DATA POINTS
C   9.  K2           NUMBER OF INTERPOLATED POINTS DESIRED
C  10.  X2(K)        VECTOR OF X-VALUES WHERE SMOOTHED DATA IS DESIRED
C  11.  P            WORKING VECTOR
C   SEE RALSTON, PG 259
C
C
      DO 23000 I=1,M+2
      OMEGA(I)=0.0
C
23000 CONTINUE
23001 CONTINUE
      DO 23002 I=1,N
      P(I,2)=1.0
      P(I,1)=0.0
      YVALUE=0.0
23002 CONTINUE
23003 CONTINUE
      GAMMA(2)=N
      BETA(2)=0.0
      DO 23004 J=2,M+2
      DO 23006 K=1,N
      OMEGA(J)=OMEGA(J)+FVALUE(K)*P(K,J)
23006 CONTINUE
23007 CONTINUE
      BCOEF(J)=OMEGA(J)/GAMMA(J)
      DO 23008 I=1,N
      YVALUE=YVALUE+BCOEF(J)*P(I,J)
23008 CONTINUE
23009 CONTINUE
      IF(.NOT.(J.EQ.M+2))GOTO 23010
      GOTO 23005
23010 CONTINUE
      ALPHA(J+1)=0.0
      DO 23012 K=1,N
      ALPHA(J+1)=ALPHA(J+1)+XVALUE(K)*P(K,J)**2/GAMMA(J)
23012 CONTINUE
23013 CONTINUE
      DO 23014 I=1,N
      P(I,J+1)=(XVALUE(I)-ALPHA(J+1))*P(I,J)-BETA(J)*P(I,J-1)
23014 CONTINUE
23015 CONTINUE
      GAMMA(J+1)=0.0
      DO 23016 I=1,N
      GAMMA(J+1)=GAMMA(J+1)+P(I,J+1)**2
23016 CONTINUE
23017 CONTINUE
      BETA(J+1)=GAMMA(J+1)/GAMMA(J)
23004 CONTINUE
23005 CONTINUE
      DO 23018 I=1,N

```

```

        DELTA2(M)=0.0
        DO 23020 J=1,M+2
        SUM=SUM+BCOEF(J)*P(I,J)
23020 CONTINUE
23021 CONTINUE
        DELTA2(M)=DELTA2(M)+(FVALUE(I)-SUM)**2
23018 CONTINUE
23019 CONTINUE
        SIGMA2(M)=DELTA2(M)/(N-M-1)
        DO 23022 J=1,M
        DELTA2(M)=0.0
        DO 23024 I=1,N
        SUM=0.0
        DO 23026 K=1,J
        SUM=SUM+BCOEF(K)*P(I,K)
23026 CONTINUE
23027 CONTINUE
        DELTA2(J)=DELTA2(J)+(FVALUE(I)-SUM)**2
23024 CONTINUE
23025 CONTINUE
        SIGMA2(J)=DELTA2(J)/(N-J-1)
23022 CONTINUE
23023 CONTINUE
        DO 10 I=1,K2
        DO 20 IJ=1,M+2
            Q(IJ)=0.0
20 CONTINUE
        DO 30 J=1,M+1
            K=M+3-J
            Q(K)=BCOEF(K)+(X2(I)-ALPHA(K+1))*Q(K+1)-BETA(K+1)*
                Q(K+2)
30 CONTINUE
        Z(I)=Q(2)
10 CONTINUE
        RETURN
        END

```

C.2.6 F. TABLE

PURPOSE:

To 1) correct engine test data from a thrust run and calculate the airflow and specific fuel consumption for the actual engine and 2) provide the corresponding values of η , the ratio between the thrust run and deck values of TSFC, for each engine.

APPROACH:

The program prompted the user for the values of test rpm, fuel flow, thrust, pressure, and temperature. All corrected values corresponding to the entered values were then displayed and, upon confirmation, the program continued with calculations which produced corrected airflow and corrected specific fuel consumption. Sub-routines then interpolated these values at even breakpoints for comparison with the engine deck values obtained from F. EXTRA.

```

C *****
C *
C * ORGANIZATION: UNIVERSITY OF KANSAS CENTER FOR RESEARCH INC. *
C * PROGRAM : F.TABLE *
C * SUBROUTINE : *
C * AUTHORS : FILE, DAVID J. AND LOVETT, MICHAEL *
C * COMPUTER : SEL 32/77 *
C * O/S : M.P.X. 1.3 *
C * COMPILER : ANSI-77 STANDARD FORTRAN (FORT77) *
C *
C * REVISIONS *
C *
C * I-----I-----I-----I-----I *
C * I PR# I VER/REV I NAME I DATE I *
C * I-----I-----I-----I-----I *
C * I I 1/0 I FILE/LOVETT I 12/23/82I *
C * I-----I-----I-----I-----I *
C *****
C
C DIMENSION RPMN1(100), XN1(100), TFG(100), FG(100), TWA(100),
&CWA(100), TFF(100), CFF(100), TSFC(100), TTSFC(100), DELFG(100),
&DELFF(100), DELWA(100), ETA(100), TFF1(100), X2(100), TFG1(100),
&DY(100), THETA(100), THETA2(100), ETA1(100), CWA1(100), CFF1(100),
&TSFC1(100), TWA1(100), TSFC0(100), CFG1(100), DELTA(100), TSFCA(100),
&TFFA(100), TFFA1(100), TSFCA(100), CFFA(100), CFFA1(100), ETAA(100)
&, TSFCX(100), TSFC2(100)
C THIS PROGRAM IS THE COMBINED EFFORT OF DAVID FILE AND MIKE LOVETT
C DEFINES HEADING FOR OUTPUT TABLE
C CHARACTER IDENT*40, FILENAME*8, WORDS(7)*11, A*1
5 FORMAT(A)
C OPEN(UNIT='UT')
C *****CONSTANTS FOLLOW *****
WORDS(1)= 'PRESSURE'
WORDS(2)= 'PRESSURE'
WORDS(3)= ' DELTA'
WORDS(5)= ' TEMP '
WORDS(4)= 'LAST CHANCE'
WORDS(6)= ' TEMP '
WORDS(7)= 'THETA*.5'
IFLAG=5
SEAPRES=29.92
SEATEMP=518.7
C *****IE. LEFT AND RIGHT ENGINE*****
TYPE *, '*****^*****'
TYPE *, 'RUN LINESIZE 132 AND OPTION 7 BEFORE RUNNING THIS PROGRAM'
TYPE *, '*****'
TYPE 20
20 FORMAT(/, 'S', 5X, 'INPUT TABLE IDENTIFICATIONS (MAX 40); ')
ACCEPT S, IDENT
C *****
C *****INPUT OF DATA FROM TEST RUN*****
C *****
TYPE 50
50 FORMAT(/, 'S', 5X, '*****ENGINE RUN DATA TO BE CORRECTED AND CURVE

```

```

&FITTED;  ')
55  TYPE 70
70  FORMAT(/, ' $$', 5X, 'INPUT # OF ENGINE STABILIZATIONS;  ')
    ACCEPT *, NNN
    TYPE 60
60  FORMAT(/, 5X, 'INPUT RPM-N1, ', 2X, 'FUEL FLOW-WF, ', 2X, 'GROSS THRUST-
&-FG, ', 2X, 'RUN PRESS AND TEMP')
C  ***** RPM-N1 *****
    TYPE *, ' '
    TYPE *, 'ENTER THE VALUES OF RPM-N1'
75  DO 80 I=1, NNN
    TYPE 77, I
77  FORMAT(/, '$', 5X, 'INPUT RPM-N1', I3, '=')
    ACCEPT *, RPMN1(I)
80  CONTINUE
C  ***** FUEL FLOW - TFF *****
    TYPE *, 'ENTER THE VALUES OF FUEL FLOW- LBS/HOUR'
82  DO 87 I=1, NNN
    TYPE 85, I
85  FORMAT(/, '$', 5X, 'INPUT FF', I3, '=')
    ACCEPT *, TFF(I)
87  CONTINUE
C  ***** GROSS THRUST *****
    TYPE *, 'ENTER THE VALUES OF GROSS THRUST'
90  DO 93 I=1, NNN
    TYPE 92, I
92  FORMAT(/, '$', 5X, 'INPUT FG', I3, '=')
    ACCEPT *, TFG(I)
93  CONTINUE
C  ***** PRESSURE FOR DELTA *****
    TYPE *, 'ENTER THE VALUES OF PRESSURE ( IN HG )'
180 DO 183 I=1, NNN
    TYPE 182, I
182 FORMAT(/, '$', 5X, 'INPUT PRESS. *IN HG*', I3, '=')
    ACCEPT *, DELTA(I)
183 CONTINUE
C  ***** TEMPERATURE FOR THETA *****
    TYPE *, 'ENTER THE VALUES OF TEMPERATURE (FAHRENHEIT)'
190 DO 193 I=1, NNN
    TYPE 192, I
192 FORMAT(/, '$', 5X, 'INPUT TEMP. *F*', I3, '=')
    ACCEPT *, THETA(I)
193 CONTINUE
C  ^^^^^^ IFLAGS CONTROL CORRECTION OF CORRECT VALUES (5,6 THEN 7)
    GOTO 95
94  IFLAG=IFLAG + 1
    TYPE *, '***** CORRECTED VALUES AT TEST CONDITIONS *****'
95  WRITE('UT', 96)(WORDS(IFLAG-4), WORDS(IFLAG))
C  ***** PRINT OUT OF TABLES ON SCREEN *****
96  FORMAT(5X, '#', 2X, 'RPM VALUE', 3X, 'FUEL FLOW VALUE',
&3X, 'GROSS THRUST VALUE', 3X, A9, 2X, A9)
    DO 130 I=1, NNN
    IF(IFLAG.LE.6)GOTO 97
    THETA(I)=SQRT((THETA(I)+459.6)/SEATEMP)
    DELTA(I)=DELTA(I)/SEAPRES*.995

```


[illegible]

```

      GOTO 850
C
150  TYPE 151
151  FORMAT(/,'S',5X,'CHANGES IN ** PRESS ** ; Y/N ')
      ACCEPT 230,A
      IF(A.EQ.'N')GOTO 120
      TYPE 153
153  FORMAT(/,'S',5X, 'WHICH ** PRESS ** ?? ')
      ACCEPT *,K
      TYPE 155,K
155  FORMAT(/,'S',5X,'INPUT NEW PRESS',I3,'= ')
      ACCEPT *, DELTA(K)
      GOTO 150
C
120  TYPE 121
121  FORMAT(/,'S',5X,'CHANGES IN ** TEMP ** ; Y/N ')
      ACCEPT 230,A
      IF(A.EQ.'N')GOTO 94
      TYPE 123
123  FORMAT(/,'S',5X,'WHICH ** TEMP ** ?? ')
      ACCEPT *,K
      TYPE 125,K
125  FORMAT(/,'S',5X,'INPUT NEW TEMP',I3,'= ')
      ACCEPT *, THETA(K)
      GOTO 120
999  TYPE *,' >>>>>>>>> DETERMINING BREAKPOINTS <<<<<<<<<'
C
*****
C*  THIS GROUP OF STATEMENTS DETERMINES THE RPM BREAKPOINTS
C
*****
C  ^^^^^^^^^ N11 IS THE FIRST BREAKPOINT AND IS DETERMINED ^^^^^^^^^
      N11=ANINT(RPMN1(1)/1000)
      N11=N11*1000
      IF(N11.GT.RPMN1(1)) GOTO 1010
      N11=N11+500
C  ^^^^^^^^^ N12 IS THE LAST BREAKPOINT AND IS DETERMINED ^^^^^^^^^
1010 N12=ANINT(RPMN1(NNN)/1000)
      N12=N12*1000
      IF(N12.LT.RPMN1(NNN))GOTO 1020
      N12=N12-500
C  ^^^^^^^^^ THE NUMBER OF POINTS TO BE WORKED WITH IS FOUND ^^^^^^^^^
1020 N=( N12 -N11)/500+1
      DO 1000 I=1,N
1000 X2(I)=N11+500*(I-1)
C*  THE SUBROUTINE WACSUB IS CALLED TO INTERPOLATE
C*  THE TEST DATA TO THE RPM BREAKPOINTS.
C
      CALL WACSUB(RPMN1,TFG,TFG1,DY,X2,N,IERR,NNN)
      CALL WACSUB(RPMN1,TFF,TFF1,DY,X2,N,IERR,NNN)
      CALL WACSUB(RPMN1,TFFA,TFFA1,DY,X2,N,IERR,NNN)
C
C*  THE FOLLOWING STATEMENTS ACCESS THE FILE CONTAINING THE
C*  DECK DATA, AND STORES THE NUMBER OF DATA POINTS AS NUAL.
C
      TYPE 1100
1100  FORMAT(/,'S',5X,'INPUT FILENAME CONTAINING DECK DATA:')

```

```

ACCEPT 8000,FILENAME
OPEN(UNIT=9,FILE=FILENAME,USER='BRAMAN',STATUS='OLD',FORM=
&'FORMATTED',BLOCKED=.TRUE.,ACCESS='SEQUENTIAL',IOSTAT=I3,
&ERR=8300)
DO 1250 I=1,7
  READ(9,1200)
1200  FORMAT(' ',A)
1250  CONTINUE
C      ***** ENGINE DECK DATA IS READ FROM THE FILE *****
  READ(9,1300,END=1400)(XN1(I),FG(I),CFF(I),CWA(I),TSFC(I),
&I=1,100)
1300  FORMAT(5G15.7)
      GOTO 1500
1400  NVAL=I-1
1500  CONTINUE
C
C*    THE DECK DATA IS SEARCHED TO FIND THE N1
C*    CORRESPONDING TO THE INITIAL BREAKPOINT.
C
      IF(ANINT(X2(1)).GE.ANINT(XN1(1))) GOTO 1750
      TYPE *, 'FIRST RPM FROM TEST DATA IS TOO LOW; REENTER DATA'
      IFLAG=5
      GOTO 55
1750  CONTINUE
      DO 1800 I=1,NVAL
        IF(ANINT(XN1(I)).EQ.ANINT(X2(1))) GOTO 1900
1800  CONTINUE
      TYPE 1850
1850  FORMAT(/, ' ERROR IN N1 COMPARISON, PROGRAM TERMINATED')
      STOP
1900  L=I
C
C*    THIS LOOP DETERMINES WHICH TEST POINTS LIE WITHIN THE
C*    RANGE OF RPM'S FROM THE DECK DATA
C
      DO 1930 I=1,(NNN+1)
        IF(RPMN1(NNN-I+1).LE.XN1(NVAL))GOTO 1940
1930  CONTINUE
1940  MUAL=NNN-I+1
C
C      *****
C      >>>>>> INTERPOLATES ALL CHARACTERISTICS TO TEST ** RPM'S ** <<
C      >>>>>> FOR AIRFLOW DETERMINATION <<<<<<<<
C      *****
C
      CALL WACSUB(XN1,FG,CFG1,DY,RPMN1,MUAL,IERR,NVAL)
      CALL WACSUB(XN1,CWA,CWA1,DY,RPMN1,MUAL,IERR,NVAL)
      CALL WACSUB(XN1,CFF,CFF1,DY,RPMN1,MUAL,IRRR,NVAL)
      CALL WACSUB(XN1,TSFC,TSFC1,DY,RPMN1,MUAL,IERR,NVAL)
C      *****
C      ***** DETERMINE VALUES OF AIR FLOW *****
C      *****
      DO 1950 J=1,NNN
        ETA1(J)=TSFCA(J)/TSFC1(J)
        TSFC2(J)=TSFC1(J)*DELTA(J)**.97/DELTA(J)

```

```

      TWA1(J)=TFFA(J)*THETA(J)**2*((CWA1(J)*3600.0/(CFF1(J)
&*THETA(J)**2*ETA1(J)))+1/ETA1(J)-1)/3600.0
1950  CONTINUE
      DO 1960 I=1,N
      IF(X2(N-I+1).LE.RPMN1(MUAL))GOTO 1970
1960  CONTINUE
1970  IVAL=N-I+1
C      >>>>>> INTERPOLATES AIRFLOW BACK TO DECK BREAKPOINTS <<<<<<<<
      CALL WACSUB(RPMN1,TWA1,TWA,DY,X2,IVAL,IERR,MUAL)
      CALL WACSUB(RPMN1,TSFC2,TSFCX,DY,X2,IVAL,IERR,MUAL)
      DO 2000 J=1,N
        K=J+L-1
        DELFG(J)=TFG1(J)-FG(K)
        DELFF(J)=TFFA1(J)-CFF(K)
        TTSFC(J)=TFF1(J)/TFG1(J)
        TTSFCA(J)=TFFA1(J)/TFG1(J)
        ETA(J)=TTSFC(J)/TSFCX(J)
        ETAA(J)=TTSFCA(J)/TSFC(K)
2000  DELWA(J)=TWA(J)-CWA(K)
C      -----
C
C*     REST OF PROGRAM STORES THE DATA IN A FILE.
C*     IF THE USER DESIRES
C
C      THE RESULTS ARE OBTAINED BY LISTING THE CREATED FILE.
C
C      -----
2100  FORMAT(///,18X,'CORRECTED TEST VALUES * DELTA*.97')
2105  FORMAT(///,23X,'EXTRAPOLATED TEST VALUES')
2110  FORMAT(///,26X,'CORRECTION FACTORS')
2150  FORMAT(///,10X,A8,7X,A40)
2200  FORMAT(///,6X,'N1',11X,'FG',11X,'WA',11X,'FF',10X,'TSFC',7X,
&'TFSC @ .97')
2220  FORMAT(///, 6X,'N1',10X,'DELF',10X,'DELWA',8X,'DELFF',8X,'ETA',8X,
&'ETA - .97')
2250  FORMAT(//,5X,'RPM',11X,'LBS',9X,'LBS/SEC',6X,'LBS/HR',7X,'1/HR'
&,8X,'1/HR')
2260  FORMAT(//,5X,'RPM',11X,'LBS',10X,'LBS/SEC',7X,'LBS/HR')
      M=N
2300  FORMAT(/,3X,F7.0,5X,F9.3,4X,F9.3,4X,F9.3,4X,F9.7,4X,F9.7)
2323  FORMAT(/,3X,F7.0,5X,F9.3,5X,F9.3,5X,F9.3,4X,F9.7,4X,F9.7)
      TYPE 2400
2400  FORMAT(/,'$',5X,'DO YOU WISH TO STORE THE DATA? Y/N: ')
      ACCEPT 8010,A
      IF(A.EQ.'N') STOP
      GOTO 2490
2790  TYPE 2800
2800  FORMAT(/,5X,'FILENAME ALREADY EXISTS' )
2490  TYPE 2500
2500  FORMAT(/,'$',5X,'INPUT FILENAME TO STORE DATA IN: ')
      ACCEPT 8000,FILENAME
      OPEN(UNIT=7,FILE=FILENAME,USER='BRAMAN',STATUS='NEW',
&FILESIZE=40,FORM='FORMATTED',BLOCKED=.TRUE.,IOSTAT=I6,
&ERR=2600,CLEAR=.TRUE.)
2600  IF(I6.EQ.0)GOTO 2900

```

```

      IF(I6.GT.1)GOTO 8100
      IF(I6.EQ.1)GOTO 2790
2900  WRITE(7,2150,IOSTAT=I5,ERR=8200)(FILENAME,IDENT)
      WRITE(7,2100,IOSTAT=I5,ERR=8200)
      WRITE(7,2310,IOSTAT=I5,ERR=8200)
      WRITE(7,2320,IOSTAT=I5,ERR=8200)
      WRITE(7,2330,IOSTAT=I5,ERR=8200)(RPMN1(I),TFG(I),TWA1(I),TFFA(I)
&,TSFC(I),TSFCA(I), I=1,NNN)
      WRITE(7,2305,IOSTAT=I5,ERR=8200)
      WRITE(7,2315,IOSTAT=I5,ERR=8200)
      WRITE(7,2325,IOSTAT=I5,ERR=8200)
      WRITE(7,2335,IOSTAT=I5,ERR=8200)(RPMN1(I),CFG1(I),CWA1(I),CFF1(I)
&,TSFC1(I), I=1,NNN )
      WRITE(7,2105,IOSTAT=I5,ERR=8200)
      WRITE(7,2200,IOSTAT=I5,ERR=8200)
      WRITE(7,2250,IOSTAT=I5,ERR=8200)
      WRITE(7,2300,IOSTAT=I5,ERR=8200)(X2(I),TFG1(I),TWA(I),
&TFFA1(I),TTSFC(I),TTSFCA(I), I=1,M)
      WRITE(7,2110,IOSTAT=I5,ERR=8200)
      WRITE(7,2220,IOSTAT=I5,ERR=8200)
      WRITE(7,2260,IOSTAT=I5,ERR=8200)
      WRITE(7,2323,IOSTAT=I5,ERR=8200)(X2(I),DELFG(I),DELWA(I),DELFF(I)
&,ETA(I),ETAA(I),I=1,M)
      WRITE(7,4999,IOSTAT=I5,ERR=8200)
      WRITE(7,5000,IOSTAT=I5,ERR=8200)(X2(I),ETAA(I), I=1,M)
4999  FORMAT('1')
5000  FORMAT(T6,F7.0,T23,F9.7)
      TYPE *, '***** DATA SAVED *****'
      STOP
8000  FORMAT(A8)
8010  FORMAT(A1)
8100  TYPE*, 'ERROR IN OPEN 7', I6
8200  TYPE*, 'ERROR IN WRITE 7', I5
8300  TYPE*, 'ERROR IN OPEN 9', I3
2125  FORMAT(//,44X, 'DEL-TERMS ARE TEST VALUES MINUS DECK VALUES')
2305  FORMAT(//, '*** CORRECTED DECK VALUES AT TEST RPM S *** @ .97 ***',
&'*****')
2310  FORMAT(//,5X, 'CN1', 7X, 'CFG(TEST)', 5X, 'CWA(TEST)', 4X, 'CFF(TEST)',
&2X, 'CTSFC(TEST)', 2X, 'CTSFC @ .97')
2315  FORMAT(//,4X, 'CN1', 7X, 'FG(DECK)', 7X, 'WA(DECK)', 5X, 'FF(DECK)', 4X,
&'TSFC(DECK)')
2330  FORMAT(/,2X,F9.3,3X,F9.3,4X,F9.3,4X,F9.3,4X,F9.7,4X,F9.7)
2335  FORMAT(/,2X,F7.0,4X,F9.3,5X,F9.3,4X,F9.3,4X,F9.7)
2320  FORMAT(/,5X, 'RPM', 10X, 'LBS', 8X, 'LBS/SEC', 7X, 'LBS/HR', 8X,
&'1/HR', 8X, '1/HR')
2325  FORMAT(/,4X, 'RPM', 10X, 'LBS', 9X, 'LBS/SEC', 6X, 'LBS/HR', 8X, '1/HR')
      END
      SUBROUTINE WACSUB(X,Y,Z,DY,X2,K,IERR,NVAL)
C      COMMON/ORDER/IDUM(4),NVAL
C      DOUBLE PRECISION AUGXL,AUGYL,FACTOR
      DIMENSION H(150),X(1),X2(1),Y(1),DY(1)
C
C      SCALE THE X DATA SO THAT THE X'S AND Y'S ARE OF THE SAME MAGNITUDE
C
      AUGXL=0.

```



```

C      D(J) = DSQRT( H(J)*H(J) + U1*U1)
C      D(J) = SQRT( H(J)*H(J) + U1*U1)
10 CONTINUE
GO TO 40
C 20 WRITE (6, 30 ) J, (XJ(I),YJ(I),I=1,M)
C 30 FORMAT (1H0,38H***ERROR IN DATA GIVEN TO ROUTINE WAC.,
C 135H INTERVAL SIZE IN X IS ZERO AT THE ,I3,9HTH POINT. ,
C 2/, (2E16.5))
C      M = J-1
C      M1 = M-1
C      M2 = M-2
20 IERR=1
DO 11 I=1,M
11 CONTINUE
RETURN
40 CONTINUE
C
C* NOW STORE G VALUES AND PUT INPUT VALUES INTO F (FOR CONVENIENCE)
C
DO 50 J=2,M1
U1 = (D(J)*F(J-1) + D(J-1)*F(J)) / ( D(J) + D(J-1) )
C      G(J)= DTAN(U1)
C      G(J) = TAN(U1)
F(J-1) = YJ(J-1)
50 CONTINUE
F(M1) = YJ(M1)
F(M) = YJ(M)
C
C* (5)
C* NOW FIND CONSTS AND HOLD INTEGRAL AT J STATIONS IN YJ. FIRST AND
C* LAST ARE EXCEPTIONAL (QUADRATIC).
C
IF (IFLAG.EQ. 0) GO TO 60
C* FORCE FIRST POINT SLOPE TO ZERO IF IFLAG.NE. 0
G(1) = Z0
J1 = 1
GO TO 70
60 J1 = 2
A(1)=Z0
C*****
B(1)=(F(1)-F(2)+G(2)*H(1))/(H(1)*H(1))
C*****
C(1)=(Z2*(F(2)-F(1))-G(2)*H(1))/H(1)
D(1)=F(1)
70 A(M1) = Z0
B(M1)=(F(M)-F(M1)-G(M1)*H(M1))/(H(M1)*H(M1))
C(M1)=G(M1)
D(M1)=F(M1)
D(M)=F(M)
DO 80 J=J1,M2
A(J)=(H(J)*(G(J+1)+G(J))-Z2*(F(J+1)-F(J)))/(H(J)**3)
B(J)=(Z3*(F(J+1)-F(J))-H(J)*(G(J+1)+Z2*G(J)))/(H(J)*H(J))
C(J)=G(J)
D(J)=F(J)
80 CONTINUE
C
C (6)

```

```

C*   NOW CALC INTEGRAL.(SEE (5))
C
      YJ(1)=Z0
      YJ(2)=YJ(1)+H(1)*(F(1)+Z2*F(2)-G(2)*H(1)/Z2)/Z3
      DO 90 J=3,M1
      YJ(J)=YJ(J-1)+H(J-1)*(F(J-1)+F(J)+H(J-1)*(G(J-1)-G(J))/Z6)/Z2
90  CONTINUE
      YJ(M)=YJ(M1)+H(M1)*(Z2*F(M1)+F(M)+G(M1)*H(M1)/Z2)/Z3
C
C*   DONE. NOW FOR FINAL INTERP VALUES
C
      I=0
      J=2
100  I=I+1
110  IF (XI(I).LE.XJ(J)) GO TO 120
      IF (J.EQ.M) GO TO L20
      J=J+1
      GO TO 110
120  ZI=XI(I)-XJ(J-1)
      ZI2=ZI*ZI
      ZI3=ZI2*ZI
      ZI4=ZI3*ZI
      UA=A(J-1)
      UB=B(J-1)
      UC=C(J-1)
      UD=D(J-1)
      G(I)=Z3*UA*ZI2+Z2*UB*ZI+UC
      F(I)=UA*ZI3+UB*ZI2+UC*ZI+UD
      H(I)=UA*ZI4/Z4+UB*ZI3/Z3+UC*ZI2/Z2+UD*ZI+YJ(J-1)
      IF (I.LT.N)GO TO 100
C
C**  RESTORE DESTROYED YJ VALUES
C
      IF (ISAVE .EQ. 1) GO TO 140
      DO 130 J=1,M
      YJ(J)=D(J)
130  CONTINUE
      RETURN
140  CONTINUE
C*   DUMP ANSWERS BACK INTO YJ ARRAY IF ISAVE = 1
      DO 150 J=1,N
      YJ(J) = F(J)
150  CONTINUE
      RETURN
      END

```

(7)

C.3 FLIGHT TEST DATA REDUCTION

Figure C.3 illustrates the routines and their execution order to process flight test data. These programs had many automatic as well as interactive features. A description and listing (if available) for each program is included.

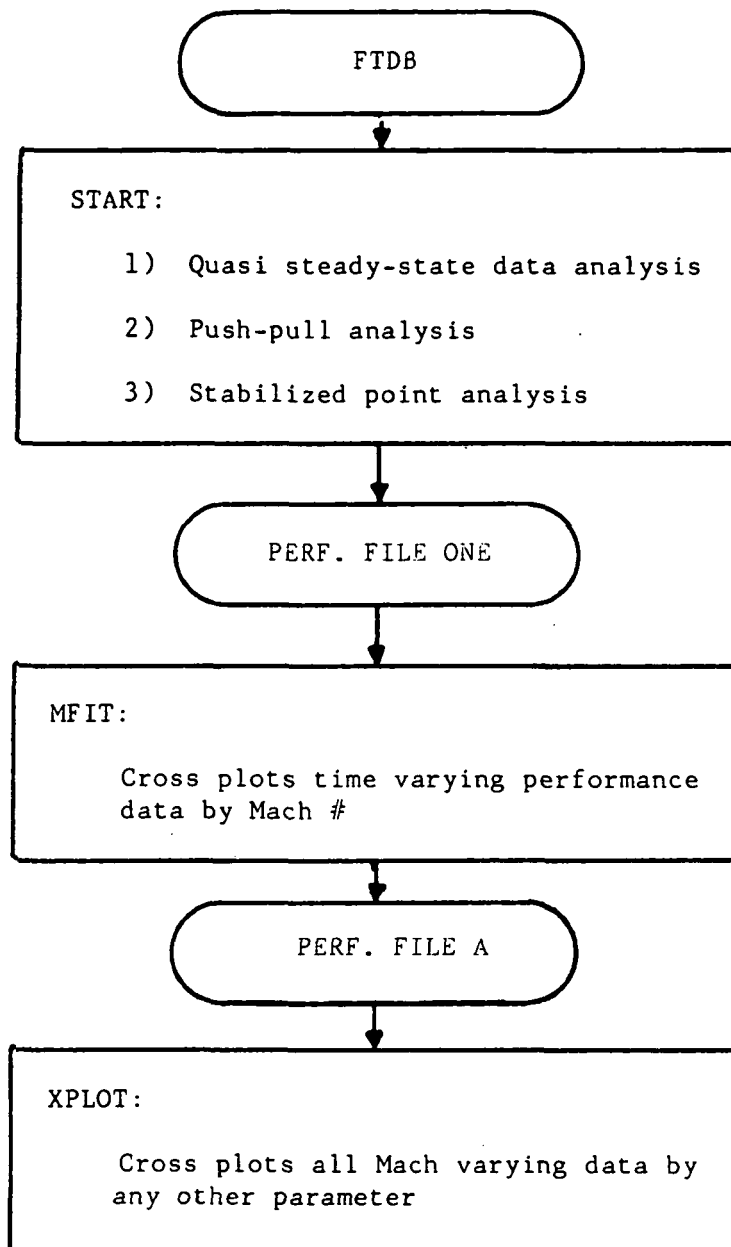


Figure C.3: Logic flow for performance data processing

C.3.1 START

PURPOSE:

This program processed the time varying parameters contained in flight test data base files and created performance file one. The program incorporated the quasi steady-state performance relationships needed for the analysis of those data. START was an interactive program designed as a generic routine suitable for the analysis of a number of aircraft configurations. Also, the analysis algorithm for conventional speed power and push-pull maneuvers were accomplished with the appropriate subroutines.

APPROACH:

The program read the flight test data base file (which were formatted as random access files) one time increment at a time, and then processed and stored that time increment in a direct access file known as performance data file one. This algorithm continued until the entire run for a particular maneuver had been processed. Subroutine STAB and PUSH/PULL were only called to reduce conventional speed-power and push-over, pull-up data.

```

C *****
C *
C * ORGANIZATION: UNIVERSITY OF KANSAS CENTER FOR RESEARCH INC. *
C * PROGRAM : F.START *
C * SUBROUTINE : HEDOT / STAB / PUSH/PULL / CONVEN / *
C * : REYNOLDS / TLU1 / TLU2 / RECOVERY / *
C * : GRANDIN / GRISTAT / GRLOWAIT *
C * AUTHOR : BRAMAN, KEITH *
C * COMPUTER : SEL 32/77 *
C * O/S : M.P.X. 1.3 *
C * COMPILER : ANSI-77 STANDARD FORTRAN(FORT77) *
C *
C * DATA FILE 1: D.##AREA (AIRCRAFT WETTED AREA AND LENGTH *
C * DATA) *
C *
C * 2: D4.##DAT (AIRCRAFT GEOMETRY DATA) *
C *
C * 3: D.##CLDE (CHANGE IN LIFT COEFFICIENT DUE TO *
C * ELEVATOR DEFLECTION) *
C *
C * 4: D.##CLIH (CHANGE IN LIFT COEFFICIENT DUE TO *
C * STABILIZER DEFLECTION) *
C *
C * 5: D4.##THR (DECK THRUST DATA) *
C *
C * 6: D4.##AIR (DECK AIRFLOW DATA) *
C *
C * 7: D.##CMDE (COEFFICIENT OF PITCHING MOMENT DUE *
C * ELEVATOR DEFLECTION) *
C *
C * 8: D.##CMG (COEFFICIENT OF PITCHING MOMENT DUE *
C * TO PITCH RATE) *
C *
C * ## = AIRCRAFT CODE *
C *
C * REVISIONS *
C *
C * I-----I-----I-----I-----I *
C * I PR# I VER/REV I NAME I DATE I *
C * I-----I-----I-----I-----I *
C * I I 2/4 I KEITH BRAMAN I 7/11/83 I *
C * I-----I-----I-----I-----I *
C *
C *****
C *****
C **
C ** THIS PROGRAM PROCESSES THE TIME VARYING PARAMETERS CONTAINED **
C ** IN FLIGHT TEST DATA BASE FILES, AND CREATES PERFORMANCE **
C ** FILE ONE. THE PROGRAM INCORPORATES THE QUASI STEADY-STATE **
C ** PERFORMANCE RELATIONSHIPS NEEDED FOR THE ANALYSIS OF **
C ** THOSE DATA. ALSO, THE ANALYSIS OF CONVENTIONAL SPEED- **
C ** POWER AND PUSH-PULL MANEUVERS ARE ACCOMPLISHED WITH THE **
C ** ATTACHED SUBROUTINES. **

```

```

C  **
C  **      EQUATION NUMBERING >   EQ.#   #/APPENDIX
C  **
C  **      APPENDIX REF. TO REPORT # KU-FRL-5770-1
C  **
C  *****
C
      CHARACTER*1 FILENUM,CONFIG,FLTCODE,SEGMENT,C
      CHARACTER*2 RUN
      CHARACTER*3 FLIGHT
      CHARACTER*8 FILENAME,USERNAME,NAME,ACIN,FILENAM1
      CHARACTER*48 NOTHING
      CHARACTER*7 MANEUVR/'JOPKSI0'/
      CHARACTER*8 ALLFLT(6) /'183','184','185','187','188','189'/
      CHARACTER*6 FLTCODE/'123456'/
      REAL*4 MAC,LT,WAREA(9),LENGTH(9),CMDE(50),CMQ(19),CLDE(50),
&      CLIH(21),GEOMETRY(40),MAXN1
      INTEGER*4 INPFCB(16) /3RINP,15*0/
      INTEGER*1 CLEAR/28/,ESC/27/
      INTEGER*4 FILESIZ,RECD
      DIMENSION A(192),THRUST(1000),WA(1000),B(60)
      COMMON/CONV/ AURPM1,WATOT,FGTOT,FRTOT,ANXW,THRUST,WA
      COMMON/GEOM/ALPHA,ALAMDA,QBAR,S,MAC,WAREA,LENGTH
      COMMON/OUT1/RCSTD(3)
      COMMON/OUT2/RF,SR,SRP
      COMMON/OUT3/PS,RERR,HDOT,HE(5),P1(5)
      COMMON/OUT4/CLS4,CDS4,CALPHA
      EQUIVALENCE      (A(1),ESB),      (A(2),ASB1),      (A(3),TIME),
&      (A(7),P),      (A(8),Q),      (A(9),R),      (A(33),FU),
&      (A(38),AN1L),  (A(39),AN1R),  (A(40),AN2L),  (A(41),AN2R),
&      (A(138),WFL),  (A(139),WFR),  (A(47),FTL),  (A(48),FTR),
&      (A(58),AMCT),  (A(59),HCT),  (A(63),ALPHAC),  (A(67),QCT),
&      (A(68),QBART), (A(77),FGL),  (A(78),FGR),  (A(79),FRL),
&      (A(80),FRR),  (A(81),FNL),  (A(82),FNR),  (A(83),AFL),
&      (A(84),AFR),  (A(85),DLTT2), (A(86),WT),  (A(87),XBAR),
&      (A(88),YBAR),  (A(89),ZBAR),  (A(94),PCTMAC), (A(96),ISUBYY),
&      (A(112),ANXC), (A(113),ANYC), (A(114),ANZC), (A(131),HCS),
&      (A(134),AMIC), (A(135),DLHPC), (A(62),UTT),  (A(71),TATK),
&      (A(76),RTHT2T), (A(122),TASK), (A(127),RTHT2S), (A(130),UTS),
&      (A(117),PAS),  (A(119),QCS),  (A(65),DAT),  (A(72),THAT),
&      (A(27),BETAU), (A(115),DLTE), (A(18),DLTS),  (A(49),TTSL),
&      (A(50),TTSR)
      ICOUNT=J=I=0
      PS=RERR=HDOT=A=THRUST=WA=B=WAREA=LENGTH=CMDE=CMQ=CLDE=CLIH=0.
      GEOMETRY=0.
C
      WRITE('UT',1000)ESC,CLEAR
C
C  THIS PROGRAM IS CAPABLE OF PROCESSING PERFORMACE DATA FOR THREE
C  AIRCRAFT WITHOUT RECONFIGURING THE CODE.(I.E. LEAR35,LEAR55,
C  CITATION II)
C
C  OPEN AND READ THE ENGINEERING UNITS DATA FILE
C
      OPEN(UNIT='UT')
1     TYPE 3

```

```

3  FORMAT(5(/),/,'$',15X,'INPUT AIRCRAFT TYPE CODE :',/,
&      20X,'A/C CODE',10X,'AIRCRAFT',/,
&      22X,'L3',18X,'LEAR35',/,
&      22X,'L5',18X,'LEAR55',/,
&      22X,'C2',18X,'CITATION II',/,
&      15X,'A/C CODE = ')
      ACCEPT 999,ACIN
      IF(ACIN.EQ.'L3')USERNAME='LEAR35'
      IF(ACIN.EQ.'L5')USERNAME='LEAR55'
      IF(ACIN.EQ.'C2')USERNAME='CITAT2'
C
C  READ ALL AIRCRAFT DATA FILES
C
C
C  OPEN AND READ WETTED AREA/LENGTH DATA FILE FOR THE REYNOLDS NUMBER
C  CORRECTION ON DRAG COEFFICIENT.
C
      FILENAME(1:2)='D.'
      FILENAME(3:4)=ACIN
      FILENAME(5:8)='AREA'
      OPEN(UNIT=1,STATUS='OLD',USER='BRAMAN',FORM='FORMATTED',
&         BLOCKED=.TRUE.,IOSTAT=I1,ERR=500,FILE=FILENAME)
      DO I=1,5
        READ(1,102)                                ! READ PAST BANNER
      END DO
      DO I=1,9
        READ(1,200)NAME,WAREA(I),LENGTH(I)
      END DO
      CLOSE(UNIT=1)
X      TYPE *,WAREA= ',WAREA
X      TYPE *,LENGTH= ',LENGTH
200  FORMAT(2X,A8,12X,F10.4,6X,F10.4)
C
C  OPEN AND READ AIRCRAFT GEOMETRY DATA FILE
C
      FILENAME(2:3)='4.'
      FILENAME(4:5)=ACIN
      FILENAME(6:8)='DAT'
      OPEN(UNIT=4,USER=USERNAME,FILE=FILENAME,FORM='FORMATTED',
&         BLOCKED=.TRUE.,IOSTAT=I1,ERR=503)
      DO I=1,5
        READ(4,102)                                ! READ PAST BANNER
      END DO
      DO I=1,40
        READ(4,996)NOTHING,GEOMETRY(I)
      END DO
      CLOSE(UNIT=4)
X      TYPE *,GEOMETRY= ',GEOMETRY
      S      = GEOMETRY(1)
      MAC     = GEOMETRY(10)
      HCGSTD  = GEOMETRY(26)
      ZCGSTD  = GEOMETRY(27)
      HTAIL1  = GEOMETRY(28)
      ZTAIL1  = GEOMETRY(29)
      ZT      = GEOMETRY(30)

```

```

XRAMDRAG= GEOMETRY(32)
ZRAMDRAG= GEOMETRY(33)
ALANDA  = GEOMETRY(34)*0.017453293
MAXN1   = GEOMETRY(35)
C
C OPEN AND READ CL-DELTA ELEVATOR DATA FILE
C
      FILENAME(1:2)='D.'
      FILENAME(3:4)=ACIN
      FILENAME(5:8)='CLDE'
      OPEN(UNIT=7,USER='BRAMAN',FILE=FILENAME,FORM='FORMATTED',
&        BLOCKED=.TRUE.,IOSTAT=I1,ERR=506)
      DO I=1,5
        READ(7,102)                ! READ PAST BANNER
      END DO
      DO I=1,50
        READ(7,*,END=666)CLDE(I)
      END DO
666      CONTINUE
      CLOSE(UNIT=7)
X      TYPE *, 'CLDE= ',CLDE
C
C OPEN AND READ CL-IH DATA FILE
C
      FILENAME(5:8)='CLIH'
      OPEN(UNIT=4,USER='BRAMAN',FILE=FILENAME,FORM='FORMATTED',
&        BLOCKED=.TRUE.,IOSTAT=I1,ERR=508)
      DO I=1,5
        READ(4,102)                ! READ PAST BANNER
      END DO
      READ(4,*)N2
      CLIH(1)=N2
      N3=N2+1
      READ(4,*)(CLIH(I),CLIH(I+N2),I=2,N3)
      CLOSE(UNIT=4)
X      TYPE *, 'CLIH= ',CLIH
C
C OPEN AND READ THRUST AND AIRFLOW DATA FILES
C
      FILENAME(2:3)='4.'
      FILENAME(4:5)=ACIN
      FILENAME(6:8)='THR'
      OPEN(UNIT=9,USER=USERNAME,STATUS='OLD',FORM='FORMATTED',
&        BLOCKED=.TRUE.,IOSTAT=I1,ERR=501,FILE=FILENAME)
C
      FILENAME(6:8)='AIR'
      OPEN(UNIT=10,USER=USERNAME,STATUS='OLD',FORM='FORMATTED',
&        BLOCKED=.TRUE.,IOSTAT=I1,ERR=502,FILE=FILENAME)
C
      DO I=1,5
        READ(9,102)                ! READ PAST BANNER
      END DO
      DO I=1,5
        READ(10,102)               ! READ PAST BANNER
      END DO

```

```

102  FORMAT(' ')
      READ(9,101,END=103)(THRUST(I),I=1,1000)
103  READ(10,101,END=104)(WA(I),I=1,1000)
104  CLOSE(UNIT=9)
      CLOSE(UNIT=10)
X    TYPE *, 'TRUST= ', THRUST
X    TYPE *, 'WA= ', WA
101  FORMAT(5G15.7)
C
C  OPEN AND READ DATA FILE FOR PUSH PULL MANEUVER(CMDE,CMQ)
C
      FILENAME(1:2)='D.'
      FILENAME(3:4)=ACIN
      FILENAME(5:8)='CMDE'
      OPEN(UNIT=5,USER='BRAMAN',FILE=FILENAME,FORM='FORMATTED',
&        BLOCKED=.TRUE.,IOSTAT=I1,ERR=504)
      DO I=1,5
        READ(5,102)                ! READ PAST BANNER
      END DO
      DO I=1,50
        READ(5,*,END=667)CMDE(I)
      END DO
667  CONTINUE
      CLOSE(UNIT=5)
X    TYPE *, 'CMDE= ', CMDE
C
      FILENAME(5:8)='CMQ'
      OPEN(UNIT=8,USER='BRAMAN',FILE=FILENAME,FORM='FORMATTED',
&        BLOCKED=.TRUE.,IOSTAT=I1,ERR=505)
      DO I=1,5
        READ(8,102)                ! READ PAST BANNER
      END DO
      READ(8,*)N2
      CMQ(1)=N2
      N3=N2+1
      READ(8,*)(CMQ(I),CMQ(I+N2),I=2,N3)
      CLOSE(UNIT=8)
X    TYPE *, 'CMQ= ', CMQ
C
C  CREATE FLIGHT TEST DATA FILE NAME AND OPEN WITH LOGICAL UNIT 'INP'
C
11  TYPE *, ' '
      TYPE *, 'INPUT FLT. # (999 IF NOT PERF FLT.) > '
      ACCEPT 999,FLIGHT
      IF(FLIGHT.EQ.'999')GO TO 2
      TYPE *, ' '
      TYPE *, '                                INPUT RUN # > '
      ACCEPT 999,RUN
      FILENAME(1:2)=ACIN
      FILENAME(3:4)=FLIGHT(2:3)
      FILENAME(6:7)=RUN
      FILENAME(8:8)='A'
      DO I=1,7
        FILENAME(5:5)=MANEUVR(I:I)

```



```

      OPEN(UNIT='INP',FILE=FILENAME,USER=USERNAME,STATUS='OLD',
      &      FORM='UNFORMATTED',BLOCKED=.FALSE.,IOSTAT=I1,ERR=90)
      K1=I
      GO TO 91
90      IF(I1.EQ.10)THEN
          CONTINUE
      ELSE
          GO TO 300
      END IF
      END DO

C
C IF NO DATA FOR THE SPECIFIED FLIGHT AND RUN CAN BE FOUND ON THE
C SYSTEM,NOTIFY THE USER AND RETURN TO THE FILE NAME INPUT(STATEMENT 11)
C
      TYPE 13,FLIGHT,RUN
13      FORMAT(/,5X,'THERE WERE NO PERF. DATA FILES FOUND FROM FLT.
      &      ',A3,'FOR RUN',A2)
      GO TO 11

C
C THIS OPTION IS USED IF THE FTDB FILE NAME DOES NOT CONFORM TO THE
C PERFORMANCE FILE NAMEING CONVENTION IN WHICH CASE THE FILE NAME
C IS INPUT MANUALLY
C
2      TYPE *,' '
      TYPE *,'INPUT FLIGHT TEST DATA FILE NAME > '
      ACCEPT 999,FILENAME
      OPEN(UNIT='INP',FILE=FILENAME,USER=USERNAME,STATUS='OLD',
      &      FORM='UNFORMATTED',BLOCKED=.FALSE.,IOSTAT=I1,ERR=92)
      GO TO 91
92      IF(I1.EQ.10)THEN
          TYPE *,'***** FTDB FILE NAME CAN NOT BE FOUND *****'
          GO TO 2
      END IF
      IF(I1.GT.1)GO TO 300

C
C TEST FILESIZE OF THE FTDB FILE AND CALC. FILESIZE FOR PERF. FILE ONE
C
91      INQUIRE(UNIT='INP',USER= USERNAME ,FILESIZE=FILESIZ)
      WRITE('UT',1000)ESC,CLEAR
      TYPE *,' '
      TYPE 18,FILENAME
      TYPE *,'      FILESIZE = ',FILESIZ

C
C IDENTIFY THE STARTING AND ENDING BLOCK NUMBERS TO BE PROCESSED
C
10      TYPE 100
100     FORMAT(5(/),'S',5X,'INPUT STARTING BLOCK NUMBER > ')
      ACCEPT *,N
      TYPE 110
110     FORMAT(/,'S',5X,'INPUT ENDING BLOCK NUMBER OF FLT DATA BASE > ')
      ACCEPT *,N1
      FILESIZ=ANINT((FLOAT(N1-N)/3.+5))

C
C CREATE PERFORMANCE DATA FILE ONE
C

```

```

WRITE('UT',1000)ESC,CLEAR
14 IF(FLIGHT.EQ.'999')THEN
    TYPE *,' '
    TYPE *,'INPUT PERFORMANCE FILE #1 FILENAME > '
    ACCEPT 999,FILENAM1
ELSE
    TYPE *,' INPUT PERF. FILE # (I.E. 1,2,3...) > '
    ACCEPT 999,FILENUM
    TYPE 12
12    FORMAT(2(/),'$',15X,'INPUT CONFIGURATION CODE :',/,
&        20X,'CODE',10X,'GEAR',10X,'FLAP(DEG)',/,
&        22X,'6',15X,'UP',15X,'0',/,
&        22X,'7',15X,'UP',15X,'8',/,
&        22X,'8',15X,'DN',15X,'8',/,
&        22X,'9',15X,'DN',15X,'40',/,
&        22X,'0',15X,'UP',15X,'0 SPOILER EVAL (FLT. 351)',/,
&        20X,'CODE > ')
    ACCEPT 999,CONFIG
    TYPE *,' '
    TYPE *,' INPUT DATA SEGMENT (I.E. A,B,C,...) > '
    ACCEPT 999,SEGMENT
    DO I=1,6
        IF(FLIGHT.EQ.ALLFLT(I))THEN
            K3=I
            GO TO 17
        END IF
    END DO
17    FILENAM1(1:1)='Q'
    FILENAM1(2:2)=FILENUM
    FILENAM1(3:3)=CONFIG
    FILENAM1(4:4)=FLTCODE(K3:K3)
    FILENAM1(5:6)=RUN
    FILENAM1(7:7)=MANEUUR(K1:K1)
    FILENAM1(8:8)=SEGMENT
    TYPE 18,FILENAM1
END IF

C
C OPEN PERFORMANCE FILE ONE
C
    OPEN(UNIT='OUT',STATUS='NEW',USER='BRAMAN',FORM='UNFORMATTED',
&        BLOCKED=.TRUE.,FILE=FILENAM1,IOSTAT=I2,ERR=301,
&        FILESIZE=FILESIZ,ACCESS='DIRECT',RECL=240,CLEAR=.TRUE.)
    GO TO 4
301 IF(I2.GT.1)GO TO 997
    IF(I2.EQ.1)THEN
        WRITE('UT',1000)ESC,CLEAR
        TYPE 998
        GO TO 14
    END IF

C *****
C *****
C ***** START CALCULATIONS *****
C *****
C *****
C

```

```

C READ FLIGHT TEST DATA FILE
C
4 RECD=1
  IBLK=0
  TYPE *, 'START CALC.'
C
C SUBROUTINE "GRANDIN" IS A SYSTEM LIBRARY ROUTINE. EACH TIME CALLED
C "GRANDIN" WILL READ ONE BLOCK OF DATA INTO ARRAY "A" . HERE A
C BLOCK OF DATA IS DEFINED AS ONE TIME SLICE OF DATA CONSISTING OF
C 192 VARIABLES. THE PROGRAM GETS THE NEW VALUE OF EACH OF ITS 56
C VARIABLES THROUGH THE EQUIVALENCE STATEMENT AT THE VARIABLE
C DECLARATION STATEMENT.
C
DO 5000 K=N,N1
120 CALL GRANDIN(INPFCB,A,192,K)
130 CALL QRISTAT(INPFCB,ISTAT,ICOUNT)
  IF(ISTAT.EQ.1)THEN
    CALL QRIOWAIT(INPFCB)
    GO TO 130
  END IF
  IF(A(2).EQ.600)GO TO 180
C
  ALPHA=ALPHAC*.017453293
  BETA = BETAU*.017453293
C
C CALCULATE WIND AXIS LOAD FACTOR
C
  ANXW=ANXC*COS(ALPHA)*COS(BETA)-ANZC*SIN(ALPHA)*COS(BETA)
  & -ANYC*SIN(BETA) !EQ.# 12D
  ANZW=ANXC*SIN(ALPHA)+ANZC*COS(ALPHA) !EQ.# 13D
C
C CALCULATE TOTAL THRUST PARAMETERS AND AVERAGE RPM(THRUST IN LBS)
C
  FGTOT=FGR+FGL !EQ.# 14D
  FRTOT=FRR+FRL !EQ.# 15D
  WFTOT=WFR+WFL !EQ.# 30D
C
C CALCULATE TOTAL AIRFLOW IN LBS/HR
C
  WATOT=AFR+AFL !EQ.# 49D
C
C CONVERT % RPM TO RPM AND AVERAGE LEFT AND RIGHT ENGINE
C
  AN1R=AN1R*MAXN1 /100.
  AN1L=AN1L*MAXN1 /100.
  AN2L=AN2L*29692./100.
  AN2R=AN2R*29692./100.
  AURPM1=(AN1R+AN1L)/2. !EQ.# 16D
  AURPM2=(AN2R+AN2L)/2. !EQ.# 17D
C
C CALC Q-BAR
C
  QBARS=(1.4 *DAT*2116.22*S*(AMCT**2))/2. !EQ.# 18D
  QBAR=QBARS/S
C

```

```

C THE AIRCRAFT DRAG COEFFICIENT CAN NOW BE CALC.
C
C 16 CD=(FGTOT*COS(ALPHA+ALAMDA)-FRTOT-WT*ANXW)/QBARS !EQ.# 19D
C
C CALC. REYNOLDS NUMBER CORRECTION FOR CD
C
C CALL REYNOLDS(CD,CDS,AMCT,TATK,THAT,DAT)
C
C THE POWER OFF LIFT COEFFICIENT (NOT CORRECTED) WILL BE
C
C CLAC=(WT*ANZW -FGTOT*SIN(ALPHA+ALAMDA))/QBARS !EQ.# 20D
C
C CALC. UNTRIMMED LIFT COEFFICIENT (DE=IH=0)
C
C L1=L2=L3=0
C CALL TLU2(CLDE,AMCT,QBAR,CLDE1,L1,L2)
C CLDE1=CLDE1/57.3
C CALL TLU1(CLIH,AMCT,CLIH1,L3)
C CLIH1=CLIH1/57.3
C CLIHDE02=CLAC-CLDE1*DLTE-CLIH1*DLTS
C
C CORRECTING LIFT COEFFICIENT (CLAC) FOR THRUST MOMENT EFFECTS
C
C ALL VARIABLES AND METHODOLOGY HAVE BEEN DEFINED IN KU REPORT
C KU-FRL-5770-1
C
C HCG=XBAR/12.
C ZCG=ZBAR/12.
C DCGH=HCG-HCGSTD !EQ.# 10D
C DCGU=ZCG-ZCGSTD !EQ.# 11D
C X1=XRAMDRAG-DCGH !EQ.# 32D
C Z1=ZRAMDRAG-DCGU !EQ.# 33D
C HR=Z1*COS(ALPHA)-X1*SIN(ALPHA) !EQ.# 34D
C A1=SQRT(DCGH**2+DCGU**2) !EQ.# 35D
C GAMMA=ATAN2(ABS(DCGU/DCGH)) !EQ.# 36D
C IF(DCGH.GE.0)THEN
C ZTHRUST=ZT-A1*SIN(ALAMDA+GAMMA)
C END IF
C IF(DCGH.LT.0)THEN
C ZTHRUST=ZT+A1*SIN(GAMMA+ALAMDA)
C END IF
C XTAIL=HTAIL1-DCGH !EQ.# 39D
C ZTAIL=ZTAIL1-DCGU !EQ.# 40D
C LT=XTAIL*COS(ALPHA)+ZTAIL*SIN(ALPHA) !EQ.# 41D
C
C THE CHANGE IN LIFT COEFFICIENT DUE TO THRUST IS:
C
C DCLT=(FGTOT*ZTRUST-FRTOT*HR)/LT/QBARS !EQ.# 42D
C
C THE AIRCRAFT LIFT COEFFICIENT CORRECTED FOR THRUST MOMENT EFFECTS
C BECOMES:
C
C CLTAC=CLAC+DCLT !EQ.# 43D
C

```

```

C CORRECTING LIFT COEFFICIENT FOR C.G. POSITION
C
  Z=HTAIL1*COS(ALPHA)+ZTAIL1*SIN(ALPHA)      !EQ.# 44D
  DCG=Z-LT                                     !EQ.# 45D
  DCLCG=- (CLTAC*DCG)/(LT+DCG)               !EQ.# 46D
C
C DELTA CG CORRECTION FOR POWER OFF CL WELL BE :
C
  DCLCG2=(CLAC*DCG)/(LT+DCG)
C
C THE TOTAL STEADY-STATE POWER OFF LIFT COEFFICIENT WILL BE:
C
  CLS=CLTAC+DCLCG                             !EQ.# 47D
C
C THE STEADY STATE POWER OFF LIFT COEFFICIENT WILL BE:
C
  CLSCG=CLAC+DCLCG2
C
C *****
C *
C * CALCULATE ALL REMAINING VALUES FOR DATA FILE NUMBER ONE *
C *
C *****
C
C CORRECT RPM
C
  CRPM1=AURPM1/RTHT2T                          !EQ.# 26D
  CRPM2=AURPM2/RTHT2T                          !EQ.# 48D
C
C CALCULATE CORRECTED ENGINE PARAMETERS
C
  CALL RECOVERY( CRPM1,PRF)
  DT2ENG=PRF*DLTT2                             !EQ.# 28D
  CFG=FGTOT/DT2ENG                             !EQ.# 29D
  CWA=(WATOT*RTHT2T)/DT2ENG                   !EQ.# 50D
  CFF=WFTOT/(RTHT2T*DT2ENG)
  WFR00TT2=WFTOT/RTHT2T
  WOD=WT/DAT                                  !EQ.# 25D
  TT5=(TTSL+TT5R)/2
  CTT5=TT5/(RTHT2T**2)
C
C CONVERT KNOTS TO FT/SEC
C
  UTT=UTT*1.689
  UTS=UTS*1.689
C
C TEST FOR MANEUVER TYPE AND CALL PROPER SUBROUTINE
C
  GO TO (21,21,23,22,21)K1
21 CALL HEDOT(ICNT,HCT,UTT,ANXW,TATK,TASK)
  CD_E=(FGTOT*COS(ALPHA+ALAMDA)-FRTOT-(WT*HDOT)/UTT)/QBARS !EQ. 11
  GO TO 24
22 CALL STAB(WFTOT,UTT,WT,DAT)
  GO TO 25
23 CALL PUSHPULL(Q,CLTAC,CDS,AMCT,CMDE,CMQ,CLDE,UTT,DCG,XBAR)

```

```

      GO TO 25
24  CALL CONVEN(RTHT29,RTHT2T,UTS,UTT,TASK,TATK,DT2ENG,AMCT,WT)
C
C *****
C *
C *          CREATE DATA FILE NUMBER ONE
C *
C *****
C
C  STUF CALC DATA INTO ARRAY "B" FOR RANDOUT WRITE
C
25  B(1)=      ESB      ! PILOT/ENGINEER EVENT
    B(2)=      ASB1     ! AIRCRAFT STATUS BYTE
    B(3)=      TIME     ! TIME
    B(4)=      AMCT     ! MACH NUMBER
    B(5)=      HCT      ! PRESSURE ALTITUDE (FT)
    B(6)=      ALPHAC    ! CORRECTED ANGLE OF ATTACK (DEG)
    B(7)=      BETAU    ! SIDE SLIP ANGLE
    B(8)=      CD       ! A/C DRAG COEFFICIENT
    B(54)=     CDS      ! CORRECTED FOR REYNOLDS NUMBER
    B(9)=      CLS      ! CORRECTED FOR THRUST MOMENT AND
                        C.G EFFECTS
C
    B(10)=     CLAC     ! POWER OFF LIFT COEFFICIENT
    B(11)=     CLSCG    ! CORRECTED FOR OFF STD. C.G. ONLY
    B(12)=     CLIHDEO  ! UNTRIMMED CL (CLDE/CLIH PREDICTED)
    B(13)=     CLIHDEO1 ! UNTRIMMED CL (CLDE/CLIH MMLE VALUES)
    B(14)=     CLIHDEO2 ! UNTRIMMED CL (CLDE/CLIH MMLE FROM
                        LEAR 35)
C
    B(15)=     AURPM1   ! AVERAGE N1 RPM
    B(16)=     AURPM2   ! AVERAGE N2 RPM
    B(17)=     CRPM1    ! CORRECTED AVERAGE N1 (RPM)
    B(18)=     CFG      ! CORRECTED GROSS THUST (LBS)
    B(19)=     CFF      ! CORRECTED FUEL FLOW (LBS/HR)
    B(20)=     CWA      ! CORRECTED AIR FLOW (LBS/HR)
    B(21)=     WFR00TT2 ! FUEL FLOW/ROOT THETA-T2 (LBS/HR)
    B(22)=     CTT5     ! CORRECTED TURBINE TEMP. (DEG C)
    B(23)=     ANXW     ! WIND AXES X ACCELERATION (G'S)
    B(24)=     ANZW     ! WIND AXES Z ACCELERATION (G'S)
    B(25)=     UTT      ! TRUE VELOCITY (FT/SEC)
    B(26)=     WOD      ! WEIGHT/DELTA (LBS)
    B(27)=     WT       ! A/C WEIGHT (LBS)
    B(28)=     QBARS    ! DYNAMIC PRESSURE * WING AERA (LBS)
    B(29)=     TATK     ! AMBIENT TEMP. (DEG K)
    B(30)=     RTHT2T   ! SQUARE ROOT THETA-T2
    B(31)=     DLTT2    ! CORRECTED PRESSURE RATIO
    B(32)=     XBAR     ! BODY AXIS X C.G. POSITION (INCHES)
    B(33)=     YBAR     ! BODY AXIS Y C.G. POSITION (INCHES)
    B(34)=     ZBAR     ! BODY AXIS Z C.G. POSITION (INCHES)
    B(35)=     DLTS     ! STABILIZER POSITION (DEG)
    B(36)=     DLTE     ! ELEVATOR POSITION (DEG)
      GO TO (30,30,50,40,30)K1
C
C  ADD DATA TO FILE 1 FOR ACCEL/DECCEL
C
30  B(37)=     PS      ! SPECIFIC EXCESS POWER (FT/SEC)

```

```

      B(38)=      HDOT      ! RATE OF CHANGE IN ENERGY HEIGHT
                           (FT/SEC)
      B(39)=      RERR      ! RELATIVE ERROR
      B(40)=      CD_E      ! CD CALC. FOR HDOT
      GO TO 60
C
C  ADD DATA TO FILE 1 FOR STABILIZED PIONTS
C
40  B(41)=      RF          ! RANGE FACTOR          (FT)
      B(42)=      SR          ! SPECIFIC RANGE      (NMPP)
      B(43)=      SRP        ! SPECIFIC RANGE PARAMETER (NM)
      GO TO 70
C
C  ADD DATA TO FILE 1 FOR PUSH PULL
C
50  B(44)=      CLS4        ! LIFT COEFF. CORRECTED FOR RATES
      B(45)=      CDS4        ! DRAG COEFF. CORRECTED FOR RATES
      B(46)=      CALPHA      ! ALPHA CORRECTED FOR RATES
      GO TO 70
C
C  ADD DATA TO FILE 1 FOR CONVENTIONAL
C
60  B(46)=      RCSTD(1)     ! STD WT = 12000 (FT/SEC)
      B(47)=      RCSTD(2)     ! STD WT = 14500 (FT/SEC)
      B(48)=      RCSTD(3)     ! STD WT = 17000 (FT/SEC)
      B(49)=      UTS         ! STD. TRUE VELOCITY (KNOTS)
      B(50)=      HCS         ! STD. PRESSURE ALTITUDE (FT)
      B(51)=      TASK        ! STD. AMBIENT TEMP (DEG. K)
      B(52)=      QCS         ! STD. COMPRESS. Q (LBS/F**2)
      B(53)=      PAS         ! STD. AMBIENT PRESSURE (LBS/FT**2)
      GO TO 70
70  CONTINUE
C
C  WRITE ALL DATA FOR THIS TIME SLICE TO PERFORMANCE FILE ONE
C
      WRITE('OUT',REC=RECD)B
C
C  INCREMENT INPUT AND OUTPUT FILE COUNTERS AND BEGIN PROCESSING
C  ON NEXT TIME SLICE.
C
      RECD=RECD+1
      IBLK=IBLK+1
5000 CONTINUE
1000 FORMAT(1X,2A1)
150  FORMAT(16G10.3)
180  TYPE 181,FILENAME1
181  FORMAT(5X,'PROGRAM START HAS BEEN COMPLETED SUCCESSFULLY AND',/,
& ' DATA FILE ONE HAS BEEN CREATED BY THE NAME: ',A8)
      TYPE *,' '
      TYPE *,' DO YOU WISH TO PROCESS ANOTHER FLT/RUN (Y/N) > '
      ACCEPT 999,C
      IF(C.EQ.'Y')THEN
        WRITE('UT',1000)ESC,CLEAR
        CLOSE(UNIT='INP')
        CLOSE(UNIT=4)
        CLOSE(UNIT=1)

```

```

        CLOSE(UNIT=5)
        CLOSE(UNIT=9)
        CLOSE(UNIT=8)
        CLOSE(UNIT=10)
        CLOSE(UNIT='OUT')
        CLOSE(UNIT=7)
        GO TO 11
    END IF
    CALL EXIT
300  TYPE *, '*** ERROR IN OPEN 5 **', I1
    CALL EXIT
302  TYPE *, '*** ERROR IN READ 5 **', I1
    CALL EXIT
303  TYPE *, '*** ERROR IN NAMELIST READ **', I8
    CALL EXIT
500  TYPE *, '*** ERROR IN OPEN # 1 **', I1
    CALL EXIT
501  TYPE *, '*** ERROR IN OPEN # 9 **', I1
    CALL EXIT
502  TYPE *, '*** ERROR IN OPEN # 10 **', I1
    CALL EXIT
503  TYPE *, '*** ERROR IN OPEN 4 **', I1
    CALL EXIT
504  TYPE *, '*** ERROR IN OPEN 5 **', I1
    CALL EXIT
505  TYPE *, '*** ERROR IN OPEN 8 **', I1
    CALL EXIT
506  TYPE *, '*** ERROR IN OPEN 7 **', I1
    CALL EXIT
507  TYPE *, '*** ERROR IN OPEN 4 (CLDE) **', I1
    CALL EXIT
508  TYPE *, '*** ERROR IN OPEN 4 (CLIH) **', I1
    CALL EXIT
997  TYPE *, '*** ERROR IN OPEN 6 **', I2
    CALL EXIT
996  FORMAT(A48,F15.6)
998  FORMAT(/,5X,'*** FILE NAME ALREADY EXISTS ***')
999  FORMAT(A)
    18  FORMAT(6X,'FILENAME = ',A8,/)
    END

```


C.3.1.1 PUSH/PULL

PURPOSE:

This subroutine, called by START, was used to reduce the push-over, pull-up, push-over maneuvers to coefficient form.

APPROACH:

The routine corrected for aircraft angular rates encountered throughout the maneuver as discussed in Section 3.2.3

```

C *****
C *
C * ORGANIZATION: UNIVERSITY OF KANSAS CENTER FOR RESEARCH INC. *
C * PROGRAM : ----- *
C * SUBROUTINE : F.PUSH *
C * AUTHOR : BRAMAN , KEITH *
C * COMPUTER : SEL 32/77 *
C * O/S : M.P.X. 1.3 *
C * COMPILER : ANSI-77 STANDARD FORTRAN (FORT77) *
C *
C * REVISIONS *
C *
C * I-----I-----I-----I-----I *
C * I PR# I UER/REV I NAME I DATE I *
C * I-----I-----I-----I-----I *
C * I I 1/0 I KEITH BRAMAN I 12/15/82I *
C * I-----I-----I-----I-----I *
C *
C *****
C
C SUBROUTINE PUSHPULL(Q,CLS,CDS,AMCT,CMDE,CMQ,CLDE1,UTT,DCG,XBAR)
C
C THIS SUBROUTINE IS USED TO REDUCE THE PUSHPULL MANUEVERS
C TO COEFFICIENT FORM. IN THIS ROUTINE THE AIRCRAFT PITCH RATE
C IS TAKEN INTO CONSIDERATION.
C
C COMMON/GEOM/ALPHA,ALAMDA,QBARS,S,MAC,WAREA,LENGTH
C COMMON/OUT4/CLS4,CDS4
C REAL*4 CMDE(1),CMQ(1),CLDE1(1),MAC
C
C ALL RATES AND ANGLES ARE IN DEGREES IN THE CALC.
C
C J=J1=L1=L2=L3=L4=0
C QBAR=QBARS/S
C CALL TLU2(CMDE ,AMCT,QBAR,CMDE1,L3,L4)
C CALL TLU1(CMQ,AMCT,CMQ1,J1)
C CALL TLU2(CLDE1,AMCT,QBAR,CLDE1,L1,L2)
C CMDE1=CMDE1/57.3
C CMQ1=CMQ1/57.3
C CLDE1=CLDE1/57.3
C
C CALC. CMQ-DOT
C
C CMQDOT = CMQ1
C QDOT=0.
C CDDE=0.
C DELMCG=-CLTAC*QBAR *DCG
C
C CALC. DELTA DELTA ELEVATOR
C
C DDE = (CMQDOT*Q*MAC)/(CMDE1*2*UTT)
C Z=-(IYY*QDOT)/(QBARS*MAC*CMDE1)
C Z=-(DELMCG)/(QBARS*MAC*CMDE1)
C
C THE CORRECTED LEFT AND DRAG COEFFICIENTS BECOME:

```

```
C      DCLDE01=CLDE01*DDE
      DCDDE=CDDE*DDE
C      CLS4=CLS+DCLDE01
      CDS4=CDS+DCDDE
C      RETURN
      END
```

C.3.1.2 STAB

PURPOSE:

This subroutine, called by START, calculated the performance parameters associated with a stabilized speed-power test point.

APPROACH:

This routine simply passed aircraft fuel flow, weight, true velocity, and ambient pressure ratio and calculated Range Factor (RF), Specific Range (SR), and Specific Range Parameter (SRP).

```

C *****
C *
C * ORGANIZATION: UNIVERSITY OF KANSAS CENTER FOR RESEARCH INC. *
C * PROGRAM : ----- *
C * SUBROUTINE : STAB *
C * AUTHOR : BRAMAN , KEITH *
C * COMPUTER : SEL 32/77 *
C * O/S : M.P.X. 1.3 *
C * COMPILER : ANSI-77 STANDARD FORTRAN (FORT77) *
C *
C * REVISIONS *
C *
C * I-----I-----I-----I-----I *
C * I PR# I VER/REV I NAME I DATE I *
C * I-----I-----I-----I-----I *
C * I I 1/0 I KEITH BRAMAN I 2/12/83 I *
C * I-----I-----I-----I-----I *
C *****
C
C SUBROUTINE STAB(WFTOT,UTT,WT,DAT)
C COMMON/OUT2/RF,SR,SRP
C
C THIS SUBROUTINE CALCULATES THE
C STABILIZED POINT PERFORMANCE PARAMETERS
C
C CALCULATE RANGE FACTOR
C
C RF=(UTT*WT)/WFTOT/1.689
C
C CALCULATE SPECIFIC RANGE
C
C SR=(UTT)/WFTOT/1.689
C
C CALCULATE SPECIFIC RANGE PARAMETER
C
C SRP=(UTT*DAT)/WFTOT/1.689
C RETURN
C END

```

C.3.2 MFIT

PURPOSE:

This program plotted time varying performance data against Mach number and generated a second and third order orthogonal polynomial through the data.

APPROACH:

The program read START output files and created performance file A. These files were manually built by the user of MFIT for every cardinal Mach number. The user had two options in building A files. The first was to simply use the calculated value at a cardinal Mach number of either the second or third order curve fit. The second allowed the user to manually interpolate a value for a particular Mach number and input that number to the A file. This program was considered proprietary to Kohlman Systems Research. For this reason a listing is not presented.

C.3.3 XPLOT

PURPOSE:

This routine cross plotted any parameter in performance file A to any other parameter of that file by any combination of Mach or power setting.

APPROACH:

This program was simply a file manipulation and plotting routine. This routine was considered proprietary to Kohlman Systems Research and for this reason a listing is not presented.

C.4 CRUISE AND TRAJECTORY MODELING

This area consisted of two main programs, ITERATE and MODEL.

Program ITERATE was use to predict the cruise performance of the modeled aircraft. Its description an approach can be found in section 3.2.4.1.

The second program, MODEL, was a trajectory following routine which was modified from the Air Force Flight Test Center's Digital Performance Simulation program. Due to the volume and the proprietary nature of this routine, the listing is not included. However, two routines were written which describe the baseline aerodynamic and engine characteristics to MODEL (DRAGA AND THRUST). Their description and listing are included.

C.4.1 ITERATE

PURPOSE:

This program was developed to calculate steady-state, constant-weight pressure ratio cruise performance from aircraft engine/aerodynamic characteristics generated from flight test quasi steady-state maneuvers.

APPROACH:

Since steady-state performance parameters cannot be explicitly solved for, it was necessary to develop an iterative routine which would converge upon the steady-state solution. This routine iterates on lift coefficient to obtain the steady-state values of C_D , C_L , F_G , F_N , ALPHA, RF, SR, SRP, and N_1 at a constant weight/pressure ratio for the entire Mach envelope. Section 3.2.4.1 presents an expanded description of this program.

```

C *****
C *
C * ORGANIZATION: UNIVERSITY OF KANSAS CENTER FOR RESEARCH INC. *
C * PROGRAM : F.ITERAT (ITERATE) *
C * SUBROUTINE : RECOVERY / REYNOLDS / STAB / TABINT *
C * AUTHOR : BRAMAN , KEITH *
C * COMPUTER : SEL 32/77 *
C * O/S : M.P.X. 1.3 *
C * COMPILER : ANSI-77 STANDARD FORTRAN (FORT77) *
C *
C * REVISIONS *
C *
C * I-----I-----I-----I-----I *
C * I PR# I VER/REV I NAME I DATE I *
C * I-----I-----I-----I-----I *
C * I I 1/0 I KEITH BRAMAN I 6/17/83 I *
C * I-----I-----I-----I-----I *
C *****
C
C PROGRAM ITERATE (ITERAT)
C BY:
C KEITH BRAMAN
C TOM YECHOUT
C
C THIS PROGRAM ITERATES ON LIFT COEFFICIENT TO OBTAIN
C STEADY STATE VALUES OF CORRECTED RPM ,RF,SR,SRP,CL,CD
C FG,WA,AND WF AT VARIOUS WEIGHT/DELTA RATIO
C *****
C *****
C
C PROGRAM INPUT:
C
C 1:FOUR-D TABLE LOOK-UP FOR DRAG COEFFICIENT AS A FUNCTION
C OF POWER , MACH, AND ALPHA (FOR MACH # LESS THAN OR
C EQUAL TO 0.60)
C
C 2:TWO-D TABLE LOOK-UP FOR DRAG COEFFICIENT AS A FUNCTION
C OF MACH AND ALPHA (FOR MACH # GREATER THAN 0.60)
C
C 3:TWO-D TABLE LOOK-UP FOR ALPHA AS A FUNCTION OF POWER
C AND LIFT COEFFICIENT FOR MACH # LESS THAN 0.65
C
C 4:TWO-D TABLE LOOK-UP FOR ALPHA AS A FUNCTION OF MACH
C AND LIFT COEFFICIENT FOR MACH # GREATER THAN 0.65
C
C 5:FLIGHT TEST ENGINE GROSS THRUST MODEL
C (AS A FUNCTION OF MACH AND RPM )
C
C 6:FLIGHT TEST ENGINE AIRFLOW MODEL
C (AS A FUNCTION OF MACH AND RPM )
C
C 7:FLIGHT TEST FUELFLOW ENGINE MODEL
C (AS A FUNCTION OF MACH AND RPM)

```



```

C
C THIS PROGRAM WAS DEVELOPED TO CALCULATE STEADY-STATE, CONSTANT-
C WEIGHT PRESURE RATIO CRUISE PERFORMANCE FROM AIRCRAFT ENGINE/
C AERODYNAMIC CHARACTERISTICS GENERATED FROM FLIGHT TEST QUASI STEADY
C STATE MANEUVERS. SINCE STEADY-STATE PERFORMANCE PARAMETERS CANNOT
C BE EXPLICITLY SOLVED FOR, IT WAS NECESSARY TO DEVELOP AN ITERATIVE
C ROUTINE WHICH WOULD CONVERGE UPON THE STEADY STATE SOLUTION. THIS
C ROUTINE ITERATES ON LIFT COEFFICIENT TO OBTAIN THE STEADY-STATE
C VALUES OF CD, CL, FG, FN, FR, ALPHA, RF, SR, SRP, AND N1 AT A CONSTANT
C WEIGHT/PRESURE RATIO FOR THE ENTIRE MACH ENVELOPE.
C
C ( "X'S" IN THE FIRST COLUMN ARE EXECUTABLE STATEMENTS DURING
C PROGRAM DEBUGGING)
C
CHARACTER*1 AAA
CHARACTER*8 FILENAME
INTEGER*1 FRMFD/220C/
REAL MAC, LT, KK, WAREA(9), LENGTH(9), NCURV(50)
COMMON/GEOM/ALPHA, ALANDA, QBARS, S, MAC, WAREA, LENGTH
COMMON/OUT2/RF, SR, SRP
DIMENSION CRPM(100), CALPHA(100), CCL(100), CCD(100),
& CCLAC(100), CM(100), CRF(100), GEOMETRY(40),
& CFG(100), CWA(100), CWF(100)
DIMENSION CORRPM(300), WA(300), FFL(350), CDARRAY(1150),
& CLPOWER(120), CLMACH(120), CSR(100), CSRP(100),
& ANEWCD(500)
C
C OPEN PRINTER OUTPUT FILE
C
OPEN(UNIT='UT')
OPEN(UNIT=6, FILE='SLO', SPOOLFILE=.TRUE., USER='BRAMAN',
& IOSTAT=I4, BLOCKED=.TRUE., FILESIZE=100,
& ERR=304)
IF(I4.GT.0)CLOSE(UNIT=6)
C
TYPE *, ' DO YOU WISH A HARD COPY ? Y/N > '
ACCEPT 999, AAA
IF(AAA.EQ.'Y')THEN
1 IXXX=6
ELSE
IXXX=3
2 TYPE *, 'OUTUT FILE NAME > '
ACCEPT 999, FILENAME
C
C OPEN DISC OUTPUT FILE
C
OPEN(UNIT=3, FILE=FILENAME, USER='BRAMAN', STATUS='NEW',
& FORM='FORMATTED', BLOCKED=.TRUE., IOSTAT=I15, ERR=92,
& FILESIZE=50)
GO TO 91
92 IF(I15.EQ.10)THEN
TYPE *, '***** FILE NAME ALL READY EXISTS *****'
GO TO 2
END IF
IF(I15.GT.1)GO TO 505

```

```

        END IF
C
C OPEN AND READ WETTED AREA/LENGTH DATA
C
91  FILENAME(1:2)='D.'
    FILENAME(3:4)='L3'
    FILENAME(5:8)='AREA'
    OPEN(UNIT=1,STATUS='OLD',USER='BRAMAN',FORM='FORMATTED',
      &   BLOCKED=.TRUE.,IOSTAT=I1,ERR=500,FILE=FILENAME)
      DO I=1,5
        READ(1,102)                                ! READ PAST BANNER
      END DO
      DO I=1,9
        READ(1,200)NAME,WAREA(I),LENGTH(I)
      END DO
      CLOSE(UNIT=1)
X    TYPE *, 'WAREA= ',WAREA
X    TYPE *, 'LENGTH= ',LENGTH
C
C OPEN AND READ POWER OF DELTA CURVE FOR FUELFLOW CORRECTION
C
      OPEN(UNIT=17,STATUS='OLD',USER='LEAR35',FORM='FORMATTED',
      &   BLOCKED=.TRUE.,FILE='D4.L3NNN',IOSTAT=I1,ERR=515)
      DO I=1,5
        READ(17,510)
      END DO
510  FORMAT(' ')
      DO I=1,17
        READ(17,*)NCURV(I),NCURV(I+17)
      END DO
      CLOSE(UNIT=17)
C
C OPEN AND READ RPM VS THRUST TABLE
C
      COPRPM =0.
      OPEN(UNIT=8,FILE='D.CRPM48',USER='BRAMAN',FORM='FORMATTED',
      &   BLOCKED=.TRUE.,IOSTAT=I6,ERR=400)
      READ(8,1000,END=402)(CORRPM(I),I=1,300)
402  CLOSE(UNIT=8)
X    TYPE *, 'THRUST= ',CORRPM
C
C OPEN AND READ AIRFLOW TABLE
C
      WA=0.
      OPEN(UNIT=9,FILE='AIRFL048',USER='BRAMAN',FORM='FORMATTED',
      &   BLOCKED=.TRUE.,IOSTAT=I7,ERR=401)
      READ(9,1000,END=404)(WA(I),I=1,300)
404  CLOSE(UNIT=9)
X    TYPE *, 'AIRFLOW= ',WA
C
C OPEN AND READ FUELFLOW TABLE
C
      FFL=0.
      OPEN(UNIT=10,FILE='FUELFLOW',USER='BRAMAN',FORM='FORMATTED',
      &   BLOCKED=.TRUE.,IOSTAT=I11,ERR=500)

```

```

      READ(10,1000,END=406)(FFL(I),I=1,350)
406  CLOSE(UNIT=10)
X    TYPE *, 'FUEL FLOW =', FFL
C
C  OPEN AND READ ALPHA AS A FUNCTION OF POWER AND CL TABLE
C
      CLPOWER=0.
      OPEN(UNIT=11,FILE='D.CLPOWR',USER='BRAMAN',FORM='FORMATTED',
&        BLOCKED=.TRUE.,IOSTAT=I9,ERR=501)
      READ(11,1000,END=408)(CLPOWER(I),I=1,120)
408  CLOSE(UNIT=11)
X    TYPE *, 'CLPOWER= ', CLPOWER
C
C  OPEN AND READ APLHA AS A FUNCTION OF MACH AND CL TABLE
C
      CLMACH=0.
      OPEN(UNIT=12,FILE='D.CLMACH',USER='BRAMAN',FORM='FORMATTED',
&        IOSTAT=I10,ERR=502,BLOCKED=.TRUE.)
      READ(12,1000,END=409)(CLMACH(I),I=1,120)
409  CLOSE(UNIT=12)
X    TYPE *, 'CLMACH= ', CLMACH
C
C  OPEN AND READ FOUR-D DRAG TABLE (FOR MACH# LESS THAN OR EQUAL TO .6)
C
      CDARRAY=0.
      OPEN(UNIT=13,FILE='D.CDARRY',USER='BRAMAN',FORM='FORMATTED',
&        IOSTAT=I11,ERR=503,BLOCKED=.TRUE.)
      READ(13,1000,END=506)(CDARRAY(I),I=1,1150)
506  CLOSE(UNIT=13)
X    TYPE *, 'CDARRAY= ', CDARRAY
C
C  OPEN AND READ DRAG AS A FUNCTION OF MACH AND ALPHA (MACH LT .6)
C
      OPEN(UNIT=13,FILE='NWCDS' ,USER='BRAMAN',FORM='FORMATTED',
&        IOSTAT=I11,ERR=503,BLOCKED=.TRUE.)
      READ(13,1000,END=509)(ANEWCD(I),I=1,1150)
509  CLOSE(UNIT=13)
C
C  OPEN AND READ AIRCRAFT GEOMETRY DATA
C
      DEBUG=0.
      OPEN(UNIT=4,USER='BRAMAN',FILE='D4.L3DAT',FORM='FORMATTED',
&        BLOCKED=.TRUE.,IOSTAT=I1,ERR=555)
      DO I=1,5
         READ(4,102)                ! READ PAST BANNER
      END DO
      DO I=1,40
         READ(4,996)NOTHING,GEOMETRY(I)
      END DO
      CLOSE(UNIT=4)
X    TYPE *, 'GEOMETRY= ', GEOMETRY
      S      = GEOMETRY(1)
      MAC    = GEOMETRY(10)
      HCGSTD = GEOMETRY(26)
      ZCGSTD = GEOMETRY(27)

```

```

        HTAIL1 = GEOMETRY(28)
        ZTAIL1 = GEOMETRY(29)
        ZT      = GEOMETRY(30)
        XRAMDRAG= GEOMETRY(32)
        ZRAMDRAG= GEOMETRY(33)
        ALAMDA  = GEOMETRY(34)*0.017453293
        MAXN1   = GEOMETRY(35)
1      I=1
        DM= -0.01
C
C      SEA LEVEL PRESSURE = 2116.22 LB/SQ FT.
C
        PZERO=2116.22
C
        CM=CRPM=CWF=CWA=CCL=CCD=CRF=CSR=CSRP=CALPHA=CCLAC=0.0
C
C THIS STARTS THE INTERACTIVE VARIABLE INPUT OF THE PROGRAM
C
        TYPE 50
50      FORMAT(/,'S',5X,'INPUT STEADY STATE CORRECTED RPM: ')
        ACCEPT *,ARPM
        TYPE 70
70      FORMAT(/,'S',5X,'INPUT STEADY STATE WT/DELTA: ')
        ACCEPT *,WOD
        TYPE 80
80      FORMAT(/,'S',5X,'INPUT BEGINNING MACH #: ')
        ACCEPT *,AM
        TYPE 100
100     FORMAT(/,'S',5X,'INPUT THETA: ')
        ACCEPT *,THETA
        TYPE 110
110     FORMAT(/,'S',5X,'INPUT DELTA: ')
        ACCEPT *,DELTA
        TYPE 111
111     FORMAT(/,'S',5X,'INPUT HORIZONTAL C.G. DELTA: ')
        ACCEPT *,DCGH
        TYPE 112
112     FORMAT(/,'S',5X,'INPUT VERTICAL C.G. DELTA: ')
        ACCEPT *,DCGU
C
C CALC. SONIC VELOCITY (FPS)
C
        A=1116.4*SQRT(THETA)
C
C THE ROUTINE NORMALLY STARTS WITH DESIRED STEADY-STATE VALUES
C OF WT/DELTA , N1, AND MACH NUMBER. THE ITERATION BEGINS BY
C FIRST APPROXIMATING LIFT COEFFICIENT WITH :
C
5      L=0
        CL=WOD*( 2./((1.4*PZERO*S*(AM**2)))
        THETA1 = THETA*(1.+.2*(AM**2))
        DELTA2 = DELTA*((1.+.2*(AM**2))**3.5)
        QBARS = (1.4*DELTA*PZERO*S*(AM**2))/2.
        PCTRPM=((ARPM*SQRT(THETA*(1.+.2*(AM**2))))/20689.0)*100.0
C

```

```

C   THE ITERATION LOOP BEGINS HERE WITH THE CALC. OF ALPHA BASED ON THE
C   APPROXIMATION OF LIFT COEFFICIENT .
C
C   THE FIRST CALCULATION WILL BE FOR ALPHA. THIS IS DONE WITH A TABLE
C   LOOK-UP OF CL VS ALPHA . HOWEVER FOR MACH # LESS THAN OR EQUAL TO
C   .65 THE CL VS ALPHA CURVE BREAKS OUT BY POWER, ABOVE .65 THE
C   CURVE BREAKS OUT BY MACH NUMBER.
C
10   IF(AM.LE.0.65)THEN
      L1=L2=0
      CALL TLU2(CLPOWER,CL,PCTRPM,ALPHA,L1,L2)
    ELSE
      L3=L4=0
      CALL TLU2(CLMACH,CL,AM,ALPHA,L3,L4)
    END IF
C
C   THE DRAG COEFFECIENT IS KNOW CALC. WITH A FOUR-D TABLE
C   LOOK-UP ON POWER,MACH AND ALPHA FOR MACH NUMBERS LESS THAN .6.
C   FOR MACH NUMBERS GREATER THAN OR EQUAL TO .6 A TWO-D LOOK-UP IS DONE
C   WITH MACH AND ALPHA.
C
      L1=L2=L3=0
      IF(AM.GE..60)THEN
        CALL TLU2(ANEWCD ,ALPHA,AM,CDS,L1,L2)
      ELSE
        CALL TLU3( CDARRAY,ALPHA,PCTRPM,AM,CDS,L1,L2,L3)
      END IF
      ALPHA=ALPHA*0.017453293
      CALL RECOVERY(ARPM,PRF)
C
C   CORRECT CD FOR REYNOLDS  NUMBER EFFECT
C
      CALL REYNOLDS(CD,CDS,AM,THETA,DELTA)
C
C   THE CORRECTED AIR FLOW IS NOW CALC.
C
      L1=L2=0
      CALL TLU2(WA,ARPM,AM,CAIRFL,L1,L2)
C
C   CALAULATE CORRECTED RAM DRAM FOR ONE  ENGINE
C
      FRODT2=((CAIRFL*AM*A)/(SQRT(THETA1)*32.2))
C
C   CALCULATE RAM DRAG OVER DELTA (MULT. BY 2 FOR BOTH ENGINES)
C
      FROD=FRODT2*((1.+2*(AM**2))**3.5)*PRF*2.
C
C   CALC. DRAG/DELTA
C
      DOD = (CD *1.4*PZERO*S*(AM**2))/2.
C
      FGOD= (DOD +FROD)/(COS(ALPHA+ALAMDA))
C

```



```

C  CALCULATE CORRECTED GROSS THRUST FOR ONE ENGINE
C
C      FGODT2=(FGOD/(((1.+2*(AM**2))**3.5)*PRF))/2.
C
C  WITH CORRECTED THRUST GO INTO THE FLIGHT TEST RPM VS THRUST
C  CORRECTED CURVES AND GET A NEW CORRECTED RPM
C
C      L1=L2=0
C      CALL TLU2(CORRPM,FGODT2,AM,ARPM,L1,L2)
C      PCTRPM=((ARPM*SQRT(THETA*(1.+2*(AM**2))))/20688.0)*100.0
C
C  CALC. THRUST/DELTA
C
C      FOD = FGOD
C
C  CALC. NEW LIFT COEFFICIENT
C
C      CL1=((WOD-FOD*(SIN(ALPHA+ALAMDA)))/QBARS)*DELTA
C
C  CORRECTING LIFT COEFFICIENT FOR THRUST MOMENT EFFECTS
C
C      X1=XRAMDRAG-DCGH
C      Z1=ZRAMDRAG-DCGU
C      HR=Z1*COS(ALPHA)-X1*SIN(ALPHA)
C      A1=SQRT(DCGH**2+DCGU**2)
C      GAMMA1=ATAN2(ABS(DCGU/DCGH))
C
C      IF(DCGH.GE.0)THEN
C          ZTHRUST=ZT-A1*SIN(ALAMDA+GAMMA1)
C      END IF
C
C      IF(DCGH.LT.0)THEN
C          ZTHRUST=ZT+A1*SIN(GAMMA1+ALAMDA)
C      END IF
C
C      XTAIL=HTAIL1-DCGH
C      ZTAIL=ZTAIL1-DCGU
C      LT=XTAIL*COS(ALPHA)+ZTAIL*SIN(ALPHA)
C
C  THE CHANGE IN LIFT COEFFICIENT DUE TO THRUST FOR
C  BOTH ENGINES BECOMES:
C
C      DCLT=2.*(FGODT2*ZTHRUST-FRODT2*HR)*DELTA2/LT/QBARS
C
C  THE AIRCRAFT LIFT COEFFICIENT CORRECTED FOR THRUST MOMENT
C  EFFECTS BECOMES :
C
C      CLTAC=CL1+DCLT
C
C  CORRECTING LIFT COEFFICIENT FOR OFF STANDARD C.G. POSITION
C
C      Z=HTAIL1*COS(ALPHA)+ZTAIL1*SIN(ALPHA)
C      DCG=Z-LT
C      DCLCG=-((CLTAC*DCG)/(LT+DCG))

```

!EQ.# 32D
 !EQ.# 33D
 !EQ.# 34D
 !EQ.# 35D
 !EQ.# 36D

!EQ.# 39D
 !EQ.# 40D
 !EQ.# 41D

!EQ.# 44D
 !EQ.# 45D
 !EQ.# 46D

```

C THE TOTAL STEADY STATE POWER OFF LIFT COEFFICIENT WILL BE:
C
C     CLS=CLTAC+DCLCG
C
C     TEST CLS WITH CL FOR CONVERGENCE, IF THEY ARE WITHIN .00001
C     OF EACH OTHER IT WILL BE ASSUMED THEY HAVE CONVERGED
C     ONTO A STABILIZED POINT
C
C     IF(CLS.LE.CL+.00001.AND.CLS.GE.CL-.00001)GOTO 1100
C     CL=CLS
C     L=L+1
C     IF(L.GE.20)GO TO 1100
C
C CONTINUE ITERATION
C
C     GOTO 10
C
1100 CONTINUE
C
C
C     IF(I.GT.100) GOTO 2000
C     CRPM(I)= ARPM
C     CCL(I)= CLS
C     CALPHA(I) =ALPHA*57.3
C     CM(I)= AM
C     CCD(I)= CDS
C     CCLAC(I)=CL1
C     L1=L2=0
C
C CLAC. FUEL FLOW FOR BOTH ENGINES
C
C     CALL TLU2(FFL,ARPM,AM,CFFLOW,L1,L2)
C     CALL TABINT(AM,FULN,0,17,0,NCURV,IND)
C     FFLOW=CFFLOW*SQRT(THETA1)*(DELTA2**FULN)
C     FFLOW=(FFLOW+ADDFFL)*2.
C
C CALL STAB TO CALC. RANGE FACTORS
C
C     WT=WOD*DELTA
C     UTT= AM*(49.04*SQRT(518.67*THETA))
C     CALL STAB(FFLOW,UTT,WT,DELTA)
C
C     CFG(I)=FGODT2
C     CWA(I)=CAIRFL
C     CWF(I)=CFFLOW
C     CSR(I)=SR
C     CRF(I)=RF
C     CSRP(I)=SRP
C
C IF THE MACH NUMBER IS LESS THAN .2 STOP THE ITERATION
C
C     IF(AM.LE.0.2.OR.L.GE.20)GO TO 2000
C
C INCREMENT MACH NUMBER TO FIND A NEW STEADY STATE POINT

```

```

C      AM = AM + DM
      I=I+1
      GOTO 5
2000  CONTINUE
      TYPE *, ' '
      TYPE 215,WOD
      TYPE 221
      N=I
      DO J=1,N
        TYPE 300,
&      CM(J),CALPHA(J),CCL(J),CCD(J),CRPH(J),CRF(J),CSR(J),CSRP(J)
      END DO
      IF(L.GE.20)TYPE 216
C
C WRITE OUT THE SOLUTIONS TO THE PROPER DEVICE
C
      IF(IXXX.EQ.6)THEN
        WRITE(IXXX,3000)FRMFD
      END IF
      WRITE(IXXX,215)WOD
      WRITE(IXXX,220)
      N=1
      DO 250 J=1,N
        WRITE(IXXX,305,IOSTAT=12,ERR=556)
&      CM(J),CALPHA(J),CCL(J),CCD(J),CCLAC(J),CRPH(J),CFG(J),CHF(J),
&      CWA(J),CRF(J),CSR(J),CSRP(J)
250  CONTINUE
      IF(L.GE.20)WRITE(IXXX,216)
      IF(IXXX.EQ.6)THEN
        WRITE(IXXX,3000)FRMFD
      END IF
C
C START NEW ITERATION
C
      GO TO 1
102  FORMAT(' ')
200  FORMAT(2X,A8,12X,F10.4,6X,F10.4)
215  FORMAT(/,T32,'PROGRAM ITERATE',/,T18,'CALCULATEDFOR A WT/DELTA
& RATIO OF : ',F7.1,/)
216  FORMAT(8X,'THE LAST ITERATION HAS EXCEEDED THE ITERATION ',
& 'LIMIT OF TWENTY',/,22X,'AND THE PROGRAM HAS BEEN TERMINATED')
221  FORMAT(T2,'MACH',T11,'ALPHA',T22,'CLS',T32,'CDS',T43,'RPM',
& T53,'RF',T63,'SR',T73,'SRP',/)
220  FORMAT(T2,'MACH #',T14,'ALPHA',T26,'CLS',T38,'CDS',T50,'CL1',
& T62,'RPM',T68,'FGODT2',T76,'CFFLOW',T88,'CWA',T98,'RF',
& T111,'SR',T125,'SRP',/)
230  FORMAT( 20X,'DELTA FUEL FLOW IS = ',F10.4,/)
300  FORMAT(8(1X,G9.4))
304  TYPE *, 'ERROR',I4,'IN OPEN 6'
      CALL EXIT
305  FORMAT(12(1X,G10.4))
333  FORMAT(1X,I4)
400  TYPE *, 'ERROR IN OPEN 8 (THRUST) ',I6
      CALL EXIT

```

```

401  TYPE *, 'ERROR IN OPEN 9 (AIRFLOW) ', I7
      CALL EXIT
500  TYPE *, 'ERROR IN OPEN 10 (FUELFLOW) ', I8
      CALL EXIT
501  TYPE *, 'ERROR IN OPEN 11 (D.CLPOWR) ', I9
      CALL EXIT
502  TYPE *, 'ERROR IN OPEN 12 (D.CLMACH) ', I10
      CALL EXIT
503  TYPE *, 'ERROR IN OPEN 13 (D.CDARRY) ', I11
      CALL EXIT
505  TYPE *, 'ERROR IN OPEN 3 (OUTPUT FILE) ', I15
515  TYPE *, 'ERROR IN OPEN 17', I1
      CALL EXIT
555  TYPE *, 'ERROR IN GEOMETRY READ, ERR=', I1
      CALL EXIT
556  TYPE *, 'ERROR IN WRITE 5, ERR=', I2
      CALL EXIT
996  FORMAT(A48,F15.6)
999  FORMAT(A)
1000 FORMAT(6G13.6)
3000 FORMAT(1X,1A1)
      END
C
1
      SUBROUTINE REYNOLDS(CD,CDS,AM,THETA,DELTA)
C
C REYNOLDS NUMBER CORRECTION SUBROUTINE
C
C THIS ROUTINE WAS DEVELOPED BY MAJ. TOM YECHOUT AND
C CODED BY KEITH BRAMAN
C
C THE ANALYSIS REF.
C      1: AFFTC-TR-81-3
C          "EVALUATION OF THE EFFECT OF WINGLETS ON THE PERFORMANCE
C            OF A KC-135A AIRCRAFT"
C
C      2: "AIRPLANE AERODYNAMICS AND PERFORMANCE"
C          BY LAN/ROSKAM
C
C
C      COMMON/GEOM/ALPHA,ALAMDA,QBARS,S,MAC,WAREA,LENGTH
C      REAL*4 WAREA(9),LENGTH(9),MAC
C      REAL*4 RETEST(9),RE25K(9),K
C
C CALC. CONSTANT FOR ALL 25K FEET REYNOLDS NUMBER
C
C      TATK=286.16*THETA
C      CONSTANT=3362674.6*AM
C
C CALC. 25K FEET REYNOLDS NUMBER
C
C      DO I=1,7
C      RE25K(I)=CONSTANT*LENGTH(I)
C      END DO

```

```

C
C  CALC. CONSTANT FOR TEST ALTITUDE REYNOLDS NUMBER
C
      CONTTEST=(7100000.0*DELTA*AM*(TATK+110.4))/(398.55*THETA**2)
C
C  CALC. TEST ALTITUDE REYNOLDS NUMBER
C
      DO I=1,7
        RETEST(I)=CONTTEST*LENGTH(I)
      END DO
C
C  CALC. K-FACTOR
C
      K=.455/S/((1.+.144*AM**2)**.65)
C
C  CALC. CD PRIMED AT 25K FEET
C
      CDP25K=K*(WAREA(1)/(LOG10(RE25K(1)))**2.58
&      +WAREA(2)/(LOG10(RE25K(2)))**2.58
&      +WAREA(3)/(LOG10(RE25K(3)))**2.58
&      +WAREA(4)/(LOG10(RE25K(4)))**2.58
&      +WAREA(5)/(LOG10(RE25K(5)))**2.58
&      +WAREA(6)/(LOG10(RE25K(6)))**2.58
&      +WAREA(7)/(LOG10(RE25K(7)))**2.58)
C
C  CALC. CD PRIMED TEST ALTITUDE
C
      CDPTEST=K*(WAREA(1)/(LOG10(RETEST(1)))**2.58
&      +WAREA(2)/(LOG10(RETEST(2)))**2.58
&      +WAREA(3)/(LOG10(RETEST(3)))**2.58
&      +WAREA(4)/(LOG10(RETEST(4)))**2.58
&      +WAREA(5)/(LOG10(RETEST(5)))**2.58
&      +WAREA(6)/(LOG10(RETEST(6)))**2.58
&      +WAREA(7)/(LOG10(RETEST(7)))**2.58)
C
C  CALC. DELTA CD
C
      DELCDP=CDP25K-CDPTEST
C
C  CALC. CD CORRECTED
C
      CD=CDS-DELCDP
C
      RETURN
      END
1
      SUBROUTINE STAB(WFTOT,UTT,WT,DAT)
        COMMON/OUT2/RF,SR,SRP
C
C  THIS SUBROUTINE CALCULATES THE
C  STABILIZED POINT PERFORMANCE PARAMETERS
C
C  CALCULATE RANGE FACTOR
C

```

```

      RF=(UTT*WT)/WFTOT/1.689
C
C      CALCULATE SPECIFIC RANGE
C
      SR=(UTT)/WFTOT/1.689
C
C      CALCULATE SPECIFIC RANGE PARAMETER
C
      SRP=(UTT*DAT)/WFTOT/1.689
      RETURN
      END
C
1
      SUBROUTINE TABINT(X,Y,Z,NX,NZ,CURVE,INDIC)
C
C      TABLE LOOK-UP SUBROUTINE
C
      DIMENSION CURVE(1)
      KX=NX
      INDIC=1
15      DO 30 I=1,NX
          IF (X-CURVE(I))16,28,30
16          IF (I-1) 17,17,20
17          INDIC=2
          KX=2
          GO TO 32
20          KX=I
          GO TO 32
28          IF (I-NX) 30,20,20
30          CONTINUE
69          FORMAT (5X,'CURVE(I) = ',F10.5)
          INDIC=3
32          XL=CURVE(KX-1)
          XH=CURVE(KX)
40          J=KX+NX
          IF (NZ-1) 42,42,44
42          ASSIGN 95 TO NFORK
          GO TO 75
44          M=NZ+NX
          KZ=M
          J=NX+1
          DO 70 I=J,M
              IF (Z-CURVE(I)) 45,68,70
45              IF (I-NX-1) 46,46,50
46              INDIC=4
              KZ=J+1
              GO TO 72
50              KZ=I
              GO TO 72
68              IF (I-M) 70,50,50
70              CONTINUE
              INDIC=5
72              ZL=CURVE(KZ-1)
              ZH=CURVE(KZ)
              ASSIGN 80 TO NFORK

```

```

J=(KZ-NX-1)*NX+KX+NZ
75 Y=CURVE(J-1)+((X-XL)/(XH-XL))*(CURVE(J)-CURVE(J-1))
GO TO NFORK,(80,90,95)
80 J=J+NX
ASSIGN 90 TO NFORK
YLO=Y
GO TO 75
90 Y=YLO+((Z-ZL)/(ZH-ZL))*(Y-YLO)
95 RETURN
END

```

C.4.2 MODEL

PURPOSE:

To predict flight trajectory performance from baseline aerodynamic and engine characteristics.

APPROACH:

The overall approach used in MODEL is described in Section 3.2.4.2.

C.4.2.1 DRAGA

PURPOSE:

This subroutine was used with the MODEL program to calculate drag coefficient and angle of attack. The problem here was the aerodynamic data used to calculate C_D and α (i.e. C_{L_S} vs. α and C_{D_S} vs. α) were defined with all thrust moment, and c.g. effect taken into account. Therefore, an iteration on alpha was required to determine a C_{L_S} which correlated to the $C_{L_{A/C}}$ passed by MODEL. With alpha defined, a drag coefficient could then be calculated from the C_{D_S} vs. α curve.

APPROACH:

The iteration routine was started by first approximating an angle of attack with the aircraft lift coefficient provided by MODEL. The angle of attack will not be correct since the table look-up for C_{L_S} vs. α requires a C_L corrected for thrust moment effects. With the first approximation of alpha and the aircraft C_L , the standard thrust moment correction was calculated to obtain a C_{L_S} from which a new alpha could be determined. A convergence test for alpha was then performed requiring agreement to within .0001 degree. If the convergence test was not satisfied, α is set equal to α_2 and a new C_{L_S} was then calculated. If convergence had occurred, the drag coefficient (C_{D_S}) was then calculated, and the Reynold number corrections subtracted out to yield the C_D and alpha needed for MODEL.

```

C *****
C *
C * ORGANIZATION: UNIVERSITY OF KANSAS CENTER FOR RESEARCH INC. *
C * PROGRAM : ----- *
C * SUBROUTINE : DRAGA *
C * AUTHOR : BRAMAN , KEITH *
C * COMPUTER : SEL 32/77 *
C * O/S : M.P.X. 1.3 *
C * COMPILER : ANSI-77 STANDARD FORTRAN (FORT77) *
C *
C * REVISIONS
C *
C * I-----I-----I-----I-----I
C * I PR# I VER/REV I NAME I DATE I
C * I-----I-----I-----I-----I
C * I I 1/0 I KEITH BRAMAN I 7/20/83 I
C * I-----I-----I-----I-----I
C *****
C
C SUBROUTINE DRAGA(CD, ALPHA, AM, CL, DELTA, THETA, PCTRPM)
C COMMON/DDDD/DEBUG
C COMMON/DPS1/DHI, DIST, DMI, DNM, ENM, EDEG, DEG, DDEG, S, AMF
C COMMON/DPS5/AIT, IALF, AMC, ANZ, ANZZ, FEX, H, HTDOT, PITCH, R
C COMMON/DPS16/CURVE1(200), CURVE2(200), CURVE3(200), CURVE4(200)
C & , ITABLE
C COMMON/USER1/THRUST1(300), WA(300), FFL(350), CDARRAY(1150),
C & CLPOWER(120), CLMACH(120), ANEWCD(1150), ANCURV(50)
C COMMON/USER2/HCGSTD, VCGSTD, HTAIL1, UTAIL1, YT, XRAMDRAG, YRAMDRAG
C & DCGH, DCGU
C REAL*4 LT
C IF(DEBUG.EQ.1)TYPE *, 'SUBROUTINE DRAGA'
C CL1=CL
C L1=L2=L3=L4=0
C IND=KATM=1
C IF(AM.LE.0.65)THEN
C IF(ITABLE.GT.2)THEN
C DD=DELTA*2116.22
C CALL HGRP(HT, DD, IND, KATM)
C L1=0
C CALL TLU1(CURVE4(1), HT, PCTRPM, L1)
C END IF
C CALL TLU2(CLPOWER, CL1, PCTRPM, ALPHA1, L1, L2)
C ELSE
C CALL TLU2(CLMACH, CL1, AM, ALPHA1, L3, L4)
C END IF
C X1=XRAMDRAG-DCGH !EQ.# 32D
C Y1=YRAMDRAG-DCGU !EQ.# 33D
C CALL TH(FG, FE, WF, FN, ALPHA, DELTA, AM, THETA)
C HR=Y1*COS(ALPHA1*.01745329)-X1*SIN(ALPHA1*.01745329)
C A1=SQRT(DCGH**2+DCGU**2) !EQ.# 35D
C IF(DCGH.EQ.0..AND.DCGU.LE.0.) THEN
C YTHRUST=TY+A1*COS(AIT*.01745329)
C GO TO 6
C END IF

```

```

IF(DCGH.EQ.0..AND.DCGU.GT.0)THEN
  YTHRUST=YT-A1*COS(AIT*.01745329)
  GO TO 6
END IF
  GAMMA1=ATAN2(ABS(DCGU/DCGH))
  IF(DCGH.GE.0)THEN
    YTHRUST=YT-A1*SIN(AIT*.01745329+GAMMA1)
  END IF
  IF(DCGH.LT.0)THEN
    YTHRUST=YT+A1*SIN(GAMMA1+AIT *.01745329)
  END IF
6  XTAIL=HTAIL1-DCGH
   YTAIL=UTAIL1-DCGU
   LT=XTAIL*COS(ALPHA1*.01745329)+YTAIL*SIN(ALPHA1*.01745329)
C
C THE CHANGE IN LIFT COEFFICIENT DUE TO THRUST IS:
C
C CALC. DELTA CL FOR BOTH ENGINES
C
  QBARS=((1.4*DELTA*2116.22*S*(AM**2))/2.
  DCLT= 2.0*(FG*YTHRUST - FE*HR)/LT/QBARS
C
C THE LIFT COEFFICIENT NOW BECOMES:
C
  CLTAC=CL1+DCLT
C
C CORRECTING LIFT COEFFICIENT FOR C.G. POSITION
C
  Z=HTAIL1*COS(ALPHA1*.01745329)+UTAIL1*SIN(ALPHA1*.01745329)
  DCG=Z-LT
  DCLCG=-(CLTAC*DCG)/(LT+DCG)
C
C THE TOTAL STEADY STATE POWER OFF LIFT COEFFICIENT WILL BE:
C
  CLS=CLTAC+DCLCG
C
C THE FIRST CALCULATION WELL BE FOR ALPHA. THIS IS DONE WITH A TABL
C LOOK-UP OF CL VS ALPHA . HOWEVER FOR MACH # LESS THEN OR EQUAL TO
C .65 THE CL VS ALPHA CURVE BREAKS OUT BY POWER, ABOVE .65 THE
C CURVE BREAKS OUT BY MACH NUMBER.
C
  L1=L2=L3=L4=0
  IF(AM.LE.0.65)THEN
    CALL TLU2(CLPWR,CLS,PCTRPM,ALPHA2,L1,L2)
  ELSE
    CALL TLU2(CLMACH,CLS,AM,ALPHA2,L3,L4)
  END IF
  IF(ALPHA2.LE.ALPHA1+.0001.AND.ALPHA2.GE.ALPHA1-.0001)GO TO 10
  ALPHA1=ALPHA2
GO TO 5
C
C WITH ALPHA KNOWN DRAG CAN NOW BE CALAULATED. THIS IS DONE WITH
C A FOUR-D TABLE LOOK-UP ON MACH,POWER AND, ALPHA FOR MACH LESS

```

```

C   THEN .6 AND A 2-D LOOK-UP ON MACH AND ALPHA FOR MACH # > .6
C
10  L1=L2=L3=0
    ALPHA=ALPHA2
    IF(AM.GE..6)THEN
      CALL TLU2(ANEWCD,ALPHA,AM,CDS,L1,L2)
    ELSE
      CALL TLU3(CDARRAY,ALPHA,PCTRPM,AM,CDS,L1,L2,L3)
    END IF
    CALL REYNOLDS(CD,CDS,AM,THETA,DELTA)
C
    RETURN
    END

```

C.4.2.2 THRUST

PURPOSE:

This routine was used by the MODEL program to describe the in-flight test engine characteristics.

APPROACH:

The program inputs were simply percent engine RPM and Mach number. The routine performed a number of table look-ups and output F_g , F_r , W_a , and W_f .

```

C *****
C *
C * ORGANIZATION: UNIVERSITY OF KANSAS CENTER FOR RESEARCH INC. *
C * PROGRAM : ----- *
C * SUBROUTINE : THRUST *
C * AUTHOR : BRAMAN , KEITH *
C * COMPUTER : SEL 32/77 *
C * O/S : M.P.X. 1.3 *
C * COMPILER : ANSI-77 STANDARD FORTRAN (FORT77) *
C *
C *
C * REVISIONS
C *
C * I-----I-----I-----I-----I
C * I PR# I VER/REV I NAME I DATE I
C * I-----I-----I-----I-----I
C * I I 1/0 I KEITH BRAMAN I 7/20/83 I
C * I-----I-----I-----I-----I
C *****
C
C SUBROUTINE THRUST(PCTRPM,FG,FE,FNZ,WF,ALPHA,AM,DELTA,THETA)
C
C SUBROUTINE TO CALC. GROSS THRUST,NET THRUST
C AND FUEL FLOW FOR THE GARRETT FTE 731-3 ENGINE
C
C COMMON/DDDD/DEBUG
C COMMON/USER1/THRUST1(300),WA(300),FFL(350),CDARRAY(1150),
C & CLPOWER(120),CLMACH(120),ANEWCD(1150)
C IF(DEBUG.EQ.1.)TYPE *, 'DEBUG SUB THRUST'
C
C THETA2=THETA*(1+.2*(AM**2))
C DELTA2=DELTA*(1+.2*(AM**2))**3.5
C RPM=PCTRPM*20688./100.0
C CRPM=RPM/SQRT(THETA2)
C L1=L2=L3=L4=L5=L6=0
C
C CALL SUB. TO LOOK-UP THE CORRECTED AIRFLOW
C
C CALL TLU2(WA,CRPM,AM,CAIRFL,L1,L2)
C
C CALC. RAM DRAG
C
C FE=((CAIRFL*AM*1116.4*SQRT(THETA))/(SQRT(THETA2)*32.2))*DELTA2
C
C CALL SUB. TO LOOK-UP THE CORRECTED ENGINE THRUST
C
C CALL TLU2(THRUST1,CRPM,AM,FGODT2,L3,L4)
C
C CALC. GROSS THRUST
C
C FG=FGODT2*DELTA2
C
C CALL SUBR. TO LOOK-UP CORRECTED FUEL FLOW
C
C CALL TLU2(FFL,CRPM,AM,FFLOW,L5,L6)

```

```
C
C  CALC. FUEL FLOW
C
C      WF=(FFLOW*DELTA2*SQRT(THETA2))
C
C      RETURN
C      END
```

C.5 UTILITIES

A number of software utility routines were developed and used throughout the program. The scope of this effort ranged from calculating the in-flight thrust characteristics to plotting data files. Only two will be presented here. However, the following is a list of the most used routines with a brief description of each.

- a) WD - Calculated constant W/δ altitude/weight profiles with fuel burn.
- b) Least - Least squares curve fit routine.
- c) PETIME - Plotted time histories of performance file one.
- d) THIST2 - Plotted time histories of flight test data base files.
- e) Look B - Screened/edited and hardcopy of performance file one.
- f) Look 9 - Screened/edited and hardcopy of flight test data base files.
- g) M1PLOT - Plotted engine deck characteristics vs. $N_1/\sqrt{\theta_{t_2}}$.
- h) ERROR - Calculated error analysis of any engineering units parameter.
- i) TLU1 - 2-D table look-up
- j) TLU2 - 3-D table look-up
- h) TLU3 - 4-D table look-up

C.4.1 THRUST1

PURPOSE:

This subroutine calculated all the in-flight engine characteristics. Incorporated in this calculation were the η and fuel flow ratio corrections defined in the thrust modeling section (3.2.1.2).

APPROACH:

The routine performed table look-ups to determine in deck engine characteristics and made the necessary η and fuel flow ratio corrections. A fuel temperature correction to test fuel flow was also accomplished.

```

C *****
C *
C * ORGANIZATION: UNIVERSITY OF KANSAS CENTER FOR RESEARCH INC. *
C * PROGRAM : ----- *
C * SUBROUTINE : THRUST1 *
C * AUTHOR : BRAMAN , KEITH *
C * COMPUTER : SEL 32/77 *
C * O/S : M.P.X. 1.3 *
C * COMPILER : ANSI-77 STANDARD FORTRAN (FORT77) *
C *
C * REVISIONS
C *
C * I-----I-----I-----I-----I
C * I PR# I VER/REV I NAME I DATE I
C * I-----I-----I-----I-----I
C * I I 1/0 I KEITH BRAMAN I 12/5/82 I
C * I-----I-----I-----I-----I
C *
C *****
C
C CURRENT MODIFICATIONS (INSTALLED) :
C A CORRECTION TO FUEL FLOW FOR TEMP. HAS BEEN ADDED
C AND THE FLIGHT TEST DATA BASE INCREASED BY TWO VALUES
C NUM 138 AND 139 CWFL AND CEFR IN LBS.
C MOD DATE 01/18/83
C
C COMMON/INPUT/ ANSUBX,ANSUBY,ANSUBN,PP,QQ,RR,THETAD,FUEL,AN1L,
C & AN1R,PHID,ALPHAD,DLTAL,DLTAR,DLTEL,DLTER,BETAD,QCIC1,TIC,PS1,
C & CURUP1,SWING,MAC,LEPOS,MAXN1,YSUBA,XSUBA,ZSUBA,EXD,EZD
C & ,PALPH,PBETA,PALBET,CORALPHA,NCURU,BETACURU
C COMMON/OUTPUT/PROUT1,PROUT2,INOUT,EUF1,BITOT,THROT
C COMMON/DATAL2/
C & AMCT ,AMIC ,CAS ,DAT ,DLHPC ,DLMPC
C & ,DLUPC ,HCS ,HCT ,HIC ,HICL ,HICP
C & ,PAS ,PAT ,PS ,PTOS ,PTOT ,QBART
C & ,QCIC ,QCS ,QCT ,RCHIC ,RCVIC ,RHOS
C & ,RHOT ,RRTH2S ,RRTH2T ,RTHAS ,RTHAT ,RTH2S
C & ,RTH2T ,SIGAS ,SIGAT ,SIGIC ,TAIC ,TAS
C & ,TASK ,TAT ,TATK ,THAS ,THAT ,TH2S
C & ,TH2T ,TT2T ,TT2TK ,TT2S ,TT2SK ,UCS
C & ,UCT ,VES ,VET ,VIC ,VICL ,UTS
C & ,UTT ,WT ,XNZM ,PT ,CLIC ,CLT
C COMMON/THRU2/THRU(1000),WA1(1000),WF1(1000),WFLT,WFRT,THRCL(72),
C & THRCR(72)
C COMMON/INERTT/WT,S,DENS,FT1,FTL,FTR,TUF,XBAR1,YBAR1,ZBAR1,
C & IXX,IYY,IZZ,IXZ,OWE,DELTP,FUELP,FULBSTOT
C INTEGER PTSX,PTSY,ENG
C
C REAL*4 CURUP1(20,7)
C REAL*4 PROUT1(17)
C REAL*4 PROUT2(44)
C REAL*4 INOUT(15)
C REAL*4 EUF1(72)

```

```

REAL*4 BITOT(8)
REAL*4 THROT(11)
REAL*4 NCURV(50)
REAL*4 BETACURV(50)
REAL*4 CORALPHA(30)
REAL*4 MAXN1
C
LAMDAD=1.
ENG=2
IL=0
IND=0
C
C THE CORRECTED FUEL FLOWS IN LBS. ARE
C
CWFL=WFLT*(-.00309* FTL +6.89)
CWFR=WFR*(-.00309* FTR +6.89)
C
C CONV. %RPM TO RPM (LEFT)
C
N1=AN1L*MAXN1/100.
CN1=N1/RTH2T
C
C CONV KNOTS TO FT/SEC
C
UTT1=UTT*1.689
C
C FIND CORRECTION FACTOR FOR TEST ENGINE
C
CALL TABINT(CN1,EFACTOR,0,36,0,THRCL,IND)
C
WFT=CWFL
C
C CALC. PT2 IN PSF BY MULT. PTOT BY RECOVERY FACTER AND THEN
C CONVERTING FROM IN. HG TO PSF
C
PT2=PTOT*.995*70.73
DLT2=PT2/2116.8
DO 10 I=1,ENG
IP0IN=0
C
C CALCULATE THE FUEL FLOW
C
CALL TLU2(WF1,CN1,AMCT,WFP0,L1,L2)
CALL TABINT(AMCT,FULN,0,17,0,NCURV,IND)
WFP=WFP0*((DLT2**FULN)*RTH2T)
C
C CALC. GROSS THRUST
C
CALL TLU2(THRUS,CN1,AMCT,FGP0,L1,L2)
FGP=FGP0*DLT2
C
C CALC. AIRFLOW
C
CALL TLU2(WA1,CN1,AMCT,WA0,L1,L2)
WAD=WA0*(DLT2/RTH2T)

```

```

      WA=(WFT/3600.)*(WAD*3600./EFACTOR/WFP+1./EFACTOR-1.)
C
      FG=WFT/WFP*FGP/EFACTOR
      FR=((WA*UTT1)/32.174)
      RAD=(ALPHAD+LAMDAD)*(3.141592654/180)
      FN=FG*(COS(RAD))-FR
C
C
C
C
C  CONV. %RPM TO RPM(RIGHT)
C
      N1=AN1R*MAXN1/100
      CN1=N1/RTH2T
      IF (IL.EQ.1) GO TO 5
      THROT(1)=FG
      THROT(3)=FR
      THROT(5)=FN
      THROT(7)=WA
      IL=1
C
      WFT=CWFR
C
C  CALC. EFACTOR FOR RIGHT ENGINE
C
      CALL TABINT(CN1,EFACTOR,0.36,0,THRCR,IND)
10  CONTINUE
5   THROT(2)=FG
      THROT(4)=FR
      THROT(6)=FN
      THROT(8)=WA
      THROT(9)=DLT2
      THROT(10)=CWFL
      THROT(11)=CWFR
      RETURN
      END

```

C.4.2 REYNOLDS

PURPOSE:

This routine calculated the change in drag coefficient due to Reynolds number standardized to 25,000 ft. Reynolds was used by START, ITERATE, and MODEL.

APPROACH:

A component build-up of the aircraft surfaces was performed to determine C_f for the aircraft from which a delta C_D due to skin friction was computed. START added this effect to the drag coefficient to obtain C_{D_S} . However, ITERATE and MODEL required a C_D from C_{D_S} so this correction was subtracted. The ITERATE listing incorporates a modified version of REYNOLDS to account for the difference.

```

C *****
C *
C * ORGANIZATION: UNIVERSITY OF KANSAS CENTER FOR RESEARCH INC. *
C * PROGRAM : ----- *
C * SUBROUTINE : REYNOLDS *
C * AUTHOR : BRAMAN , KEITH *
C * COMPUTER : SEL 32/77 *
C * O/S : M.P.X. 1.3 *
C * COMPILER : ANSI-77 STANDARD FORTRAN (FORT77) *
C *
C *
C * REVISIONS
C *
C * I-----I-----I-----I-----I
C * I PR# I VER/REV I NAME I DATE I
C * I-----I-----I-----I-----I
C * I I 1/0 I KEITH BRAMAN I 3/03/83 I
C * I-----I-----I-----I-----I
C *
C *****
C
C SUBROUTINE REYNOLDS(CD,CDS,AMCT,TATK,THAT,DAT)
C
C REYNOLDS NUMBER CORRECTION SUBROUTINE
C
C THIS ROUTINE WAS DEVELOPED BY MAJ. TOM YECHOUT AND
C CODED BY KEITH BRAMAN
C
C THE ANALYSIS REF.
C 1: AFFTC-TR-81-3
C "EVALUATION OF THE EFFECT OF WINGLETS ON THE PERFORMANCE
C OF A KC-135A AIRCRAFT"
C
C 2:"AIRPLANE AERODYNAMICS AND PERFORMANCE"
C BY LAN/ROSKAM
C
C
C COMMON/GEOM/ALPHA,ALAMDA,QBARS,S,MAC,WAREA,LENGTH
C REAL*4 WAREA(9),LENGTH(9),MAC
C REAL*4 RETEST(9),RE25K(9),K
C
C CAL CONSTANT FOR ALL 25K FEET REYNOLDS NUMBER
C
C CONSTANT=3362674.6*AMCT
C
C CALC. 25K FEET REYNOLDS NUMBER
C
C DO I=1,7
C RE25K(I)=CONSTANT*LENGTH(I)
C END DO
C
C CALC. CONSTANT FOR TEST ALTITUDE REYNOLDS NUMBER
C
C CONTTEST=(7100000.0*DAT*AMCT*(TATK+110.4))/(398.55*THAT**2)
C

```

```

C CALC. TEST ALTITUDE REYNOLDS NUMBER
C
  DO I=1,7
    RETEST(I)=CONTTEST*LENGTH(I)
  END DO
C
C CALC. K-FACTOR
C
  K=.455/S/((1+.144*AMCT**2)**.65)
C
C CALC. CD PRIMED AT 25K FEET
C
  CDP25K=K*(WAREA(1)/(LOG10(RE25K(1)))**2.58
&      +WAREA(2)/(LOG10(RE25K(2)))**2.58
&      +WAREA(3)/(LOG10(RE25K(3)))**2.58
&      +WAREA(4)/(LOG10(RE25K(4)))**2.58
&      +WAREA(5)/(LOG10(RE25K(5)))**2.58
&      +WAREA(6)/(LOG10(RE25K(6)))**2.58
&      +WAREA(7)/(LOG10(RE25K(7)))**2.58)
C
C CALC. CD PRIMED TEST ALTITUDE
C
  CDPTEST=K*(WAREA(1)/(LOG10(RETEST(1)))**2.58
&      +WAREA(2)/(LOG10(RETEST(2)))**2.58
&      +WAREA(3)/(LOG10(RETEST(3)))**2.58
&      +WAREA(4)/(LOG10(RETEST(4)))**2.58
&      +WAREA(5)/(LOG10(RETEST(5)))**2.58
&      +WAREA(6)/(LOG10(RETEST(6)))**2.58
&      +WAREA(7)/(LOG10(RETEST(7)))**2.58)
C
C CALC. DELTA CD
C
  DELCDP=CDP25K-CDPTEST
C
C CALC. CD CORRECTED
C
  CDS=CD+DELCDP
C
  RETURN
  END

```

APPENDIX D

TFE 731-2 ENGINE PREDICTION DECK FINAL THRUST,
FUEL FLOW AND AIRFLOW CHARACTERISTICS

APPENDIX D SUMMARY

<u>Figure No.</u>	<u>Title</u>
D.1	Engine Deck Corrected Gross Thrust Summary
D.2	Engine Deck Nonstandard Corrected Fuel Flow Summary
D.3	Engine Deck Corrected Airflow Summary

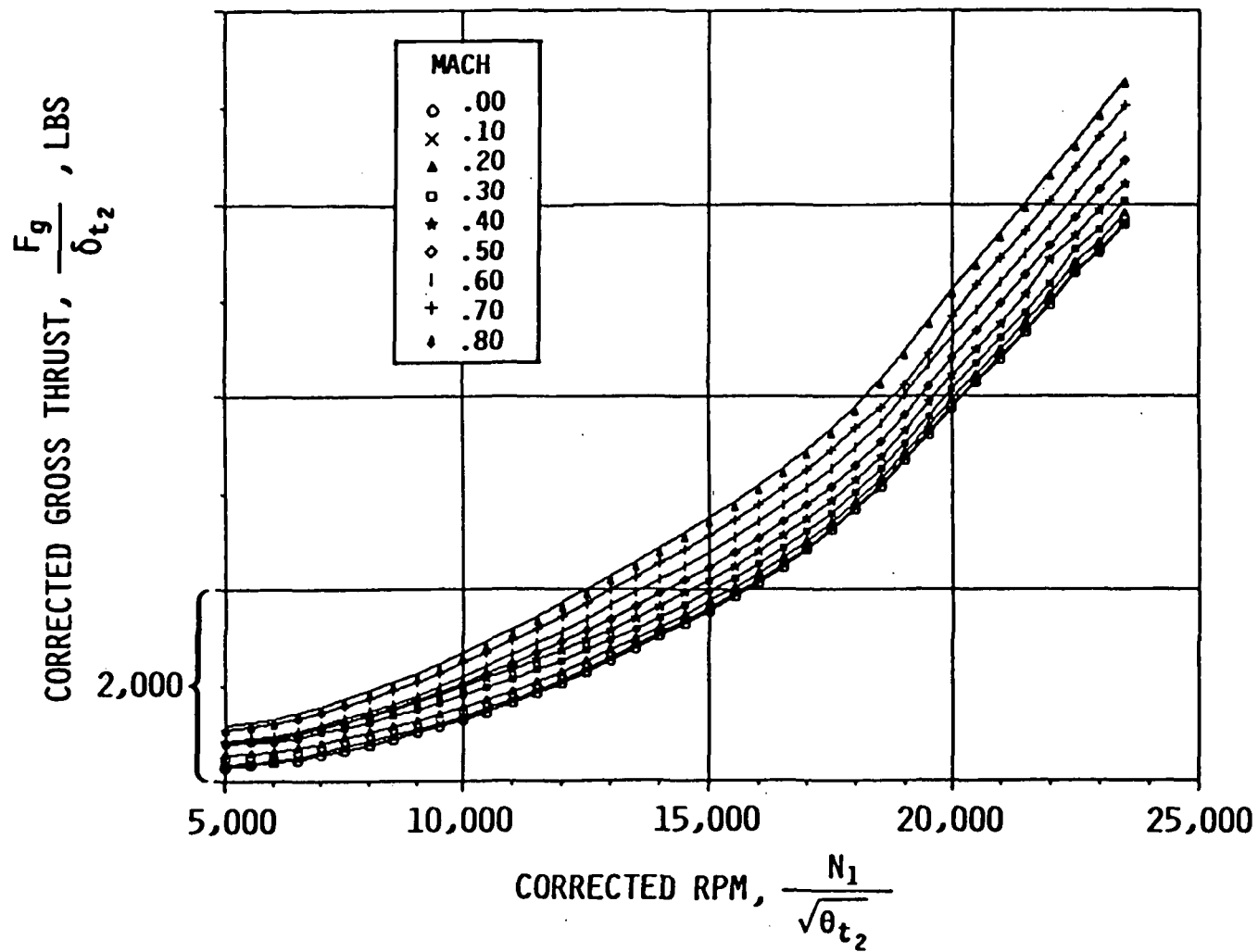


Figure D.1: Engine Deck Corrected Gross Thrust Summary

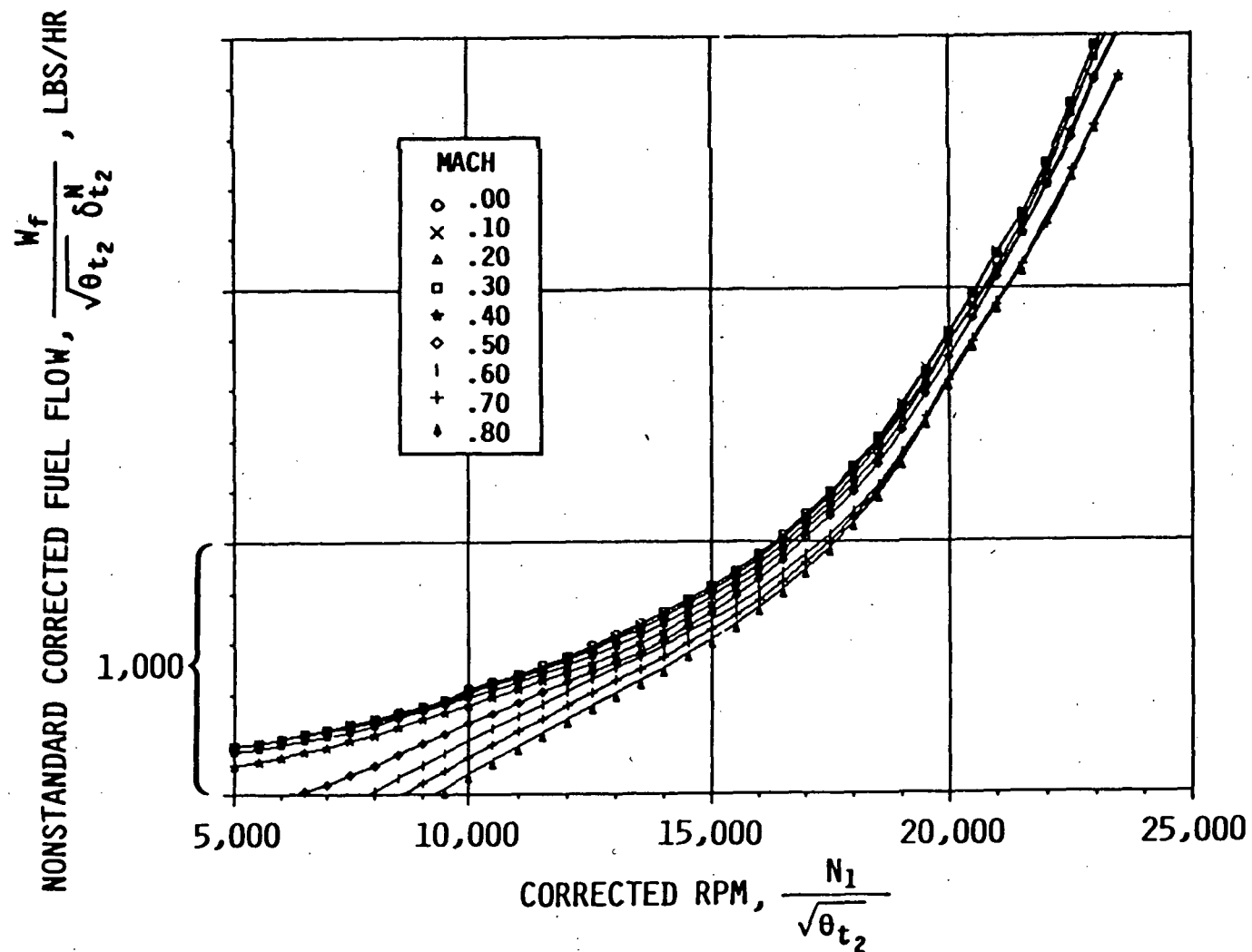


Figure D.2: Engine Deck Nonstandard Corrected Fuel Flow Summary

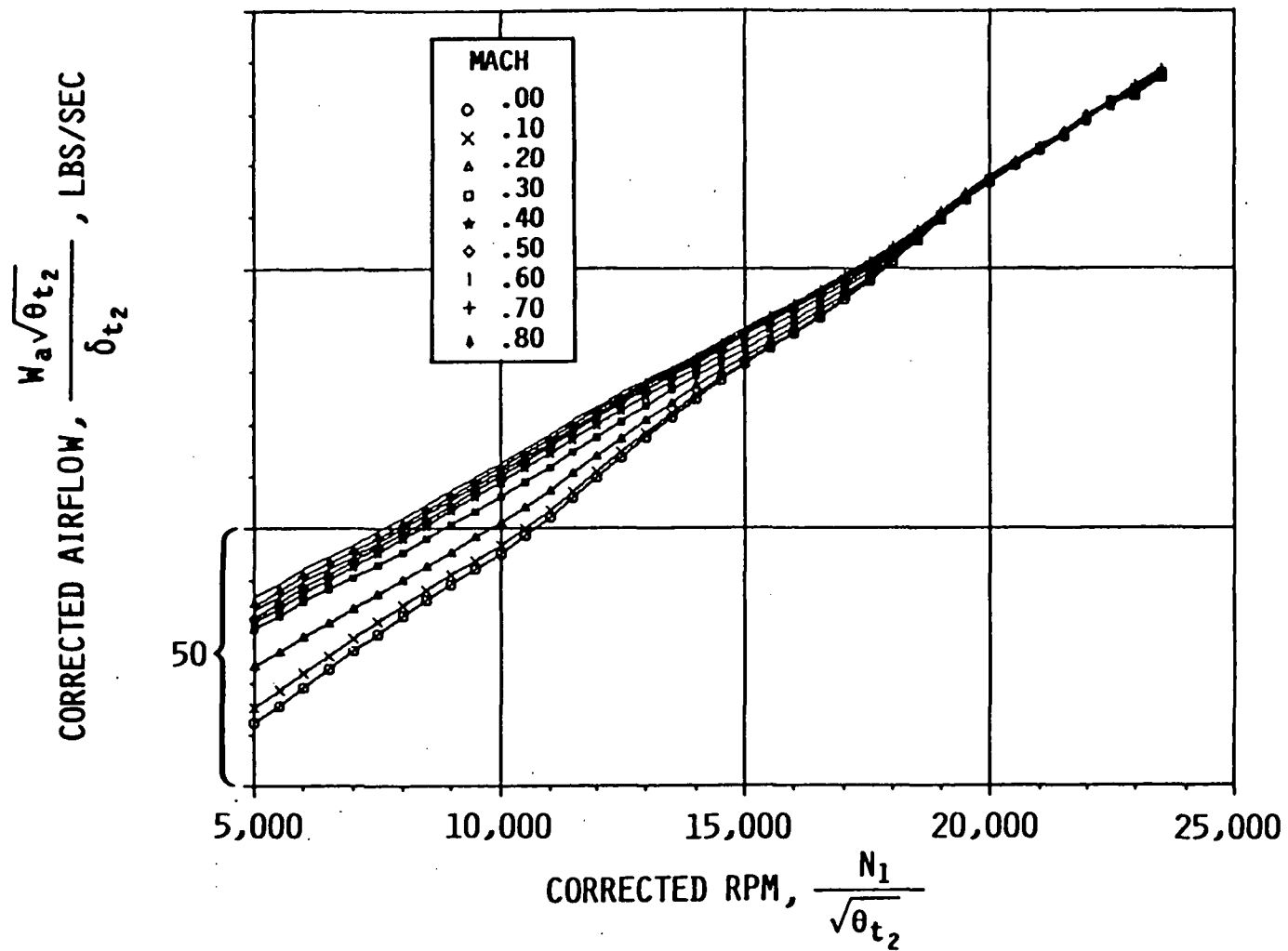


Figure D.3: Engine Deck Corrected Airflow Summary

APPENDIX E

LEAR 55 THRUST RUN

A thrust run was accomplished using a Lear 55 aircraft (S/N N552GL) and the Edwards AFB thrust stand facility on February 28, 1983. This thrust run defined a calibration correction curve for the load cell/tie down arrangement used during the Lear 35 thrust run. A calibration correction curve was needed due to the difficulty of estimating the frictional forces between the landing gear and the ground which affect the load cell reading. The Lear 55 aircraft was tested on the Edwards thrust stand rather than the Lear 35, since the Lear 35 flight program had been completed prior to facility availability and Singer Corporation funding to support the trip to Edwards from Wichita was available only for the Lear 55 (an active flight test program at the time).

Table E.1 presents the target stabilized engine test points for each engine. The aircraft was secured to the Edwards thrust stand, a 15' x 425' load table supported on steel flexures, using the load cell/tie down arrangement of Figure 3.17. Load cell and thrust table loads were recorded for each test point and a correction curve developed based on the difference between the thrust stand value and the load cell reading for sequence 1 through 9 test points. Figure E.1 presents the correction factor data for each engine which was applied to the data for the Lear 35 program. A load cell reading for the high thrust point on the right engine was not obtained due to a malfunction of the cable tie down. Figure E.2 presents data for the entire left engine thrust run in which the test points in Table E.1 were accomplished in ascending order by RPM and then repeated in descending order, as indi-

cated by the sequence number, to check for the repeatability and overall hysteresis of the load cell/tie down arrangement. As can be seen from the figure, considerable hysteresis was observed and, as a result, the Lear 35 thrust run was accomplished by sequencing the test points in ascending order. The calibration correction curve was based on data obtained during the ascending portion of the Lear 55 thrust run.

Table E.1: Lear 55 Thrust Run Target Test Points,
Stabilized Engine (Based on N_1)

	<u>Sequence</u>
IDLE	1, 17
50	2, 16
60	3, 15
70	4, 14
75	5, 13
80	6, 12, 18
85	7, 11, 19
90	8, 10
TAKEOFF POWER	9, 20

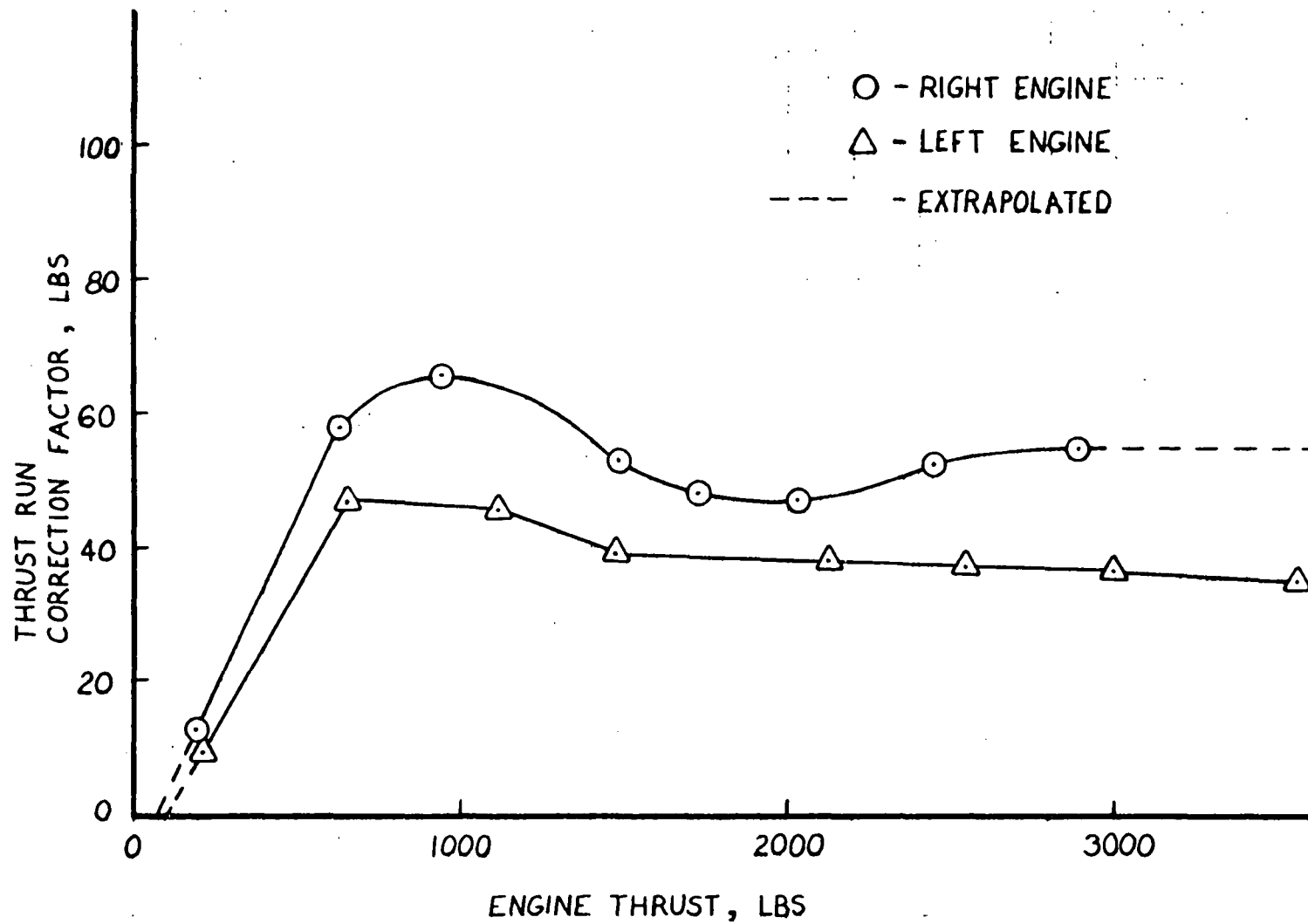


Figure E.1: Thrust Run Correction Factor

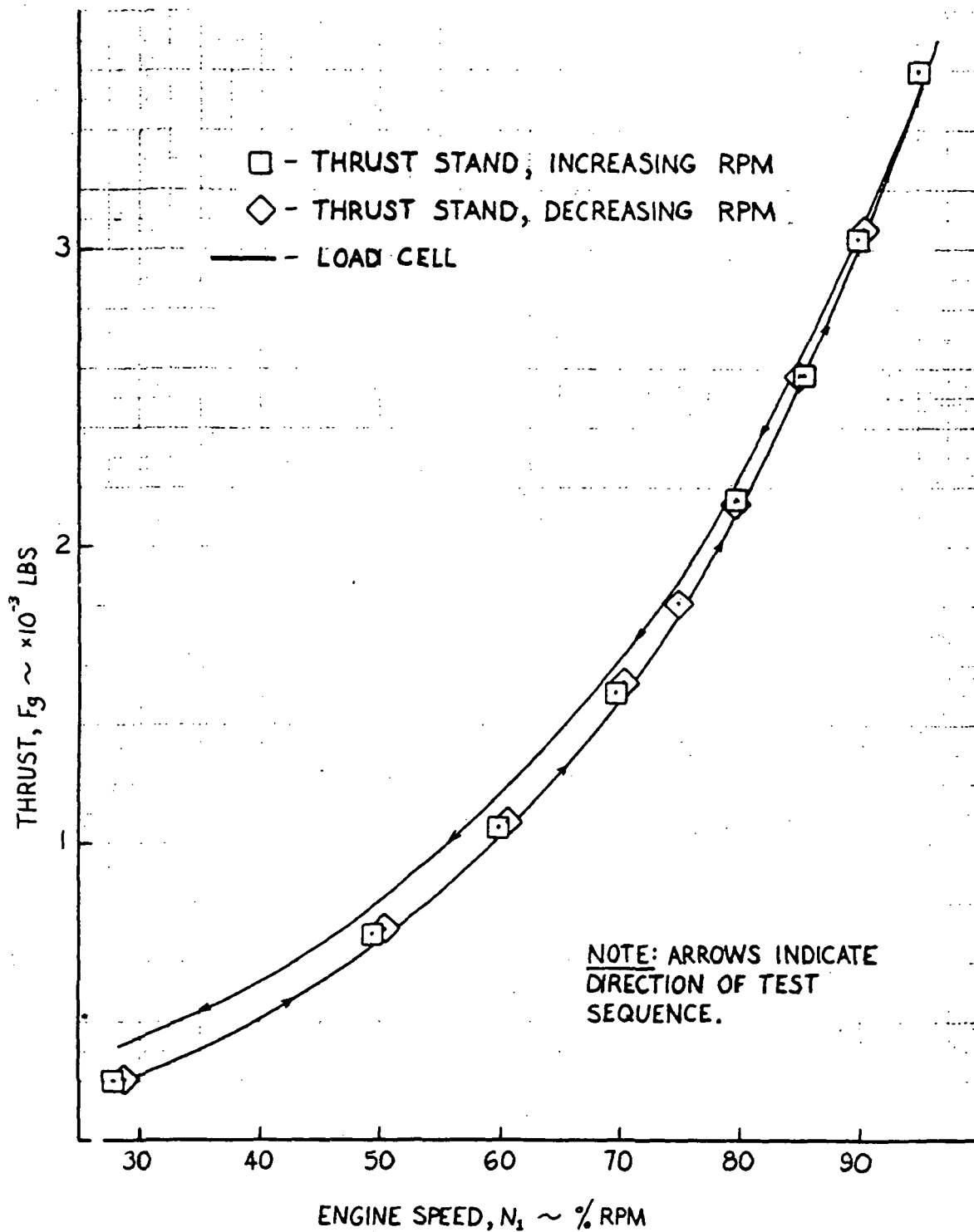


Figure E.2: Load Cell and Thrust Stand Comparison, Left Engine

APPENDIX F

DATA PLOTS:

BASELINE AERODYNAMIC CHARACTERISTICS

SUMMARY

<u>Figure No.</u>	<u>Title</u>
F.1	Lift Characteristics, $M = .65$, All Available Powers
F.2	Lift Characteristics, $M = .7$, All Available Powers
F.3	Lift Characteristics, $M = .75$, All Available Powers
F.4	Lift Characteristics, $M \leq .65$, $95\% \geq N_1 \geq 75\%$
F.5	Lift Characteristics, $M \leq .65$, $N_1 = 70\%$
F.6	Lift Characteristics, $M \leq .65$, $60\% \geq N_1 \geq 50\%$
F.7	Drag Characteristics, $M = .6$, All Available Powers
F.8	Drag Characteristics, $M = .65$, All Available Powers
F.9	Drag Characteristics, $M = .7$, All Available Powers
F.10	Drag Characteristics, $M = .75$, All Available Powers
F.11	Drag Characteristics, $M \leq .55$, $N_1 = 95\%$
F.12	Drag Characteristics, $M \leq .55$, $N_1 = 90\%$
F.13	Drag Characteristics, $M \leq .55$, $85\% \leq N_1 \leq 70\%$
F.14	Drag Characteristics, $M \leq .55$, $N_1 = 60\%$
F.15	Drag Characteristics, $M \leq .55$, $N_1 = 50\%$

Page intentionally left blank

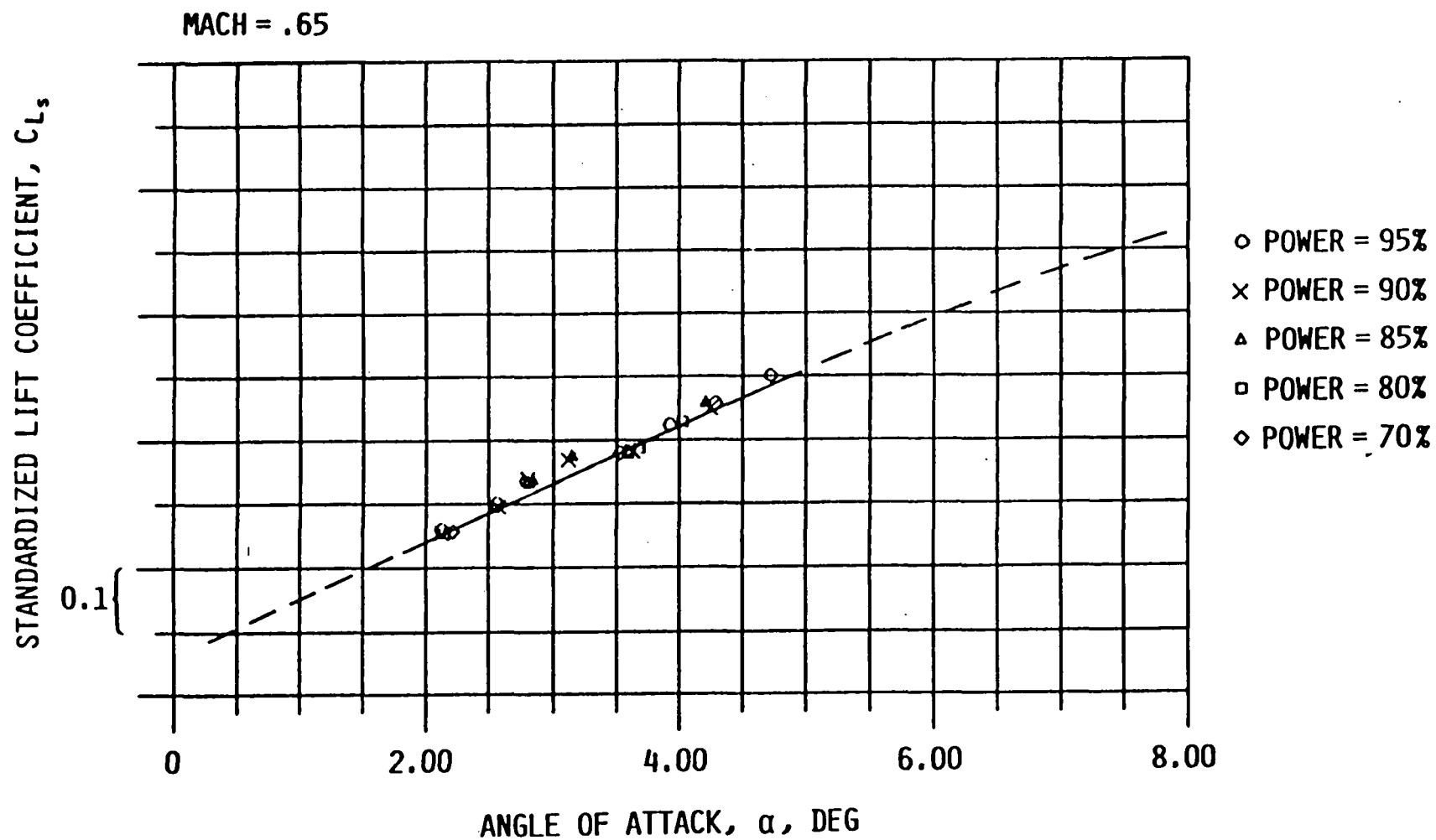


Figure F.1: Lift Characteristics, $M = .65$, All Available Powers

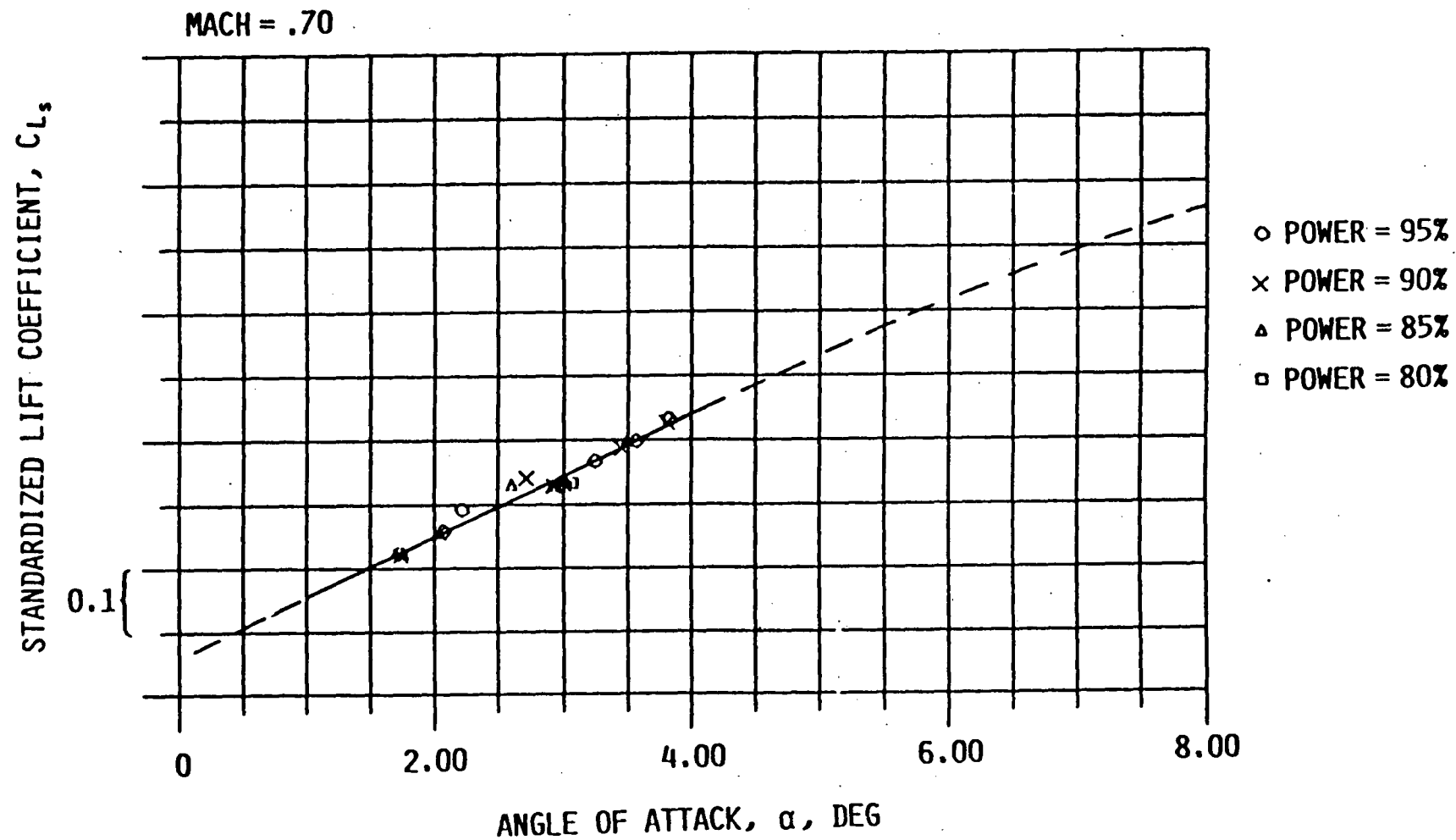


Figure F.2: Lift Characteristics, $M = .7$, All Available Powers

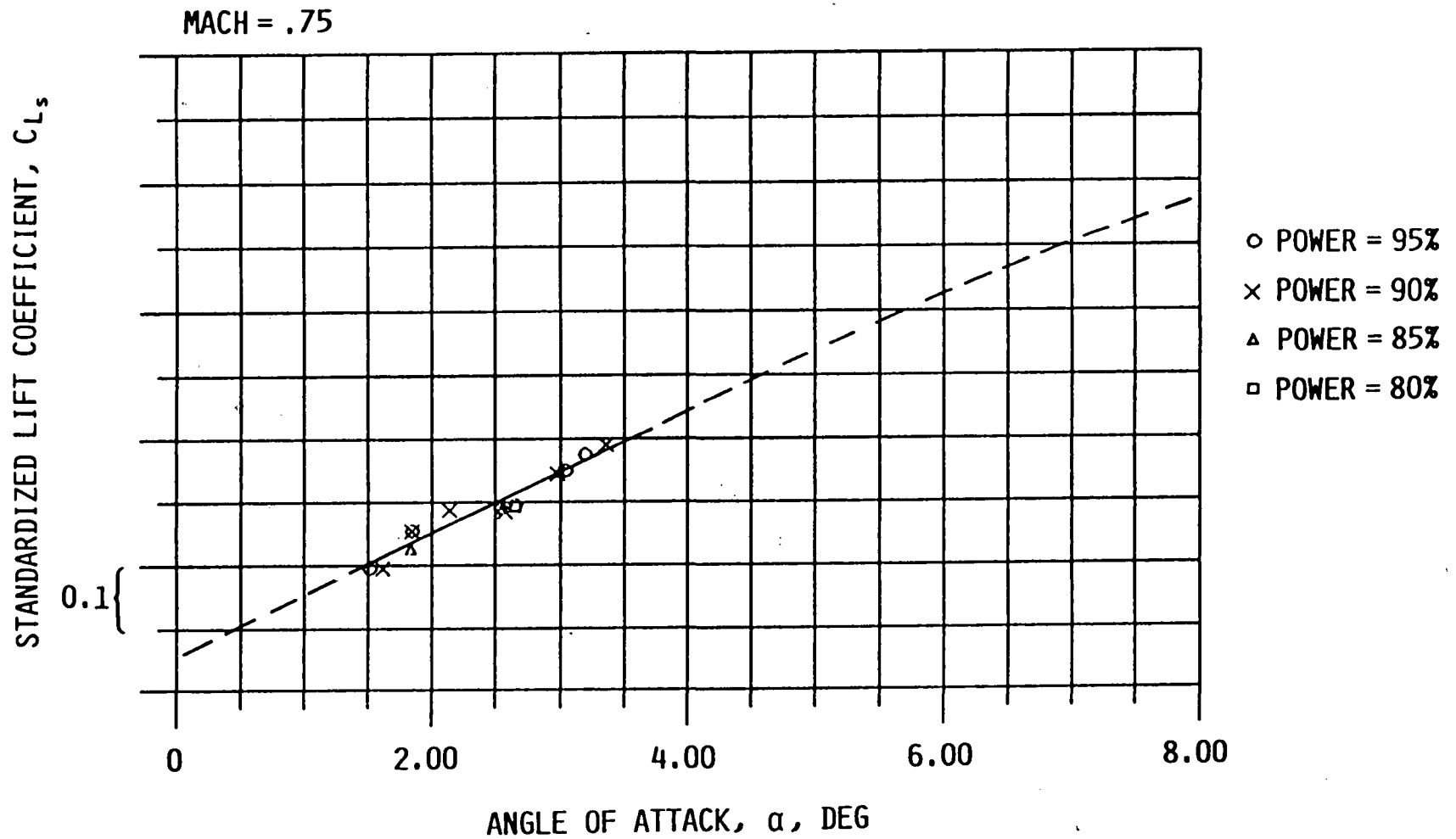


Figure F.3: Lift Characteristics, $M = .75$, All Available Powers

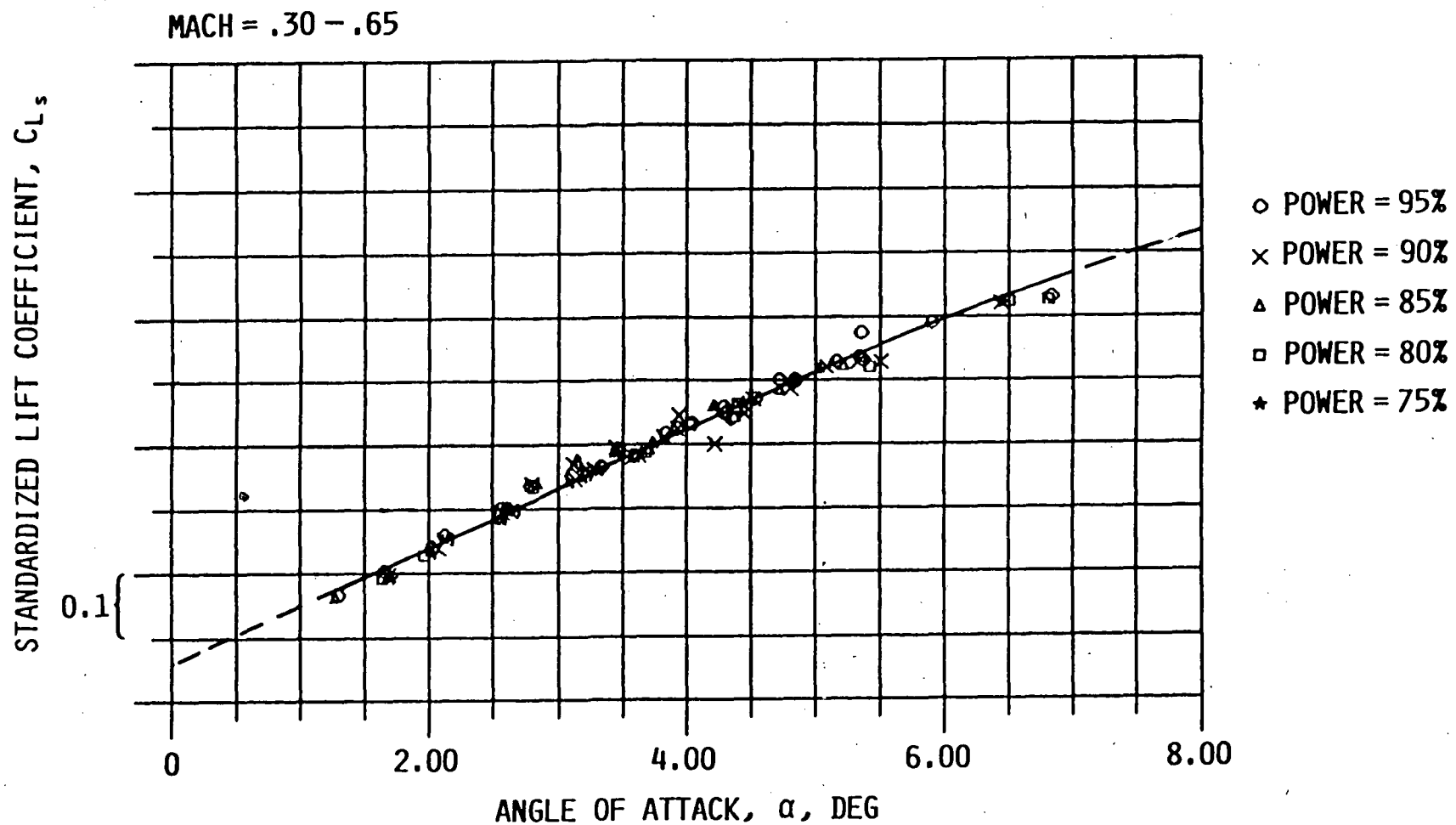


Figure F.4: Lift Characteristics, $M \leq .65$, $95\% \leq N_1 \leq 75\%$

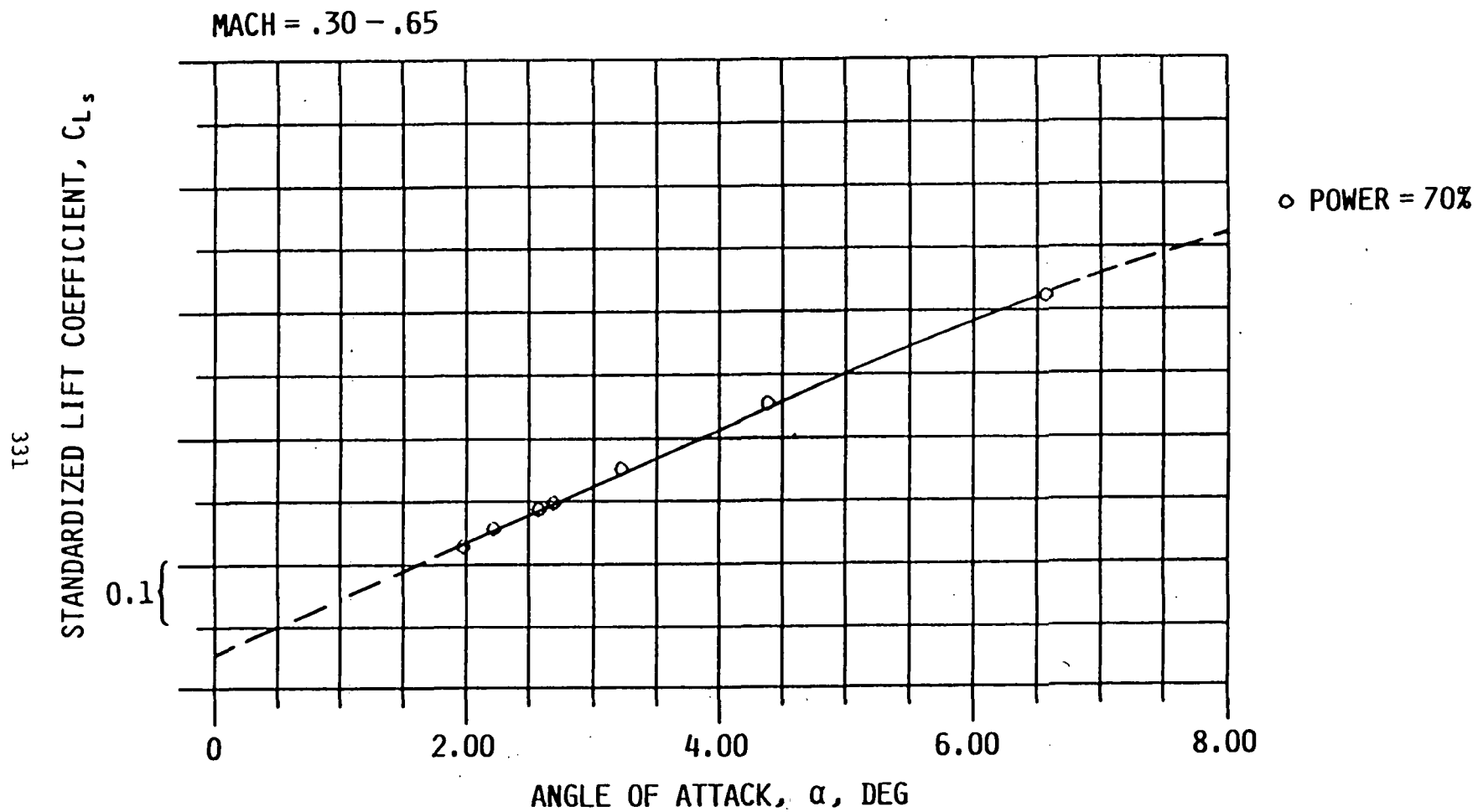


Figure F.5: Lift Characteristics, $M \leq .65$, $N_1 = 70\%$

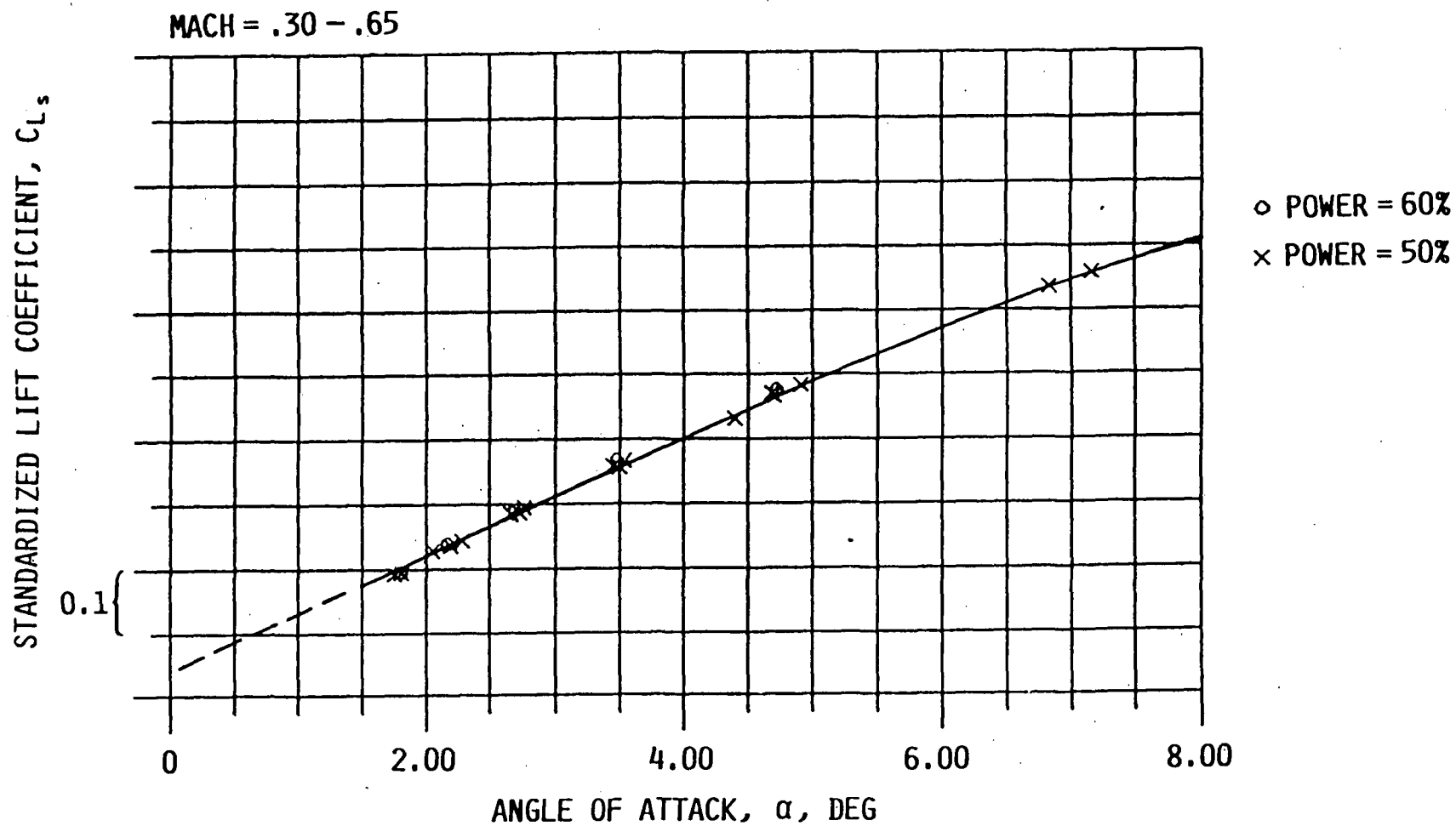


Figure F.6: Lift Characteristics, $M \leq .65$, $60\% \geq N_1 \geq 50\%$

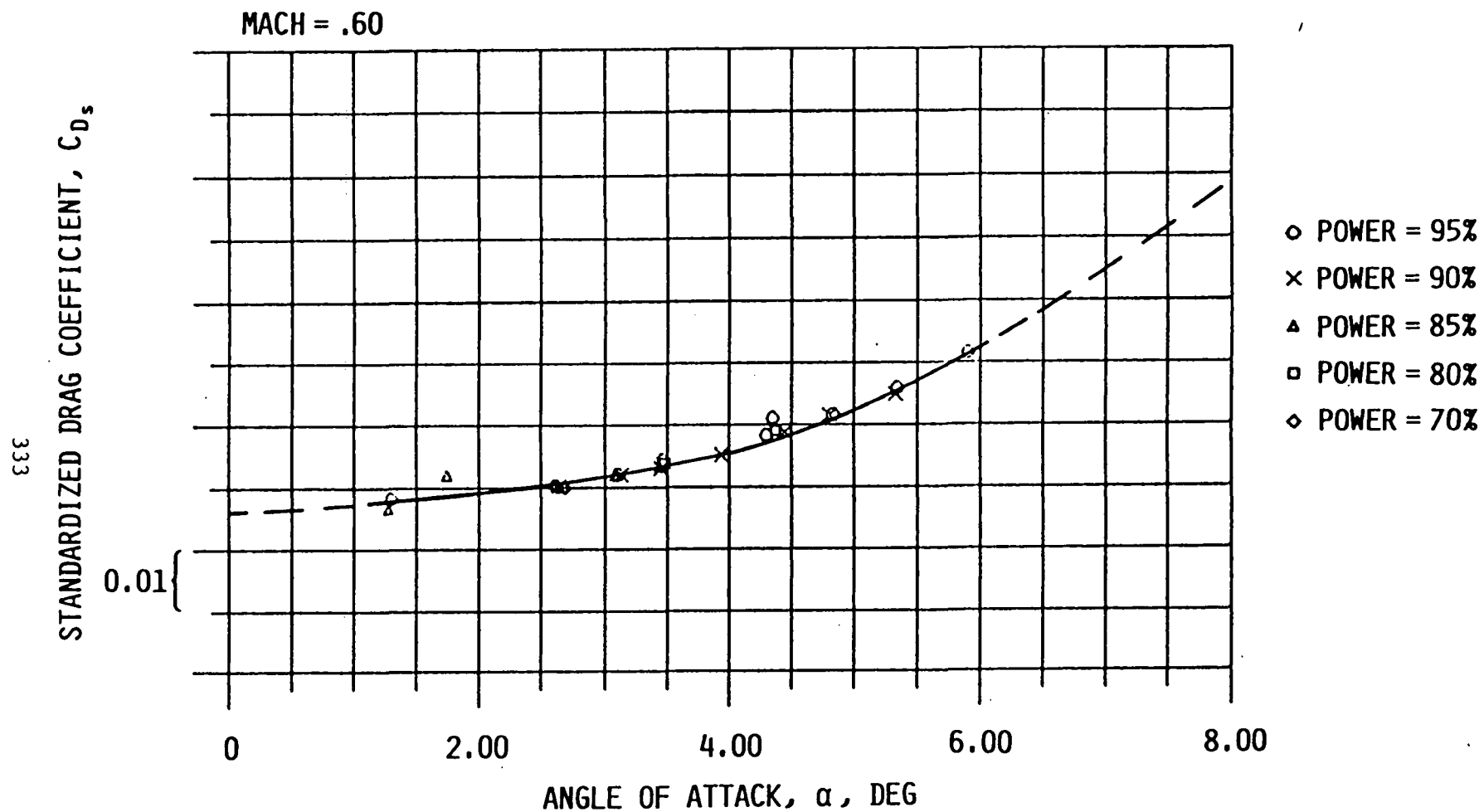


Figure F.7: Drag Characteristics, $M = .6$, All Available Powers

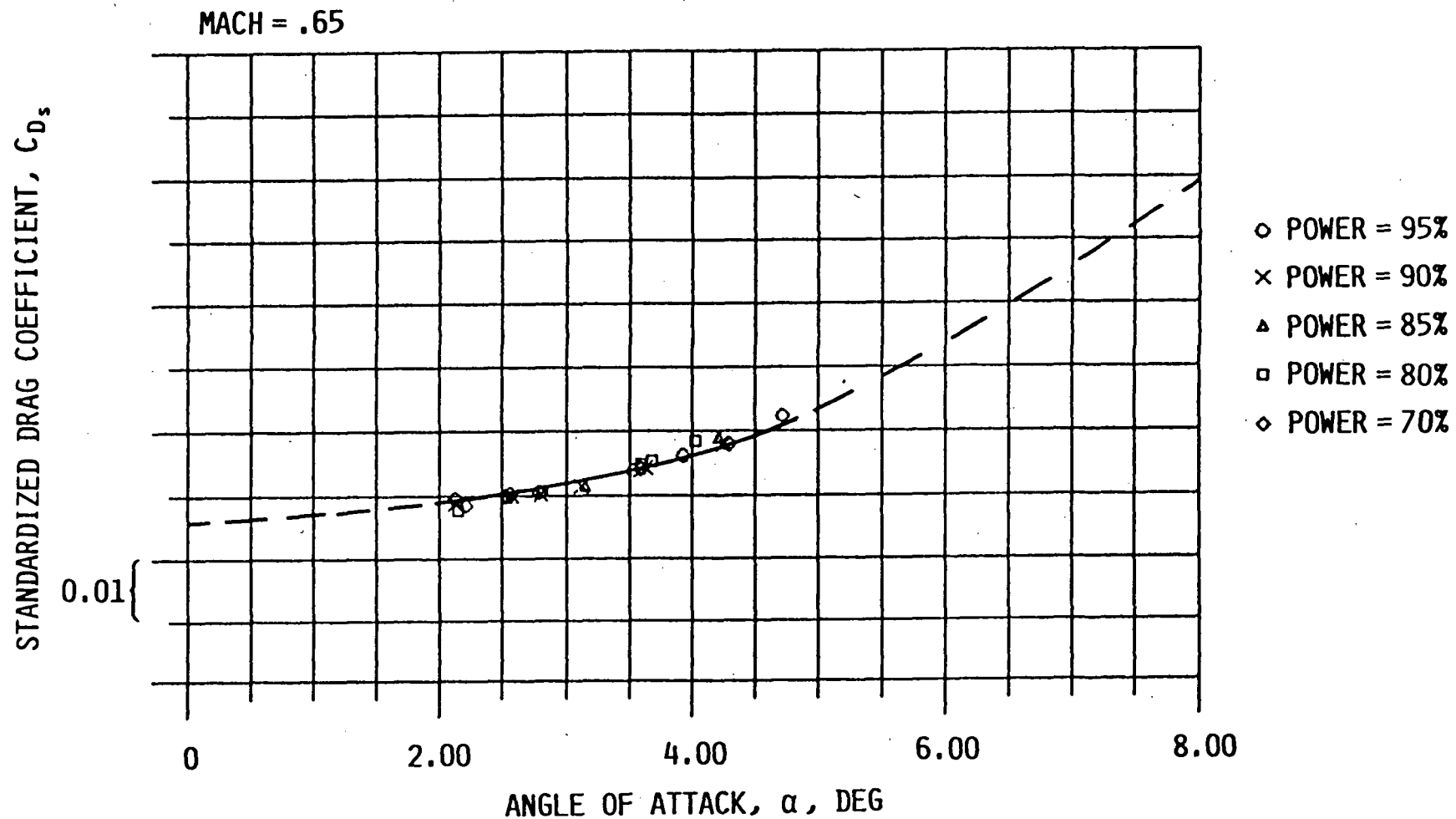


Figure F.8: Drag Characteristics, $M = .65$, All Available Powers

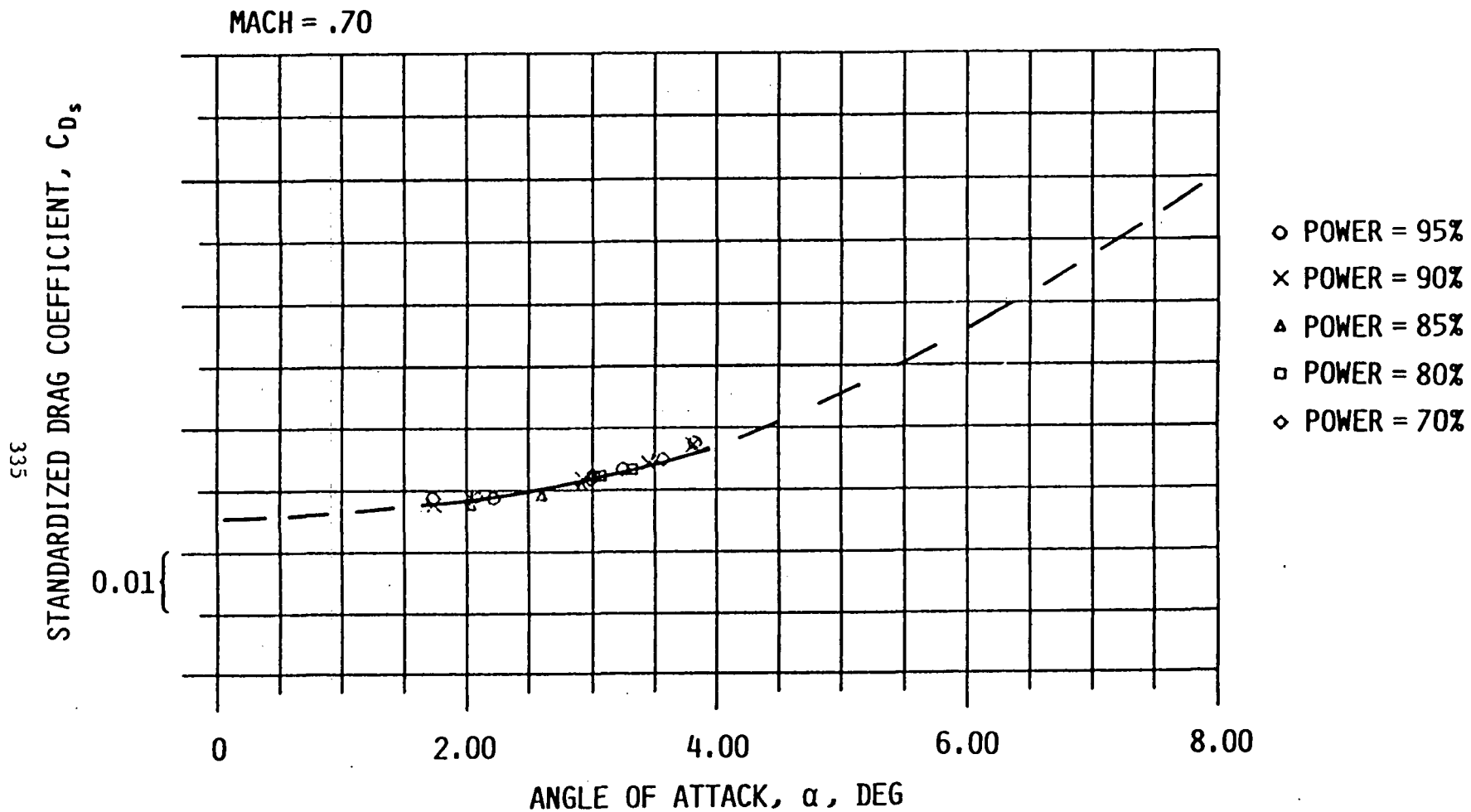


Figure F.9: Drag Characteristics, $M = .7$, All Available Powers

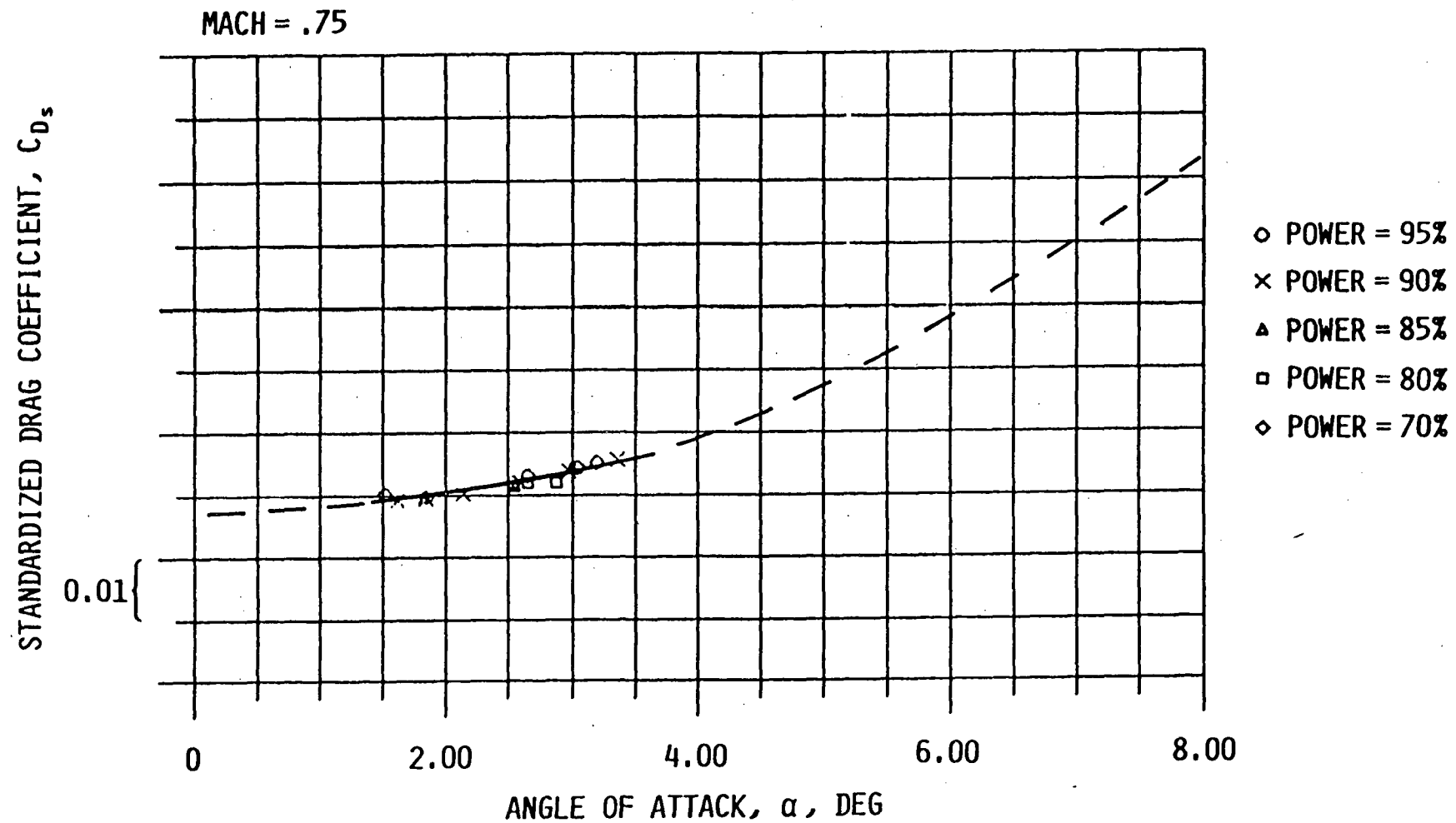


Figure F.10: Drag Characteristics, $M = .75$, All Available Powers

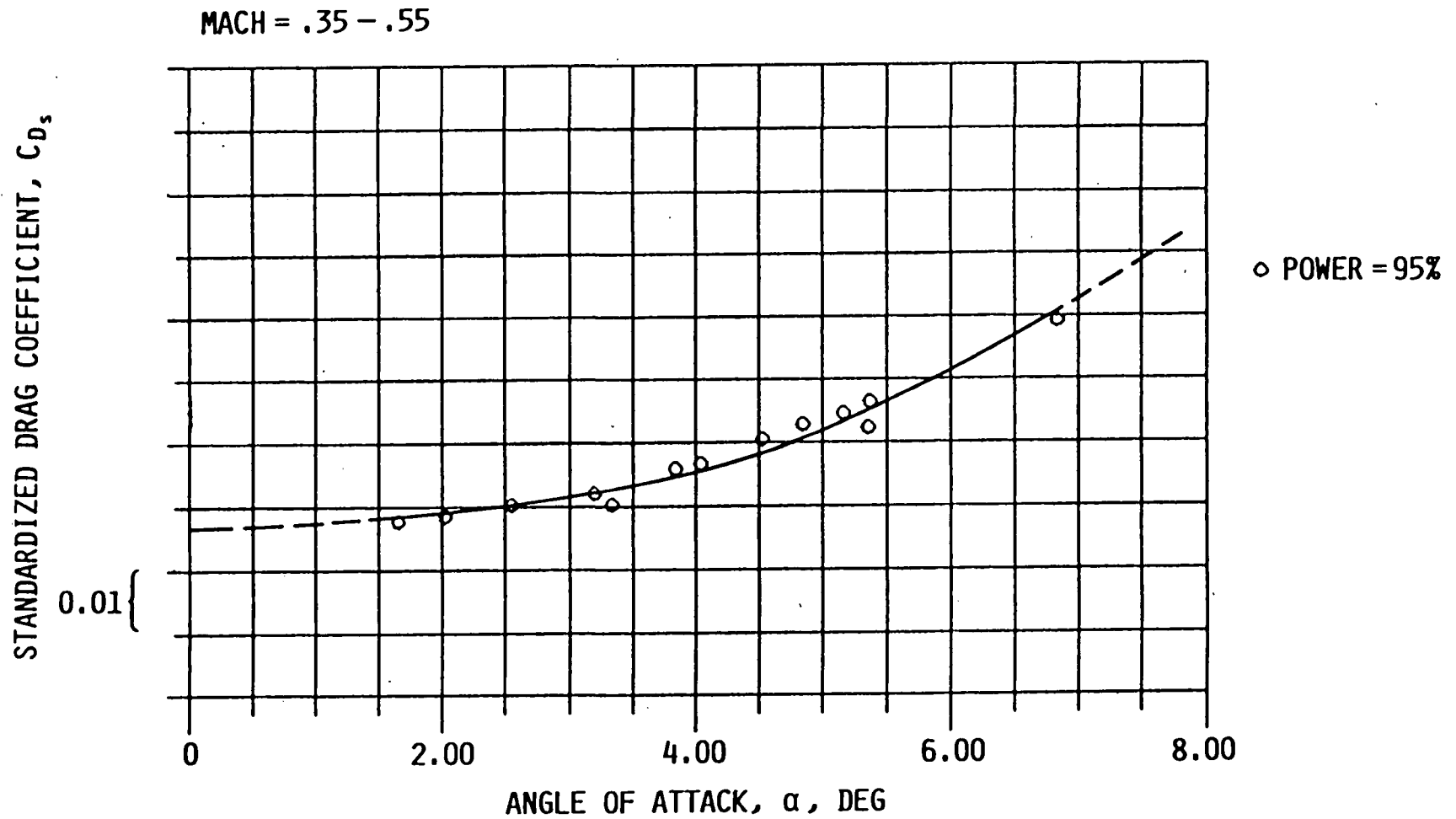


Figure F.11: Drag Characteristics, $M \leq .55$, $N_1 = 95\%$

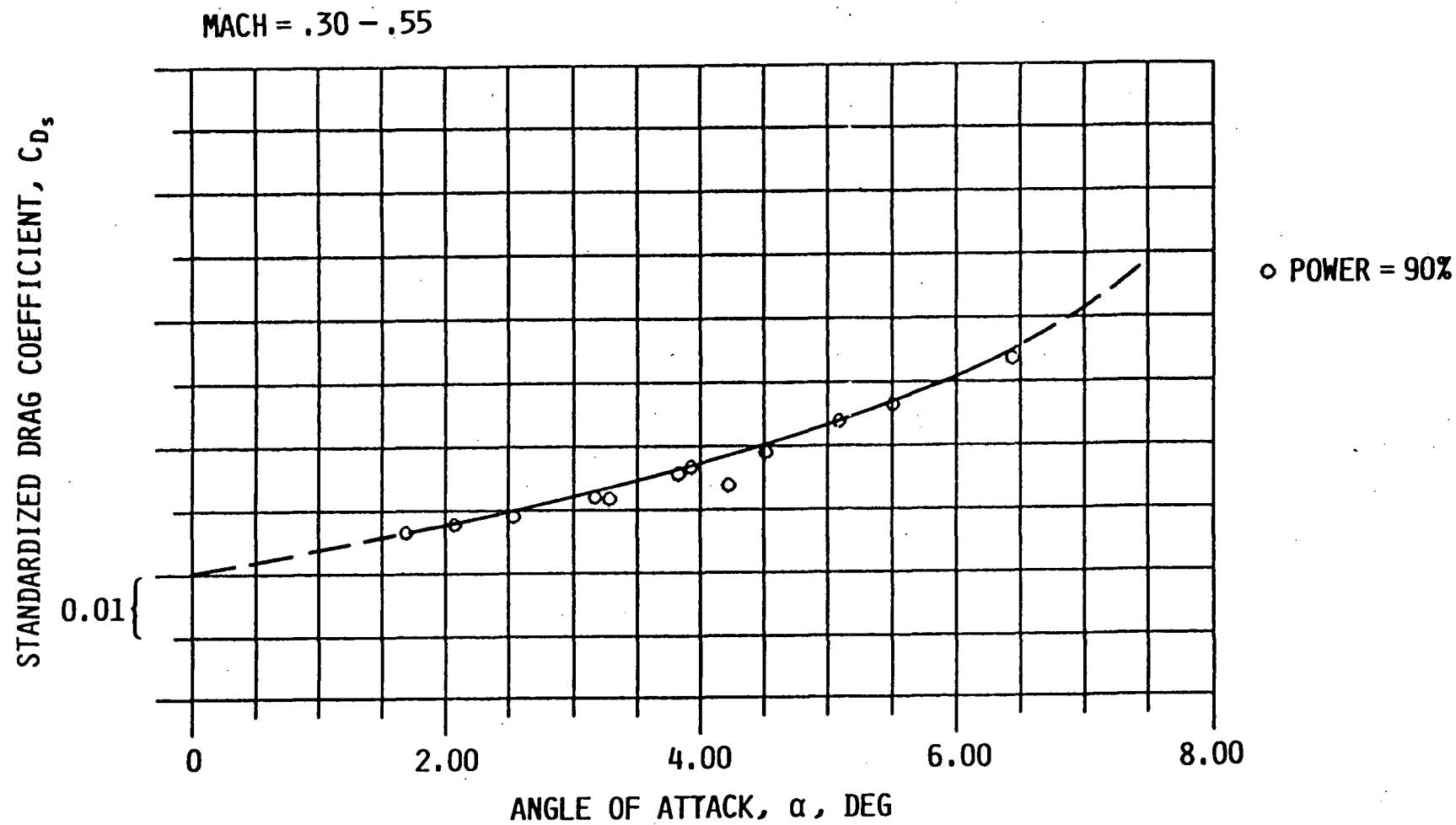


Figure F.12: Drag Characteristics, $M \leq .55$, $N_1 = 90\%$

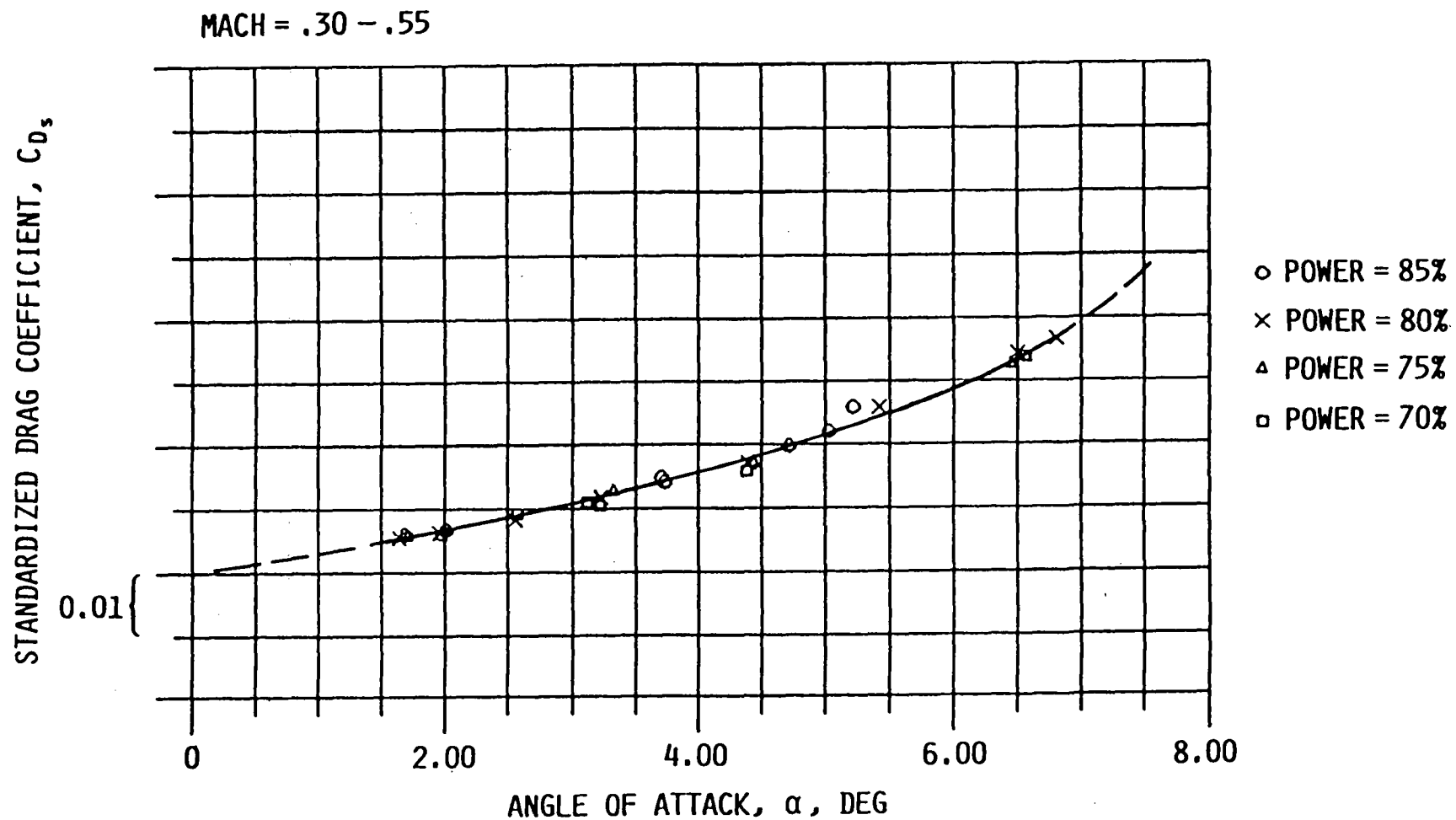


Figure F.13: Drag Characteristics, $M \leq .55$, $85\% \leq N_1 \leq 70\%$

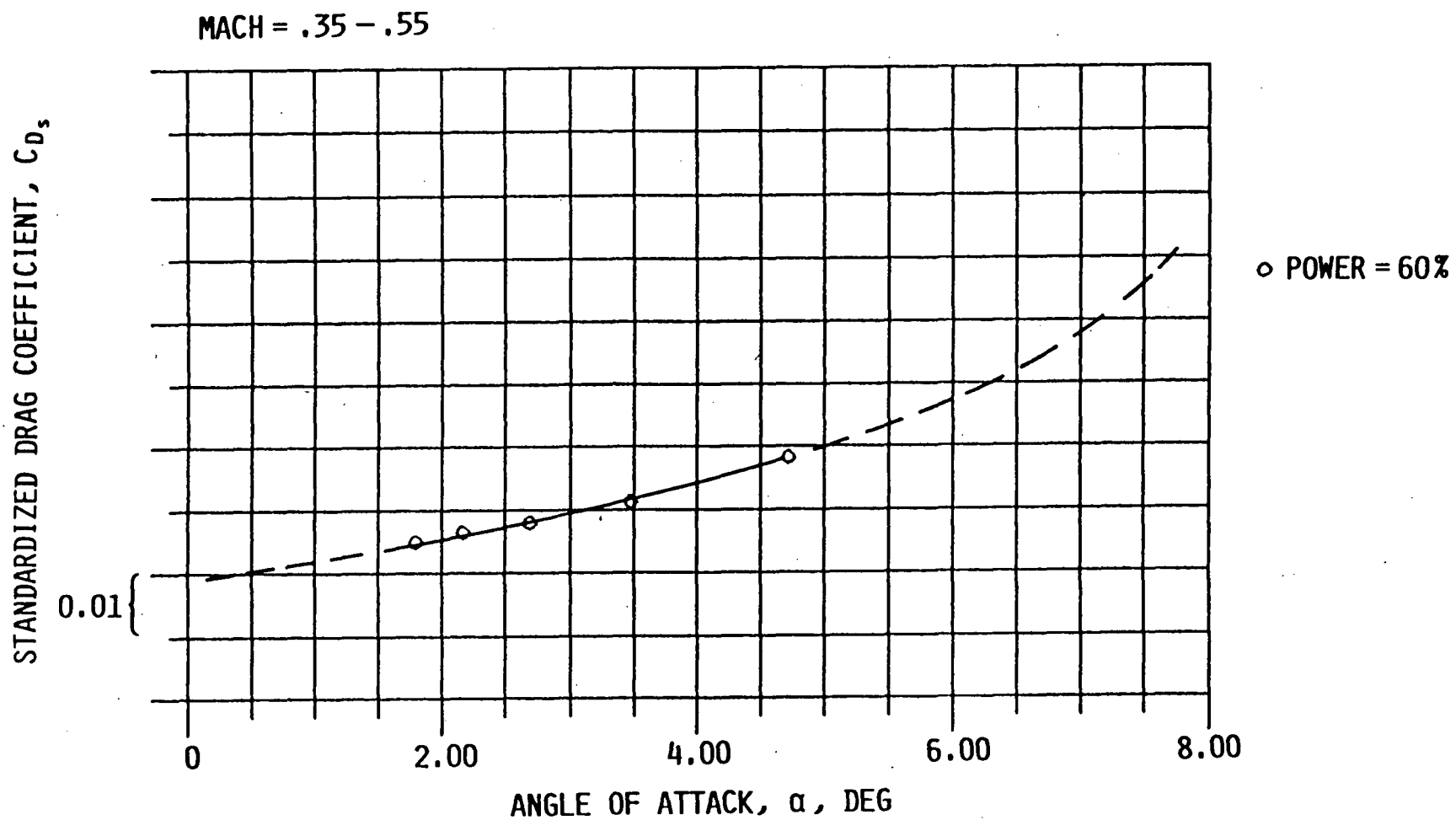


Figure F.14: Drag Characteristics, $M \leq .55$, $N_1 = 60\%$

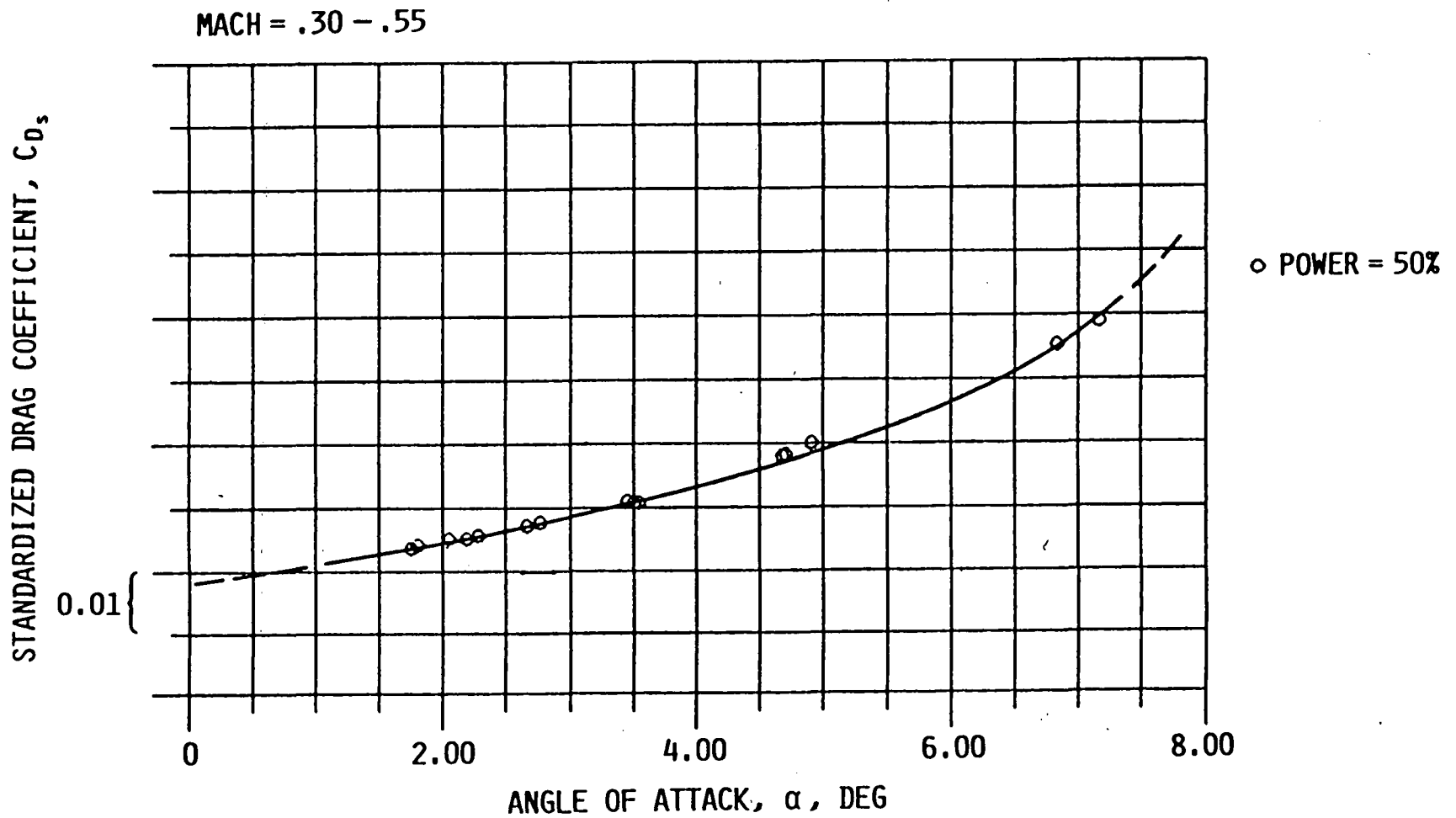


Figure F.15: Drag Characteristics, $M \leq .55$, $N_1 = 50\%$

APPENDIX G

LEAR 55 BASELINE ENGINE CHARACTERISTICS

A complete flight test program was accomplished using a Lear 55 aircraft in conjunction with a subsequent Singer Corporation contract. This flight test program extended from February through March 1983 and used the same performance modeling test approach developed in this report. A thrust run was accomplished on this aircraft using the Edwards AFB thrust facility as discussed in Appendix E. The purpose of this Appendix is to present the data plots for selected Lear 55 baseline in-flight engine characteristics to illustrate the lower degree of scatter that can be expected when compared to the Lear 35 program. The engine prediction deck curve is included on each of the plots for comparison to the final curve that was faired through the data. Figures G.1 through G.5 present the corrected gross thrust data plots. The maximum scatter experienced for corrected gross thrust was approximately ± 200 pounds which was primarily observed in the mid-Mach range (.45-.55). Figures G.6 through G.10 present the corrected fuel flow data plots. For corrected fuel flow, the same normalization techniques using the N power of δ discussed in Section 3.2.1.2 was used to eliminate the altitude dependency. N was generally not the same value as that used on the Lear 35, since the engines were not the same. The maximum scatter experienced for corrected fuel flow was approximately ± 70 lbs/hour which was again primarily experienced in the mid-Mach range. Figures G.11 through G.15 present the corrected

airflow data plots. The maximum scatter experienced was approximately ± 3 lbs/sec again in the mid-Mach range.

APPENDIX G SUMMARY

<u>Figure No.</u>	<u>Title</u>
G.1	Lear 55 Corrected Gross Thrust Characteristics, $M = .35$
G.2	Lear 55 Corrected Gross Thrust Characteristics, $M = .45$
G.3	Lear 55 Corrected Gross Thrust Characteristics, $M = .55$
G.4	Lear 55 Corrected Gross Thrust Characteristics, $M = .65$
G.5	Lear 55 Corrected Gross Thrust Characteristics, $M = .75$
G.6	Lear 55 Nonstandard Corrected Fuel Flow Characteristics, $M = .35$
G.7	Lear 55 Nonstandard Corrected Fuel Flow Characteristics, $M = .45$
G.8	Lear 55 Nonstandard Corrected Fuel Flow Characteristics, $M = .55$
G.9	Lear 55 Nonstandard Corrected Fuel Flow Characteristics, $M = .65$
G.10	Lear 55 Nonstandard Corrected Fuel Flow Characteristics, $M = .75$
G.11	Lear 55 Corrected Airflow Characteristics, $M = .35$
G.12	Lear 55 Corrected Airflow Characteristics, $M = .45$
G.13	Lear 55 Corrected Airflow Characteristics, $M = .55$
G.14	Lear 55 Corrected Airflow Characteristics, $M = .65$
G.15	Lear 55 Corrected Airflow Characteristics, $M = .75$

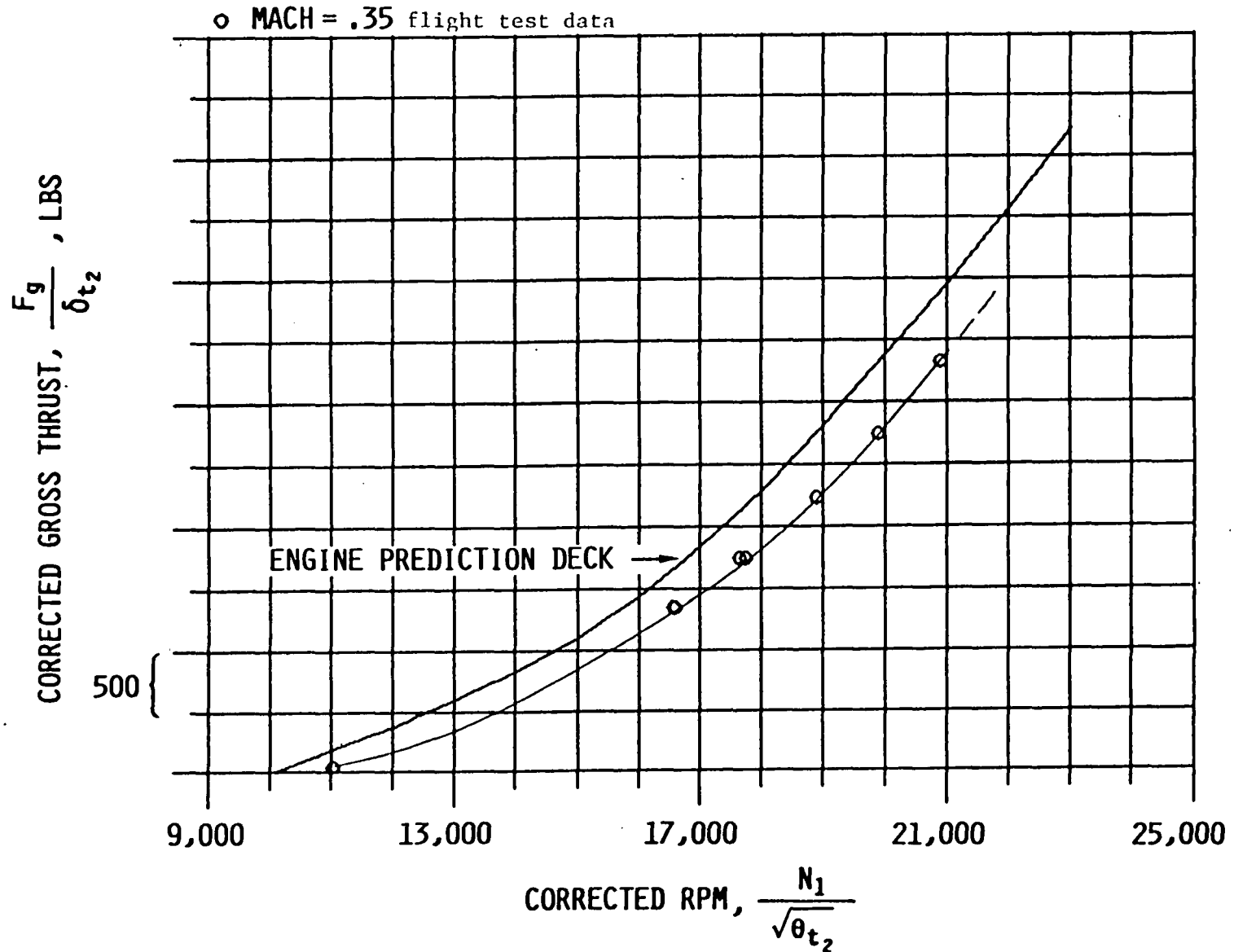


Figure G.1: Lear 55 Corrected Gross Thrust Characteristics, M = .35

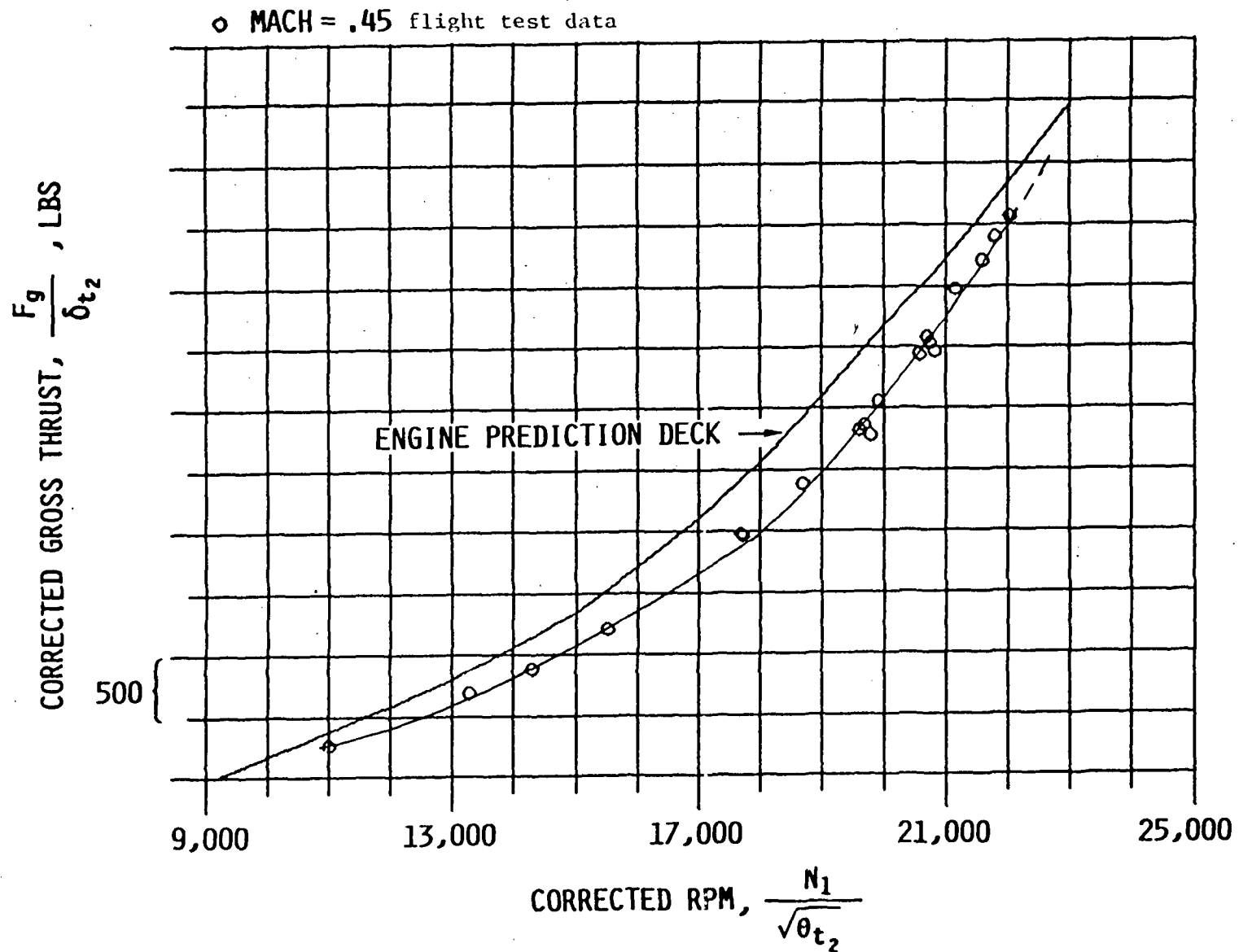


Figure G.2: Lear 55 Corrected Gross Thrust Characteristics, M = .45

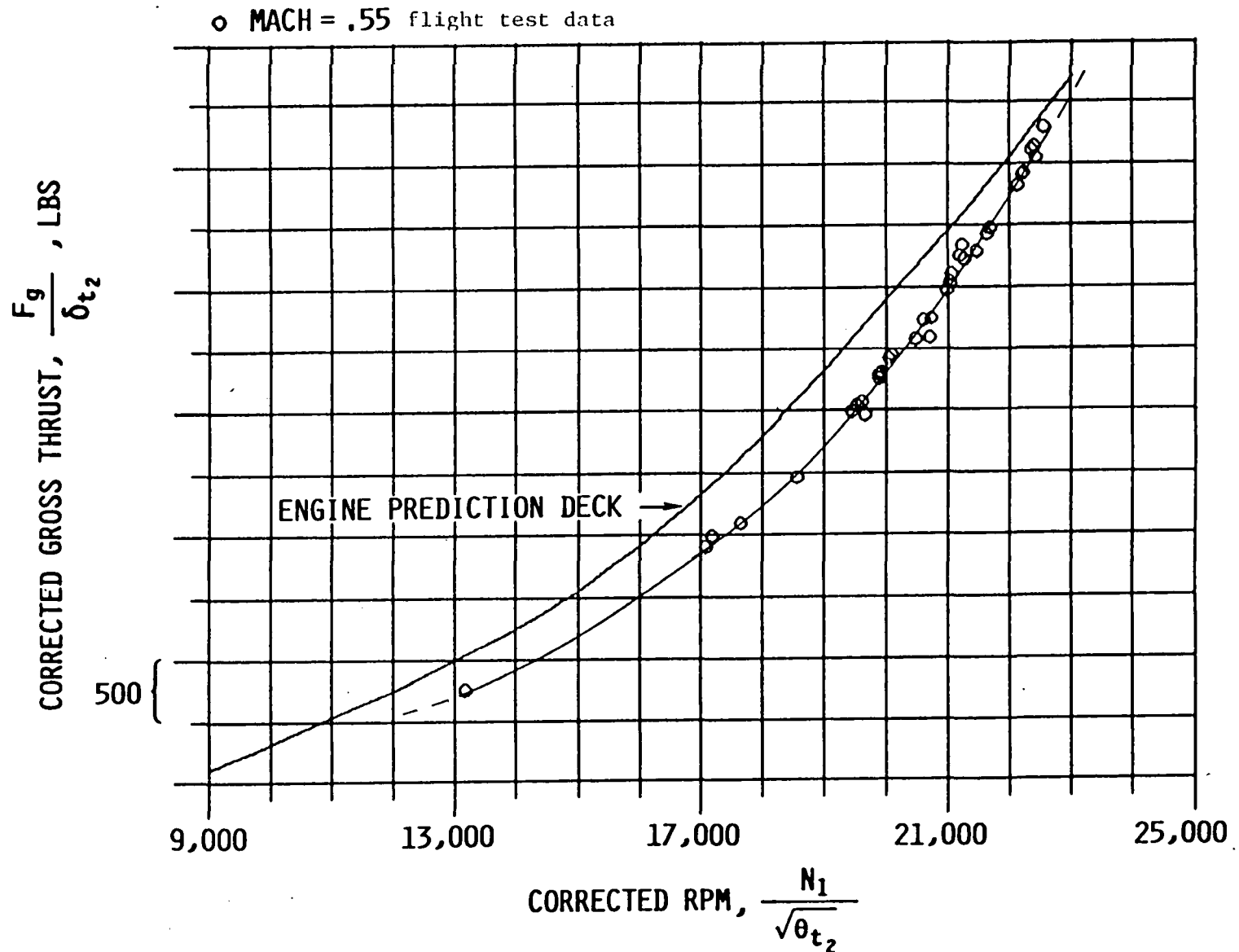


Figure G.3: Lear 55 Corrected Gross Thrust Characteristics, $M = .55$

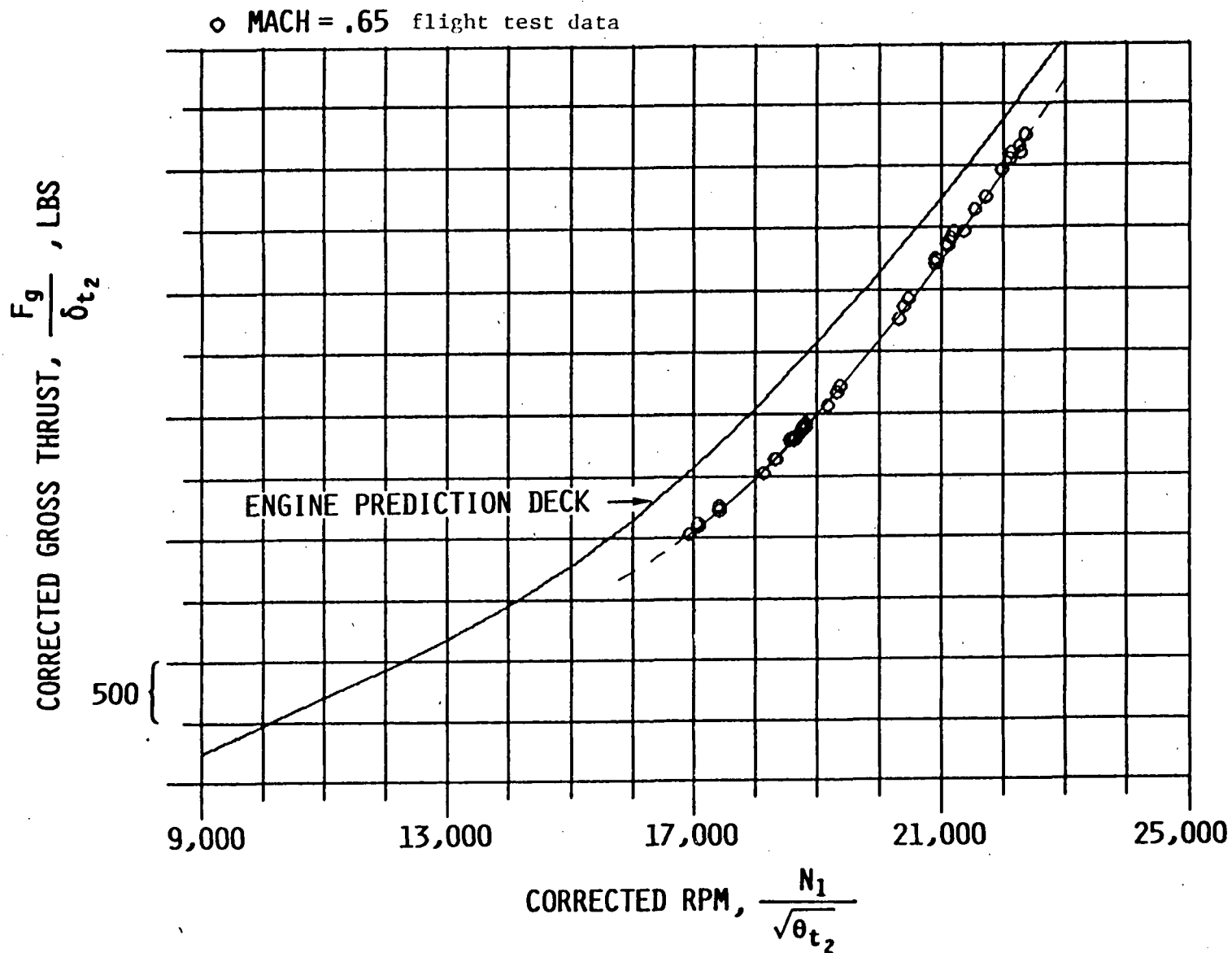


Figure G.4: Lear 55 Corrected Gross Thrust Characteristics, M = .65

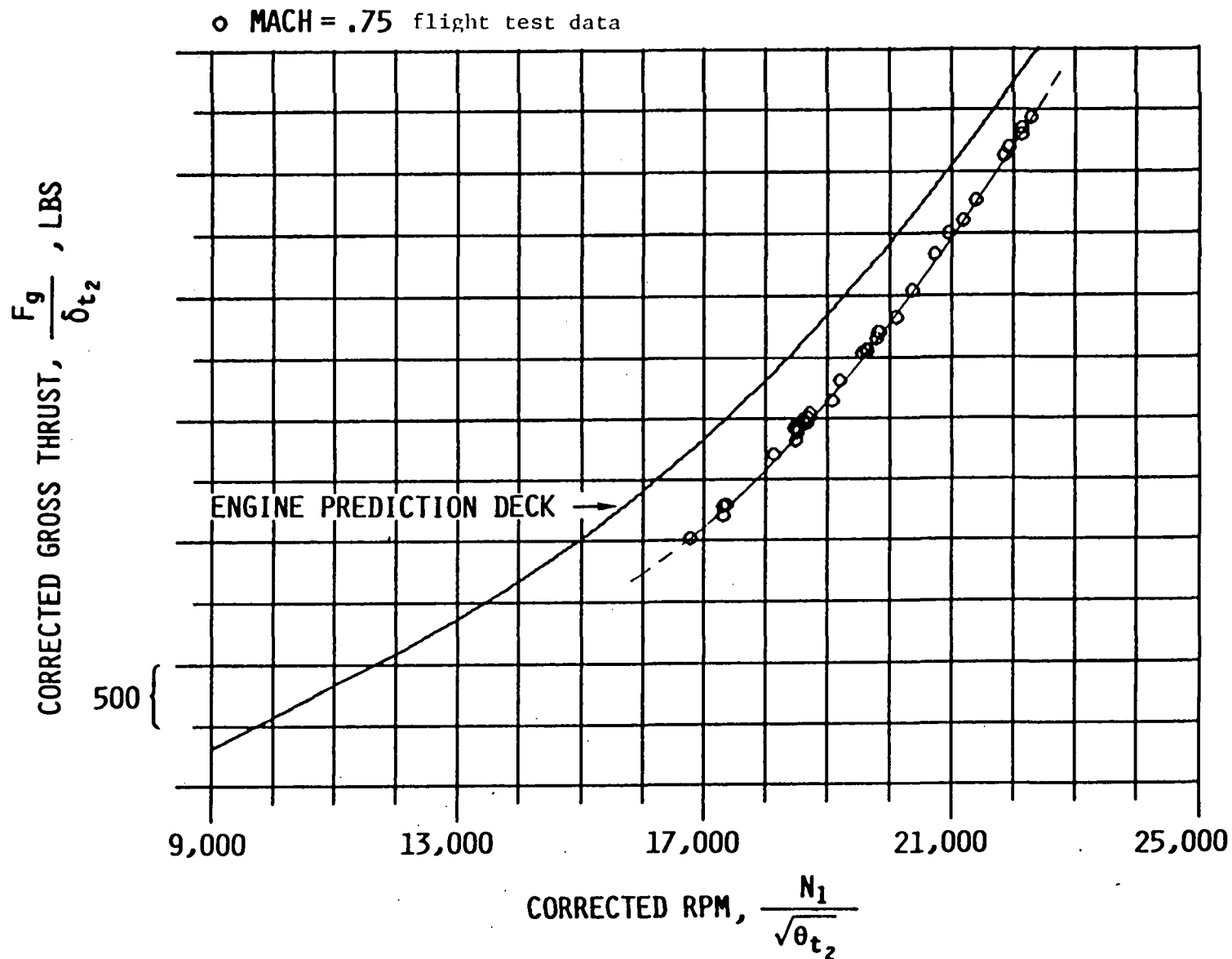


Figure G.5: Lear 55 Corrected Gross Thrust Characteristics, $M = .75$

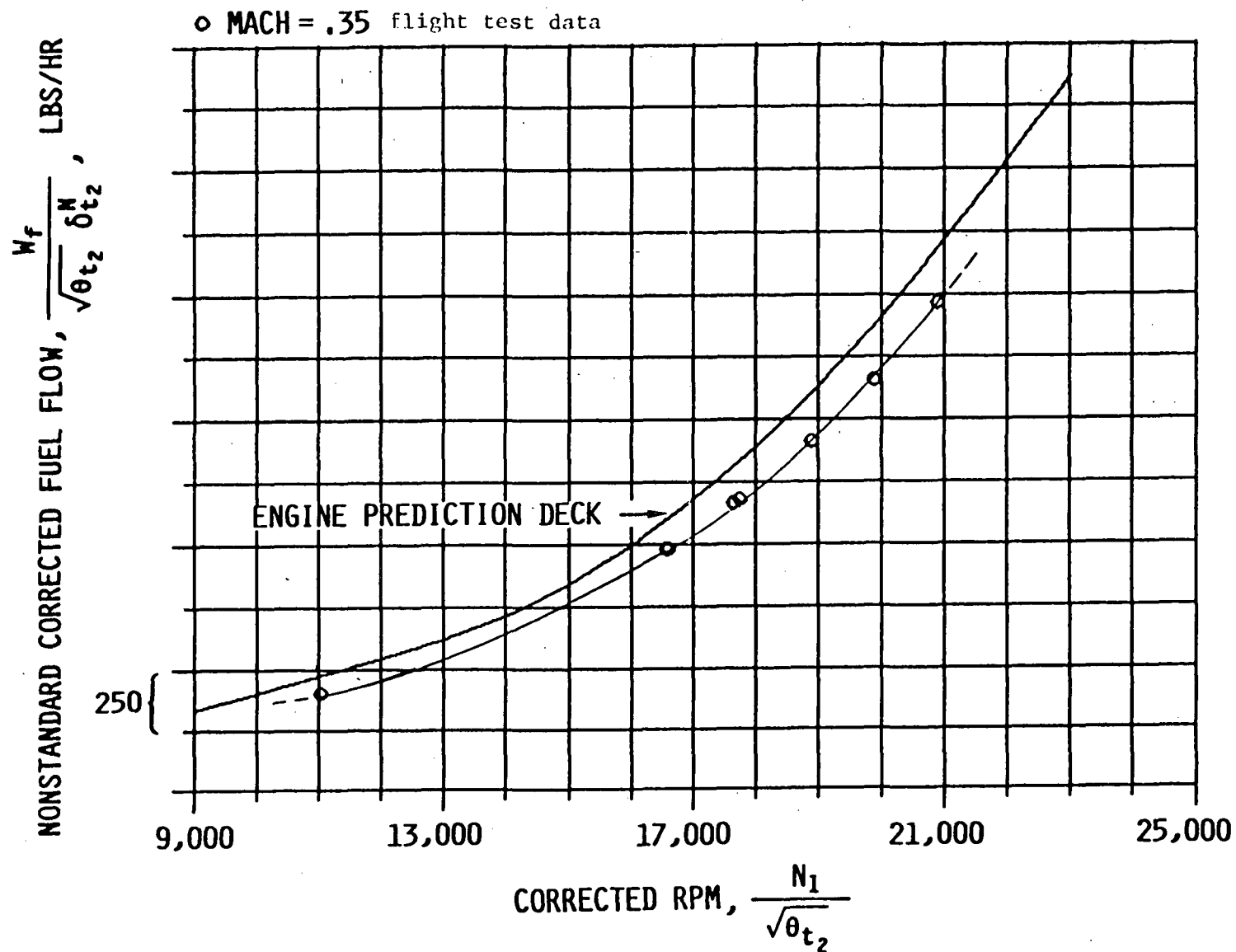


Figure G.6: Lear 55 Nonstandard Corrected Fuel Flow Characteristics, M = .35

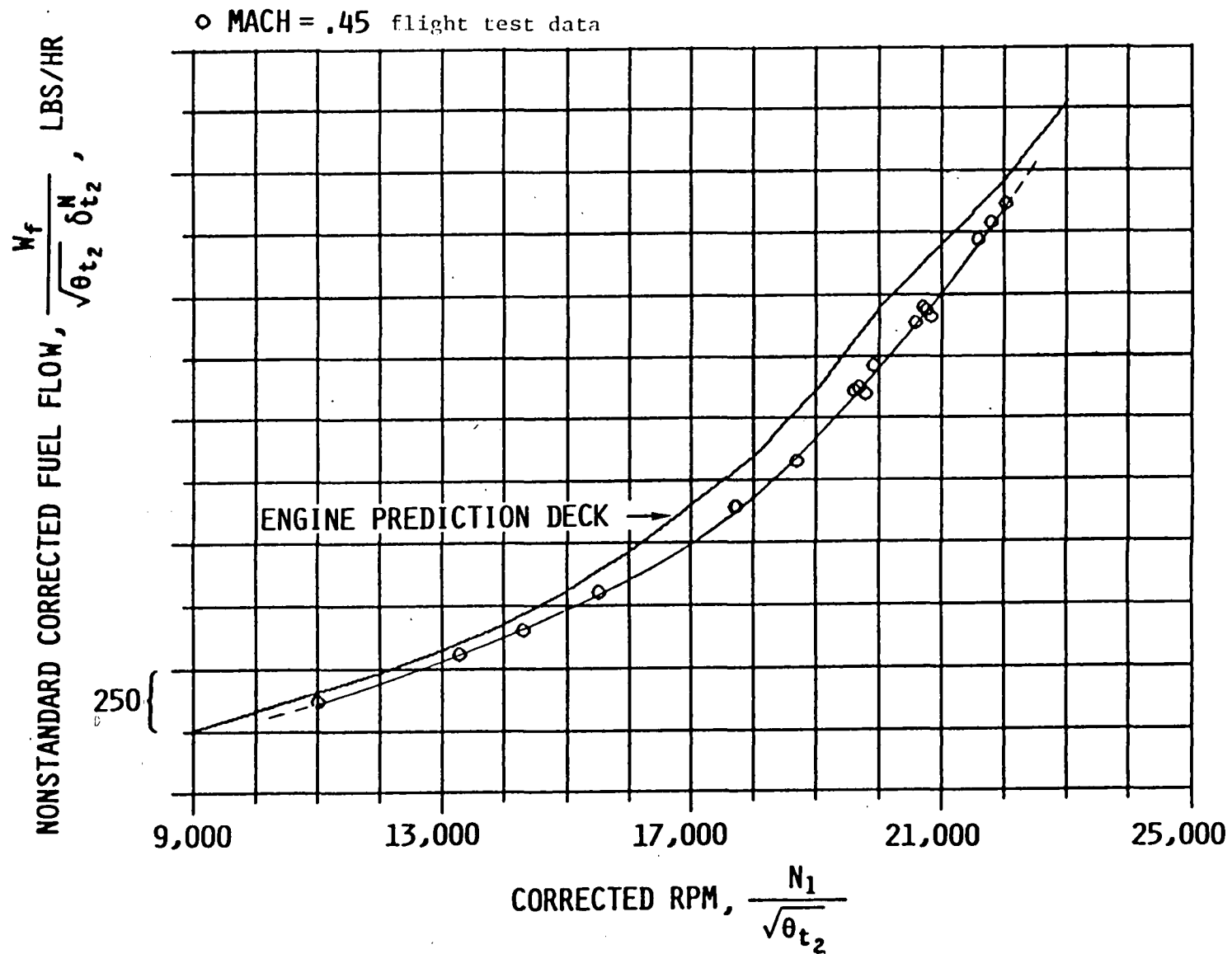


Figure G.7: Lear 55 Nonstandard Corrected Fuel Flow Characteristics, M = .45

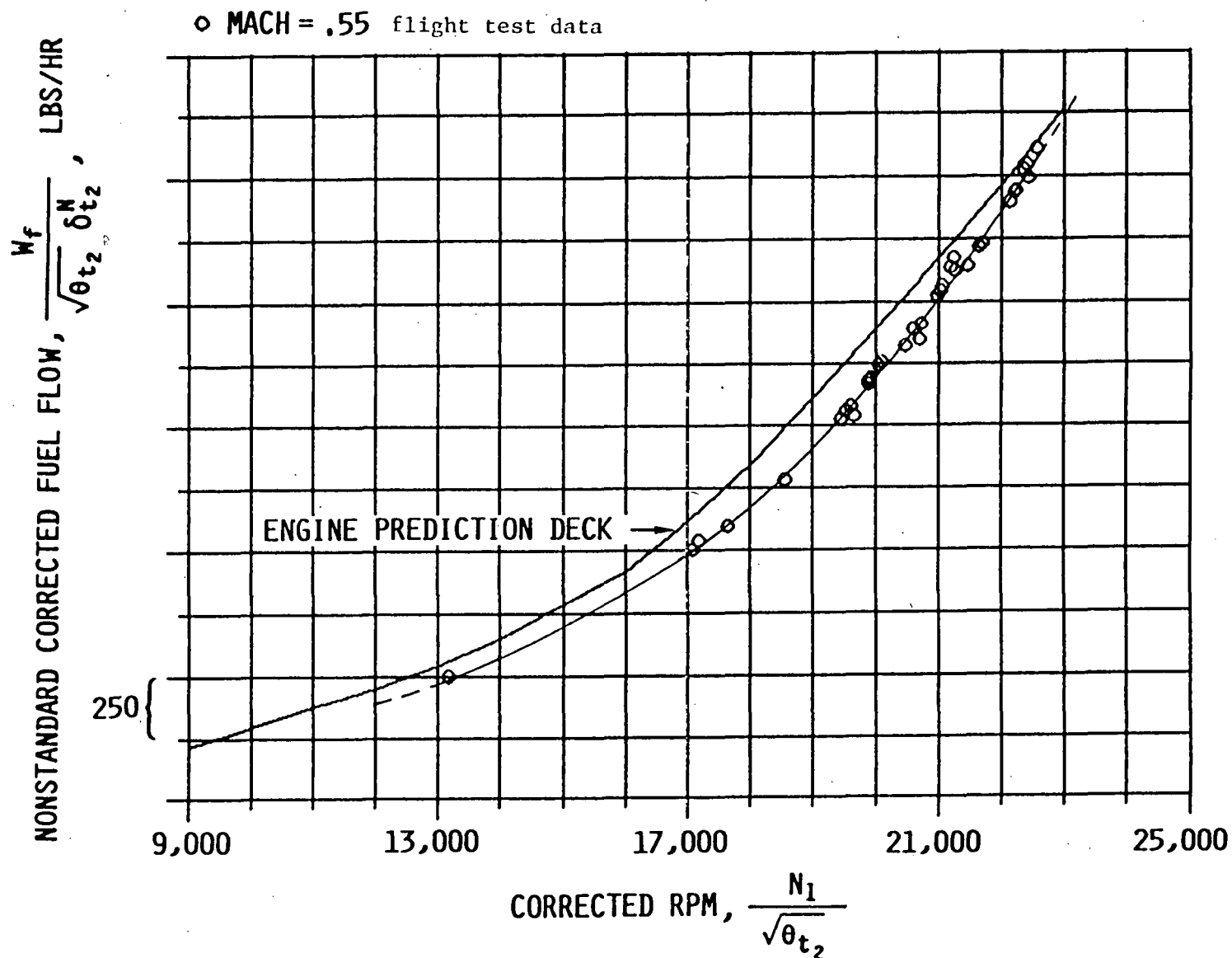


Figure G.8: Lear 55 Nonstandard Corrected Fuel Flow Characteristics, $M = .55$

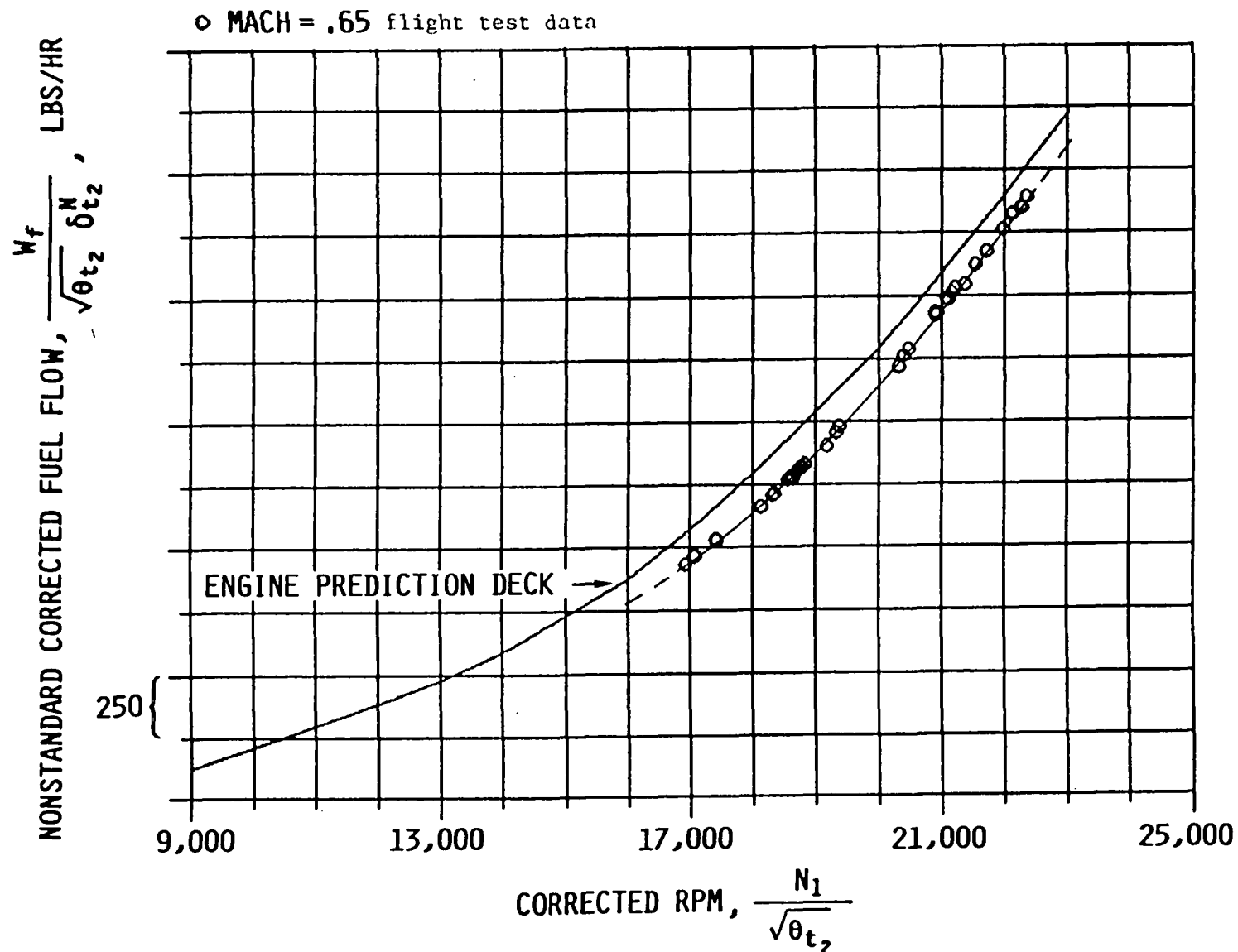


Figure G.9: Lear 55 Nonstandard Corrected Fuel Flow Characteristics, M = .65

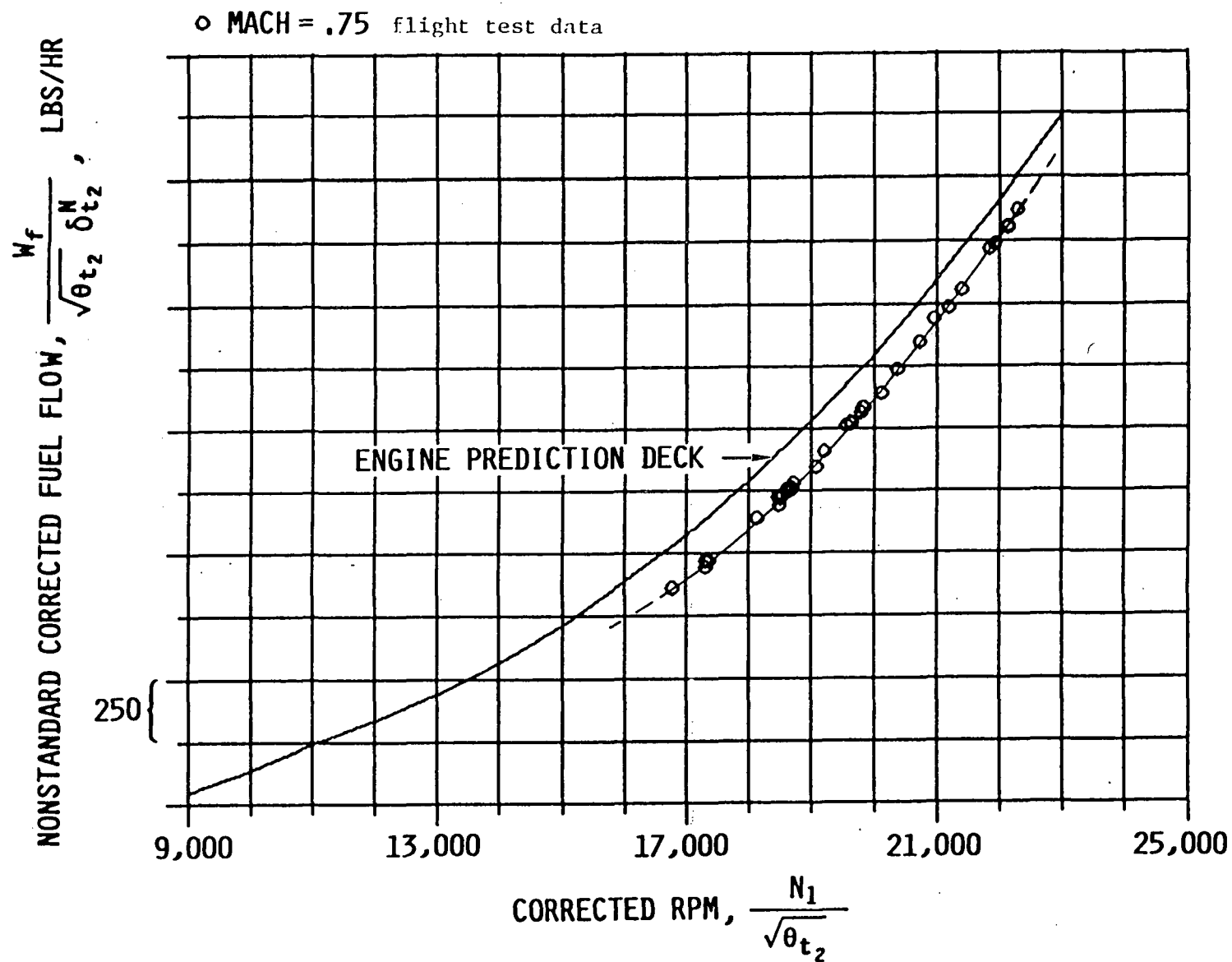


Figure G.10: Lear 55 Nonstandard Corrected Fuel Flow Characteristics, $M = .75$

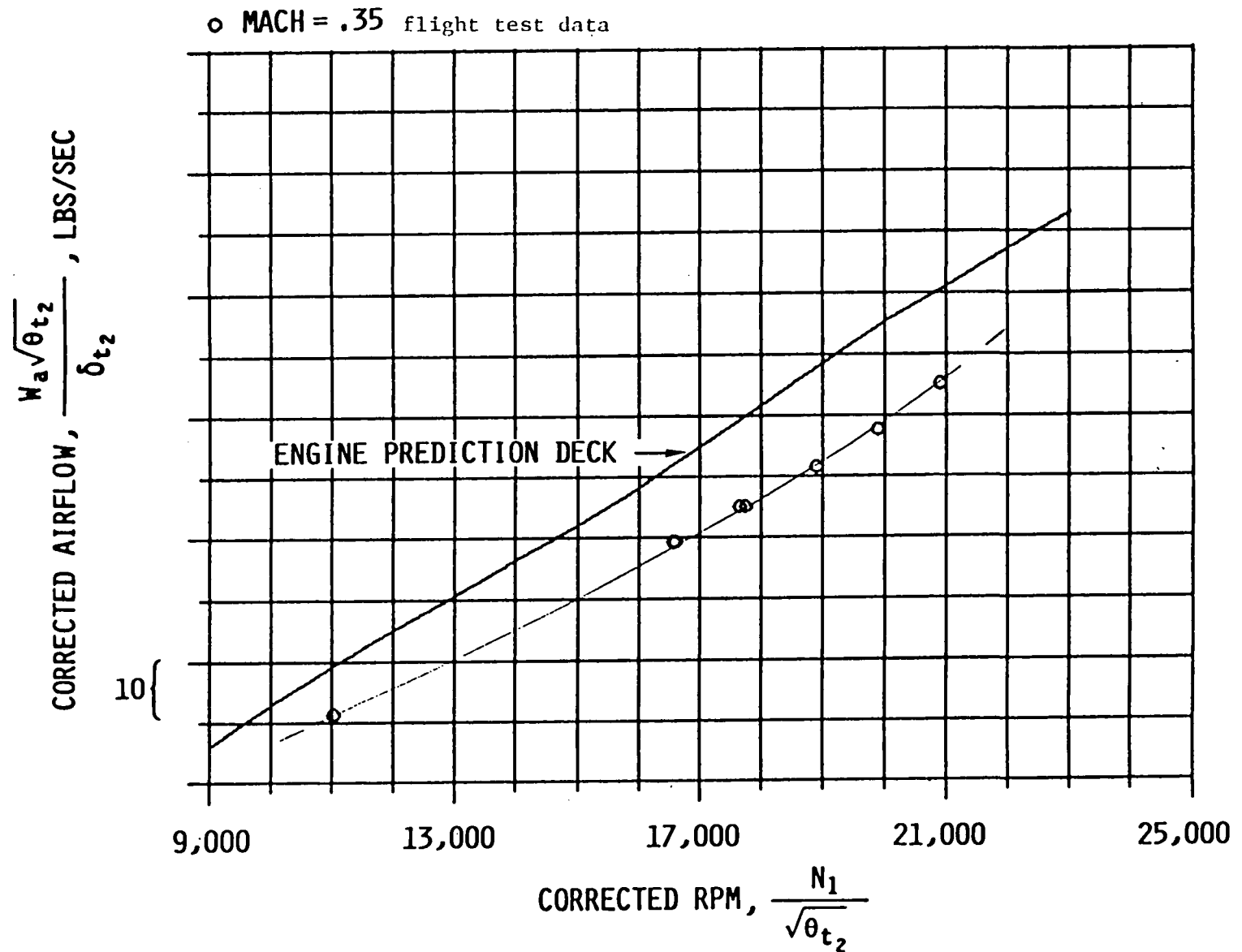


Figure G.11: Lear 55 Corrected Airflow Characteristics, M = .35

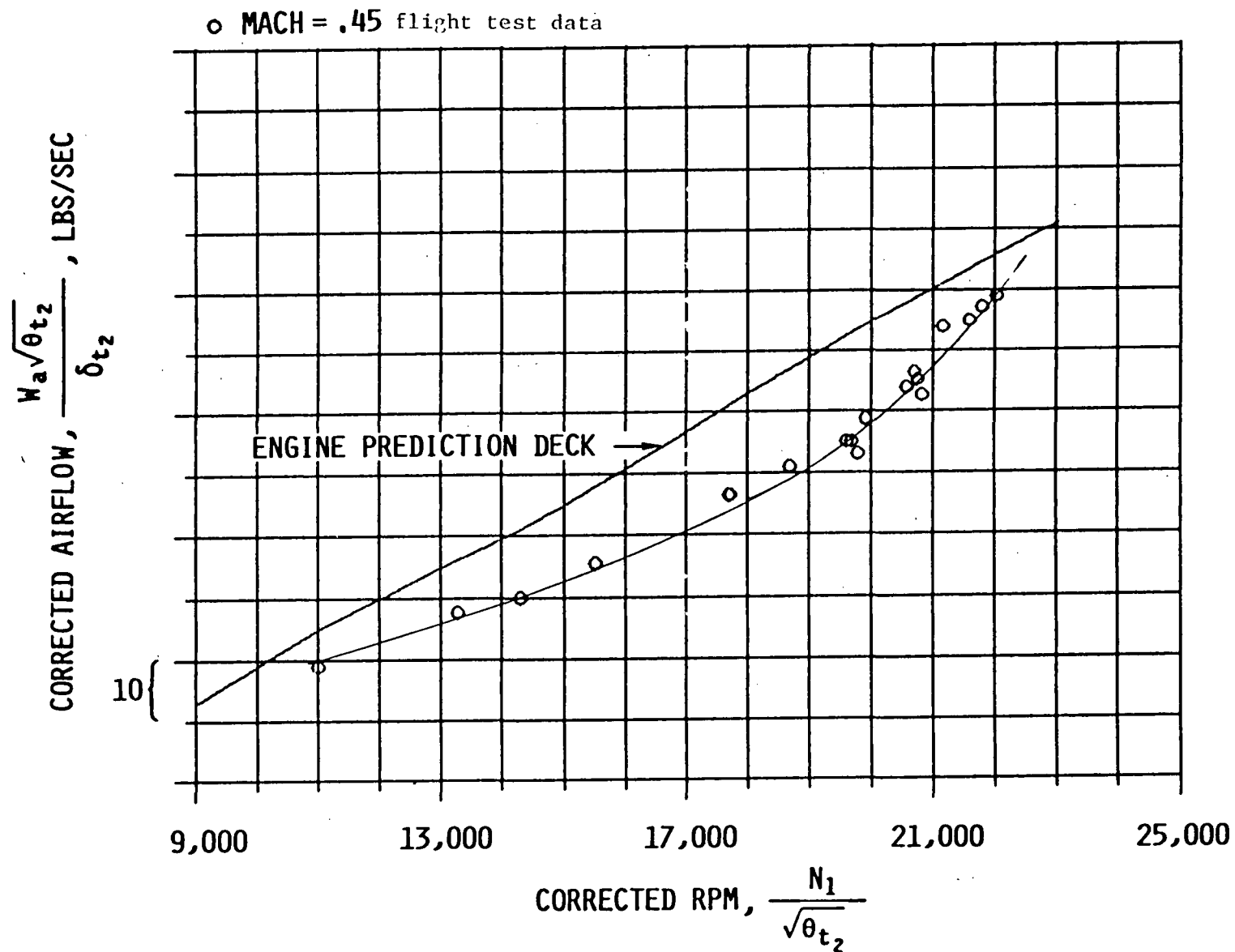


Figure G.12: Lear 55 Corrected Airflow Characteristics, $M = .45$

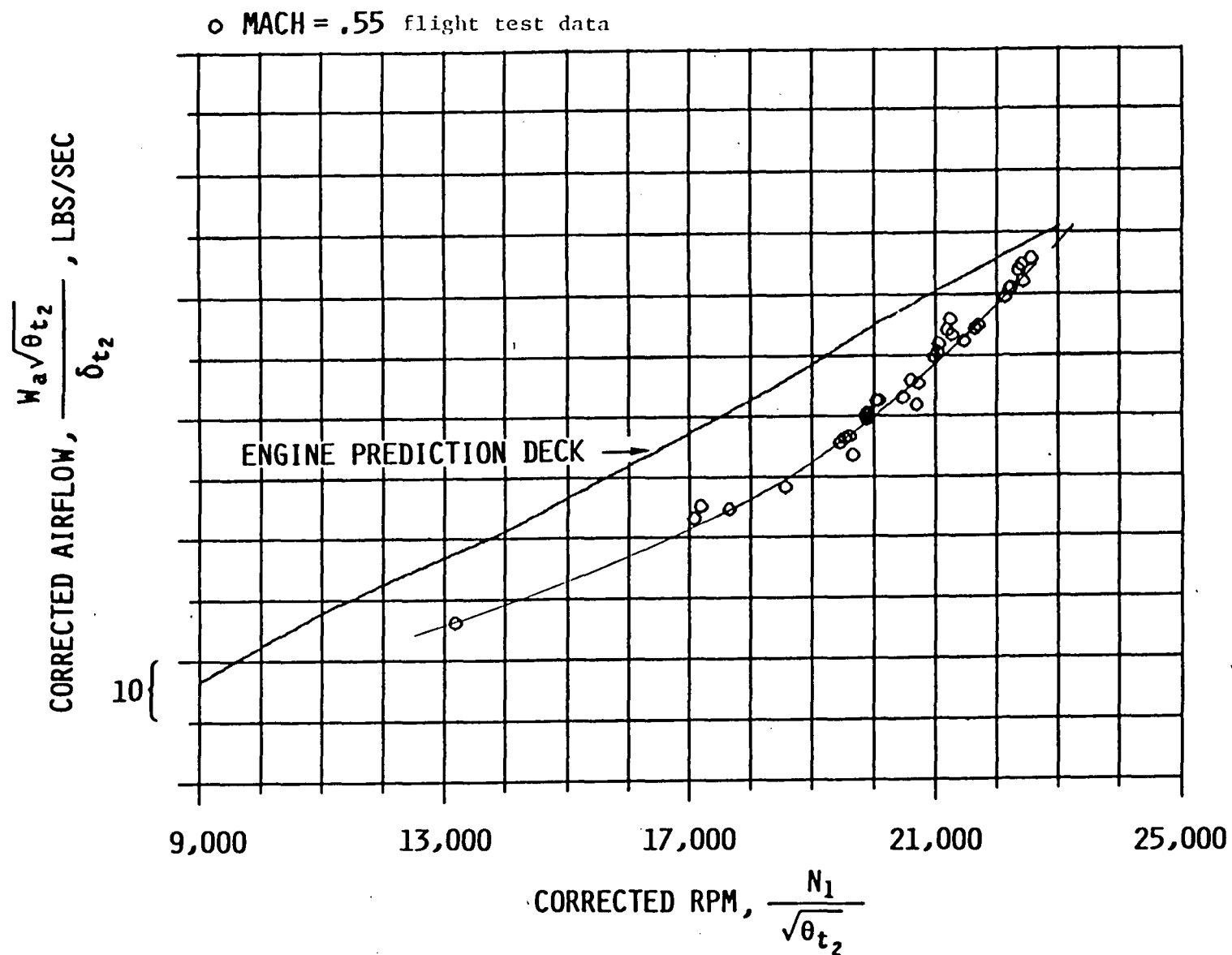


Figure G.13: Lear 55 Corrected Airflow Characteristics, M = .55

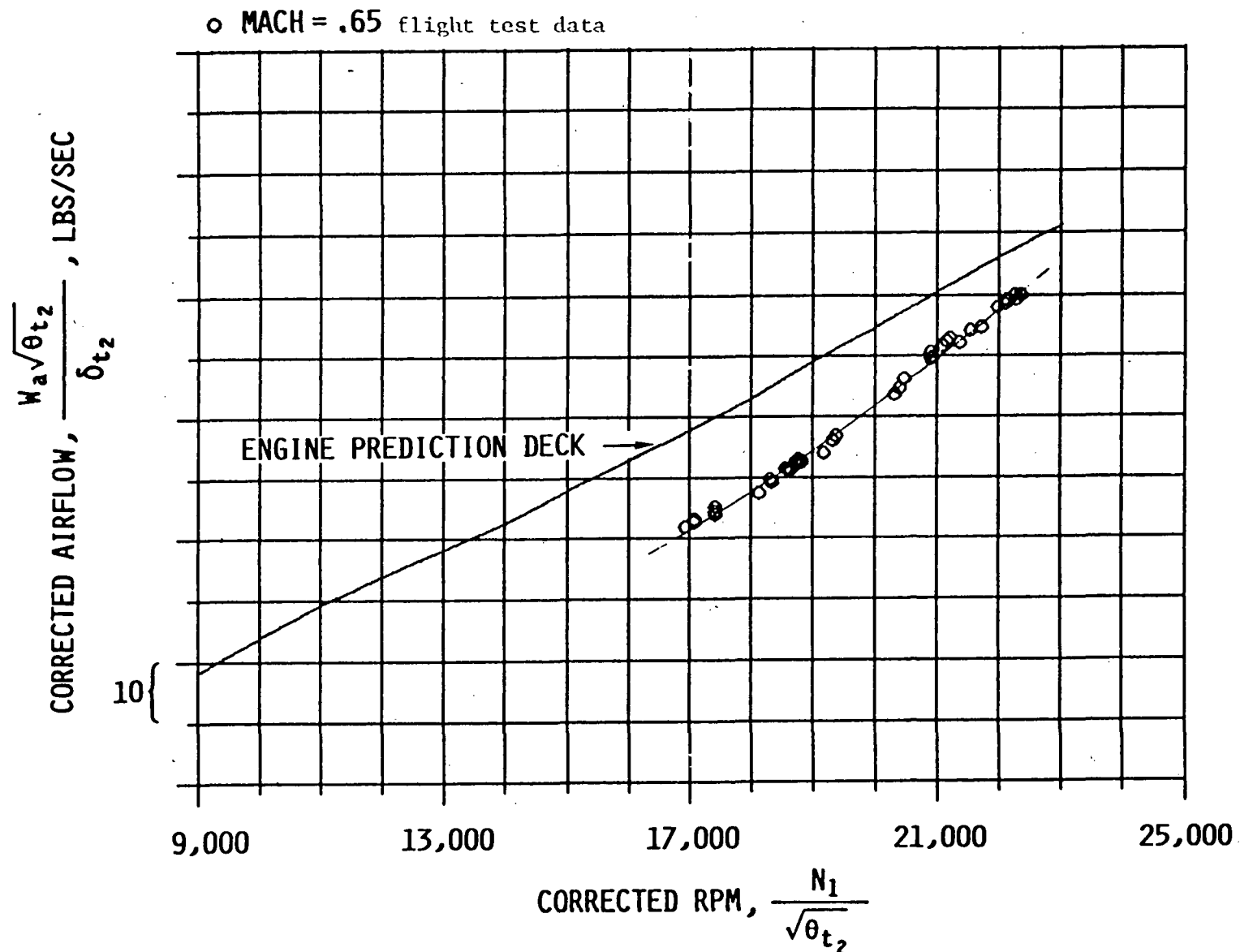


Figure G.14: Lear 55 Corrected Airflow Characteristics, M = .65

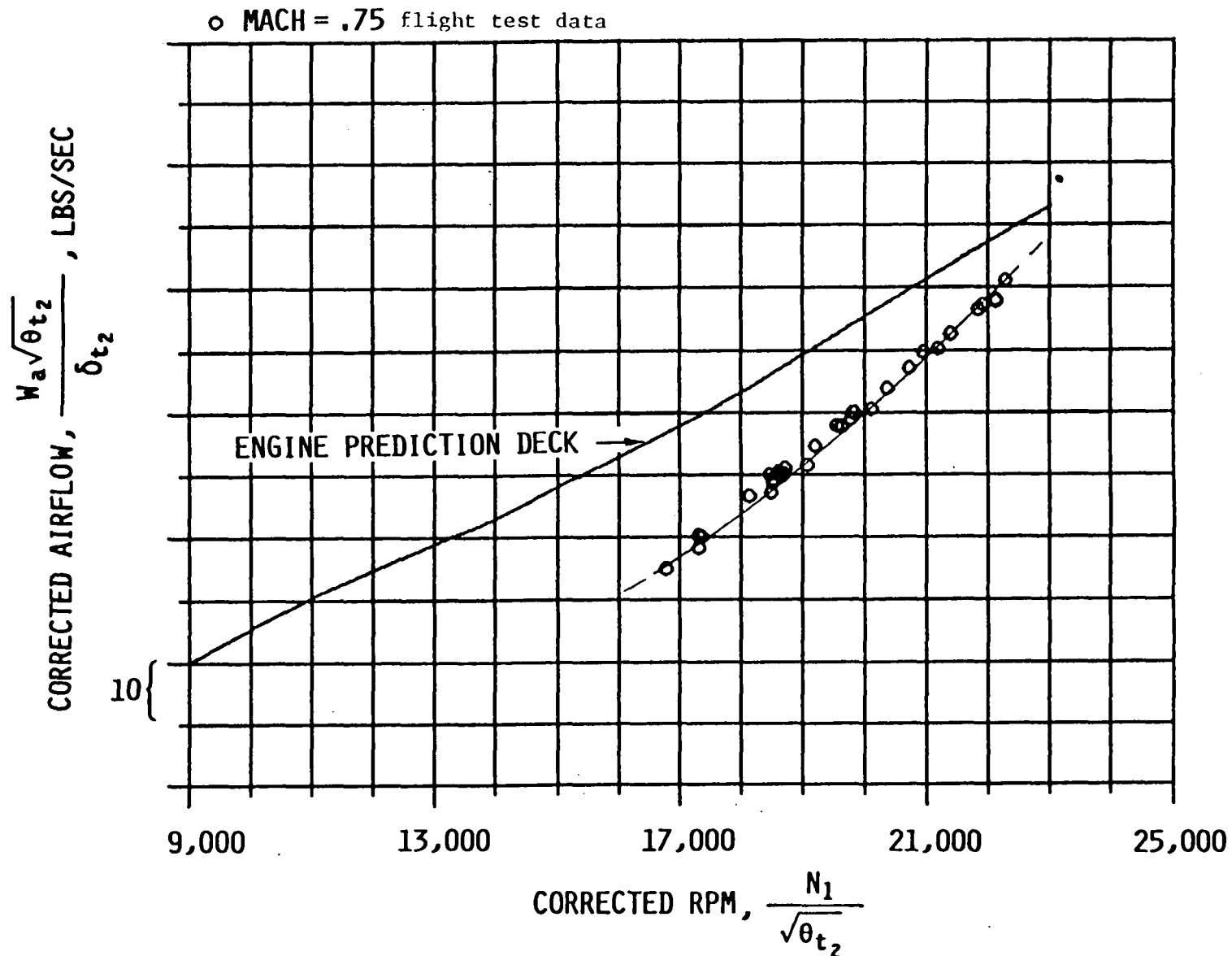


Figure G.15: Lear 55 Corrected Airflow Characteristics, $M = .75$

APPENDIX H

LEAR 35

BASELINE ENGINE CHARACTERISTICS

APPENDIX H SUMMARY

<u>Figure No.</u>	<u>Title</u>
H.1	Corrected Gross Thrust Characteristics, $M = .3$
H.2	Corrected Gross Thrust Characteristics, $M = .35$
H.3	Corrected Gross Thrust Characteristics, $M = .4$
H.4	Corrected Gross Thrust Characteristics, $M = .45$
H.5	Corrected Gross Thrust Characteristics, $M = .5$
H.6	Corrected Gross Thrust Characteristics, $M = .6$
H.7	Corrected Gross Thrust Characteristics, $M = .65$
H.8	Corrected Gross Thrust Characteristics, $M = .7$
H.9	Corrected Gross Thrust Characteristics, $M = .75$
H.10	Nonstandard Corrected Fuel Flow Characteristics, $M = .3$
H.11	Nonstandard Corrected Fuel Flow Characteristics, $M = .35$
H.12	Nonstandard Corrected Fuel Flow Characteristics, $M = .4$
H.13	Nonstandard Corrected Fuel Flow Characteristics, $M = .45$
H.14	Nonstandard Corrected Fuel Flow Characteristics, $M = .5$
H.15	Nonstandard Corrected Fuel Flow Characteristics, $M = .6$
H.16	Nonstandard Corrected Fuel Flow Characteristics, $M = .65$
H.17	Nonstandard Corrected Fuel Flow Characteristics, $M = .7$
H.18	Nonstandard Corrected Fuel Flow Characteristics, $M = .75$

APPENDIX H SUMMARY (continued)

<u>Figure No.</u>	<u>Title</u>
H.19	Corrected Airflow Characteristics, $M = .3$
H.20	Corrected Airflow Characteristics, $M = .35$
H.21	Corrected Airflow Characteristics, $M = .4$
H.22	Corrected Airflow Characteristics, $M = .45$
H.23	Corrected Airflow Characteristics, $M = .5$
H.24	Corrected Airflow Characteristics, $M = .6$
H.25	Corrected Airflow Characteristics, $M = .65$
H.26	Corrected Airflow Characteristics, $M = .7$
H.27	Corrected Airflow Characteristics, $M = .75$

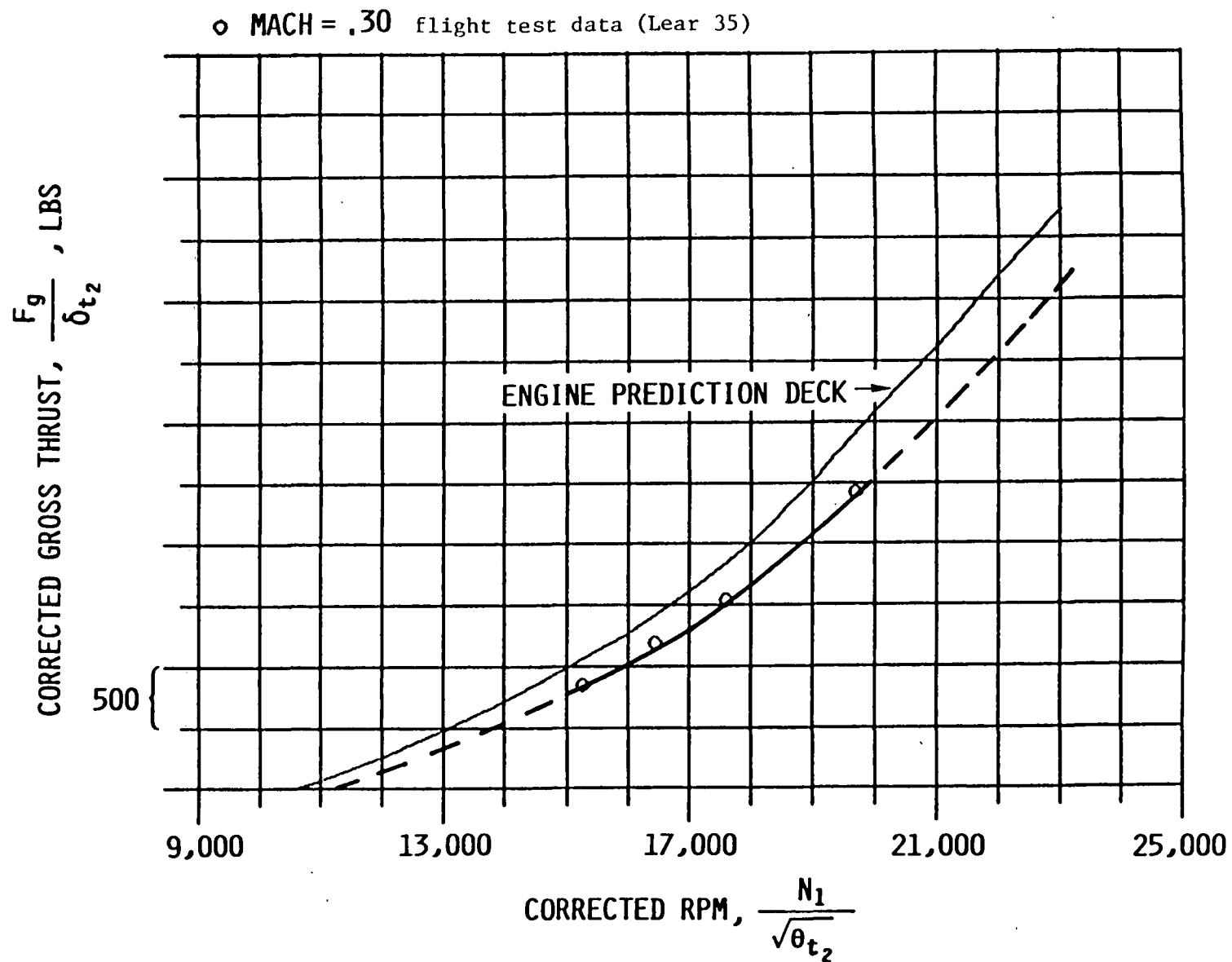


Figure H.1: Corrected Gross Thrust Characteristics, M = .30

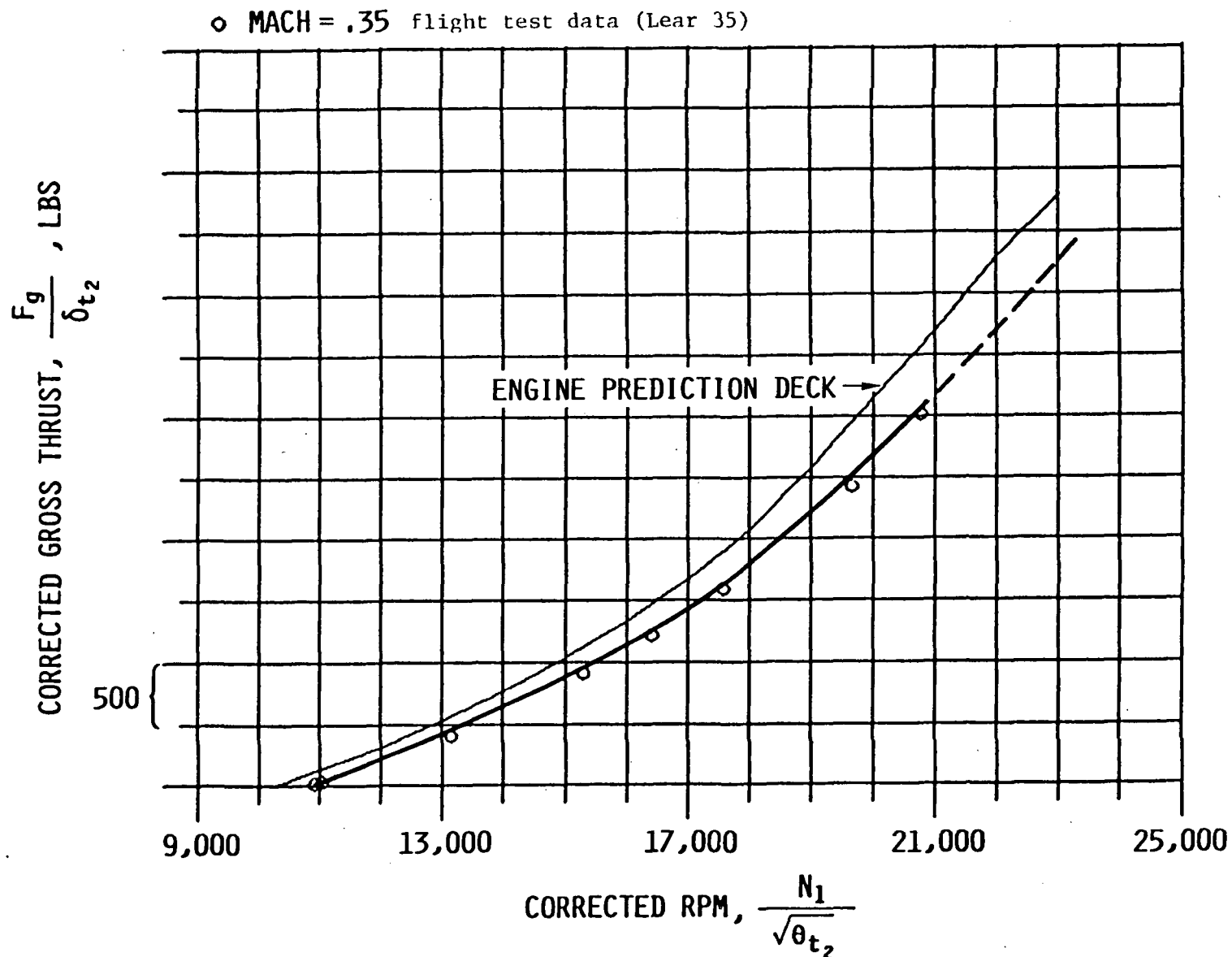


Figure H.2: Corrected Gross Thrust Characteristics, M = .35

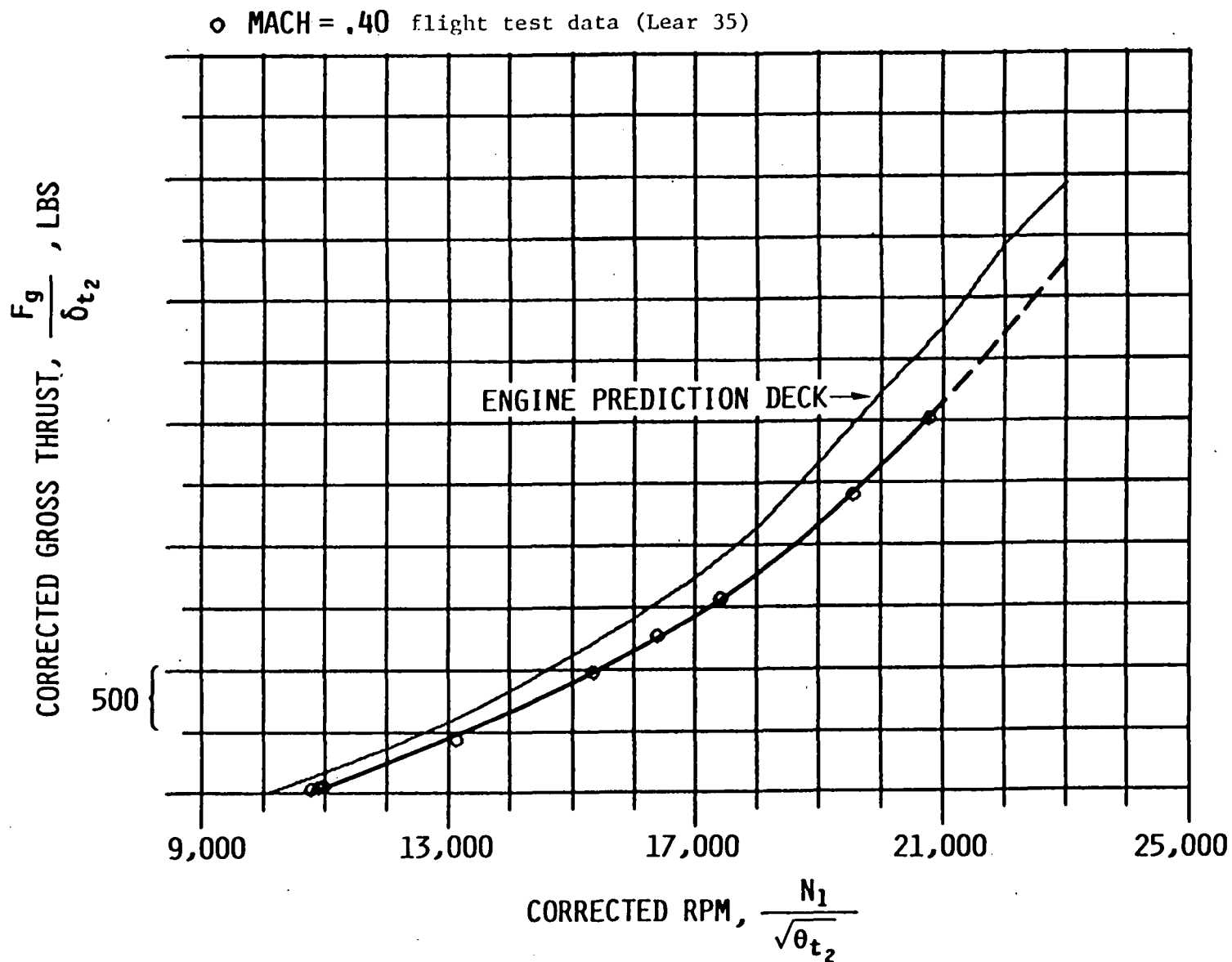


Figure II.3: Corrected Gross Thrust Characteristics, $M = .40$

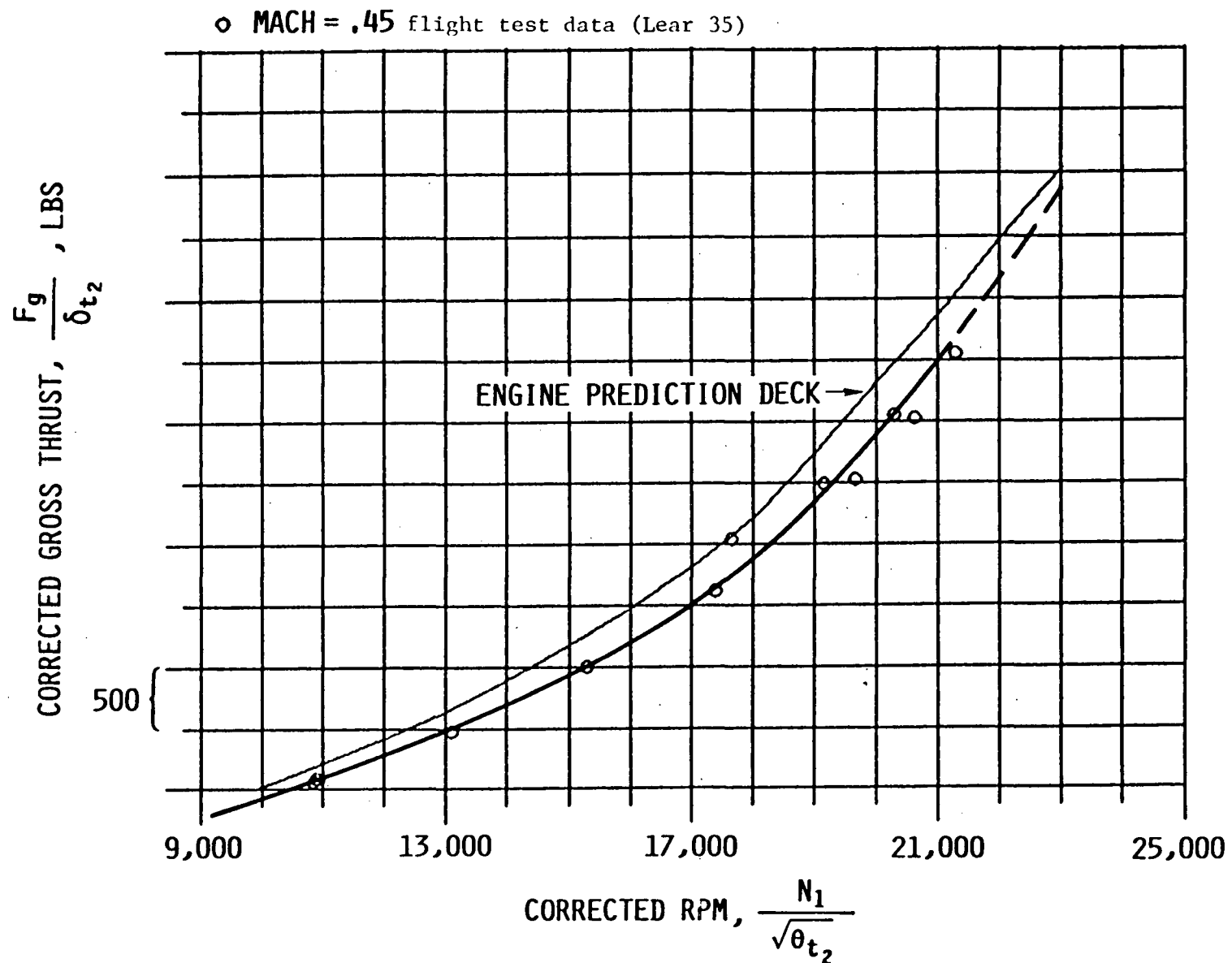


Figure H.4: Corrected Gross Thrust Characteristics, M = .45

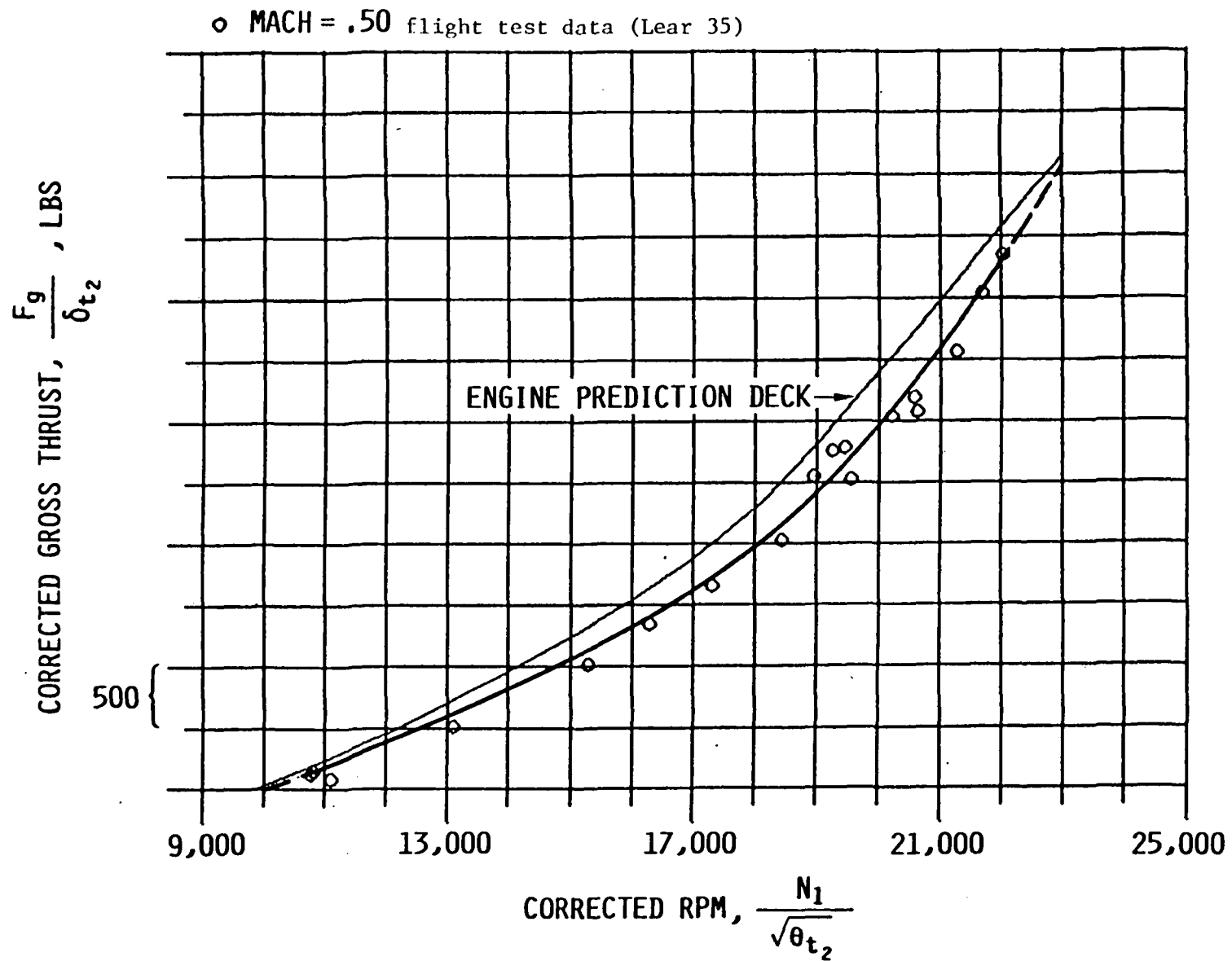


Figure H.5: Corrected Gross Thrust Characteristics, M = .50

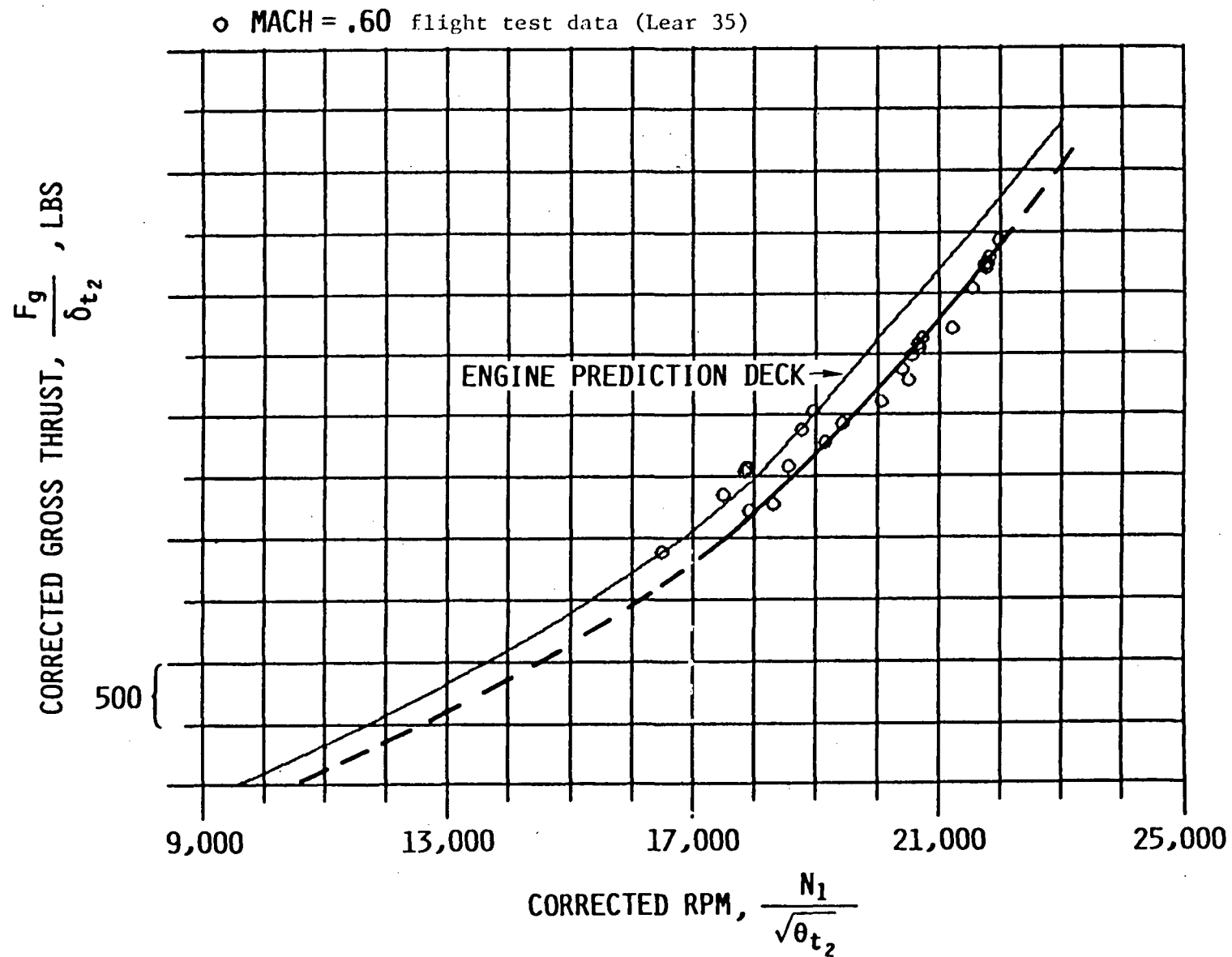


Figure H.6: Corrected Gross Thrust Characteristics, M = .60

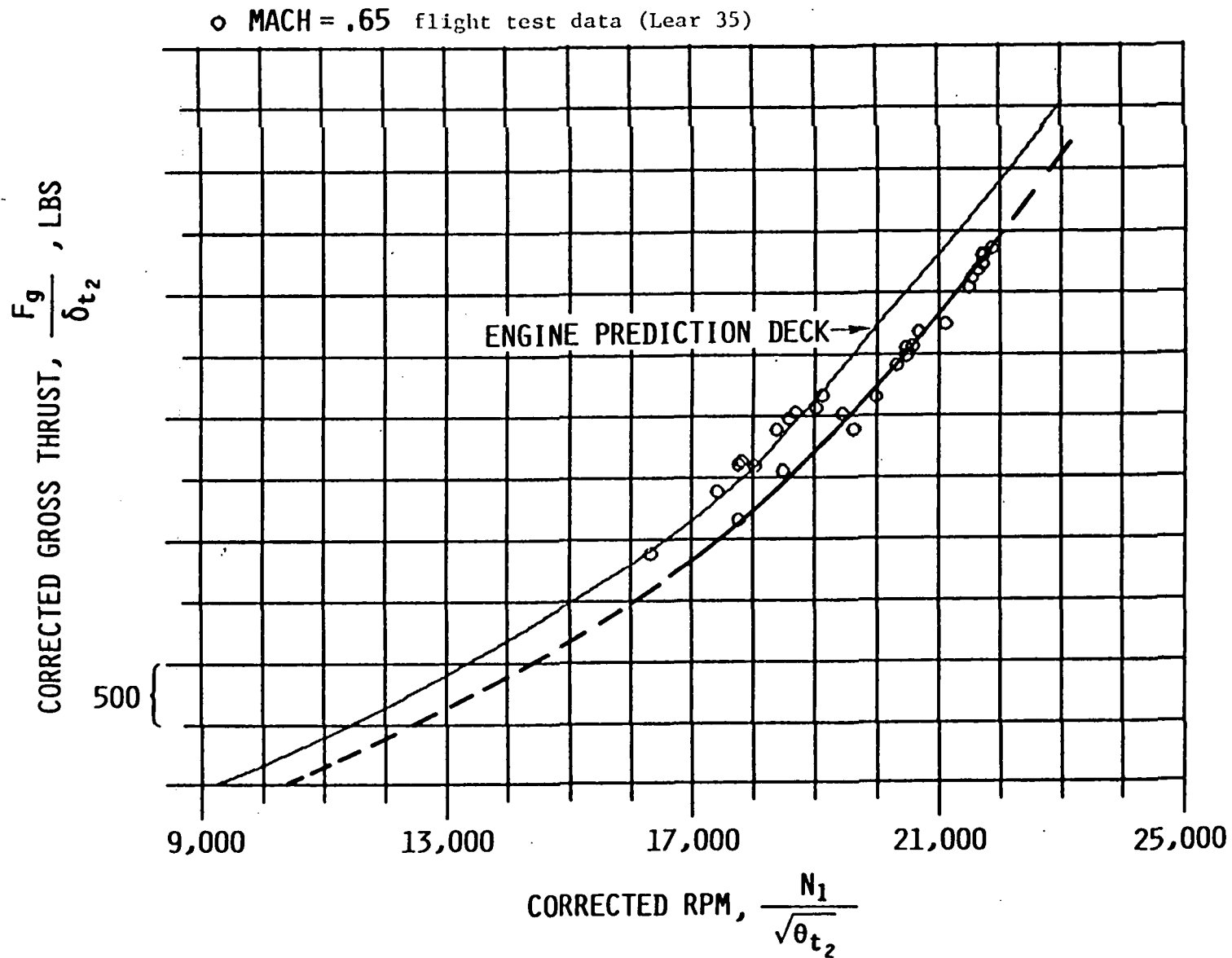


Figure H.7: Corrected Gross Thrust Characteristics, $M = .65$

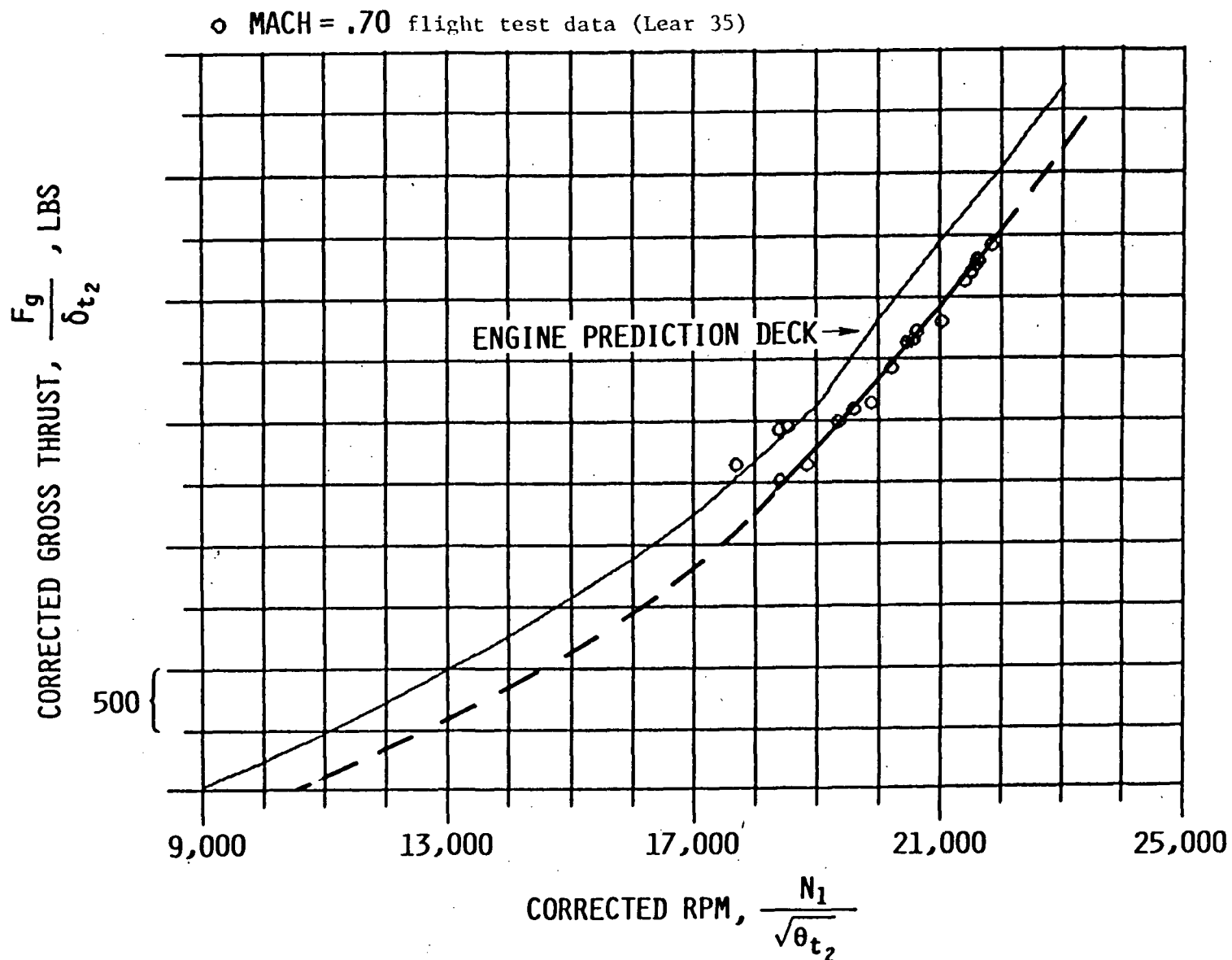


Figure 11.8: Corrected Gross Thrust Characteristics, M = .70

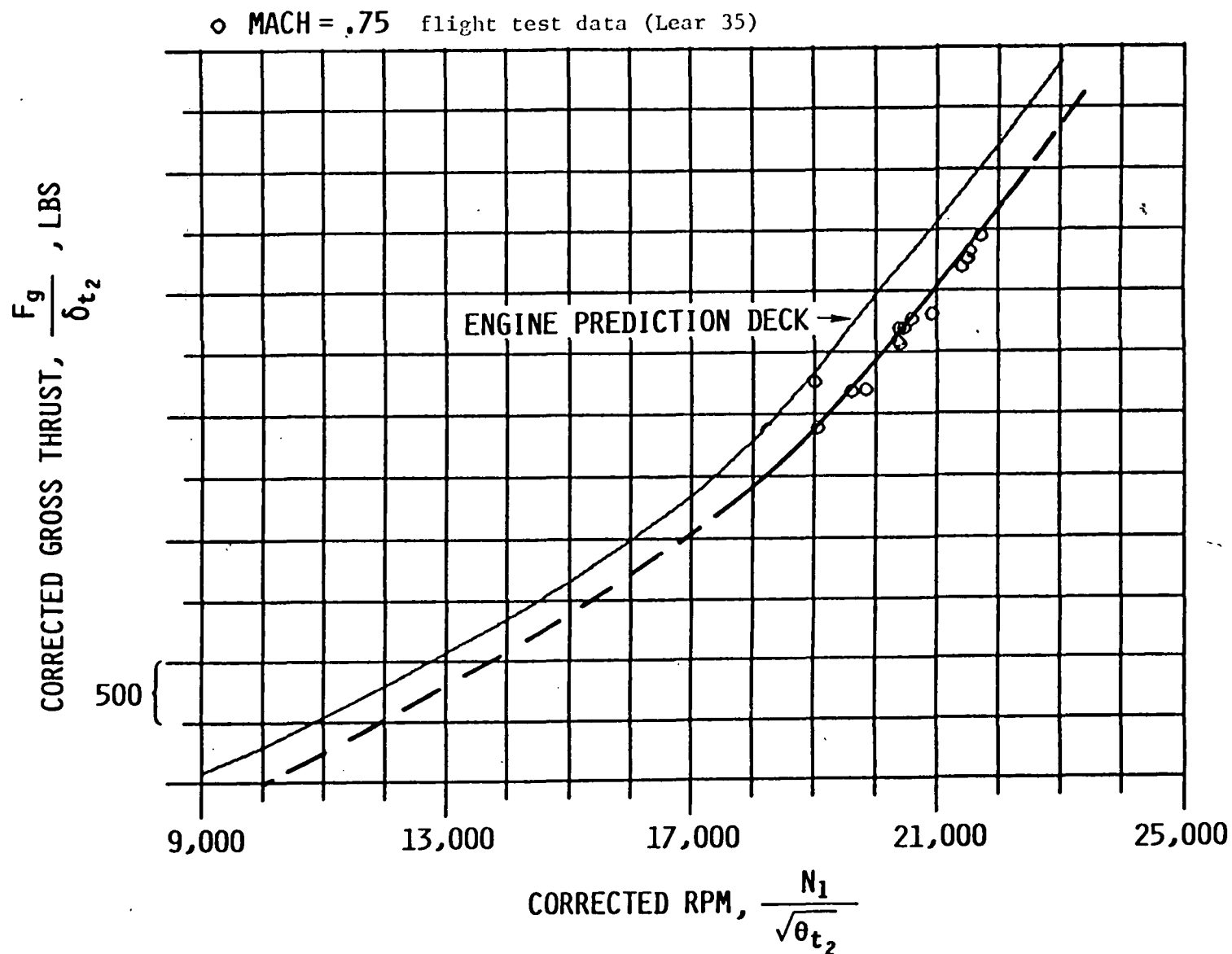


Figure II.9: Corrected Gross Thrust Characteristics, M = .75

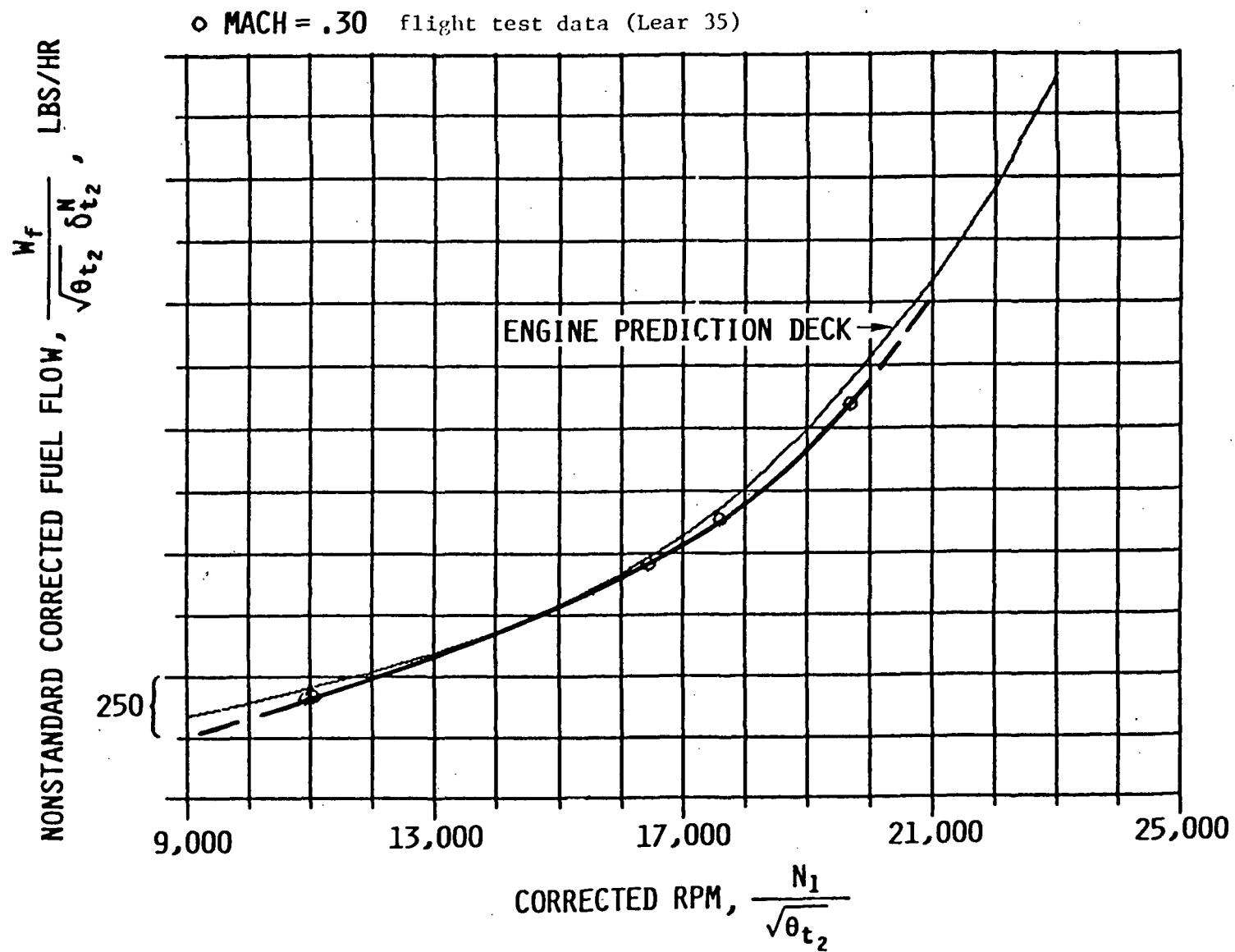


Figure H.10: Nonstandard Corrected Fuel Flow Characteristics, M = .30

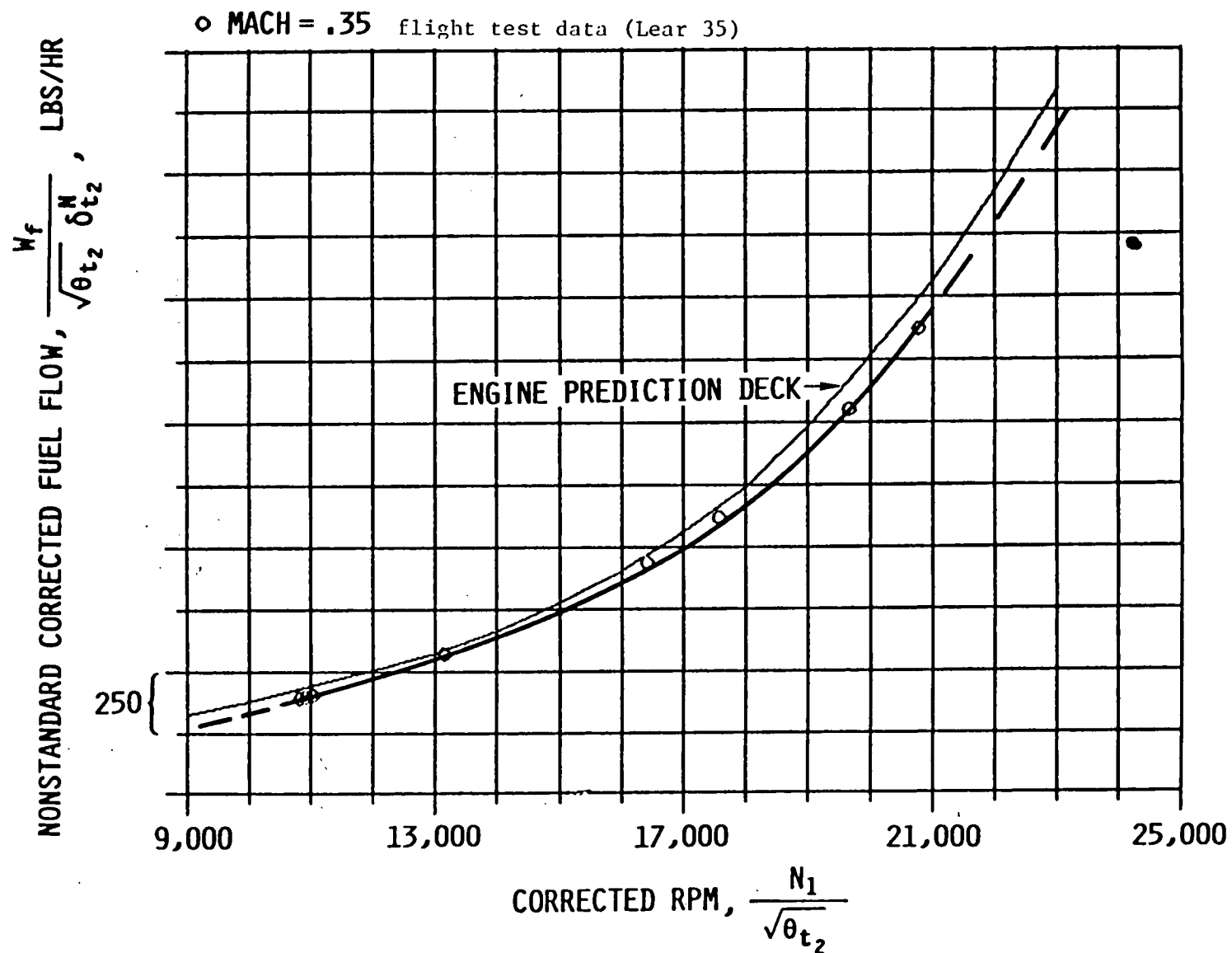


Figure H.11: Nonstandard Corrected Fuel Flow Characteristics, M = .35

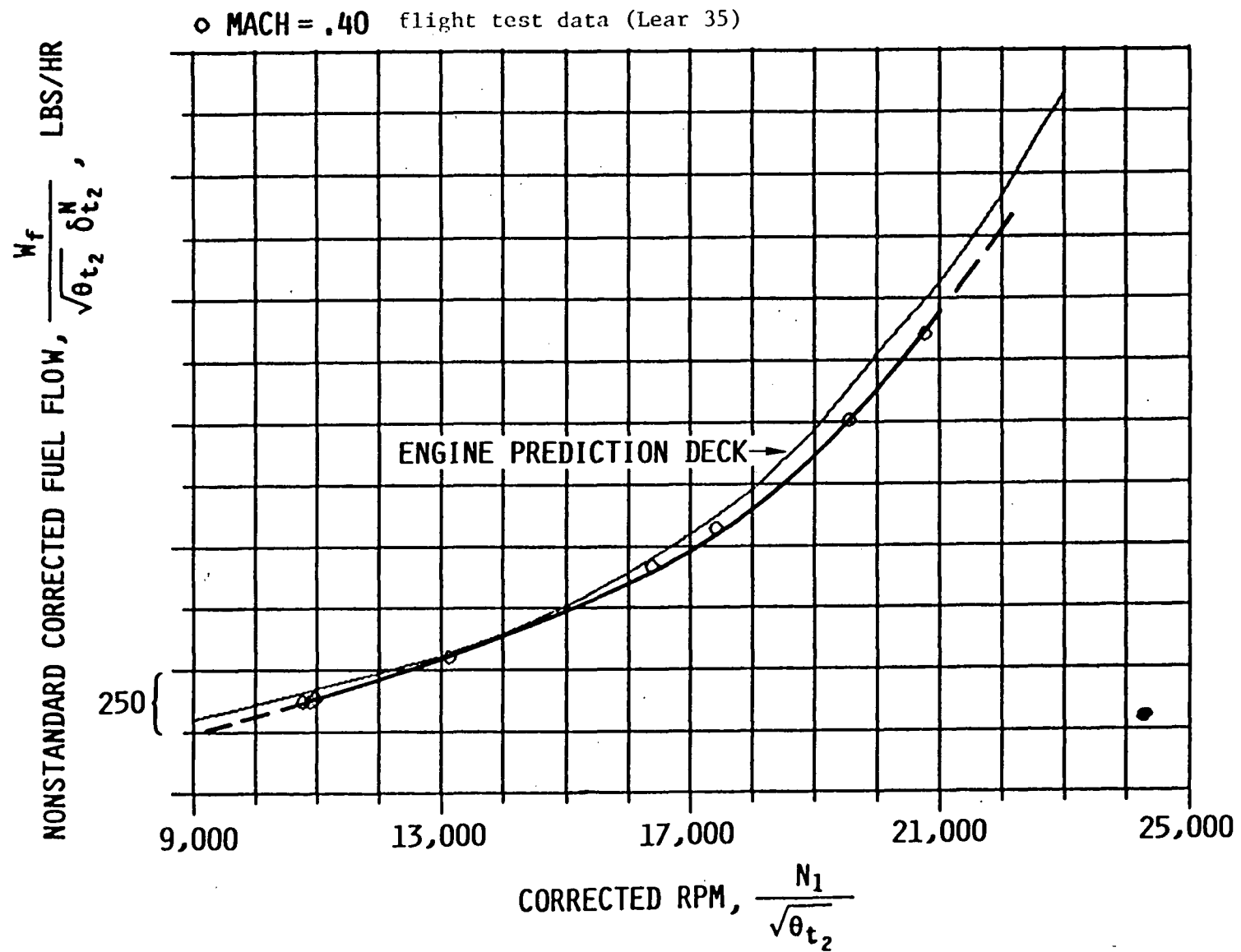


Figure H.12: Nonstandard Corrected Fuel Flow Characteristics, M = .40

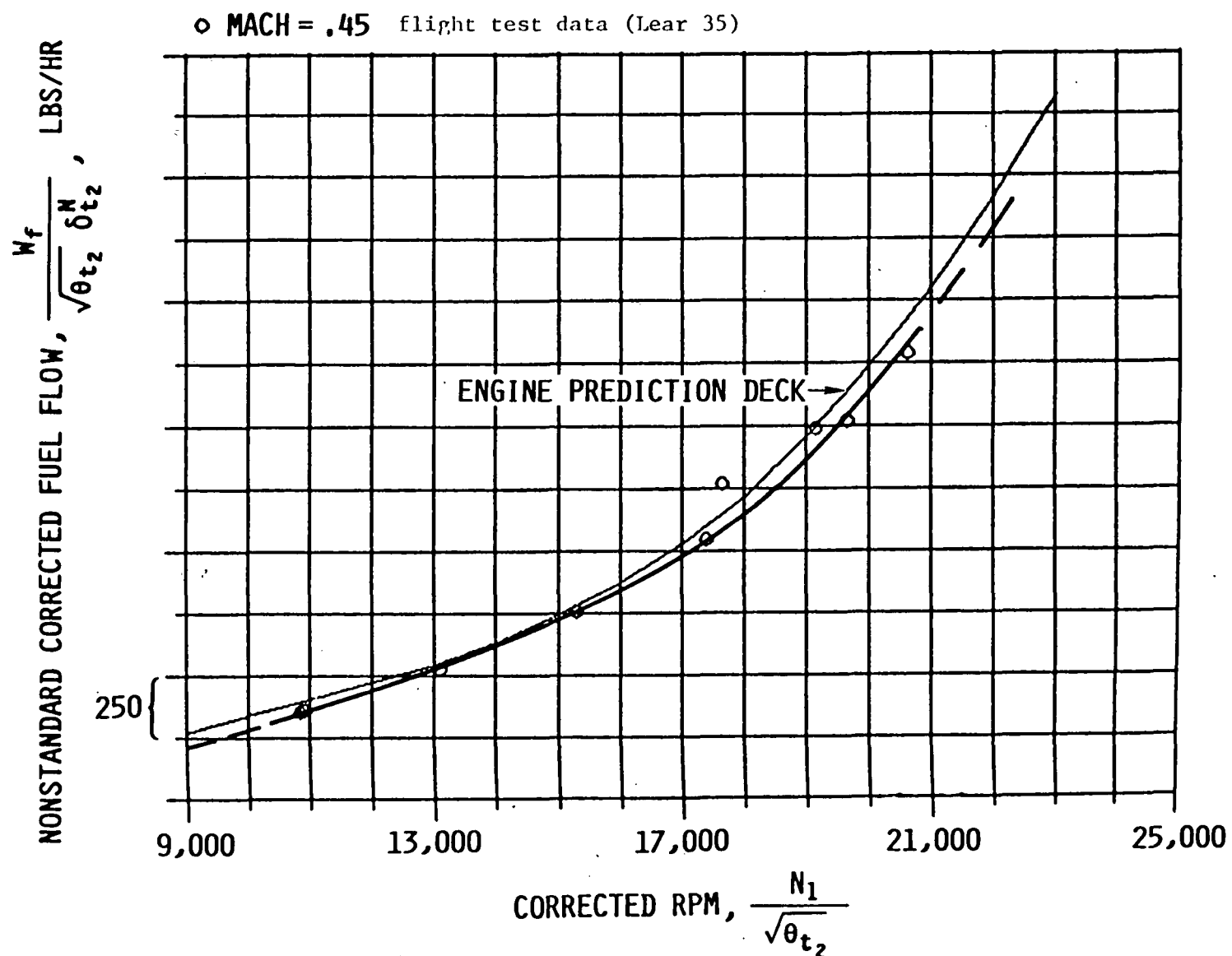


Figure H.13: Nonstandard Corrected Fuel Flow Characteristics, M = .45

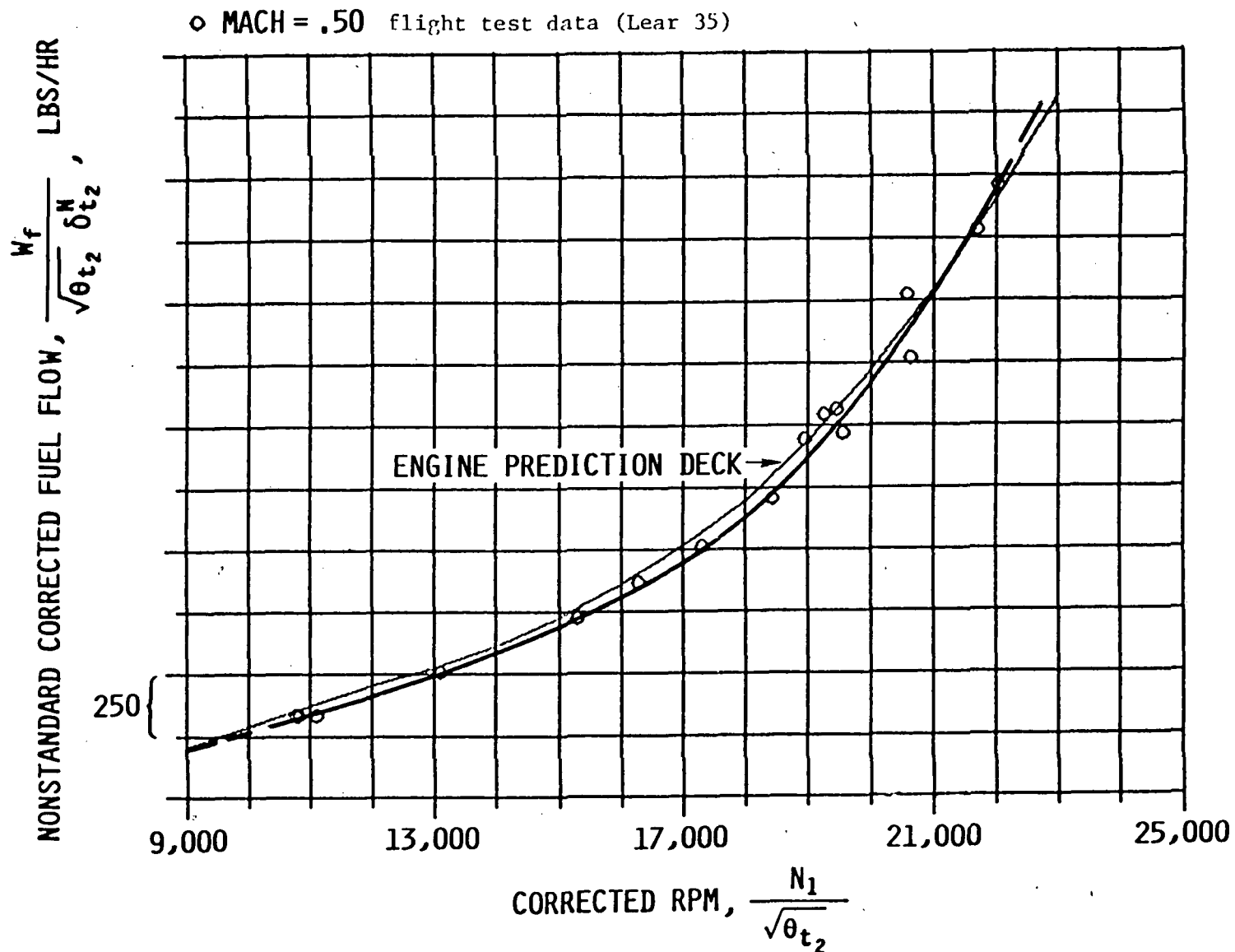


Figure H.14: Nonstandard Corrected Fuel Flow Characteristics, M = .50

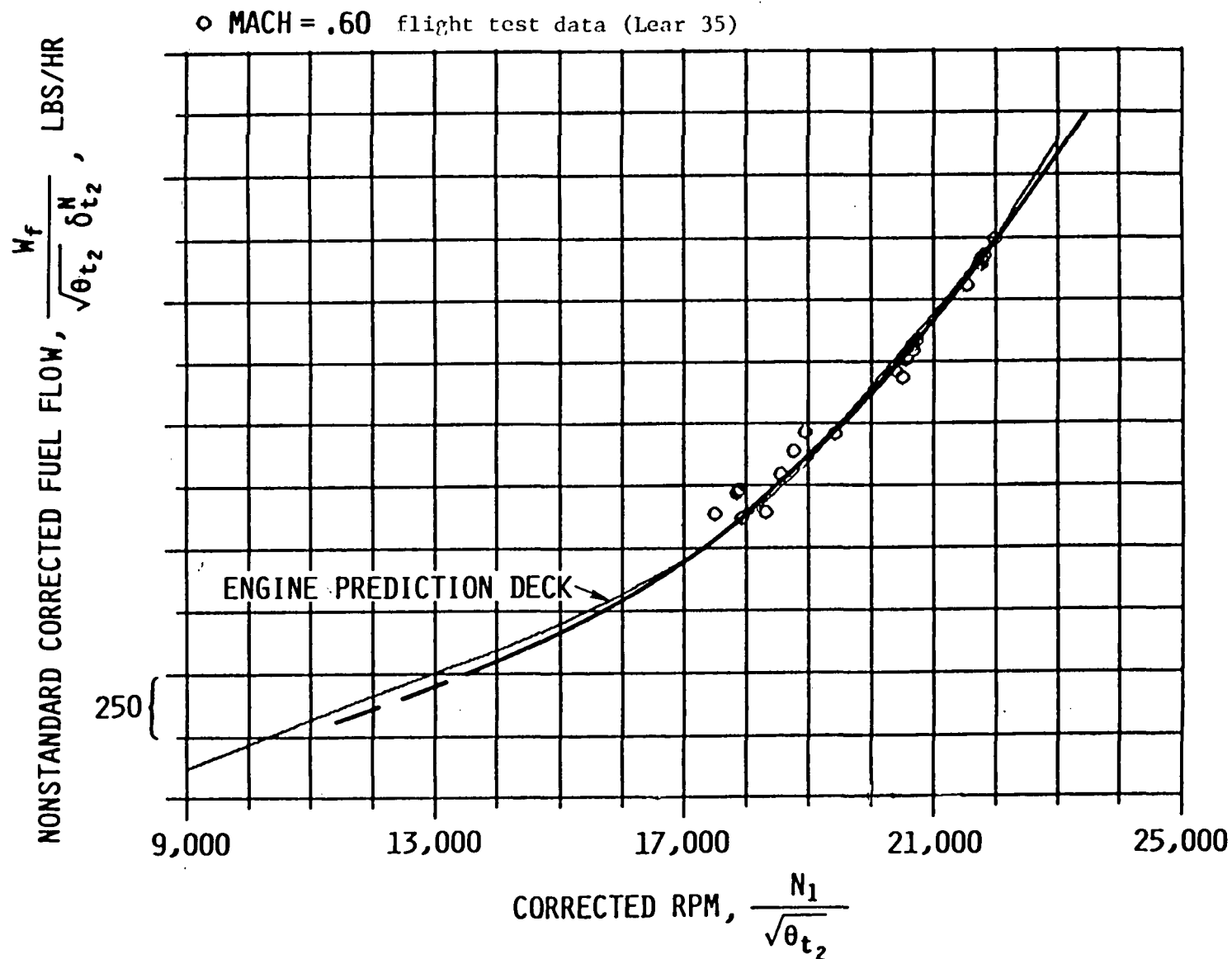


Figure H.15: Nonstandard Corrected Fuel Flow Characteristics, M = .60

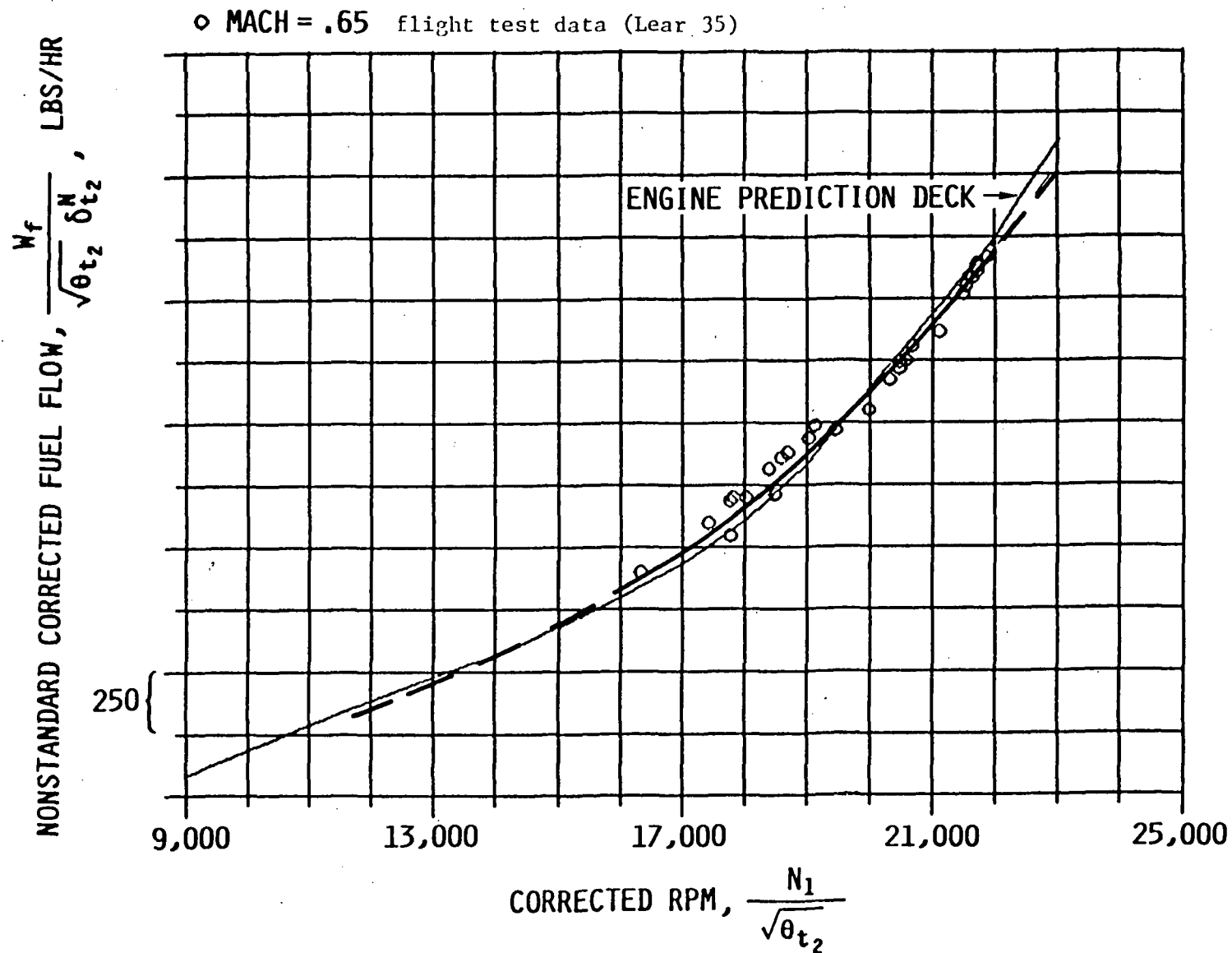


Figure H.16: Nonstandard Corrected Fuel Flow Characteristics, M = .65

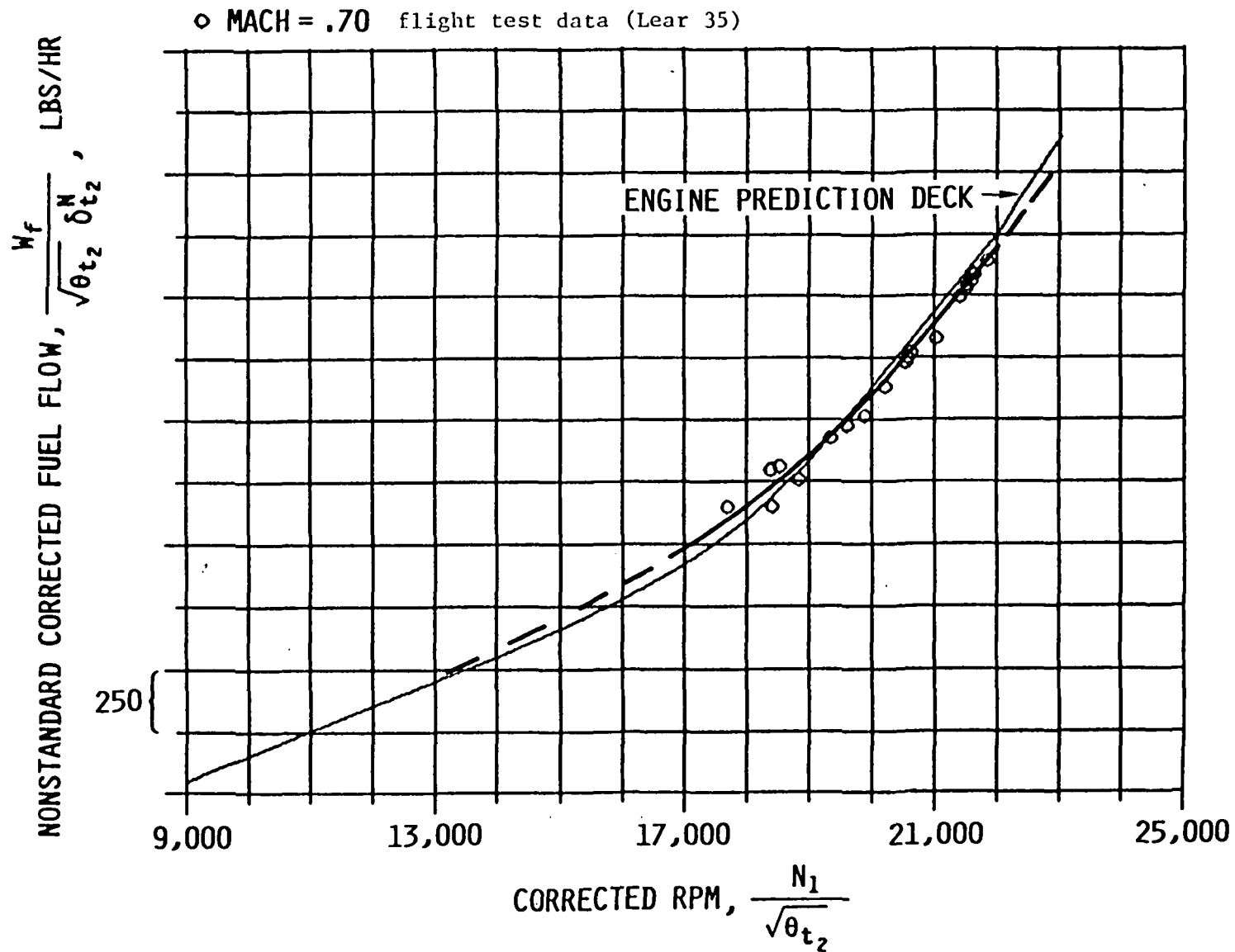


Figure H.17: Nonstandard Corrected Fuel Flow Characteristics, M = .70

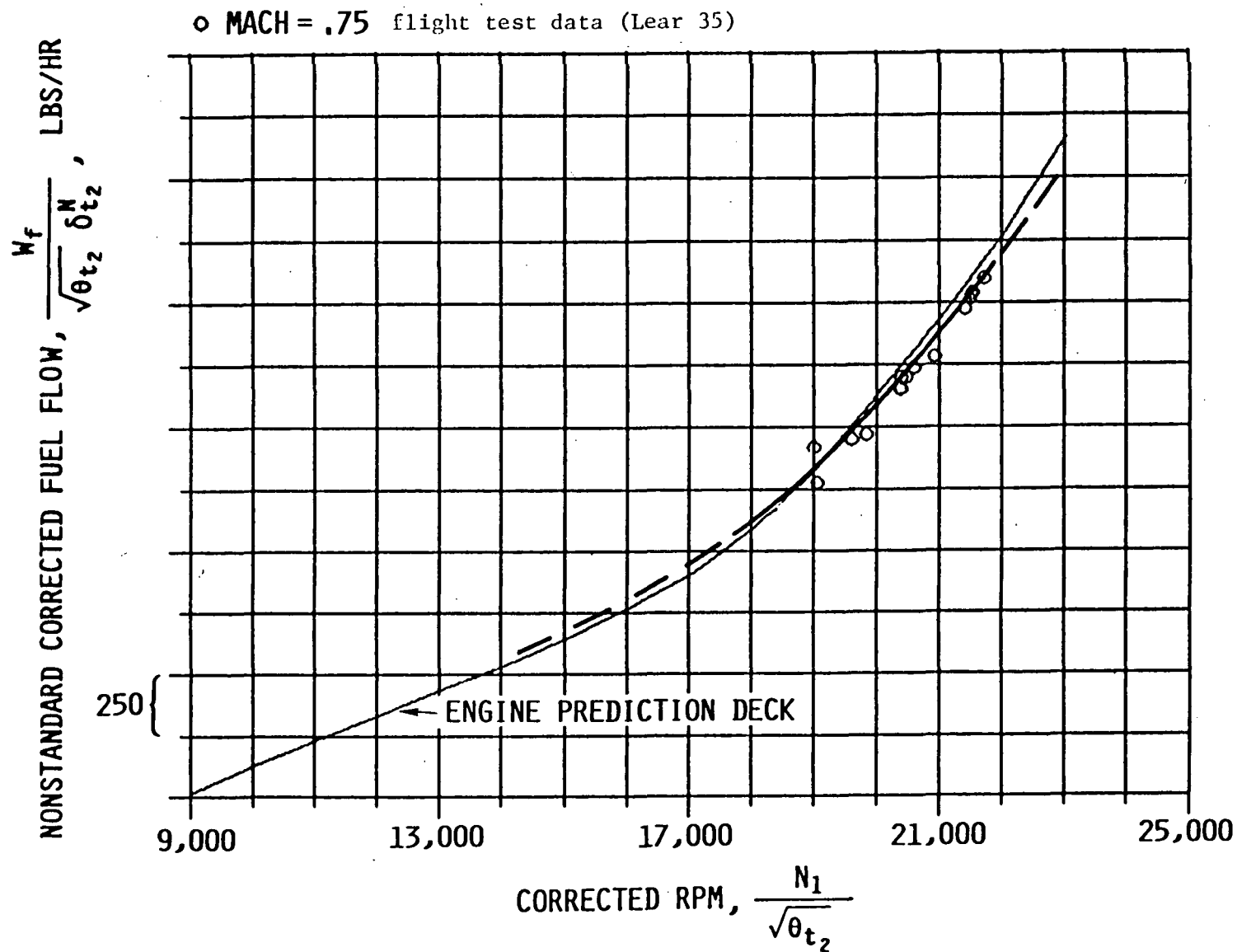


Figure H.18: Nonstandard Corrected Fuel Flow Characteristics, M = .75

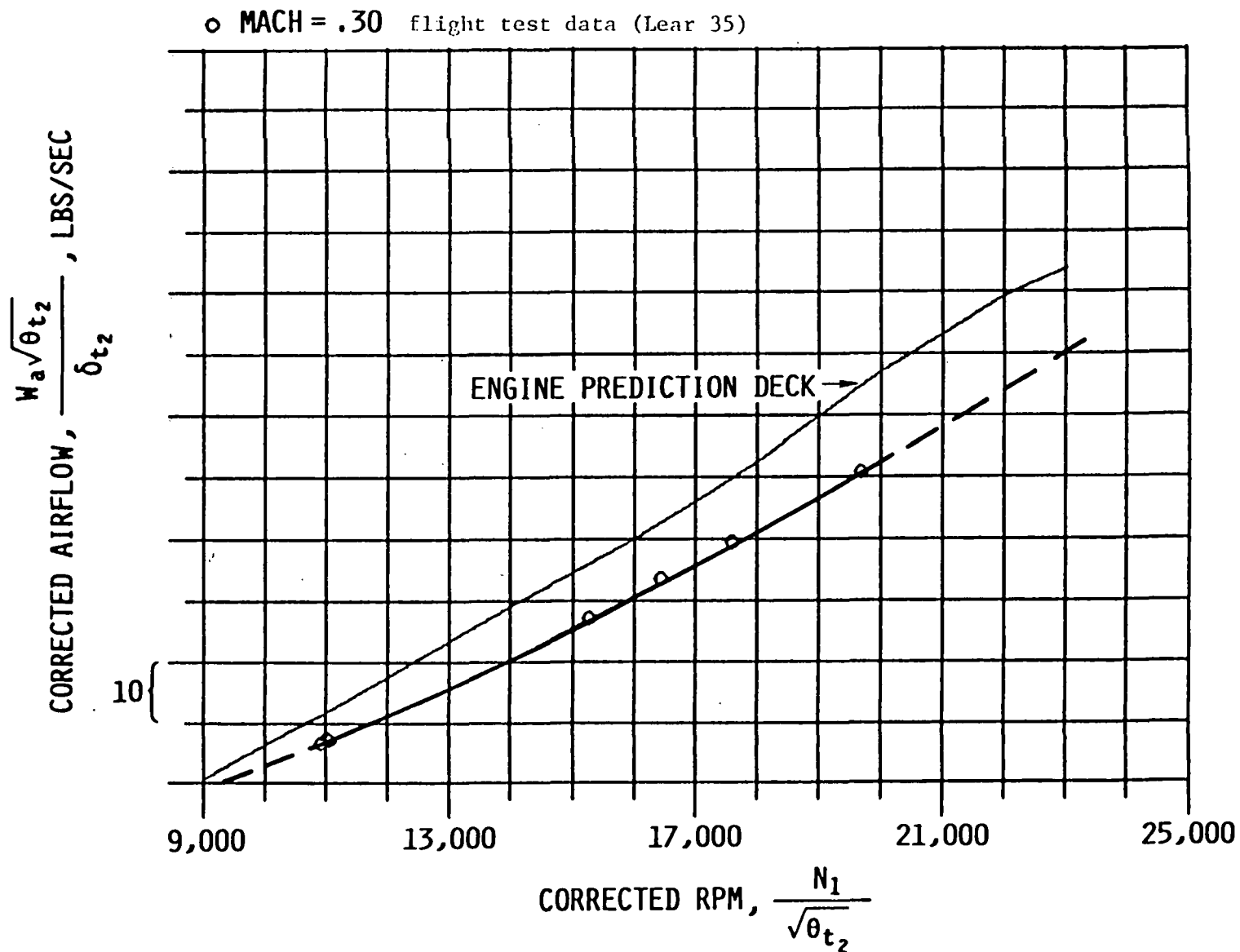


Figure H.19: Corrected Airflow Characteristics, M = .30

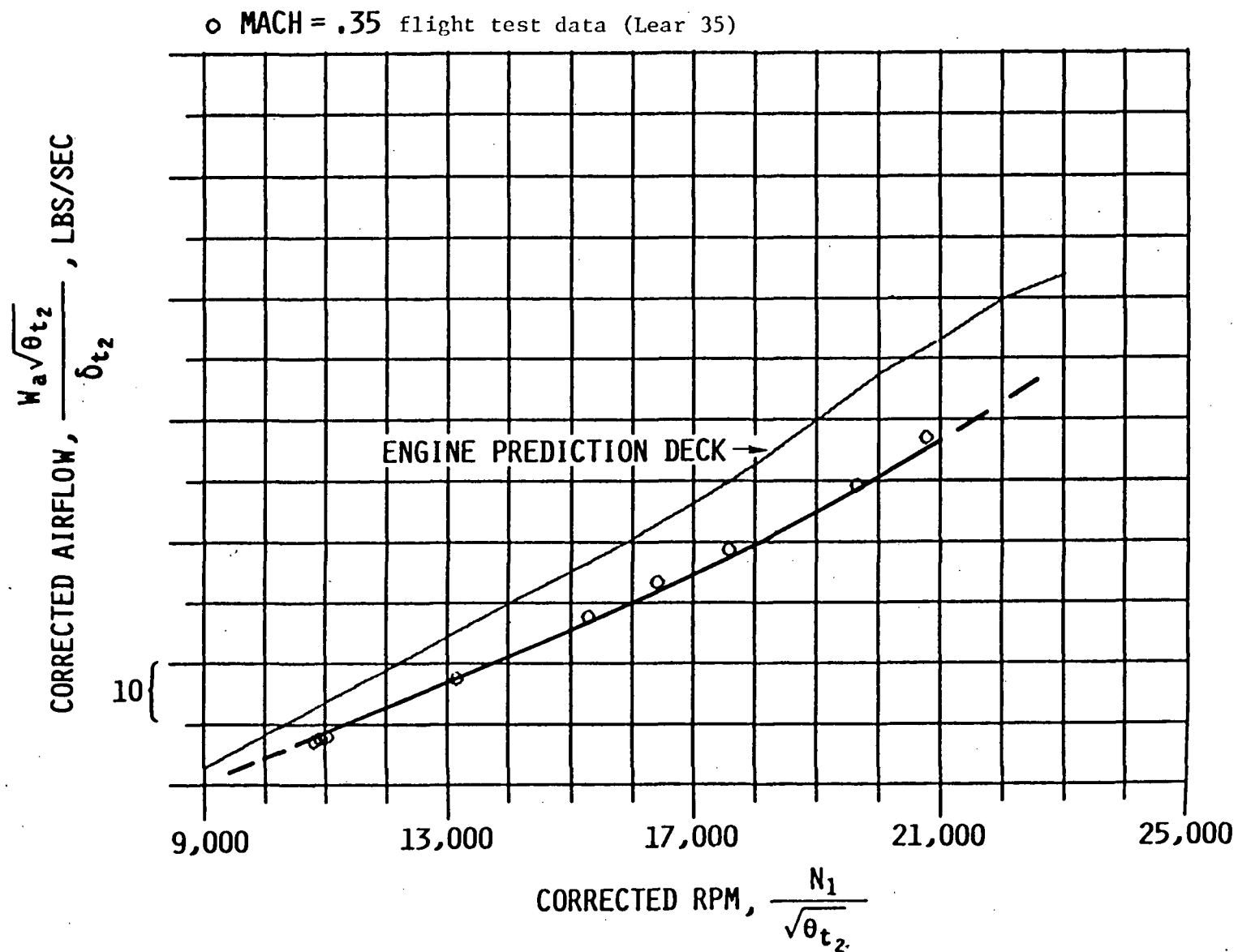


Figure H.20: Corrected Airflow Characteristics, M = .35

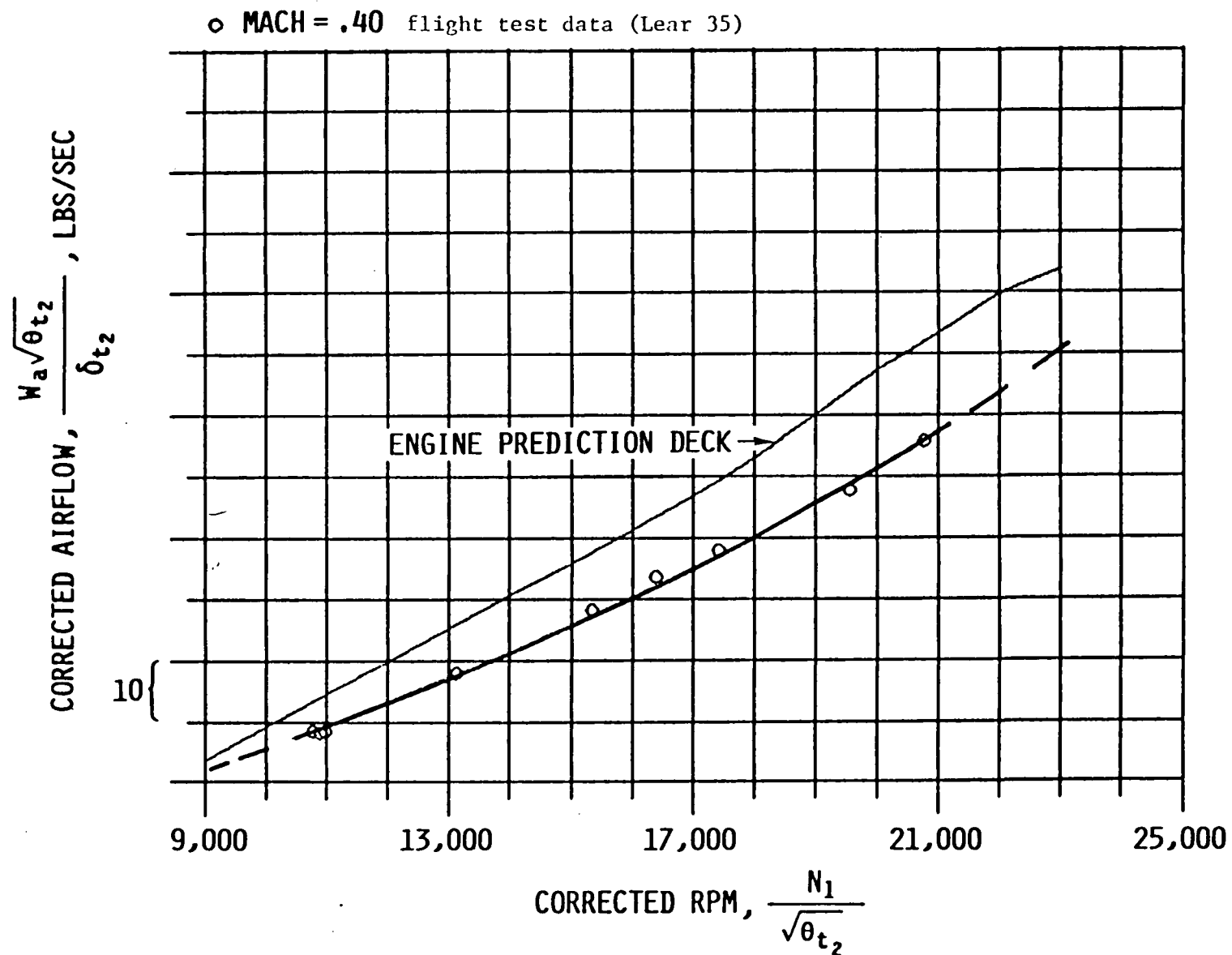


Figure H.21: Corrected Airflow Characteristics, M = .40

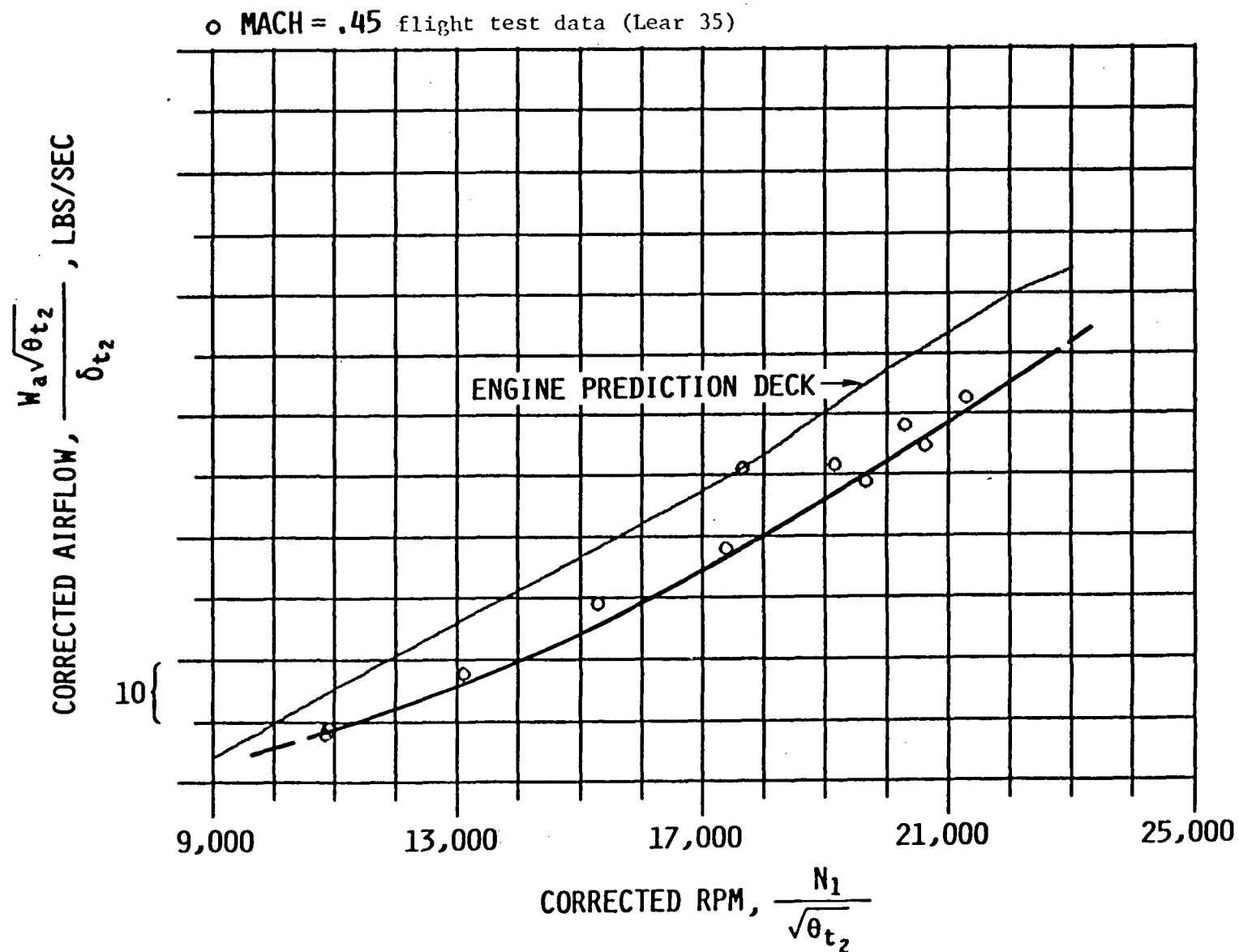


Figure H.22: Corrected Airflow Characteristics, M = .45

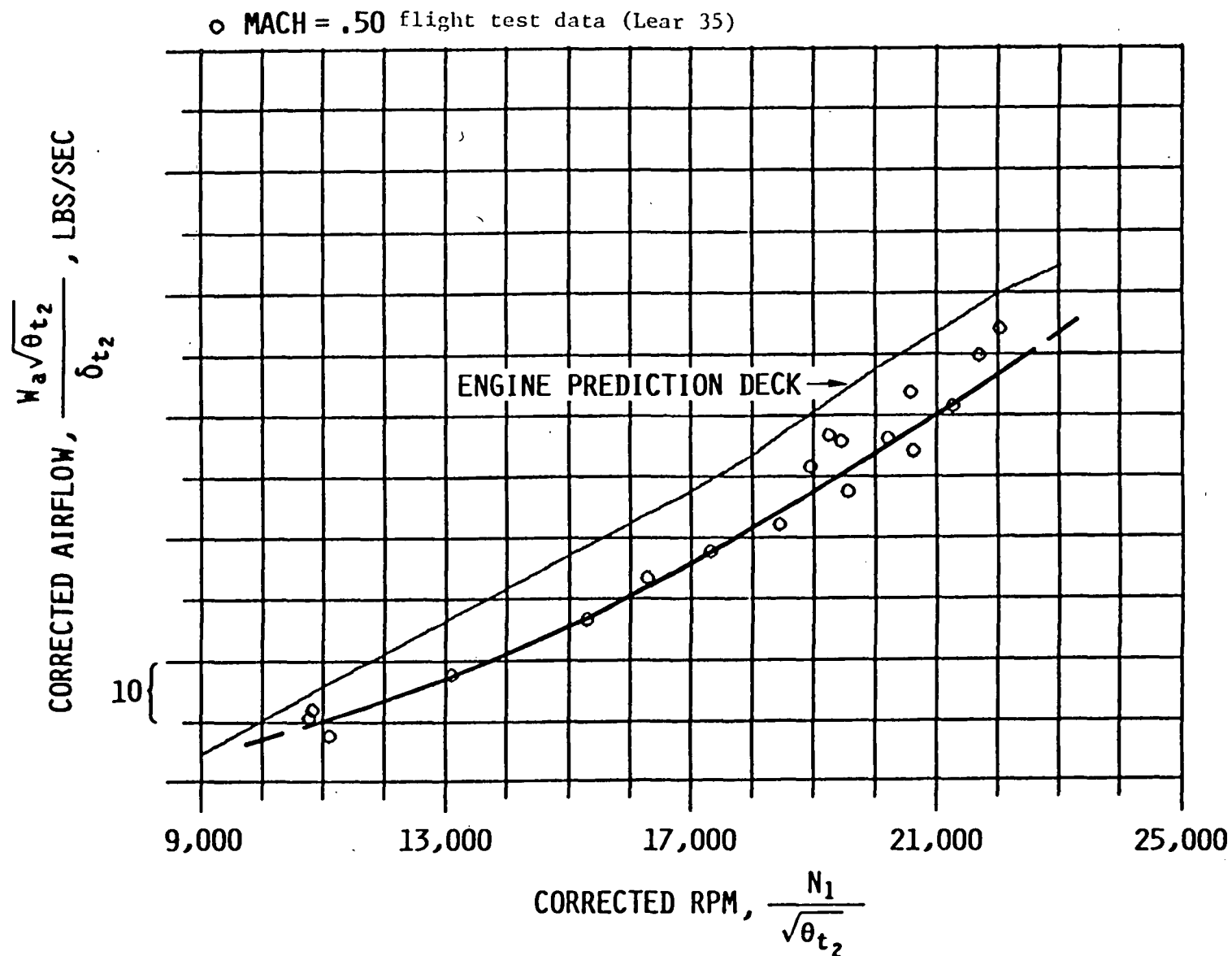


Figure H.23: Corrected Airflow Characteristics, M = .50

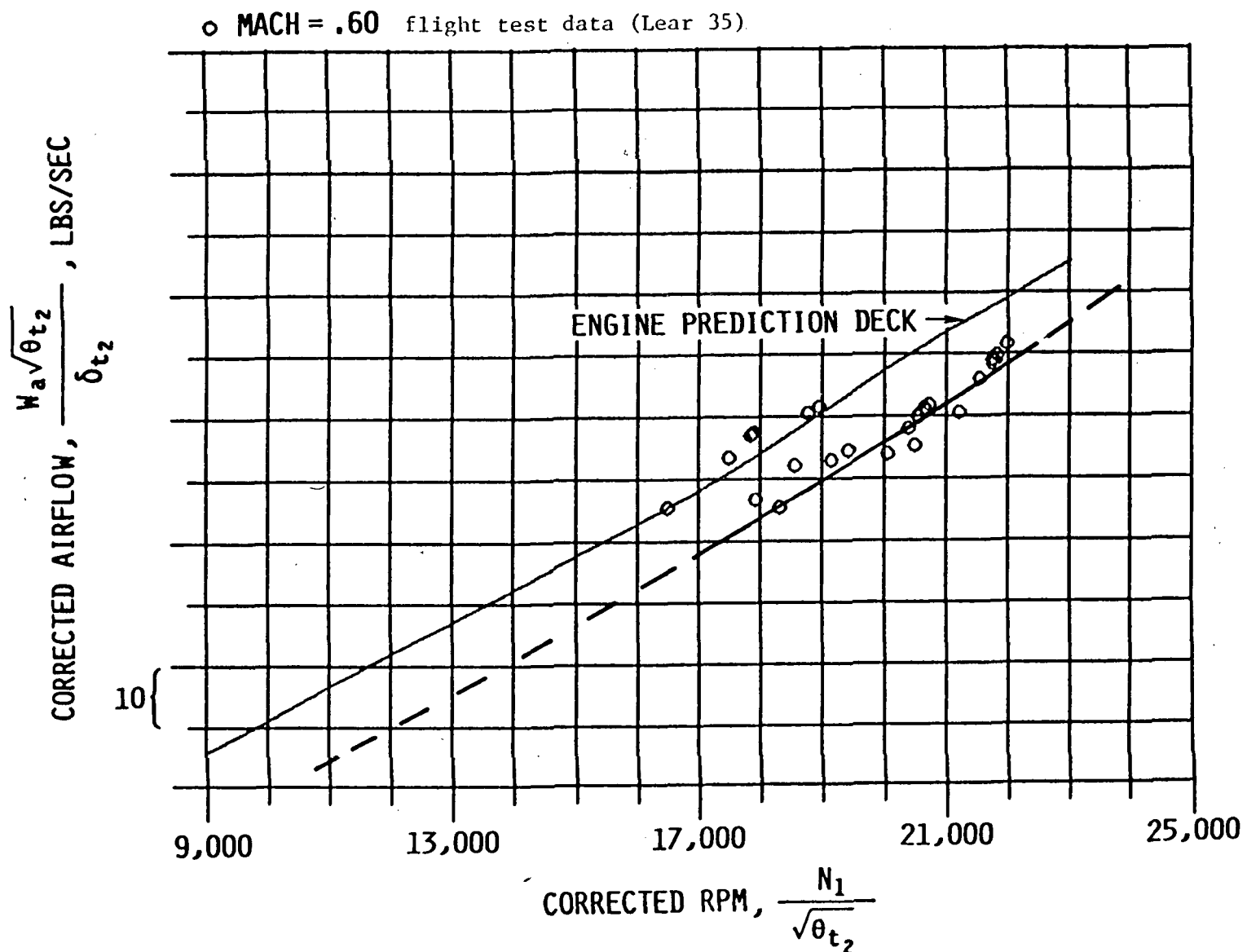


Figure H.24: Corrected Airflow Characteristics, M = .60

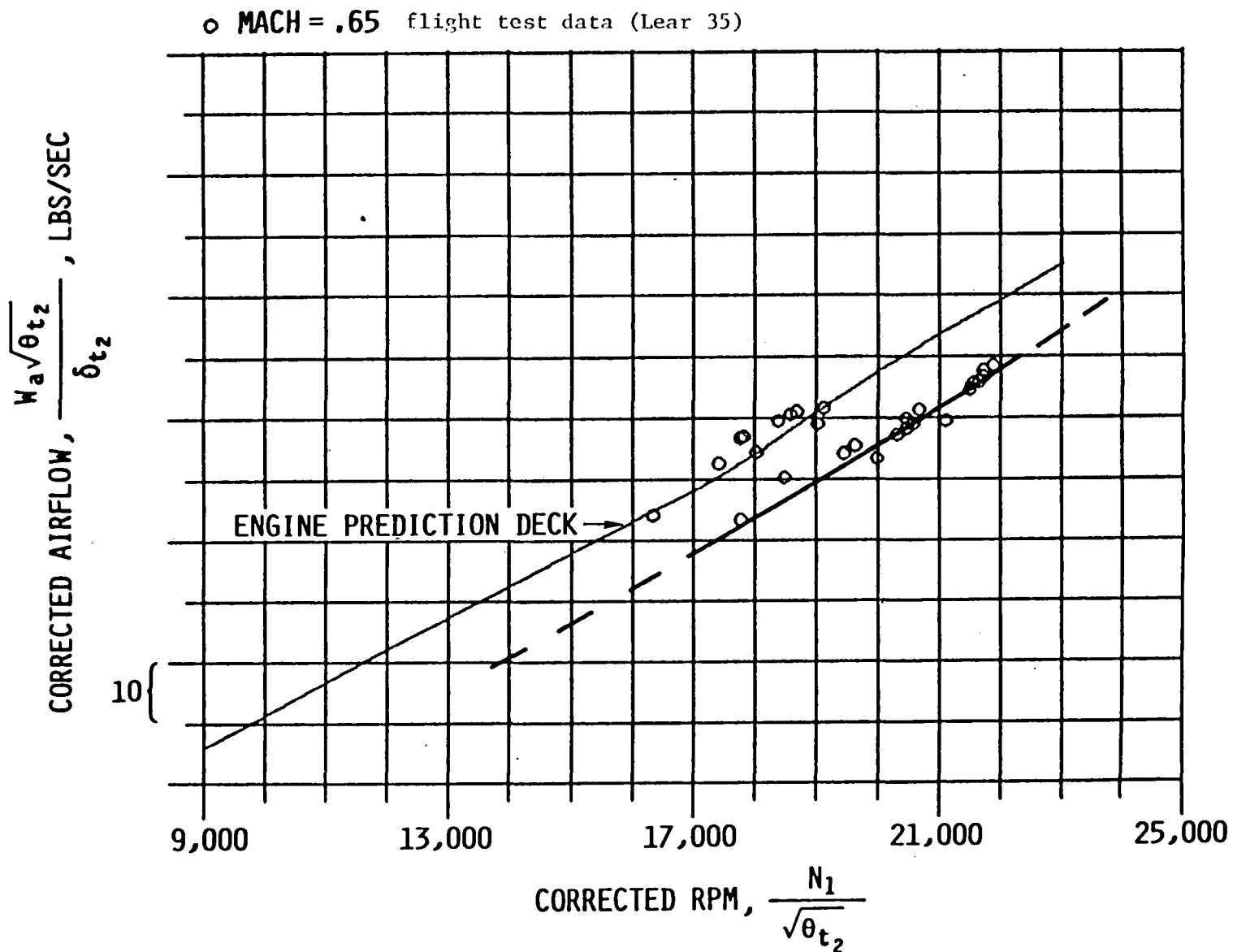


Figure H.25: Corrected Airflow Characteristics, M = .65

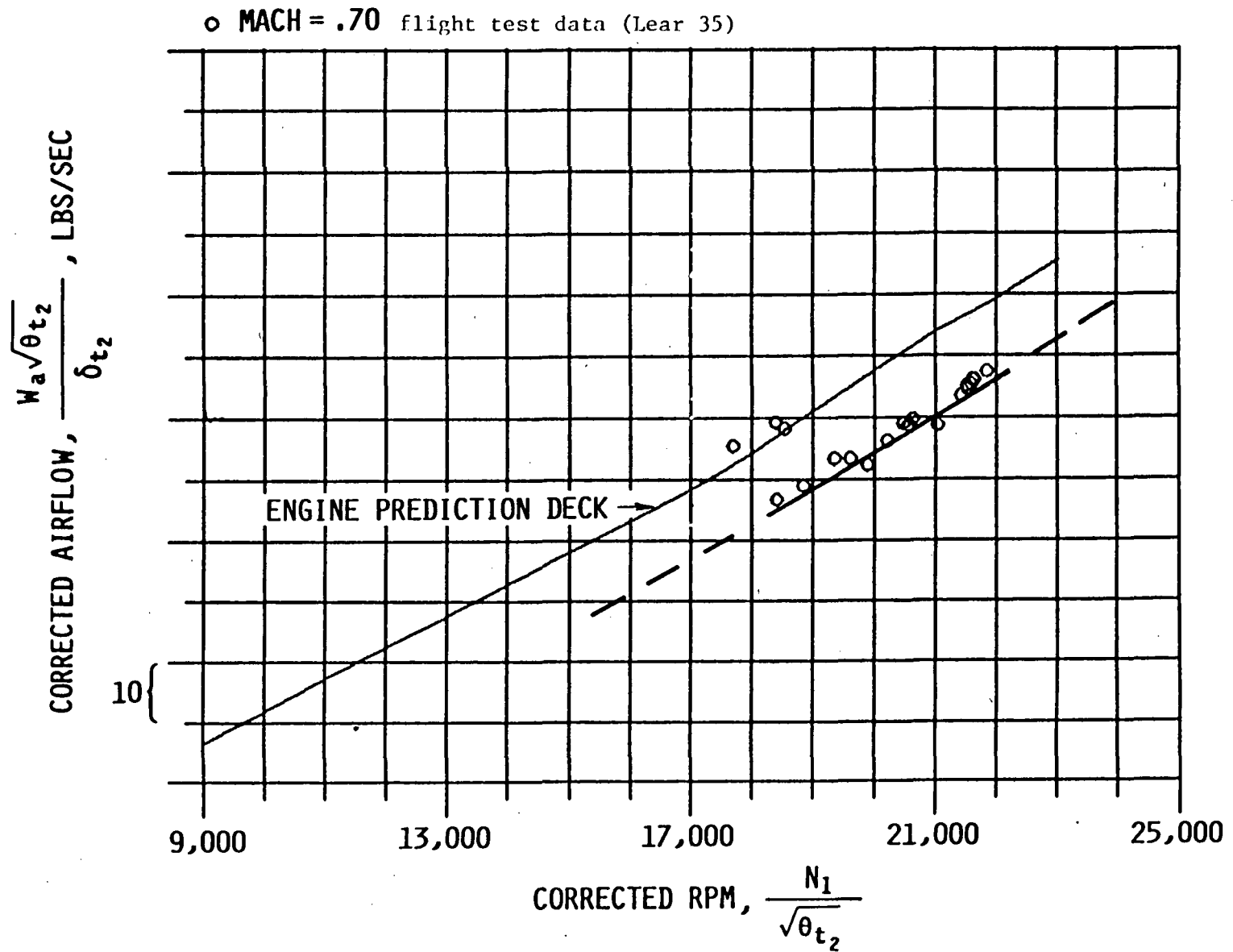


Figure H.26: Corrected Airflow Characteristics, M = .70

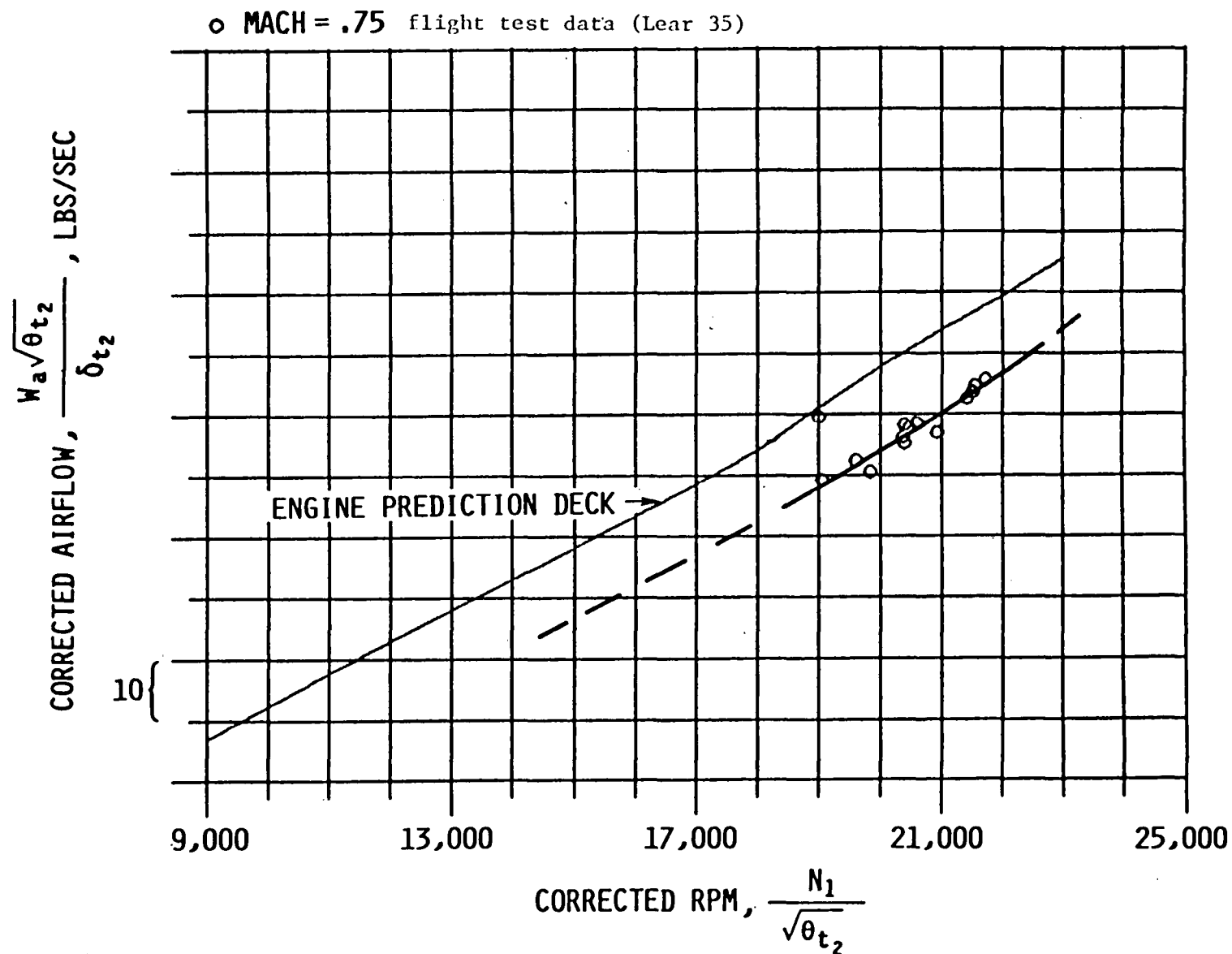


Figure H.27: Corrected Airflow Characteristics, M = .75

APPENDIX I
FLIGHT TRAJECTORY
PREDICTIONS

APPENDIX I SUMMARY

<u>Figure No.</u>	<u>Title</u>
I.1	MODEL Time Prediction, Profile 4
I.2	MODEL Fuel Used Prediction, Profile 4
I.3	MODEL P_S Prediction, Profile 4
I.4	MODEL Time Prediction, Profile 5
I.5	MODEL Fuel Used Prediction, Profile 5
I.6	MODEL P_S Prediction, Profile 5
I.7	MODEL Time Prediction, Profile 8
I.8	MODEL Fuel Used Prediction, Profile 8
I.9	MODEL P_S Prediction, Profile 8
I.10	MODEL Time Prediction, Profile 9
I.11	MODEL Fuel Used Prediction, Profile 9
I.12	MODEL P_S Prediction, Profile 9
I.13	MODEL Time Prediction, Profile 10
I.14	MODEL Fuel Used Prediction, Profile 10
I.15	MODEL P_S Prediction, Profile 10

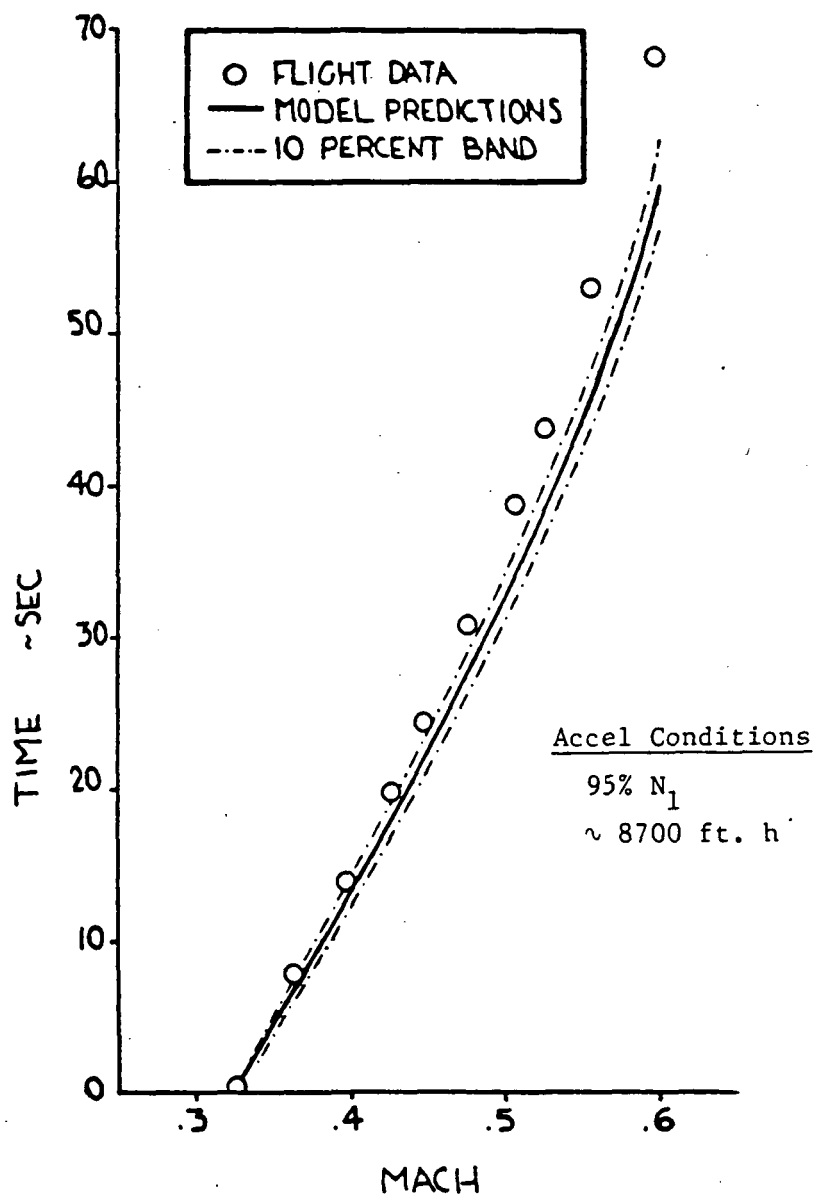


Figure I.1: MODEL Time Prediction, Profile 4

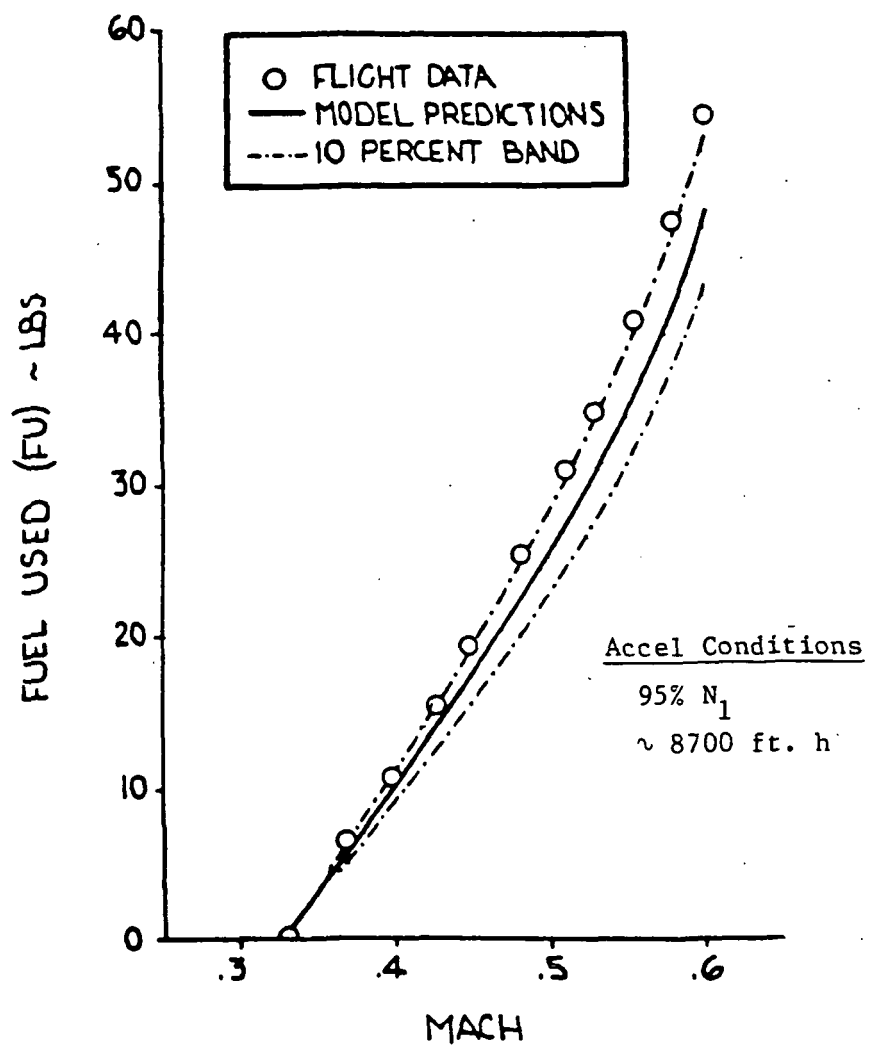


Figure I.2: MODEL Fuel Used Prediction, Profile 4

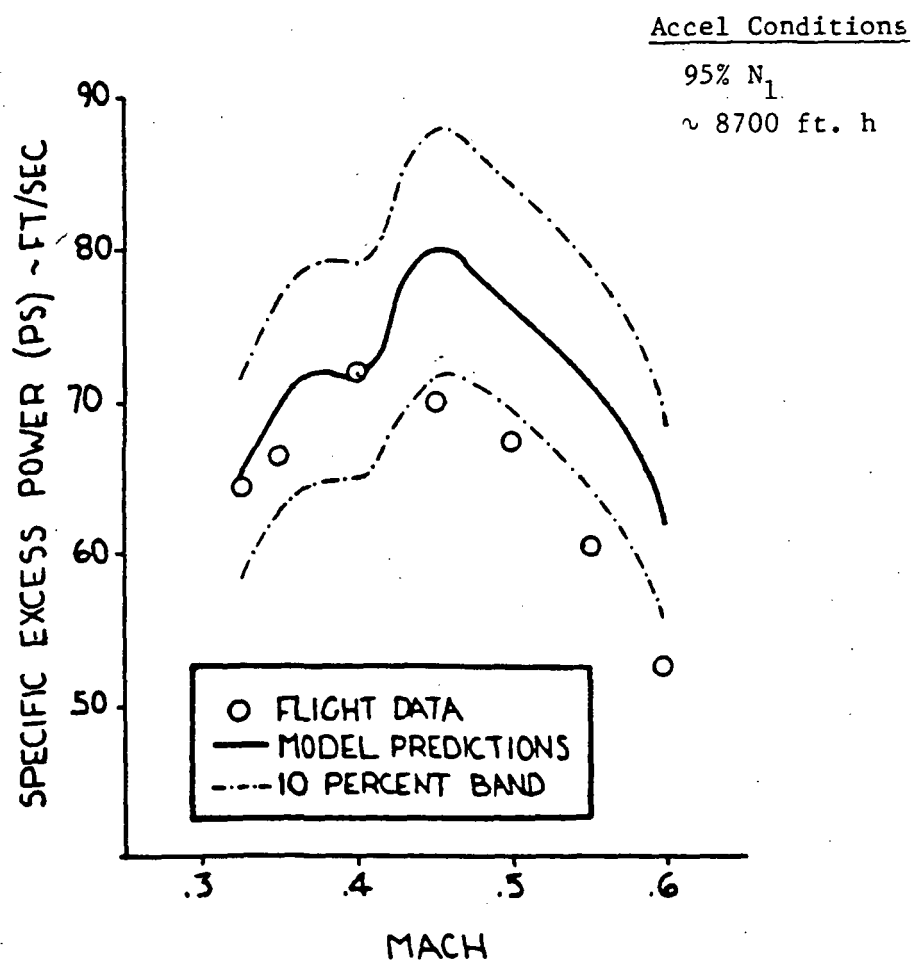


Figure I.3: MODEL P_S Prediction, Profile 4

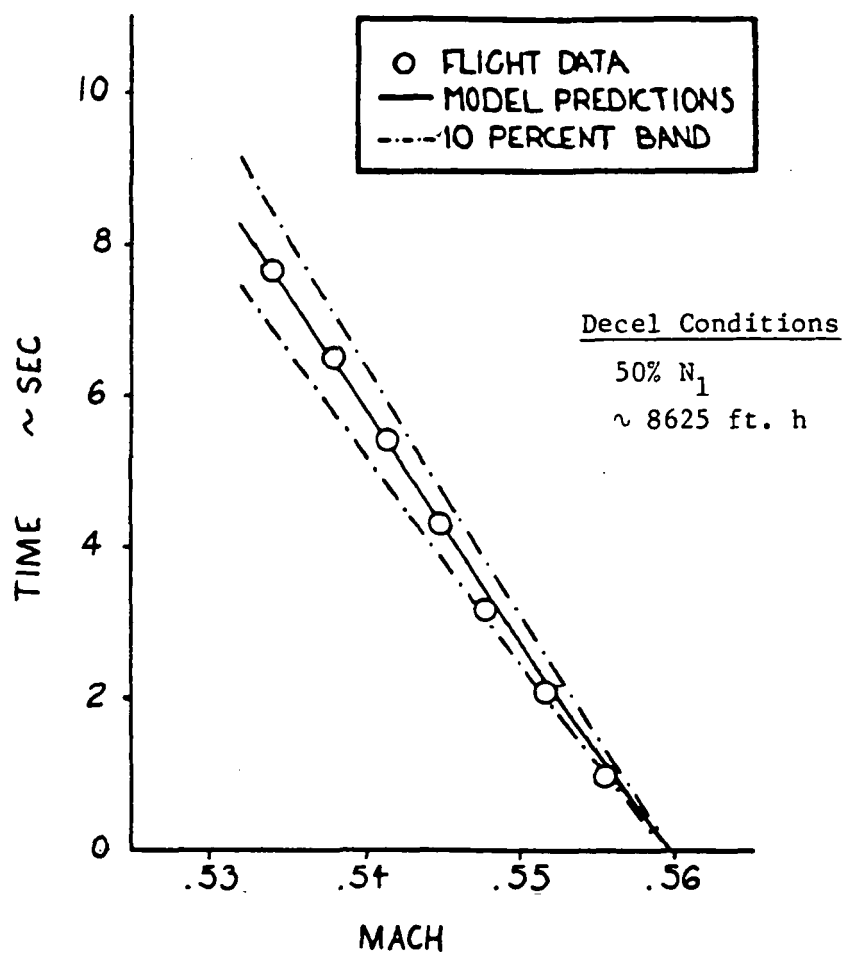


Figure I.4: MODEL Time Prediction, Profile 5

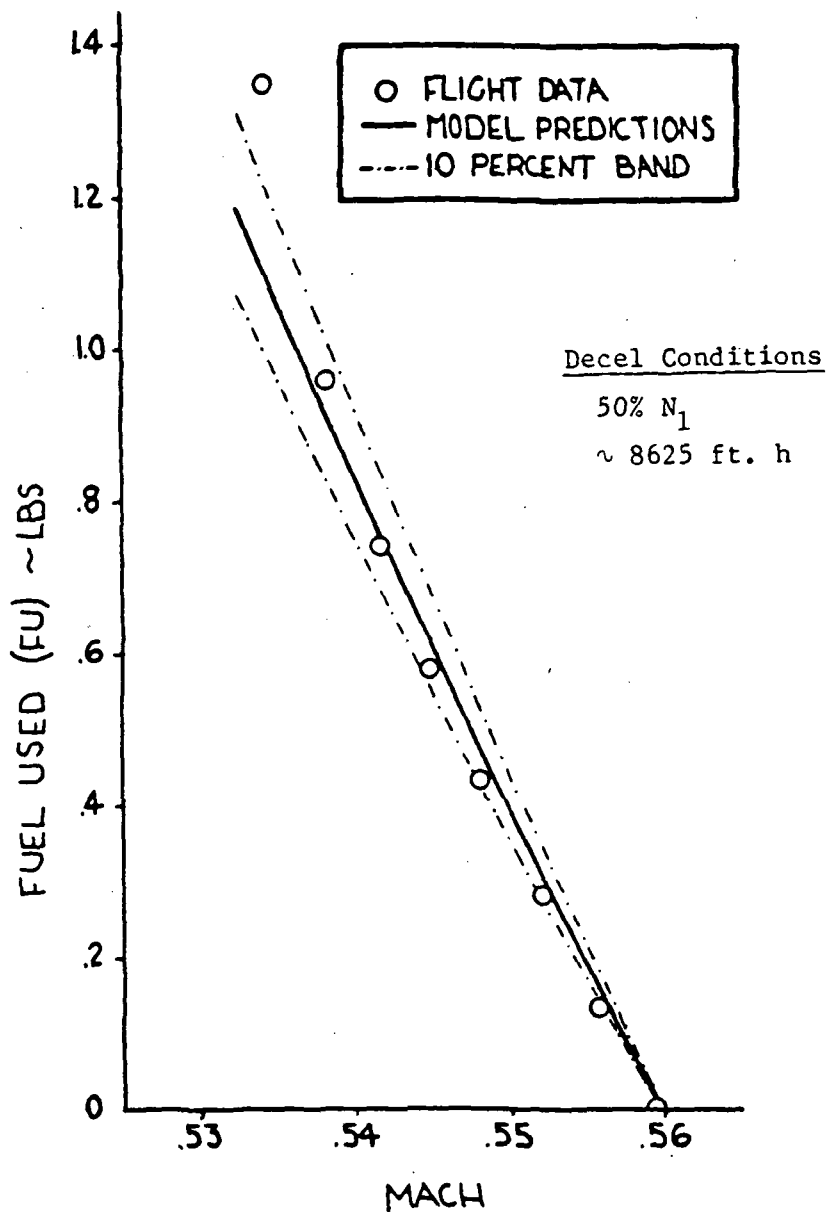


Figure I.5: MODEL Fuel Used Prediction, Profile 5

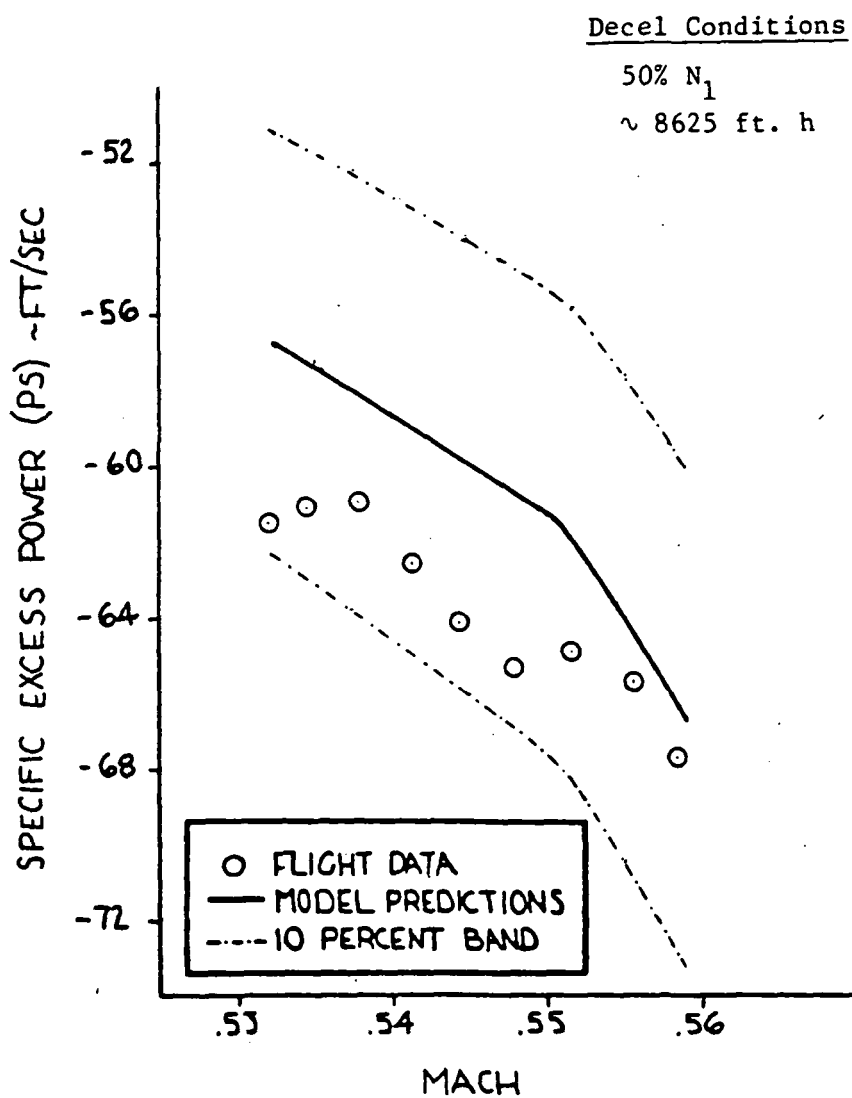


Figure I.6: MODEL P_S Prediction, Profile 5

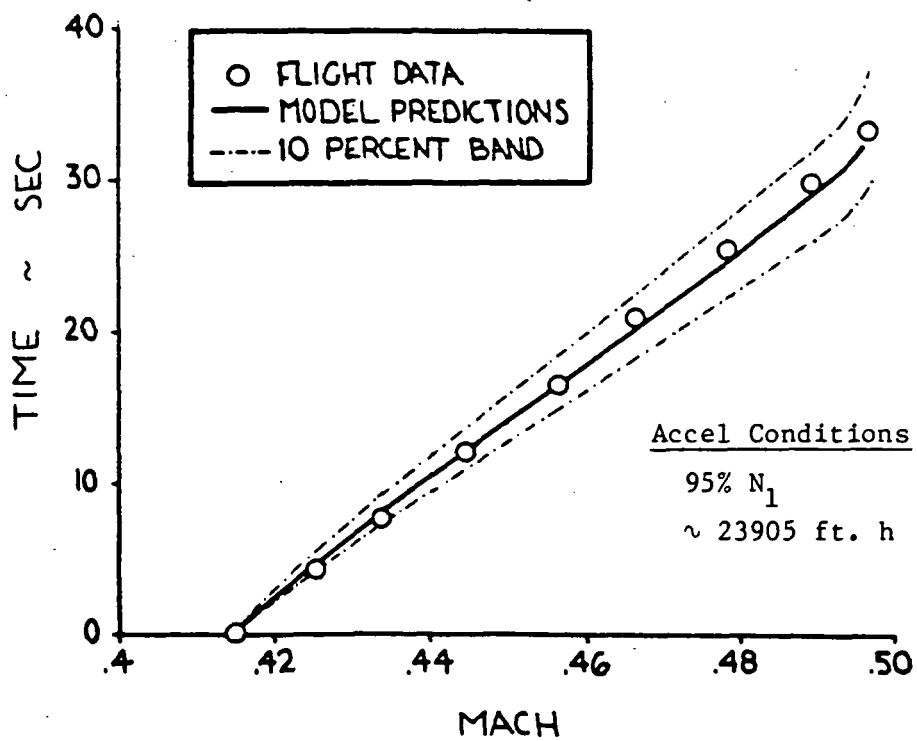


Figure I.7: MODEL Time Prediction, Profile 8

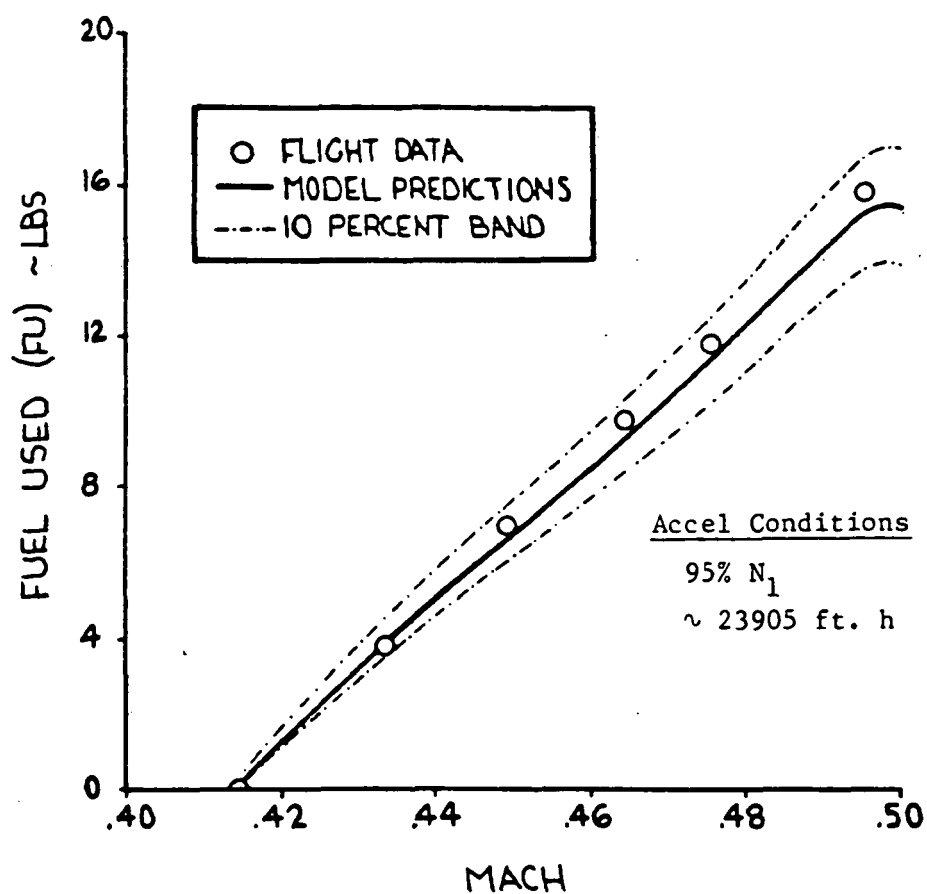


Figure I.8: MODEL Fuel Used Prediction, Profile 8

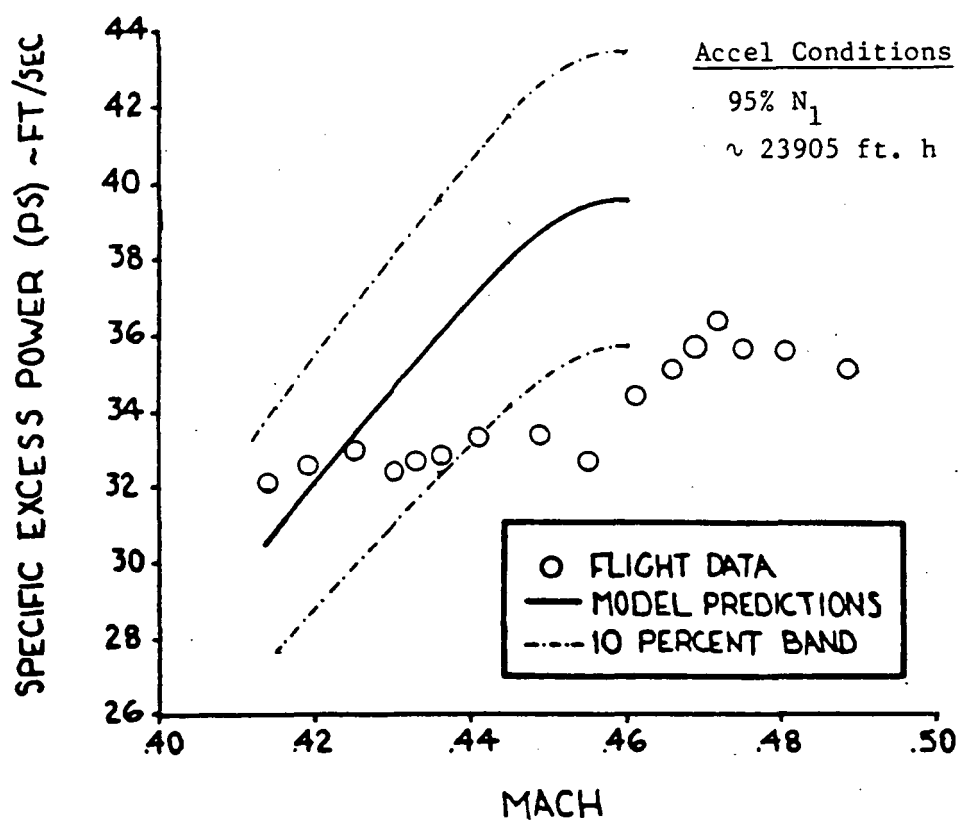


Figure I.9: MODEL P_s Prediction, Profile 8

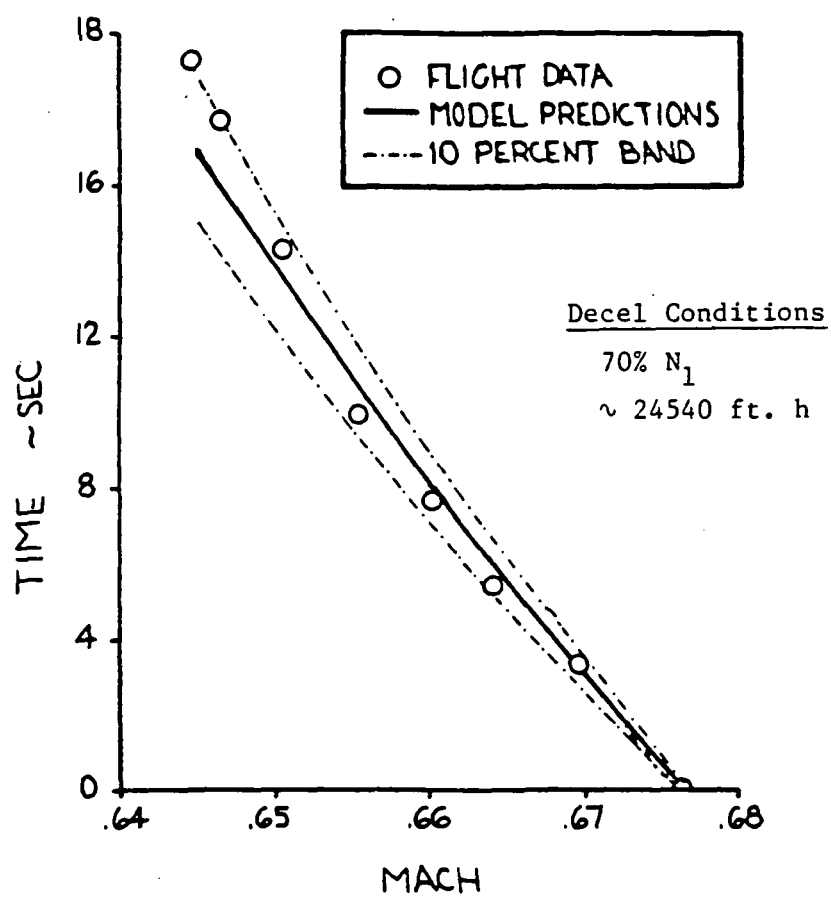


Figure I.10: MODEL Time Prediction, Profile 9

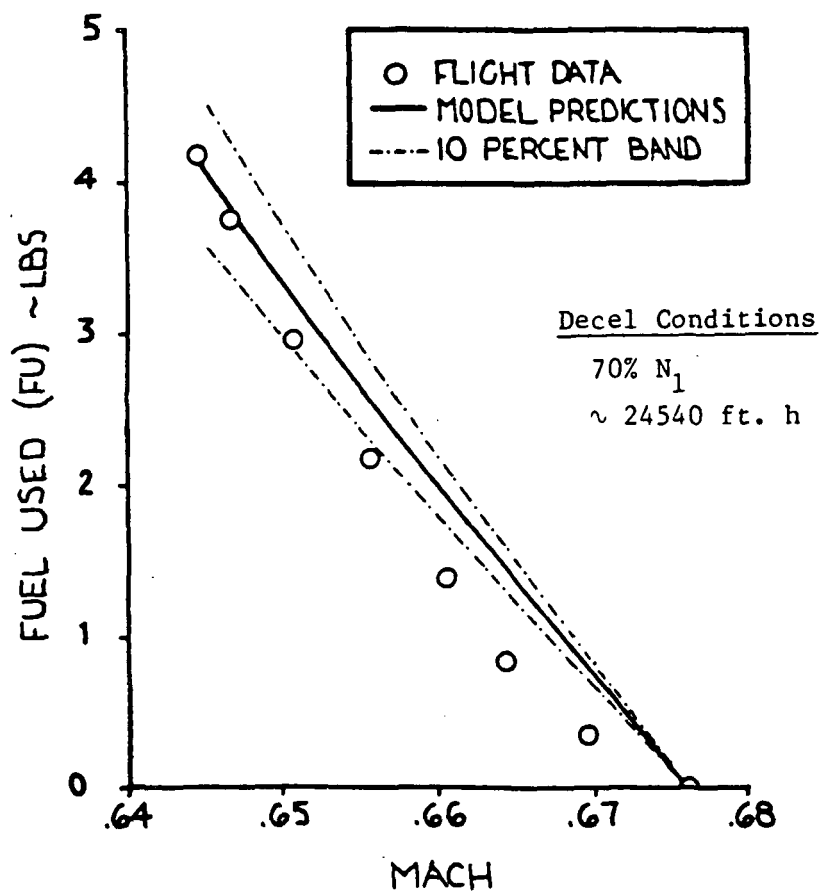


Figure I.11: MODEL Fuel Used Prediction, Profile 9

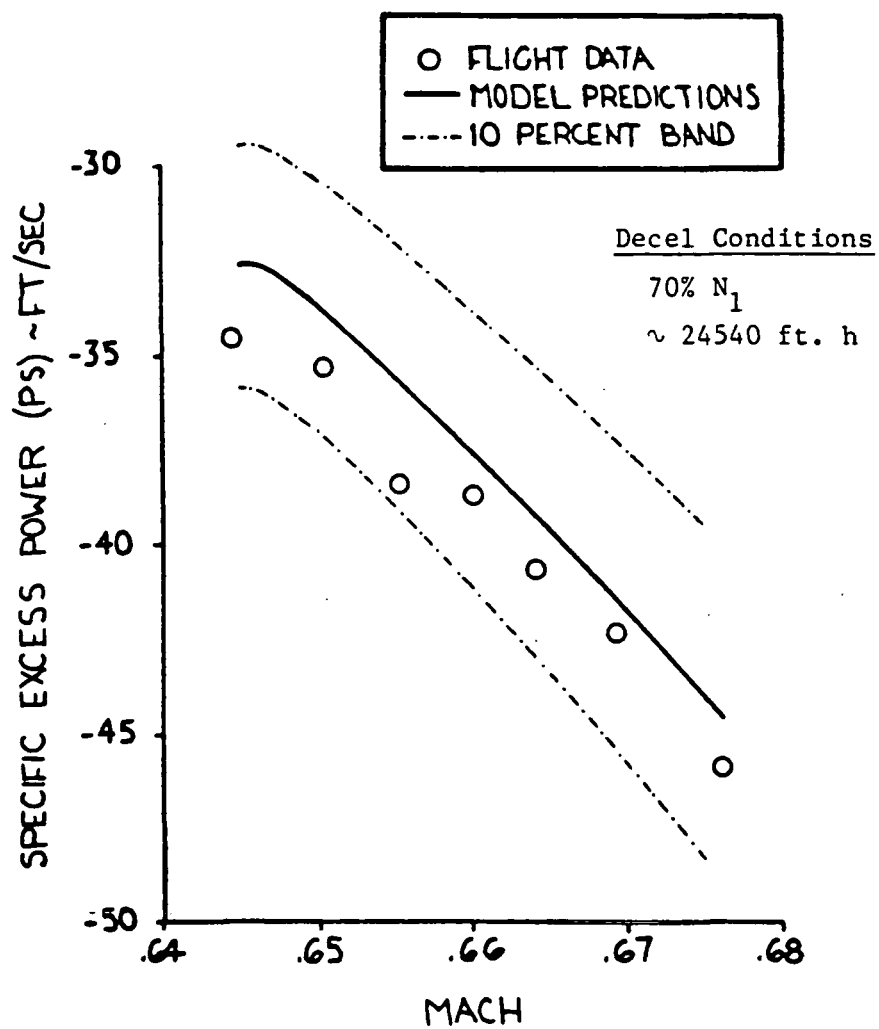


Figure I.12: MODEL P_s Prediction, Profile 9

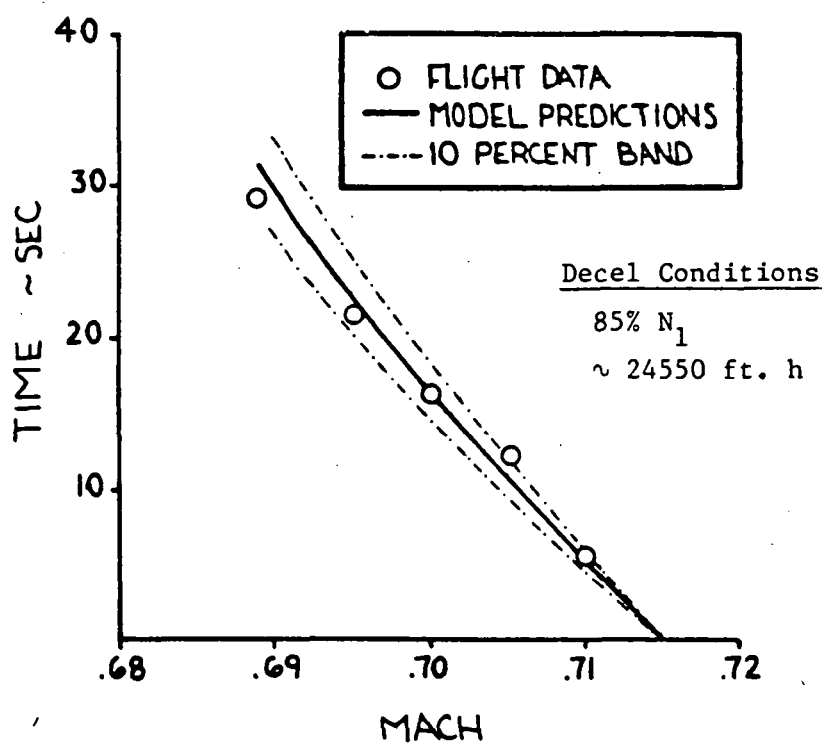


Figure I.13: MODEL Time Prediction, Profile 10

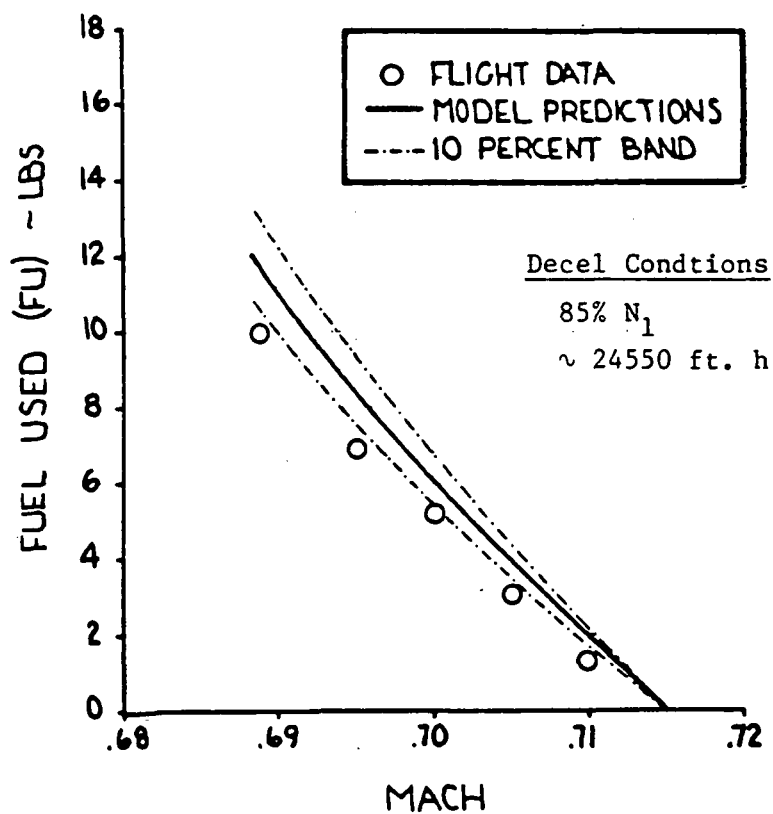


Figure I.14: MODEL Fuel Used Prediction, Profile 10

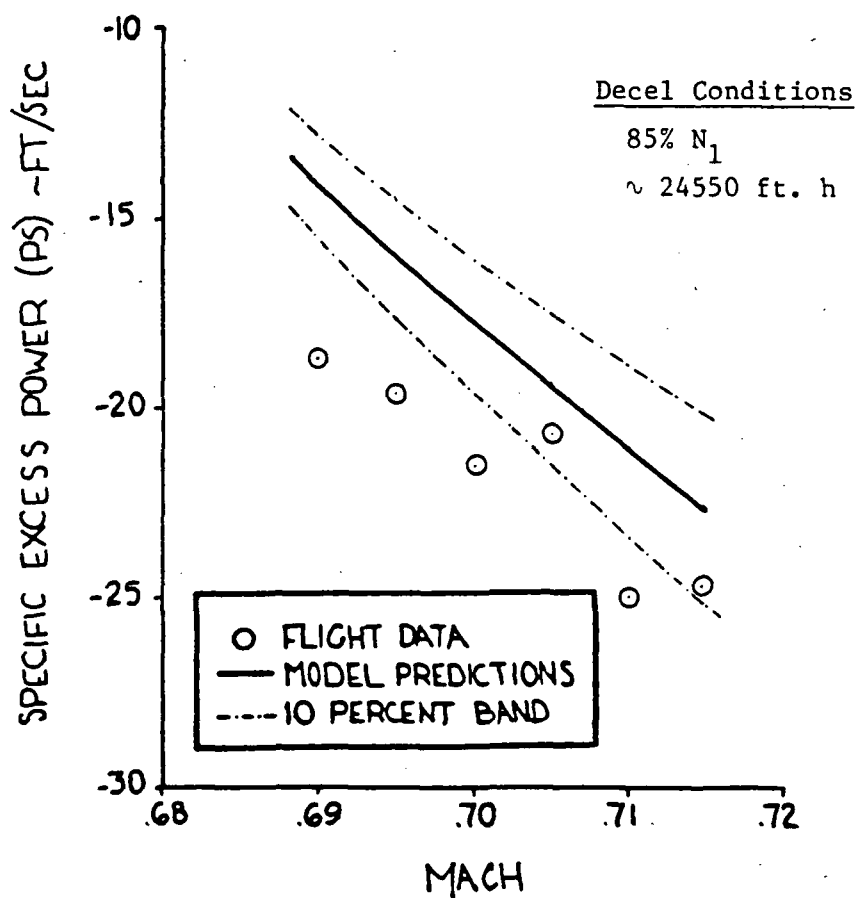


Figure I.15: MODEL P_s Prediction, Profile 10

1. Report No. NASA CR-170414	2. Government Accession No.	3. Recipient's Catalog No.	
4. Title and Subtitle Development and Evaluation of a Performance Modeling Flight Test Approach Based on Quasi Steady-State Maneuvers		5. Report Date April 1984	
		6. Performing Organization Code	
7. Author(s) Thomas R. Yechout and Keith B. Braman		8. Performing Organization Report No.	
		10. Work Unit No.	
9. Performing Organization Name and Address Flight Research Laboratory University of Kansas Center for Research, Inc. Laurence, Kansas 66045		11. Contract or Grant No. NSG-4028	
		13. Type of Report and Period Covered Contractor Report-Final	
12. Sponsoring Agency Name and Address National Aeronautics and Space Administration Washington, D.C. 20546		14. Sponsoring Agency Code RTOP 505-36-21	
15. Supplementary Notes NASA Technical Monitor: Paul C. Redin, Ames Research Center, Dryden Flight Research Facility, Edwards, California 93523.			
16. Abstract This report describes the development, implementation and flight test evaluation of a performance modeling technique which required a limited amount of quasi steady-state flight test data to predict the overall one g performance characteristics of an aircraft. A saving in flight time of up to 60 percent over classical methods was projected, and the technique provided significantly more information. The concept definition phase of the program included development of 1) the relationship for defining aerodynamic characteristics from quasi steady-state maneuvers, 2) a simplified in-flight thrust and airflow prediction technique, 3) a flight test maneuvering sequence which efficiently provided definition of baseline aerodynamic and engine characteristics including power effects on lift and drag, and 4) the algorithms necessary for cruise and flight trajectory predictions. Implementation of the concept included 1) design of the overall flight test data flow, 2) definition of instrumentation system and ground test requirements, 3) development and verification of all applicable software and 4) consolidation of the overall requirements in a flight test plan. A flight test evaluation which included over 17 flying hours was then conducted using a Learjet Model 35 aircraft to verify the concept and provide an overall methodology.			
17. Key Words (Suggested by Author(s)) Performance modeling Thrust modeling Learjet 35 Flight test Computer modeling		18. Distribution Statement Unclassified-Unlimited STAR category 05	
19. Security Classif. (of this report) Unclassified	20. Security Classif. (of this page) Unclassified	21. No. of Pages 425	22. Price* A18

*For sale by the National Technical Information Service, Springfield, Virginia 22161.